Monitoring as a tool for the assessment of wastewater quality dynamics

Rémy Schilperoort

Printed by Gildeprint drukkerijen - Enschede, the Netherlands
Published by Water Management Academic Press - Delft, the Netherlands
ISBN/EAN 978-90-8957-021-5
NUR 956

Keywords: sewer system, monitoring, wastewater quality dynamics, spectroscopy, distributed temperature sensing, wastewater treatment plant influent

Monitoring as a tool for the assessment of wastewater quality dynamics

Proefschrift

ter verkrijging van de graad van doctor
aan de Technische Universiteit Delft,
op gezag van de Rector Magnificus prof.ir. K.C.A.M. Luyben,
voorzitter van het College voor Promoties,
in het openbaar te verdedigen op vrijdag 17 juni 2011 om 15.00 uur
door Rémy Peter Sander SCHILPEROORT
civiel ingenieur
geboren te Delft

Dit proefschrift is goedgekeurd door de promotoren:
Prof.dr.ir. F.H.L.R. Clemens
Prof.ir. J.H.J.M. van der Graaf

Samenstelling promotiecommissie:

Rector Magnificus	voorzitter
Prof.dr.ir. F.H.L.R. Clemens	Technische Universiteit Delft, promotor
Prof.ir. J.H.J.M. van der Graaf	Technische Universiteit Delft, promotor
Prof.dr. J.-L. Bertrand-Krajewski	INSA de Lyon
Ass.Prof. Dipl.-Ing. Dr.techn. G. Gruber	Technische Universität Graz
Prof.dr.ir. I. Nopens	Universiteit Gent
Prof.dr. S.J. Tait	University of Bradford
Prof.dr.ir. N.C. van de Giesen	Technische Universiteit Delft
Prof.dr.ir. J.B. van Lier	Technische Universiteit Delft, reservelid

Dit proefschrift is tot stand gekomen met (financiële) ondersteuning van:
Arcadis
Grontmij
Hoogheemraadschap Hollands Noorderkwartier
Royal Haskoning
Tauw
Waternet
Waterschap de Dommel
Waterschap Groot Salland
Witteveen+Bos

‘But he continued to look and it was all as wonderful to him and it moved him as it had when he was eighteen years old and had seen it first, understanding nothing of it and only knowing that it was beautiful.’

Ernest Hemingway, Across the River and into the Trees

“If I’d go on and become prime minister I would not see my children grow up. That’s not worth it to me."

Wouter Bos, resigning as leader of the PvdA (Dutch Labor Party) in March 2010

Table of contents

Chapter 1. Introduction

1.1 Broad context of the thesis

Sewer systems serve two purposes. Their first objective is the collection of wastewater and its removal from urban areas. By removing it, exposure of inhabitants to faecally contaminated water is largely avoided hence reducing the number of water-borne diseases in urban areas. Their second objective is the collection of excess stormwater and its removal from urban areas in order to prevent flooding. Both types of water are generally collected in underground sewer pipes and directed towards a central point of discharge which is often located near local surface water downstream the urban area. In the Netherlands the large-scale development of sewer systems has begun at the beginning of the 20th century, see Figure 1-1. Nearly a century later, over 99% of Dutch households are connected to some form of wastewater handling. The construction of sewer systems has been very successful in the sense that its two purposes have been largely fulfilled: water-borne diseases as well as stormwater-related urban flooding have become (relatively) rare in the Netherlands.

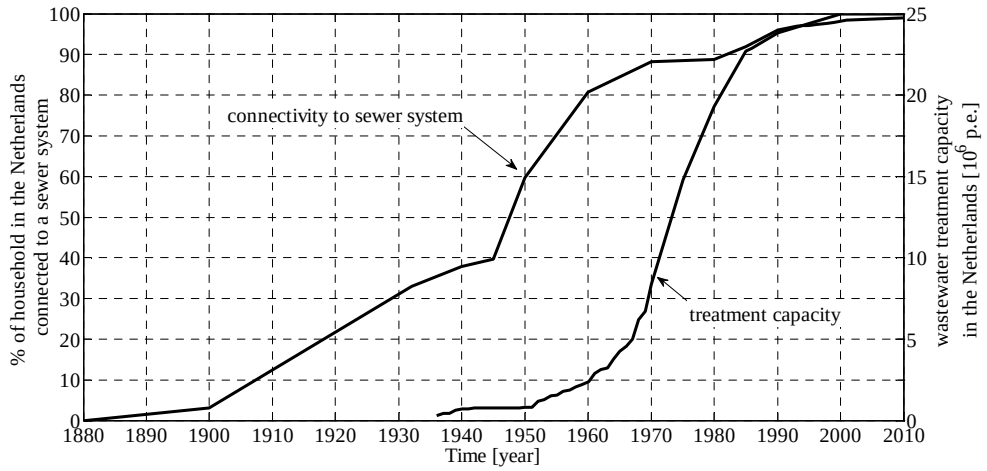

Figure 1-1: Development in the 20th century of connectivity of households in the Netherlands to a sewer system and wastewater treatment capacity (reproduced with permission from Langeveld, 2004).

An important drawback of sewer systems has originally been the centralized discharge of large amounts of raw sewage to receiving waters. As early as the end of the 19th century it became apparent in and around major European cities that

discharging untreated wastewater can cause a severe deterioration of surface water quality and a wide variety of associated negative effects. To mitigate this problem water pollution control measures have been implemented. The most important measure has been the wide-spread construction of wastewater treatment plants (wwtp). These facilities aim at reducing pollutant loads in wastewater prior to its discharge to receiving waters. Large-scale construction in the Netherlands started in the 1940s with especially in the 1960s and 1970s a major increase in treatment capacity, see Figure 1-1. Since the 1990s nearly all collected domestic wastewater in the Netherlands receives treatment at a wwtp.

Just considering Figure 1-1 it might be concluded that current wastewater infrastructure in the Netherlands is 'complete' in the sense that almost the entire population is connected to a sewer system and nearly all wastewater is being treated. Nevertheless, surface water quality problems have not ceased to exist. Implemented measures (such as the construction of wwtps) have largely improved surface water quality compared to several decades ago, but many surface waters in the Netherlands are yet to meet the set water quality target levels. More specifically, a survey for implementation of the European Water Framework Directive (WFD) shows that roughly 20% of samples collected from the 724 identified surface water bodies in the Netherlands do not meet the requirements in terms of good chemical and/or ecological status (Min.V&W, 2010). Discharges of (untreated) wastewater into receiving water are still a major contributor to high pollution levels in surface waters. It should be noted, however, that other factors such as wash out from agricultural lands, resuspension from contaminated sediment layers and pollutants in precipitation also contribute. Especially for small urban surface waters RIONED (2009a) shows that the contribution of sources other than from wastewater infrastructure can be non-negligible.

Wastewater and its associated pollutants can reach surface waters via a number of routes. A major contributor is wwtp effluent. Annual mean treatment efficiencies for key pollutant parameters are less than 100% (e.g. BOD ~98%; COD ~90%; N_{total} and P_{total} ~80%, see RIONED, 2009b) resulting in non-zero pollutant concentration levels in discharged effluent. Treatment efficiencies can further deteriorate under, for instance, specific wet weather conditions (Langeveld, 2004). A second route is via combined sewer overflows (CSO) that serve as emergency outlets in case a sewer system is nearly flooded. In areas with separated sewer systems a third route is via the outlets of stormwater sewers. Pollutant levels in discharged 'stormwater' can be significant especially if the system holds one or multiple illicit connections. Foul water is then erroneously discharged to the stormwater sewer.

Over the last decades large efforts have been made in both practice and science to find ways to improve the performance of wastewater infrastructure. Essentially, the

ultimate objective of many of these optimization efforts is to reduce the impact of wastewater infrastructure on its environment. Often, this translates into an effort to reduce the amount of pollutants discharged via (one of) the aforementioned routes. This can be achieved by, for instance, adding or improving treatment technologies at the wwtp in order to improve treatment efficiencies, applying control to a sewer system to reduce the number of CSO events, the installation of forms of effluent treatment installations such as storage and settling tanks and the search for and removal of illicit connections.

The contents of this thesis fit this 'tradition': its ultimate goal is to contribute to the reduction of impact of wastewater infrastructure on its environment. In the next paragraphs this is further narrowed down to arrive at a more specific research objective.

1.2 Integrated system optimization accounting for water quality

Optimization programs are a frequently applied means to improve wastewater system performance. Many of these programs essentially follow the same principle: a number of alternative optimization measures are evaluated against one or multiple criteria. Examples of such measures are the construction of settling and storage tanks near CSOs, increasing the available pumping capacity from a sewer system into a wwtp and installation of additional treatment steps at a wwtp. Predominantly, the criteria used in an evaluation are performance with respect to set emission standards (e.g. annual CSO volume, wwtp effluent pollutant concentrations) and investment costs. Hence, changing standards often requires new optimization efforts. Historically, sewer systems in the Netherlands are operated by municipalities whereas wastewater treatment plants are the concern of dedicated water authorities. As a result of this organizational separation, optimization programs were (and still are) often developed for each system separately. Also, most optimization programs were volume based, not taking into account any water quality aspects. The need to change this approach to an integrated assessment became apparent with a growing awareness in the 1990s that emissions from both sewer systems and treatment plants are responsible for deterioration of receiving water quality (Lijklema *et al.*, 1993). At first, the term 'integrated optimization' included wastewater infrastructure only focusing on emissions from sewers and wwtps; further on system limits were extended to also include receiving waters with an associated shift in focus towards impact-based optimization. Apart from system integration the idea grew that optimization measures that were optimal in a volume based approach might not be optimal, or even detrimental, when considering water quality aspects. Also, the *dynamics* of both water quantity and quality parameters were expected to play an important role in attaining a better system performance.

In 1999 a research program was initiated at TU Delft to investigate possible benefits of an integrated approach to wastewater system optimization accounting for possible water quality variations. The program comprised a PhD-position that was co-financed by university and engineering firms (and later joined by water authorities). The first phase of the research program (1999-2004) aimed at *"identifying the possibilities to extend today's Dutch volume based approach for wastewater system optimization to a water quality based approach by taking into account the dynamic interactions within wastewater systems"* (Langeveld, 2004). Based on literature assessment, model simulations and data analyses, a first conclusion of the study was that dynamic interactions are indeed important for wastewater system performance: wwtp effluent quality is truly affected by quantitative as well as qualitative fluctuations in wwtp influent, which are in turn determined to a large extend by characteristics of the contributing sewer system. Hence, the operation and state of maintenance of a sewer system was found to be a key element in wastewater system optimization as it not only affects CSO performance but also wwtp effluent quality. Second, using a semi-hypothetical integrated model, multiple optimization strategies such as 'additional storage' and 'altering pumping capacity' were tested. It was found that the optimal configuration largely depends on the quality parameter selected to describe wastewater system performance. In addition, it was shown that the characteristics of storm events play an important role in the selection of the best optimization strategy. Also, model simulations showed that the volume of wastewater present in a sewer system (pressure mains, lost storage) can exert a significant influence on wastewater system performance by its pollution potential.

Knowledge of the actual state of wastewater infrastructure and the characteristics of the processes that take place inside are indispensible for proper system optimization. For sewer systems much effort has been put into *modeling* of hydrodynamics and water quality processes. The basic in-sewer processes that determine the (variation in) quantity and quality parameters are hydrodynamics, transport of soluble pollutants, transport of suspended solids, and in-sewer transformations. However knowing the general mechanisms of all of these processes, efforts to model in-sewer wastewater *quality* parameters have hitherto not resulted in accurate predictions (Willems, 2006, 2008; Clemens *et al.*, in preparation). Many factors that have an influence on the shape of pollutographs have not (yet) or only partially been incorporated into water quality models. Examples are an incomplete knowledge of parameter behavior governing important processes (resuspension processes, the composition of in-sewer sediment layers, etc.), the manner in which a sewer system is operated (set points of pumps, the use and performance of storage facilities, etc.) and maintained (frequency of gully pot cleaning, presence of dead storage, etc.) or errors in the database describing the structure of the sewer system and the geometry of its components. Also, important determining factors such as the number and location of illicit connections in

separate sewer systems are not likely to be included in a model. As a result, wastewater quality modeling is in some cases not (yet) an appropriate tool to study the behavior of wastewater quality parameters.

Partly because models need data for calibration and validation purposes and partly because some processes appear to be too complex to be correctly modeled, a tendency towards *monitoring* of wastewater processes can be observed. Data are generally used as a diagnostic tool to directly assess a process or condition parameter, or indirectly calibrating a model that simulates the considered process or condition parameter. Also, sensors can be part of an automatic control system for which they provide the input. Application of monitoring equipment in wastewater systems is however not straightforward, which is further elaborated on in the next paragraph. The second phase of the aforementioned TU Delft research program (2004-2009) has therefore focused on monitoring in wastewater systems. In cooperation with a water authority a monitoring network has been installed in a large wastewater system to gather data on a number of water quality parameters at a variety of locations throughout the system. This thesis describes and analyzes a *part* of the results, namely the results of quantity and quality monitoring at a wwtp influent pumping station. In addition, a novel monitoring technique that targets wastewater temperature has been tested in three municipalities. Results of these tests have also been included in this thesis.

1.3 Wastewater monitoring

1.3.1 Introduction

Monitoring is increasingly applied in wastewater infrastructure. Recent developments in sensor technology in combination with efforts to apply this technology in wastewater systems have led to a rapid increase in the availability of data sets describing a wide variety of parameters in and around wastewater infrastructure. Modern sensors often allow the collection of continuous and high-frequent data sets, which offers an advantage over the short-term and low-frequent sets generated with ‘traditional’ methods such as (composite) grab sample collection. This thesis describes two of such sensor developments that aim at high-frequent monitoring of wastewater quality: UV/VIS sensing (using UltraViolet and VISible light) and DTS monitoring (Distributed Temperature Sensing) with fiber-optics.

Wastewater monitoring can aim at a wide variety of parameters. These parameters either describe the *condition* of (a component of) the wastewater system or *processes* that take place in the system. An example of (in-sewer) monitoring of condition parameters is the inspection of sewer pipes with CCTV cameras, the data of which often play a role in sewer pipe renovation. However widely applied, the

objectiveness, consistency and reproducibility of human interpretation of CCTV footage are under discussion (Dirksen *et al.*, 2011). As a result, developments to use digital image processing and additional sensor types (lasers, ultrasound) in order to obtain a more objective representation of the condition of the sewer system, are wide-spread (e.g. Teichgräber *et al.*, 2006; Guo *et al.*, 2009). Measurements to determine the condition of a sewer system are *not* topic of this thesis; measurements of process parameters to study system performance are. Monitoring of *process* parameters aims at determining the quantity or quality of wastewater either in the sewer or transport system or at the treatment facility.

Wastewater monitoring in the context of this thesis is monitoring of *raw and untreated* wastewater which is typically found in sewer systems. Monitoring of wastewater at a wastewater treatment plant (wwtp) differs from monitoring of wastewater in sewer systems in a sense that a wwtp provides relatively *steady* and *controlled* monitoring conditions. Sensors in sewers, however, are exposed to a much larger variation in flows and ambient conditions. For instance, solids (e.g. sediments, toilet paper, branches, sanitary products, etc.) that often cause contamination problems for sensors installed in sewer systems, are generally directly targeted upon arrival at a wwtp reducing contamination problems for wwtp sensors. Also, most sensors at treatment facilities have easy access and can hence be frequently checked upon by wwtp personnel whereas access to in-sewer sensors can be difficult, time consuming and expensive (Scheer and Schilling, 2003). The data described in this thesis have been collected in combined and separate sewer systems (DTS sensing) as well as in the influent pumping station of a treatment plant (UV/VIS sensing). The latter location combines the raw quality of in-sewer wastewater with the favorable monitoring conditions of a wwtp.

1.3.2 In-sewer wastewater quantity monitoring

In-sewer water *quantity* data sets are a basic requirement for many analyses on in-sewer processes. Therefore, for many decades effort has been put into the development of monitoring techniques that are able to accurately determine the amount of wastewater passing an in-sewer location. Nevertheless, determining the amount of water that flows through a sewer pipe remains a challenge. Sensors for *full pipe* flow measurements are generally installed around the targeted pipe (such as around a pressure main or around the discharge line of a pump in a pumping station). Due to a relatively steady velocity profile inside the pipe these sensor types have limited uncertainty bands on the order of a few percent. Common monitoring equipment for flow measurements in *part-full pipes* however, suffer from uncertainty bands that are an order of magnitude larger with reported errors up to 50% (Watt and Jefferies, 1996; Smits *et al.*, 2007). The bottleneck is the water *velocity* monitoring that is mostly based on an ultrasonic or electromagnetic

measurement principle. Water velocity profiles change rapidly with a variation in water levels and other monitoring conditions, rendering calibration parameters for one set of conditions invalid for other sets of conditions (de Man, 2008; de Man *et al.*, 2008). Moreover, these types of sensors are often installed in the sewer pipe at invert level and hence suffer from sedimentation and debris on and around the sensor that can hamper the signal. Alternative approaches such as velocity estimation using image analyses are being developed (Jeanbourquin *et al.*, 2010). In practice, part-full sewer pipes are generally targeted with more robust water *level* measurements that show much smaller uncertainty bands. Water levels are often measured with pressure inducers installed at or around a sewer pipe invert level. Ultrasonic and radar type measurements are also used. Measured water levels can subsequently be combined with hydrodynamic sewer models to calculate in-sewer flows.

One chapter of this thesis is dedicated to wastewater quantity monitoring. Results of electromagnetic full-pipe flow measurements are used to derive flows arriving at a wwtp influent pumping station. An elaborate assessment of these flow data is included in the thesis to *support* the actual objective of the thesis which is the assessment of dynamics of wastewater *quality* parameters. Flow is a key explanatory parameter for (variations in) water quality values. Also, using the flow data, measured concentration values of quality parameters can be transformed into quality parameter pollutant *loads* arriving at the treatment plant. Hence, while presenting the results of wastewater quantity monitoring is not an objective of the present study, results of flow monitoring are necessarily included.

1.3.3 In-sewer wastewater quality monitoring

Wastewater quality monitoring has long been an issue only at wastewater treatment plants. Results of quality measurements were and still are used for a variety of purposes such as process control, regulatory monitoring and model calibration. Since the 1970s the concept of instrumentation, control and automation (ICA, i.e. basing operational decisions on data from sensors installed in the process) at treatment plants has become gradually accepted as a means of maintaining control over increasingly complex plants (Olsson, 2002). Developments in instrumentation technology, improved actuators, enhanced data collection and data processing and a gradual familiarization of operators with the techniques have all contributed to the increasing and successful implementation of ICA at treatment facilities.

Large-scale trials to monitor wastewater quality in *sewer systems* are of more recent date. For long, an incentive to monitor in-sewer wastewater quality has been absent. Instead, wastewater *quantity* has been the main concern: real-time control of sewer systems has focused predominantly on wastewater levels and volumes

(e.g. Weyand, 2002; Schütze *et al.*, 2004), combined sewer overflow (CSO) regulations have long concerned overflow frequencies or volumes only (e.g. Langeveld, 2004) and in the field of in-sewer process modeling correct hydrodynamic modeling has been of primary concern (Clemens, 2001). Moreover, as earlier described, requirements for in-sewer quality monitoring in terms of robustness of sensor systems and maintenance frequencies are harder to fulfill. Combined with the fact that sewer managers in the Netherlands are generally part of relatively small organizations that often lack the means to maintain and operate advanced sensor systems, it can be understood that the development of in-sewer quality monitoring lags behind its equivalent at wastewater treatment plants. With an increasing interest in the actual spilled pollutant concentration or even load from CSOs and with the appearance of concepts such as pollution-based real-time control of wastewater (treatment) systems, the desire to monitor wastewater quality at various locations in the sewer system has emerged. As a result, a number of large-scale projects that implement quality sensors in sewer systems have been initiated (e.g. Grüning and Orth, 2002; Gruber *et al.*, 2005; Bertrand-Krajewski *et al.*, 2007)

In terms of technical approaches of wastewater quality monitoring, the main development lies in the transition from discontinuous, low-frequency, manual or automated grab sampling with subsequent laboratory analysis to continuous, high-frequency and fully automatic online monitoring with dedicated sensors. This new approach has become available with the development of alternatives to the traditional chemical analysis methods. Examples of such alternatives that have been applied in sewer systems are optical measurements (UV and UV/VIS absorption), ion selective electrodes (NH_4^+) and biosensors (Vanrolleghem *et al.*, 1999; Bourgeois *et al*., 2001).

This thesis presents the results of the application of two types of modern wastewater quality sensors in sewer systems in the Netherlands. The first type (UV/VIS sensors) consists of optical measurements that provide continuous and high-frequent results of the quality parameters *TSS*, *total COD* and *soluble COD*. These sensors have been applied in the influent pumping station of a wwtp for the purpose of long-term monitoring of the quality of wastewater from three distinct catchment areas. The second type (DTS monitoring) also consists of optical measurements, but resulting in data sets of the water quality parameter *temperature*. Measuring with a fiber-optic cable that is installed along a sewer section the temperature of the wastewater can be determined with a high frequency and simultaneously over many individual parts of the cable.

1.3.4 Measuring frequency, large data sets and data validation

The measuring frequency of the data sets discussed in this thesis is on the order of once per minute (UV/VIS sensors: 2 minutes^{-1}; flow sensors: 1 minute^{-1}; DTS sensors: 30 seconds^{-1}). The selection of frequencies has *not* been based on an assessment of minimal characteristic time-scales of processes that need observation, but merely on practical arguments. For the UV/VIS and DTS sensors the smallest possible frequency (in terms of practical operation of the sensor) has been selected to include as many data points as possible. The added value of observing water quality parameters with a measurement interval of 1 minute (as opposed to 15 or 60 minutes intervals as mostly used for grab sampling campaigns) is shown by e.g. Henckens and Schuit (2002) and Veldkamp *et al.* (2003) and illustrated in Figure 1-2. The graph shows two time-series of NO_3^- measurements collected from the same wwtp influent wastewater over a time-span of 24 hours. The first time-series comprises results of 24 grab samples (i.e. one per hour) with subsequent laboratory analysis; the second time-series comprises 720 measurements (i.e. one per 2 minutes) with an online UV/VIS sensor. The large nitrate peak during night hours can be well observed with the UV/VIS sensor. Based only on laboratory results the peak value of around 45 mg/L would not have been noticed. Moreover, without the sensor results the lab result at 22h30 (25.4 mg/L) might erroneously be identified as an outlier since the value lies (for instance) more than 4 times the standard deviation from the mean.

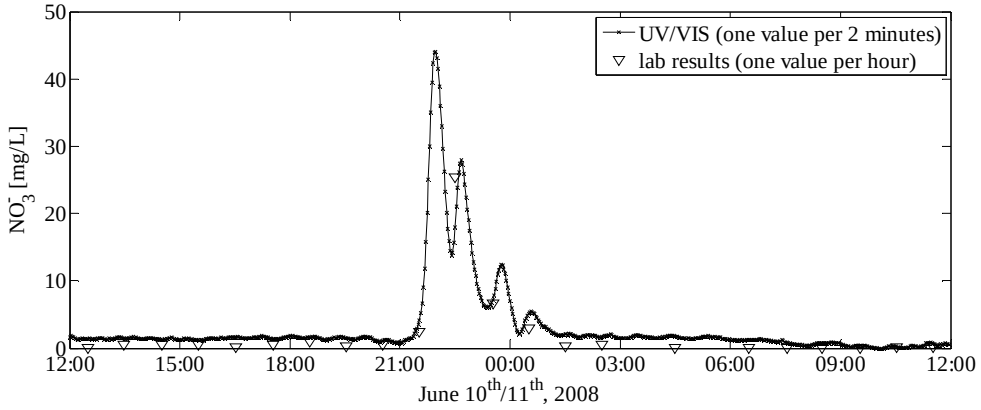

Figure 1-2: NO3 measurements in wwtp influent wastewater with a UV/VIS sensor (one value per 2 minutes) vs. with lab analysis (one value per hour).

The application of sensors with high measuring frequencies results in the generation of (much) larger data sets than in the past. With this development, the ratio between time invested in data gathering and generated number of data points

has decreased. This is illustrated by an inventory made by Brombach and Fuchs (2003) of measured pollution levels in combined and separate sewer systems. An extensive search over the time-span 1968 - 2001 has yielded a collection of data comprising approximately 16 million individual data points, distributed over 34 pollution parameters. The majority of these data points have been generated using grab samples and laboratory analysis. The authors estimate that the dataset represents roughly 2000 man-years of work which equals 15 minutes per measurement. In contrast, the data presented in this thesis add to an order of 50 - 100 million individual data points for which - very roughly estimated - 12 man-years of work were invested. In other words, each measurement in this thesis corresponds to (on average) approximately 1 second of work, reducing the aforementioned 15 minutes by a factor of 1000.

With the generation of such large data sets using modern sensor technology, the need for large-scale data *validation* is introduced. With traditional grab sampling and subsequent laboratory analysis each measurement receives 'personal attention' allowing for immediate quality control. A sensor, however, performs measurements largely unattended. Hence, data sets require a *posteriori* quality check to exclude any data points that do not correctly represent the targeted parameter. Generally, such data anomalies must be identified using the data themselves, using other sources of information, or a combination of both. This way, data validation procedures play an important role in the transfer from raw data to information and knowledge. Basing data analyses on correct data only reduces the chance of false conclusions. In this thesis for each of the data sets presented an elaborate data quality assessment has been included prior to use of the data in data analyses.

1.3.5 Wastewater monitoring in the Eindhoven area

Waterschap de Dommel (WDD) is one of 26 dedicated water boards in the Netherlands. One of its responsibilities is the operation and maintenance of the wastewater treatment plant of Eindhoven and its contributing wastewater transport system. The wwtp Eindhoven discharges its effluent to the river Dommel, which is relatively small receiving water. Especially in summer months, wwtp effluent can make up a large fraction of the total flow in the river. As a result, (emergency) discharges of wwtp effluent can easily cause exceeding of surface water quality standards and cause severe damage to the ecology in the river. The vulnerability of the receiving water is reflected in the wwtp discharge permit: it forced WDD in 2003 to start a "research program into the further optimization of the wwtp and in particular into an improved nutrient removal" (WDD, 2004). The water board subsequently expressed the ambition to investigate the possibilities for implementation of (pollution-based) real-time control (RTC) as a possible means for wastewater system optimization.

To study possibilities for RTC, a monitoring program in the wastewater system of the wwtp Eindhoven was initiated in September 2005. TU Delft participated in the design of the sensor network and aided in data analyses. In the first months of 2006 a monitoring program was conceived. It was decided to focus the program on water quantity and quality parameters of wwtp influent as well as on water quantity parameters in the wastewater transport system. An overview of the monitoring network with installed sensors and monitoring locations can be found in appendix A. In autumn of 2006 most sensors were installed at the selected monitoring locations. In the following months, many monitoring stations required (sometimes substantial) improvements to the sensor set-up, to the maintenance schedule or to the data communication and storage system. After implementation of all improvement works, on April 1st, 2007 long-term monitoring was started. Three months later, in July 2007, a network for precipitation monitoring was added to the program. The data sets considered in this thesis cover a 19-months time-span from April 1st, 2007 till November 1st, 2008. Not all data sets are presented in the thesis: the selection is limited to precipitation (chapter 3), flow measurements at the wwtp influent pumping station (chapter 4) and water quality measurements using UV/VIS sensors also at the wwtp influent pumping station (chapter 5).

In 2009 it has been decided by WDD to further extend the monitoring network in the Eindhoven wastewater system. A new set-up for precipitation monitoring as well as additional sensors in the surface water system, at the Eindhoven treatment plant, in the contributing transport systems and at CSOs will complete the data collection system. The objectives of the project (referred to as Kallisto-project) are the improvement of wwtp effluent quality in terms of N and P, and the prevention of oxygen depletion and ammonium peaks in the river Dommel due to wwtp effluent and CSO spills. An elaborate description of the Kallisto-project can be found in Weijers *et al.* (accepted).

1.4 Thesis objective

The objective of this thesis is twofold. The first objective is the further development of in-sewer wastewater metrology. More specifically, it aims at a description of in-sewer application of two novel types of sensors: UV/VIS spectroscopy and DTS with fiber optics. As field applications of both sensor types are rare, a thorough documentation of monitoring set-ups is included in the thesis. Given the used installations, research questions associated with both monitoring techniques are:

- What sensor calibration is required and how can it be implemented?
- What is the data uncertainty?
- What is the data quality?

The second objective of the thesis is the assessment of in-sewer wastewater quality dynamics. More specifically, using the UV/VIS data it aims at an understanding of the variability of influent loads from three distinct catchment areas to a wastewater treatment plant. Using the DTS data it aims at an understanding of small-scale spatial and temporal temperature variations in combined and separate sewer systems. Associated research questions are:

- What are the characteristics of the observed dry and wet weather pollutographs?
- What processes can be distinguished that influence the shape of the pollutographs? Are the observed processes site-specific or do these have a more general validity?
- Are illicit connections in stormwater sewers detectable with high-resolution temperature data sets?
- What possible uses of high-resolution temperature data sets in combined sewer systems can be conceived?

1.5 Thesis outline

The thesis comprises two parts that can be read independently. The first part (chapters 2 to 6) presents the results of wastewater quality monitoring using UV/VIS sensors in the influent pumping station of the wwtp Eindhoven. The second part (chapter 7) presents the results of wastewater quality monitoring using the DTS monitoring technique in combined and separate sewer systems in three municipalities in the Netherlands.

Chapter 2 provides an introduction into the Eindhoven area wastewater system. The vulnerability of local receiving waters - which is the driving force behind the present study - is demonstrated comparing effluent standards to receiving water standards. The characteristics of the wwtp, of the interceptor sewers Riool-Zuid and Nuenen/Son and of the contributing municipal sewer systems are presented.

Chapter 3 presents the results of precipitation monitoring in the Eindhoven area. A network comprising 22 tipping-bucket gauges has been used to generate data on rainfall in the distinct catchment areas. Prior to data analysis an extensive data quality assessment has been performed using external data sources. The derived data sets are used as key (explanatory) parameters in data analyses of wwtp influent variations in chapter 6.

Chapter 4 describes water quantity measurements at the wwtp Eindhoven influent pumping station. Inflow data sets per catchment area are derived using the raw data sets of 9 flow sensors observing the same number of influent pumps. Again, a data

quality assessment has been included. The uncertainty associated with the derived data sets is discussed and estimated. The water quantity data sets are used for influent pollutant load calculations in chapter 6.

Chapter 5 presents water quality measurements with UV/VIS sensors, also at the wwtp Eindhoven influent pumping station. Monitoring principle and constructed by-pass installations as well as sensors calibration procedures and uncertainty estimates are included in the chapter. Also for these water quality data sets an extensive data quality assessment has been performed. The resulting data sets have been used in chapter 6 to derive influent loading data sets.

Chapter 6 uses the data sets as derived in chapters 3 through 5 to study the dynamics of wwtp Eindhoven influent. With a selection of dry weather data typical dry weather patterns are derived for flow and quality parameters TSS_{eq}, COD_{eq} and $CODf_{eq}$. Also, long-term and weekday variations of the DWF patterns are studied. For wet weather conditions data associated with a large number of storm events are considered. Per catchment area and per quality parameter peak load factors are derived allowing for comparison of results. Also, the 'extreme loading event' of May 7th, 2007 is presented and discussed.

Chapter 7 describes the application of the DTS monitoring technique in sewer systems. The principle of fiber-optic distributed temperature sensing and the installation of fiber-optic cables in sewer systems are discussed. Two distinct applications of the technique are presented. First, the application in separate sewer systems aims at locating illicit connections in storm water sewers. Second, the application of DTS in a combined sewer system allows the spatially distributed observation of in-sewer processes that influence in-sewer temperatures.

Chapter 8 presents a final discussion of results, conclusions and outlook. The experienced data loss during the monitoring programs is discussed as well as opportunities for data yield improvement. Observed peak loadings as reported in chapter 6 are confronted with climate change scenarios. Finally, the use of highly detailed in-sewer data sets (as generated by the DTS technique) introduces the need to consider privacy issues.

Chapter 2. Eindhoven area wastewater system

2.1 Introduction

Water board De Dommel (in Dutch: Waterschap De Dommel, referred to as WDD) is a water board governing an area in the southern part of the Netherlands, see Figure 2-1. A water board is a regional government body that is charged with managing water barriers, waterways, and water quantity and quality in (parts of) the surface water and wastewater system in its region. Currently (2011), there are 26 water boards in the Netherlands.

Figure 2-1: Water board De Dommel governing area in the Netherlands. The catchment area of wwtp Eindhoven is part of this area.

WDD manages a total of eight wastewater treatment plants in its region. The wwtp Eindhoven is the largest WDD plant with its catchment area located in and around the city of Eindhoven. The wwtp Eindhoven treats wastewater from a total of ten municipalities comprising many urban areas, see Figure 2-2. The scattered character of the urban areas necessitates an extensive wastewater collection and transport system to direct all wastewater towards the central wwtp.

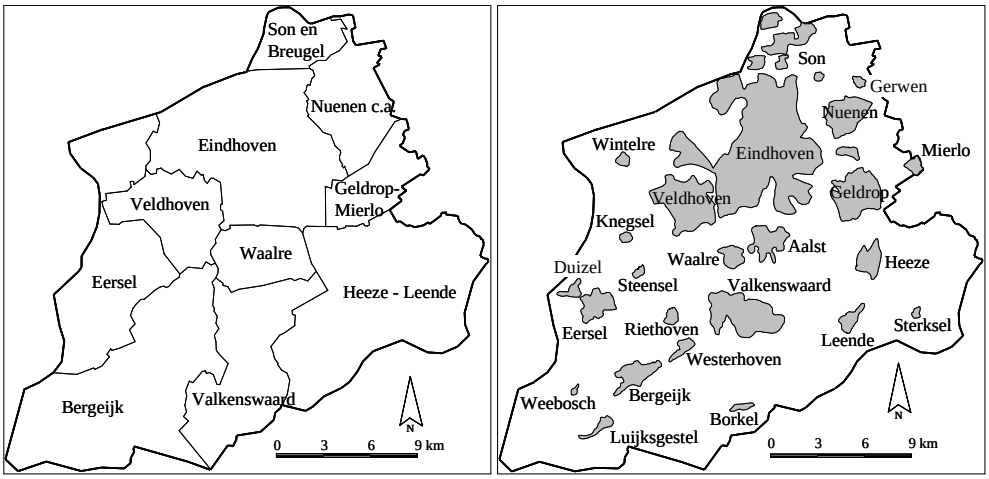

Figure 2-2: (left figure) 10 municipalities in the catchment area of wwtp Eindhoven; (right figure) urban areas in the catchment area of wwtp Eindhoven.

In this chapter, the Eindhoven area and its wastewater system are introduced. First, in paragraph 2.2 an overview is given of the surface waters in and around the city of Eindhoven relating to the historic development of the Eindhoven area wastewater system. All subsequent paragraphs describe a specific component of the wastewater system. Paragraph 2.3 provides an overview of the wastewater system lay-out. The basic characteristics of the wwtp Eindhoven are presented in paragraph 2.4. Subsequently, paragraph 2.5 describes the characteristics of the transport mains of Riool-Zuid and Nuenen/Son. Finally, the municipal sewer systems and their catchment areas are the topic of paragraph 2.6.

2.2 Surface waters around Eindhoven

The Eindhoven area can be characterized by a lack of large surface water bodies. Approximately 7 km^2 or 1.2% of a total of 600 km^2 (see appendix B) is surface water, which is limited compared to an average of 18.7% for all municipalities in the Netherlands (CBS, 2007). The majority of surface waters are small rivers and

creeks. The largest river in the area is the river Dommel, see Figure 2-3. The river originates in north-eastern Belgium, flows in a northerly direction for approximately 150 km, passes the city of Eindhoven and ultimately spills into the river Meuse near the city of Den Bosch. River flows are relatively small: up to 300 days of the year values range between 1 m^3/s and 10 m^3/s as measured at a monitoring location just downstream of the city (and the wwtp) of Eindhoven. The remaining part of the year values are larger, with maximum values around 40 m^3/s (Arcadis, 2007). These values imply that, especially in dry summer months, wwtp effluent (mean dry weather flow roughly 4,500 m^3/h or 1.25 m^3/s) can make up a large fraction (~50%) of the total flow in the river Dommel. For wet weather situations with an increased effluent rate up to 35,000 m^3/h or 9.75 m^3/s, the share of wwtp effluent in the river can increase up to 90%.

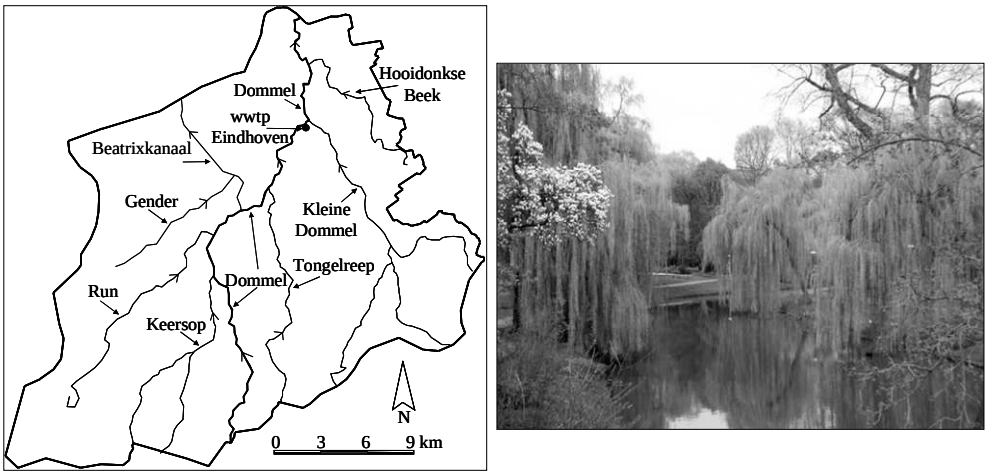

Figure 2-3: (left picture) Major surface waters in the Eindhoven area; (right picture) river Dommel near the wwtp Eindhoven.

Historically, the rivers and creeks in the area have long served as receiving waters for all (untreated) wastewater from adjacent communities. In the 20th century, with increasing urban activities in the area, the quality of surface waters deteriorated. As a result, in the 1950s the surface waters in and around the city of Eindhoven were highly polluted. In 1963 a wastewater treatment plant was constructed in the city of Eindhoven, back then servicing a catchment area much smaller than the current one. In the 1970s and 1980s the wastewater system gradually expanded with the construction of transport mains Riool-Zuid and Nuenen/Son. Nowadays, these two interceptor sewers transport the wastewater of nine surrounding municipalities to the wwtp Eindhoven. Only discharges from CSOs are still directed towards local surface waters.

2.3 Overview of wastewater system lay-out

The Eindhoven area wastewater system comprises municipal sewer systems, pumping stations and transport mains, one central wastewater treatment plant and a separate sludge processing installation. Each municipality collects wastewater in its own sewer system for which it bears responsibility for operation and maintenance. At the outlet of each municipal sewer system the responsibility for wastewater handling is transferred to water board De Dommel. By means of a WDD operated wastewater transport system (transport mains and pumping stations) all wastewater is transported to the wwtp, which is also operated by WDD. The entire system comprises an area of about 23 km in east-west direction and about 28 km in north-south direction (≈ 600 km^2) in and around the city of Eindhoven.

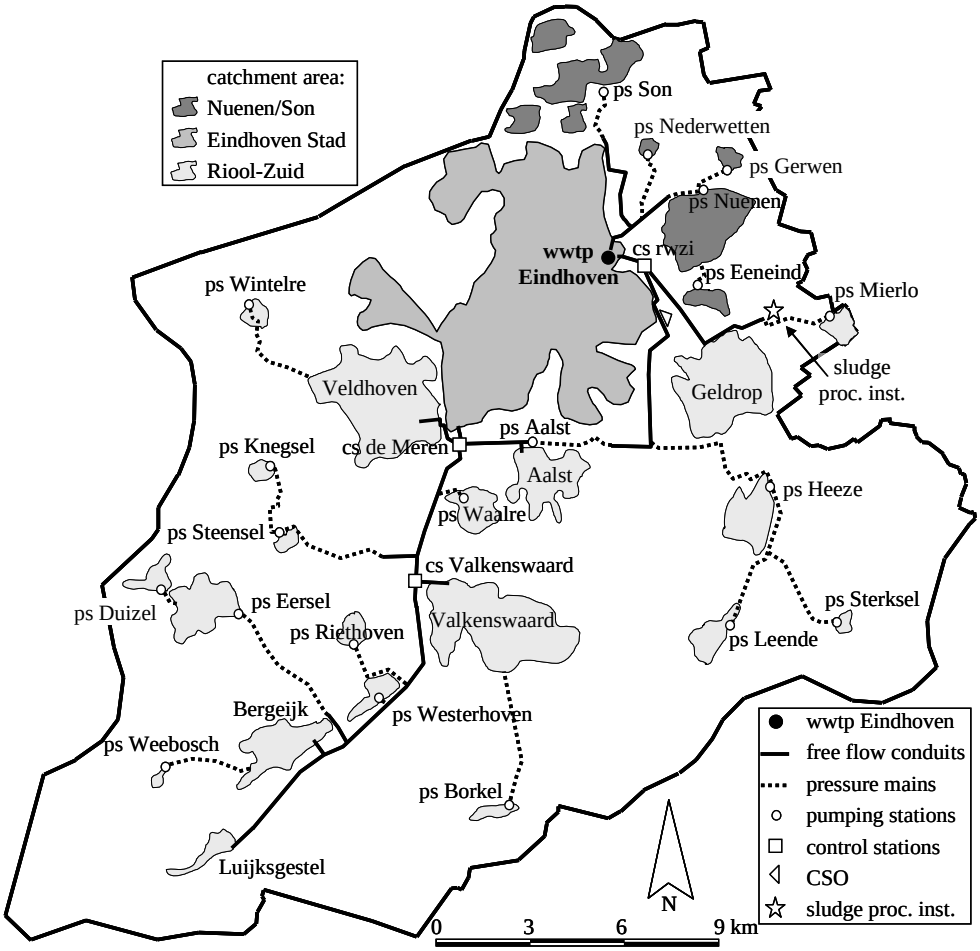

Figure 2-4: The main components of the Eindhoven area wastewater system.

At the wwtp influent pumping station three wastewater flows from three distinct catchment areas arrive. These are (see Figure 2-4):

1. wastewater from the municipality of Eindhoven (referred to as 'Eindhoven Stad' or 'ES');
2. wastewater from the municipalities of Son en Breugel and Nuenen, arriving in a free-flow transport main (referred to as 'Nuenen/Son' or 'NS');
3. wastewater from seven municipalities south of Eindhoven, also arriving at the wwtp in a transport main (referred to as 'Riool-Zuid' or 'RZ').

Under normal dry weather flow conditions, the inflow from Eindhoven Stad accounts for approximately 50% of the daily hydraulic loading to the wwtp; Riool-Zuid and Nuenen/Son contribute about 40% and 10%, respectively (see Table 6-2).

2.4 Characteristics of wwtp Eindhoven

The wastewater treatment plant Eindhoven has a design capacity of 750,000 population equivalents (p.e.) on an area population of about 425,000. This makes it the third largest wwtp in the Netherlands after wwtp Harnaschpolder (1.35 million p.e.) and wwtp Amsterdam-West (1.30 million p.e.). Between 2003 and 2006 the wwtp has undergone a renovation to comply with nutrient removal standards.

The wwtp Eindhoven is a treatment plant with an activated sludge system set up according to the UCT process. The lay-out of the plant is presented in Figure 2-5. In the plant, wastewater undergoes both a mechanical treatment and a biological treatment. In the influent pumping station 25 mm and 6 mm bar screens remove large solid particles, after which the wastewater is led through 2 parallel sand traps (400 m^2 each) and 3 primary clarifiers (8,750 m^3 each). The influent pumping station is limited to 35,000 m^3/h, which is the hydraulic capacity of the plant up to the primary clarifiers, at which stage the hydraulic capacity reduces to 26,250 m^3/h. In case total flow exceeds this value, the surplus is sent to an 8,750 m^3 stormwater storage tank (SST). Any surplus water exceeding the tank volume is discharged from the tank into the river Dommel.

After the primary clarifiers, wastewater is pumped into the biological treatment process by means of an intermediate pumping station. The biological treatment consists of 3 activated sludge tanks (of each 30,300 m^3) with anaerobic, aerated and denitrification zones. Each activated sludge tank is connected through a cascade system to four secondary clarifiers of each 6,300 m^3. Finally, the effluent of the secondary clarifiers is discharged to the river Dommel. Water quality demands for wwtp effluent are presented in Table 2-1.

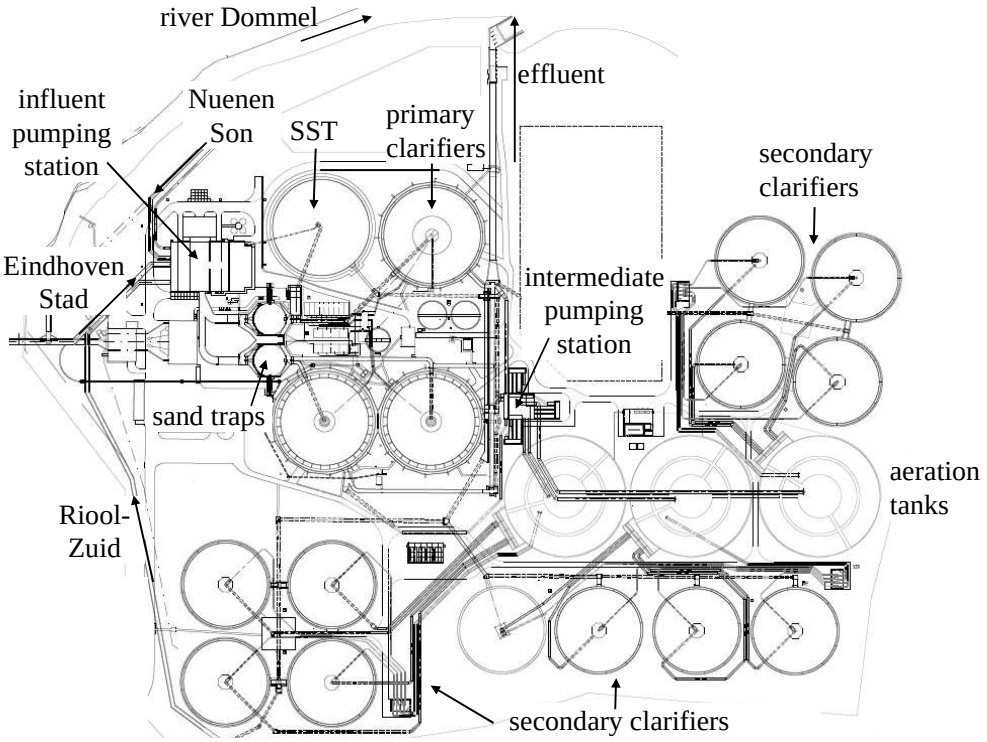

Figure 2-5: Lay-out of wwtp Eindhoven

The river Dommel has been designated as "fish water for cypriniformes" in the Provincial and Water board Water Plans (WDD, 2004). As a result, the surface water quality standards for this type of surface water as described in BKMO (1994, see Table 2-2) apply for the river Dommel. These standards are relatively strict when compared to the water quality standards for wwtp effluent. As a result, during dry months when effluent can constitute up to 50% of river flow downstream the Eindhoven treatment plant, wwtp effluent that meets its quality standards can nevertheless cause exceeding of surface water quality standards. As an example: for an ammonium concentration of 3 mg/L in wwtp effluent the ammonium concentration in the river Dommel is - with a dilution factor of 2 - at best 1.5 mg/L, which is larger than the 0.8 mg/L surface water standard.

Each year approximately 650,000 m^3 of sludge is produced, roughly corresponding to 15,000 tons of dry matter content. For reasons of odor nuisance, the sludge is not treated at the wwtp, but transported via a 7 km pipe system to a sludge processing installation near Mierlo. In Mierlo, the sludge is centrifuged for dewatering; the

centrate is discharged back into the Mierlo sewer system while the dewatered sludge is transported to an incinerator in Moerdijk (~60,000 m^3/year).

Table 2-1: The main water quality demands for effluent of wwtp Eindhoven (WDD, 2004). Samples are 24h volume-proportional samples.

Parameter	maximum concentration per sample [mg/L]	maximum concentration of moving average over 10 samples [mg/L]	mean annual concentration (over 60 samples) [mg/L]	any sample
COD	125			
BOD_5	20			
TSS	30		<10	
N-total			<10	
P-total		1.0		
NH_4-N	3			
pH				6.5 < x < 9
temperature				< 25°C
DO				> 5 mg/L

Table 2-2: A selection of water quality demands for surface water with the function of "fish water for cypriniformes" (BKMO, 1994). A total of 12 samples per year are required; one sample may exceed the stated limits, but not by more than 50%.

Parameter	limit per sample
BOD_5	< 10 mg/L
TSS	< 50 mg/L (mean of 12 samples)
NH_4-N	< 0.8 mg/L
pH	6.5 < x < 9
temperature	< 3°C temperature increase with respect to natural temperature
DO	> 6 mg/L

2.5 Characteristics of transport mains Riool-Zuid and Nuenen/Son

All wastewater from catchment areas Riool-Zuid and Nuenen/Son are transported to the treatment plant by means of two transport mains, see Figure 2-4 for a topographical map and Figure 2-6 for a schematic representation.

The northern transport main, Nuenen/Son or NS, transports the wastewater originating from the municipalities of Son en Breugel and Nuenen located north and north-east of the city of Eindhoven. It is constructed as a branched, predominantly free-flow system. The downstream branch has a length of roughly 1.5 km (average slope of 0.3 cm/m^1), the Son branch 5 km (slope of 0.2 cm/m^1) and the Nuenen branch 1.7 km (average slope of 0.1 cm/m^1). The Son branch is fed by two pumping stations only; the Nuenen branch receives wastewater from

several free-flow and pressurized connections. Pipe diameters range from ø600mm in the upstream sections of the Son and Nuenen branches to ø1400mm near the wwtp. The total in-sewer volume of the Nuenen/Son transport main is roughly 5,100 m^3. The transport main is free of CSOs.

The southern transport main is called Riool-Zuid or RZ, which literally translates as 'Sewer-South', indicating it transports all wastewater originating from the area mainly south of the city of Eindhoven to the wwtp. With a total of 13 large connections it services 7 municipalities:

1. Geldrop-Mierlo;
2. Heeze-Leende;
3. Waalre (includes the village of Aalst);
4. Veldhoven;
5. Valkenswaard;
6. Eersel (includes the village of Steensel) and
7. Bergeijk (includes the villages of Luijksgestel, Riethoven and Westerhoven).

The four largest contributaries (Geldrop, Veldhoven, Valkenswaard and Bergeijk) discharge to Riool-Zuid in free-flow pipes without any control barriers; an additional six connections are equipped with pumping stations and three connections are fitted with special structures (Archimedes' screw and vortex valves). A few connections to the transport main have not been considered separately in this study. These include (very) small connections from a sports canteen, a recreational area, a mobile home center and an eel farm. Flows and pollution loads are included in the data for the nearest large connection.

Riool-Zuid has a total length of nearly 31 km from its origin near the village of Luijksgestel to the influent pumping station at the wwtp. An intermediate pumping station near the village of Aalst divides the transport system into two main parts. Upstream from pumping station Aalst, Riool-Zuid is an 18.6 km long free-flow conduit with pipe diameters ranging from ø300mm at Luijksgestel up to 1900x1500mm directly upstream the Aalst pumping station. The invert level difference over the upstream section is 18.6 m, yielding an average slope of 0.1 cm/m^1. The total in-sewer volume of the upstream section of Riool-Zuid adds to 24,000 m^3. At the Aalst pumping station (7,500 m^3/h) wastewater is pumped into two parallel ø1000mm pressure mains by means of four parallel pumps. The pressure mains transport the wastewater over a length of approximately 3 km (in-sewer volume 5,600 m^3) from the 'valley' of the river Dommel into the 'valley' of the river Kleine Dommel. The last 9 km section of Riool-Zuid consists of free-flow pipes with pipe measures ranging from 1900x1500mm to 2250x1800mm. The total in-sewer volume of the downstream section of Riool-Zuid adds to 35,000 m^3.

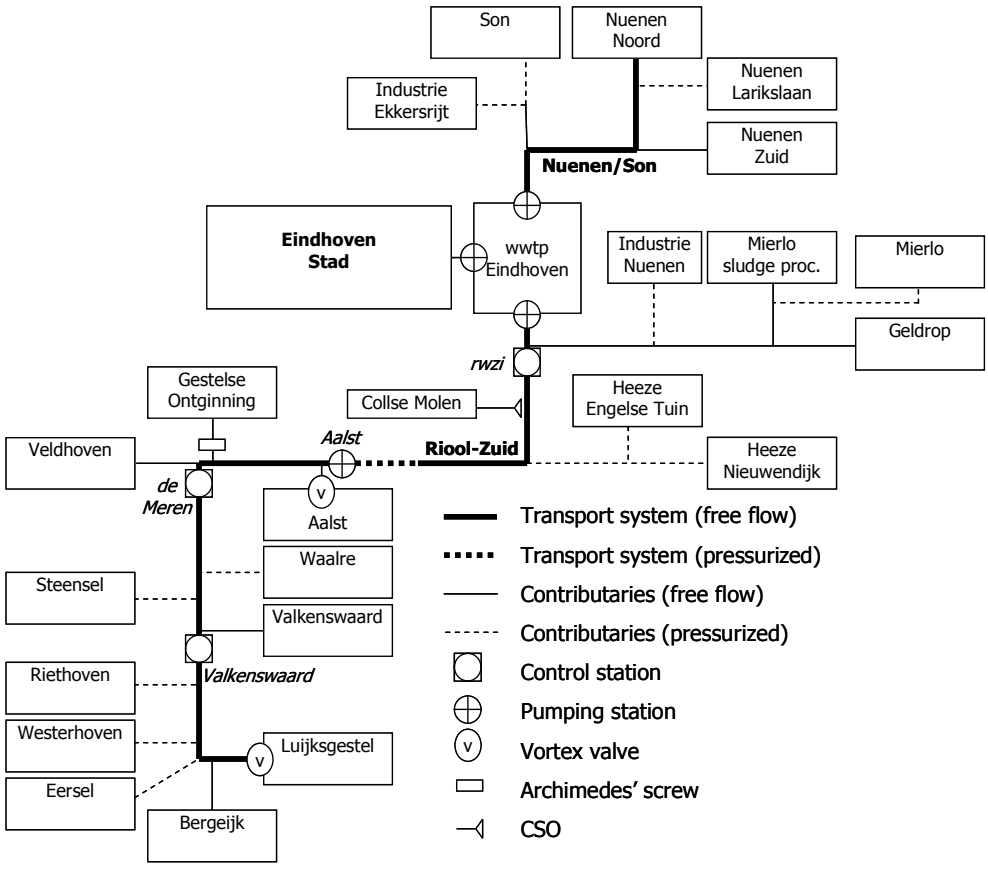

Figure 2-6: Schematic representation of the Eindhoven area wastewater system

Riool-Zuid is equipped with three control stations. These were included in the design of Riool-Zuid to be able to control the amount of flow in the transport system during (large) storm events. The main objective for flow control was guaranteeing a minimum flow from the three largest free-flow contributaries by restricting flow in the transport system. The control stations are therefore located directly upstream the respective confluences: control station 'rwzi' directly upstream contributary Geldrop, control station 'de Meeren' directly upstream contributary Veldhoven and control station 'Valkenswaard' directly upstream contributary Valkenswaard. All control stations are fitted with parallel pipes, see Figure 2-7. The main pipe (left pipe in the figure) serves for normal free-flow regimes and can be completely closed off at a critical water level. At that moment the right pipe starts serving as a by-pass with a full-pipe flow regime, allowing relatively accurate flow measurements. Flow in the by-pass can consequently be regulated using a valve. The original algorithm (implemented at the time of

construction in the 1970s) aimed at an optimal use of the storage capacity of the transport system. The control stations 'Valkenswaard' and 'rwzi' are no longer in use; control station 'de Meeren' limits flow in Riool-Zuid to 4,500 m^3/h to guarantee sufficient capacity for the municipality of Veldhoven.

Transport main Riool-Zuid is equipped with one CSO structure at Collse Molen which has not functioned during the time-span considered in this thesis.

Figure 2-7: Control station Valkenswaard. The left pipe is the main transport line; in case of active flow control all wastewater can be by-passed via the right pipe.

2.6 Characteristics of municipal sewer systems and catchment areas

An overview of characteristics of the 10 municipalities and municipal sewer systems that discharge wastewater to the wwtp Eindhoven is given in appendix B. The total municipal surface area adds to nearly 600 km^2 of which approximately 40 km^2 or 7.1% is qualified as impervious area that discharges storm water to the sewer systems. Receiving waters make up an area of just under 7 km^2 or 1.2%. The total number of inhabitants in the area equals roughly 425,000. Eindhoven is the largest municipality in terms of inhabitants with about half of the area's total

(210,000); Heeze-Leende, Son en Breugel, Waalre, Eersel and Bergeijk are the five smallest municipalities each with 15,000 to 20,000 inhabitants. Industrial activities add approximately 150,000 p.e. of wastewater to the wastewater system. The municipalities of Son en Breugel and Geldrop-Mierlo show the largest relative contributions of industrial wastewater (inhabitants-to-industry ratio ≈ 1:1). For Geldrop-Mierlo this is mainly due to the presence of the wwtp sludge processing installation that adds nearly 2,500 m^3/day to the municipal sewer system. The municipality of Nuenen produces almost no industrial wastewater.

Total length of all municipal sewers adds to about 2,400 km of which, on average, 78% are combined sewers and 22% separate sewers. The largest shares of separate sewer systems are found in the largest municipal sewer systems (Eindhoven and Veldhoven, 29%). In total, 182 combined sewer overflows are found in municipal sewer systems.

Appendix C partly presents the same information as appendix B, but data are considered at catchment area scale instead of municipal scale. Catchment area Eindhoven Stad consists of the largest part of the municipal sewer system of the city of Eindhoven. It is a largely looped network serving just over 200,000 inhabitants, over 65,000 p.e. worth of industrial activities and nearly 20 km^2 of impermeable area. Total storage in the sewer system is 6.4 mm. At the moment, no storage in additional storage facilities is available; in 2010/2011, however, a settling tank with a capacity of 8,000 m^3 will be built.

Catchment area Riool-Zuid consists of the sewer systems of seven municipalities that are each connected to transport main Riool-Zuid. The area has a population of around 188,000 people, nearly 70,000 p.e. of industrial activities and 17 km^2 of impermeable area. Total storage in the sewer system is 6.7 mm and in external storage facilities 4.1 mm.

Lastly, catchment area Nuenen/Son consists of the sewer systems of the municipalities of Son en Breugel and Nuenen that both transport wastewater to the wwtp Eindhoven via transport main Nuenen/Son. The catchment area services a population of 38,000 inhabitants, approximately 14,000 p.e. of industry and 4.6 km^2 of impermeable area. Total in-sewer storage is 5.0 mm and additional storage adds to 1.4 mm.

Chapter 3. Precipitation monitoring

3.1 Introduction

Precipitation measurements are an important source of information for studies on urban wastewater systems. Rainfall is by far the most important input variable that drives urban surface run-off (Schilling, 1991), which is in turn an important driving factor for variations of in-sewer wastewater quantity and quality parameters. As a result, knowledge of the amount and temporal distribution of precipitation is important to study in-sewer processes during wet weather situations. Precipitation measurements have therefore been included in the WDD monitoring campaign.

A total of 22 tipping-bucket raingauges (TBRGs) have been used to monitor rainfall in the Eindhoven area within the WDD monitoring project. For the data quality assessment data of 9 other raingauges in the Eindhoven area have been used: 3 other tipping-bucket raingauges that belong to a monitoring project of the municipality of Eindhoven (referred to as NM gauges) and 6 Hellmann type raingauges operated by the Royal Netherlands Meteorological Institute (referred to as KNMI gauges).

The objective of this chapter is to obtain three time-series that, as accurately as possible, represent 'mean area precipitation' of the three considered catchment areas: one time-series for Riool-Zuid, one time-series for Eindhoven Stad and one time-series for Nuenen/Son. These time-series are used in data analyses in chapter 6 to calculate mean area precipitation depths during storm events, to determine antecedent dry weather periods, and to aid in distinguishing between dry weather flow and wet weather flow data. The three time-series are derived combining the data of WDD (and NM) gauges, but only after data quality assessment.

To meet the objective, precipitation measurements in the Eindhoven area are firstly introduced in paragraph 3.2 reporting on sensor types and other monitoring details such as data availability, monitoring locations, data communication and storage, and log book details. Secondly, before using the data, the quality of the WDD TBRG data is assessed in paragraphs 3.4 and 3.5. Before the assessment, paragraph 3.3 introduces the selected method for quality assessment and discusses the relation of the considered data sources to 'true' precipitation and the use of reference data sets. Paragraph 3.4 focuses on the detection and removal of data errors based on cross-correlations of TBRG results by means of both manual and automatic checks. Paragraph 3.5 briefly describes a comparison between WDD and NM tipping-bucket raingauge data to the KNMI Hellmann gauge data. The complete comparison and assessment of differences can be found in appendix E. Finally, in

paragraph 3.6 the desired area precipitation time-series are derived using the inverse distance weighting method. Resulting time-series are valued for their use in other chapters.

3.2 Rain gauges and monitoring locations

3.2.1 WDD gauges

For the WDD monitoring campaign in the Eindhoven area, tipping-bucket raingauges have been selected to monitor precipitation. The main reason for selecting this type of gauge was the possibility to gather high-frequent (min^{-1}) data. Also, the automatic operation of the gauges has favored TBRGs over for instance Hellmann gauges that need to be read manually. The principle of a tipping-bucket raingauge is described in detail in e.g. Marsalek (1981). The gauges are of type RAIN-GER of manufacturer FlowTronic (Belgium). The funnel area is 200 cm^2 and the nominal bucket size equals 0.1 mm. The gauges are not equipped with siphons nor have they been fitted with heater-systems for snow melt purposes.

For the Eindhoven area data, April 1st, 2007 - November 1st, 2008 is the 19-month time-span considered for data analysis. WDD raingauges, however, were only installed in July 2007 and started data yield around July 11th, 2007. Prior to this date, the derived time-series are based on NM gauge data only. The raw WDD data consist of equidistant, 1-minute interval data with a 0.1 mm resolution, cumulative over 24 hours, reset to zero at 09h00. The raw data sets contain data gaps, defined here as those entries with a time stamp but without a precipitation value.

WDD gauges have been installed at or nearby WDD property (mainly pumping stations and control stations) throughout the Eindhoven area. A map showing the locations of all 22 WDD raingauges can be found in Figure 3-1. After cost considerations, creating monitoring stations near existing electricity and, in some cases, data communication facilities was preferred over creating entirely new monitoring stations. As a result, at most locations optimal monitoring conditions could not be attained due to lack of space and the presence of trees, buildings or other obstructions. As an example, Figure 3-2 shows a WDD raingauge at pumping station Heeze Nieuwendijk that was positioned directly next to the pumping station building. The effects of these monitoring conditions on data results are considered in section 3.4.2 and appendix E.

Studying Figure 3-1 it can be observed that WDD gauges do not monitor the urban area of the city of Eindhoven. For an improved areal representation, three gauges operated by the municipality of Eindhoven (NM gauges) are included in the data analyses. NM sensors are described in the next section.

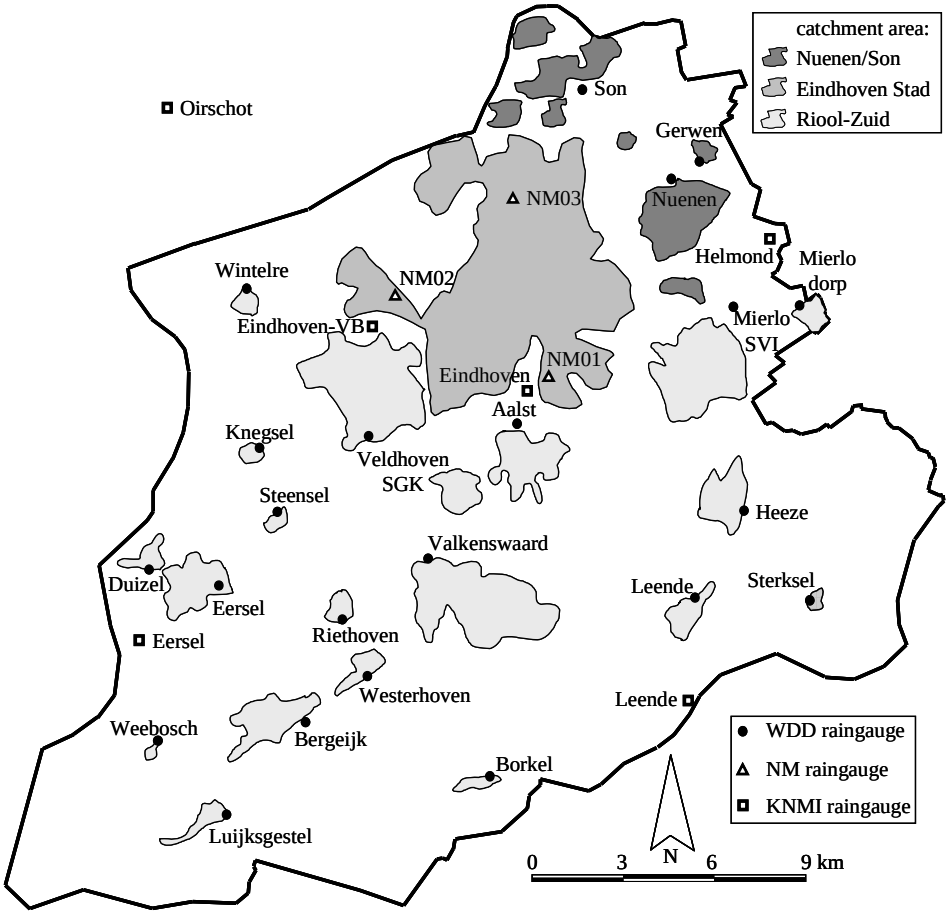

Figure 3-1: Catchment area of wwtp Eindhoven with WDD, NM and KNMI raingauges

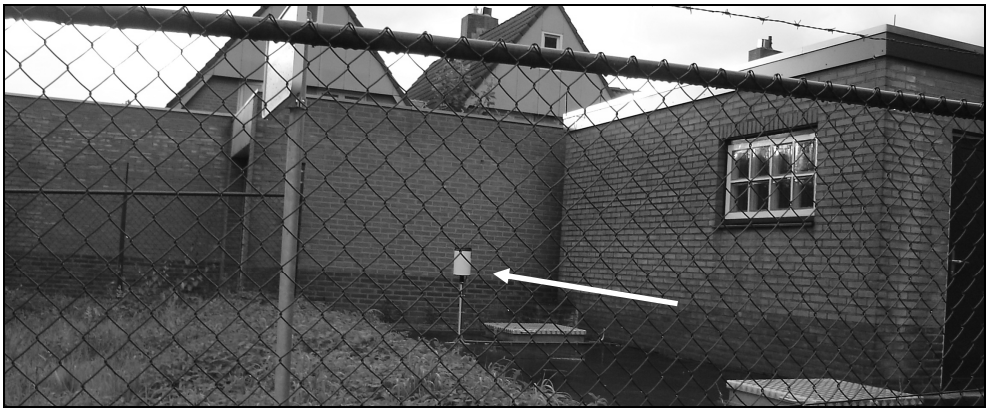

Figure 3-2: WDD raingauge in Heeze placed directly next to the pumping station building

Each WDD raingauge is connected to a local router that sends precipitation data via a General Packet Radio Service (GPRS) connection to a central router located outside the Eindhoven area, see Figure 3-3. The central router is connected to a computer server that stores the data in a database. Once per 15 minutes the data are 'pushed' by the local router (one-way communication) instead of 'requested' by the central router (two-way communication) to reduce the amount of data transfer. At the moment of sending, the local router adds a time-stamp to the data using its own clock-time. Hence, to be able to guarantee a synchronous dataset, all local router clock-times should be equal. For this, the central router synchronises the clock-times of all local routers once per day, using the central time registration of the server. In turn, the server is synchronised to UTC (Coordinated Universal Time) via the internet. The use of UTC has the advantage of the exclusion of day-light saving time which can cause difficulties in handling time-series. The importance of synchronous precipitation data sets (or any other data sets that are used in combination) has been shown by Schilling (1991): a modelled peak run-off deviated already 16% with only a 2-minute synchronization error. Also, synchronization errors between raingauges generate a pseudo spatial variability which might for instance corrupt RTC investigations. Local data storage has not been installed at the precipitation monitoring locations. As a result, any failure in data communication has led to immediate loss of data.

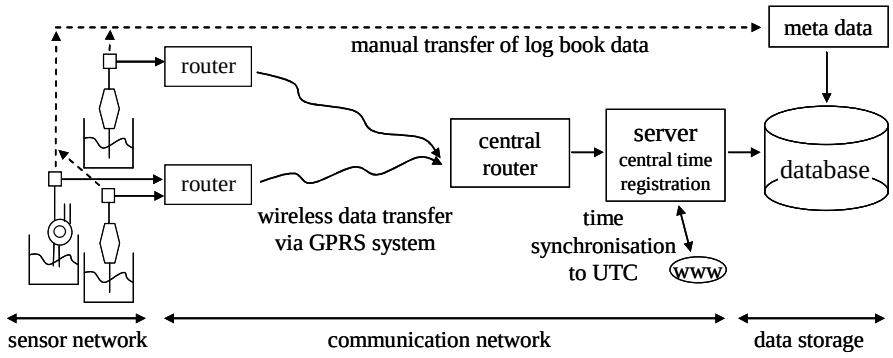

Figure 3-3: Data communication and storage of WDD raingauges

At each WDD monitoring location, a log book was provided. All maintenance personnel were instructed to fill in a log book page during each site visit. The log book reports on general visit information (location, date, time, name inspector, weather conditions), the status of the equipment upon arrival (clogged sensor, pollution of sensor, failure of local router), and any actions performed on the equipment (cleaning of sensor, on/off-switching of router, calibration, etc.). After studying anomalies in the WDD data sets (see paragraph 3.4) and comparing these

to the log book entries, the quality and completeness of the log book is judged as fair. Many anomalies in the data can be explained using the log book. However, inconsistencies do occur. On a specific dry weather day, for instance, all raingauges have been cleaned (isolated peaks of ~5-10 mm throughout the day in all data sets), but metadata on cleaning are missing for several sensors. Vice versa, on a few occasions the cleaning of the sensor is reported, but no anomalies are found in the data.

3.2.2 NM gauges

The *municipality* of Eindhoven operates three raingauges in the Eindhoven area. The gauges are referred to as the NM01, NM02 and NM03, with NM as the abbreviation for the Dutch word for raingauge (NeerslagMeter). Data of these gauges have been made available for use in this study. NM gauges are tipping-bucket raingauges of type OMC-212 of manufacturer Observator Instruments (Netherlands). The gauge catchment area is 400 cm^2 and the nominal bucket size equals 0.2 mm. The locations of NM gauges are indicated in Figure 3-1. Figure 3-4 presents the monitoring location of sensor NM01.

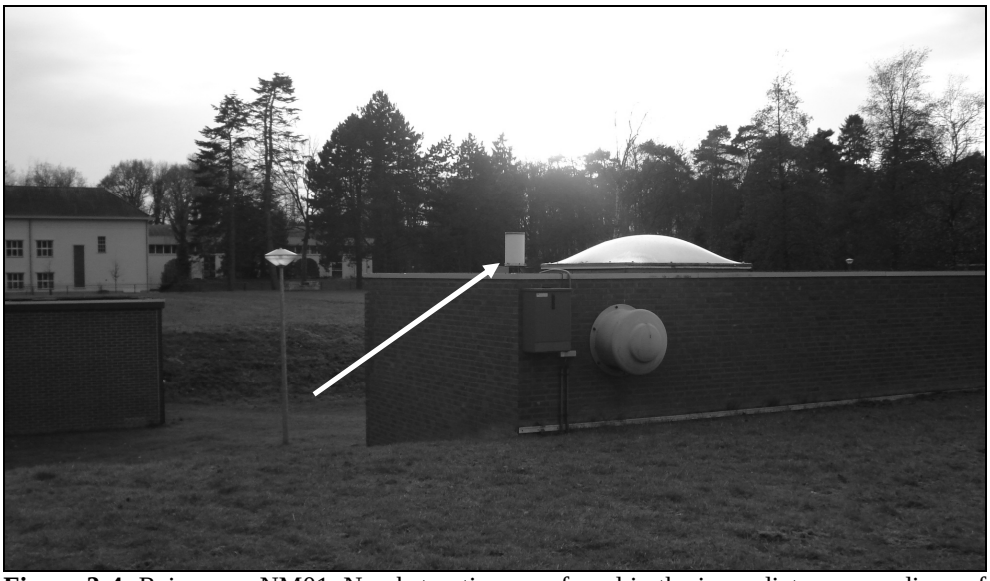

Figure 3-4: Raingauge NM01. No obstructions are found in the immediate surroundings of the sensor.

Data for NM gauges are available for the full time-span that is considered for analysis of Eindhoven area data (April 1st, 2007 - November 1st, 2008). The raw

data sets of NM gauges have a variable time-interval: time-stamps are generated every 5 minutes in case of dry weather and for every tip of 0.2 mm in case of wet weather. Precipitation values are cumulative over 24 hours, reset to zero every day at midnight. Data validation of NM data sets was performed by a third party, commissioned by the municipality of Eindhoven. For NM gauges both details of the validation procedure and log book information are not available.

3.2.3 KNMI gauges

The Royal Netherlands Meteorological Institute (Koninklijk Nederlands Meteorologisch Instituut, KNMI) studies precipitation in the Netherlands using (among others) a network of 325 monitoring stations that measure precipitation day sums. Six of these monitoring stations are in the Eindhoven area. Gauges are of the Hellmann type with a 200 cm^2 catchment area positioned 40 cm above ground level. Manual registration of day sums occurs daily at 08h00 UCT (09h00 local time, 10h00 in summer). Validated data are freely available at the website (www.knmi.nl). The location of KNMI gauges in the Eindhoven area can be found in Figure 3-1. Data of KNMI gauges are also available for the full considered time-span (April 1st, 2007 - November 1st, 2008). The raw data sets consist of day sums (08h00 UCT - 08h00 UCT) of precipitation at a 0.1 mm resolution.

3.3 Introduction to quality assessment of WDD gauge results

The quality of data of the 22 WDD tipping-bucket raingauges has been assessed before data analysis. The need for a proper data quality assessment of TBRG results is widely acknowledged; for instance Steiner *et al.* (1999) demonstrate that the use of all their raingauge data, as opposed to using good data only, would have resulted in a 25% underestimation of rain depths. Many different approaches for quality control are suggested in literature. For instance, Jørgensen *et al.* (1998) use an automatic rejection of intensities over 2 mm/min and a manual comparison of daily TBRG precipitation sums with nearby Hellmann gauge results and weather charts. Upton and Rahimi (2003) recognize the need for further automation of quality assessment of large TBRG data sets. For individual gauges, their algorithms search for excessively fast tipping and typical behavior of partially blocked gauges. For gauge networks, comparisons based on number of tips and inter-tip times are used in their analyses.

The data quality assessment of WDD TBRG results in this study comprises two steps. In the first step (paragraph 3.4) the performance of gauges is assessed cross-checking results of all 25 tipping-bucket raingauges (22 WDD gauges + 3 NM gauges). The performance of each sensor is evaluated using the results of other

TBRGs in the gauge network. The assessment is divided into two parts: a manual cross-check, described in section 3.4.1 and an automated cross-check, described in section 3.4.2 and appendix D. However considered the best available reference data set (see hereafter), the KNMI data have not been used in paragraph 3.4 due to incompatibility: KNMI data are available as day sums only whereas the cross-checks are performed per storm event requiring short-interval data. In the second step of the quality assessment a comparison is made between on one hand the long-term performance of WDD and NM gauges and on the other hand the long-term performance of KNMI gauges. A brief description of this comparison is found in paragraph 3.5; an elaborate presentation as well as an assessment of differences can be found in appendix E.

In this chapter, three data sources are considered: WDD data, NM data and KNMI data. It is important to notice that none of these data sources present 'true' precipitation: they all have their respective errors compared to 'true' values. Ideally, for data quality assessment, all data are evaluated against 'true' precipitation but no such data source is available (or even exists). Hence, the 'next best solution' is to consider an existing data source as 'true' precipitation. In this study, the KNMI data sets are considered to represent 'true' precipitation. Two arguments support this choice. The first argument is that KNMI gauges are of the Hellmann type. Generally, differences between Hellmann gauge results and 'true' precipitation are smaller than differences between TBRG results and 'true' precipitation since instrumentation errors associated with the latter type are often not found with Hellmann type gauges. In several publications on this topic, data produced by Hellmann gauges are even considered synonymous to 'true' precipitation (for instance in Rauch *et al.*, 1998). The second argument is that KNMI gauges are operated by the Royal Netherlands Meteorological Institute and therefore receive professional attention by experienced personnel. KNMI gauges are visited daily, are well-positioned and all data are thoroughly validated before publication and subsequent usage in this chapter.

KNMI data and NM data are both used as reference values for the quality assessment of WDD data. For this, the quality of both data sources should be sufficient. The good quality of KNMI data has been argued and is not further considered in this chapter; the quality of NM data, however, was *a priori* unknown since only little information was available on factors such as sensor maintenance and data collection and storage. Therefore, NM data has been included in the data quality assessments in paragraphs 3.4 and 3.5. The former paragraph demonstrates that NM data sets are nearly free of data gaps and erroneous data. The latter paragraph (and appendix E) shows that lumped sums of NM gauges correspond well to (assumedly correct) lumped sums of KNMI gauges. Therefore, retrospectively, it can be concluded that NM data have been rightfully used as reference values for the quality assessment of WDD data.

3.4 Data quality assessment of WDD gauges: cross-check of TBRG data

3.4.1 Manual cross-check of TBRG results

For a manual assessment of WDD and NM TBRG results, the raw and cumulative data of all 25 gauges have been plotted per month. Visually inspecting and comparing the plots, obviously erroneous data are detected and marked. Largely similar precipitation patterns of neighboring gauges in combination with anomalous behavior of a single raingauge, suggests a malfunctioning sensor.

The Sterksel and Luijksgestel gauges consistently show anomalous behavior when compared to the other WDD and NM sensors. During a site visit it was found that basic requirements for proper raingauge installation were severely violated: the sensors were installed directly beneath trees, see Figure 3-5. Therefore, all data of the Sterksel and Luijksgestel gauges have been discarded and are not used in any further data analyses.

Figure 3-5: Incorrectly installed tipping-bucket raingauge in Sterksel. The left picture gives a situation overview showing the raingauge attached to a small pumping station; the picture on the right gives the view upwards as seen from the sensor.

For the other 23 TBRG data sets all observed anomalies can be fit into one of the following five categories:

i. Data gaps of more than 1 hour during which no monitoring data are available. Most of these gaps are caused by a failing data communication system. The Weebosch data in Figure 3-6 show an example of a data gap of approximately 6 days.

ii. Data recorded during sensor cleaning, often indicated by a large (~10mm), instantaneous increase in precipitation depth which has not been recorded by any of the other raingauges, see the Riethoven data in Figure 3-6. In fact, spot-checks in the WDD and NM data sets have confirmed that any observed rain intensity larger than 3 mm/min is associated with an isolated 1 or 2-minute event observed by a single gauge and is not associated with a storm event. Therefore, any data entries larger than 3 mm/min have been removed from the data sets.

iii. Data recorded during sensor malfunctioning, indicated by a non-response to storm events. Figure 3-6 shows a series of storm events on August 19th-23rd, 2007 recorded by the Weebosch, Aalst and Eersel gauges with a total sum of approximately 20mm. The Riethoven gauge shows (nearly) no response to the storm events. Only after sensor cleaning on August 29th does the raingauge again respond to a minor storm event on August 31st. For each supposed non-response it has been verified using the closest available in-sewer flow data whether the non-response is really due to sensor malfunctioning instead of the absence of precipitation. Anomalous data entries have been removed from the data sets.

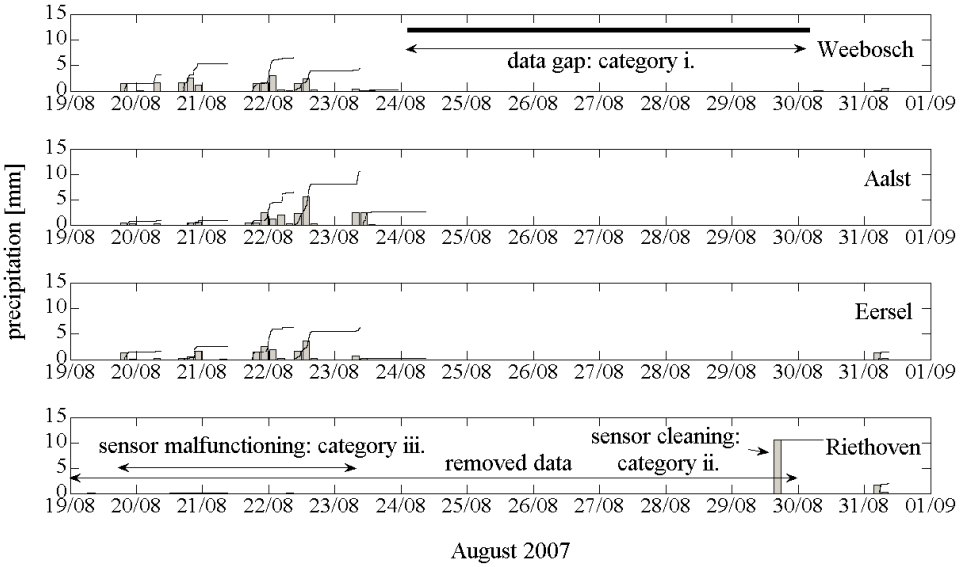

Figure 3-6: Data results of raingauges Weebosch, Aalst, Eersel and Riethoven for 19 - 31 August 2007. The black lines represent raw cumulative 1-minute interval data per 24 hours, reset to zero every day at 09h00. Grey bars represent the same data, but in blocks of precipitation depth per 3 hours.

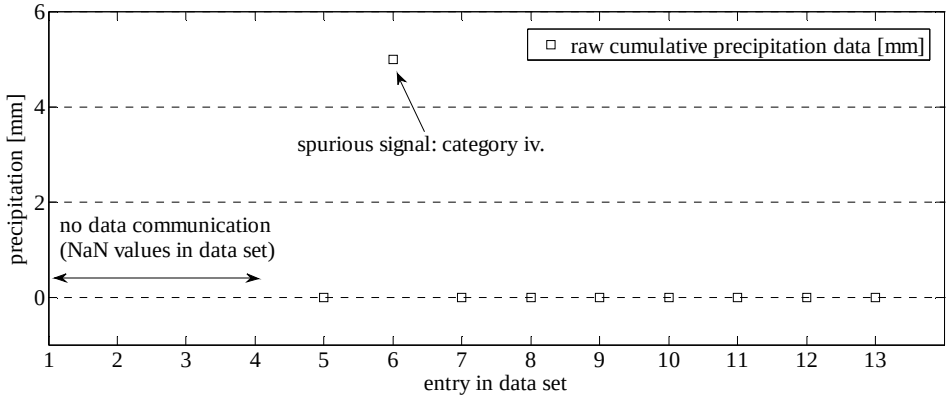

Figure 3-7: A spurious signal (5 mm) in raw cumulative precipitation data after an interruption in data communication.

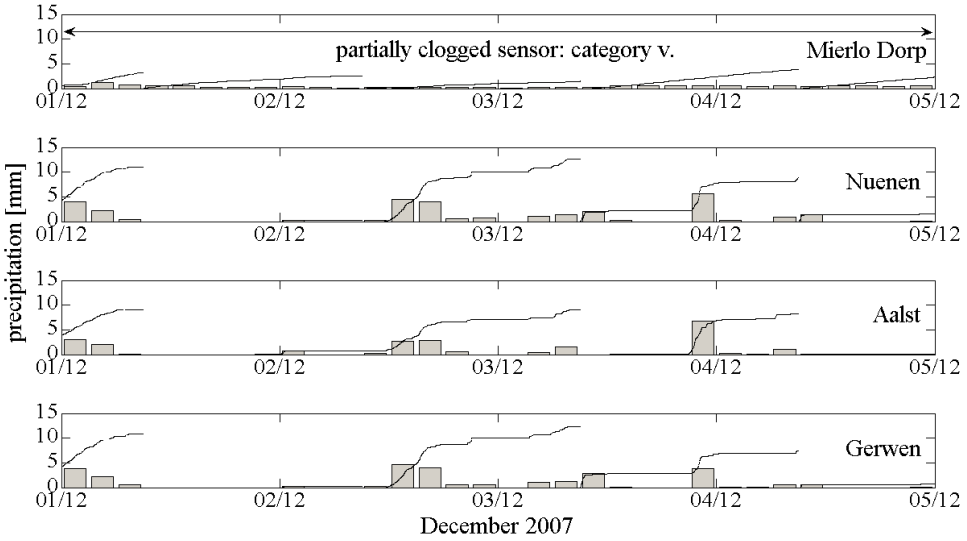

Figure 3-8: Data results of raingauges Mierlo Dorp, Nuenen, Aalst and Gerwen for 1 - 4 December 2007. Partial obstruction of the gauge in Mierlo Dorp results in data characteristics that resemble those of a slowly emptying water vessel, losing the intermittent character of precipitation as observed at the other three sensors.

iv. Data recorded after a restart of the data communication system. The restart occasionally produces a spurious signal that, as shown in Figure 3-7, does not add to the cumulative data. Since the signal has no relation with precipitation it is removed.

v. Data recorded during partial obstruction of the funnel, indicated by data characteristics as shown for gauge Mierlo Dorp in Figure 3-8. Due to an

obstruction, the capacity of the outlet from the funnel into the tipping-bucket mechanism is largely reduced which causes stormwater to accumulate in the collector funnel. The funnel empties only slowly, hence losing the temporal distribution of the precipitation data as recorded by the other three gauges. Particularly sensors downwind clusters of birch trees have encountered these problems. The seeds and twigs of this type of tree have regularly been removed from the sensor funnels and tipping-buckets. All data entries showing this anomaly have been removed from the data sets.

Table 3-1: Result of manual data assessment of 20 WDD and 3 NM tipping-bucket raingauges. For the sensors in bold (much) less than the mean 59% of the total data set is considered good data; these sensors are not used in any further data analyses. Percentages are fractions of the total data sets (489 days for WDD gauges, 580 days for NM gauges).

	total data set	data gaps > 1 hour *category (i)*			anomalous data *categories (ii) - (v)*		remaining data set	
		number of gaps	length	fraction	length	fraction	length	fraction
WDD gauges	[days]	[#]	[days]	[%]	[days]	[%]	[days]	[%]
Aalst	489	25	66	13	30	6	393	80
Bergeijk	489	29	116	24	82	17	291	60
Borkel	489	22	116	24	74	15	299	61
Duizel	489	26	65	13	24	5	399	82
Eersel	489	25	68	14	59	12	362	74
Gerwen	489	24	64	13	79	16	346	71
Heeze	489	7	317	65	85	17	88	**18**
Knegsel	489	142	140	29	118	24	231	**47**
Leende	489	26	128	26	115	23	246	**50**
Mierlo-D.	489	15	236	48	72	15	181	**37**
Mierlo-SVI	489	11	231	47	57	12	201	**41**
Nuenen	489	19	63	13	112	23	314	64
Riethoven	489	36	68	14	74	15	347	71
Son	489	20	68	14	72	15	349	71
Steensel	489	21	67	14	79	16	343	70
Valkensw.	489	17	218	45	55	11	216	**44**
Veldh. SGK	489	11	229	47	40	8	220	**45**
Weebosch	489	46	113	23	47	10	329	67
Westerh.	489	24	65	13	66	14	358	73
Wintelre	489	43	67	14	165	34	257	**53**
						mean (all 20 gauges)		*59*
					mean (12 non-bold gauges)			*70*
NM gauges								
NM01	580	15	2	0,3	0	0	578	99,7
NM02	580	13	4	0,7	0	0	576	99,3
NM03	580	15	2	0,3	0	0	578	99,7

Table 3-1 presents the results of the manual data assessment, specifying the amount and total length of data gaps and the total length of anomalous data. Figure 3-9 shows the location in time of these gaps and rejected anomalous data. The total length of WDD data sets is 489 days (July 1st, 2007 - November 1st, 2008). The number of data gaps longer than 1 hour ranges between 7 and 142; the associated relative data loss ranges between 13% and 65% of the total data sets. The majority of these are caused by a malfunctioning data communication system. WDD gauges have approximately 60 days of data gaps in common, attributable to failures of a central part of that communication system. The largest shared gaps lasted 27 days (March 4th-31st, 2008) and 15 days (April 28th - May 19th, 2008) owing to server problems and lack of communication signal. Studying Figure 3-9, it can be observed that the longest data gaps by individual gauges are due to termination of sensor operation. A mere 7 out of 20 sensors cease operation during the 19-month time-span. In most cases, the local router suffered a break-down after which it was decided not to replace the router. Hence, while the raingauge still functioned, the data could no longer be sent to the data server.

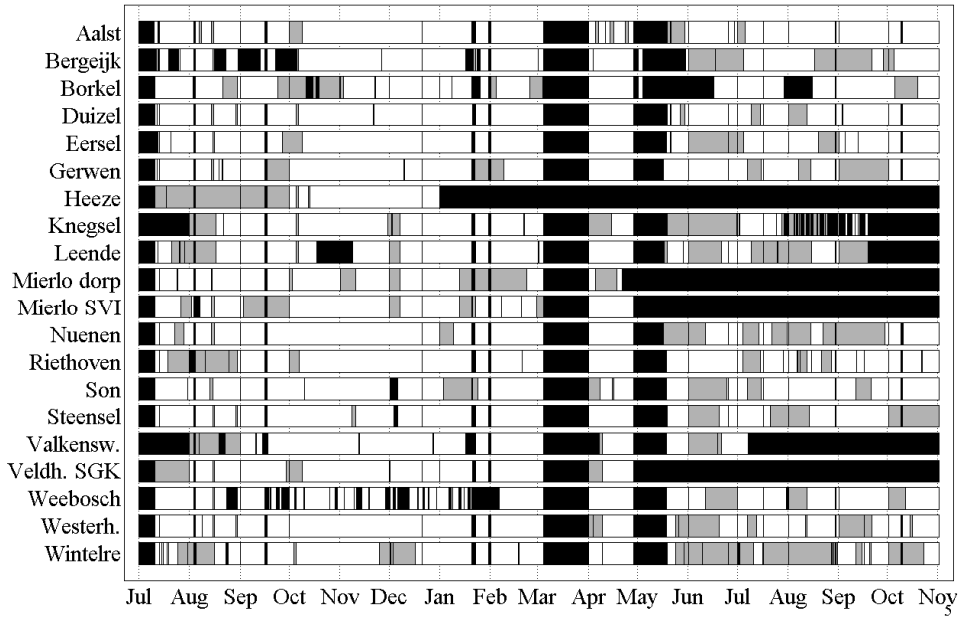

Figure 3-9: Data gaps (in black) and anomalous data (in grey) based on manual data assessment of 20 WDD TBRG data sets for the time-span 1 July 2007 - 1 November 2008.

Anomalous data in categories (ii) through (v) represent a second source of significant data loss. Again, a wide variation of values can be observed: a minimum of 24 days (or 5%) with anomalous data for the Duizel gauge up to a

maximum of 165 days (or 34%) for the Wintelre gauge. Studying Figure 3-9 it can be seen that the majority of anomalous data can be found within the last 5 months. By contrast, only few data are rejected over the first half year of operation. This suggests that the sensors become more prone to anomalous behavior over time, due to slow and gradual fouling and due to a decreasingly stringent cleaning strategy.

After removal of data gaps and anomalous data, the WDD TBRG data sets contain on average 288 days or nearly 60% of data of the original data sets. This percentage varies between 18% and 82%; in other words, after manual assessment of the quality of TBRG data, at best 18% and at worst 82% of the data sets is considered *unfit* for further consideration. For a total of eight WDD TBRGs (much) less than the mean 59% of the total data set is available for data analyses. To prevent working with too fragmented data sets, it was decided to discard the complete data sets of these sensors and to work with the data of the remaining 12 WDD and 3 NM raingauges. Further considerations on this poor performance of the WDD precipitation monitoring network can be found in chapter 8.

The results of manual assessment of NM data sets are included in Table 3-1. The Eindhoven municipality gauges have been in operation during the full considered time-span: April 1st, 2007 - November 1st, 2008 (580 days). NM gauges show a much better performance with no observed anomalous data and an average loss of 3 days (or 0.4%) due to data gaps. For these gauges more than 99% of data can be used for data analyses. A better functioning data communication system, a proper cleaning strategy and a superior placement of sensors prevent the majority of problems encountered with the WDD monitoring system.

3.4.2 Automatic cross-check of TBRG results

Like any non-automated validation of data, a manual assessment of TBRG data results is subjective and poorly reproducible. To enhance objectiveness and reproducibility, the results of the manual assessment are confronted with the results of an automated data quality assessment. The applied automated data quality assessment is an adapted form of the method as presented by Upton and Rahimi (2003). The details of the method are given in appendix D. The results of the assessment are also given in the appendix as well as a comparison of results with the results of the manual data quality assessment. In this section, results are only summarized and briefly discussed.

Using the automated procedures, a total of 325 tip sequences have been identified that may not be representing the precipitation process correctly, see Table 3-2. Of these, approximately 50% lie within a manually rejected sequence, the other half has not been identified in the manual assessment (i.e. false positive results of the

automated procedure). Of the 137 manually rejected sequences, 81 (or 59%) contain at least one automatically detected doubtful tip sequence. The other 56 manually rejected sequences are not detected by the automated procedure and hence constitute false negative results.

Table 3-2: Automatically detected versus manually rejected sequences with false positives and false negatives

automatically detected sequences			manually rejected sequences		
total	within manually rejected sequence	outside manually rejected sequence (false positive)	total	noticed by automatic detection	unnoticed by automatic detection (false negative)
325	169 (52%)	156 (48%)	137	81 (59%)	56 (41%)

Finding 59% of the manually rejected sequences, the performance of the automatic tests on the Eindhoven area data is poor compared to the 90% obtained by Upton and Rahimi (2003) for their test data. Also, the number of false positives is significant for the Eindhoven data. Upon closer consideration of false positives and false negatives it is found that the general poor performance of the Eindhoven raingauge network stands at the basis of many false identifications. Using the proposed procedures, it is relatively straightforward to detect an anomaly amidst good data. However, confronted with a hampering data communication, incomplete metadata files and simultaneous blockages of multiple gauges the success rate falls, introducing many false negatives. Only applying an automated procedure would leave approximately 40% of all erroneous data unnoticed. On the other hand, studying false positives reported by the automated procedure leads to the identification of doubtful sequences that were overlooked during the manual assessment. Therefore, the application of an automated procedure is useful to complement the results of a manual data assessment.

3.5 Data quality assessment of WDD gauges: WDD versus KNMI data

The second step in the data quality assessment of WDD gauges is the comparison of WDD TBRG results with KNMI Hellmann gauge results. The objective is to valuate the WDD TBRG results using the ‘true’ KNMI data. Also, any structural differences between both data sources are assessed. The complete comparison is presented in appendix E; in this paragraph a short resume of results is given.

Comparing long-term sums of precipitation, the WDD tipping-bucket raingauges systematically underestimate precipitation by 20% to 25% when compared to the Hellmann type KNMI raingauges. Figure 3-10 shows the differences in (equivalent) annual sums between WDD and other gauges. Comparing data on a monthly basis

yields comparable results. Searching for an explanation of these large differences it appeared that the WDD sensors had not been calibrated directly after installation. Hence, a calibration was performed two years after installation. It has shown that approximately half of the underestimation is accounted for by the lacking calibration. The WDD data sets have been corrected for this deficiency, reducing the difference to 10-15%. The other half of the observed underestimation may be explained by systematic errors related to observation conditions. Mainly, the poor installation of WDD gauges has likely caused large-scale wind shading. Also, intrinsic differences in wind-induced errors exist between Hellmann gauges and TBRGs. For the latter two error sources no quantification is possible; as a result, WDD data cannot be corrected for these errors.

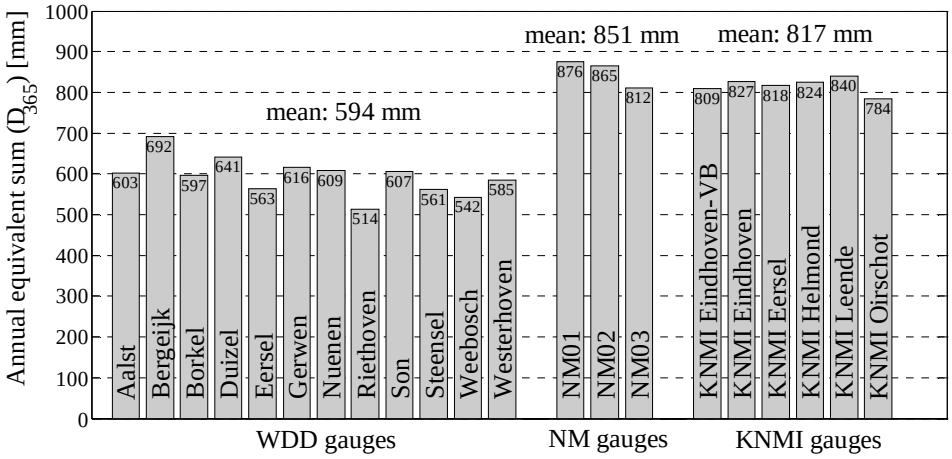

Figure 3-10: Annual equivalent sums of precipitation (D_{365}) of 12 WDD, 3 NM and 6 KNMI raingauges. The definition of an equivalent sum can be found in appendix E.

3.6 Calculation of areal time-series

Briefly restating, the main objective of this chapter is to obtain three time-series that, as accurately as possible, represent precipitation in the three catchment areas Riool-Zuid, Eindhoven Stad and Nuenen/Son. In this paragraph, results of the 12 WDD gauges with sufficient data yield and the 3 NM data sets are used to derive the desired time-series by means of the inverse distance weighting method. To limit calculation time, the calculation is based on 1-hour lumped data (see appendix E.1) instead of the original 1-minute data.

The data results of the TBRGs are point observations and represent as such a limited number of single draws from geographically distributed events. In fact, the

total catchment area of the 15 TBRGs equals 3600 cm^2 which is approximately one billionth of the 600 km^2 catchment area of the wwtp Eindhoven. Estimated values at non-observed locations can be obtained by means of interpolation techniques. The technique used in this paragraph is the inverse distance weighting method (idw-method). The estimate at any point without observation is obtained from the sum of weighted observations in the neighborhood. The weights are inverse proportional to the distance from those observations. The description of the idw-method in this section is based on Luxemburg and Savenije (2007).

To be able to apply the idw-method on the Eindhoven area a grid has been superimposed, see Figure 3-11. Each cell represents 36" along latitude lines (east-west) and 18" along longitude lines (north-south) which (at the Eindhoven latitude) corresponds to an area of approximately 695m x 556m. Cells that contribute stormwater to one of the considered sewer systems (combining cells to make fully shaded cells) are included in the calculation. For Riool-Zuid a total of 175 cells or ~ 68 km^2 are included, for Eindhoven Stad 143 cells or ~ 55 km^2 and 45 cells or ~ 17 km^2 for Nuenen/Son. For each cell in the grid precipitation per hour has been calculated as a weighted average of available TBRG data:

$$z'(x_0) = \sum(\lambda_i \cdot z(x_i)) \tag{3.1}$$

with $z'(x_0)$ = precipitation depth estimate at x_0;
$z(x_i)$ = precipitation depth observation at x_i and
λ_i = weight for observation $z(x_i)$.

Weights are based on inverse distances to the available observations:

$$\lambda_i = \frac{1/D_i^b}{\sum_{j=1}^{n} 1/D_j^b} \tag{3.2}$$

with D_i = distance between x_0 and x_i;
b = exponent (= 2) and
n = number of raingauges with a data value.

For cells with a raingauge, the weight of that gauge is set at 1 and all other gauges are ignored. All raingauges are assumed to be centrally located in their cells. Finally, after calculation of precipitation values per cell, precipitation depths per hour for the Riool-Zuid, Eindhoven Stad and Nuenen/Son catchment areas are calculated as arithmetic means of the results of all contributing cells. This way, the areal time-series are derived.

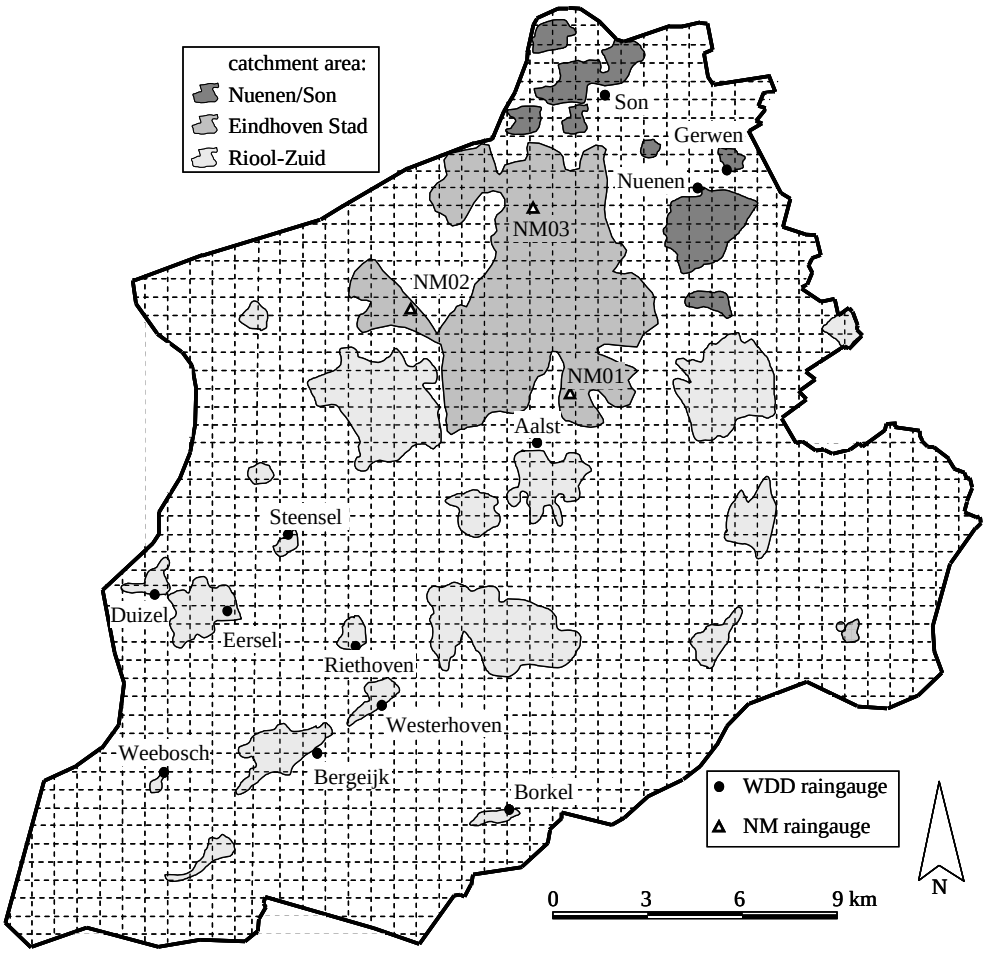

Figure 3-11: Catchment area of the wwtp Eindhoven with a superimposed grid. Each cell has a width of 36" along latitude lines (or 695m) and a height of 18" along longitude lines (or 556m). The locations are indicated of the 12 WDD gauges and 3 NM gauges used in the calculation of areal time-series.

Since the WDD TBRG data sets are far from complete (see Table 3-1), areal calculations are regularly based on a limited number of gauges (*n* in equation 3.2). During prolonged data communication problems in the WDD system (during which no data are available for all WDD gauges) the areal calculations are based on NM gauge results only. This is particularly the case for 1 April - 11 July 2007 (102 days), 4 - 31 March 2008 (27 days) and 28 April - 19 May 2008 (21 days). During a total of 123 hours (~0.9% of total data set) WDD nor NM sensors have yielded precipitation data. During these hours, no areal precipitation values have been calculated.

3.7 Conclusions and evaluation of areal precipitation time-series

Waterschap De Dommel (WDD) installed 22 tipping-bucket raingauges to monitor precipitation in the three catchment areas contributing wastewater to wwtp Eindhoven. The purpose of the gauges was to generate data that could be used to derive high-frequent time-series of precipitation per catchment area.

A thorough data quality assessment has been applied on the WDD data sets. For this, the data sets have been cross-checked with both manual and automatic procedures. The data of two WDD gauges have been rejected all together since the gauges were located beneath trees. The other 20 WDD data sets have been examined for data gaps and erroneous data. For 8 WDD gauges between 40% and 80% of data did not correctly represent the precipitation process; these gauges were excluded from further processing. Accounting for data gaps and erroneous data, the remaining 12 WDD gauges have a mean data yield of 70%.

For comparison of long-term performance of WDD gauges, the data of nine other raingauges (6 Hellmann gauges and 3 other tipping-bucket gauges) have been used as reference values. It was concluded that WDD gauges underestimate precipitation depths by approximately 20% to 25%. The explanation for this bias in data results is twofold. Firstly, WDD gauges were initially not calibrated. An *a posteriori* calibration demonstrated that about half of the underestimation can be attributed to the lacking calibration. Secondly, the other half can be explained mainly by observation conditions. Intrinsic differences in wind-induced errors exist between Hellmann gauges and TBRGs and a poor installation of WDD gauges has caused large-scale wind shading. For lack of quantification of errors explaining the latter half, the WDD data sets have only been corrected for the bias due to the missing calibration.

Altogether, of the more than 18 million data points in the 22 raw WDD data sets, approximately 8.5 million data points (or 46%) have been rejected in the data quality assessment. Moreover, the assessment in paragraph 3.5 and appendix E has shown that the data of the remaining 12 WDD gauges are biased. Also, WDD data sets are incomplete due to data gaps and the removal of erroneous data described in paragraph 3.4. As a result, and especially during data gaps shared among all WDD sensors, the calculation of areal time-series can be based on a limited number of gauges reducing the chance of correctly representing precipitation over a catchment area. For instance, in case the Riool-Zuid time-series is based on NM gauges only, a storm event traveling in north-easterly direction will pass the Riool-Zuid catchment area earlier than observed by the NM gauges. Even with all TBRGs in operation, the gauges are not evenly distributed over the area: sensors are overrepresented in the south-western and north-eastern part of the area, whereas the

eastern and south-eastern areas are not observed. Again, this is likely to reduce the chance of correctly representing precipitation over the entire catchment area.

In all, it can be concluded that the overall performance of the WDD raingauge network has been poor. Having based the areal time-series primarily on these WDD data sets, the accuracy and correctness of the derived RZ, ES and NS precipitation time-series can be disputed. However, the use of the precipitation data in chapter 6 is such that a bias in values and a (small) error in timing are not of the utmost importance. The data are used to select dry weather and wet weather data from wwtp influent quantity and quality data sets. A bias in values might lead to a different number of e.g. dry weather days, but a sensitivity analysis (see sections 6.2.1) has shown that results are little sensitive to the exact definition of a dry weather flow day. Also, the applied definition of wet weather conditions is such that a small timing error in the onset or ending of a storm event will not largely influence results. More important than the bias or timing error, the use of the aggregated 1-hour data instead of the original 1-minute data has meant losing short-term precipitation intensity information. As a result, it has not been possible to search for relations between peak loadings arriving at the wwtp Eindhoven and short-term precipitation intensities.

Further considerations on the poor performance of the WDD precipitation monitoring network can be found in chapter 8.

Chapter 4. Flow monitoring

4.1 Introduction

The calculation of pollution loads in wastewater arriving at the wwtp Eindhoven requires time-series of both wastewater quantity and quality. This chapter focuses on the water *quantity* time-series; chapter 5 presents the water *quality* time-series. In chapter 6 both time-series are combined into pollution load time-series.

At the influent pumping station of the wwtp Eindhoven wastewater arrives from the three contributing catchment areas Riool-Zuid, Eindhoven Stad and Nuenen/Son (Q_{RZ}, Q_{ES} and Q_{NS} in Figure 4-1). At the pumping station a total of nine pumps transport the wastewater further into the treatment plant. Nine flow sensors monitor the amounts of water that pass the pumps (Q_{pump1} through Q_{pump9}). These flow sensor data sets form the basis for the calculation of the flow time-series for each of the three catchment areas. The transition from nine flow sensor data sets to three areal inflow time-series is, however, not straightforward. A number of data modifications are required to obtain three accurate and correct time-series that represent the inflow of wastewater from the contributing sewer systems into the treatment plant. Monitoring at the interface between sewer system and treatment plant, the resulting flow values are both catchment area *outflows* and wwtp *inflows*.

The objective of this chapter is to derive three time-series that represent - as accurately as possible and with an uncertainty estimate - the *quantity* of wastewater that arrives at the wwtp Eindhoven originating from the three contributing catchment areas (Q_{RZ}, Q_{ES} and Q_{NS}). For this, paragraph 4.2 introduces the influent pumping station and the characteristics of its pumps and flow sensors. Next, the quality of the raw flow sensor data sets is assessed in paragraph 4.3. Observed data errors that need removal or correction include data gaps, zero values, and a non-zero baseline. In paragraph 4.4 the validated flow sensor data sets are used to calculate the three areal inflow time-series. Preceding the actual calculation which is presented in paragraph 4.4.3, the contribution of pump 6 is assigned to the correct influent chamber in section 4.4.1 and the inter-chamber flow between the influent chambers of Riool-Zuid and Eindhoven Stad is calculated in section 4.4.2. Some considerations on discrepancies between pump behavior and ‘expected’ areal inflow patterns are discussed in section 4.4.4. Finally, section 4.4.5 presents an estimation of uncertainty of the areal inflow data sets.

4.2 The influent pumping station: pumps and flow sensors

This paragraph describes the wwtp Eindhoven influent pumping station. First, the lay-out of the pumping station is presented in section 4.2.1. Subsequently, the installed pumps and flow sensors are topic of sections 4.2.2 and 4.2.3, respectively.

4.2.1 Lay-out of influent pumping station

At the influent pumping station of the wwtp Eindhoven separate influent chambers receive the wastewater from the three catchment areas Riool-Zuid, Eindhoven Stad and Nuenen/Son, see Figure 4-1.

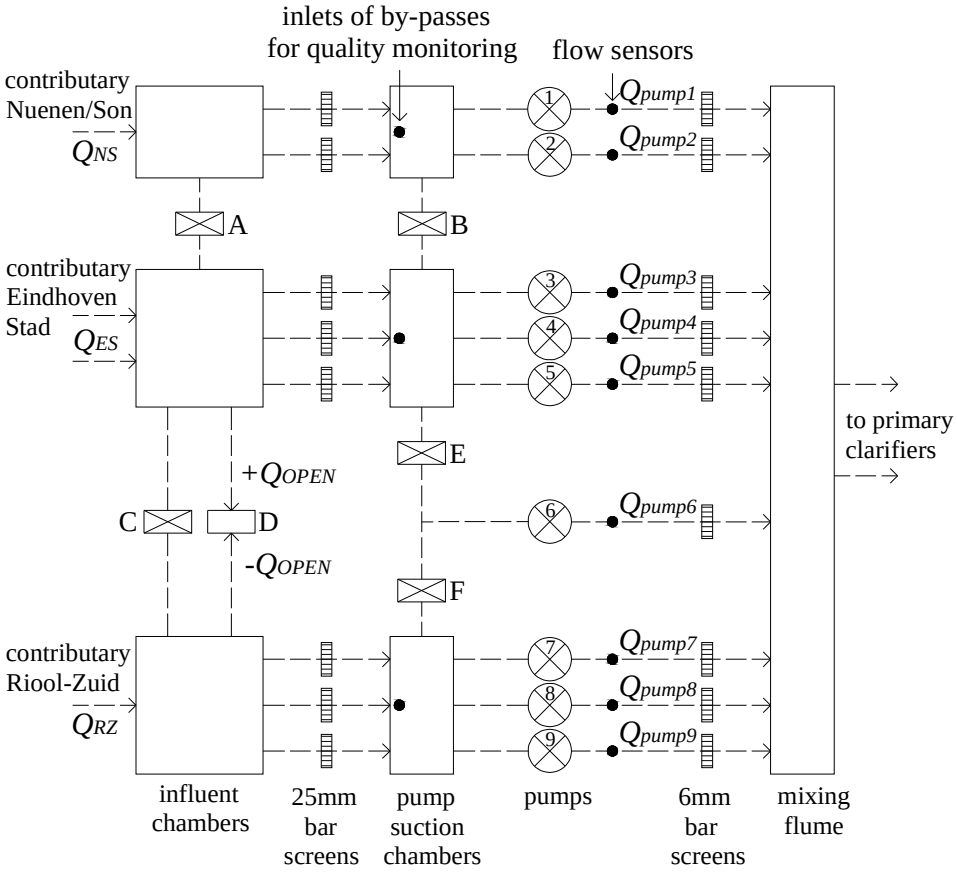

Figure 4-1: Schematic lay-out of the influent pumping station at wwtp Eindhoven. Wastewater flows from left to right. Nine flow sensors monitor flow directly downstream each of the nine influent pumps.

The wastewater passes 25 mm bar screens before being pumped up by one of nine influent pumps. Subsequently, 6 mm bar screens further remove gross solids from the wastewater after which the three hitherto separate wastewater flows are combined in a mixing flume. Under dry weather conditions all wastewater in the mixing flume is directed towards the primary clarifiers.

The three influent chambers are interconnected by means of gates A and C. The gates are movable, but were continuously closed during the collecting of data considered in this chapter. Gate D, however, represents an opening in the concrete wall that separates the influent chamber of Eindhoven Stad from the influent chamber of Riool-Zuid. At specific water levels in the influent chambers, wastewater can freely flow from one chamber into the other (Q_{OPEN}). This inter-chamber flow is further addressed in section 4.4.2.

4.2.2 Influent pumps

Lay-out
Nine pumps are used to pump wastewater from the pump suction chambers towards the primary clarifiers, see Figure 4-1 and Figure 4-2. The nine influent pumps are positioned such that pumps 1 and 2 service influent chamber Nuenen/Son, pumps 3, 4 and 5 service chamber Eindhoven Stad and pumps 7, 8 and 9 service chamber Riool-Zuid. Pump 6 services a separate section of the pumping station that is either connected to the influent chamber of Eindhoven Stad (in case moveable gate E is open) or to the influent chamber of Riool-Zuid (in case moveable gate F is open). Gates E and F are never simultaneously opened. Registrations of gate operations are unavailable for the time-span of data considered in this chapter. Instead, the assignment of pump 6 to either one influent chamber is based on flow data, as presented in section 4.4.1.

Types and capacity
All pumps are by manufacturer Nijhuis Pompen (the Netherlands) and are of the impellor type. The capacities per pump, as presented in Table 4-1, are for the presented head differences which equal the level differences between the respective (design) set-points of the influent chamber water levels and the (design) set-points of the water levels just before the 6 mm bar screens. In case of decreasing differential head (e.g. an increasing water level in the influent chambers during wet weather flow) the realized flows per pump can increase up to levels as shown in Table 4-1. When pumping in combination, the pumps are electrically limited such that the total flow to the wwtp does not exceed 35,000 m^3/h. Additionally, the inflows from each of the three catchment areas are limited to the indicated maximum values. The main reason behind the latter restriction is that, during large storm events, the inflow from catchment area Eindhoven Stad can increase quickly

and up to a level that, without the limitation, only a very limited fraction of the hydraulic capacity of the wwtp would be left available for the more delayed inflow from catchment areas Nuenen/Son and Riool-Zuid.

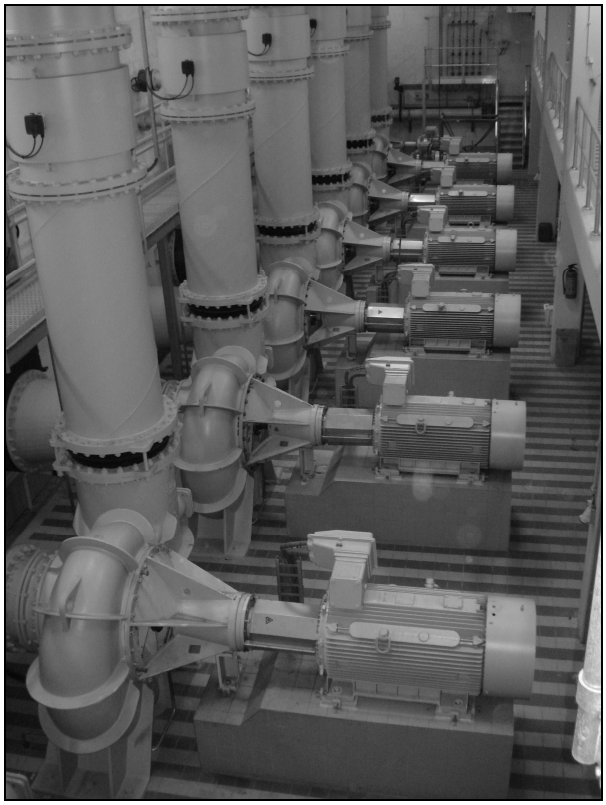

Figure 4-2: Influent pumps at the influent pumping station of wwtp Eindhoven. On top, the electromagnetic flow sensors in separate flanges build into the discharge lines of the pumps.

Table 4-1: Characteristics of influent pumps

		pumps 1 - 2 Q_{NS}	pumps 3 - 5 $\approx Q_{ES}$*	pumps 6 - 9 $\approx Q_{RZ}$*
pump type	[-]	RW1-400.525A	HMFr1-8070	HMFr1-8070
capacity per pump	[m^3/h]	1,700	5,100	5,800
differential head	[mLC]	10.6	9.07	9.49
realized maximum flow per pump	[m^3/h]	2,000	6,000	6,200
maximum allowed total flow from catchment area	[m^3/h]	3,290	14,000	17,710

*Q_{RZ} and Q_{ES} also depend on the assignment of pump 6 and Q_{OPEN}, see paragraph 4.4.1.

All pumps have been installed in 1998. Prior to installation the pumps have been tested for Q-H and efficiency relations according to ISO (1975). Proactive maintenance on pumps includes a regular inspection and maintenance of engines and moving pump parts. Maintenance activities as well as other irregularities on pumps are recorded in a database.

4.2.3 Flow sensors

Type and settings
Nine electromagnetic sensors measure flow directly after the influent pumps, see Figure 4-2. The sensors are pipe-mounted and attached to the discharge lines of the pumps and hence constitute closed conduit full pipe measurements. The distances between pump and sensor are approximately four times the pipe diameter, which is less than the recommended value of ten pipe diameters between sensor and the last upstream flow disturbance (ISO, 1992b). The sensors are of type MAG3100 by manufacturer Danfoss (Denmark). The principles of flow sensing using electromagnetic induction are also described in ISO (1992b). The sensors at pumps 1 and 2 have a programmed range of [0-2,000] m^3/h; the other seven sensors monitoring pumps 3 through 9 have a programmed range of [0-6,200] m^3/h. For ease of reference the flow sensor monitoring pump 1 is referred to as "flow sensor 1", the sensor monitoring pump 2 is referred to as "flow sensor 2", etc.

Data and data communication
Every minute the nine flow sensors each produce an analogue 4-20 mA signal. This signal is converted to a digital signal by a 12-bits ADC (analogue-to-digital convertor). The digital bit-signal is communicated to a central server and stored as such. Before data analyses and visualization, the digital signal is translated back to flow data using the aforementioned sensor ranges. A 12-bits ADC allows a total of 2^{12} possible bit-signal values. Hence, in combination with the programmed ranges, the values of flow sensors 1 and 2 have a resolution of 0.49 m^3/h and the values of flow sensors 3 through 9 a resolution of 1.51 m^3/h.

The nine raw data sets of flow data consist of 1-minute interval time-series, available for the time-span April 1st, 2007 - November 1st, 2008.

Metadata information
Most maintenance and repair activities on flow sensors have been recorded in a database. However, often due to lack of time, activities during large-scale malfunctioning of the wwtp or influent pumping station have not been recorded. Some large-scale events have been added to the metadata file after interviewing operators on this topic.

4.3 Quality assessment of flow sensor data sets

The quality of raw data sets as measured by the nine flow sensors is assessed before the data sets are used to derive areal inflow time-series. The flow sensor data sets suffer from data gaps, "zero"-values, values outside sensor ranges, inter-resolution values and non-zero baselines. The assessment of raw data sets presented in this paragraph aims at the detection and, where possible, correction of erroneous data.

4.3.1 Data gaps

The raw data sets contain a limited amount of data gaps (i.e. time-stamps without data values). Each data set misses 385 minutes of data (or 0.05% of the data sets), divided over 32 data gaps shared by all sensors. The longest data gap lasted 151 minutes; the length of the other gaps range between 1 and 20 minutes with a mean length of 7.5 minute. Flow sensor 1 has one extra data gap lasting 16 minutes, not shared by any of the other sensors. Metadata files do not provide information on the reasons behind the data gaps; however, since nearly all data gaps coincide, it is assumed that the gaps are caused by data communication errors. Data gaps have not been corrected for.

4.3.2 "Zero"-values

The raw flow sensor data sets contain a limited number of "zero"-values, i.e. time-stamps with a flow value of exactly 0 m^3/h. Metadata files show that maintenance activities are the main reason behind these particular entries. In other words, "zero"-values in the data sets are associated with a non-operation of the sensor, not with the non-operation of pumps. For eight flow sensors the number of "zero"-values ranges between 72 and 119 (≈ 0.03% of the data sets), divided over 5 specific days during which maintenance on the sensors has taken place. The data set of flow sensor 3 contains 1552 "zero"-values (≈ 0.4%) due to a prolonged maintenance event. All 0 m^3/h values have been replaced by empty time-stamps to differentiate between a non-operational sensor and a non-operational pump.

4.3.3 Values outside sensor range and inter-resolution values

All entries in the data sets should be within the programmed sensor ranges. For flow sensors 1 and 2 the range is [0-2,000] m^3/h; sensors 3 though 9 have a programmed range of [0-6,200] m^3/h. Studying the data sets, a total of four entries contain values outside the programmed ranges (all larger than the maximum value).

Also, all values in the data sets should be multitudes of the signal resolution (0.49 m^3/h for sensors 1 and 2; 1.51 m^3/h for sensors 3 - 9). A total of 16 values, however, are not. Metadata files provide no information as to the reason behind the observed anomalies. All values outside sensor ranges and inter-resolution values have been replaced by empty time-stamps.

4.3.4 Non-zero baseline

Plotting all data per flow sensor in ascending order yields graphs with a clear distinction between entries during which the pump was in operation and entries associated with non-operation or "zero flow". Figure 4-3 presents an example for flow sensor 8. For this sensor approximately 540,000 entries (or 65% of the data set) lie within the "zero flow" area. Zooming in on this area (Figure 4-4) it can be observed that all "zero flow" values are actually larger than zero: values range between 2 and 10 m^3/h and are multitudes of the resolution of the flow sensor signal (for pump 8: 1.51 m^3/h).

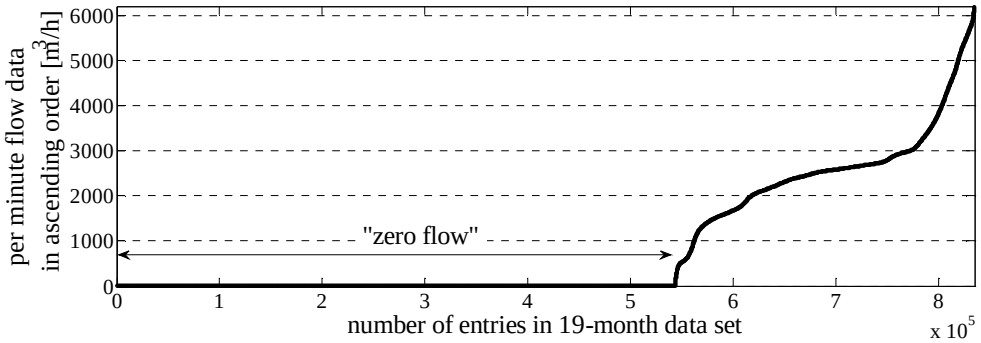

Figure 4-3: All data of flow sensor 8 in ascending order (per minute data over time-span April 1st, 2007 - November 1st, 2008)

Despite the non-operation of pump 8, the surface area under the graph in Figure 4-4 represents approximately 62,000 m^3 of transported wastewater. The question arises whether this amount of water has been truly transported through the pipe monitored by flow sensor 8 or that the signal is wrongfully created by the flow sensor. At some treatment plants, non-operational pumps are not fully switched off to prevent sedimentation in and around the pump's casing. However, at the wwtp Eindhoven influent pumping station non-operational pumps are fully switched off (Weijers, 2009). Hence, it is concluded that the non-zero values are a bias in the flow sensor and should be corrected for. Similar biases have been observed for all

nine flow sensors. Flow sensors 1 and 2 show "zero flow" values on the order of 0 to 3 m^3/h; flow sensors 3 through 9 on the order of 0 to 24 m^3/h.

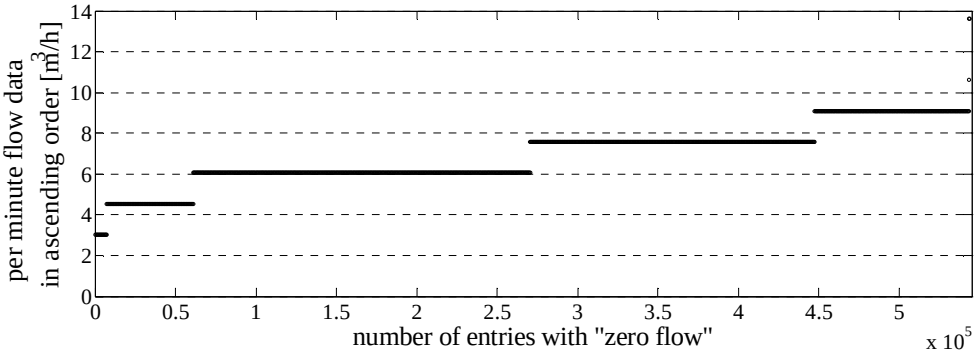

Figure 4-4: Zoom of "zero flow" area in Figure 4-3. Values are multitudes of 1.51 m^3/h, the resolution of the flow sensor signal.

To be able to correct for the non-zero baselines, the temporal distribution of biases is important. Figure 4-5 shows "zero flow" values plotted chronologically for flow sensor 8. The figure presents the per-minute data in black (again, as multitudes of the flow sensor signal resolution) and in grey the daily mean values of all "zero values" for each of the 580 presented days. For this particular sensor, the mean values are fairly constant over specific time-spans; at certain moments in time (in the figure indicated with "A" through "D"), however, a change in signal behavior can be observed. Metadata files show that these moments of change coincide with maintenance work and an interruption of sensor signals.

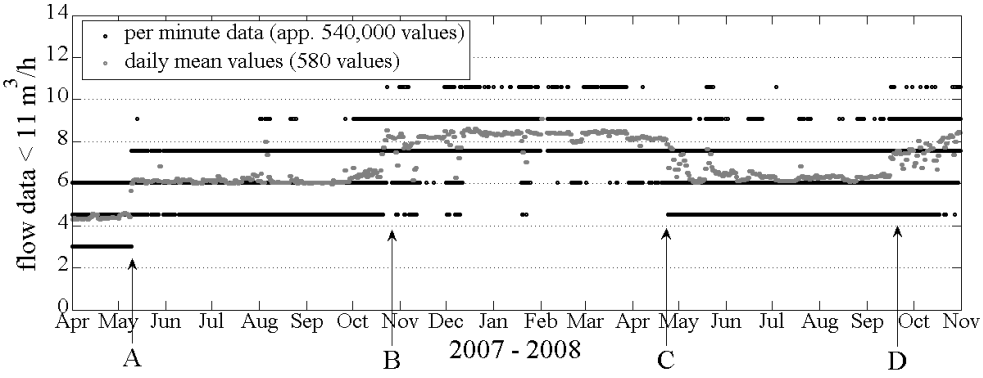

Figure 4-5: "Zero flow" data (i.e. values < 11 m^3/h) for flow sensor 8 for the considered 19-month time-span. In black the per-minute data from the raw data sets; in grey the 580 daily mean values. At moments A through D a change in signal behavior can be observed.

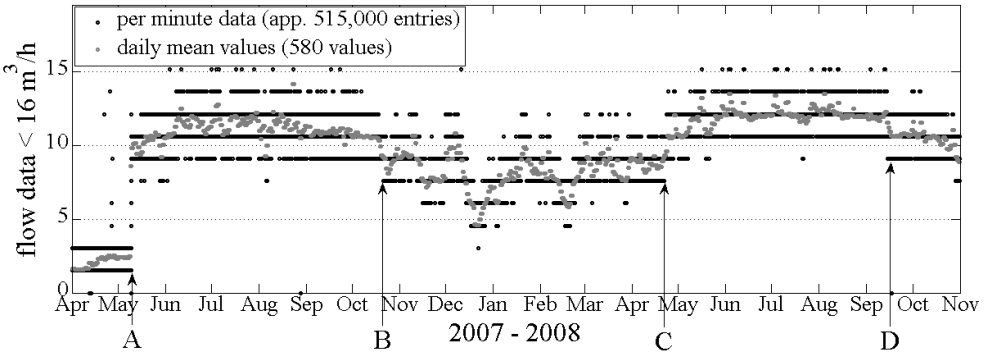

Figure 4-6: "Zero flow" data (i.e. values < 16 m^3/h) for flow sensor 5 for the considered 19-month time-span. In black the per-minute data from the raw data sets; in grey the 580 daily mean values. At moments A through D a change in signal behavior can be observed.

The variation of mean values differs per sensor. For instance, flow sensor 5 shows in Figure 4-6 a different pattern of mean "zero flow" values. The moments of change, however, are the same for the two sensors, confirming the notion that an external factor must have caused the changes. Other sensors show still other changes and variations in the daily mean values of "zero entries". It can be concluded that the studied flow sensors do not suffer from constant baseline drift, but suffer from an irregular baseline variation that differs per sensor.

Based on the previous diagnosis of variations of the non-zero baseline in flow sensor data sets, the following modifications to the data sets have been made:

1. all "zero flow" values in the flow sensor data sets are set to 0 m^3/h;
2. all other values in the flow sensor data sets are corrected using the daily mean values of "zero flow" (the grey values in Figure 4-5 and 4-6).

Since all "zero flow" values are larger than zero, the aforementioned corrections are in fact subtractions and lead to a reduction in measured volumes. Table 4-2 presents the volume reductions per flow sensor as percentages of the total volumes of the raw 19-month data sets. These reductions range between 0.8% and 5.2%.

Table 4-2: Reductions in total measured volume after correction for baseline variations.

	volume reduction [%]		volume reduction [%]
flow sensor 1	0.9	flow sensor 6	1.5
flow sensor 2	1.9	flow sensor 7	5.2
flow sensor 3	2.1	flow sensor 8	2.2
flow sensor 4	0.8	flow sensor 9	2.3
flow sensor 5	1.1		

4.4 From data per flow sensor to areal inflow data

After quality assessment in the previous paragraph, the validated results of flow sensors are used in this section to calculate the total flow from the three catchment areas Nuenen/Son (Q_{NS}, pumps 1+2), Eindhoven Stad (Q_{ES}, pumps 3+4+5) and Riool-Zuid (Q_{RZ}, pumps 7+8+9). A straightforward summation of sensor results is not possible for two reasons. First, no metadata information on the contribution of pump 6 is available which makes it unclear when this pump should be added to Q_{RZ} and when to Q_{ES}. Second, an opening in the concrete wall between the influent chambers of Riool-Zuid and Eindhoven Stad makes it necessary to correct Q_{RZ} and Q_{ES} for Q_{OPEN}, the flow through the opening. Sections 4.4.1 and 4.4.2 consider these two problems and present the required data manipulations for a proper calculation of areal inflow data. The actual equations with which the areal data are derived are presented in section 4.4.3. In section 4.4.4 some considerations are presented on discrepancies between pump behavior and 'expected' areal inflow patterns. Finally, in section 4.4.5 the uncertainty in the areal inflow time-series is addressed.

4.4.1 Contributions of pump 6

Pump 6 is used to pump wastewater from either influent chamber Eindhoven Stad or influent chamber Riool-Zuid, see Figure 4-1. Since no *metadata* are available on the operation of gates E and F, all *flow sensor data* have been plotted and manually assessed to determine to which flow (Q_{RZ} or Q_{ES}) pump 6 contributes. Figure 4-7 presents a 4-day example in September 2007. During the first day (September 2nd) the graph that presents the summation of data of pumps 3, 4 and 5 is gradual and continuous whereas the graph presenting the summation of data of pumps 7, 8 and 9 resembles a block pulse function. During zero flow for the latter, pump 6 is in operation. The addition of pump 6 to the Riool-Zuid summation would yield a gradual and continuous function, as expected for wastewater flow from a large catchment area. Therefore, it is concluded that - for this day - pump 6 should be added to Q_{RZ}. Reasoning analogously, pump 6 contributes to Q_{ES} on September 4th and 5th. On September 3rd the positions of gates E and F must have been reversed during the non-operation in the morning: the peak-flow of Eindhoven Stad during a storm event suddenly decreases around 12h30 by the same magnitude as the increase in pump 6.

Studying all flow sensor data this way, for the complete 19-months time-span the contribution of pump 6 has been determined, see Table 4-3. In total, the contribution of pump 6 changes five times between the influent chambers of Riool-Zuid and Eindhoven Stad.

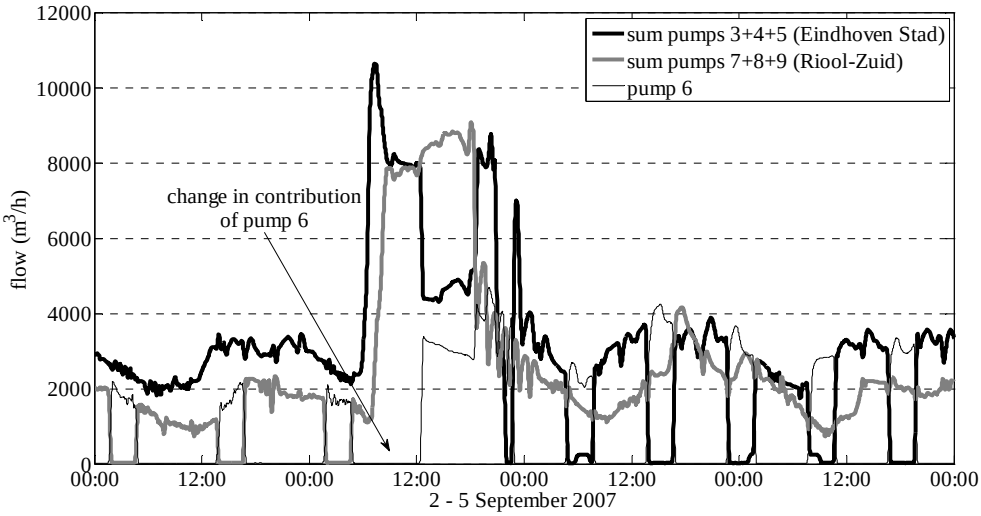

Figure 4-7: Summation of data for Eindhoven Stad and Riool-Zuid and the data of pump 6. All data have been smoothed with a 30-minute window for the purpose of clear presentation.

Table 4-3: Assignment of pump 6 to Q_{RZ} or Q_{ES}

from	till	pump 6 contributes to
April 1st, 2007 00h00	May 27th, 2007 09h00	Q_{RZ} (Riool-Zuid)
May 27th, 2007 09h00	June 9th, 2007 11h30	Q_{ES} (Eindhoven Stad)
June 9th, 2007 11h30	September 3rd, 2007 12h00	Q_{RZ} (Riool-Zuid)
September 3rd, 2007 12h00	January 29th, 2008 12h00	Q_{ES} (Eindhoven Stad)
January 29th, 2008 12h00	April 24th, 2008 12h00	Q_{RZ} (Riool-Zuid)
April 24th, 2008 12h00	November 1st, 2008 00h00	Q_{ES} (Eindhoven Stad)

4.4.2 Inter-chamber flow Q_{OPEN}

A rectangular opening of 1.50 m wide and 0.70 m high in the concrete wall between the influent chambers of Riool-Zuid and Eindhoven Stad (gate D in Figure 4-1) allows wastewater to flow from one chamber into the other. This is the case if water levels in one or both influent chambers exceed the crest level of the opening at +13.30 mNAP, which occasionally occurs during a large storm event. The resulting flow is referred to as Q_{OPEN} and is defined as a positive value if water flows from the chamber of Eindhoven Stad into the Riool-Zuid chamber. Per combination of water levels different flow conditions occur. Appendix F describes these flow conditions and the associated equations to calculate Q_{OPEN}.

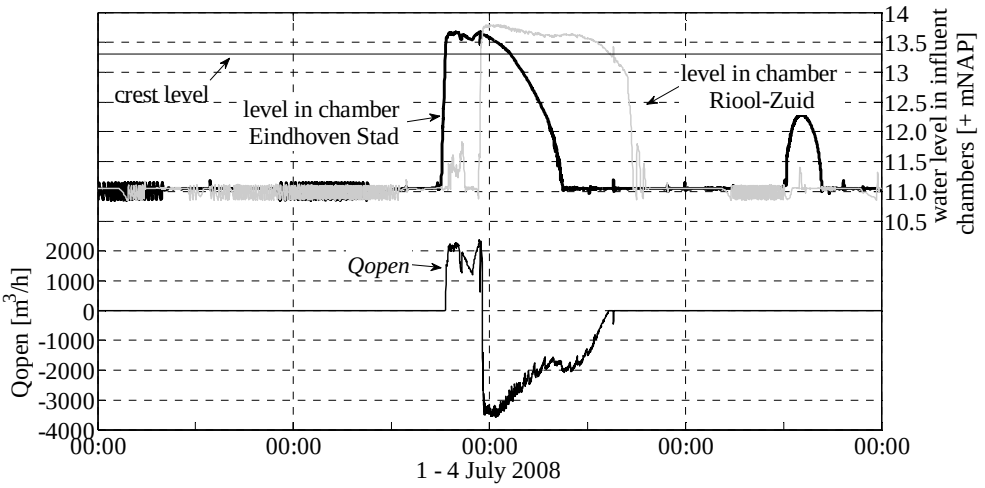

Figure 4-8: Inter-chamber flow (Q_{OPEN}) when water levels in influent chambers Riool-Zuid and Eindhoven Stad exceed the crest level of the opening that connects both influent chambers.

Figure 4-8 presents an example for a 4-day period in July 2008. An increase in influent chamber water levels is caused by a storm event on July 2nd and 3rd. First, the level in chamber Eindhoven Stad increases beyond crest level, resulting in a Q_{OPEN} up to 2,000 m^3/h. A few hours later an increase in water level in the Riool-Zuid chamber results in an opposite flow of up to -3,000 m^3/h, which slowly reduces to zero as the water level in the influent chamber sinks back to crest level. In this example, the volume of water spilled from chamber Eindhoven Stad to chamber Riool-Zuid (V_{OPEN}, the integral of all $+Q_{OPEN}$ values) equals 8,000 m^3; the volume of water transferred in the other direction equals 32,000 m^3. Hence, the net flux between the two chambers amounts to 24,000 m^3 for this storm event. During the same time-span (i.e. as long as $Q_{OPEN} \neq 0$), a total of 136,000 m^3 of wastewater has arrived at the wwtp from catchment area Riool-Zuid (V_{RZ}) and a total of 234,000 m^3 from area Eindhoven Stad (V_{ES}). Accounting for Q_{OPEN} these values change to 160,000 m^3 and 210,000 m^3, respectively. In other words, for this example, the inter-chamber flow has a large effect (respectively 18% and 10% changes) on calculated volumes and must therefore be incorporated for a correct calculation of areal inflow data.

During the time-span April 1st, 2007 - November 1st, 2008 for a total of 40 (storm) events wastewater has spilled through the opening. The total spilled volume equals approximately 490,000 m^3, divided almost evenly over V_{OPEN} and $-V_{OPEN}$.

4.4.3 Calculation of areal inflow time-series

Considering the data manipulations as presented in the previous two sections, the inflow from catchment areas Riool-Zuid (Q_{RZ}), Eindhoven Stad (Q_{ES}) and Nuenen/Son (Q_{NS}), can be calculated as follows (see Figure 4-1 for explanation of parameters):

$$Q_{NS} = Q_{pump1} + Q_{pump2} \tag{4.1}$$

$$Q_{ES} = Q_{pump3} + Q_{pump4} + Q_{pump5}(+Q_{pump6}) + Q_{OPEN} \tag{4.2}$$

$$Q_{RZ} = (Q_{pump6}+)Q_{pump7} + Q_{pump8} + Q_{pump9} - Q_{OPEN} \tag{4.3}$$

4.4.4 Pump behavior versus 'expected' areal inflow patterns

As flow sensors monitor *pumped* flows, their data sets occasionally show 'typical' pump behavior. As a result, the calculated areal inflow time-series sometimes do not resemble an 'expected' pattern of wastewater entering a wastewater treatment plant from a free flow connection. In this section, three such data 'anomalies' are considered: high-frequent on/off switching of pumps, varying speed of pumps during wet weather flow, and prolonged non-operation of pumps.

High-frequent on/off switching of pumps

Figure 4-9 presents the first encountered anomaly in the pump data sets. During the operation of a specific pump, flow values change between 0 and approximately 3,000 m^3/h every few minutes for the duration of several hours (areas "A" in the figure). This has no relation with the actual inflow of wastewater to the treatment plant, but is the result of the (unintended) high-frequent on/off switching of the pump due to an error in pump control settings. Application of a (nearly) flow-conservative filter over the data (a symmetrical moving average filter with a span of 31 minutes) shows that the total amount of pumped wastewater over a higher aggregate level is in accordance with the expected inflow pattern. Hence, it is assumed that for this type of data anomaly - while pump *behavior* may be anomalous over a certain time-span - the *total amount* of pumped wastewater over the same time-span is nevertheless correct. Also, when studying the pollutograph of TSS in Figure 4-9 for the considered time-span, it can be concluded that the high-frequent on/off switching of pumps does not have a distinguishable effect on water quality parameters as measured at the wwtp influent pumping station. This means that data analyses over time-spans shorter than the duration of the anomaly

do not yield valid results, but analyses at higher aggregate levels still can be performed. Therefore, these data anomalies have *not* been removed from the pump data sets.

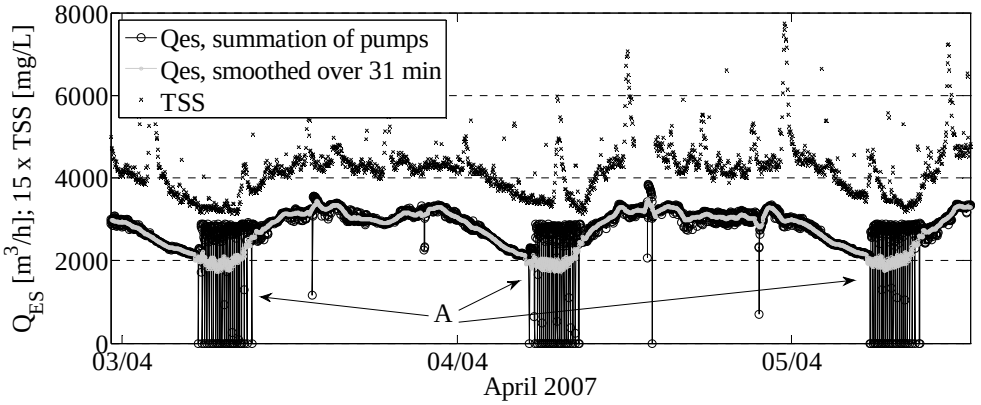

Figure 4-9: Pump data during high-frequent on/off switching of a pump (areas "A") and the same data set after application of a 31-minutes moving average filter.

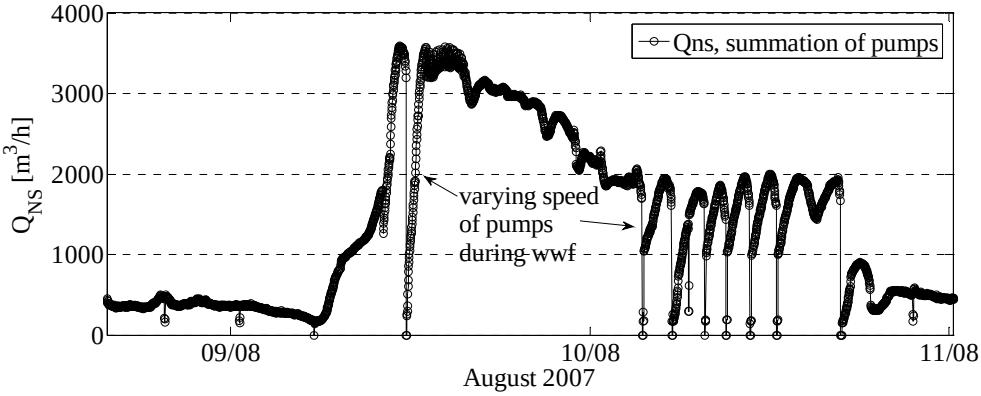

Figure 4-10: Large variations in pump speeds during wet weather flow.

Varying speed of pumps during wet weather flow

The moment additional pumps are switched on or off to accommodate for the increase or decrease in wastewater flow during wet weather situations, it is often observed that the speed of pumps varies strongly; see Figure 4-10 for an example. For several hours on end, the control algorithm of the pumps is not able to attain a steady and only slowly varying flow. Instead, it unnecessarily speeds the pumps up and down with a frequency of approximately 1 hour reaching values as low as zero

and as high as full-flow regime. Again, this flow pattern is very unlikely to resemble the arrival of the stormwater at the wwtp. Nevertheless, the data anomalies have also *not* been removed from the pump data sets for the same two reasons as the previous anomaly: (1) the sum of pumped flows over the time-span of the anomaly is assumed to be correct and (2) no influences on data quality parameters have been observed during occurrences of the anomaly. As a result, data analyses over aggregate levels higher than the duration of the anomaly can successfully be performed.

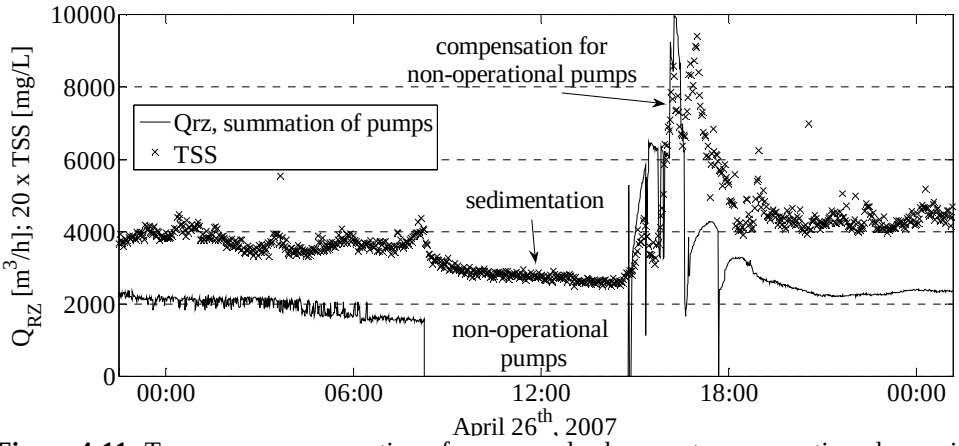

Figure 4-11: Temporary non-operation of pumps and subsequent compensation phase with the effect on TSS measurements.

Non-operation of pumps

A third data anomaly found in the data sets is the temporary non-operation of pumps, see Figure 4-11. In the example, all pumps servicing catchment area Riool-Zuid are non-operational for a period of approximately 8 hours. During this time-span, wastewater from the catchment area is temporarily stored in the influent chamber and, with increasing water level, in the contributing sewer system. After pumps resume operation, for a few hours the total flux is significantly larger than normal to compensate for the preceding non-operation and to empty the sewer system and bring the water level in the influent chamber back to the target level. Both during the non-operational phase as well as the compensation phase, the pump data does not correctly represent the amount of wastewater from the catchment area arriving at the wwtp, but the day sum of Q_{RZ} remains unchanged. More importantly (when considering the multiplication of flow data with quality data in chapter 6), during the non-operation of pumps water quality sensors no longer monitor the wastewater that newly arrives from the catchment area since this wastewater does not reach the quality monitoring installation in the influent

chamber due to the increased storage (see chapter 5 for details). As presented in Figure 4-11 sedimentation processes during the non-operational phase and resuspension processes during the compensation phase influence data quality parameters. If the rates of sedimentation and resuspension differ significantly (i.e. if a sediment layer is build up or removed during the data anomaly) the wwtp influent pollutant loads no longer represent normal values due to the temporary non-operation of pumps. Therefore, all flow data during the non-operation and during the subsequent compensation phase have been removed from the data sets.

4.4.5 Data uncertainty

Uncertainty of data in the areal inflow time-series is determined by the uncertainty in the raw flow sensor data sets and the subsequent summation of values. This is illustrated in Figure 4-12 for the calculation of areal inflow from catchment area Eindhoven Stad. As earlier presented in equation 4.2, the calculation of Q_{ES} is based on the results of 1, 2, 3 or 4 flow sensors and the (calculated) values of Q_{OPEN}. Each of these "raw" data sets has an associated uncertainty. The summation of data requires consideration to derive a suitable uncertainty associated with the flow values in the areal inflow time-series. These considerations are discussed hereafter.

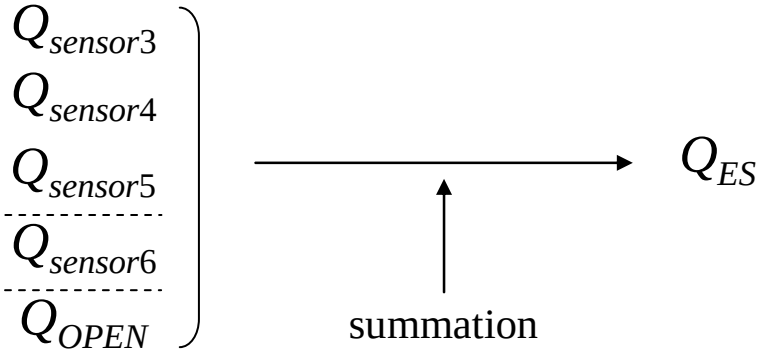

Figure 4-12: The combination of flow sensor data en Q_{OPEN} to calculate Q_{ES}.

Uncertainty in raw flow sensor data sets
Prior to installation in 1998 all nine flow sensors have been calibrated in test rigs ("wet calibration") that operate according to the static weighing method, as described in ISO (1980). Each sensor has been subjected twice to flows of 25% and 90% of the full scale flow-rate of the used rig. For flow sensors 1 and 2 a rig with a full scale flow of 200 l/s has been used (25% = 180 m^3/h; 90% = 650 m^3/h); for flow sensors 3 through 9 a rig with a capacity of 1,200 l/s has been used (25% =

1,080 m^3/h; 90% = 3,900 m^3/h). Table 4-4 presents the results of the calibration procedure. Presented values are the differences between the flow sensor results and the true flow that passed the sensor as determined by a weighing mechanism. Positive errors are overestimations of the true value by the sensors.

The limited number of calibration results per flow sensor hampers uncertainty calculations per flow sensor. ISO (1991) recommends at least three tests per flow rate at five distinctive flow rates (10%, 25%, 50%, 75% and 100% of full scale flow), but only two tests at two distinctive flow rates are available. It was therefore decided to group calibration results of all flow sensors that service the same catchment area, calculate uncertainty with the grouped values and consider the results representative for each sensor in the group. This way, the calibration results of for instance sensors 1 and 2 are used to calculate the uncertainty associated with each of both flow sensors servicing catchment area Nuenen/Son. Also, the uncertainty is assumed to be a constant percentage over the full ranges of the flow sensors. With this assumption the calibration results obtained at 25% of full scale flow can be combined with the results obtained at 90% of full scale flow. The resulting uncertainty values per flow sensor data set can also be found in Table 4-4. Assuming that errors follow a Gaussian distribution it can be concluded that the mean error is a bias in the data sets and that (with 95% confidence) random errors remain within a range of twice the standard deviation of observed errors. The data sets have been corrected for the calculated biases. The remaining uncertainty for all data sets is around 0.2%, which is of the same order of magnitude as values in literature for electromagnetic induction flow measurements in closed conduits (e.g. a value of ~0.5% in STOWA, 1996).

Table 4-4: Errors in flow sensor results when compared to true flows, determined in an ISO (1980) calibration rig; based on combined errors, the uncertainty in flow sensor data sets per group of sensors.

	at 90% of full scale flow		at 25% of full scale flow		uncertainty in data sets (based on calibration results)	
# flow sensor	test 1 [%]	test 2 [%]	test 1 [%]	test 2 [%]	bias [%]	random error [%]
sensor 1	-0.07	-0.01	0.06	0.08	0.02	±0.13
sensor 2	0.02	-0.03	0.12	-0.03		
sensor 3	0.10	0.09	0.13	0.23		
sensor 4	-0.00	0.01	0.03	-0.10	0.09	±0.21
sensor 5	0.04	-0.03	0.12	0.07		
sensor 6	0.07	0.13	0.34	0.18		
sensor 7	0.02	0.22	0.17	0.08		
sensor 8	-0.04	0.07	0.19	0.08	0.10	±0.22
sensor 9	-0.12	0.09	0.03	0.05		

After installation of the sensors in 1998 no additional wet calibrations have taken place (i.e. the sensors have not been removed from their installations in the influent pumping station to be tested in a test rig). The result of comparable electromagnetic flow sensors that have been in operation over a prolonged period of time (~ 10 years) generally show an increase in bias whereas random errors hardly change (Pothof, 2010). For lack of test results, however, the magnitudes of these biases of flow sensors in the influent pumping station are unknown and cannot be corrected for. The results of annual *verifications* of signal translation in the flow sensors (from artificially induced voltage signal to resulting mA output signal, i.e. a partial "dry calibration") show no deterioration of signal translation.

Uncertainty in Q_{OPEN}

The values of Q_{OPEN} are based on Q/h-relations as presented in appendix F as well as on measurements of water levels in the influent chambers of Riool-Zuid and Eindhoven Stad. Consequently, the uncertainty in calculated values of Q_{OPEN} is a combination of the uncertainty in the level measurements and the uncertainty in the calibration function between Q and h. Clemens (2001) shows that for overflow weirs typical uncertainty (95% confidence range) for flow values derived with a well-established calibration function can add to ±5%. For the weir in the wwtp Eindhoven influent pumping station, however, no combination of level and flow measurements over the weir are available (no pairs of Q/h values). Therefore, neither calibration function nor its associated uncertainty can be estimated and 'standard' Q/h-relations are used instead, see appendix F. In an extensive testing procedure Bos and Kruger - van der Griendt (2007) show that these 'standard' equations result in only small deviations from the actual Q/h-relations for a number of tested weirs. It is therefore assumed that using standardized Q/h-equations for the calculation of Q_{OPEN} results in uncertainty bands that are larger than the aforementioned typical values, but to a limited extent. The uncertainty of values for Q_{OPEN} is estimated at ±10%.

Summation of data sets: combining uncertainties

As illustrated in Figure 4-12 values for Q_{ES} are obtained by summing the data sets of sensors 3 through 6 and Q_{OPEN}. Assuming no interdependencies exist among sensor data sets as well as between sensor data sets and Q_{OPEN}, the application of the law of propagation of uncertainty on equation 4.2 yields the following uncertainty for the combined data set:

$$\sigma^2_{Q_{ES}} = \sigma^2_{Q_{sensor\,3}} + \sigma^2_{Q_{sensor\,4}} + \sigma^2_{Q_{sensor\,5}} + \sigma^2_{Q_{sensor\,6}} + \sigma^2_{Q_{OPEN}} \qquad (4.6)$$

Considering the equation it can be observed that the uncertainty in Q_{ES} strongly depends on the number of pumps in operation and whether or not inter-chamber

flow is present, see Table 4-5. For normal dry weather situations with only a single pump running, the uncertainty in Q_{ES} is relatively small and equal to the uncertainty of the associated flow sensor. For wet weather situations with multiple pumps running simultaneously, the uncertainty in Q_{ES} is multiplied by the number of pumps in operation, but remains relatively small. In case $Q_{OPEN} \neq 0$ (which is the case for approximately 40 storm events during the 19 months time-span, or roughly 1.5% of the total data set) the relatively large uncertainty in Q_{OPEN} becomes dominant in equation 4.5, yielding an uncertainty in Q_{ES} values of the same order of magnitude. Thus, with the onset of inter-chamber flow the uncertainty in Q_{ES} values (and hence in Q_{RZ} values as well) shifts from ~0.5% to ~11%. For catchment area Nuenen/Son no such shift is present for lack of inter-chamber flow.

Table 4-5: Uncertainties associated with the areal inflow time-series of catchment area Eindhoven Stad and percentage of the data set for which the uncertainty applies.

operation	uncertainty	share of Q_{ES} data set
1 pump	~0.2%	66%
2 pumps	~0.4%	22%
3 pumps	~0.6%	7%
4 pumps	~0.8%	3%
$Q_{OPEN} > 0$	~10%	1.5%

4.5 Conclusions

In this chapter three time-series have been derived that represent the inflow of wastewater from catchment areas Riool-Zuid (Q_{RZ}), Eindhoven Stad (Q_{ES}) and Nuenen/Son (Q_{NS}) into the wwtp Eindhoven. The data sets of nine flow sensors in the discharge lines of the influent pumps at the wwtp Eindhoven form the basis for the calculation. All subsequent data modifications aim at combining and altering the data such that the resulting time-series represent areal inflow as accurately and as realistically as possible.

The raw data sets are of relatively good quality: only a small number of data errors such as data gaps, “zero”-values and values outside the sensor ranges were found. All flow sensor data sets have been corrected for non-zero baselines (i.e. non-zero values for non-operational pumps). With these corrections the total sum the data sets have been reduced by between 0.8% and 5.2%.

The validated flow sensor data sets have been combined to calculate the three areal inflow time-series. The contribution of pump 6 to either Q_{RZ} or Q_{ES} has been determined based on the interpretation of flow data. The inter-chamber flow between the influent chambers of Riool-Zuid and Eindhoven Stad has been derived

and incorporated in the calculation of Q_{RZ} and Q_{ES}. After summation of the flow sensor data sets, the areal inflow time-series have been considered for discrepancies between pump behavior and 'expected' areal inflow patterns. Discrepancies are due to high-frequent on/off switching of individual pumps, large variations in pump speeds during wet weather flow, and the prolonged non-operation of pumps. Only for the last data anomaly all data have been removed from the data sets; for the first two anomalies the data cannot be used for analyses considering time-spans shorter than the observed anomaly.

The uncertainties in the areal inflow data sets have been considered. Influencing parameters are the observed uncertainty of the raw flow sensor data sets, the number of operational pumps and possible inter-chamber flow. In case inter-chamber flow occurs, the uncertainty largely increases from ~0.5% to an estimated ~11%.

The resulting wastewater quantity time-series, in combination with the wastewater quality time-series derived in chapter 5, are used for pollution load calculations in chapter 6.

Chapter 5. Water quality monitoring

5.1 Introduction

In the previous chapter wastewater *quantity* data sets have been studied that have been generated by flow sensors at the wwtp Eindhoven influent pumping station. In this chapter wastewater *quality* data sets are studied that have been generated in the same influent pumping station. In chapter 6 both types of data sets are combined to derive wastewater pollutant loads arriving at the wwtp.

In analogy to the objective of chapter 4, the objective of this chapter is to derive time-series that represent - as accurately as possible and with an uncertainty estimate - the *quality* of wastewater that arrives at the wwtp Eindhoven originating from the three contributing catchment areas. For the WDD monitoring campaign various water quality sensors have been installed at a number of locations (see appendix A). In this chapter, the focus is on three quality parameters (TSS, COD and CODf) all measured by one sensor type (UV/VIS spectrometer) at one location (wwtp Eindhoven influent pumping station) in three different inflows of wastewater to the wwtp (Riool-Zuid, Eindhoven Stad and Nuenen/Son). Hence, a total of nine wastewater quality time-series are considered in the chapter. The selected quality parameters are among the most frequently used parameters to characterize the quality of wastewater. The parameter TSS (total suspended solids) describes the particulate content of the water, total COD (chemical oxygen demand) is a measure for oxygen consumption related to the presence of organic matter in the water and filtered or soluble COD (CODf) presents the same for wastewater after filtration over a 0.45 μm filter.

Paragraph 5.2 presents the sensor type as well as the monitoring set-up that have been used for wastewater quality monitoring. The focus is on the monitoring principle and the lay-out of the constructed by-pass installations. Local calibration of the UV/VIS sensors is the topic of paragraph 5.3. Firstly, section 5.3.1 presents the selected method of calibration as well as a pre-selection of wastewater matrices used in the calibration procedure. Secondly, sections 5.3.2 and 5.3.3 focus on the results of, respectively, dry and wet weather sampling campaigns that have generated references samples for the local calibration. The actual calibration procedure is described in section 5.3.4. Based on calibration results, an uncertainty estimate for each parameter time-series can be calculated. The method of calculation is illustrated in section 5.3.5. Finally, paragraph 5.4 focuses on the quality assessment of the UV/VIS data sets. Erroneous data due to a variety of error mechanisms have been detected and removed from the data sets.

5.2 Sensors and monitoring set-up

This paragraph successively presents a description of the UV/VIS spectrophotometer and its monitoring principle (section 5.2.1), the by-pass installations in which the UV/VIS sensors have been installed (section 5.2.2.) and the characteristics of the data sets generated by the spectrophotometers (section 5.2.3).

5.2.1 UV/VIS sensors

The applied sensors for wastewater quality monitoring are in-situ UV/VIS spectrometers (type spectro::lyser by manufacturer s::can, Austria). The sensor, its measuring principle, its method of calibration and its practical applications have been extensively documented in Langergraber *et al.* (2003, 2004), Hochedlinger (2005) and Gruber *et al.* (2006). The following description is largely based on these sources.

The spectrometer is a probe measuring 44 mm in diameter and roughly 0.6 m in length. It is submersible and can hence be installed directly in the wastewater. In the mid-section of the sensor, an opening ('envelope') perpendicular to the longitudinal axis of the probe is provided where measurements take place, see Figure 5-1. On one side of the envelope a 2-beam 256 pixel xenon flash lamp serves as the light source for the optical measurements. On the other side of the opening detectors are installed to measure the incident light. The measuring beam is transmitted through the opening, hence passing the targeted wastewater; the other beam is a reference beam and remains within the sensor. As a result of this configuration, the difference in incident light from both beams is only due to the passage through the wastewater accounting for ageing of the light source. The width of the opening ('optical path length') of the used sensors is 2 mm. The lenses on both sides of the opening are cleaned by means of an automated pressurized air system. Every 2 minutes for the duration of 15 seconds, air is blown through nozzles into the envelope and along the lenses removing pollutants that have attached to the lenses or larger particles that are stuck in the opening.

The xenon light source emits light in the ultraviolet (UV) and visible (VIS) range with wavelengths ranging from 200 nm up to 750 nm. Each light signal that is emitted into the wastewater suffers from gradual attenuation that is the result of absorption and scattering of light by constituents in the wastewater. The absorbance is wavelength dependent and is recorded by the sensor with a resolution of 2.5 nm. The measurement principle of the UV/VIS sensor is based on the correlation between on one hand the absorbance of light at certain wavelengths and on the other hand pollutant concentrations in the wastewater. These relations are

extensively documented in Perkampus (1992). In this thesis only the parameters TSS, COD and CODf are considered.

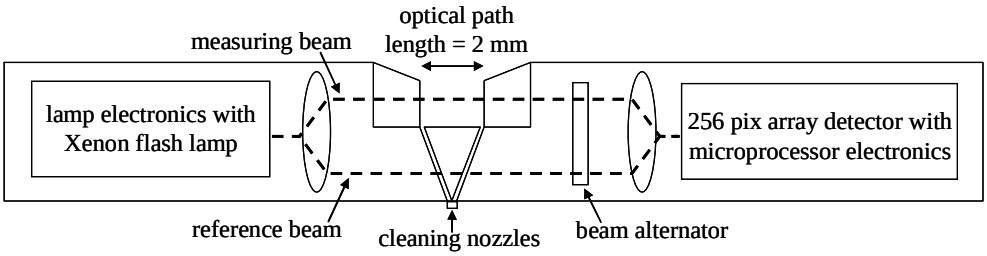

Figure 5-1: Cross-section of UV/VIS spectrometer with principle of operation (after Langergraber *et al.*, 2003)

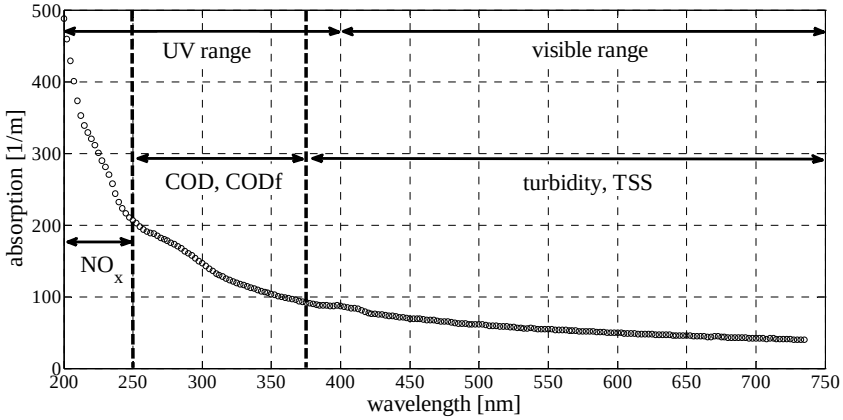

Figure 5-2: Typical absorbance spectrum of wastewater (example from the Eindhoven area) with wavelength ranges associated with NO_x (200-250 nm in the UV range), organic compounds (such as the aggregate parameters COD and CODf: 250-380 nm) and turbidity (380-750 nm, predominantly in the visible light range) (after Rieger *et al.*, 2004)

Figure 5-2 shows an example of a measured absorbance spectrum of wastewater from the Eindhoven area. Absorbencies in the range 200 - 250 nm in the UV spectrum can be used for the determination of nitrite and nitrate (NO_x), the concentration values of organic substances (such as the aggregate parameters COD and CODf) are associated with results in the 250 - 380 nm range and results in the visible range (~ 400 - 750 nm) are used for the derivation of TSS values. Pollutant parameter concentrations are calculated using the absorption values at a number of wavelengths, using a weighing factor per wavelength and an overall off-set factor:

$$c_{eq} = \sum_{i=1}^{n} \left(w_i A_{\lambda i} \right) + K \qquad (5.1)$$

with c_{eq} = equivalent pollutant concentration [mg/L];
n = number of wavelengths used [-];
$A_{\lambda i}$ = absorbance at wavelength λ_i [m^{-1}];
w_i = weighing factor [m·mg/L];
K = off-set factor [mg/L].

The suffix -eq indicates that the calculated concentration value is an equivalent value based on optical measurements and not the result of a 'standard' laboratory analysis. A calibration set describes which wavelengths to include in the calculation as well as the values of weighing and off-set factors.

The relation between wastewater pollutants and absorbance spectra is wastewater and condition specific. Upon purchase, all sensors are provided with a manufacturer calibration set ('global calibration'): a set of calibration parameters that relate absorbencies to pollutant parameters for a 'typical' municipal wastewater composition. For applications that require high precision (such as treatment plant control), the global calibration often delivers sufficient results (Langergraber *et al.*, 2003). The matrix or composition of wastewater can (and often does) deviate from this 'mean' set of values and can change depending on, among others, the relative mix of domestic and industrial wastes and the social-economic profile of the community. For instance, the type of food consumed and the availability and composition of drinking water are among the factors that affect the composition (and hence the matrix) of domestic wastewater (Pons *et al.*, 2004). To account for the deviating matrix (with respect to the global matrix) and to thus enhance the accuracy of results, a calibration to local wastewater circumstances ('local calibration') is required. The local calibration of the UV/VIS sensors in the influent pumping station of the wwtp Eindhoven is described in paragraph 5.3.

5.2.2 Monitoring set-up

In the search for appropriate monitoring locations and well-functioning monitoring station designs, a number of different set-ups have been tried. In fact, the monitoring set-up that is presented in this section and that has been used during collection of the data sets studied in this chapter, is the third applied design. Two earlier designs have been rejected for a variety of reasons. Appendix G presents the design process, the rejected designs and the reasons for rejection.

Each UV/VIS sensor has been installed in its own by-pass installation. Each by-pass is fed by a pump that is positioned in the pump suction chambers of the influent pumping station, see Figure 5-3. Figure 5-4 provides a longitudinal profile of the pumping station showing the location of the by-pass pumps. The pumps are suspended from the ceiling of the chamber by means of steel chains. The suction mouths of the pumps are located at a height of approximately 0.6 m from the chamber floor, which is - for normal DWF situations and for the parameter TSS - in accordance with ISO (1992a) that recommends a sampling height of one third of the water level to obtain a value representative of the solids present within the flow. As the pump can rotate freely around its point of suspension, the elevation height slightly changes with an increased drag force for larger flows. Researching possible concentration gradients over a cross-sectional area, Larrarte (2008) concludes that using a one-point sampler (such as the used pumps) yields good results that are representative of the mean concentration over the cross-section. Flexible supply pipes (ø 6cm) transport the wastewater to the by-pass installations.

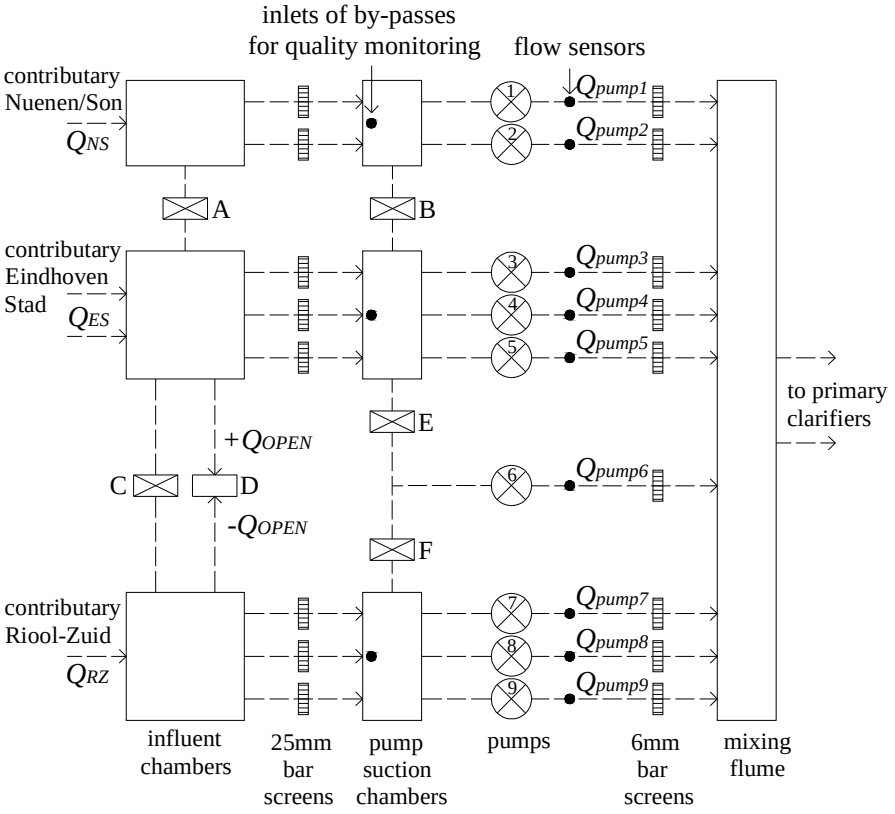

Figure 5-3: Schematic lay-out of the influent pumping station at the wwtp Eindhoven. Pumps installed in the three pump suction chambers feed the by-pass installations.

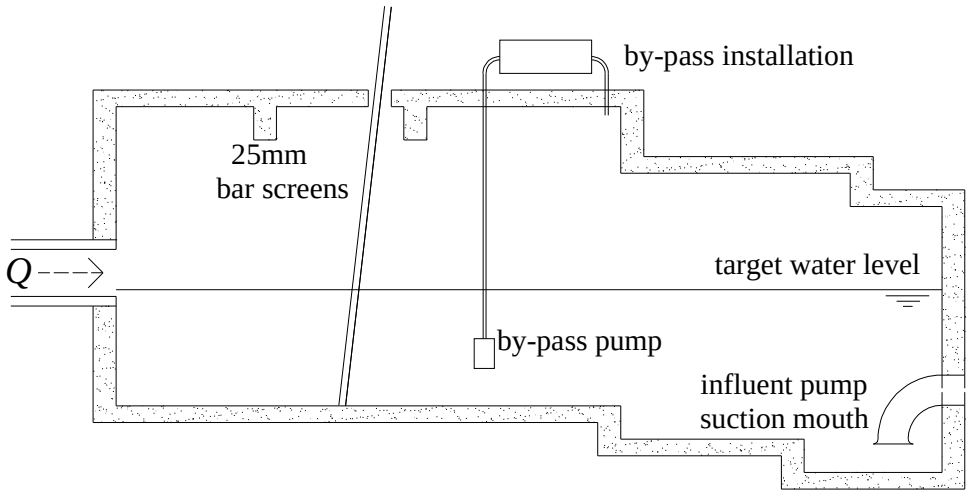

Figure 5-4: Longitudinal profile of the influent pumping station (not on scale) showing the location of the by-pass pumps and installation holding the UV/VIS sensors.

Each by-pass installation consists of two measurement vessels in series, see Figure 5-5. Each vessel is fed with wastewater near the bottom of the vessel and the outflows are designed as overflow constructions near the top of the vessel. This way, short-circuit flows that would leave the sensor in stagnant water are prevented. The vessels have a diameter of 0.75 m with a water column of ~0.50 m between inflow and outflow level. Holding a total of approximately 0.35 m^3, the retention time of each vessel is one minute. In the first vessel the UV/VIS sensor is installed half way between the inflow and outflow levels. The second vessel allows for additional sensors. For instance, in the second vessel of the by-pass installation for inflow Eindhoven Stad an ammonium sensor is installed, see Figure 5-5.

The presented set-up has an important drawback: sediment gathers on the bottom of the vessels. The flow velocity in the vessels is too low to transport all coarse particles in the wastewater to the outflow level, resulting in the gradual build-up of a sediment layer on the bottom of the vessel, see Figure 5-6. This is unwanted since velocity variations in the supply pipes might cause resuspension of particles, leading to higher levels of suspended solids in the measurement vessel than in the targeted wastewater. Such velocity variations could be the result of water level variations in the pump suction chambers with wet weather conditions. To reduce peaks in particulate matter due to this phenomenon, vessels have been cleaned once per week, each time removing all sediment from the vessels. Despite this stringent cleaning strategy, sediment layers have frequently been observed. Hence, it cannot be ruled out that resuspension of sediment in the vessels has influenced some of the measurements. To annul this error source from future measurements, a fourth

monitoring set-up has been implemented in 2010 (hence, *after* the collection of data sets presented in this chapter) replacing the vessels with rectangular flumes and providing means to prevent sedimentation of particles in the flumes. Details of all designs can be found in appendix G.

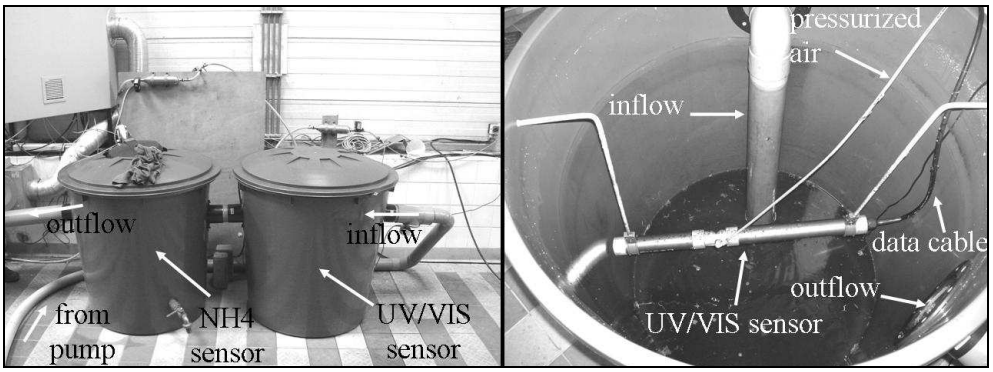

Figure 5-5: (left picture) by-pass installation for inflow Eindhoven Stad with two measurement vessels; (right picture) inside the first vessel the UV/VIS sensor is installed

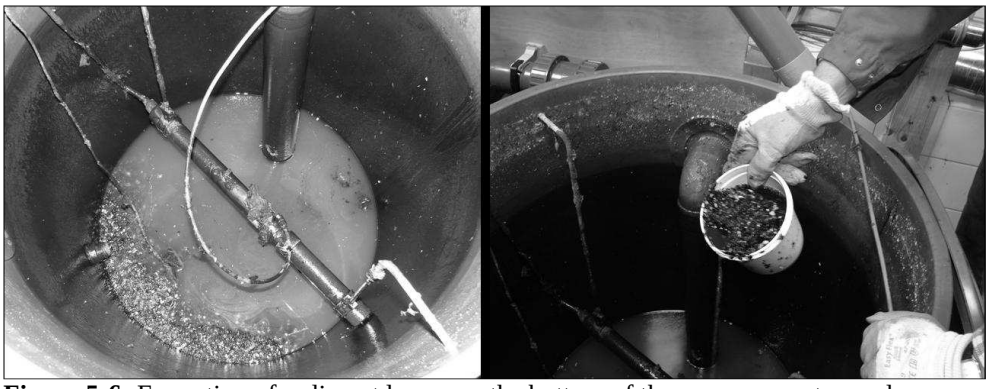

Figure 5-6: Formation of sediment layers on the bottom of the measurement vessel

Monitoring wastewater in a pump-fed by-pass installation comes at the risk of altering the wastewater composition due to the passage of the wastewater through the pump. Hochedlinger *et al.* (2005) have observed “no loss of solids” when using a peristaltic pump to feed a sampler installation (hypothesizing that large particles may be underrepresented in the samples due to a larger inertia). The pumps used in the wwtp Eindhoven pumping station, however, are of the shredding type. The shredder aims at grinding materials that could block the suction mouth, hence possibly influencing the composition of the water. Since no comparative sampling has been performed (simultaneous sampling directly from the wwtp influent

chambers and from the measurement vessels) any influence of the shredding pump on the wastewater composition is unknown. The wastewater in the measurement vessels is assumed to be identical to the targeted wastewater in the wwtp influent chambers.

5.2.3 Data sets

UV/VIS sensors produce two types of data files. Fingerprint (.fp) files contain the measured light absorbance [m^{-1}] per time step and per wavelength. Emitting 221 different wavelengths, fingerprint files contain the same number of values per time-step. Parameter files (.par) contain the user-selected pollutant parameter concentration values [mg/L], in this thesis TSS_{eq}, COD_{eq} and $CODf_{eq}$. These are derived from the fingerprint files using the calibration set. Parameter files contain one concentration value per parameter per time-step.

The three UV/VIS sensors at the wwtp Eindhoven influent pumping station have yielded data for the full 19-month time-span considered in this thesis (April 1st, 2007 - November 1st, 2008). The data files consist of equidistant, 2-minute interval data. A 2-minute monitoring interval was selected to allow the sensor sufficient time for the automated cleaning procedure. With a 1-minute monitoring interval it could not be ruled out that remnants of the air-cleaning are still present in the measuring envelope (in the form of air bubbles that get stuck near the lenses).

Each parameter file contains 417,600 entries per pollutant parameter, making a total of 1.25 million data points per UV/VIS sensor for the 19-month time-span. With 3 three installed sensors this adds to a total of nearly 3.8 million water quality data points.

Data sets have been transferred to a central data server by means of the data communication and storage system as described earlier in paragraph 3.2. This means that all data sets are synchronous to UTC time and can be compared using the same time axis.

5.3 Local calibration of UV/VIS sensors

This paragraph successively presents the selection of a method for the local calibration of the UV/VIS photospectrometers as well as calibration matrix considerations (section 5.3.1), the results of a dry weather flow sampling campaign (section 5.3.2.), the results of a wet weather flow sampling campaign (section 5.3.3), the applied procedure for the actual local calibration (section 5.3.4) and the

calculation of an uncertainty estimate for each parameter time-series based on calibration results (section 5.3.5).

5.3.1 Selection of method and matrices for local calibration

Prior to calibration of UV/VIS sensors two choices need to be made. First, the method of calibration must be selected. Second, a (preliminary) decision must be made for which wastewater matrices separate calibration sets are to be derived. Hereafter both aspects are discussed.

Method of calibration
The UV/VIS sensors calculate pollutant parameter concentrations using the absorption values at a number of wavelengths, applying a weighing factor per used wavelength and an overall off-set factor:

$$c_{eq} = \sum_{i=1}^{n} \left(w_i A_{\lambda i} \right) + K \qquad (5.2)$$

with c_{eq} = equivalent pollutant concentration [mg/L];
n = number of wavelengths used [-];
$A_{\lambda i}$ = absorbance at wavelength λ_i [m^{-1}];
w_i = weighing factor [m·mg/L];
K = off-set factor [mg/L].

The manufacturer global calibration set describes which wavelengths to include in the calculation as well as the values of weighing and off-set factors.

The objective of a local calibration is to minimize the error between on one hand sensor values of the targeted wastewater (as generated based on the global calibration set) and on the other hand the results of laboratory analysis of reference samples of the same wastewater. In essence, this minimization problem can be solved using two distinct approaches:

(1) use the raw absorbance values to derive an improved set of calibration parameters (with respect to the global calibration set) specifying which (possibly different set of) wavelengths to include in the calculation as well as the values of (possibly different) weighing and off-set factors;
(2) use the equivalent pollutant concentration values as calculated with the global calibration set and construct a polynomial function between these and the laboratory measurement results.

Langergraber *et al.* (2003) describe a procedure for the first type approach. Their method consists of an initial plausibility check of spectra after which the approved spectra are corrected for turbidity. This correction is done by curve fitting based on the relation between scattering intensity on one hand and wavelength and particle diameter on the other hand as described by Huber and Frost (1998). Subsequently, outliers in the laboratory reference values are detected and removed. The actual improved local calibration set is obtained using a PLS (Partial Least Squares) technique. A local calibration using this first type approach yields better results (in terms of residuals between sensor and laboratory values) than the second type approach or than using an unaltered global calibration set (Hochedlinger, 2005; Torres and Bertrand-Krajewski, 2008). However, the application of the first type approach is hampered by the lack of detailed information on the calibration process provided in the manufacturer's documentation. As a result, the global calibration results cannot be easily reproduced and improvement of the calibration set requires the (resources-intensive) development of a proper calibration procedure. Such an alternative method (also using PLS regression) is presented by Torres and Bertrand-Krajewski (2008).

The second calibration approach has been used in this thesis. The approach constitutes the straightforward construction of a relation between equivalent pollutant concentrations (as yielded by the UV/VIS sensors based on the global calibration set) and the laboratory reference values. Details of the method as well as the application on the results of the three UV/VIS sensors can be found in section 5.3.4.

Matrix considerations

The manufacturer global calibration set comprises a set of calibration parameters that relate absorbencies to pollutant parameters for a 'typical' municipal wastewater composition or matrix. The matrices of wastewater from catchment areas Riool-Zuid, Eindhoven Stad and Nuenen/Son, however, deviate from this 'default' type of wastewater. Local calibration aims at adjusting sensor values such that they better represent the areal wastewater matrices. These areal matrices are not static entities but change with different circumstances in the wastewater system. The circumstances during which grab samples have been collected that are used to generate reference values in the local calibration procedure, determine for which wastewater matrix the calibration set is valid.

For typical municipal wastewater, a matrix change is often observed with the transition from dry weather flow to wet weather flow. Examples in literature show different local calibration sets for DWF conditions and for WWF conditions (Hochedlinger, 2005; Gruber *et al.*, 2006; Torres and Bertrand-Krajewski, 2008). Even within a set of observations that are all associated with DWF conditions, matrix differences can be present. For instance Gruber *et al.* (2006) and Maribas *et*

al. (2008) report a matrix change between dry weather *day* flow and dry weather *night* flow that is attributed to the change of the relative contribution of infiltration water to total wastewater flow. Also for wet weather flow conditions there is no single matrix that can be associated with all storm events. Stumwöhrer *et al*. (2003) show that WWF calibration sets based on information from one particular storm event lead to erroneous results for a different storm event. This is attributed to the - sometimes large - variation of composition of the wastewater/stormwater mix depending on parameters such as length of the antecedent dry weather period and the maximum storm intensity. The introduction of industrial discharges in the wastewater can also influence the wastewater matrix significantly. Maribas *et al.* (2008) show that rapid composition changes due to the insertion of (highly polluted) reject waters at a wwtp cause difficulties in establishing a consistent calibration set.

For practical applications, the extent to which matrix variations can be taken into account during the local calibration process is often determined by budget constraints. With each additional local calibration set the UV/VIS sensor will be able to more accurately represent pollutant concentrations for a wider variety of circumstances (i.e. for more distinct wastewater matrices). For each additional set, however, reference samples must be gathered for those specific circumstances requiring a costly collection of representative grab samples and ditto proper laboratory analysis. As a result, with an increasing number of wastewater matrices to be studied, the effort and costs of calibration also increase.

For this thesis, it was assumed that the most important matrix change occurs in the transition from dry to wet weather conditions. Therefore, it was decided to perform sampling campaigns for both situations. The details and results of the sampling campaigns can be found in the next two sections. The results of the sampling campaigns suggest that other matrix changes also occur in the three inflows to the wwtp Eindhoven. The decision for which matrices separate local calibration sets are derived is discussed in section 5.3.4.

5.3.2 Dry weather sampling campaign

The main objective of the sampling campaign is to obtain laboratory reference values that correctly represent the considered DWF matrix, for all three parameters (TSS, COD and CODf) and for all three wastewater flows (RZ, ES and NS). Any samples not correctly representing the targeted wastewater are to be removed from the data set with laboratory reference values to prevent an erroneous calibration set. The results of samples associated with clear indications of erroneous laboratory analysis (e.g. observed non-compliance with procedures during the laboratory work) have been immediately removed from the data sets before presentation in this section. All other results are presented, but are further assessed for quality.

Consequently, additional samples have been excluded from the calibration procedure for suspicion of misrepresentation of the targeted wastewater.

In analogy to examples found in literature (Hochedlinger, 2005; Gruber *et al.*, 2006), it was decided to perform a dry weather sampling campaign taking one wastewater sample per wwtp inflow and per hour over a time-span of 24 hours. This way, the typical range of pollutant concentrations for a normal dry weather day is likely to be represented in the local calibration reference set. The DWF campaign took place the 10th and 11th of June, 2008 from noon till noon. The last recorded rainfall in the Eindhoven area was on June 5th, 2008 (~ 3 mm), allowing for 4 days without precipitation prior to sampling. Hence, conditions for normal dry weather situations as described in section 6.2.1 have been fulfilled.

Figure 5-7: (left picture) taking a grab sample from a measurement vessel holding a UV/VIS sensor; (right picture) samples from inflows Riool-Zuid, Eindhoven Stad and Nuenen/Son at the magnetic stirrer ready for laboratory analysis (at the far end, samples from a fourth location 'tussengemaal', results of which are not presented in this thesis)

To sample the same wastewater as observed by the sensors, grab samples were taken directly from the vessels containing the UV/VIS sensors in the by-pass installation, see Figure 5-7. Samples were immediately transported to the dedicated laboratory next to the wwtp influent pumping station. Upon arrival, samples were directly analyzed for the parameters TSS, COD and CODf. Since the laboratory was in operation for the full time-spans of both the DWF and WWF sampling campaigns, all samples have been directly processed (maximum delay between sample collection and start of the analysis ≈ 10 minutes) and no sample preservation has been needed. Samples have been analyzed for total suspended solids (TSS_{lab}) using filtration over 0.45 μm glass-fiber disk filters in a vacuum set-up and subsequent filter drying at 103°C-105°C (procedure 2540D in Standard

Methods, 1998). Analyses for COD_{lab} have used the colorimetric method (procedure 5220D, using the Merck Nova60 photospectrometer with cell test 14541). For $CODf_{lab}$ analyses, samples have first been filtered using 0.45 μm filters, after which the same cell test as for COD_{lab} has been applied on the filtrate.

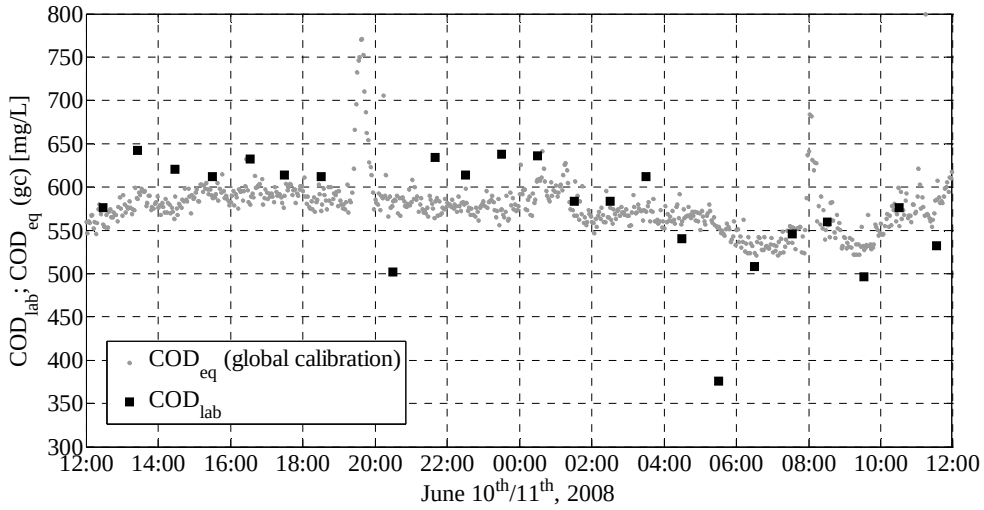

Figure 5-8: Results of DWF sampling campaign: COD_{eq} (as measured by the UV/VIS sensor at a 2-minutes interval, global calibration) versus COD_{lab} (1 grab sample per hour) for wastewater from catchment area Eindhoven Stad. The results of grab samples taken at 19h30 (non-existent), 20h30 (unrepresentative sample) and 05h30 (wrong lab analysis) have been excluded from use in the local calibration.

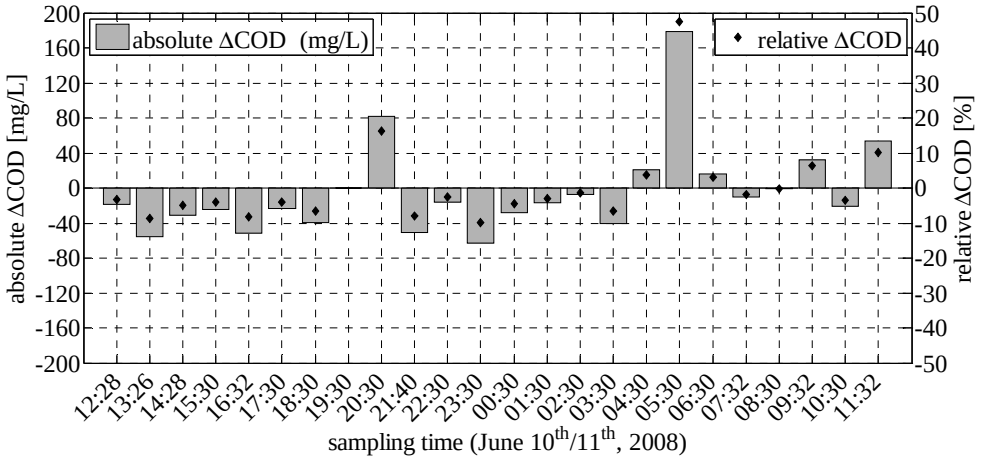

Figure 5-9: Absolute (COD_{eq} - COD_{lab}, left axis) and relative (with respect to COD_{lab}, right axis) differences between COD results as presented in Figure 5-8.

All results of the dry weather sampling campaign are presented in appendix H. Hereafter, some exemplary results of the dry weather campaign are presented and discussed.

The results for parameter COD for wastewater from inflow Eindhoven Stad are presented in Figure 5-8 and Figure 5-9. Except for the samples taken at 20h30 and 05h30 the laboratory analyses remain within a limited range around the UV/VIS sensor results: absolute differences remain within ±60 mg/L, relative differences within ±10%. The small 05h30 COD_{lab} value is likely due to an erroneous laboratory analysis (however unnoticed during the laboratory work) and is therefore not used as reference value in the local calibration. Also, the laboratory result of the 20h30 sample is inconsistent compared to directly neighboring results. The same inconsistency for the TSS_{lab} result of the same sample (see figure H-7 in appendix H) suggests that - due to an unknown cause - the grab sample itself misrepresents the wastewater as observed by the UV/VIS sensor. Also this result is excluded from the local calibration process. Finally, at 19h30 no grab sample was taken from inflow Eindhoven Stad due to problems with the by-pass installation. The other 21 sampling results are considered fit to be used as reference values in the local calibration for the DWF matrix of inflow Eindhoven Stad.

For catchment area Riool-Zuid a daily recurring large peak in pollutant concentrations can be observed around noon lasting for approximately one hour; see Figure 5-10 for the example of TSS values. The peak is due to the arrival of an amount of highly polluted reject water from the sludge processing installation of the wwtp (for details, see section 6.2.3). The TSS_{lab} value of the 11h32 sample collected during the peak has a relatively large absolute difference of 90 mg/L with the sensor value, but the relative difference is on the same order as for several other samples collected during the 24-hour time-span (not shown here, see figure H-2 in appendix H). Possibly, considering Maribas *et al.* (2008), a matrix change occurs with the arrival of the reject water, which would require a different local calibration set for the duration of the peak. However, since only one sample has been collected during the peak, insufficient data is available to fully appreciate the necessity of a separate calibration set as well as to derive such a ‘peak’ DWF calibration set. The result of the 11h32 sample has therefore been included in the ‘mean’ DWF calibration set.

For catchment area Nuenen/Son a possible matrix effect can be observed between day and night conditions, see Figure 5-11. For this catchment area low flows (associated with the night minimum) arrive at the treatment plant between 05h00 and 09h00. During this time-span, absolute differences between TSS_{eq} and TSS_{lab} values become increasingly large, perhaps owing to a wastewater matrix change due to the (known) relatively large contribution of industrial discharges in night flow from this catchment area. Again, since only few samples have been collected

during the time-span, insufficient data is available to fully appreciate the necessity of a separate calibration set. As a result, all results have been included in a 'mean' DWF calibration set.

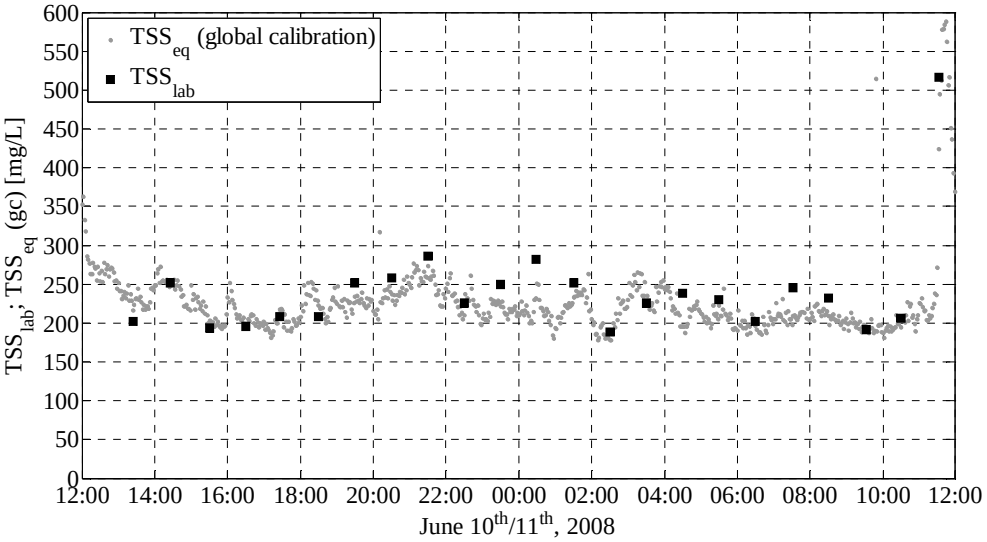

Figure 5-10: Results of DWF sampling campaign: TSS_{eq} versus TSS_{lab} for wastewater from catchment area Riool-Zuid. Despite a possible matrix change, the 11h32 sample has been included in the DWF calibration procedure.

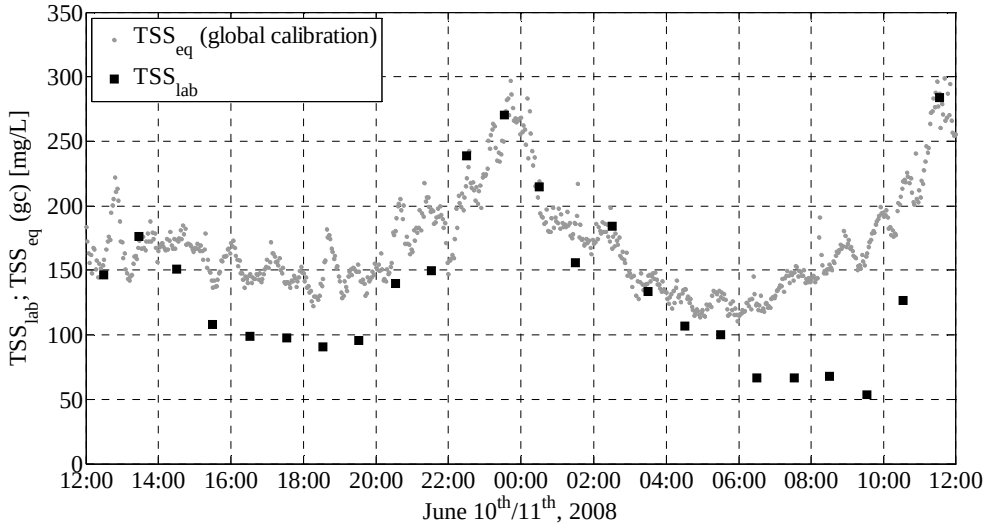

Figure 5-11: Results of DWF sampling campaign: TSS_{eq} versus TSS_{lab} for wastewater from catchment area Nuenen/Son.

During the dry weather sampling campaign, the wrong filter membrane material has been used for the filtering procedure prior to the $CODf_{lab}$ analysis. Instead of using filters with polyethersulfone membranes, cellulose acetate membranes have been used resulting in a significant increase of $CODf_{lab}$ values. Since the magnitude of the increase depends on the (unknown and varying) contact time between filter and filtrate, no correction is possible. As a result, none of the $CODf_{lab}$ values determined during the DWF sampling campaign can be used for the local calibration of the UV/VIS sensors. To nevertheless be able to compare $CODf_{eq}$ with $CODf_{lab}$ values under dry weather conditions, it was decided to start the WWF sampling campaign a few hours earlier than necessary to obtain a (limited) number of results for dry weather flow conditions.

5.3.3 Wet weather sampling campaign

A wet weather sampling campaign was performed on September 12th, 2008. A storm event (~16 mm) has been recorded on that day between 11h00 and 19h00, leading to large increases in Q_{RZ}, Q_{ES} and Q_{NS}; see Figure 5-12 for the example of Q_{RZ}. Around 12h00 flow values start deviating from mean DWF values, the pattern of which can be observed in the preceding dry weather days. After the large storm event, the recovery to dry weather flow is interrupted by a subsequent smaller storm event (~2 mm) on September 13th, after which flow values return to typical dry weather values in the early hours of September 14th.

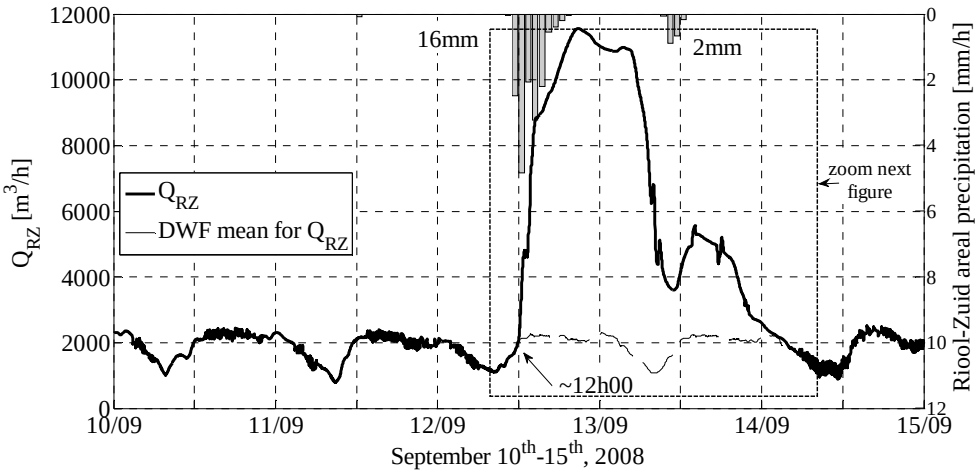

Figure 5-12: Overview of wwtp inflow from catchment area Riool-Zuid during the September 12th and 13th, 2008 storm events. On September 12th after 12h00 Q_{RZ} starts deviating from mean DWF flow.

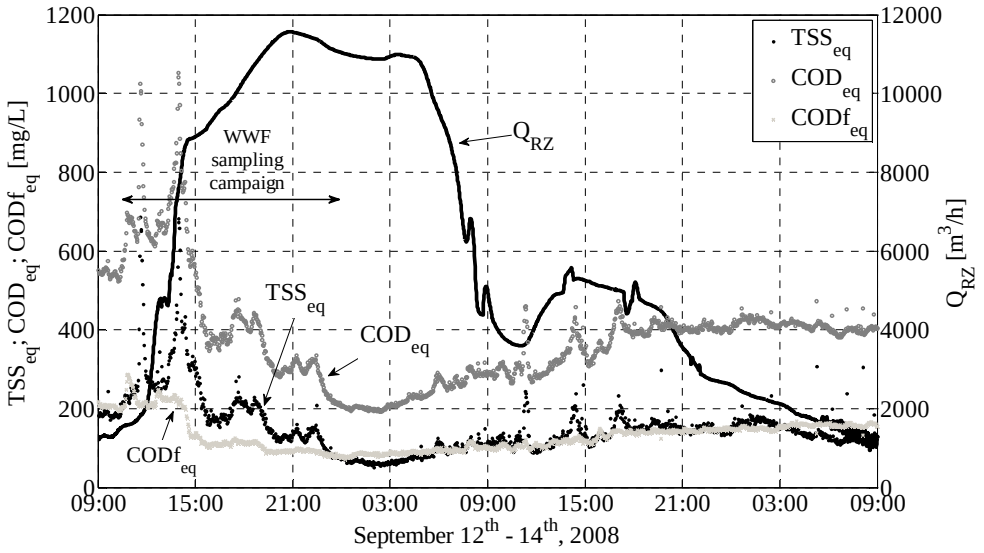

Figure 5-13: Overview of behavior of Q_{RZ} and UV/VIS parameters during the storm events on September 12th and 13th, 2008. Samples for the WWF campaign have been taken during the first 12 hours of the storm event.

The behavior of pollution parameter concentrations during the storm events can be found in Figure 5-13 for the same example of Riool-Zuid. A typical initial peak in TSS_{eq} and COD_{eq} concentrations can be observed between 13h00 and 15h00 (the earlier peak around 12h00 is the daily recurring DWF peak for catchment area Riool-Zuid) after which all three parameters dilute by a factor 2 to 3. Minimum concentration values are reached early on September 13th. Subsequently, pollutant concentrations slowly recover towards DWF values.

For the WWF sampling campaign, per inflow a total of 14 grab samples have been collected between 10h00 and 23h00 (one sample per hour). Assuming dry weather conditions until the moment flow starts deviating from mean DWF values (as presented in Figure 5-12), the samples taken around 10h00 and 11h00 are assumed to be associated with DWF. The 12h00 sample has been collected during the transition from DWF to WWF and is therefore associated with neither flow condition. All samples taken from 13h00 onwards are assumed to be associated with wet weather flow conditions. As a result, a maximum of 11 reference samples are available for local calibration during WWF conditions.

All results of the wet weather flow sampling campaign can be found in appendix J. Hereafter, some exemplary results of the WWF sampling campaign are presented and discussed.

Results for parameter TSS for wastewater from inflow Eindhoven Stad are presented in Figure 5-14. Between 12h00 and 15h00 an initial peak in TSS_{eq} values can be observed, directly following the flow increase around 11h30 (see figure J-10 in appendix J). After 15h00, TSS_{eq} values are diluted to approximately 100 mg/L. Comparing TSS_{eq} to TSS_{lab} values it can be seen that during the initial peak the sensor *under*estimates TSS values. Then, when the wastewater starts diluting, the sensor tends to *over*estimate values. This pattern is typical sensor behavior under WWF conditions for all three inflows and for both TSS and COD values: a (large) underestimation of values for the few samples collected during the initial concentration peak and a subsequent transition to a relatively good fit (Riool-Zuid and Nuenen/Son) or even overestimation of values (Eindhoven Stad) further into the storm event when pollutant concentrations are low.

Possibly, in analogy to DWF conditions, a matrix change occurs in the transition between peak values and the lower, diluted wastewater values. If so, two distinct WWF local calibration sets would be required each covering their respective in-sewer conditions. However, since only a limited number of samples have been collected during peak conditions, insufficient data are available to derive such a separate calibration set. Moreover, basing 'peak' calibration sets on a small number of laboratory results comes at the risk of including undetected outliers and other non-representative samples in the set. Therefore, no distinction is made and all TSS and COD laboratory results associated with WWF are included in the data sets used for the local calibration procedure.

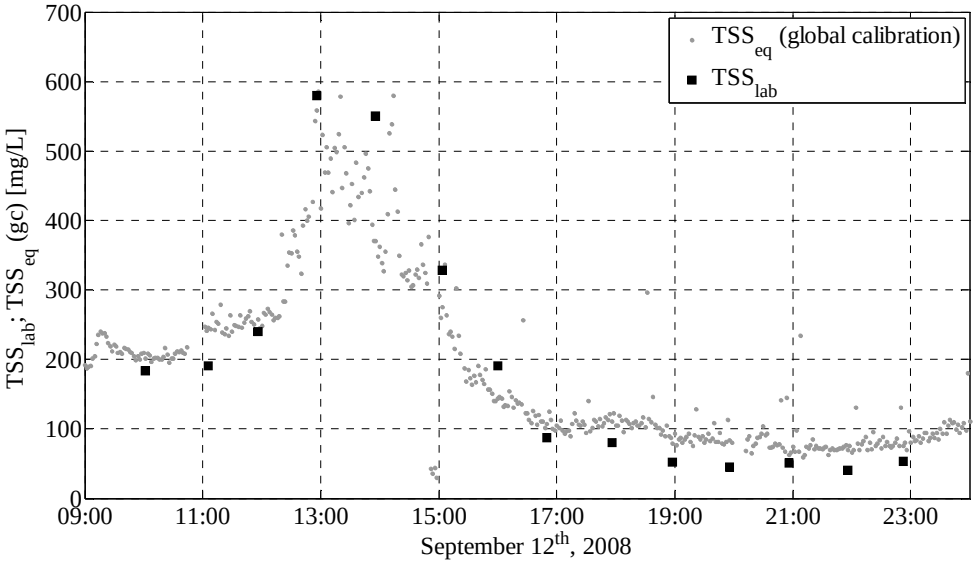

Figure 5-14: Results of WWF sampling campaign: TSS_{eq} versus TSS_{lab} for wastewater from catchment area Eindhoven Stad.

Noteworthy is the difference between the dilution process of on one hand catchment areas Eindhoven Stad and Nuenen/Son and on the other hand catchment area Riool-Zuid (compare e.g. figures J-10 and J-18 in appendix J). It can be observed that for Eindhoven Stad and Nuenen/Son the lowest diluted concentration values lay well within the sampling time-span. In other words: for these two catchment areas collected grab samples cover the initial peak phase of the storm event, the dilution phase and a part of the recovery phase. Considering Figure 5-13 it can be seen that for catchment Riool-Zuid the lowest diluted concentration values are reached only *after* the last sample (around 23h00) has been collected. The prolonged dilution process for this catchment can be understood considering the long transportation times in the transport sewer Riool-Zuid. Well into the storm event plug flows holding e.g. the DWF content of the Aalst pressure main arrive at the wwtp and interrupt the dilution process. As a result, for this particular catchment area the set of collected grab samples largely covers the combined peak/dilution phase of the storm event, but cannot provide data on the subsequent recovery phase. For the latter phase the WWF calibration set is assumed to be valid, but additional sampling should confirm this assumption.

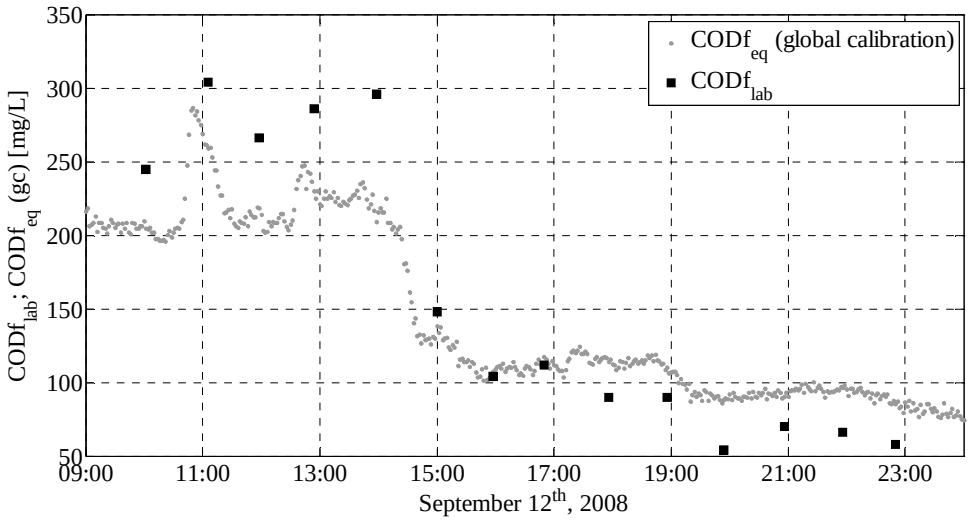

Figure 5-15: Results of WWF sampling campaign: $CODf_{eq}$ versus $CODf_{lab}$ for wastewater from catchment area Riool-Zuid.

For CODf values a clear matrix change can be observed that coincides with the dilution of wastewater, see Figure 5-15 for the example of inflow Riool-Zuid. The UV/VIS sensor underestimates $CODf_{lab}$ values prior to dilution whereas most sensor results after the main dilution process between 14h00 and 15h00 are equal to or higher than $CODf_{lab}$ values. This phenomenon can also be observed for

catchment area Nuenen/Son. For WWF local calibration of CODf values only laboratory results of samples collected after the main dilution process (i.e. after 15h00 in Figure 5-15) have been included. Results of samples collected prior to dilution have been used to calibrate the UV/VIS sensors for CODf under dry weather flow conditions for lack of good results obtained during the DWF campaign.

5.3.4 Local calibration

The UV/VIS sensors in the influent pumping station of the wwtp Eindhoven have been calibrated constructing a polynomial function between on one hand sensor results (based on the global calibration set) and on the other hand laboratory results of grab samples. The approach is similar to the method for local calibration provided in the sensor software (van den Broeke, 2009). Also, various authors report the use of this approach for the local calibration of their UV/VIS sensors (Gruber *et al*., 2006; Maribas *et al.*, 2008).

The approach leaves the relation between measured absorption values and pollutant parameters unaltered. In other words, no different set of wavelengths, weighing factors and off-set factors are applied. Instead, locally calibrated equivalent pollutant concentrations (c_l) are obtained by means of a linear regression model that adjusts the globally calibrated values (c_g) using a multiplication factor (b_1) and an off-set factor (b_2):

$$c_l = f(c_g) = b_1 c_g + b_2 \tag{5.3}$$

The values for b_1 and b_2 are calculated using linear least squares fitting, minimizing the root mean squared error (*RMSE*) between regression model and target values (i.e. the laboratory analysis results c_{lab}). Minimizing the *RMSE* is equivalent to solving an overdetermined system of n simultaneous linear first order equations for two unknown coefficients (Otto, 1999):

$$\begin{bmatrix} y_1 \\ y_2 \\ \dots \\ y_n \end{bmatrix} = \begin{bmatrix} x_1 & 1 \\ x_2 & 1 \\ \dots & \dots \\ x_n & 1 \end{bmatrix} \times \begin{bmatrix} b_1 & b_2 \end{bmatrix} \tag{5.4}$$

or:

$$y = Xb \tag{5.5}$$

with y = n-by-1 vector of laboratory reference (target) values (c_{lab}) [mg/L];
X = n-by-m design matrix of the model (c_g) [mg/L];
b = m-by-1 vector with unknown coefficients b_1 and b_2 [-];
n = number of available samples [-];

An example of the derived linear regression model for inflow Riool-Zuid, parameter COD, DWF matrix is given in Figure 5-16. The 95% confidence interval values y_0 of the model fit is indicated in the figure and is calculated for a value x_0 as (Otto, 1999):

$$y_0 = x_0 b \pm \sqrt{F(\alpha;1,n-p)\, s_R^2 \left(x_0 \left(X^T X \right)^{-1} x_0^T \right)} \tag{5.6}$$

with X = n-by-m design matrix of the model;
F = F-statistic at probability α with 1 and (n-p) degrees of freedom;
s^2_R = mean sum of squares of the residuals.

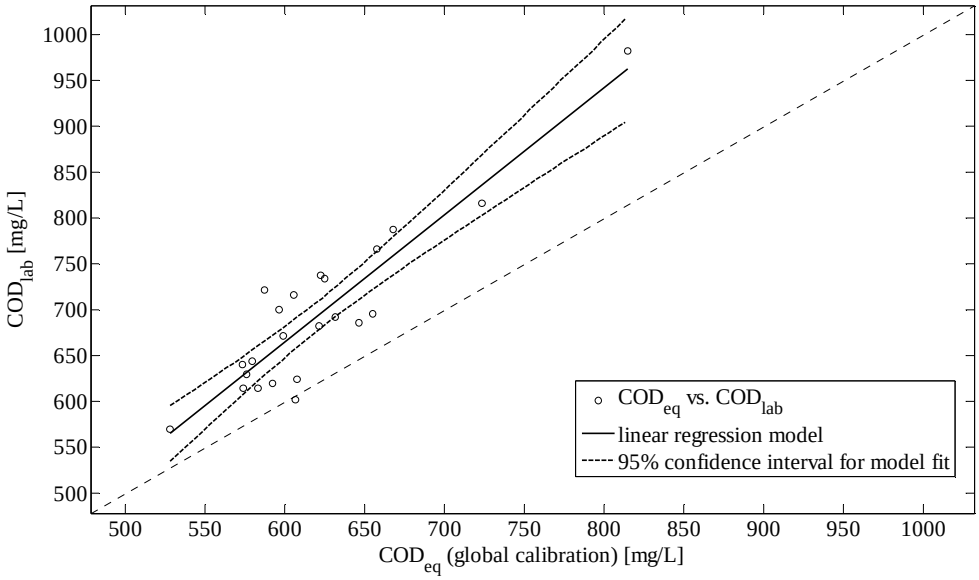

Figure 5-16: For inflow Riool-Zuid, DWF matrix: COD_{eq} (global calibration) vs. COD_{lab} with linear regression model and confidence bounds.

Application of model parameters b_1 and b_2 on raw sensor data yields locally calibrated pollutant concentration values, see Figure 5-17. The locally calibrated values show a closer agreement with the laboratory reference values than the original raw sensor data based on the global calibration set. The improved performance can be expressed using the root mean squared error between lab and sensor values as a performance indicator:

$$RMSE = \sqrt{\frac{1}{n}\sum_{i=1}^{n}\left(c_{lab} - c_{sensor}\right)^2} \tag{5.7}$$

with c_{lab} = reference value determined in laboratory analysis [mg/L];
c_{sensor} = sensor value, either globally or locally calibrated [mg/L];
n = number of available samples [-].

For the example presented in Figure 5-17 the $RMSE_g$ = 84 mg/L for the raw sensor values decreases to $RMSE_c$ = 35 mg/L for the locally calibrated sensor values. All results of the local calibration of UV/VIS sensors can be found in appendix K; the associated *RMSE* values can be found in Table 5-1. As can be observed in the table, all local calibrations lead to improvement of performance of the UV/VIS sensors.

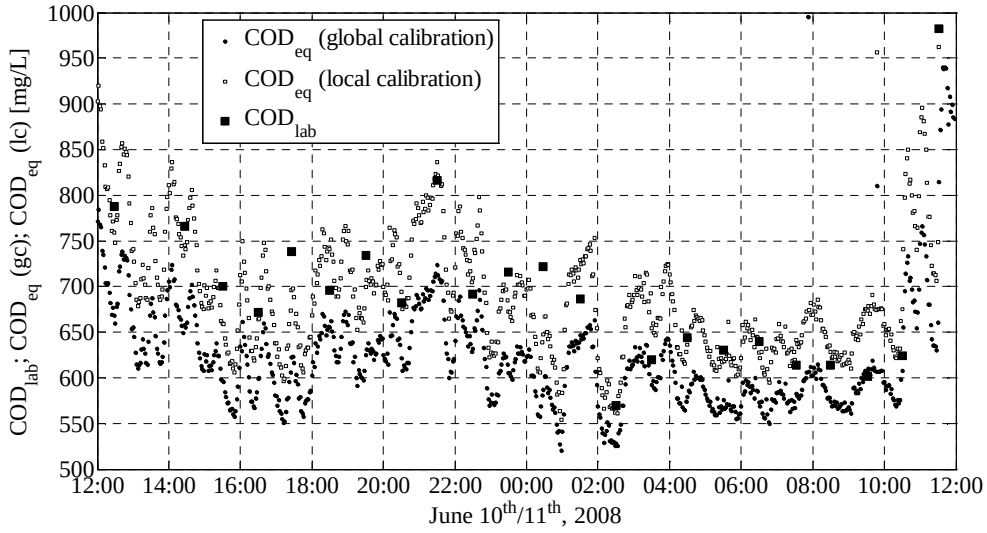

Figure 5-17: Results of local calibration for DWF matrix of inflow Riool-Zuid: COD_{eq} (global calibration, 2-minute interval) transposed to COD_{eq} (local calibration, 2-minute interval) and compared to COD_{lab} (1 sample per hour).

Table 5-1: Per wastewater matrix the agreement between an indicated number of laboratory results and sensor values on global and local calibration sets.

			# of samples	*RMSE* global calibration	*RMSE* local calibration
inflow	param.	matrix	[-]	[mg/L]	[mg/L]
RZ	TSS	DWF	23	28	18
RZ	TSS	WWF	10	117	42
RZ	COD	DWF	23	84	35
RZ	COD	WWF	10	109	31
RZ	CODf	DWF	4	48	6
RZ	CODf	WWF	9	22	8
ES	TSS	DWF	22	46	14
ES	TSS	WWF	10	65	23
ES	COD	DWF	21	34	26
ES	COD	WWF	9	40	17
ES	CODf	DWF	3	14	5
ES	CODf	WWF	10	11	10
NS	TSS	DWF	24	49	31
NS	TSS	WWF	9	73	34
NS	COD	DWF	24	97	34
NS	COD	WWF	9	80	24
NS	CODf	DWF	4	34	6
NS	CODf	WWF	9	5	3

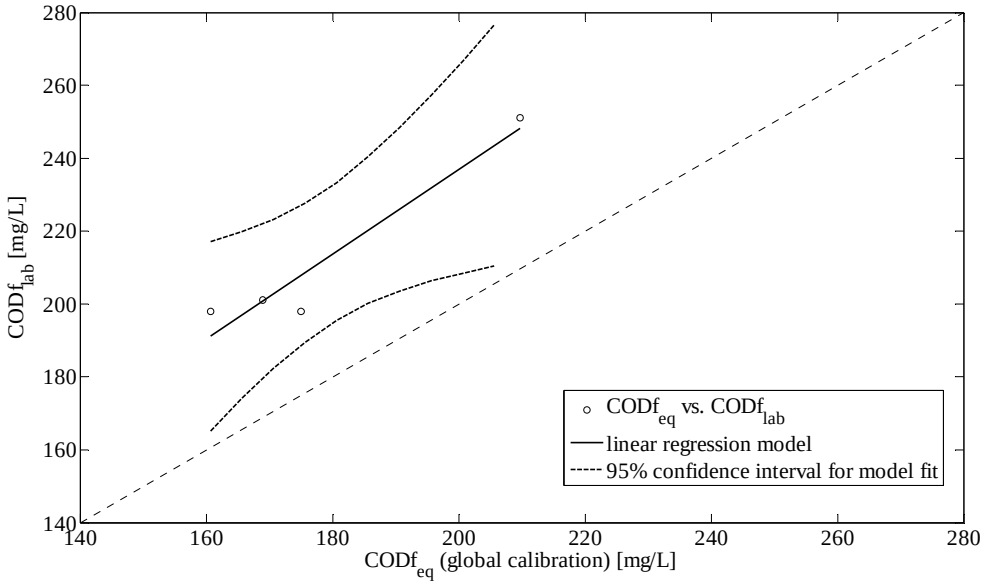

Figure 5-18: For inflow Nuenen/Son, DWF matrix: $CODf_{eq}$ (global calibration) vs. $CODf_{lab}$ with linear regression model and confidence bounds.

Figure 5-18 presents the linear regression model for inflow Nuenen/Son, parameter CODf, DWF matrix. The model is based on four available reference grab samples only. As a result, the uncertainties in the regression model parameters are relatively large compared to the other DWF models that are based on more than 20 reference samples. These large uncertainties show up in the figure as relatively wide 95% confidence bands. Basing calibration sets on such small numbers of laboratory results comes at the (unquantifiable) risk of including undetected outliers and other non-representative samples in the set. Moreover, the samples collected for this matrix only cover a small bandwidth, introducing large uncertainties with the calibration of values outside the bandwidth. The same problem is associated with the models for inflows Riool-Zuid and Eindhoven Stad for the same parameter/matrix combinations. For these three matrices additional sampling is required to better fund the local calibration sets.

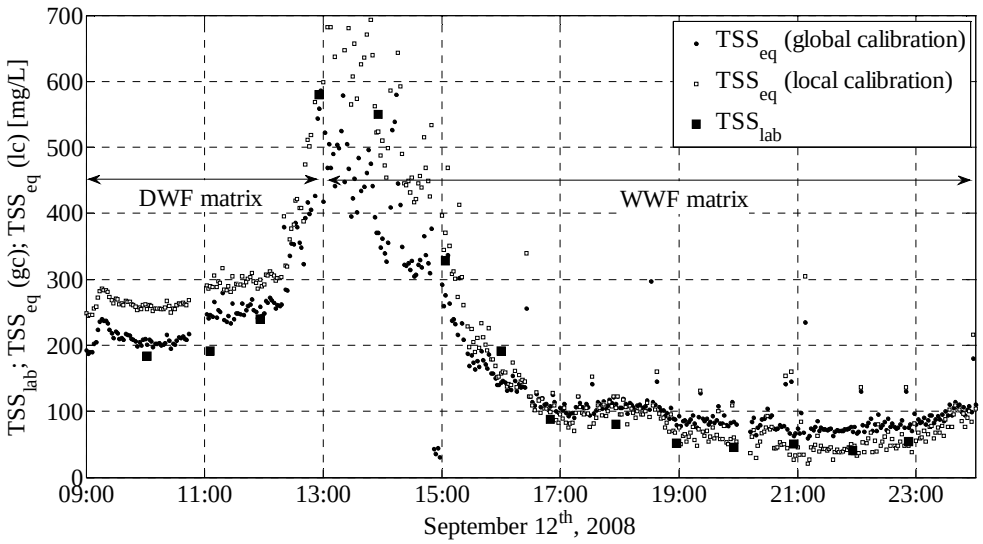

Figure 5-19: Results of calibration for WWF matrix of inflow Eindhoven Stad: TSS_{eq} (global calibration, 2-minute interval) converted into TSS_{eq} (local calibration, 2-minute interval) and compared to TSS_{lab} (1 sample per hour).

Figure 5-19 presents the results of calibration of inflow Eindhoven Stad, parameter TSS, WWF matrix. As earlier described in section 5.3.2 it was decided to start the WWF sampling campaign a few hours earlier than necessary to obtain results for dry weather flow conditions for parameter CODf. The collected grab samples have also been analyzed for the parameter TSS resulting in additional DWF laboratory reference values for this parameters. Since these values have not been used to derive the DWF calibrations sets, these values can be used to *validate* the derived

DWF models. Considering the DWF data presented in Figure 5-19 it can be concluded that the laboratory results agree better with the raw sensor data than with the locally calibrated values. In other words, the application of the regression model has led to a *deterioration* of the agreement between sensor and lab values. Apparently, the set of reference samples collected during the DWF sampling campaign (in June) on which the DWF model has been based does not (fully) cover the matrix conditions experienced during the dry weather period prior to the storm event (in September) in Figure 5-19. Possibly, a seasonal matrix change introduces this error. Additional sampling is required to better fund these local calibration sets.

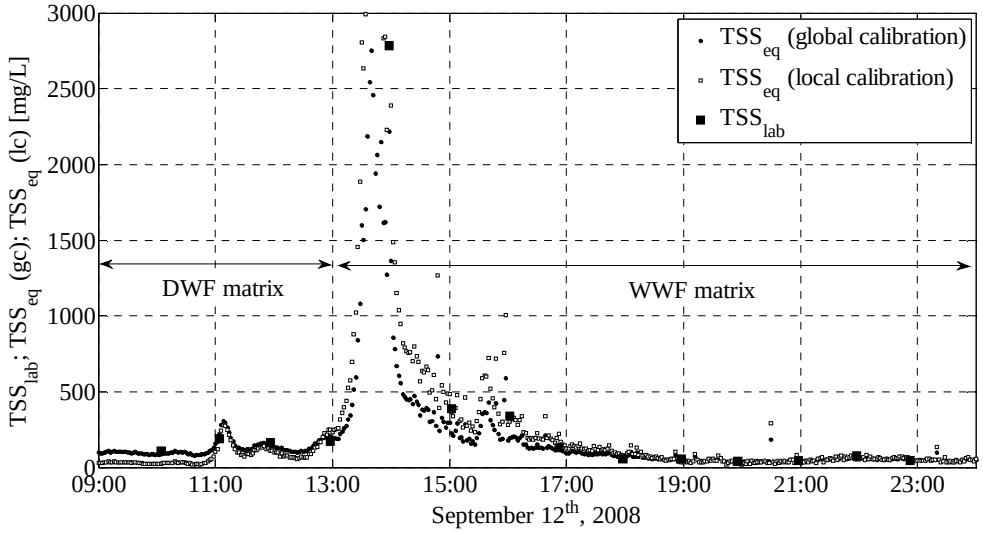

Figure 5-20: Results of calibration for WWF matrix of inflow Nuenen/Son: TSS_{eq} (global calibration, 2-minute interval) converted into TSS_{eq} (local calibration, 2-minute interval) and compared to TSS_{lab} (1 sample per hour). Before 13h00, the DWF local calibration set has been applied. The sample collected at 13h58 has been removed from the WWF laboratory data set prior to calibration.

The results of local calibration for area Nuenen/Son (also WWF matrix, parameter TSS) can be observed in Figure 5-20. Samples collected from 13h00 onwards are considered to be associated with WWF. Between 13h00 and 16h00 a peak in TSS_{eq} values can be observed with a maximum around 2,800 mg/L which is roughly 20 times larger than normal DWF concentrations. The sample collected during the concentration peak at 13h58 shows a large absolute error of approximately 600 mg/L corresponding to a relative error of ~20%, the latter being comparable with other samples from this set. Due to its absolute magnitude, however (and due to the model fitting procedure that minimizes absolute errors), this single peak value

largely deteriorates the fit of all other WWF values. The overall fit of all but the peak value is (much) better when excluding the peak sample from the calibration set. Therefore, the peak sample has been removed from the reference data set prior to calibration. The same applies for the laboratory data sets of parameters COD and CODf for this catchment area.

Despite the reservations made in this section (limited number of samples, small bandwidth of values, etc.), local calibration as described by equation 5.3 has been applied for all considered wastewater matrices. Hence, all wastewater quality values presented in chapter 6 represent locally calibrated values.

5.3.5 Uncertainty assessment

The uncertainty in the locally calibrated UV/VIS data sets is derived considering the equation with which values are calculated (see equation 5.3):

$$c_l = f(c_g) = b_1 c_g + b_2 \tag{5.8}$$

The uncertainty in the locally calibrated time-series (σ_{Cl}^2) is a combination of three sources of uncertainty (Métadier and Bertrand-Krajewski, 2009). The in-situ uncertainty describes a possible error due to monitoring in a by-pass installation instead of in the main wastewater flow. This error source has been studied nor quantified and is therefore excluded from the uncertainty assessment (i.e. assumed to be negligible, see also section 5.2.2). The other two sources of uncertainty are:

1. Uncertainty in the original, globally calibrated values (σ_{Cg}^2). This type of uncertainty is also referred to as sensor uncertainty. It describes the variation in the sensor signal when observing a homogenous medium. It has been determined placing the UV/VIS sensors in a vessel holding tap water and taking a long-term measurement. The result for parameter TSS_{eq} of the sensor in inflow Riool-Zuid can be observed in Figure 5-21. The upper graph presents 136 observations (at a 2-minute interval) scattered around its linear regression line. The lower graph shows the residuals between observations and regression model. The residuals are normally distributed with a standard error of σ_{Cg} = 1.9 mg/L.

2. Uncertainty in the application of regression coefficients b_1 and b_2. This type of uncertainty is also referred to as calibration function uncertainty and is illustrated in Figure 5-16 and Figure 5-18. Variances of coefficients b_1 and b_2 as well as the covariance between the two coefficients determine a 95% confidence bound for the regression function. Values for σ_{b1}^2, σ_{b2}^2 and σ^2_{b1b2} follow from the variance-covariance matrix (Otto, 1999):

$$C = s_R^2 (X^T X)^{-1} = \begin{pmatrix} \sigma_{b_1}^2 & \sigma_{b_1 b_2}^2 \\ \sigma_{b_2 b_1}^2 & \sigma_{b_2}^2 \end{pmatrix} \tag{5.9}$$

with: X = design matrix of the model;
s_R^2 = mean sum of squares of the residuals;
σ_{b1}^2 = variance in parameter b_1;
σ_{b2}^2 = variance in parameter b_2;
σ_{b1b2}^2 = covariance between parameters b_1 and b_2;

It should be noted that the uncertainty of the calibration function cannot account for a poor representation of the considered wastewater matrix. For instance for WWF matrices (of which the calibration sets consist of samples collected during a single storm event only) the inter-event variation in wastewater composition (as earlier described in section 5.3.1) can be such that deviations between sensor and laboratory values are larger than expected based on the calibration function. Also, calibration sets not fully covering the range of normal concentration values for the considered wastewater matrix can lead to additional errors.

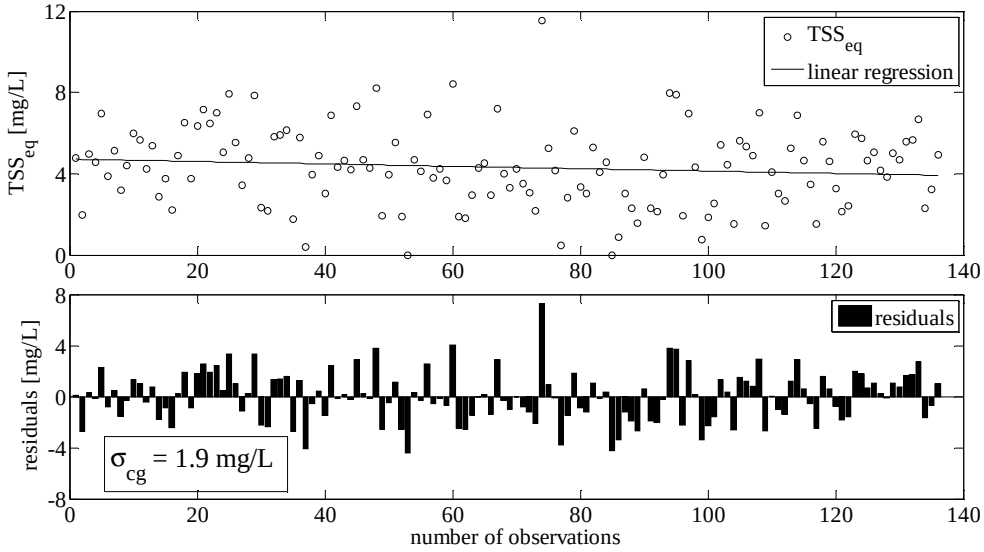

Figure 5-21: Result of a long-term TSS_{eq} measurement (≈ 4.5 hours) of tap water with the Riool-Zuid UV/VIS sensor. Observations and linear regression model are presented in the upper graph; residuals are presented in the lower graph. The residuals are normally distributed with standard error σ_{Cg} = 1.9 mg/L.

The sources of uncertainty can be combined through the law of propagation of uncertainty using the Taylor series of the first order of the function for c_l (Bertrand-Krajewksi and Bardin, 2002):

$$\sigma_{c_l}^2 = \left(\frac{\partial f}{\partial c_g}\right)^2 \sigma_{c_g}^2 + \left(\frac{\partial f}{\partial b_1}\right)^2 \sigma_{b_1}^2 + \left(\frac{\partial f}{\partial b_2}\right)^2 \sigma_{b_2}^2 + 2\left(\frac{\partial f}{\partial b_1}\right)\left(\frac{\partial f}{\partial b_2}\right)\sigma_{b_1 b_2}^2 \quad (5.10)$$

or:

$$\sigma_{c_l}^2 = {b_1}^2\sigma_{c_g}^2 + {c_g}^2\sigma_{b_1}^2 + \sigma_{b_2}^2 + 2c_g\sigma_{b_1 b_2}^2 \quad (5.11)$$

The standard error in locally calibrated values is a second order function of globally calibrated concentration values. For the example of inflow Riool-Zuid, parameter TSS, DWF matrix equation 5.10 yields a standard error in locally calibrated values as illustrated in Figure 5-22. In this example, relative standard errors range between 2-4%.

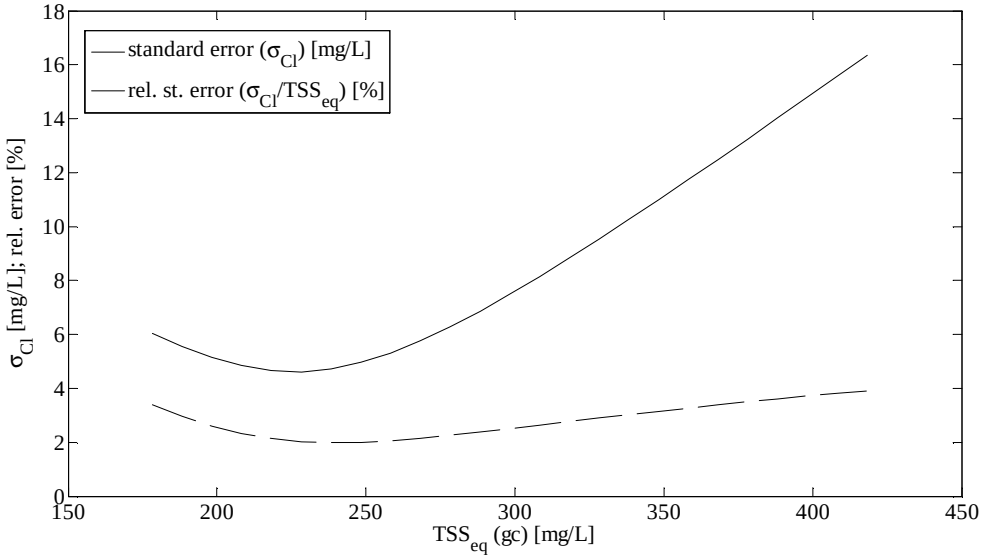

Figure 5-22: Standard error and relative standard error as a function of globally calibrated TSS_{eq} concentration values for inflow Riool-Zuid, DWF matrix.

5.4 Quality assessment of UV/VIS data sets

5.4.1 Introduction

The 19-months data sets of the three UV/VIS sensors have been assessed for quality of the data. The objective of the quality assessment is to exclude any data from the data sets that do not correctly represent the measured pollutant parameter. Including such erroneous data in the data sets could lead to incorrect conclusions during data analysis.

The data quality assessment in this paragraph consists of the following steps, successively described in the next sections:

1. Assessment of large gaps in the data sets
2. Removal of data related to sensor and by-pass cleaning
3. Removal of data related to by-pass pump failure
4. Removal of data related to envelop obstruction
5. Removal of data related to auto-cleaning system failure
6. Removal of outliers

The basic assumption during the assessment is that the data are good unless otherwise indicated by one of the tests. The search for data gaps and outliers has been done automatically; the other errors have been found during a manual search. This manual search comprised two iterations. In a first sweep four error mechanisms (steps 2 through 5 in the above list) were determined based on all log book entries indicating an anomaly from normal operation. In a second sweep the complete data sets were assessed for these error mechanisms, yielding a number of erroneous data sequences for which no log book entries were found.

The data sets have also been analyzed for data values that are outside the physically possible range. For pollutant concentration values the lower boundary value equals 0 mg/L. No values below this threshold have been found. A strict upper boundary cannot be set for pollutant concentration values. However, the detection of prolonged exceeding of *locally realistic* values (i.e. TSS_{eq} and COD_{eq} concentrations > $5 \cdot 10^3$ mg/L for several hours on end) has led to the diagnoses of the error mechanisms of envelop obstruction and auto-cleaning system failure.

5.4.2 Assessment of large gaps in the data sets

The UV/VIS data sets have been assessed for large data gaps. A large data gap is defined here as a time-span of at least 15 consecutive minutes (or 8 consecutive data points) without monitoring data. Table 5-2 presents the results.

Table 5-2: Number, total length (in minutes and days) and percentage (of total 580-days data sets) of data gaps in the UV/VIS data-sets.

	data gaps								
	15 - 60 min		1 - 6 hours		> 6 hours		all gaps > 15 min		
	num. [#]	length [min]	num. [#]	length [min]	num. [#]	length [min]	num. [#]	length [days]	perc. [%]
Riool-Zuid	45	1,326	6	718	17	65,054	68	46.6	**8.0**
Eindhoven Stad	38	1,152	10	1,076	18	63,532	66	45.7	**7.9**
Nuenen/Son	30	972	5	574	16	126,052	51	88.6	**15.3**

Large data gaps represent around 8% of the total data sets of Riool-Zuid and Eindhoven Stad and more than 15% for Nuenen/Son. The smallest considered gaps (15-60 minutes) occur most often, but contribute only marginally to the total amount of data loss. Most of these small gaps can be attributed to cleaning activities of sensors and by-pass installations during which the power to the monitoring stations was switched off. Gaps between 1 and 6 hours are generally due to small repair activities during which power was also switched off. The data sets contain a total of 16 to 18 data gaps longer than 6 hours. Large gaps that appear simultaneously for the three sensors include gaps due to data communication failures, gaps due to a week-long repair of the compressor that provides the air for the auto-cleaning devices and gaps due to software and hardware updates for the entire WDD sensor network. Furthermore, all three UV/VIS sensors have been broken down several times during the 19-months time-span. Down-times for repair have varied between 1 and 48 days, the latter being by far the largest single data gap in the data sets. This exceptional long repair time explains the large percentage of absent data for catchment area Nuenen/Son.

5.4.3 Removal of data related to sensor and by-pass cleaning

The UV/VIS sensors and the by-pass installations holding the sensors were regularly cleaned, recording the (majority of) moments of cleaning in a meta data file. By-pass installations were cleaned once per week: the pumps were stopped, the vessels holding the sensors were emptied, accumulated sediments and other dirt were removed from the vessels, and the UV/VIS sensors were hosed off. Cleaning of the sensor lenses was *not* included in this once-per-week cleaning procedure. During the cleaning procedure the power to the installations was nearly always switched off, resulting in a data gap of typically 15-30 minutes, as presented in the previous section. The data sets therefore contained almost no data collected during by-pass installation cleaning. On a few occasions, however, power to the sensors was not switched off; these data have been removed from the data sets.

Once per month an extensive lens cleaning was added to the weekly cleaning procedure. Lens cleaning consisted of initial rinsing with demineralized water and subsequent treatment with diluted hydrochloric acid or a manufacturer cleaning agent. To be able to monitor the cleaning effect of each treatment step the power supply to the monitoring stations was *not* switched off. Hence, the data-set contains data recorded during lens cleaning that needs removal. Figure 5-23 gives an example for the Nuenen/Son data. The power supply to the monitoring station was first switched off for by-pass installation cleaning between ~08h15 and ~08h50. Then, the effect of sensor lens cleaning on the monitoring data can be observed between 10h00 and 11h00. The latter time-span has been removed from the set.

During the considered 19-months time-span sensor lens cleaning has taken place 20 to 25 times, depending on the sensor. The associated data loss is limited (~0.3% of the total data sets, see Table 5-3) due to the short duration of the cleaning procedures.

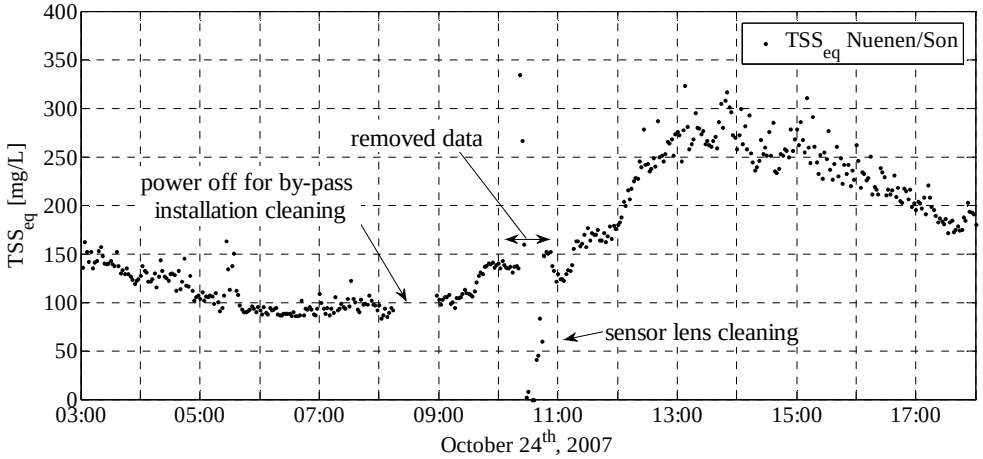

Figure 5-23: Example of influence of by-pass installation and sensor lens cleaning on data results. Results are for catchment area Nuenen/Son, TSS_{eq}, October 24th, 2007 03h00 - 18h00. Data collected between 10h00 and 11h00 have been removed from the data set.

Table 5-3: Number, total corresponding length and associated percentage of the 580-days total data sets of sensor lens and by-pass cleaning activities in the UV/VIS data-sets.

	sensor lens and by-pass cleaning		
	number [#]	total length [min]	percentage of total data sets [%]
Riool-Zuid	25	3,150	0.4
Eindhoven Stad	20	2,220	0.3
Nuenen/Son	20	2,100	0.3

5.4.4 Removal of data related to by-pass pump failures

The pumps that feed the by-pass installations occasionally fail due to clogging of the suction mouths of the pump. Without feed the wastewater in the by-pass installations is no longer renewed and hence no longer represents the wastewater in the influent pumping station correctly. Therefore, this data needs removal from the data-set. Monitoring results of stagnant wastewater in a vessel can be detected searching for a reduced signal bandwidth and gradual sedimentation of suspended particles, see Figure 5-24. By-pass pump failure has occurred three times for catchment area Riool-Zuid as well as for catchment area Eindhoven Stad, representing 0.6% and 1.1% of the total data sets, respectively. Nuenen/Son has seen no pump clogging. An overview of occurrence, total length and associated percentages can be found in Table 5-4.

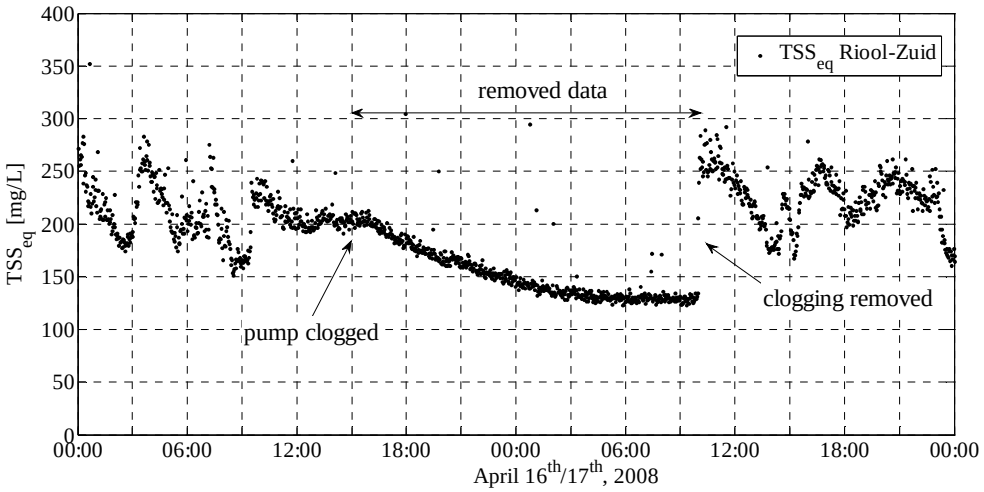

Figure 5-24: Example of influence of by-pass pump failure on data results. Results are for TSS_{eq}, Riool-Zuid, April 16th/17th, 2008. Data between April 16th 15h00 and April 17th 10h00 have been removed from the data set.

Table 5-4: Number, total corresponding length and associated percentage (of the 580-days total data sets) of by-pass pump failures in the UV/VIS data sets.

	by-pass pump failures		
	number [#]	total length [days]	percentage [%]
Riool-Zuid	3	3.6	0.6
Eindhoven Stad	3	6.7	1.1
Nuenen/Son	0	0	0

5.4.5 Removal of data related to envelop obstruction

Large particles in the wastewater regularly obstruct the measuring envelop of the UV/VIS sensors. As a result, the absorbance of light (and hence related parameter concentrations) suddenly increases to large and untypical values for domestic wastewater. Occasionally, large particles can get stuck in the envelop and unrealistic values can hence persist for a period of time, see Figure 5-25. After removal of the particles monitoring results instantly return to normal wastewater values. Data recorded during such envelop obstructions have been removed from the data sets.

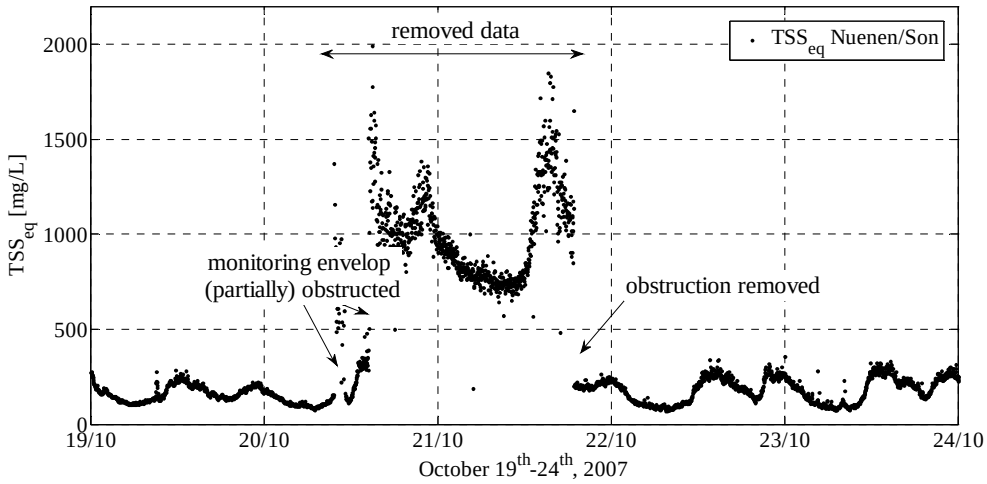

Figure 5-25: Influence of (partial) obstruction of the monitoring envelop on data results. Results are for TSS_{eq}, Nuenen/Son, October 19th-24th, 2007. Data between October 20th 09h00 and October 21st 21h00 have been removed from the data set.

Obstruction of the monitoring envelop can also be caused by entrapped air bubbles, see Figure 5-26. If the envelop is positioned in an exactly downward direction, the air produced by the auto-cleaning device cannot fully escape from the envelop and hence influences the measurements. After a lens cleaning procedure (July 4th, 2007) the Nuenen/Son sensor was unintentionally positioned as such and intermittently yielded a cloud of monitoring values. After the subsequent sensor cleaning (July 25th, 2007) the sensor was rotated and again yielded normal monitoring results, see Figure 5-26. All data between the two cleaning procedures have been removed from the data-set. In total, 13 envelop obstructions have been identified during the 19-months time-span of the data sets. These correspond to between 1.4% and 3.1% of the total UV/VIS data sets, see Table 5-5.

Table 5-5: Number, total corresponding length and associated percentage (of the 580-days total data sets) of envelop obstructions in the UV/VIS data sets.

	envelop obstructions		
	number [#]	total length [days]	percentage [%]
Riool-Zuid	7	17.9	3.1
Eindhoven Stad	2	8.0	1.4
Nuenen/Son	4	15.9	2.7

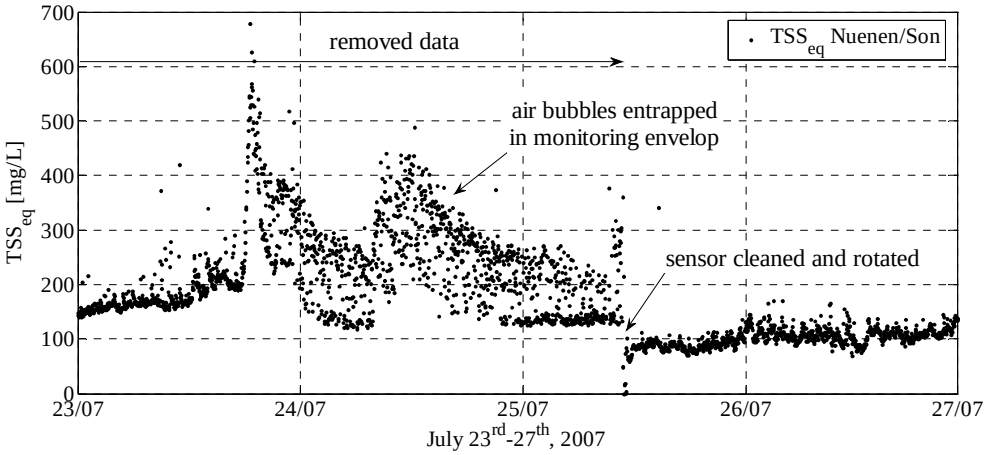

Figure 5-26: Influence of air bubble obstruction of the monitoring envelop on data results. Results are for TSS_{eq}, Nuenen/Son, July 23rd-27th, 2007.

5.4.6 Removal of data related to auto-cleaning system failure

Failure of (a part of) the sensor auto-cleaning system leads to progressive pollution of monitoring envelops and sensor lenses and hence to unreliable monitoring results. Failure of a central part of the auto-cleaning device (e.g. the compressor, a central power cut) influences the results of all three UV/VIS sensors simultaneously; failure of a single component (e.g. air nozzle, supply container) generally leads to unreliable results for one sensor only. Figure 5-27 shows an example for which metadata information confirms a compressor failure for the time-span September 1st-21st, 2007. After the breakdown on September 1st around 09h00 (see Figure 5-28) all three signals show increasing values for TSS_{eq} due to a gradual lens contamination. The rate of increase, however, differs. Eindhoven Stad and Nuenen/Son signals show an immediate reaction to the lens pollution build-up. TSS_{eq} values for Riool-Zuid only show a limited drift in the 9-days time-span following the compressor failure. These differences are likely due to differences in wastewater pollutant characteristics (e.g. the grease content of the wastewater).

Large jumps in TSS_{eq} to unrealistic values between 1000 and 5000 mg/L are visible for all three signals. These are attributable to monitoring envelop particle obstruction (or removal of the particle obstruction for jumps down). Vessel cleaning on September 5th temporarily reduces values to the normal value range, but the same pollution process can be observed immediately afterwards. Repair of the compressor on September 19th in combination with vessel and sensor lens cleaning brings back monitoring values to the normal value range. After minor final adjustments on September 20th/21st the three UV/VIS sensors again yielded representative monitoring data.

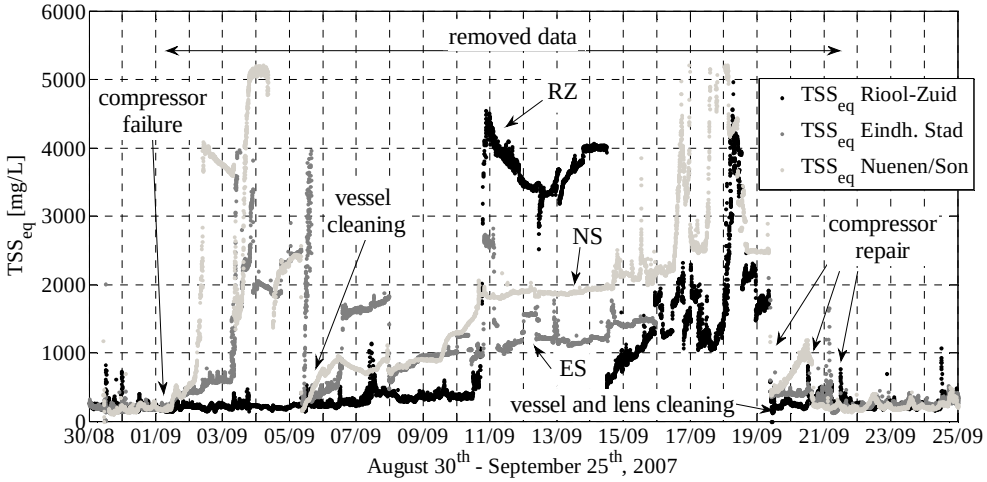

Figure 5-27: Influence of air compressor failure on data results. Results are for TSS_{eq}, all three inflows, August 30th - September 25th, 2007. Data between September 1st 9h00 and September 21st 12h00 have been removed from the data sets.

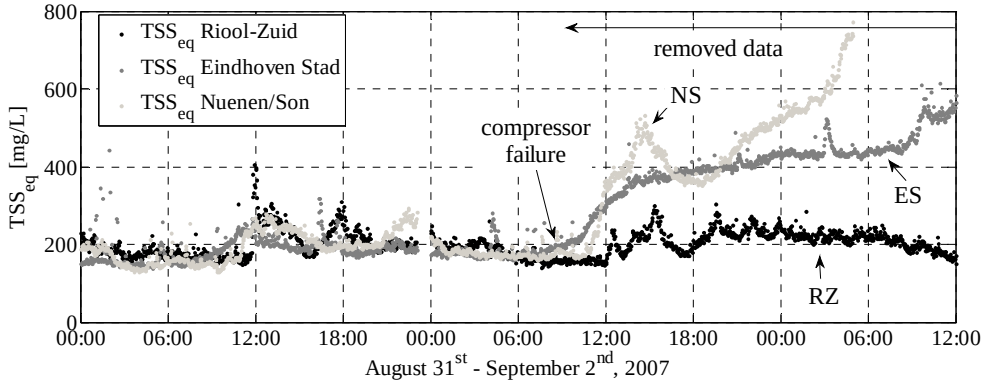

Figure 5-28: Zoom of Figure 5-27 on the moment of compressor failure. Immediate reactions for TSS_{eq} values can be observed for Eindhoven Stad and Nuenen/Son. Influence of the failure on Riool-Zuid results is not distinguishable in this graph.

Figure 5-29 shows a second example of the influence of air compressor failure on data results. Within a time-span of a week two compressor failures have caused large and simultaneous increases in TSS_{eq} monitoring results for all three catchment areas. On February 18th, after resetting the compressor and cleaning the vessels and sensors lenses, the sensors resume normal behavior. Zooming in on these cleaning activities (Figure 5-30) it can be seen that each large reduction in concentration values coincides with vessel cleaning and not with sensor lens cleaning. Apparently, the simple action of hosing off the sensor and its measuring envelop removes the envelop obstructing particles that are responsible for the large peaks in pollutant concentrations. The subsequent action of intensive sensor lens cleaning with demineralized water and diluted hydrochloric acid (or a manufacturer cleaning agent) only has a limited effect on measurement values.

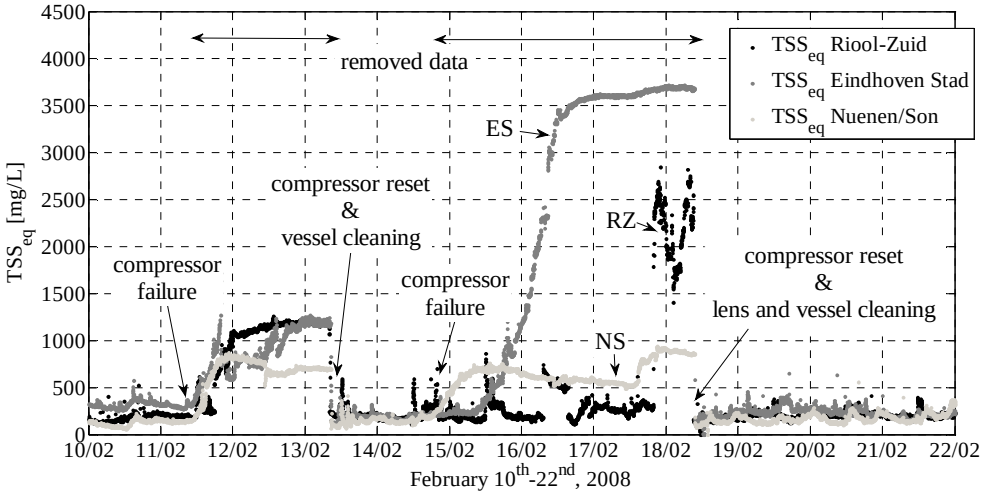

Figure 5-29: Influence of air compressor failure on data results. Results are for TSS_{eq}, all three inflows, February 10th-22nd, 2008.

Due to persistent problems with the auto-cleaning system, the UV/VIS data-sets contain a large number (14, 19 and 20) of peaks such as depicted in Figure 5-27 and Figure 5-29. Shares of 13.8% (Riool-Zuid), 36.2% (Eindhoven Stad) and 16.3% (Nuenen/Son) of the total data sets have been removed for reasons of auto-cleaning system failure, see Table 5-6. Due to missing entries, metadata information could not confirm a causal relationship between all peaks and a malfunctioning cleaning system, but - since signal behavior is similar for nearly all peaks - it is assumed that a malfunctioning auto-cleaning system is the probable cause of all identified large peaks.

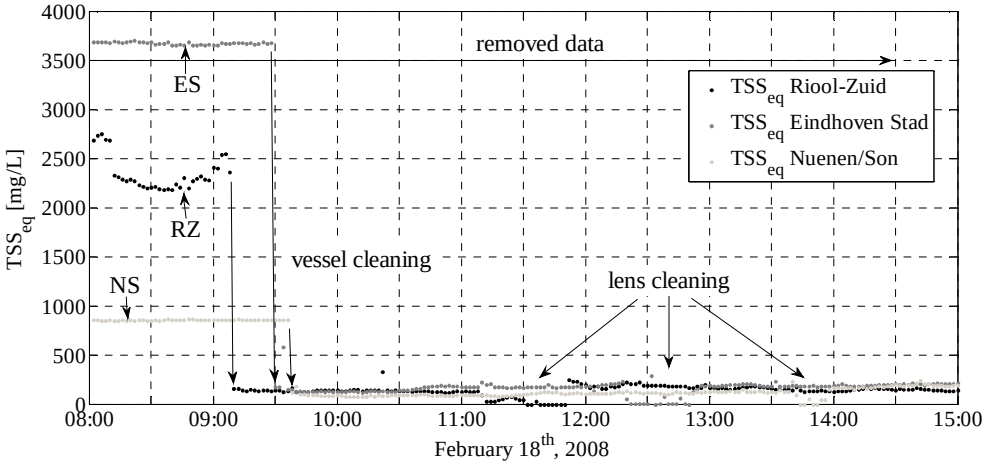

Figure 5-30: Zoom of Figure 5-29 on the moment of vessel and lens cleaning. The former process is mainly responsible for the large reduction in monitoring values.

Table 5-6: Number, total corresponding length and associated percentage (of the 580-days total data sets) of auto-cleaning system failures in the UV/VIS data sets.

	auto-cleaning system failures		
	number [#]	total length [days]	percentage [%]
Riool-Zuid	19	80.3	13.8
Eindhoven Stad	14	210.1	36.2
Nuenen/Son	20	94.5	16.3

5.4.7 Removal of outliers

The UV/VIS data sets contain outliers: a small number of data points that show a sudden and relatively large increase or decrease with respect to the main signal, see Figure 5-31 upper graph. These values are often due to a short and temporary obstruction of the measurement envelop, which leads to an increase in concentration values. Detection of outliers has been done with the Page-Hinkley (PH) algorithm described in e.g. Mourad and Bertrand-Krajewski (2002). The algorithm aims at detecting values that differ from the average of a Gaussian signal. The Gaussian signal is the difference between the original signal and the central moving average filtered signal, see Figure 5-31 (lower graph). By filtering the original signal over a short span, single or small numbers of outlying values become apparent through relatively large residuals (ε_k) that deviate from the mean residual μ_n (≈ 0) over the preceding time-span of length n. The required deviation to be characterized as 'outlier' can be altered through a user-defined amplitude value (δ) and detection level (λ). The test statistics are:

$$U_n = \sum_{k=1}^{n}\left(\varepsilon_k - \mu_n - \frac{\delta}{2}\right) \text{with } U_0 = 0;\ m_n = \min_{0\le k\le n} U_k \tag{5.12}$$

$$V_n = \sum_{k=1}^{n}\left(\varepsilon_k - \mu_n + \frac{\delta}{2}\right) \text{with } V_0 = 0;\ M_n = \max_{0\le k\le n} V_k \tag{5.13}$$

Outliers are detected when $U_n - m_n > \lambda$ (for outliers larger than μ_n) or when $M_n - V_n > \lambda$ (for outliers smaller than μ_n). The test needs to be reinitialized following each detection. Results of the PH algorithm can be observed in Figure 5-31.

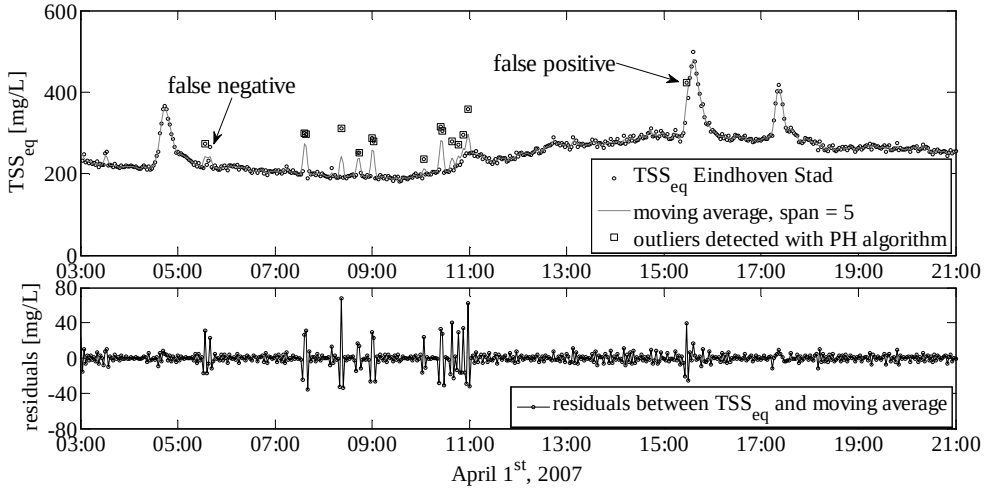

Figure 5-31: TSS_{eq} monitoring data (upper graph) for April 1st, 2007 03h00-21h00 for catchment area Eindhoven Stad. Outliers are detected using the Page-Hinkley algorithm based on the assessment of residuals (lower graph) between TSS_{eq} data and its moving average over (for this specific time-series) a span of 5 data points.

The values for the filter span, amplitude value and detection level need calibration for each data set separately. Setting optimum values for these parameters requires weighing the number of false positives against the number of false negatives: setting the criteria too loose yields more false positives (i.e. data points identified as outliers which are not) whereas setting the criteria too strict yields more false negatives (i.e. outliers that remain undetected). Table 5-7 presents per UV/VIS data set the number, total corresponding length and associated percentage of outliers in the. All outliers have been removed from the data sets.

Table 5-7: Number, total corresponding length and associated percentage (of the 580-days total data sets) of outliers in the UV/VIS data sets.

		outliers		
		number [#]	total length [days]	percentage [%]
Riool-Zuid	TSS	9,539	13.2	2.3
	COD	3,248	4.5	0.7
	CODf	248	0.3	<0.1
Eindhoven Stad	TSS	4,728	6.6	1.1
	COD	1,218	1.7	0.3
	CODf	156	0.2	<0.1
Nuenen/Son	TSS	3,971	5.5	1.0
	COD	1,312	1.8	0.3
	CODf	480	0.7	0.1

5.4.8 Overview data quality assessment

The data quality assessment of the 19-months UV/VIS data sets has resulted in the removal of roughly 25% to 50% of the data sets, see Table 5-8. The two main contributors to these large shares of data loss are a repeatedly malfunctioning auto-cleaning system (i.e. a repeatedly failing compressor) and the presence of large data gaps due to the (prolonged) absence of sensors for repairs. These two factors are related to the *operation* of the monitoring stations and are not intrinsic to the sensor or its set-up. Therefore, improvement of the operation is likely to produce a much better data yield. Unavoidable data loss that is intrinsic to the sensor and its set-up (such as due to cleaning, due to an occasional pump clogging, due to envelop obstruction and outliers) adds to less than 5% indicating that - with proper sensor operation - data yields over 90% can be expected. A further analysis of monitoring network performance can be found in chapter 8.

Table 5-8: Shares of data removed from the UV/VIS data sets as a percentage of the 580-days total data sets as a result of data quality assessment.

	percentage of removed data [%]		
	Riool-Zuid	Eindhoven Stad	Nuenen/Son
data gaps > 15 min	8.0	7.9	15.3
sensor/by-pass cleaning	0.4	0.4	0.3
by-pass pump failures	0.6	1.1	0
envelop obstruction	3.1	1.4	2.7
auto-cleaning system failure	13.8	36.2	16.3
outliers	~ 1.0	~ 0.5	~ 0.5
TOTAL	26.9	47.5	35.1

5.5 Conclusions

In this chapter a total of nine time-series have been derived that represent the *quality* of wastewater that arrives at the wwtp Eindhoven. For each of the three contributing catchment areas time-series are available for quality parameters TSS, COD and CODf. The data sets have been generated by means of UV/VIS sensors that provide high-frequent optical measurements of the wastewater in a dedicated by-pass installation.

Dry weather and wet weather reference sampling campaigns have demonstrated that the sensors are capable of reproducing trends in the variation of pollutant concentration values. Using the manufacturer's global calibration set relative errors between sensor and laboratory values for DWF conditions are roughly within a range of ±25% (Riool-Zuid, Eindhoven Stad) or ±50% (Nuenen/Son). For WWF conditions relatively large absolute errors have been observed during initial peak moment as well as relatively large relative errors during the dilution phase of the storm event.

Per time-series two distinct wastewater matrices have been distinguished, yielding a total of 18 studied wastewater matrices for the 9 time-series. For each matrix a local calibration set has been derived constructing a linear regression model between globally calibrated sensor values and laboratory reference values. All local calibration sets yield an improved fit between sensor and laboratory values. An error estimate of locally calibrated sensor values is obtained accounting for sensor uncertainty and uncertainty in the calibration regression function. Concerns are the limited number and possible ill-representativeness of collected samples for a number of wastewater matrices. Additional sampling would increase the confidence in the calibration functions for these matrices.

A quality assessment of the data sets has shown that data loss for this long-term monitoring campaign (19 months) has added to 25 to 50% of the data. The majority of the observed data loss is associated with (avoidable) errors non-intrinsic to the monitoring station. Hence, it is concluded that - with proper sensor and by-pass installation operation - a data yield of more than 90% is achievable for wastewater quality monitoring with this type of sensor.

In chapter 6 the resulting wastewater quality time-series are combined with the wastewater quantity time-series studied in chapter 4 to produce pollutant load time-series. This allows for a study of pollutant loads arriving at the wwtp Eindhoven.

Chapter 6. Wwtp Eindhoven influent analysis

6.1 Introduction

On May 7th, 2007 a storm event occurred in the Eindhoven area. Total precipitation depth during the event was not extremely large (28 mm, the fourth largest that year), but it was the first storm event after an exceptionally long dry period lasting 41 days. During the first few hours of wet weather flow nothing unusual occurred at the wwtp Eindhoven. The morning of May 8th, however, all 12 secondary clarifiers were covered by 15-30 cm thick layers of floating sludge. Nearly 50% of the activated sludge mass was found in the secondary clarifiers, partially floating and hence introducing a risk of activated sludge spills to the river Dommel. After a week of implementing countermeasures the layers were removed; only after five to six weeks the treatment plant was back at normal operation conditions (Tauw, 2007).

The event was - after a test phase - the first storm event monitored by the UV/VIS sensors installed in the influent pumping station of the wwtp Eindhoven. The influent quality data proved to be valuable in the search for an explanation of the origin of the floating sludge layers. A hypothesis that an extreme loading to the wwtp could stand at the basis of a series of processes leading up to the floating sludge layers, could be tested and confirmed. One evaluation (Tauw, 2007) reports on May 7th a loading of 3 million population equivalents which roughly equals five times normal dry weather flow loading (577,000 p.e., see section 6.2.2). Results in this chapter (Table 6-13) show that TSS_{eq} and COD_{eq} loads have been, respectively, a factor seven and six larger than under dry weather flow conditions, constituting by far the largest mean 24-hour inflow for these pollutant parameters over the studied 1.5 year time-span.

This example shows the added value of collecting continuous and high-frequent data on influent of a wastewater treatment plant. Proper performance assessments, good modeling of processes as well as correct scenario studies for the improvement of system operation all require a detailed knowledge of the wastewater that enters the treatment plant. This chapter scrutinizes the 19-months data sets on wastewater quantity and quality of influent to the wwtp Eindhoven from the three contributing catchment areas. It utilizes the data sets as derived in chapter 3 (precipitation), chapter 4 (wastewater quantity) and chapter 5 (wastewater quality). The objective of this chapter is to study and quantify the temporal and spatial variability of the amount and composition of wastewater. A distinction is made between dry weather conditions and wet weather conditions: for the former the focus is on the derivation

of standard dry weather patterns and variations among patterns; for the latter the focus is on 24-hour peak loadings associated with storm events.

For dry weather conditions relevant time-scales are diurnal variations as well as long-term seasonal and annual variations of mean values. For wet weather conditions the considered time-scales are mainly 24-hour mean loadings. These can be used to compare wet weather to dry weather values. More short-term mean loadings (over e.g. 1 hour or 3 hours) are not considered as these are generally of minor importance to the treatment plant. Observed dry and wet weather values are confronted with design values of the wwtp Eindhoven in paragraph 6.4. *Instantaneous* short-term variations in flow and pollutant loads can be of interest to the operation of specific wet weather infrastructure. For instance, the operation of the wwtp Eindhoven stormwater storage tank (filled up in approximately one hour at the maximum wet weather flow rate) can be optimized with information on short-term fluctuations of pollutant parameters. Also, amounts and loadings of CSO spills are largely determined by short-term variations. In paragraph 6.3 for a number of storm events short-term flow and pollutant load variations are presented showing the relation with 24-hour mean values.

Paragraph 6.2 presents the results for dry weather conditions. To start with, section 6.2.1 sets the criteria for the selection of dry weather data. Then, in three consecutive sections results are presented for dry weather *flows* (6.2.2), dry weather pollutant *concentrations* (6.2.3) and dry weather pollutant *loads* (6.2.4). For flows and pollutant loads daily patterns are derived as well as pattern variations across days of the week and long-term variation of mean values. Day sums of observed flows are compared to theoretical values and differences are assessed. Day sums of pollutant loads are compared to results based on regular composite sampling at the wwtp. Also, observed time-shifts and pattern similarities between flow and pollutant concentrations are considered. Paragraph 6.3 discusses results for wet weather conditions. Criteria for wet weather data are set in section 6.3.1. An approximate number of 65 events have been selected for wet weather data analyses. Of these, three examples are given in section 6.3.2: a single large storm event, a single small storm event without dilution and a series of storms. For each example, the behavior of flow and pollutant parameters is studied. For all observed storm events peak loadings during the event to the treatment plant are calculated and plotted in section 6.3.3. Also, a brief search for a relation between the magnitude of peak load factors and possible explanatory variables is presented. The paragraph concludes with a presentation of data on the extreme loading event of May 7th, 2007. Paragraph 6.4 discusses results and gives final conclusions.

Parts of this chapter have been based on work presented in Schilperoort *et al.* (2008).

6.2 Dry weather conditions

6.2.1 Selection of data associated with dry weather conditions

For the analysis of flow and pollutant data associated with dry weather conditions a selection has been made from the quantity and quality time-series as derived in chapters 4 and 5. The selection comprises data that correctly represent the targeted flow condition, i.e. selected data must have been collected at times that any wastewater arriving at the wwtp Eindhoven has been free of stormwater. Table 6-1 presents per catchment area the system emptying time which represents the time-span needed to empty a completely full sewer system given the maximum WWF pumping capacity. After a large storm event that completely fills up all in-sewer storage, stormwater can be removed from the system within 11 hours (Eindhoven Stad), 12 hours (Nuenen/Son) and 16 hours (Riool-Zuid). In practice, the emptying time can often be shorter when in-sewer storage has only been partly filled. In contrast, values could also be larger in case the WWF pumping capacity has deliberately been reduced by the wwtp operator. In all, the values presented in Table 6-1 are considered the maximum time-span after cessation of precipitation during which the wwtp Eindhoven influent contains stormwater. It should be noted that only directly discharged stormwater is considered here; indirect discharges of stormwater through for instance groundwater infiltration are considered to be part of normal dry weather flow conditions.

Table 6-1: System emptying times based on total in-sewer storage (sum of storage in municipal systems, additional storage facilities and transport systems) and available WWF pumping capacity (difference between total pumping capacity and mean DWF).

		Riool-Zuid	Eindhoven Stad	Nuenen/Son
municipal systems[1]	[m^3]	112,000	124,000	23,000
additional storage[1]	[m^3]	70,000	-	7,000
transport systems[2]	[m^3]	65,000	-	5,000
total in-sewer storage	[m^3]	*247,000*	*124,000*	*35,000*
total pumping capacity[3]	[m^3/h]	17,710	14,000	3,290
mean DWF[4]	[m^3/h]	1,840	2,330	360
WWF pumping capacity	[m^3/h]	*15,870*	*11,670*	*2,930*
system emptying time	[h]	16	11	12

[1] see appendix C; [2] see paragraph 2-5; [3] see Table 4-1; [4] see Table 6-2

In this paragraph data are analyzed at day-scale (00h00 - 23h59). Considering the system emptying times, the selection of data associated with dry weather conditions has been done using the following definition for all three catchments:

> *if the sum of precipitation of the current and previous day is less than 0.5 mm, the current day can be considered a dry weather day.*

For a small number of days data have been disregarded due to anomalous (e.g. during maintenance or testing of pumps) or missing flow data (> 90% of data is required). The selection of dry weather data is hence primarily based on precipitation data with a subsequent plausibility check using the flow data sets. For this, the three areal precipitation data sets as derived in chapter 3 have been used: the Riool-Zuid precipitation data set for the selection of Riool-Zuid flow and pollutant data, the Eindhoven Stad precipitation data set for the Eindhoven Stad data, etc. As a result, the number of dry weather days is different for each catchment area, as can be seen in the next section.

For the dry weather flow analyses presented hereafter, results are only little sensitive to the values used in the definition of a dry weather day. In a sensitivity analysis, threshold values of 0.1 mm and 1.0 mm and time-spans without precipitation of 3 and 4 days (the current day and the previous 2, respectively 3 days) have been studied. Results show a large difference in the *number* of dry weather days (for instance, for area Riool-Zuid the largest number of dry weather days equals 211, the smallest 52), but mean flow values across the different dry weather data sets change only marginally (< 1%). For pollutant concentration data sets considered in section 6.2.3 sensitivity of results to the used dry weather definition has not been tested.

6.2.2 Dry weather flow

Dry weather flow patterns

Application of the dry weather definition on the 580-days areal inflow data sets from chapter 4 yields a total of 192 (Riool-Zuid), 175 (Eindhoven Stad) and 221 (Nuenen/Son) dry weather days. To remove data anomalies due to the high-frequent on/off switching of pumps (section 4.4.4), a moving average filter with a span of 31 minutes has been applied on the data prior to analysis. For each 2-minute interval in a day a set of flow values equal to the number of dry weather days is available. For instance, for area Riool-Zuid a set of 192 dry weather flow values is available for any 2-minute interval in a day. Plotting mean values for all 2-minute intervals in consecutive order yields daily dry weather flow patterns. Figure 6-1 presents these patterns for the three catchment areas as well as for the total flow into the wwtp Eindhoven; key values are presented in Table 6-2. For

easy comparison, all values are normalized, i.e. divided by the mean absolute value of each dry weather data set. The random error for each individual measurement (under DWF conditions) was determined at ±0.5% (see section 4.4.5). According to Smith (1997) the amount of reduction in random error is equal to the square-root of the number of points in the average. Hence, averaging over a large number of values (~200), the random error associated with the presented dry weather flow patterns becomes negligible.

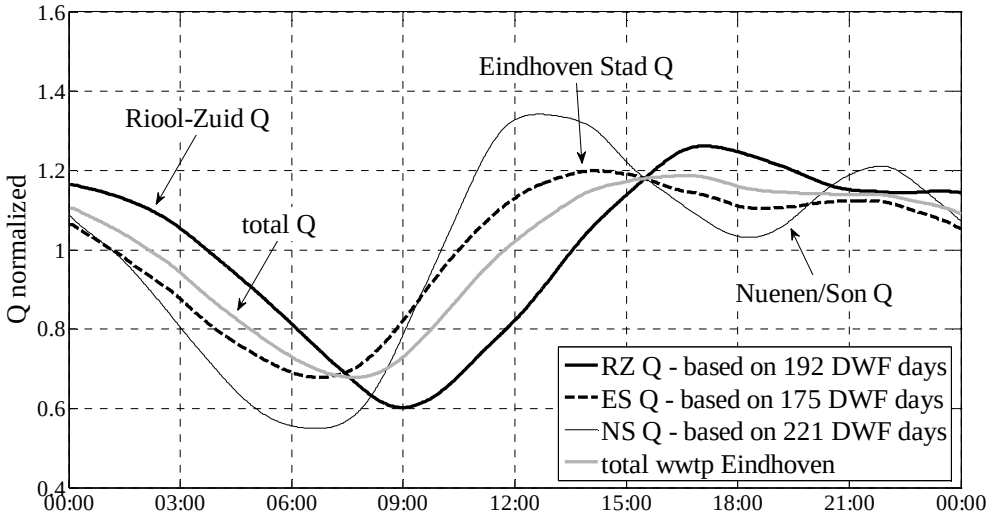

Figure 6-1: Flow patterns associated with dry weather for the three catchment areas and total flow to the wwtp Eindhoven. Values are normalized with respect to mean DWF values.

Table 6-2: Mean dry weather flow and associated minimum and maximum peak factors for catchments Riool-Zuid, Eindhoven Stad, Nuenen/Son and total inflow to the wwtp Eindhoven.

		Riool-Zuid	Eindhoven Stad	Nuenen/Son	wwtp Eindhoven
mean dry weather flow	[m^3/h]	1,840	2,330	360	4,530
peak factor: minimum	[-]	0.60	0.68	0.55	0.68
peak factor: maximum	[-]	1.27	1.20	1.34	1.19

For all three catchments a diurnal variation can be observed. The derived patterns are similar in shape to ‘standard’ textbook DWF patterns (e.g. Metcalf and Eddy, 2003; Butler and Davies, 2004), but somewhat delayed in time due to the relatively long transportation times (compared to the areas used in the textbook examples). The delay becomes larger with increasing wastewater transportation times.

Minimum flows are observed between 06h00 and 09h00; maximum values are recorded between 13h00 and 17h00. Despite the rather different lay-outs, the phase-shift between the flow patterns of Riool-Zuid and Eindhoven Stad is only small (2 to 3 hours, or roughly a tenth of the daily cycle). Mean transportation times from both areas do not largely differ, which can be understood considering the fact that major contributors to the Riool-Zuid system (Geldrop, Veldhoven, Aalst) are situated relatively close to the treatment plant, with transportation times comparable to those from several Eindhoven Stad districts (see Figure 2-4). Due to this small phase-shift and due to the fact that Riool-Zuid and Eindhoven Stad contribute about 90% of wwtp influent, total inflow to the wwtp also follows a diurnal variation with minimum values around 08h00 and maximum values around 16h00 and with similar peak factors, see Table 6-2.

Peak factors reduce with increasing catchment size. The smallest area (Nuenen/Son) shows a daily minimum of 55% and a daily maximum of 134% of mean dry weather flow whereas values for the largest area Eindhoven Stad are 68% and 120%, respectively. This catchment size effect has its origin in a combination of factors. Most important factor is the number of connections with their associated transport times: the larger the catchment, the larger the number of connections with a wider range of transport times which leads to a larger smoothing of peak values. Metcalf and Eddy (2003) mention the economic and social makeup of a community that often changes with its size: smaller communities often show a more uniform discharge pattern whereas in larger cities economic activities with a 24-hour continuity are not uncommon. Also, longer mean transport times in large catchments allow for a continued dispersion of peak flows. The observed peak values for the three catchment areas in the Eindhoven area are of the same order as for catchment areas of similar sizes found in literature (e.g. CIRIA, 1998; Krebs *et al.*, 1999a).

Comparing DWF mean values with other sources it should be noted that values in Table 6-2 are 24-hour means. Other sources may have a different definition of ‘mean DWF value’. For instance, van der Graaf (1995) mentions a representative DWF value of wwtp influent that is calculated dividing total day sum by 12 or 14, depending on the catchment size.

Observed vs. theoretical DWF

Mean observed dry weather flows are again presented in Table 6-3. As earlier stated, these values are the arithmetic mean values of the complete dry weather data sets. For instance, the Riool-Zuid value is the mean of a total of 192 x 720 values (respectively the number of selected dry weather days and the number of 2-minute intervals in a day). The table further presents the theoretical dry weather flows. These are based on the number of inhabitants in the area plus population

equivalents (p.e.) for industrial activities (see appendix C). Inhabitants represent roughly two thirds of the total sum, industrial sources one third. Total p.e. have been multiplied by the mean drinking water consumption per inhabitant in the Netherlands of 0.130 $m^3/(d \cdot p.e.)$ (de Moel *et al.*, 2004) and divided by 24 to obtain values in m^3/h. Differences between theoretical and observed DWF are roughly 25% (for Riool-Zuid and Nuenen/Son) and 40% (for Eindhoven Stad) which results in a 31% difference for the total inflow to the wwtp Eindhoven.

Table 6-3: Observed mean versus theoretical dry weather flows for the three catchment areas and wwtp Eindhoven. See text for calculation details.

	observed mean DWF[1] [m^3/h]	p.e.[2] [#]	theoretical DWF [m^3/h]
Riool-Zuid	1,840	257,000	1,390 (-24%)
Eindhoven Stad	2,330	268,000	1,450 (-38%)
Nuenen/Son	360	52,000	280 (-23%)
wwtp Eindhoven	4,530	577,000	3,130 (-31%)

[1] see Table 6-2; [2] see appendix C

The observed differences could be (partly) explained by a discrepancy between the *administrative* number of population equivalents in the area (as reported in Table 6-3) and the *actual* number of p.e. The latter number is derived using data from a data set holding the results of 24-hour flow proportional composite samples collected for 5 randomly selected days each month. The number of p.e. are calculated assuming a constant pollutant load per population equivalent. Samples are taken from the mixing flume in the influent pumping station and hence represent mean wwtp influent. Of a total of 96 samples (for April 1st, 2007 - November 1st, 2008) a total of 28 samples are associated with dry weather conditions. For each dry weather sample the population equivalent has been calculated using (van der Graaf, 1995):

$$p.e. = Q(COD + 4.57N_{kj})/136 \qquad (6.1)$$

with: p.e. = population equivalent [#];
Q = flow [m^3/d];
COD = chemical oxygen demand [mg O_2/L];
N_{kj} = Kjeldahl nitrogen [mg N/L];
136 = mean daily total oxygen demand per inhabitant [g O_2/d].

Results show a variation between 400,000 and 750,000 p.e. with a mean value of 580,000 p.e. Considering the near-identical administrative p.e. value in Table 6-3

(577,000 p.e. for wwtp Eindhoven) it can be concluded that administrative p.e. values correspond well to actual p.e. values based on Kjeldahl and COD measurements. Hence, the aforementioned discrepancy is not apparent and does not explain the differences between observed and theoretical DWF.

Another possible explanation for the differences between observed and theoretical dry weather flows is a larger contribution of wastewater from industrial sources than assumed in the calculation of theoretical values. Administration on industrial discharges (e.g. discharge permits) generally holds information on population equivalents based on pollutant loads instead of based on wastewater quantity. As a result, the *amount* of wastewater from these sources can be (much) larger than the earlier assumed 0.130 $m^3/(d \cdot p.e.)$. A further explanation is a possible contribution of infiltration and inflow (I/I) of groundwater and other water sources in the dry weather flow. Assuming infiltration and inflow stems from relatively clean water sources it enlarges wastewater quantity but does not add pollutant loads to the dry weather flow arriving at the wwtp. Many studies have shown that a fraction of 20% to 40% of extraneous flows in dry weather flow is not uncommon (e.g. Weiß *et al*., 2002).

Long-term variations and seasonality of dry weather flow

Seasonal variation of mean dry weather flows has often been observed. Metcalf and Eddy (2003) describe a relation with a change in drinking water consumption during a holiday season that results in an *increase* in wastewater production for e.g. resort areas. For the same season a *decrease* in flows can also be observed following a decline in residential and industrial activities. Thackray *et al*. (1978, cited in Butler and Davies, 2004) found that WC flushing decreases in summer whereas bathing and showering increases. According to Butler and Davies (2004) overall summer dry weather flows typically exceed winter flows by 10-20% mainly due to changes in domestic wastewater production.

The Eindhoven area dry weather flow data have been studied for long-term variations and possible seasonality. Figure 6-2 presents the DWF day sums of wastewater from catchment area Riool-Zuid for the time-span April 1st, 2007 - November 1st, 2008, normalized with respect to their mean value (≈ 44,000 m^3/day). In Table 6-4 key values can be found: the minimum and maximum values in the data set as well as the 5% and 95% percentiles. The latter values are included since these give a better representation of the variation of day sums than the former values. It can be observed that DWF day sums vary over the year: minimum values of roughly 80% to 90% of the yearly mean are mostly observed towards the end of summer (September/October) and maximum values of roughly 110% to 120% of the yearly mean are mostly observed towards the end of winter (March/April).

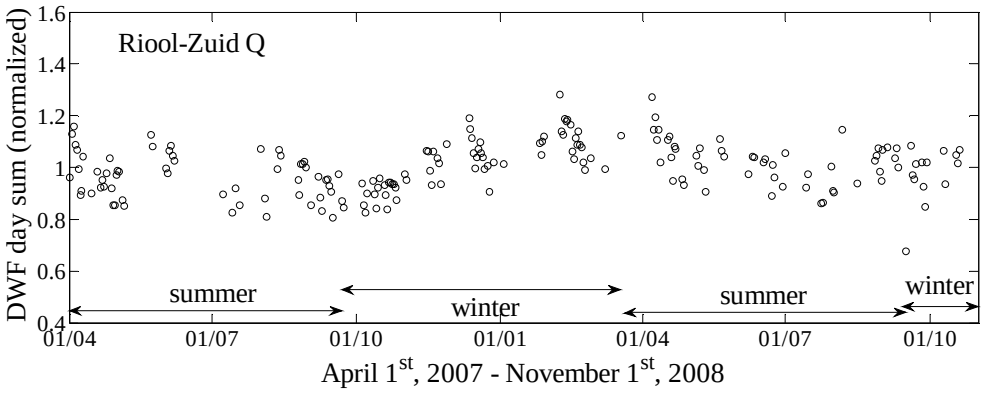

Figure 6-2: Dry weather flow day sums from catchment Riool-Zuid normalized to the mean value (≈ 44,000 m^3/day).

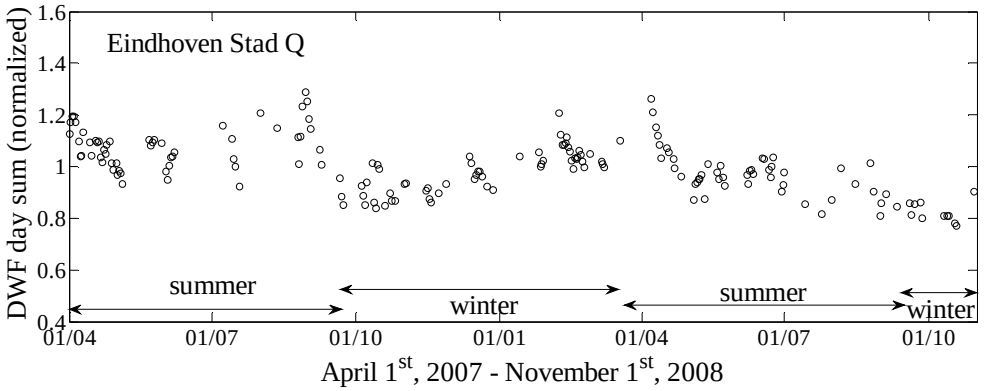

Figure 6-3: Dry weather flow day sums from catchment Eindhoven Stad normalized to the mean value (≈ 56,000 m^3/day).

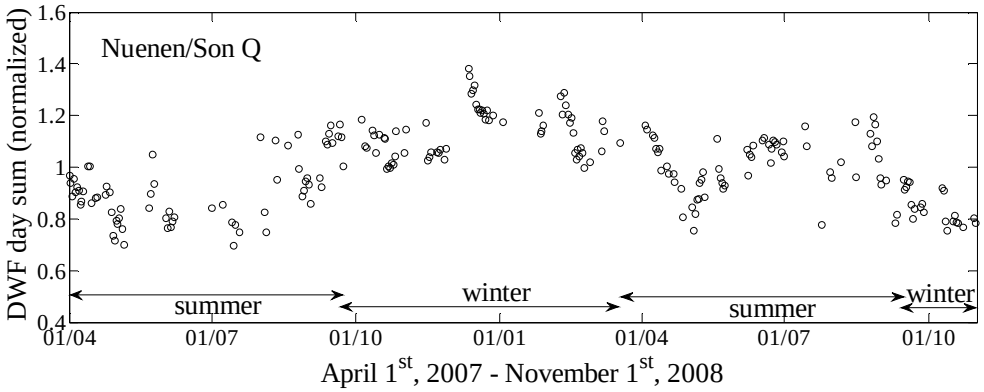

Figure 6-4: Dry weather flow day sums from catchment Nuenen/Son normalized to the mean value (≈ 8,600 m^3/day).

Table 6-4: Long-term variation of normalized dry weather flow day sums: the minimum and maximum values and the 5% and 95% percentiles over the time-span April 1st, 2007 - November 1st, 2008.

	Riool-Zuid	Eindhoven Stad	Nuenen/Son
number of days in data set	192	175	221
minimum	0.68	0.77	0.70
5% percentile	0.85	0.82	0.77
95% percentile	1.15	1.19	1.22
maximum	1.28	1.29	1.38

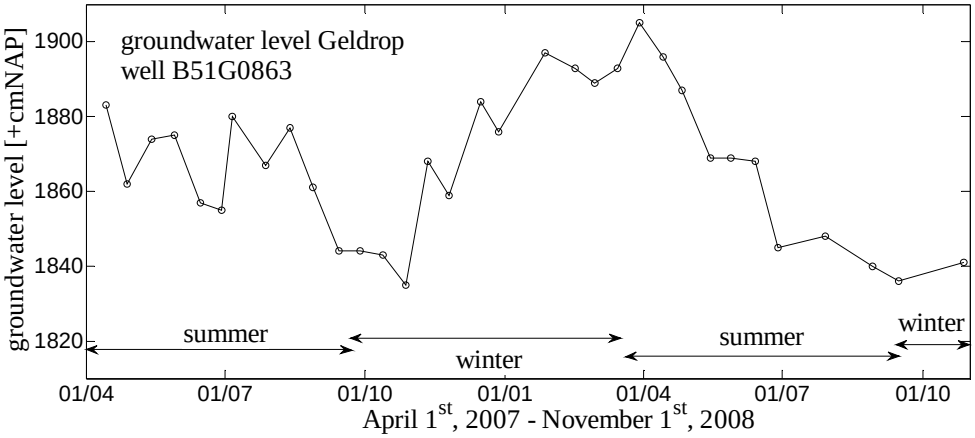

Figure 6-5: Groundwater levels in Geldrop (catchment area Riool-Zuid) for well B51G0863 (TNO, 2010).

The timing of minimum and maximum values hints at a relation with groundwater levels: the graph is somewhat similar to typical groundwater level variations in the studied area. Figure 6-5 presents an example for the groundwater level in a well in Geldrop (in the Riool-Zuid catchment area) with a shape comparable to the dry weather flow data. The association is based on the notion that higher groundwater levels may lead to an increase in infiltration of groundwater into sewer systems, but only if the groundwater table lies above invert levels. Low groundwater levels are typically found towards the end of summer after a prolonged precipitation deficit whereas high groundwater tables can be observed towards the end of winter when a precipitation surplus has refilled groundwater stocks.

The DWF day sums arriving at the wwtp Eindhoven from catchment Nuenen/Son are presented in Figure 6-4 with key values again in Table 6-4. Also in this area winter DWF day sums tend to be larger than their summer equivalents. There are, however, two differences compared to the Riool-Zuid results in Figure 6-2. Firstly,

the long-term variation of DWF day sums for Nuenen/Son is larger than for Riool-Zuid: the 5% and 95% percentiles are, respectively, about 8% smaller and 7% larger than Riool-Zuid values. Again, the smallest catchment area is associated with the largest peak factors, suggesting that a catchment size effect is also present in the long-term variation of dry weather flow day sums. Secondly, during the summer of 2008 relatively large dry weather day sums are recorded instead of gradually decreasing values. During the summer of 2007 these large values are not observed. The latter phenomenon shows that, besides seasonal variations, flow conditions are also influenced by annual variations.

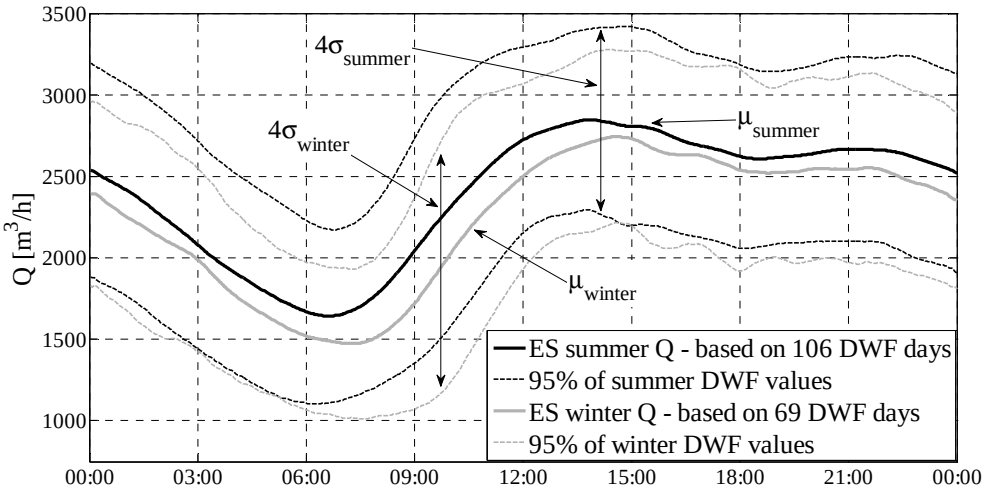

Figure 6-6: Summer and winter daily DWF patterns of flow values for wastewater from catchment area Eindhoven Stad based on data of 106 and 69 DWF days, respectively.

Results for Eindhoven Stad (Figure 6-3) show a 'typical' variation for the 2007/2008 winter values and subsequent 2008 summer values: a gradual increase in dry weather day sums in winter and a gradual decrease of values in summer. The 2007 summer values, however, deviate from typical behavior showing larger values than in the following two seasons. Apparently, also in this area annual variations are present in the dry weather flow data. Dividing the 2-minute interval Eindhoven Stad dry weather flow data set into a set associated with summer days (March 21st - September 22nd) and a set associated with winter days, DWF patterns per season can be derived, see Figure 6-6. Since the complete time-span of the flow data sets (April 1st, 2007 - November 1st, 2008) comprises roughly two summers (or 356 summer days) and one winter (or 224 winter days), summer days are better represented than winter days. The figure presents the mean values and the 4σ bands containing roughly 95% of data for both data sets. It can be observed that mean summer values are larger than mean winter values, which can be understood

considering the relatively large 2007 summer values presented in Figure 6-4. It can also be observed that the summer pattern is *shifted* in time compared to its winter counterpart. Earlier summer peak values suggest that residential and industrial activities have an earlier start in summer.

Weekday variations of dry weather flow patterns

The derived dry weather flow patterns have been studied for possible variations across days of the week. The three dry weather data sets have each been divided into 7 separate sets, each one associated with a day of the week. The results are presented in Figure 6-7 (Riool-Zuid), Figure 6-8 (Eindhoven Stad) and Figure 6-9 (Nuenen/Son) and key values are summarized in Table 6-5. Results are consistent across all three catchment areas in terms of small variations across weekdays. For each area two weekdays are plotted associated with the largest and smallest peak factors, spanning the range of values observed for weekdays. For Riool-Zuid and Nuenen/Son these days are Mondays and Thursdays, for Eindhoven Stad plotted days are Tuesdays and Fridays. Results are also consistent in terms of an observed time-shift for weekend days: in all three figures the increase in flow values in the morning is delayed on Saturdays and even more so on Sundays, suggesting ditto domestic activities. On weekdays mean dry weather flow is 1% to 3% larger than the overall mean value; on Sundays total flow is between 3% and 8% smaller. Considering Thackray *et al*. (1978, cited in Butler and Davies, 2004) and Butler (1993) who found that domestic wastewater production generally *increases* during weekends, lower total flow values during the weekend are likely due to a reduction in non-domestic activities. The absence of reject water from the sludge processing installation in Mierlo (at a rate of 325 m^3/h or roughly 15% of mean DWF) is a major contributing factor to the reduction in Riool-Zuid flow values on weekend days. For area Nuenen/Son the DWF peak value around noon increases from 1.33 on weekdays to 1.51 on weekend days suggesting a delayed, but more concentrated wastewater production on Saturdays and Sundays.

Table 6-5: Mean DWF and associated minimum and maximum daily peak factors for the complete dry weather sets as well as for weekdays, Saturdays and Sundays only.

			Riool-Zuid	Eindh. Stad	Nuenen/Son
all days	mean DWF	[m^3/h]	1,840	2,330	360
	peak factors	[min-max]	0.60 - 1.27	0.68 - 1.20	0.55 - 1.34
weekdays	mean DWF	[m^3/h]	1,900 (+3%)	2,360 (+1%)	365 (+1%)
	peak factors	[min-max]	0.61 - 1.29	0.67 - 1.19	0.55 - 1.33
Saturdays	mean DWF	[m^3/h]	1,770 (-4%)	2,280 (-2%)	365 (+1%)
	peak factors	[min-max]	0.55 - 1.24	0.64 - 1.23	0.53 - 1.51
Sundays	mean DWF	[m^3/h]	1,690 (-8%)	2,270 (-3%)	339 (-6%)
	peak factors	[min-max]	0.51 - 1.26	0.65 - 1.23	0.51 - 1.51

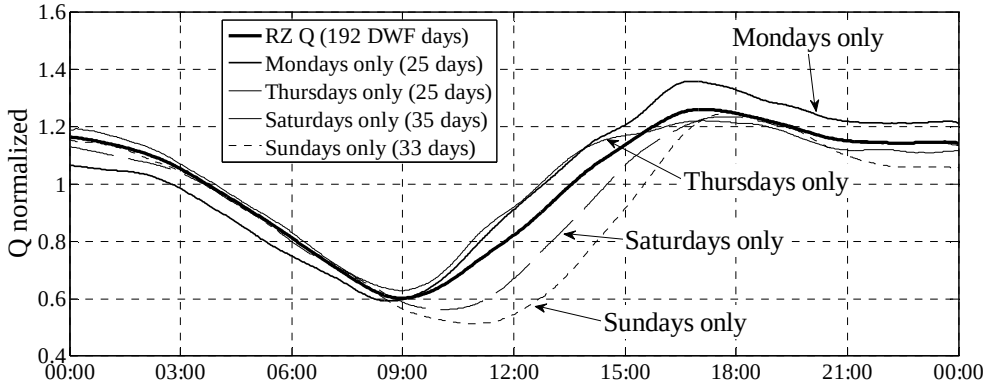

Figure 6-7: Dry weather flow patterns of wastewater from catchment area Riool-Zuid: variation across days of the week.

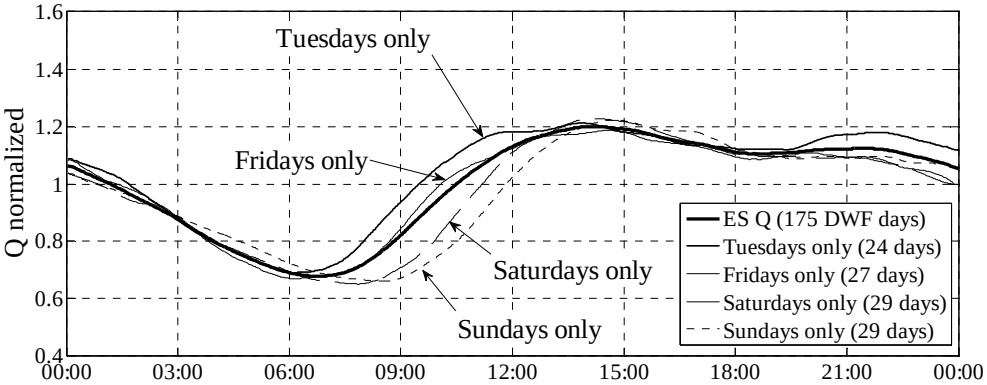

Figure 6-8: Dry weather flow patterns of wastewater from catchment area Eindhoven Stad: variation across days of the week.

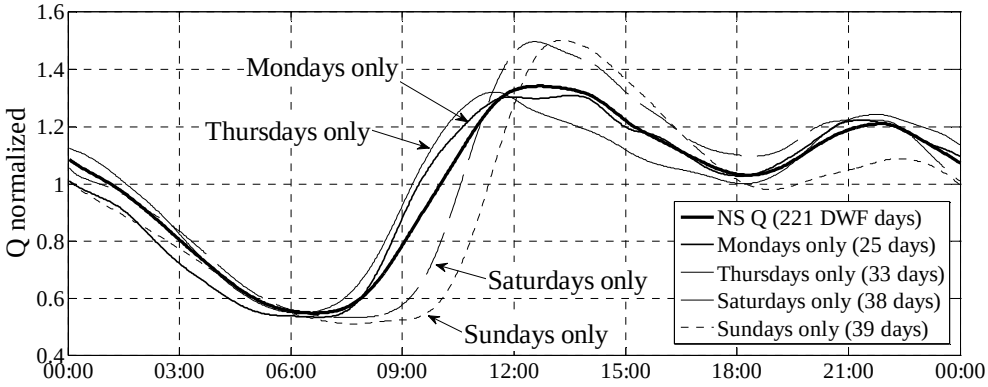

Figure 6-9: Dry weather flow patterns of wastewater from catchment area Nuenen/Son: variation across days of the week.

6.2.3 Dry weather pollutant concentrations

For a proper interpretation of pollutant measurements it should be kept in mind that parameter TSS (total suspended solids) describes the particulate content of the water which is subject to in-sewer sedimentation and resuspension processes. Parameter CODf (filtered or soluble chemical oxygen demand) is a measure for the oxygen consumption related to the presence of organic matter in the water after filtration over a 0.45 μm filter. The behavior of this parameter is hence the behavior of a dissolved pollutant. As total chemical oxygen demand is associated with both particulate as well as dissolved matter parameter COD (chemical oxygen demand) combines both characteristics. The suffix -eq indicates equivalent measurements with an optical UV/VIS sensor instead of sample laboratory analysis.

Results catchment areas Eindhoven Stad and Nuenen/Son
For the assessment of dry weather pollutant concentrations the same dry weather days as used for the assessment of flows have been studied. Application of the dry weather definition on the 580-days UV/VIS data sets yields, however, a smaller set of dry weather data than for flow. Not for all dry weather days quality data are available due to the relatively large data loss for UV/VIS data sets after data quality assessment (see paragraph 5.4). A total of 145 (Riool-Zuid), 100 (Eindhoven Stad) and 140 (Nuenen/Son) dry weather days are available for data analyses. Figure 6-10 presents the normalized mean dry weather flow patterns for catchment area Eindhoven Stad for quality parameters TSS_{eq}, COD_{eq} and $CODf_{eq}$ and (for reason of comparison) Q; key values are summarized in Table 6-6.

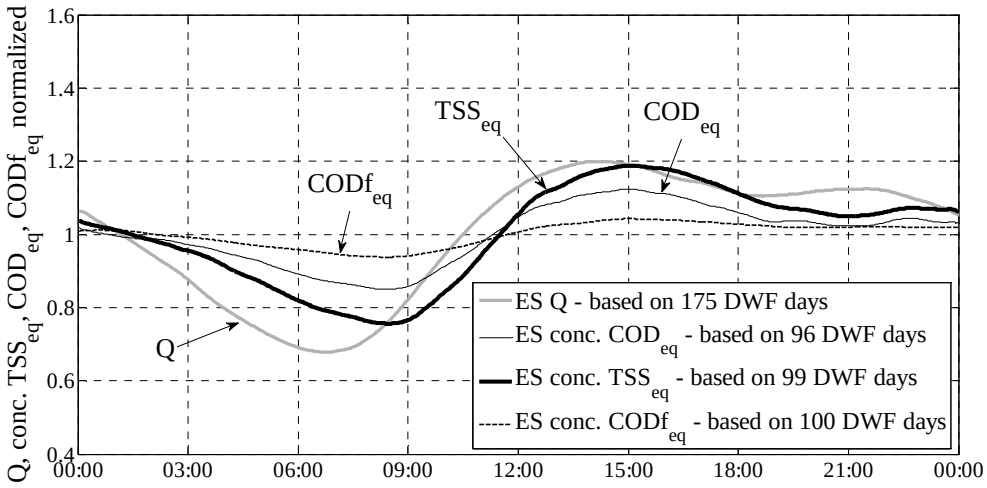

Figure 6-10: For catchment area Eindhoven Stad normalized daily patterns associated with dry weather for flow and concentration values of parameters TSS_{eq}, COD_{eq} and $CODf_{eq}$.

Table 6-6: Mean dry weather values and associated minimum and maximum peak factors for parameters Q, TSS_{eq}, COD_{eq} and $CODf_{eq}$ for catchment Eindhoven Stad.

Eindhoven Stad	Q	TSS_{eq}	COD_{eq}	$CODf_{eq}$
	[m^3/h]	[mg/L]	[mg/L]	[mg/L]
mean dry weather value	2,330	290	642	197
peak factor: minimum	0.68	0.76	0.84	0.93
peak factor: maximum	1.20	1.18	1.13	1.05

For area Eindhoven Stad, the dry weather patterns of the studied pollutant parameters show a similar diurnal variation as for flow, but with a time-shift of approximately one to two hours. Peaks are less pronounced, i.e. closer to one, especially for night-flow. $CODf_{eq}$ shows the least DWF variation over a day with peak values of 93% and 105% of the mean dry weather pollutant concentration; TSS_{eq} is associated with the largest diurnal variation with values ranging between 76% and 118%. COD_{eq}, combining the behavior of dissolved and suspended compounds, shows intermediate values. For catchment area Nuenen/Son (Figure 6-11 and Table 6-7) essentially the same results have been obtained: dry weather patterns for flow and pollutant concentrations that are similar in shape but shifted in time. For this area, however, the variation in particulate matter (TSS_{eq}) covers a larger range (62% - 145%) than for area Eindhoven Stad (76% - 118%). For dissolved pollutants a larger range of values over a day is also observed, but to a lesser extent than for TSS_{eq}. As for flow, peak factors of pollutant dry weather patterns increase with decreasing catchment size.

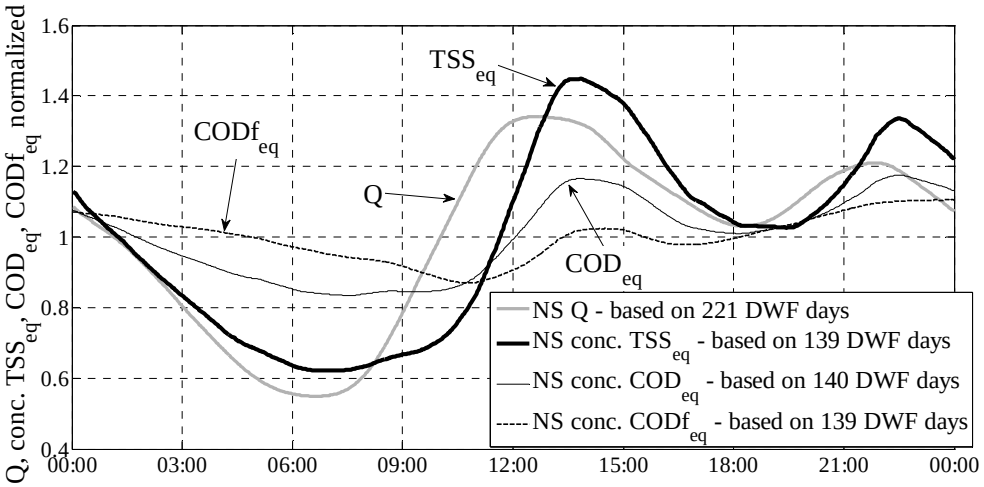

Figure 6-11: For catchment area Nuenen/Son normalized daily patterns associated with dry weather for flow and concentration values of parameters TSS_{eq}, COD_{eq} and $CODf_{eq}$.

Table 6-7: Mean dry weather values and associated minimum and maximum peak factors for parameters Q, TSS_{eq}, COD_{eq} and $CODf_{eq}$ for catchment Nuenen/Son.

Nuenen/Son	Q	TSS_{eq}	COD_{eq}	$CODf_{eq}$
	[m^3/h]	[mg/L]	[mg/L]	[mg/L]
mean dry weather value	360	176	416	193
peak factor: minimum	0.55	0.62	0.84	0.87
peak factor: maximum	1.34	1.45	1.17	1.11

Pattern similarity and time-shift

The similarity between dry weather patterns of flow and pollutant concentrations means that during dry weather conditions low flows are generally associated with relatively low pollutant concentrations and vice versa. The observed diurnal variation of pollutant parameters can be related to either at-source variations in wastewater quality and/or to one or multiple in-sewer processes that influence the pollutograph in between source and observation location. Hereafter, both influencing mechanisms are considered.

For domestic sources, Almeida *et al.* (1999) have searched for at-source diurnal variations in *concentration* values for a number of pollutant parameters using elaborate survey data in the UK. Their findings show that no "obvious diurnal pattern" can be distinguished in the pollutographs of parameters TSS and COD. Other investigations (e.g. US EPA, 1978) confirm these results. Therefore, it is concluded that at-source quality variations from domestic sources are not likely to cause the observed variations in the influent pollutographs at the wwtp Eindhoven.

A number of in-sewer processes are related to the observed variation of pollutant concentrations in wwtp influent. The first mechanism considered here is the influence of infiltration and inflow (I/I) on pollutant concentrations. Assuming that infiltration of groundwater into sewer systems is constant over short time-spans such as a day, the *relative* contribution of I/I to the total amount of wastewater is larger for low flows during the night and smaller for large flows during the day. Hence, night-flows are more diluted by the relatively clean infiltration water than day-flows, resulting in lower pollutant concentration values.

For suspended compounds a second mechanism is of importance for the realization of non-constant dry weather concentration values: *causality* between flow value variations and variations in suspended solids concentrations. An increase in flow (velocity) often stands at the basis of an increase of solids in suspension. For dry weather conditions, a fraction of suspended solids is deposited in the sewer system during lower night-flows, resulting in lower TSS concentrations at night; during the day, upon increase of flow velocities, the deposited matter (partly) erodes resulting in higher TSS concentrations for that time-span. Equations governing this effect are

for instance Velikanov's model and the Ackers-White model (Bertrand-Krajewski *et al.*, 1993; Ashley and Verbanck, 1996). These essentially relate suspended solids concentrations to mean flow velocities (or flow induced turbulence, i.e. the 'erosive' force) and particle sizes (or settling velocities, i.e. the 'depositing' force). In practice, many examples can be found of catchments that indeed show good correlations between concentrations and flow rates (e.g. Bertrand-Krajewski *et al.*, 1993), but also of catchments for which correlations are less well established (e.g. CIRIA, 1998; Krebs *et al.*, 1999a). For the Eindhoven Stad data presented in Figure 6-10 it is expected that part of the diurnal variation of TSS_{eq} concentrations can be explained by the described phenomenon. Pore water located in interstitial spaces in sewer sediments are known to contain a variety of dissolved pollutants (e.g. Ashley *et al.*, 2004). Therefore, upon resuspension of sewer sediments an increase in CODf concentrations is also expected.

Studying Figure 6-10 and Figure 6-11 it can be seen that, apart from a similarity in shape, a *time-shift* exists between the dry weather patterns of flow on one hand and pollutant concentrations on the other hand. The latter lags behind the variation of flow values by a number of hours depending on the pollutant parameter. A possible explanation for the time-shift of *dissolved compounds* lies in a phenomenon described by Krebs *et al.* (1999b) and Huisman *et al.* (2000): a wave celerity that is larger than the associated flow velocity. An upstream variation in flow values (due to the onset of a storm event, or in the present case due to the diurnal DWF variation) translates relatively quickly into a downstream variation of flow (as the process is dictated by the relatively large wave celerity), but translates relatively slowly into a variation of dissolved pollutant concentrations (as this process is dictated by the actual advection of the water body, i.e. the relatively small flow velocity). As a result, at a downstream location a flow increase can be noticed before the associated pollutant concentration increase. The fine fraction of TSS_{eq} (< 45 μm) that generally remains in suspension and hence can act as a dissolved compound is likely also influenced by this mechanism. The observed time-shift for *total suspended solids* is unexpected considering the earlier described relation between flow and suspension of particles: the highest concentration of particles is expected to coincide with the highest flow rate and not to lag one to two hours *behind* peak flows. Clemens (1988) describes an adaptation effect in the dynamics of suspension transport that could (partly) bridge the discrepancy: after a change in flow rate an adaptation time is required to reach the new suspension equilibrium.

Results catchment area Riool-Zuid

For Riool-Zuid deviating dry weather patterns for pollutant concentrations can be distinguished, see Figure 6-12. As earlier presented in Figure 6-1 flow follows a typical dry weather curve, but the patterns for the quality parameters exhibit a particular shape. A clear night minimum is lacking and around noon a sharp

increase in concentration values is observed that lasts for several hours. Then, around 18h00 a local minimum is reached. The peak is due to the arrival of an amount of highly polluted reject water from the wwtp sludge processing installation. The installation is located in Mierlo at approximately 7 km from the treatment plant (see Figure 2-4). At the installation the sludge is centrifuged for dewatering; the centrate is discharged at a mean rate of approximately 325 m^3/h into the Mierlo sewer system and hence directed back towards the wwtp Eindhoven. The installation is in full-time operation, but discharging centrate to the sewer system occurs only during working days (Monday through Friday) and working hours (08h00 - 16h00). As a result, every morning around 08h00 the night stock of centrate is spilled, arriving at the wwtp about 4 hours later which clearly shows in the quality parameter patterns. On days without centrate discharges (i.e. on weekend days) no peaks in pollutant concentrations are observed, see Figure 6-13 for the example of parameter TSS_{eq}. The weekend pattern more closely resembles the quality parameter patterns found for the other two catchment areas, except for the local minimum around 18h00, which is present on both weekend and week days. A proper explanation for this reduction in concentrations has not been found.

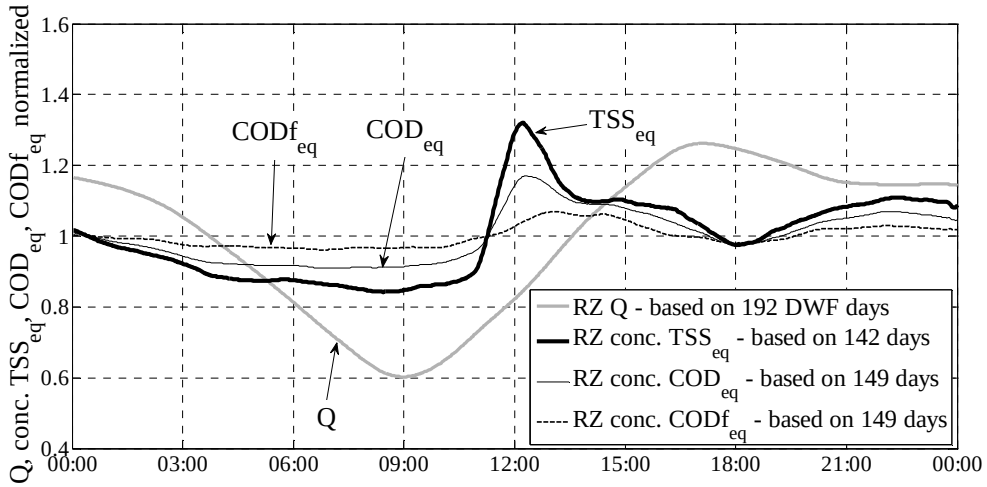

Figure 6-12: For catchment area Riool-Zuid normalized daily patterns associated with dry weather for flow and concentration values of parameters TSS_{eq}, COD_{eq} and $CODf_{eq}$.

Table 6-8: Mean dry weather values and associated minimum and maximum peak factors for parameters Q, TSS_{eq}, COD_{eq} and $CODf_{eq}$ for catchment Riool-Zuid.

Riool-Zuid	Q	TSS_{eq}	COD_{eq}	$CODf_{eq}$
	[m^3/h]	[mg/L]	[mg/L]	[mg/L]
mean dry weather value	1,840	231	675	258
peak factor: minimum	0.60	0.83	0.90	0.96
peak factor: maximum	1.27	1.33	1.17	1.08

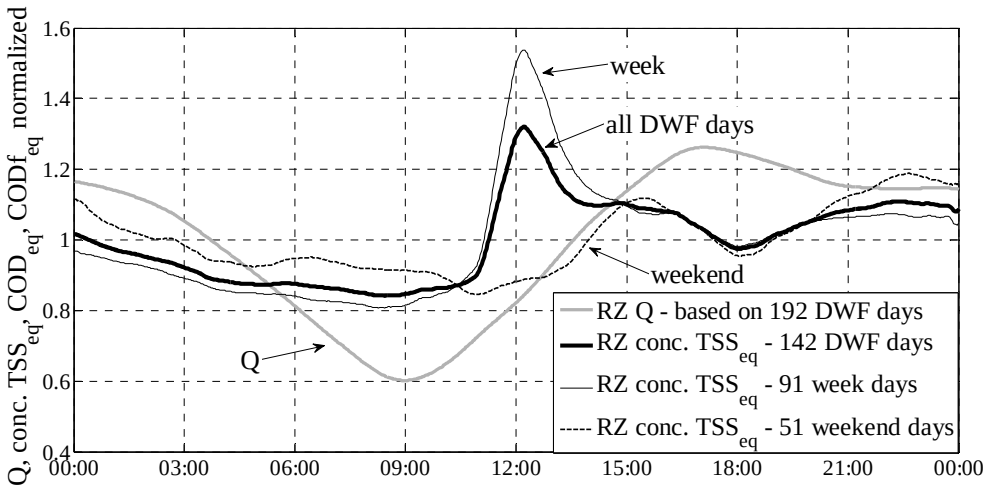

Figure 6-13: For catchment area Riool-Zuid normalized daily patterns associated with dry weather for flow and concentration values of parameter TSS_{eq} for all DWF days, week days only and weekend days only.

6.2.4 Dry weather pollutant loads

Dry weather pollutant load patterns

The combination of the (measured) flow data sets and (measured) pollutant concentrations data sets yields (calculated) pollutant loads data sets. The dynamics of the dry weather patterns of pollutant loads are hence a combination of the dynamics in the associated flow and pollutant concentration patterns. Figure 6-14, Figure 6-15 and Figure 6-16 present, respectively, for catchment areas Riool-Zuid, Eindhoven Stad and Nuenen/Son the normalized dry weather daily patterns for pollutant loads of TSS_{eq}, COD_{eq} and $CODf_{eq}$ as well as for flow. Please note that the vertical axis in the figure for Nuenen/Son has a larger range than the other figures to be able to fit all data. Key values of the presented graphs can be found in Table 6-9.

The normalized dry weather variation of pollutant loads is consistently larger than its equivalent for flow values. This, in combination with the (near-)simultaneity of peak values, leads to the in the previous section observed variations in pollutant concentrations. For quality parameters with limited daily concentration variations (such as RZ $CODf_{eq}$) load variations are dominated by flow variations. Hence, flow and load patterns are nearly identical. With increasing variations in concentration values, however, these become more apparent in the derived load patterns. For instance, the large TSS_{eq} and COD_{eq} concentration peaks for Riool-Zuid around 12h00 (see Figure 6-13) are recognizable in the load patterns, but are not associated with the maximum daily loads. Peak loads for this area are found around 17h00

when pollutant concentrations are lower than during the peak at 12h00, but flow has increased relatively more.

Dissolved compounds generally show the least DWF variation over a day whereas normalized dry weather variations of suspended solids are significantly larger than flow variations. The earlier discussed catchment size effect dictates that peak values in daily DWF patterns increase with decreasing catchment size. The effect was observed for flow values (section 6.2.2) as well as for pollutant concentrations (section 6.2.3). Logically, the phenomenon is also visible for the observed daily load patterns, leading to relatively large peak values for pollutant loads originating from the smallest catchment area Nuenen/Son and vice versa.

Table 6-9: Mean dry weather flow, pollutant fluxes and associated minimum and maximum peak factors for catchments Riool-Zuid, Eindhoven Stad, Nuenen/Son and total inflow to the wwtp Eindhoven.

		Riool-Zuid	Eindhoven Stad	Nuenen/Son	wwtp Eindhoven
Q	mean DWF [m^3/h]	1,840	2,330	360	4,530
	peak factors [-]	0.60 - 1.27	0.68 - 1.20	0.55 - 1.34	0.68 - 1.19
TSS_{eq}	mean DWF [kg/h]	432	691	69	1,191
	peak factors [-]	0.50 - 1.31	0.52 - 1.39	0.32 - 1.85	0.50 - 1.34
COD_{eq}	mean DWF [kg/h]	1,247	1,550	156	2,953
	peak factors [-]	0.55 - 1.28	0.58 - 1.33	0.45 - 1.51	0.58 - 1.27
$CODf_{eq}$	mean DWF [kg/h]	473	467	71	1,011
	peak factors [-]	0.59 - 1.25	0.64 - 1.25	0.53 - 1.34	0.61 - 1.21

Adding the contributions of the three inflows, Figure 6-17 presents normalized daily DWF patterns for flow and pollutant loads to the wwtp Eindhoven. Key values can be found in Table 6-9. The variation of total flow and pollutant loads to the wwtp is of the same order of magnitude as its two main contributaries Riool-Zuid and Eindhoven Stad. This is due to the (near-)simultaneity of peaks in flows and loads from the two catchment areas. Despite the mixing with wastewater from Eindhoven Stad and Nuenen/Son the peak load due to the arrival of reject water from the sludge processing installation can still be distinguished in the TSS_{eq} graph.

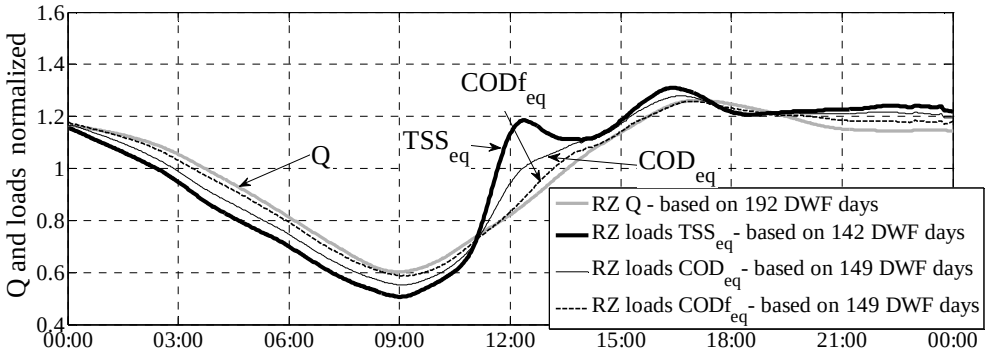

Figure 6-14: For catchment area Riool-Zuid normalized daily patterns associated with dry weather for flow and pollutant loads of parameters TSS_{eq}, COD_{eq} and $CODf_{eq}$.

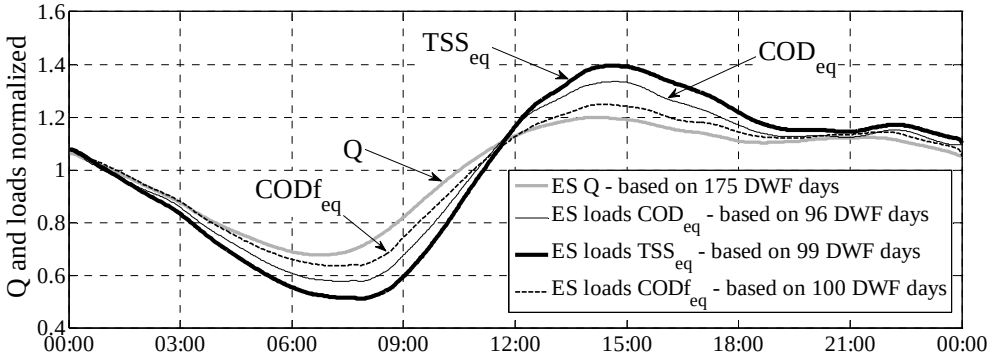

Figure 6-15: For catchment area Eindhoven Stad normalized daily patterns associated with dry weather for flow and pollutant loads of parameters TSS_{eq}, COD_{eq} and $CODf_{eq}$.

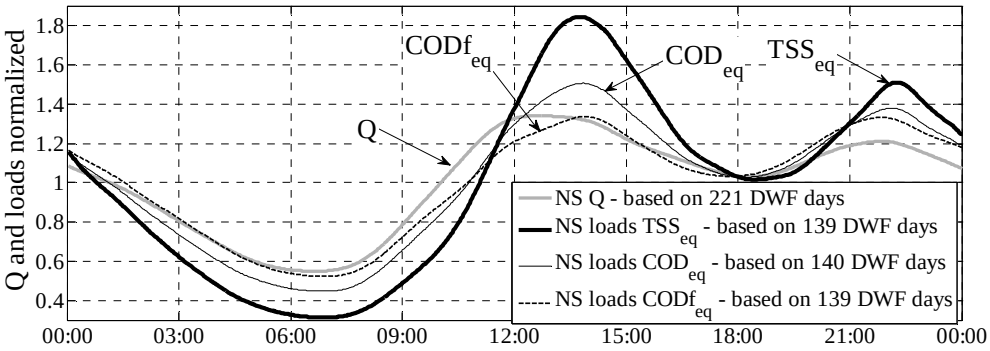

Figure 6-16: For catchment area Nuenen/Son normalized daily patterns associated with dry weather for flow and pollutant loads of parameters TSS_{eq}, COD_{eq} and $CODf_{eq}$.

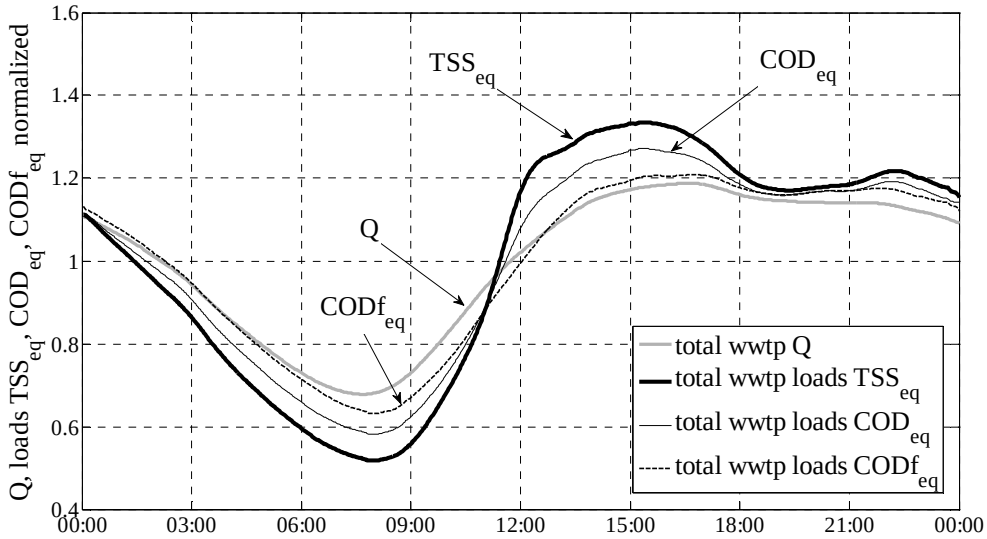

Figure 6-17: For total inflow to wwtp Eindhoven normalized daily patterns associated with dry weather for flow and pollutant loads of parameters TSS_{eq}, COD_{eq} and $CODf_{eq}$.

Long-term variations and seasonality of dry weather pollutant loads

The Eindhoven area dry weather pollutant load data sets have been studied for long-term variations and possible seasonality. For this, dry weather day sums of pollutant loads TSS_{eq} COD_{eq} and $CODf_{eq}$ have been calculated and plotted chronologically. Figure 6-18, Figure 6-19 and Figure 6-20 present results for parameter TSS_{eq}, results for $CODf_{eq}$ can be found in Figure 6-21, Figure 6-22 and Figure 6-23. Key values can be found in Table 6-10. All values are normalized with respect to their DWF mean values, see Table 6-9. The 5% and 95% percentile values are again considered the best representation of the long-term variation of pollutant load day sums; minimum and maximum values of each data set are also given in the table.

All graphs show a long-term variation of dry weather pollutant load day sums. TSS_{eq} day loads from Riool-Zuid and Eindhoven Stad vary between roughly 70% and 150% of their annual mean value. These percentages are larger than their flow equivalents (roughly 80% and 120%, respectively). For Nuenen/Son, the smallest catchment, the range of values is larger: 40%-160%. This suggests that, as observed for DWF day sums, the long-term variation of pollutant load day sums is also affected by a catchment size effect. Contrary to the observation for flow values, the TSS_{eq} graphs do not show a seasonal pattern: the magnitude of the pollutant load day sum does not seem to depend on the season. For the Eindhoven Stad results a cluster of relatively large values can be observed in the beginning of the

data set; possibly, a relation exists with the relatively long dry period during the time-span April 1st, 2007 - May 6th, 2007.

Results for parameter $CODf_{eq}$ show a narrower variation: for all catchments values range between approximately 80% and 120-130%. Hence, $CODf_{eq}$ variations are comparable to those associated with long-term flow variations. Especially for the Eindhoven Stad results a seasonal variation is apparent for this parameter: smaller day sums are generally found towards the end of summer whereas larger day sums can be found towards the end of winter. This suggests a temperature relation as in-sewer wastewater temperatures are importantly influenced by the temperature of the surrounding soils that reach their maximum at the end of summer and their minimum towards the end of winter. Possibly, higher wastewater temperatures in summer lead to a larger in-sewer transformation rate and subsequent lower CODf concentration in wwtp influent. Further notable for this parameter is the fact that the largest variations are *not* associated with the smallest catchment area; instead, day sums from Eindhoven Stad show the largest range, but differences among areas are small.

Table 6-10: Long-term variation of normalized dry weather flow and pollutant load day sums: the minimum and maximum values and the 5% and 95% percentiles over the time-span April 1st, 2007 - November 1st, 2008.

		Riool-Zuid	Eindhoven Stad	Nuenen/Son
Q	number of days in data set	192	175	221
	5% percentile (minimum)	0.85 (0.68)	0.82 (0.77)	0.77 (0.70)
	95% percentile (maximum)	1.15 (1.28)	1.19 (1.29)	1.22 (1.38)
TSS_{eq}	number of days in data set	142	99	139
	5% percentile (minimum)	0.66 (0.46)	0.69 (0.45)	0.39 (0.33)
	95% percentile (maximum)	1.55 (2.23)	1.45 (1.55)	1.58 (2.94)
COD_{eq}	number of days in data set	149	96	140
	5% percentile (minimum)	0.75 (0.66)	0.77 (0.67)	0.70 (0.62)
	95% percentile (maximum)	1.29 (1.42)	1.28 (1.32)	1.30 (1.48)
$CODf_{eq}$	number of days in data set	149	100	139
	5% percentile (minimum)	0.81 (0.71)	0.77 (0.72)	0.83 (0.75)
	95% percentile (maximum)	1.21 (1.43)	1.28 (1.38)	1.20 (1.30)

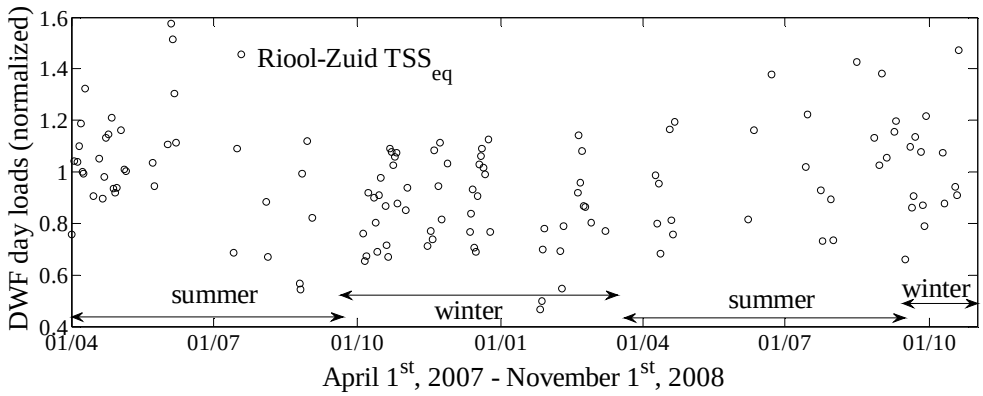

Figure 6-18: Dry weather TSS_{eq} pollutant load day sums from catchment area Riool-Zuid normalized to the mean value (≈ 10,350 kg).

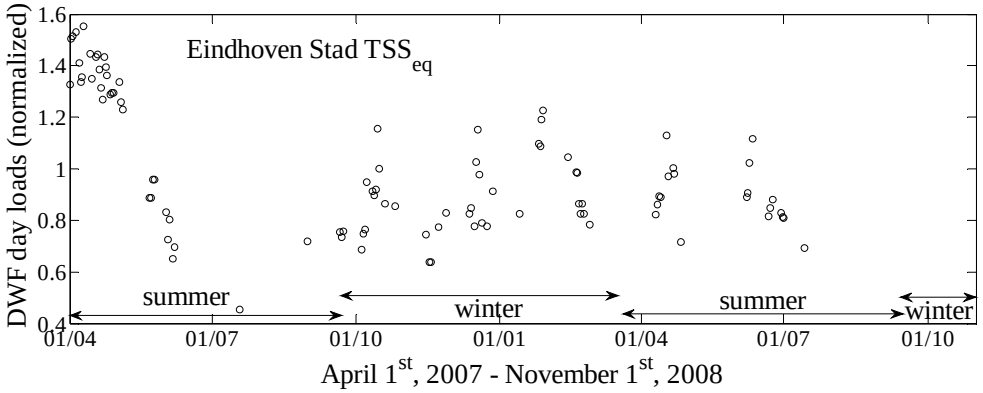

Figure 6-19: Dry weather TSS_{eq} pollutant load day sums from catchment area Eindhoven Stad normalized to the mean value (≈ 16,580 kg).

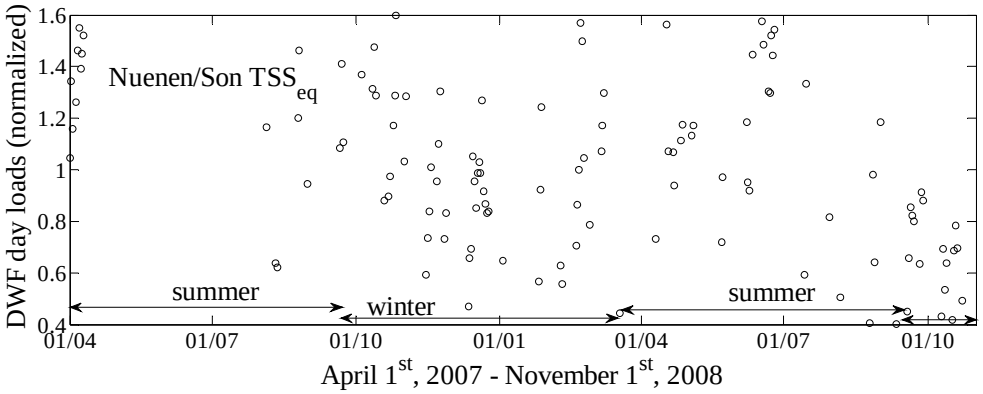

Figure 6-20: Dry weather TSS_{eq} pollutant load day sums from catchment area Nuenen/Son normalized to the mean value (≈ 1,660 kg).

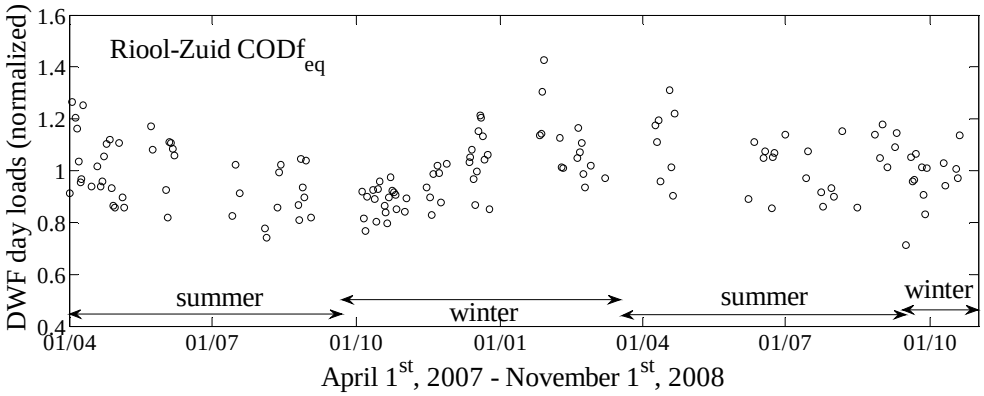

Figure 6-21: Dry weather $CODf_{eq}$ pollutant load day sums from catchment area Riool-Zuid normalized to the mean value (≈ 11,350 kg).

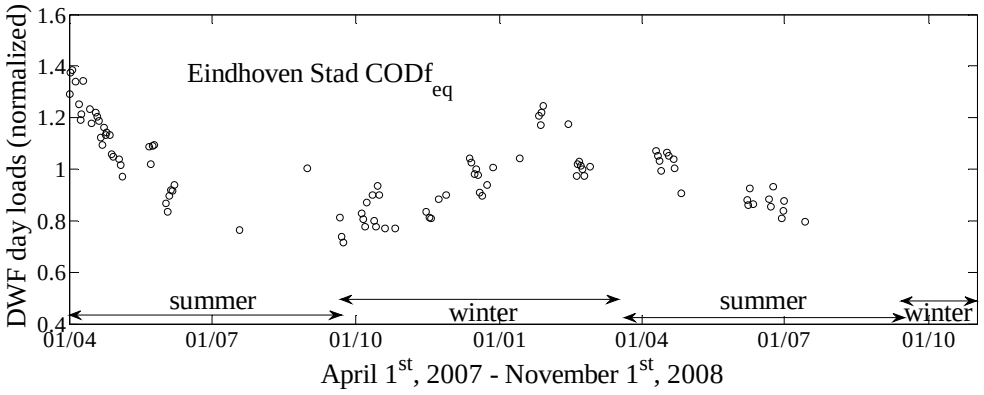

Figure 6-22: Dry weather $CODf_{eq}$ pollutant load day sums from catchment area Eindhoven Stad normalized to the mean value (≈ 11,210 kg).

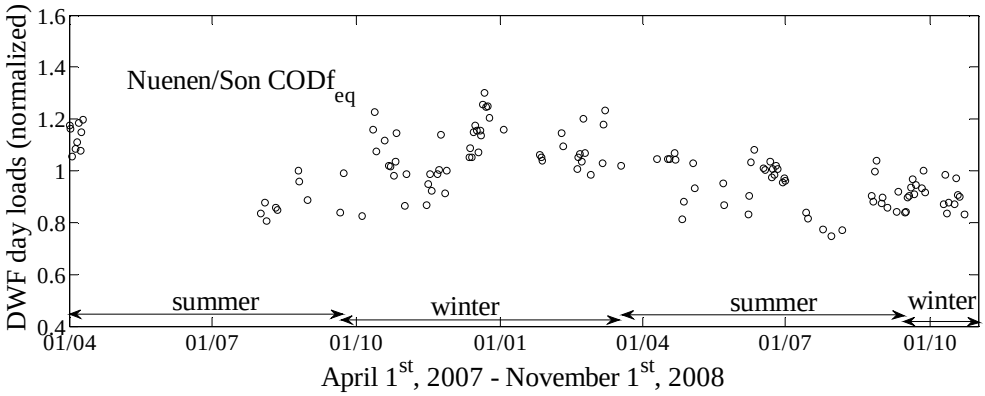

Figure 6-23: Dry weather $CODf_{eq}$ pollutant load day sums from catchment area Nuenen/Son normalized to the mean value (≈ 1,700 kg).

Weekday variations of dry weather pollutant load patterns
The derived dry weather pollutant load patterns have been studied for possible variations across days of the week. For this, the dry weather data sets have been divided into 7 separate sets, each one associated with a day of the week. The results for parameter TSS_{eq} are presented in Figure 6-24 (Riool-Zuid), Figure 6-25 (Eindhoven Stad) and Figure 6-26 (Nuenen/Son). Please note that in Figure 6-24 and Figure 6-26 the range of the vertical axis is larger than in other figures to fit all data. Key values for all parameters are summarized in Table 6-11.

For catchment area Riool-Zuid large differences can be observed between the TSS_{eq} load patterns for various days of the week. On average, total loads for weekdays are roughly 9% larger than the overall mean value (i.e. the mean of all dry weather days) whereas total loads for weekend days are about 15% to 18% smaller. This is equal to results for flow values in this area: weekday flow values are larger than weekend day flow values, see Table 6-5. In absolute terms, the difference in pollutant load flux between week and weekend days adds to about 110 kg TSS_{eq} per hour or 2,600 kg per day. According to de Jonge (2009) the Mierlo sludge processing installation discharges on weekdays roughly 2,000 kg TSS per day; the observed difference is hence largely attributable to the functioning of the Mierlo plant. Differences can also be observed across weekdays. Mondays generally show the largest values (both in terms of mean loads and peak factors), Thursdays the smallest and other week days show intermediate values. The large values on Mondays again have a probable relation with the operation of the sludge installation in Mierlo: on Mondays the entire weekend stock of reject water is discharged whereas on other weekdays only the night stock is added. A final observation for the Riool-Zuid data is the delay in onset of the morning increase in pollutant loads. Similar to flow (see Figure 6-7) the increase is delayed by approximately 1.5 hours on Saturdays and 2 hours on Sundays. Results for parameters COD_{eq} and $CODf_{eq}$ are similar in terms of differences between week days and weekend days as well as differences across week days, but relative deviations from mean values and peak factors are smaller, see Table 6-11.

For catchment area Eindhoven Stad differences across days of the week are less pronounced, see Figure 6-25. Week days do not differ much from weekend days in terms of mean dry weather loads. Again, this is in agreement with results for flow values for which weekend day values were only marginally smaller than weekday values. Fridays are the exception to this observation: on this day mean loads are on average 9% smaller than the dry weather mean value. Again similar to the flow graphs (see Figure 6-8) for weekend days a time-shift occurs and peak values around 14h00 are slightly higher than on other days.

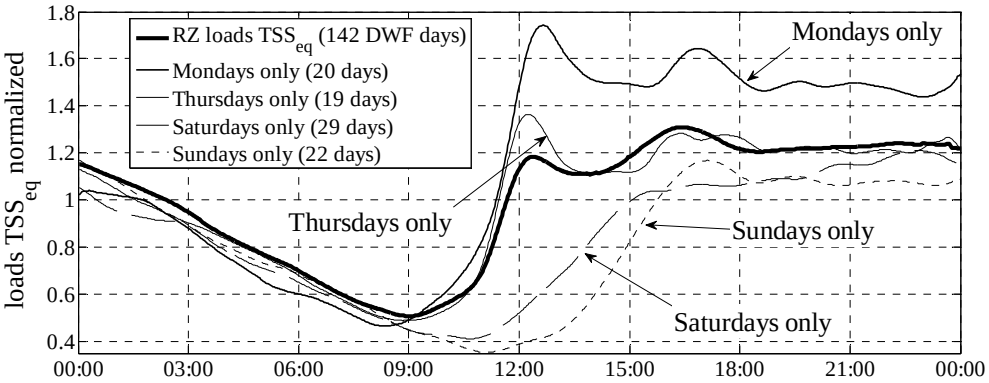

Figure 6-24: Dry weather pollutant load patterns for parameter TSS_{eq} of wastewater from catchment area Riool-Zuid: variation across days of the week.

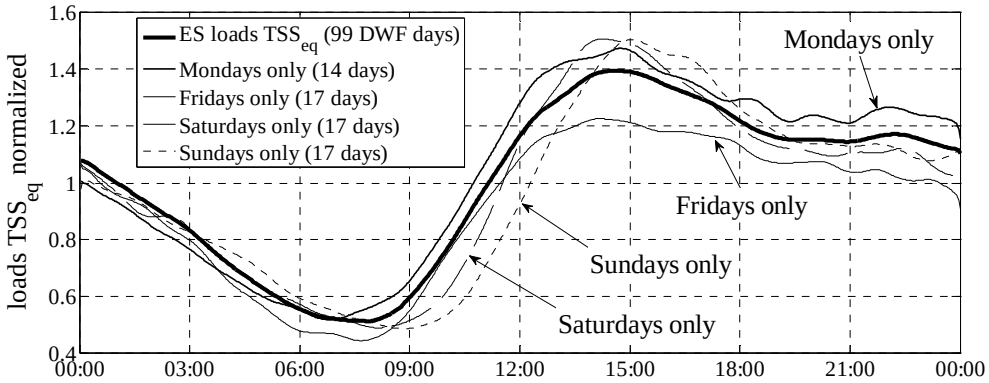

Figure 6-25: Dry weather pollutant load patterns for parameter TSS_{eq} of wastewater from catchment area Eindhoven Stad: variation across days of the week.

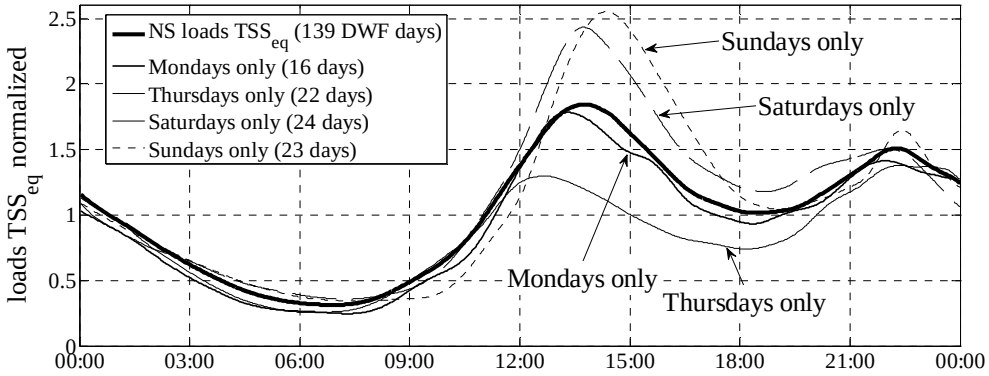

Figure 6-26: Dry weather pollutant load patterns for parameter TSS_{eq} of wastewater from catchment area Nuenen/Son: variation across days of the week.

Table 6-11: Mean dry weather pollutant loads and associated minimum and maximum peak factors per pollutant parameter for the complete dry weather sets as well as for all weekdays, relevant single weekdays, Saturdays and Sundays.

			TSS_{eq}	COD_{eq}	$CODf_{eq}$
Riool-Zuid					
all days	mean load	[kg/h]	432	1,247	473
	peak factors	[min-max]	0.50 - 1.31	0.55 - 1.28	0.59 - 1.25
weekdays	mean load	[kg/h]	471 (+9%)	1,334 (+7%)	497 (+5%)
	peak factors	[min-max]	0.52 - 1.57	0.55 - 1.39	0.59 - 1.33
Mondays	mean load	[kg/h]	493 (+14%)	1,365 (+9%)	491 (+4%)
	peak factors	[min-max]	0.46 - 1.76	0.51 - 1.54	0.52 - 1.43
Saturdays	mean load	[kg/h]	366 (-15%)	1,111(-11%)	438 (-7%)
	peak factors	[min-max]	0.40 - 1.21	0.47 - 1.19	0.51 - 1.18
Sundays	mean load	[kg/h]	353 (-18%)	1,072(-14%)	414 (-12%)
	peak factors	[min-max]	0.36 - 1.17	0.41 - 1.17	0.42 - 1.19
Eindhoven Stad					
all days	mean load	[kg/h]	691	1,550	467
	peak factors	[min-max]	0.52 - 1.39	0.58 - 1.33	0.64 - 1.25
weekdays	mean load	[kg/h]	701 (+1%)	1,570 (+1%)	477 (+2%)
	peak factors	[min-max]	0.51 - 1.36	0.58 - 1.29	0.65 - 1.25
Fridays	mean load	[kg/h]	626 (-9%)	1,490 (-4%)	454 (-3%)
	peak factors	[min-max]	0.44 - 1.23	0.55 - 1.24	0.61 - 1.20
Saturdays	mean load	[kg/h]	680 (-2%)	1,521 (-2%)	449 (-4%)
	peak factors	[min-max]	0.48 - 1.53	0.56 - 1.45	0.60 - 1.27
Sundays	mean load	[kg/h]	669 (-3%)	1,508 (-3%)	449 (-4%)
	peak factors	[min-max]	0.48 - 1.52	0.56 - 1.42	0.60 - 1.27
Nuenen/Son					
all days	mean load	[kg/h]	69	156	71
	peak factors	[min-max]	0.32 - 1.85	0.45 - 1.51	0.53 - 1.34
weekdays	mean load	[kg/h]	65 (-6%)	153 (-2%)	70 (-1%)
	peak factors	[min-max]	0.29 - 1.60	0.44 - 1.41	0.52 - 1.36
Thursdays	mean load	[kg/h]	57 (-17%)	145 (-7%)	69 (-3%)
	peak factors	[min-max]	0.25 - 1.30	0.42 - 1.36	0.51 - 1.36
Saturdays	mean load	[kg/h]	78 (+13%)	164 (+5%)	75 (+6%)
	peak factors	[min-max]	0.36 - 2.46	0.45 - 1.82	0.53 - 1.58
Sundays	mean load	[kg/h]	75 (+9%)	157 (+1%)	70 (-1%)
	peak factors	[min-max]	0.37 - 2.57	0.44 - 1.89	0.51 - 1.60

In terms of mean daily loads results for area Nuenen/Son are the opposite of the Riool-Zuid results: on average, total loads for week days are roughly 6% *smaller* than the overall means whereas total loads for weekend days are 9% to 13% *larger*. The latter is in disagreement with the observation for flow values: total flows from Nuenen/Son *decrease* on Sundays with respect to the dry weather flow mean (see Table 6-5). Weekend load peak values around 14h00 are (much) larger than their mean values, which is likely associated with the coinciding large weekend peak flows and the earlier discussed relation between flow and TSS concentrations. Consistent with all other flow and pollutant load results, weekend patterns show a delay in onset of the morning increase as well as a delay in peak values around 14h00. Differences across week days are also observed: analogous to the Riool-Zuid results Mondays generally show the largest values (both in terms of mean loads and peak factors), Thursdays the smallest and other week days intermediate values.

DWF day loads: comparison of UV/VIS data versus long-term sampling

As a final consideration of observed dry weather pollutant loads at the wwtp Eindhoven, the results collected using the UV/VIS sensors (as presented in this chapter) are compared to a distinct source of information: 24-hour reference samples. Waterschap De Dommel performs regular wastewater sampling at various locations throughout the wwtp Eindhoven. One of these locations is the mixing flume in the influent pumping station that assumedly holds mean wwtp influent wastewater. Samples are 24-hour flow proportional composite samples (NEN, 2009) collected at 5 randomly selected days each month, analyzed for (among others) pollutant parameter COD using a standard laboratory method (tube tests according to ISO, 2002). For the time-span April 1st, 2007 - November 1st, 2008 a total of 96 samples are available. The results of these 24-hour samples are compared to the aggregated high-frequent UV/VIS data sets. More specifically, the pollutant load COD that arrives at the wwtp Eindhoven during collection of the 24-hour sample is calculated using the UV/VIS data. This sensor result is compared to the sample result. Comparison is not possible for all samples due to missing data: during the collection of 71 samples (i.e. 75% of samples) at least one of the flow or UV/VIS data sets lacks more than 10% of data. Of the remaining 25 samples 14 are associated with wet weather conditions. As a result, comparison is possible for 11 dry weather flow samples only. Results are plotted in Figure 6-27.

Results show that DWF day loads of COD based on 24h samples are systematically *smaller* than those based on UV/VIS data. Using the latter as reference, the mean difference is 23%, minimum and maximum differences are 10% and 41%, respectively. Sources of the observed differences can be manifold and can be associated with systematic errors in sampling, sample storage, laboratory work and/or in the UV/VIS data. For instance, the UV/VIS sensors have been calibrated only once during the 19-months time-span for which the data are considered in this

analysis (see chapter 5). Variations in wastewater composition (i.e. matrix changes) other than accounted for by the used calibration sets may have occurred during the observation period, possibly resulting in systematic errors in UV/VIS data.

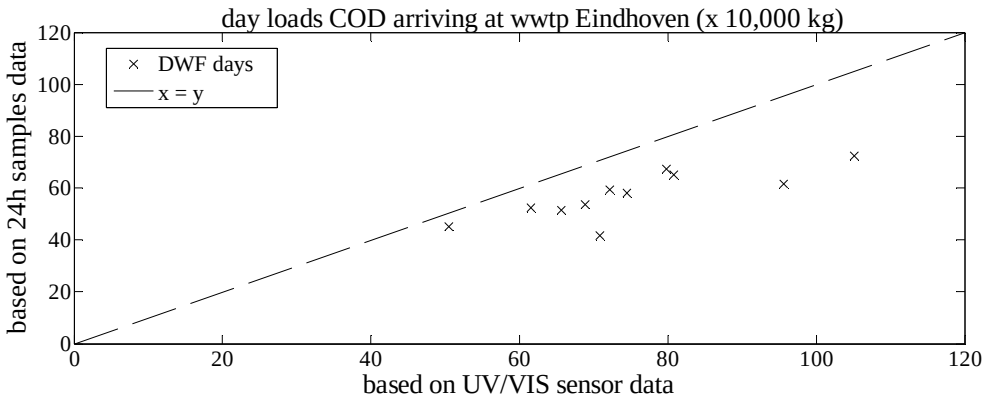

Figure 6-27: Day loads COD arriving at wwtp Eindhoven: comparison of data based on 24-hour flow proportional composite samples versus data based on the UV/VIS data sets.

6.3 Wet weather conditions

6.3.1 Selection of data associated with wet weather conditions

For the analysis of flow and pollutant data associated with wet weather conditions a selection has been made from the flow and wastewater quality time-series as derived in chapters 4 and 5. The selection comprises data that correctly represent the targeted flow condition, i.e. data associated with storm events. The selection of storm events has been done using the following set of criteria:

- flow must be larger than the 97.5% percentile of dry weather flows for a duration of at least 2 hours;
- more than 0.5 mm of precipitation must have been recorded over the preceding 24 hours;
- data sets must be nearly complete (i.e. > 99% for flow; > 90% for quality parameters) directly preceding the event, during the event, and directly following the event;
- events separated by less than 8 hours are considered to be part of the same event.

Similar to the selection of data associated with dry weather condition, wet weather data are selected using precipitation and flow data sets only. It should be noted that

the selection criteria for dry weather and wet weather conditions are such that not all data are assigned to either one condition; some data are excluded from both analyses. The criterion for completeness has been included to avoid basing results on incomplete data sets.

6.3.2 Storm events

Application of the storm event criteria on the 580-days flow and UV/VIS data sets yields a total of 65 (Riool-Zuid), 60 (Eindhoven Stad) and 67 (Nuenen/Son) storm events that can be used for data analysis. Hereafter, the behavior of flow and pollutant parameters during a number of typical events is presented: a single and isolated large storm event, a single small storm without dilution and multiple storms in series.

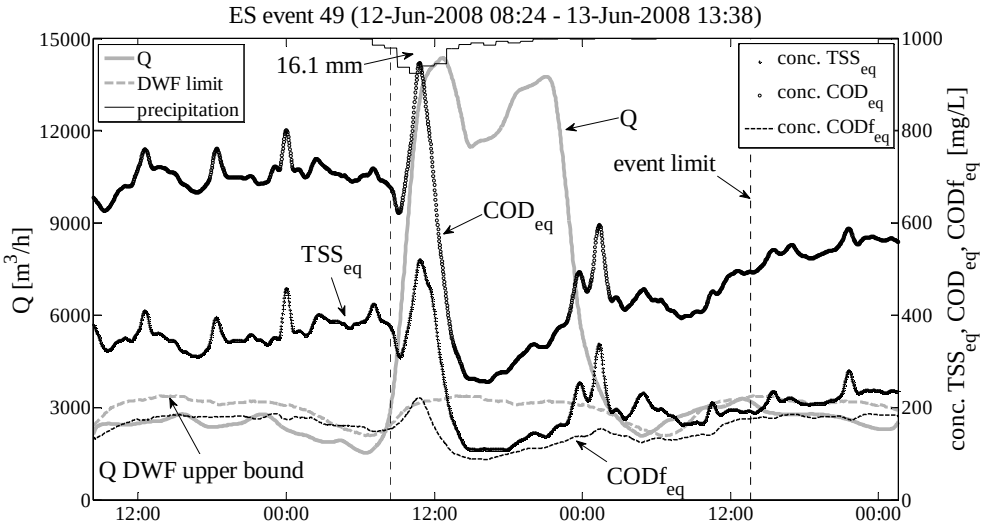

Figure 6-28: For catchment area Eindhoven Stad the reaction of flow and pollutant concentrations of TSS_{eq}, COD_{eq} and $CODf_{eq}$ to a storm on June 12th and 13th, 2008.

Single large storm

Figure 6-28 illustrates the short-term fluctuations in flow and concentration levels of pollutants in wwtp influent from catchment area Eindhoven Stad as a result of a storm on June 12th and 13th, 2008. The storm event constitutes a single large storm lasting for approximately 13 hours with a recorded precipitation depth of 16.1 mm. In reaction to the storm flow increases by a factor 5 to 6 surpassing the DWF upper bound (i.e. the 97.5% percentile of dry weather flows). The moment flow rises

above DWF levels an initial concentration peak for all quality parameters can be observed. Approximately 7 hours into the storm event all concentration levels have reduced by a factor ~ 2 with respect to pre-storm DWF values. After precipitation ceases, flow values return to DWF values within a time-span of roughly 6 hours. Pollutant concentrations, however, recover more slowly to pre-storm DWF levels. At the end of the event (as defined using the aforementioned criteria) TSS_{eq} and COD_{eq} concentrations are still below normal DWF levels and continue to recover. In other words, after the wastewater system has been emptied following a storm event, it returns to a *hydraulic* equilibrium associated with dry weather flow, but the influence of the storm event on *pollutant* concentrations extends beyond the duration of the event. This phenomenon is likely associated with a prolonged replenishment of sediments in in-sewer storages that were removed during the preceding event. At the end of the event concentration values of parameter $CODf_{eq}$ are back at dry weather values as all diluting storm water has been removed from the sewer system.

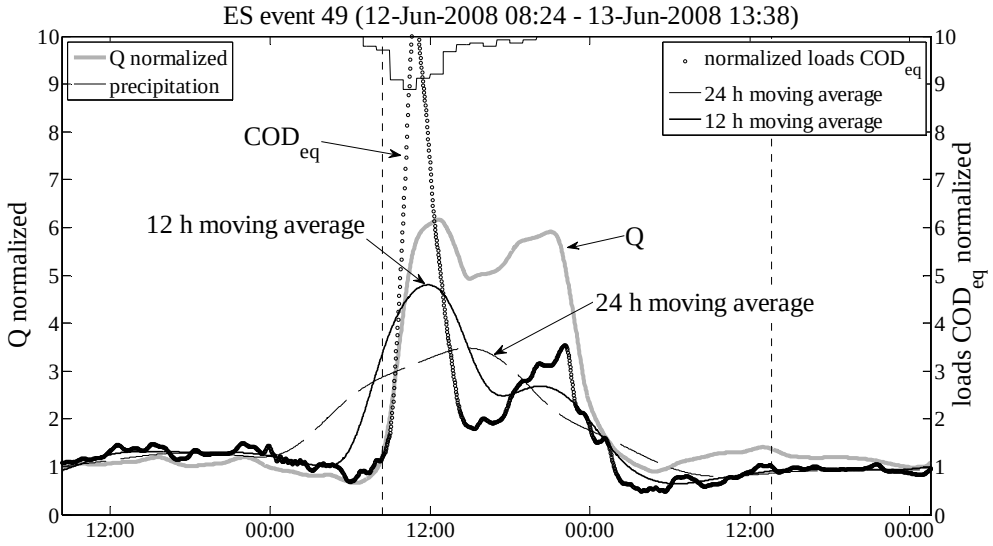

Figure 6-29: The reaction of flow and pollutant loads of COD_{eq} to the same storm as presented in Figure 6-28. Values are normalized to DWF means.

The variation of pollutant concentrations in Figure 6-28 is further studied using the data presented in Figure 6-29. The figure gives the reaction of flow and COD_{eq} *loads* to the same June $12^{th}/13^{th}$ storm event. Values are normalized to dry weather flow mean values in order to be able to compare peak values. As earlier stated, flow increases by a factor 5 to 6 and shows limited variation during the time-span of high flows (i.e. the maximum pumping capacity is maintained throughout nearly

the entire storm). The arrival of pollutant loads, however, varies over the course of the storm event. It can be observed that directly after the onset of the event COD_{eq} loads briefly increase to roughly 10 times the mean DWF load. In combination with a smaller relative flow increase, this yields the observed initial concentration peak. Then, for the remainder of the time-span with increased flows, supplied loads reduce to a level of around 3 times the DWF mean. As the relative flow increase is now larger than the relative load increase, a dilution in pollutant concentrations can be observed. Considered at larger time-scales the variation of pollutant loads during storm events is more gradual and peak load factors (PLF, i.e. the maximum attained normalized load during a storm event) are hence smaller. This is illustrated in the figure with the application of symmetrical moving average filters with spans of 12 and 24 hours. For parameters COD_{eq} this yields a PLF_{12} of 4.8 and a PLF_{24} of 3.5. Peak load factors are further discussed in the next paragraph.

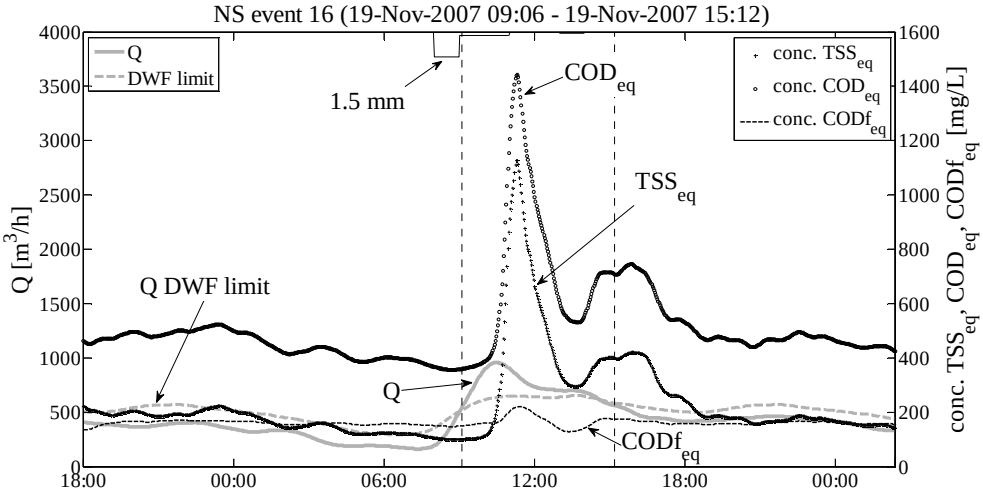

Figure 6-30: For catchment area Nuenen/Son the reaction of flow and pollutant concentrations of TSS_{eq}, COD_{eq} and $CODf_{eq}$ to a storm on November 19th, 2007.

Single small storm without dilution

Figure 6-30 presents the reaction of flow and pollutant concentrations in wwtp influent from catchment area Nuenen/Son to a storm on November 19th, 2007. The storm event constitutes a single small storm lasting for approximately 3 hours with a recorded precipitation depth of 1.5 mm. As a result of the storm, flow increases by a factor 2 to 3 surpassing the DWF upper bound for a time-span of about 6 hours. After the onset of the storm initial concentration peaks can be discerned that are possibly the result of resuspension of in-sewer sediments. Contrary to the previous example, however, no subsequent reduction in concentrations to below

DWF values is observed. The increase in flow values that has proven sufficient for the sediment resuspension is evidently insufficient to cause large-scale dilution of wastewater. Instead, for the remainder of the storm event, pollutant concentrations are recorded that are *larger* than during dry weather conditions. Apparently, after the initial peak phase, the relative increase in pollutant loads remains larger than the relative increase in flow. This effect can be observed in Figure 6-31. For the duration of the storm event flow values roughly double whereas normalized TSS_{eq} loads vary between 4 and a peak value of 24. Considering the variation of pollutant loads during the storm event again at larger time-scales, Figure 6-31 presents the moving average of TSS_{eq} loads with spans of 12h and 24h. Calculated peak load factors are 5.8 and 3.3, respectively. These values suggest that relatively small storm events are not necessarily associated with small peak load factors.

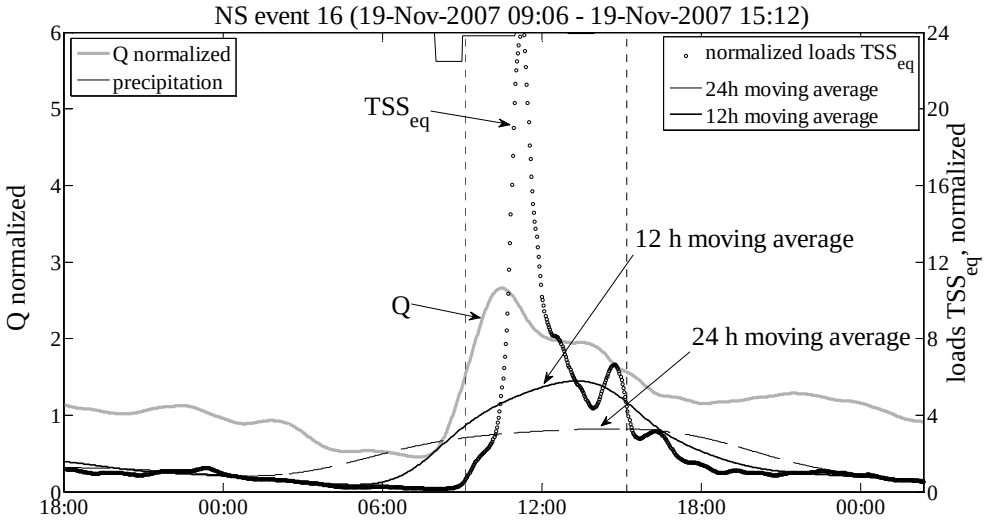

Figure 6-31: The reaction of normalized flow and pollutant loads of TSS_{eq} to the same storm as presented in Figure 6-30. Please note that the vertical axes have different ranges.

Multiple storms in series

Figure 6-32 presents the behavior of flow and COD_{eq} concentrations in wwtp influent from catchment area Riool-Zuid during a series of storms between November 30th and December 11th, 2007. The event comprises multiple small and seven large storm clusters, with the complete event lasting for about 10.5 days and a total recorded precipitation depth of 69.4 mm. For nearly the entire event flow values remain larger than the DWF upper limit. Each storm is associated with a dilution of COD_{eq} content in the wastewater, but despite the repetitive character of the storms concentrations remain larger than 100 mg/L at all times.

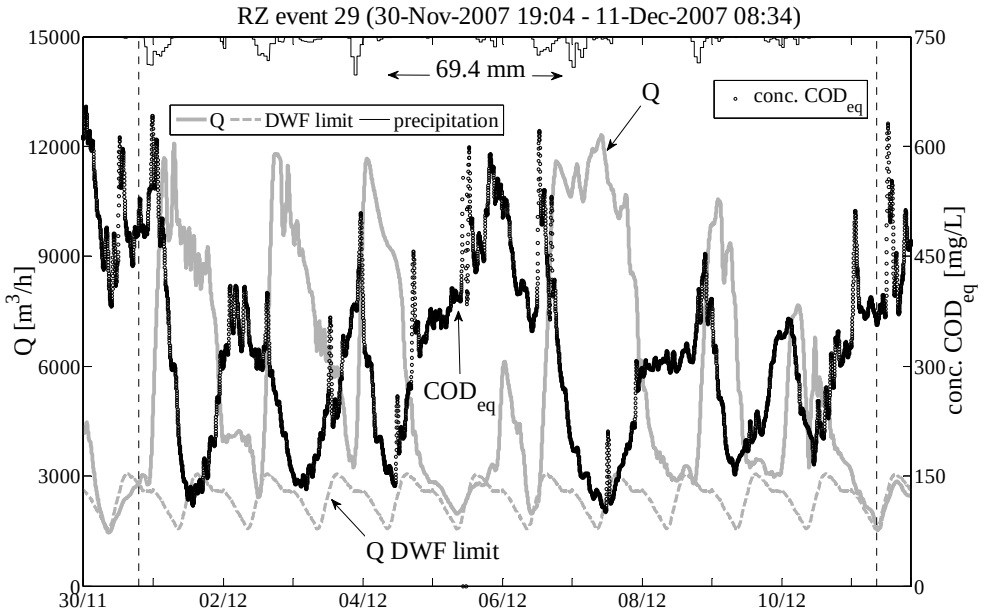

Figure 6-32: For catchment Riool-Zuid the reaction of flow and pollutant concentrations of COD_{eq} to a series of storms between November 30th and December 11th, 2007.

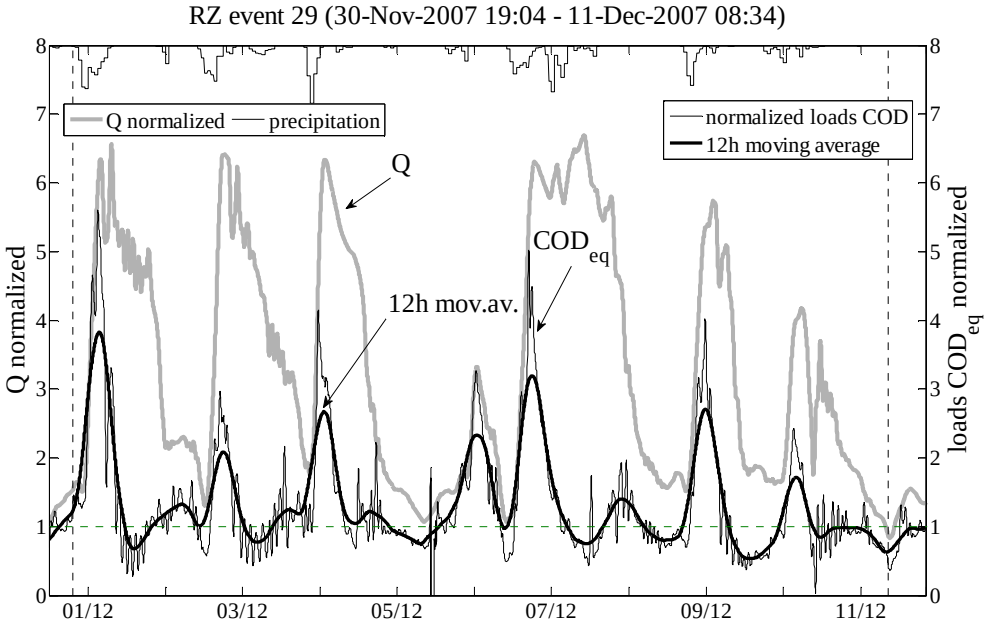

Figure 6-33: The reaction of flow and pollutant loads of COD_{eq} to the same series of storms as presented in Figure 6-32. Values are normalized to DWF means.

The explanation for this phenomenon can be found in Figure 6-33. For all individual storms within the event an initial peak in COD_{eq} *loads* can be observed that lasts for roughly 12 to 15 hours, followed by a reduction in supplied loads to values of around 1. In other words, each storm is associated with a time-span with pollutant loads arriving at the wwtp larger than DWF values, and - if flow values continue to be high - a subsequent time-span with pollutant loads arriving at the wwtp at a rate about equal to DWF values. During the latter time-span minimum concentration values are reached with dry weather pollutant loads arriving at (near-maximum) wet weather flow rates.

Figure 6-34 presents on the same scale and for the same event normalized loads for dissolved COD ($CODf_{eq}$). Peak values are smaller than for total COD_{eq}, but again peaks have a repetitive character for subsequent storms. Hence, each of the observed peak loads for total COD_{eq} has a contribution from both the particulate fraction as well as from the dissolved fraction. Also, the repetitive character of peak loads suggests that the source(s) of the additional loads during wet weather flow seems 'inexhaustible' on the considered time-scale. Even after a number of (large) storms within a time-span of a few days a peak in pollutant loads is again observed for the next storm event. This topic is further discussed in paragraph 6.4.

The result of application of a 12h moving average filter on the COD_{eq} load data yields a single global peak load factor (3.8 on December 1st), but up to 7 local maximum values, each of which is associated with an individual storm within the event, see Figure 6-33. In the analysis in the next paragraph events are only associated with the global maximum value, which is often the first observed peak.

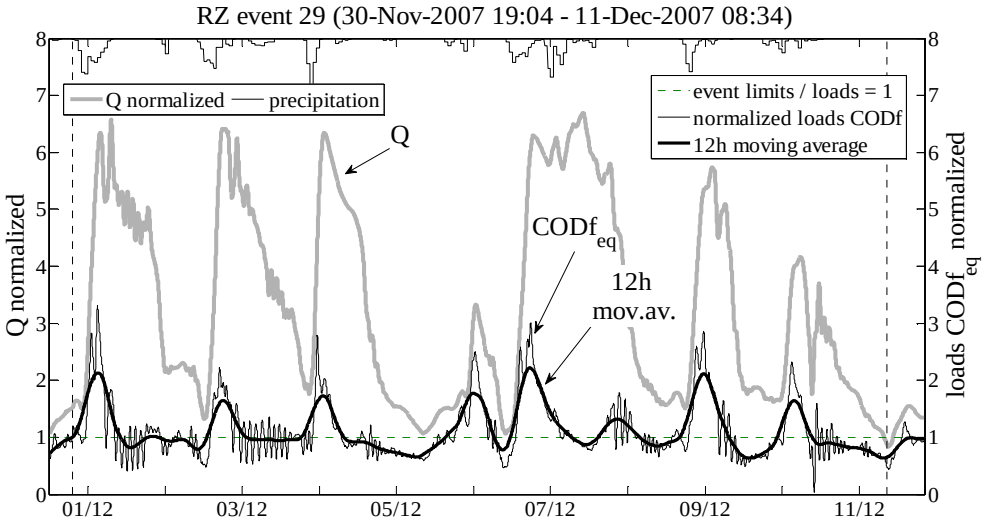

Figure 6-34: The reaction of flow and pollutant loads of $CODf_{eq}$ to the same series of storms as presented in Figure 6-32. Values are normalized to DWF means.

6.3.3 Peak load factors

A peak load factor (PLF) is the maximum attained pollutant load during a storm event after application of a moving averaging filter on the load data set and normalization of values with respect to DWF mean values. It expresses the arriving pollutant load in one of the three inflows at the wwtp Eindhoven (averaged over the span of the filter) as a multiple of its mean DWF equivalent. PLFs have been calculated for all storm events in the 19-months data sets, for each of the three catchment areas and for each of the three considered pollutant parameters. Filter lengths of 12 hours (PLF_{12}) and 24 hours (PLF_{24}) have been applied.

Figure 6-35 presents all peak load factors. Results are presented in a 3x3 matrix with Riool-Zuid results in the top row (65 storm events), those for Eindhoven Stad in the middle row (60 storm events) and Nuenen/Son results in the bottom row (67 storm events); results for parameter TSS_{eq} can be found in the left column, COD_{eq} results in the middle column and $CODf_{eq}$ results in the right column. Per matrix cell (i.e. per location/parameter combination) PLF_{12} results are plotted on the left, PLF_{24} results on the right. Each dot represents a storm event; the mean value over all storm events per category is given and its position indicated with a horizontal dash. Please note that vertical axes are the same for all graphs per location, but are different across locations. The range of values (the 5% and 95% percentiles) and its mean are given in Table 6-12 per pollutant parameter and per catchment area.

Table 6-12: Peak load factors (PLF_{12} and PLF_{24}) per pollutant parameter and per catchment area: the mean values over all storm events as well as the 5% and 95% percentiles. The data are plotted in Figure 6-35.

	Riool-Zuid		Eindhoven Stad		Nuenen/Son	
# storm events	65		60		67	
TSS_{eq}	PLF_{12}	PLF_{24}	PLF_{12}	PLF_{24}	PLF_{12}	PLF_{24}
5% percentile	1.4	1.2	1.0	0.9	1.1	0.8
mean	3.9	2.9	3.6	2.0	9.8	5.5
95% percentile	8.1	5.8	6.5	4.1	24.3	12.0
COD_{eq}						
5% percentile	1.4	1.2	0.9	0.8	1.4	1.2
mean	2.7	2.2	2.8	1.7	7.5	4.5
95% percentile	4.9	3.9	4.6	3.1	18.8	9.8
$CODf_{eq}$						
5% percentile	1.0	0.9	1.2	1.1	1.3	1.1
mean	1.9	1.6	2.5	1.7	2.8	2.0
95% percentile	3.4	2.9	3.6	2.9	5.1	3.3

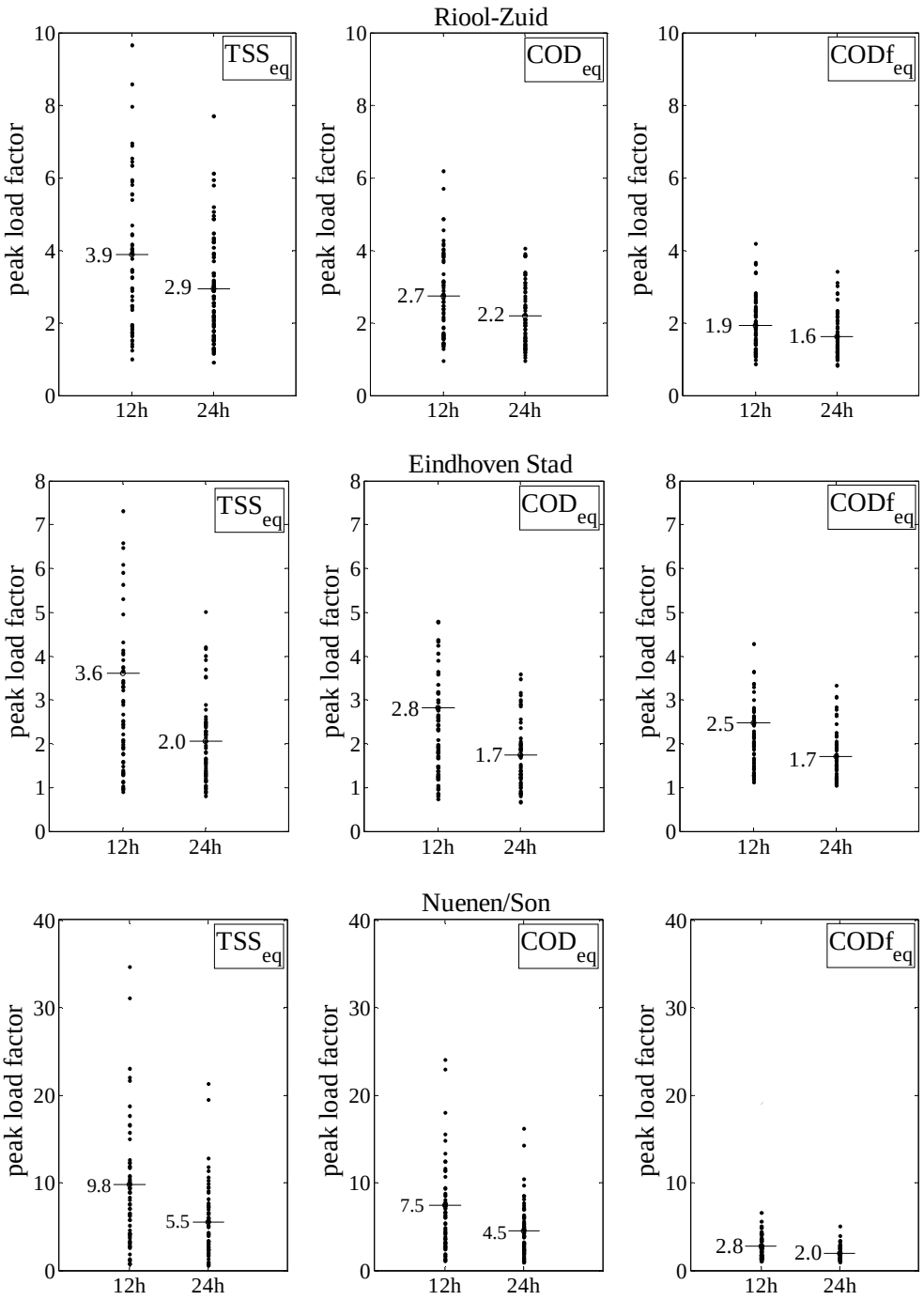

Figure 6-35: Peak load factors and their mean values for parameters TSS_{eq} (left), COD_{eq} (centre) and $CODf_{eq}$ (right) of all selected storm events of areas Riool-Zuid (top, 65 storm events), Eindhoven Stad (middle, 60 storm events) and Nuenen/Son (bottom, 67 events).

For all three catchment areas and for all three parameters mean PLF_{24} values are larger than one. This means that for a 'mean storm event' the arriving pollutant load over 24 hours from all inflows is systematically larger than during dry weather. The magnitude of this 'mean storm peak load' varies with parameter and catchment area. The largest mean PLF_{24} values are found for TSS_{eq} (2.0 - 5.5), followed by parameters COD_{eq} (1.7 - 4.5) and $CODf_{eq}$ (1.6 - 2.0). This suggests that during wet weather conditions the additional discharge of suspended solids is consistently larger than for dissolved compounds. The smallest catchment area (Nuenen/Son) shows the largest mean peak factors whereas values are smaller for Riool-Zuid and Eindhoven Stad, the largest catchments. This contradicts earlier research (Kafi *et al*., 2008) where no significant variability between catchments of different sizes could be observed. For parameter $CODf_{eq}$ the catchment size effect is less pronounced than for parameters TSS_{eq} and COD_{eq}.

All 5% percentile values are equal or close to one. In other words, for 'small storm events' arriving pollutant loads over 24 hours are on the same order of magnitude as mean dry weather loadings. For relatively large storm events (i.e. the 95% percentile values) 24h loadings can become much larger than mean DWF values: for parameter TSS_{eq} a factor 4 to 6 for large areas such as Riool-Zuid and Eindhoven Stad and a factor 12 for area Nuenen/Son. For parameters COD_{eq} and $CODf_{eq}$ these values are smaller, but remain much larger than any dry weather variation.

All nine graphs show that applying a moving average filter with a smaller span yields larger peak load factors. The values of PLF_{12} should be considered with care for its relation with time of the day. For instance, for area Riool-Zuid the same storm event will yield a larger PLF_{12} value when occurring between 09h00 and 21h00 than between 21h00 and 09h00. For PLF_{24} values this restriction does not apply.

Possible relations between the magnitude of peak load factors and the explanatory variables 'total event precipitation depth', 'antecedent dry weather period', 'mean event precipitation intensity' and 'maximum event precipitation intensity' have been studied. Results show that correlations are weak or non-existent. For variables 'total precipitation depth' and 'antecedent dry weather period' a positive correlation is observed, suggesting increasing PLFs with increasing parameter values. However, all observed relations are weak with no correlation coefficient found larger than $r^2 = 0.35$, see Figure 6-36. For the variables related to precipitation *intensity* correlations are non-existent. This is likely attributable to the fact that precipitation data sets as derived in chapter 3 have been used in the analysis. In these data sets precipitation data have been aggregated into 1 hour interval data, losing short-term intensity information. Others (e.g. Bertrand-Krajewski *et al.*, 1993) do have observed relations between precipitation intensities

and pollutant loadings. In conclusion, a straightforward relation between individual variables and averaged pollutant loads arriving at the treatment plant during a storm event has not be observed. Possibly, a combination of factors has a better predictive value. Also, other variables might play a role in the processes involved.

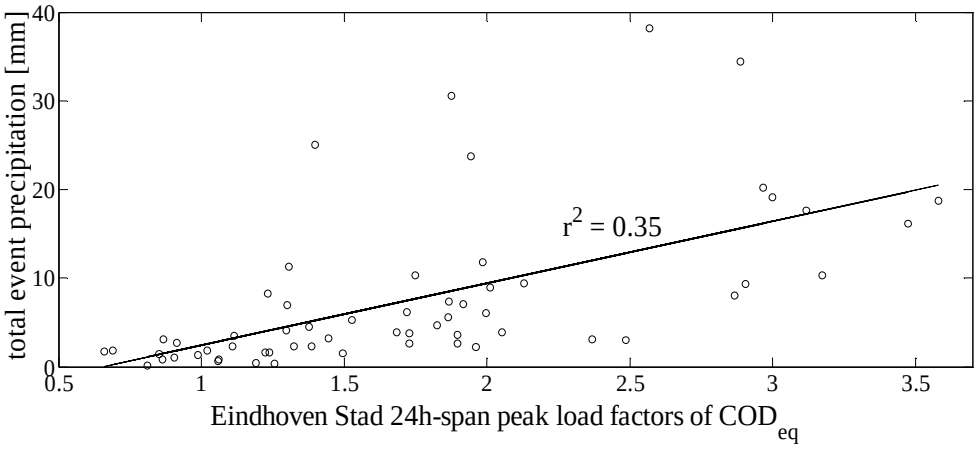

Figure 6-36: PLF_{24} of COD_{eq} for area Eindhoven Stad versus total event precipitation.

The storm event of May 7th, 2007 (that caused floating sludge layers on all secondary clarifiers of the wwtp Eindhoven, see paragraph 6.1) is presented in Figure 6-37 and Figure 6-38. In the figures, the behavior of flow and pollutant parameter TSS_{eq} during (a part of) the event can be observed for wastewater from areas Riool-Zuid and Eindhoven Stad, respectively. The storm event (that lasted for several days) has not been included in the results presented in Figure 6-35 due to lacking data towards the end of the event. Data of May 7th and 8th, however, are complete and presented in the graphs. The UV/VIS sensor for area Nuenen/Son was malfunctioning during the event.

The TSS_{eq} PLF_{24} for Eindhoven Stad adds to 6.0; its equivalent for catchment area Riool-Zuid is 9.0. Considering the range of observed PLF_{24} values of all studied storm events these are very large values and in fact the largest observed PLF_{24} values for this parameter over the considered 19-months time-span, see Table 6-13. Also for parameters COD_{eq} and $CODf_{eq}$ the PLF_{24} values on May 7th, 2007 are larger than any PLF_{24} value presented in Figure 6-35. Moreover, the gap between PLF_{24} values on May 7th and the PLF_{24} values of other large storm events (i.e. the 95% percentile values) are significant. For instance, for Riool-Zuid parameter COD_{eq} the difference adds to 2.9 which roughly equals the entire span of values for all other observed storm events.

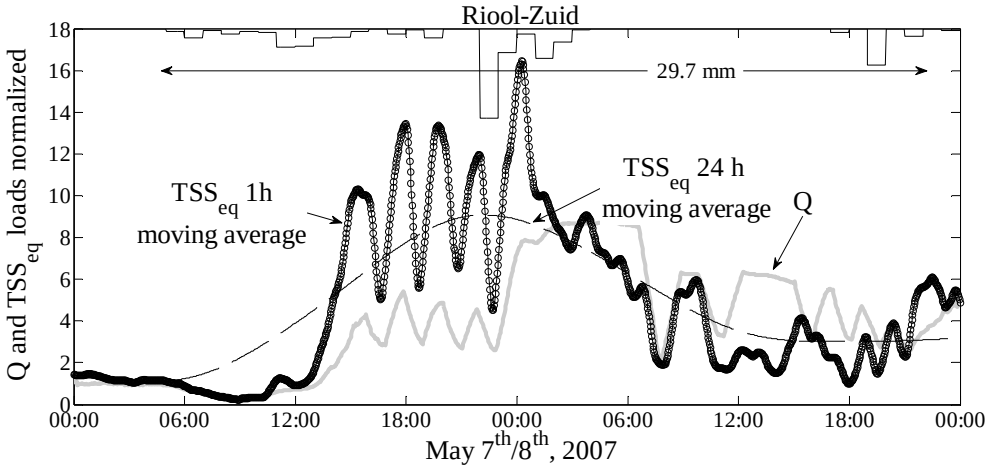

Figure 6-37: For catchment area Riool-Zuid the reaction of flow and pollutant loads of TSS_{eq} to a storm on May 7th and 8th, 2007.

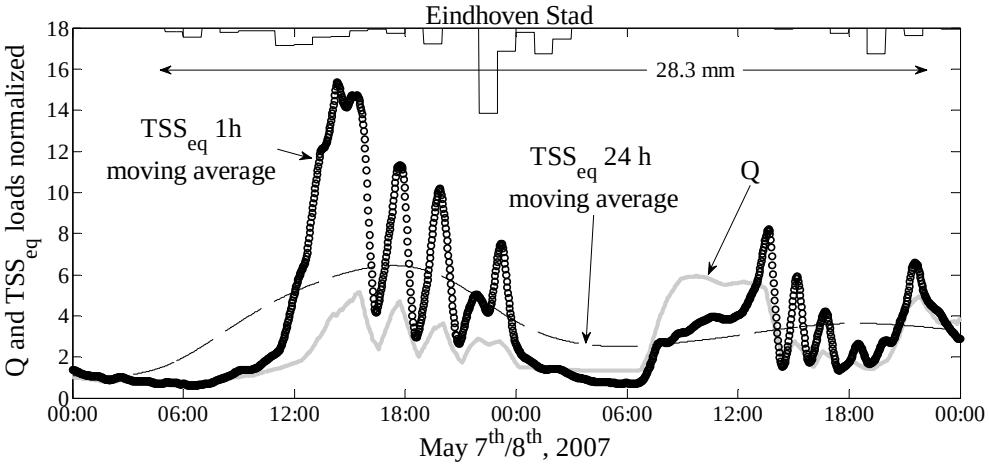

Figure 6-38: For catchment area Eindhoven Stad the reaction of flow and pollutant loads of TSS_{eq} to a storm event on May 7th and 8th, 2007.

Combining Riool-Zuid and Eindhoven Stad data yields PLF_{24} values of 6.8 (TSS_{eq}), 5.5 (COD_{eq}) and 4.3 ($CODf_{eq}$). Acknowledging that Nuenen/Son peak load factors are generally larger than Riool-Zuid and Eindhoven Stad values and are therefore likely to somewhat further increase PLF values for total wwtp influent, it can be concluded that on May 7th, 2007 the wwtp Eindhoven has received a 24-hour load of roughly 7 times the dry weather flow mean for total suspended solids, roughly 6 times for parameter COD_{eq} and roughly 4.5 times for $CODf_{eq}$. Considering all other events during the 1.5 year time-span of April 1st, 2007 - November 1st, 2008 this constitutes an exceptionally large influx of pollutant loads.

Table 6-13: PLF_{24} values for the storm event of May 7th, 2007 versus the range of observed PLF_{24} values over all storm events in the time-span April 1st, 2007 - November 1st, 2008.

	Riool-Zuid	Eindhoven Stad	RZ + ES
TSS_{eq}	PLF_{24}	PLF_{24}	
5% percentile	1.2	0.9	
mean	2.9	2.0	
95% percentile	5.8	4.1	
event May 7th, 2007	*9.0*	*6.0*	*6.8*
COD_{eq}			
5% percentile	1.2	0.8	
mean	2.2	1.7	
95% percentile	3.9	3.1	
event May 7th, 2007	*6.8*	*5.0*	*5.5*
$CODf_{eq}$			
5% percentile	0.9	1.1	
mean	1.6	1.7	
95% percentile	2.9	2.9	
event May 7th, 2007	*5.5*	*3.6*	*4.3*

6.4 Discussion and conclusions

In this chapter quantity and quality data of wastewater arriving at the wwtp Eindhoven from the three contributing catchment areas Riool-Zuid, Eindhoven Stad and Nuenen/Son have been studied. For this, the data sets as earlier derived in chapter 3 (precipitation data), chapter 4 (wastewater quantity data) and chapter 5 (wastewater quality data) have been used. A distinction is made between dry weather conditions and wet weather conditions. For both flow conditions the main findings are presented and discussed hereafter.

Dry weather conditions
For dry weather conditions wastewater *flows* have been studied using data of approximately 200 dry weather days. Firstly, diurnal variations have been observed. Minimum night flows are on the order of 60% of the overall dry weather mean value whereas maximum flows add to roughly 125%. Secondly, variations of dry weather flow patterns across days of the week have been distinguished. Weekdays do not differ much from each other, but weekend flows can be different in terms of peak factors and timing. Thirdly, a long-term variation of dry weather flow day sums has been presented. On an annual basis, day sums vary between 80% and 120% of the overall mean. For each of these three variation types a catchment size effect has been observed: the smallest catchment area (Nuenen/Son) is associated

with the largest deviations from mean values whereas the two largest catchments (Riool-Zuid and Eindhoven Stad) consistently show smaller variations.

Based on data of 100 to 150 dry weather days diurnal patterns of pollutant *concentrations* have been derived. For pollutant parameters associated with suspended solids (TSS_{eq} and COD_{eq}) these show large similarities with their flow equivalents: large flows are generally associated with relatively high pollutant concentrations and vice versa. As a result, the combination of both into dry weather patterns for pollutant *loads* yields diurnal patterns with larger variations than for flow only. For instance, for catchment area Eindhoven Stad flow varies over a day from 68% to 120% of the DWF mean whereas COD_{eq} loads show a variation between 58% and 133%. Concentration values of dissolved COD_{eq} are more constant; therefore, load variations of $CODf_{eq}$ over a day are of the same order as for flow. Long-term variations of pollutant load day sums show the same tendency: the variation of values for suspended loads is larger than for flow values whereas the variation of dissolved loads is on the same order of magnitude. Essentially, these two observations hint at the same phenomenon: suspended solids concentrations are significantly influenced by relatively small flow variations during dry weather whereas concentration values of dissolved COD_{eq} remain largely unaffected by such variations in flow values. The observed catchment size effect in pollutant loads for parameters TSS_{eq} and COD_{eq} is hence directly related to the same effect in flow values. As for flow, diurnal patterns and day sums for pollutant loads can vary for different days of the week. For this variation type the largest differences are site-specific: the discharge of centrate water from the sludge treatment facility into the Riool-Zuid sewer system on weekdays only. Other observed differences are due to typical week/weekend variations.

A survey (STOWA, 2001) among water boards in the Netherlands shows that a wide variety of methods is applied to determine the ‘design capacity’ of new or renewed wastewater treatment plants. In general, it is current practice to account for variation in hydraulic loading but to assume a constant pollutant loading. Results in this chapter show that the latter is not in accordance with observations at the wwtp Eindhoven influent pumping station. Seasonal and weekday variations are generally acknowledged, but not often incorporated in the design. Reported percentages for these variations are smaller than values observed in this chapter. A catchment size effect that was observed for both flow and pollutant loads in this chapter is not reported for any current wwtp design.

In the same STOWA (2001) report much attention is paid to a commonly encountered problem when (re)designing wwtps: a discrepancy between the *administrative* number of population equivalents in an area and the *actual* number of p.e. based on measurements. Using the same approach as in the report (i.e. using data of 24-hour composite sampling), results in this chapter show that this

discrepancy is non-existent for the wwtp Eindhoven. At the same time, however, comparison between UV/VIS data and composite sample results suggest that systematic errors are present in either one or both data sets. In the survey many respondents have expressed their doubts on full compliance with prescribed sampling and analysis methods of the composite sampling.

Wet weather conditions
Under wet weather conditions arriving pollutant loads at the wwtp Eindhoven can be an order of magnitude larger than under dry weather conditions. Using data of approximately 65 storm events the arriving pollutant loads over 24 hours have been calculated and compared to its dry weather equivalent (PLF_{24} value). Results show that 'mean storm events' lead to the arrival of 2 to 3 times the suspended solids load for areas Riool-Zuid and Eindhoven Stad and 5.5 times the load for area Nuenen/Son. For parameter $CODf_{eq}$ these values are 1.6 to 1.7 and 2.0, respectively. As for dry weather conditions, a catchment size effect is observed in the magnitude of peak loads. Also, the larger peak factors for pollutant parameters associated with suspended solids again express the strong relation between these parameters and flow: large flows during wet weather conditions cause a much larger increase in TSS_{eq} loads than in $CODf_{eq}$ loads.

For 'small storm events' (i.e. the 5% percentile value of all calculated PLF_{24} values) arriving pollutant loads are comparable to normal dry weather loads. For 'large storm events' (the 95% percentile value), however, peak loads factors can be large: roughly 4, 6 and 12 (TSS_{eq} loads), 3, 4 and 10 (COD_{eq} loads) and 3, 3 and 3.5 ($CODf_{eq}$ loads) for areas Eindhoven Stad, Riool-Zuid and Nuenen/Son, respectively. The combination of these into values for total wwtp Eindhoven influent yields 24-hour peak load factors of roughly 5 (TSS_{eq}), 3.5 (COD_{eq}) and 3 ($CODf_{eq}$) for a typical 'large storm event'. The latter values are (much) larger than peak factors used in the Eindhoven treatment plant design. For instance, the oxygen demand in the activated sludge tanks at the wwtp Eindhoven is estimated using a mean dry weather influent loading, and incorporating a substrate peak factor of 1.5 as well as an overall (wet weather) factor of 1.1 (Tauw, 2002). In other words, a variation of up to 165% of mean dry weather loading is anticipated in the design. Despite exceeding this loading during a typical 'large storm event', $COD_{eq}/CODf_{eq}$ pollutant concentrations in wwtp Eindhoven effluent are *not* known to largely deteriorate and violate effluent standards during large storms. This confirms the notion that the removal of oxygen demanding substances in wastewater is a robust process (e.g. Langeveld, 2004) that can handle peak loadings beyond its design value. The robustness is owing to processes such as a temporary reduction in endogeneous respiration and delay of substrate respiration due to prolonged adsorption instead of direct oxidation of pollutants. It should be noted that this observation does not hold for nitrogen removal processes; a peak loading in

influent is therefore often associated with peak concentrations in effluent, as is commonly observed in practice.

For the May 7th, 2007 event, however, the extreme loading in oxygen demanding pollutants seems to stand at the basis of the formation of floating sludge layers on all secondary clarifiers (see paragraph 6.1). In an evaluation Tauw (2007) concludes that denitrification in the secondary clarifiers is the most likely cause for the formation of the floating layers. Observed high concentration levels of nitrate in the secondary tanks in combination with a low oxygen concentration and the presence of substrate in the form of COD_{eq} adsorbed to sludge particles have probably led to this delayed denitrification process that should have taken place earlier in the aeration tanks. The extreme pollutant loading at an unaltered wet weather flow rate caused unusually high pollutant concentrations in inflow into the aeration tanks, resulting in a prolonged nitrification process and a residence time 'deficit' for subsequent denitrification. Retrospectively, a reduction of flow into the aeration tanks (i.e. a reduction in inflow of total pollutant loads) or a reduction in oxygen supply (i.e. limiting the nitrification process) might have prevented the occurred problems. Naturally, this would have resulted in an increased ammonium load in the wwtp effluent, but might have prevented the weeks-long restoration of normal plant operation.

Origin of additional loads during wet weather flow

An interest in the prevention of such extreme wet weather peak loadings to a wastewater treatment plant starts with a search for the origin of additional pollutant loads. The origin of additional loads has been studied by e.g. Krejci *et al*. (1987) and Gromaire *et al*. (2001). Identified sources of pollutant loads in wet weather flow are, apart from the continued dry weather flow during the storm event, loads entering the sewer system via run-off and loads from eroded in-sewer stocks (sometimes divided into sewer sediments and bio-films). For the 'typical large storm event' on June 12th/13th, 2008 (earlier presented in Figure 6-28) the contribution of in-sewer stocks to the total TSS_{eq} load from catchment area Eindhoven Stad is derived using a mass-balance equation as used by Gromaire *et al*. (2001):

$$M_T = M_S + M_R + M_D$$

with:
- M_T = total mass of pollutants at catchment outlet / wwtp inlet [kg]
- M_S = mass of pollutants from in-sewer stocks [kg]
- M_R = mass of pollutants from run-off [kg]
- M_D = mass of pollutants from dry weather flow [kg]

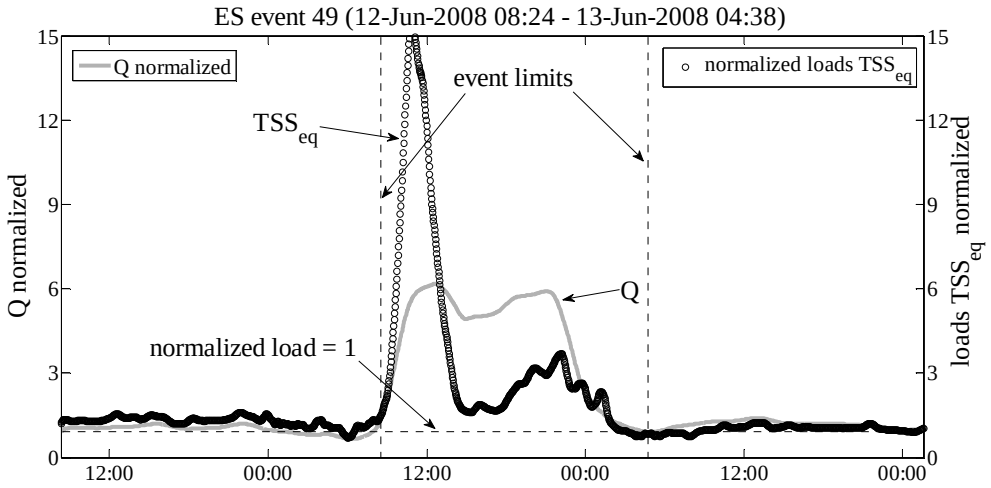

Figure 6-39: The reaction of flow and pollutant loads of TSS_{eq} to the same storm as presented in Figure 6-28. Values are normalized to DWF means.

Figure 6-39 presents the variation of TSS_{eq} loads over the course of the storm event. The surface area beneath the TSS_{eq} graph and enclosed by the event limits represents the total load of TSS_{eq} that arrives at the wwtp Eindhoven during the storm event ($M_T \approx$ 50,000 kg TSS_{eq}). The DWF load equals the surface area beneath the 'normalized load = 1' line ($M_D \approx$ 14,000 kg TSS_{eq} or 28% of total load). The contribution of run-off is calculated as $M_R \approx$ 7,500 kg TSS_{eq} or 15% of the total load. To obtain this value total run-off volume ($\approx$ 150,000 m^3, i.e. the volume larger than the DWF volume) has been multiplied by an assumed pollutant concentration in run-off equal to mean pollutant concentrations in Dutch stormwater as collected in the STOWA stormwater database (for TSS 49 mg/L, see STOWA, 2007a). The resulting mass of pollutants from in-sewer stocks is hence 28,500 kg TSS_{eq} or 57% of the total arriving load during the storm event. For the same storm event total load of parameter COD_{eq} consists of 62% originating from in-sewer stocks. All derived shares can be found in Table 6-14. Using the same approach for the 'extreme loading' event of May 7th, 2007 the share of in-sewer stocks in the total pollutant loads TSS_{eq} and COD_{eq} arriving at the wwtp Eindhoven has been calculated as 69% and 74%, respectively. For this event the share of run-off is likely underestimated as a prolonged dry period is expected to lead to larger run-off pollutant concentration values than the aforementioned mean value from the STOWA database. Calculated percentages are comparable to values found in literature, see Table 6-14. Considering the large shares of in-sewer stocks it can be concluded that these are an important source for the pollution load TSS and COD arriving at the wwtp Eindhoven during large storm events.

Table 6-14: Contributions of dry weather flow loads (M_D), run-off loads (M_R) and in-sewer stocks loads (M_S) in total observed load (M_T = 100%) for two (very) large storm events in the Eindhoven area and literature values.

		dry weather flow (M_D)	run-off (M_R)	in-sewer stocks (M_S)
TSS				
Eindhoven data:				
June 12th/13th, 2008	ES	28%	15%	57%
May 7th, 2007	RZ + ES	18%	13%	69%
literature:				
Gromaire *et al.*, 2001	median	21%	15%	64%
	10%-90%	4%-43%	9%-25%	40%-81%
Krejci *et al.*, 1987	average	6%	35%	59%
COD				
Eindhoven data:				
June 12th/13th, 2008	ES	33%	5%	62%
May 7th, 2007	RZ + RZ	22%	4%	74%
literature:				
Gromaire *et al.*, 2001	median	34%	15%	51%
	10%-90%	9%-62%	10%-29%	26%-72%
Krejci *et al.*, 1987	average	20%	22%	58%

For the May 7th, 2007 event the derived TSS_{eq} pollutant load from in-sewer stocks equals roughly 100,000 kg. With an estimated wet bulk density of around 1200 - 1700 kg/m^3 (Ashley *et al.*, 2004) this corresponds to about 70 m^3 of resuspended in-sewer sediments and biofilms. If (theoretically) spread out evenly over the 2100 km of sewer pipes in the Eindhoven area this volume corresponds to a uniform sediment/slime layer of (for instance) 1mm in height and 3cm in width. From multiple observations in the Eindhoven sewer system (as well as general observations in many other sewer systems) it is suspected that the total in-sewer storage of sediments and biofilms is (much) larger than this calculated load of eroded sediments. Hence, during the event only a fraction of total in-sewer stocks has been eroded and transported towards the wwtp. As a result, also directly following a storm event the 'pollutant reservoir' in sewer sediments is not depleted and a subsequent storm event can again be associated with a peak in pollutant loads. This repetitive character of peak pollutant loads during a series of successive storms has been observed in Figure 6-33. This observation is in line with research on the total pollution potential of sewer sediments. Ristenpart (1995, cited in Ashley *et al.*, 2004) found the pollution potential in terms of COD load in bed material in a typical sewer pipe to be 29 times higher than in the wastewater above the bed. Naturally, not all these pollutants are transported to the wwtp during a storm event as only part of the sediment is eroded and part of the remobilized pollutant load again settles further downstream in the system.

With dry weather flow being a continuous contribution to the wastewater system, the prevention of extreme wet weather peak loadings to the Eindhoven wastewater treatment plant can be achieved reducing the wet weather contributions of run-off and/or of in-sewer stocks. For this, a number of solutions are available that essentially reduce the availability of pollutant loads at many locations along the route from precipitation to wwtp inflow. For instance, more frequent street sweeping reduces pollutant loads on impervious areas, intensified gully pot cleaning ensures less pollutant entrainment by run-off entering the sewer system, and regular sewer cleaning with e.g. flushing gates prevents the resuspension of material that was deposited at an earlier stage. Ashley *et al.* (2004) present an overview of approaches that have been applied for sewer solids management showing application and effectiveness. Further research is required to evaluate the applicability of each of these techniques in the Eindhoven area wastewater system. Besides technical aspects, an important question to be answered concerns the value of a peak load reduction. Estimating the gain of smaller peak loadings to wwtp and CSOs (e.g. in terms of improved wwtp and CSO effluent quality or prevention of costs associated with a calamity such as the May 7th, 2007 event) would allow for an improved evaluation of the advantages of an intensified solids management program.

Chapter 7 In-sewer temperature monitoring

7.1 Introduction

For water quality monitoring, the advantage of using automated sensors instead of the 'traditional' method of manual sampling and laboratory analysis lies primarily in the possibility to generate high-frequent and continuous data sets. Conventional sampling campaigns typically last for a few hours or a day at intervals of 10 or 60 minutes whereas the UV/VIS spectrometer, as presented in chapter 5, can measure water quality parameters over time-spans of months or years with frequencies up to once per minute. As a result of this difference, monitoring with automated sensors provides an improved insight into the variation in time of the observed parameters. Additional knowledge on the *spatial* variation of the parameters, however, cannot be generated. A spectrometer installed somewhere in the wastewater system will yield, just like grab samples taken at that same location, data sets representing water quality at that specific location only.

Distributed temperature sensing (DTS) with fiber-optic cables is a measuring technique that allows monitoring the wastewater quality parameter 'temperature' simultaneously *at many different locations along a sewer conduit* using a single instrument. Over the last decades, the technique has been applied extensively in other fields, but has hitherto not found its way into sewer systems. This chapter presents applications of fiber-optic distributed temperature sensing in both combined and stormwater sewer systems.

The objective of this chapter is to introduce the DTS monitoring technique and to present results of its application in sewer systems. For this, paragraph 7.2 introduces the technique focusing on sensor set-up and cable installation, monitoring principle, and data uncertainty and calibration. Paragraph 7.3 describes the application of DTS in stormwater sewers for the purpose of locating illicit connections. The paragraph introduces illicit connections in stormwater systems, describes current techniques to locate these and explains why the use of temperature monitoring can be of added value. Subsequently, the results of DTS monitoring in two test sites are presented and discussed. Paragraph 7.4 describes the application of DTS in a combined sewer system. It introduces the test location and discusses data results. Also, a possible use of the data - flow ratio calculations in part-full pipes - is presented in section 7.4.4

This chapter is based on work earlier presented in two articles: Hoes *et al.* (2009) on the application of DTS in stormwater sewers (paragraph 7.3) and Schilperoort and Clemens (2009) on the application in combined sewer systems (paragraph 7.4).

7.2 Fiber-optic distributed temperature sensing

7.2.1 Introduction

Fiber-optic distributed temperature sensing is a monitoring technique developed at the beginning of the 1980s in the United Kingdom (e.g. Dakin *et al.*, 1985). The technique is a spin-off of technology developed for testing fiber-optic cables that are installed for telecommunication purposes. Since the 1980s the technique has found many applications in a wide variety of fields. For instance, DTS has been used for leakage detection in dams (Johansson, 1997), the hydrology of small streams (Selker *et al.*, 2006a,b), fire detection in cable trays in buildings (Glombitza and Hoff, 2004) and fire detection in road tunnels (e.g. the German SOLIT-project). The wide application of the technique can be understood considering a number of characteristics the technique offers in common system monitoring situations. For instance, a DTS system (with power supply and data storage at a single and easily accessible location) can replace many point sensors, hence reducing the effort for power supply and data gathering at many different locations. Since the fiber acts as both sensing element and transmission medium, a separate data communication system is not required. When *a priori* knowledge of sensor placement lacks, the near-continuous spatial resolution of the DTS system in combination with the long range of the cable allows diagnosis of small problem areas within a large observation area. Also, since there is no electrical signal in the fiber-optic cable, placement in an environment that in some cases requires explosion-proof equipment (such as sewers systems) is possible.

7.2.2 Monitoring set-up and cable installation

The application of DTS in sewer systems is performed with a fiber-optic cable in combination with a stand-alone instrument that contains a laser, sensing optoelectronics and a PC. The fiber-optic cable is laid out at the invert of a sewer pipe. At one end, the cable is connected to the computer/laser instrument that is generally stored outside the sewer system in a small container to protect it from weather and vandalism (see Figure 7-1). For the case-studies presented in this chapter, fiber-optic cables were used by manufacturer Kaiphone Technology (Taiwan). The cables carry two glass fibers, of which one is used for measurements and the other provides redundancy. The glass fibers (multimode 50/125 μm core/cladding diameter) are embedded in a gel to avoid direct stress on the fibers, as stress influences measurement results. The fibers are further protected by subsequent layers of PBT, stainless steel spiral, aramid fiber, metal braiding and PE. The laser/computer instrument used is a Halo DTS by manufacturer Sensornet (England).

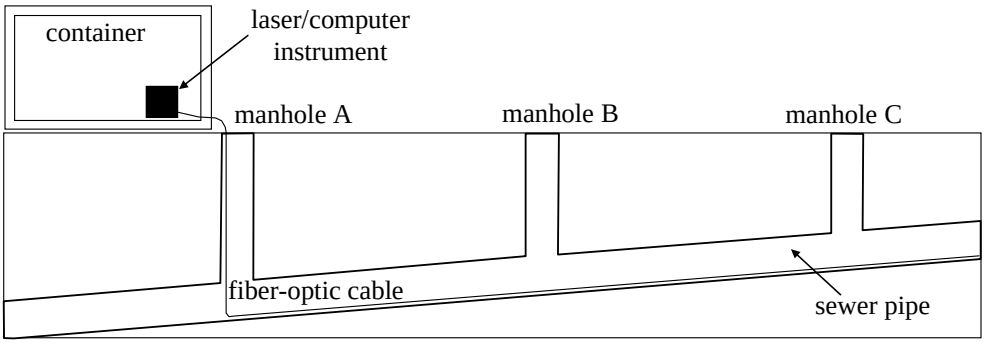

Figure 7-1: Set-up of in-sewer DTS monitoring

Installation of the cable in a sewer pipe requires pulling a rope from manhole A to manhole B (see Figure 7-1) by first letting a water-jet propelled sewer flushing device make its way from B to A and - after attachment of the rope - by mechanically pulling the device back to manhole B. Consequently, the fiber-optic cable that is attached to the end of the rope can be pulled from A to B by hand. Pulling the cable manually assures that, in case of sudden blockage, no damaging excessive forces are exerted on the cable. Steps are repeated to advance from manhole B to manhole C. Following this procedure, installation of a 1300m cable takes a 5-persons team approximately 4 hours. This can be improved by using pulleys to reduce friction in combination with a longer hose on the sewer flushing device to skip manhole B, and start from manhole C. Bends or loops in the cable with a radius less than 10 cm should be avoided to prevent loss of signal in the cladding which has a lower refractive index than the core of the fiber. Mechanical and other restrictions to be observed during installation and operation of a fiber-optic cable can be found in EN-IEC (2003).

7.2.3 Monitoring principle

For a measurement, the laser instrument emits a pulsing laser light into the fiber-optic cable through a directional coupler, see Figure 7-2. As a result of several mechanisms light is scattered as the pulse passes down the fiber. Density and composition fluctuations such as microscopic non-uniformities in the glass fiber cause Rayleigh scattering; Raman and Brillouin scattering are due to molecular and bulk vibrations, respectively (López-Higuera, 2002). Each scatter type has its effect on wavelength and intensity of the scattered light, see Figure 7-3. A proportion of the scattered light is retained in the fiber core and travels back towards the source. There, the signal is read by the optoelectronics and further processed.

The Rayleigh and Raman components of the backscattered light are used in combination to create temperature against distance profiles. The Rayleigh backscatter is the main component of the returned signal and is unshifted from the launch wavelength. Knowing the speed of light in fiber, the distance the light has travelled down the fiber can be calculated. Hence, Rayleigh backscatter provides information on the *location* of the reflection along the cable. This process is often referred to as optical time-domain reflectrometry.

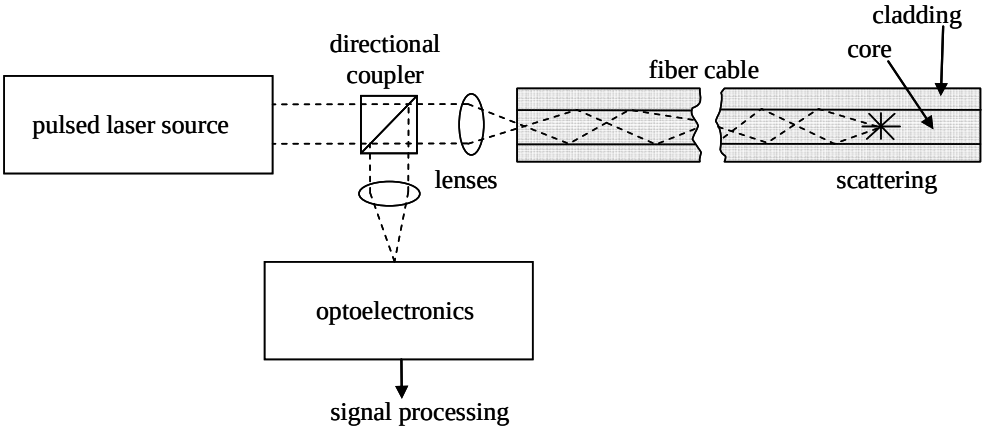

Figure 7-2: Configuration of laser, fiber cable and optoelectronics for a DTS measurement (after López-Higuera, 2002)

The Raman light comprises two elements: the Stokes and anti-Stokes signals which are shifted in wavelength compared to the Rayleigh signal and can be filtered from the dominant constituent of the total backscattered light. The intensity of the longer wavelength Stokes light is nearly independent of temperature whereas the intensity of the shorter wavelength anti-Stokes light is temperature-dependent. The *temperature* at the location of the reflection along the fiber-optic cable is determined using the ratio of the anti-Stokes and Stokes light intensities. Further details on the monitoring principle of DTS can be found in López-Higuera (2002).

The temporal and spatial resolution of the measurement can be manually adjusted. Typical temporal resolutions for in-sewer applications are 30 seconds up to several minutes; a typical spatial resolution is 2 meter, which is also the minimum value for the applied Halo instrument. Programming these resolutions yields a temperature data set every 30 seconds containing temperature values for each 2 meter section of the fiber-optic cable. Essentially, all backscattered signals originating from the targeted section of the cable are integrated over the considered time-span to derive a single temperature value for that section.

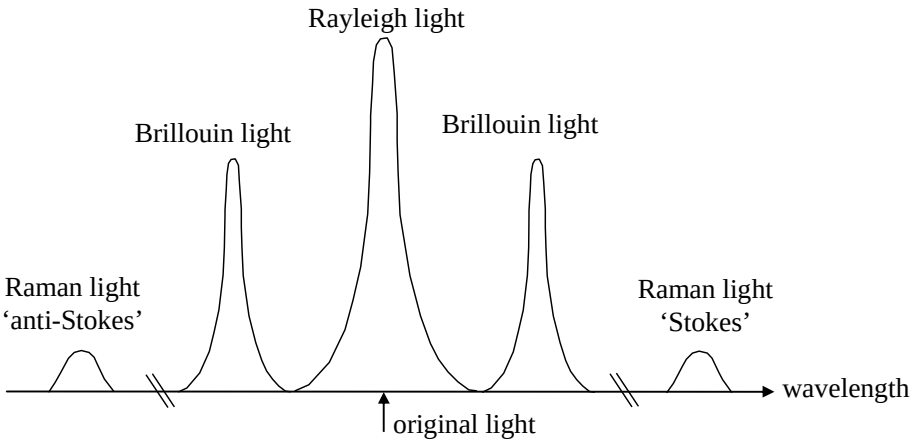

Figure 7-3: Scatter types and their spectral shifts with respect to the emitted laser light (after López-Higuera, 2002)

7.2.4 Calibration and data uncertainty

A distinction must be made between the absolute accuracy of a DTS measurement and repeatability or precision. Absolute accuracy is the ability of the DTS system to accurately measure a temperature value and is typically referenced to a standard measurement method in a calibration process (e.g. thermistors or bi-metal thermocouples). Hence, the absolute accuracy of a DTS system is limited by the accuracy of the device generating reference values during the calibration process. Calibration of the instrument requires a value for temperature offset and a slope parameter that adjusts the offset with distance from the computer/laser instrument. A calibration is ideally carried out by placing the entire cable in an environment of known constant temperature, attaching the cable to the instrument and taking a long-time integration measurement (Selker *et al.*, 2006b). Logically, this kind of calibration must be carried out before installation of the cable in a sewer system. Alternatively, after installation of the cable in a sewer system or because of any other logistical difficulty, calibration is possible inserting two well separated sections of the cable in an environment of known temperature such as an ice-bath. Recommended lengths of such calibration sections are on the order of 30m or more (Tyler *et al.*, 2009). This way, calibration of most commercial DTS systems against standard thermometers can yield absolute measurement accuracies up to ±0.1°C. Figure 7-4 gives an example of the calibration of an in-sewer DTS set-up after installation of the cable in the sewer system. Two reference measurements with 0.2°C accurate temperature sensors installed directly next to the fiber-optic cable at locations 1 and 2 give an offset and slope parameter to calibrate the raw DTS data. In this example, the two calibration sections were only 5m long and could not be

arranged at the beginning and end of the cable, but instead at locations around 500m and 800m from the instrument. Two reference measurements should be sufficient for calibration since the signal attenuation process is in theory purely log-linear. However, when irregularities such as connectors or fusion splices are found in the cable measuring an offset at more than two calibration sections gives a better understanding of the temperature offset along the cable (see e.g. Figure 7-17).

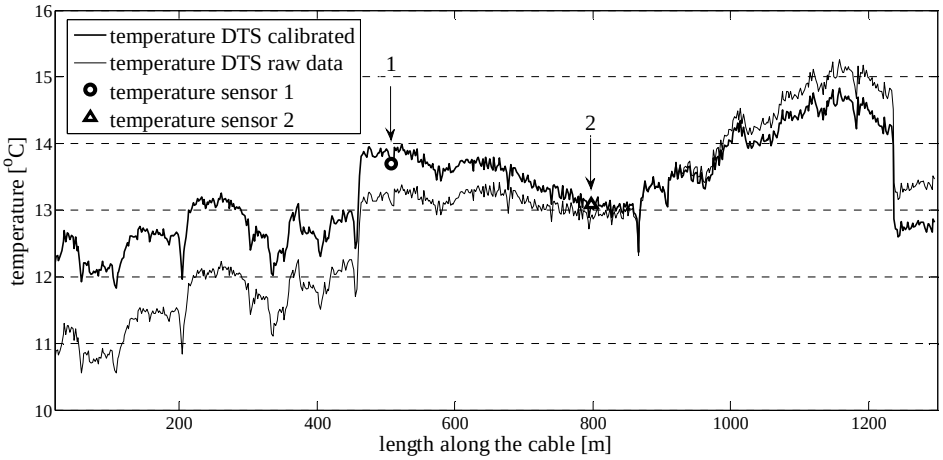

Figure 7-4: Calibration of a DTS measurement using two additional reference sensors

Repeatability or precision of measurements describes the closeness of agreement between the results of successive measurements under identical conditions. For DTS systems, repeatability can be divided into two components: temporal and spatial repeatability. In an environment with constant temperatures in both time and space temporal repeatability describes closeness of agreement between measurements over a certain time-span taken at one location whereas spatial repeatability describes the same for measurements taken at one moment in time at multiple locations along the fiber-optic cable.

Tyler *et al.* (2009) have tested both precision types for various commercially available DTS systems, among which the system used for the measurements presented in this chapter. Short-term (~2 hours) temporal repeatability tests show standard deviations ranging between 0.1°C and 0.3°C for different systems. Long-term effects such as instrument drift are not included in these values. For these effects values of ±1°C to 2°C are reported, especially for multiday experiments when the instruments are subjected to significant internal temperature variations (which can be the case for in-sewer DTS monitoring campaigns). Observed values for standard deviations of spatial repeatability over cable lengths of ~100m range

between 0.02°C and 0.08°C. Hence, small changes in temperature from one cable section to the other can easily be detected with a DTS system.

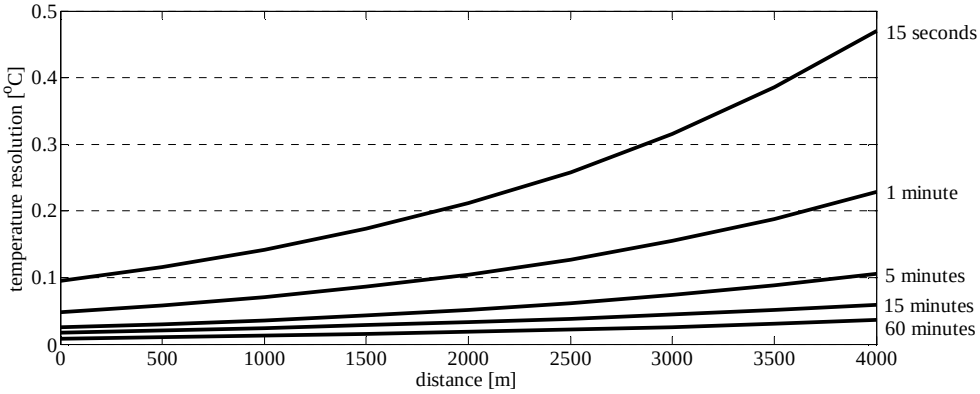

Figure 7-5: For the Sensornet Halo DTS system the temperature resolution versus distance along the fiber-optic cable at different integration times. The presented values are for a spatial resolution of 2m (Sensornet, 2009).

The precision of a DTS measurement is dependent on the distance from the instrument, the selected temporal resolution, the selected spatial resolution, and the quality of the applied instrument and cables. In general, the more reflected laser pulses can be used for a single temperature reading, the more precise the reading is. In other words, the precision of the measurement deteriorates for measurements taken further away from the instrument, for shorter integration times, for shorter integration sections and for less quality cables and connectors that generally show increased signal attenuation. For the Sensornet Halo DTS instrument the 'temperature resolution' is given in Figure 7-5 as a function of distance along the cable and programmed resolutions. Temperature resolution is defined by Sensornet (2009) as "the standard deviation of the measured temperature with respect to distance" (i.e. spatial repeatability), and should not be confused with the minimum resolvable step change that can be detected by the system.

For DTS applications in stormwater sewers, absolute accuracy of measurement is not of the utmost importance. Locating illicit connections requires the ability to observe temperature *differences* along the cable instead of generating accurate temperature values. Therefore, spatial and temporal precision are more important than an accurate calibration procedure. A calibration program has not been deemed necessary for this specific application. For the application in a combined sewer system, however, knowledge of accurate temperature values is important. Therefore, for this application a calibration program was performed.

7.3 Distributed temperature sensing in stormwater sewers

7.3.1 Introduction

Ever since the introduction of separate sewer systems system managers have been faced with illicit connections. These illicit connections are generally unintended cross-connections that connect foul water outlets from residential or industrial premises to the stormwater system and/or stormwater outlets to the foul water system. For locating stormwater outlets that are connected to the sanitary sewer system, a reliable, inexpensive, and often practically feasible method exists: introducing smoke in the sanitary sewer and searching for stormwater outlets through which smoke is released (see e.g. US EPA, 2004). Such a simple and straightforward method does not exist for the location of foul water outlets connected to stormwater systems. Most currently applied searching techniques come with disadvantages that reduce reliability, increase costs or make the method difficult to implement.

The DTS monitoring system offers a new methodology for locating illicit connections in stormwater sewers. In this paragraph the method is explained and examples of application are presented. Illicit connections are introduced in section 7.3.2 reporting on occurrence, effects on receiving waters and current detection techniques. Then, in section 7.3.3 the concept of using temperature differences and variations for the location of illicit connections is discussed. The two locations where the method has been tested are introduced in section 7.3.4. Finally, test results are presented in section 7.3.5 and discussed in section 7.3.6.

7.3.2 Illicit connections in stormwater systems

Definition

In the Netherlands separate sewer systems have been widely introduced since the early 1970s to circumvent the drawbacks of combined sewer systems. Since then, it has become clear that separate sewer systems also come with disadvantages. A major drawback is the occurrence of illicit connections. For stormwater systems the term ‘illicit connection’ has many meanings in regulations, literature and practice. The strictest definitions consider an ‘illicit connection’ a connection with a discharge that is not entirely composed of stormwater. The United States Environmental Protection Agency (US EPA, 2004), however, considers discharges to stormwater systems to be illicit only if a flow during dry-weather conditions contains pollutants and/or pathogens. By this definition, discharges of for instance groundwater (if unpolluted) are not considered improper. On the other hand, intended or accidental spills on paved areas of liquids such as oil, grease, paint or car wash water that enter the stormwater system after surface run-off through a

storm drain inlet are considered illicit discharges, but are not the result of an illicit connection. In the context of this paragraph, illicit connections to stormwater systems are defined as unintended sewer cross-connections that connect wastewater outlets from residential or industrial premises to the stormwater system. The majority of these connections are due to poor plumbing during construction or renovation of a property when outlets are connected to the closest available sewer pipe, which is not necessarily the designated sewer pipe. Infiltration and inflow of e.g. groundwater or drain water are not considered illicit discharges, but are referred to as extraneous flows.

Occurrence and effects

Illicit connections to stormwater systems are common. Schmidt and Spencer (1986) report that more than one third of over 300 inspected buildings in a drainage basin in Ann Arbor (Michigan, USA) discharged wastewater to the stormwater system. An extensive study in the Boston area (Massachusetts, USA) revealed a smaller percentage: 3% of nearly 5700 inspected buildings were found to have an illicit connection (Jewell, 2001). Other studies in the United States (US EPA, 2004) show similar percentages of illicit connections to stormwater systems. Many of these detection programs are initiated upon water quality problems at beaches and lakes (Boyd *et al.*, 2004; Dickerson *et al.*, 2007). Illicit connections lead to direct transport of raw wastewater through storm drains to receiving waters. At the outfall of a storm drain there is often no treatment or only limited treatment in the form of a settling basin or plate separator. As a result, illicit connections can represent a major source of pollution to receiving waters. After an extensive monitoring program, van Sluis *et al*. (1991) concluded for the Netherlands that mainly because of illicit connections the average annual pollution load discharged to receiving waters from stormwater systems can be on the same order of magnitude as the pollution load discharged from combined sewer systems. In other words, the anticipated pollution reduction by building a more expensive separate sewer system can be largely annulled by the presence of illicit connections. Logically, repairing illicit connections has a beneficial effect on receiving water. Taylor and Wong (2002) present the effects of illicit discharge elimination programs in various large cities. In one example, the changes of in-sewer stormwater quality before and after an elimination program were measured and analyzed using event mean concentrations averaged over 4-year intervals. The results include a reduction in event mean concentrations of 13% for total suspended solids, 17% for total phosphate and 8% for total Kjeldahl nitrogen.

Present searching techniques

Current searching techniques to locate illicit connections to stormwater sewers include (Jewell, 2001; Tuomari and Thompson, 2003; US EPA, 2004):

- Visual inspection and progressive sampling at manholes. The goal is to isolate the illicit discharge between two storm drain manholes for which

visual inspection results (e.g. presence of flow, odors, deposits) or indicator sampling results (e.g. ammonia/potassium ratio, surfactants, caffeine) differ significantly.
- Dye testing. The introduction of a non-toxic dye into toilets, sinks, shop drains and other plumbing fixtures and the subsequent discovery of dye in the storm drain suggest the existence of an illicit connection to the storm sewer and pinpoints to the specific source.
- Video reconnaissance. Guiding a mobile video camera through the storm drain pipes allows a visual inspection of sewer pipes and reveals connections that discharge during dry weather conditions.

However widely applied, these techniques come with disadvantages. Visual inspection of manholes is subjective (Dirksen *et al*., 2011) and not all water quality changes can be visually perceived. Progressive sampling at manholes requires a large number of laboratory analyses, while results cannot exactly locate illicit connections in-between manholes. For dye testing the need to enter premises makes application in some areas practically infeasible. Moreover, the method is laborious with often many plumbing fixtures per connection. Observation of an intermittent domestic wastewater flow from an illicit connection with video reconnaissance is difficult as an average household connection discharges wastewater only during ~30 minutes per person per day (Butler *et al.*, 1995). Hence, video testing mainly depends on visual observation of residues such as toilet paper.

7.3.3 Method: searching anomalous in-sewer temperatures and variations

For the detection of illicit connections in stormwater sewers the parameter 'in-sewer temperature' is considered. Temperature monitoring for the detection of extraneous flows has previously been used in other in-sewer applications (e.g. Wirahadikusumah *et al.*, 1998). For dry weather conditions, in-sewer temperatures in a stormwater system without illicit connections are determined by surrounding air and soil temperatures (Dürrenmatt and Wanner, 2008), see Figure 7-6. In the Netherlands, values for soil temperatures at 1m depth vary between roughly 5°C (winter) and 15°C (summer); average air temperatures range from approximately 3°C for winter conditions to 17°C for summer conditions (KNMI, 2008). Within these ranges, air and soil temperatures are primarily subject to daily and seasonal variations. In case of a (partially) submerged stormwater system (i.e. when surface water levels are higher than sewer invert levels) heat exchange is also possible with receiving waters. Receiving water temperatures and variations therein are comparable to soil temperatures. Considering the temperature characteristics of these two (or three) influencing entities, it can be deduced that 'expected' dry weather in-sewer temperatures for a stormwater system without illicit connections are within the same range of values showing temperature variations only on a daily

and seasonal basis. Any deviant temperature values and/or deviant temperature variations constitute an anomaly from the described dry weather conditions and suggest an additional 'influencing factor'. Results in the next section show that such irregularities in in-sewer temperatures are frequently related to an illicit connection.

The DTS technique provides a means to study temperature values in stormwater sewers. Data results give a detailed view of in-sewer temperatures and variations therein in both time and space. Hence, results allow searching for anomalous temperatures and temperature variations that point to a disruption of usual conditions inside the stormwater system.

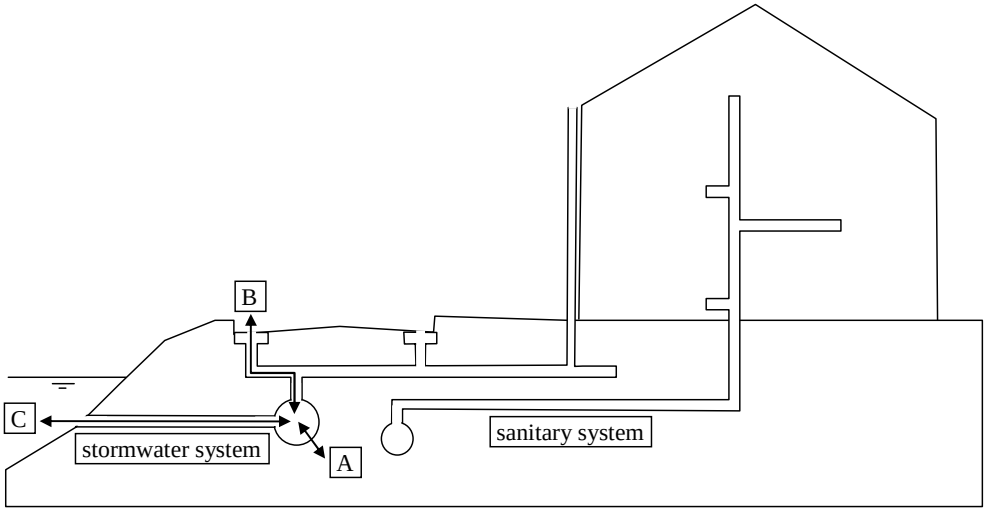

Figure 7-6: Heat exchange of a 'perfect' stormwater system: only with surrounding soils ('A'), outside air ('B') and receiving waters ('C').

7.3.4 Test areas: Korendijk and Groningen

The DTS method has been applied in the municipalities of Korendijk and Groningen in the Netherlands. Preparatory visual inspections of sewers as well as residents' complaints inventories had already revealed the presence of illicit connections in the selected areas. Their exact locations however, were unknown. Table 7-1 presents area characteristics and monitoring parameters for each catchment area. The areas differ in type which allows studying both domestic and industrial/commercial discharges. The Korendijk sewer section services a number of streets with 102 bungalows and terraced houses whereas the Groningen stormwater sewer is situated in a street with 11 large buildings each one housing multiple companies and industries. Data sets from both areas include data collected

during storm events. This opens up the possibility to study the influence of precipitation on DTS measurements in stormwater systems. Groningen data have been gathered under both submerged and empty sewer conditions, which allows observation of the differences in data results. In the context of this paragraph 'submerged' indicates that a large amount of water is present in the sewer system due to which the fiber-optic cable at the invert of the pipe is completely submerged and measures water temperatures only. 'Empty', on the other hand, does not suggest that the system is completely free of water; instead, 'empty' systems will hold small amounts of water (wastewater spills, groundwater infiltration, etc.) that could still (partially) cover the fiber-optic cable and hence influence measurements. The main difference lies in the water mass: the temperature of the small water mass in an 'empty' sewer is more easily influenced by external heat sources than the large water mass in a 'submerged' storm drain. Korendijk data are collected in an 'empty' system. Further discussions on this topic are presented in section 7.3.6.

For both areas a temporal resolution of 30s and a spatial resolution of 2m were programmed. Using the Halo instrument and the indicated cable lengths, the measurements have a precision of approximately 0.1°C, see Figure 7-5. In both areas, no instrument calibration has taken place since absolute accuracy of temperature values are not important for this application of DTS monitoring.

Table 7-1: Characteristics of test areas Korendijk and Groningen

	Korendijk	Groningen
Type of area	residential	commercial / industrial
Length of fiber-optic cable [m]	1264	1160
Premises along studied sewer section	102 bungalows and terraced houses	11 large multiple company buildings
Empty or submerged storm drains	empty	empty and submerged
Precipitation during monitoring	yes	yes

7.3.5 Results

Korendijk

Figure 7-7 presents the results for the Korendijk catchment area. The horizontal axis represents the length along the cable from x=0 m at the Halo instrument to x=1264m at the end of the cable; the vertical axis represents a time-span of 21 hours: from Thursday October 9th 18h00 until Friday October 10th 15h00. The figure consists of 632 x 2520 pixels (respectively 1264m divided by the 2m spatial resolution and 21 hours divided by the 30s temporal resolution) that each represent

a measured temperature value. The pixels are colored according to the color map on the right hand side of the graph: values of 16.5°C and lower are colored white, values of 19°C and higher are colored black and any intermediate values are a shade of gray. For this graph the range of presented temperatures has been adjusted to accentuate values other than predominant in-sewer temperatures. In appendix L (Figure L-1) the original full-color graph can be found. A longitudinal profile of the storm drains is given directly above the temperature graph. The numbers (1-26) represent manholes that vertically correspond to locations in the temperature graph. Side-connections to other storm drains are indicated by circles.

The in-sewer predominant temperature is around 16°C. At six locations ('a' through 'f') anomalous temperatures above the dominant temperature are observed. High-temperature plumes have a distinct shape: a sharp upstream temperature rise during a certain time-span with energy transfer and dissipation in the downstream direction. Note that the downstream direction differs per location. For instance, at location 'c' the slope of the sewer is from left to right whereas at location 'd' the slope of the sewer is from right to left. Between manholes 22 and 24 at locations 'e' and 'f' temperatures well over 19°C are intermittently recorded. The majority of these recordings are concentrated during early morning and evening hours, whereas almost no temperature increases occur between 00h00 and 06h00. The interpretation of results is presented in section 7.3.6.

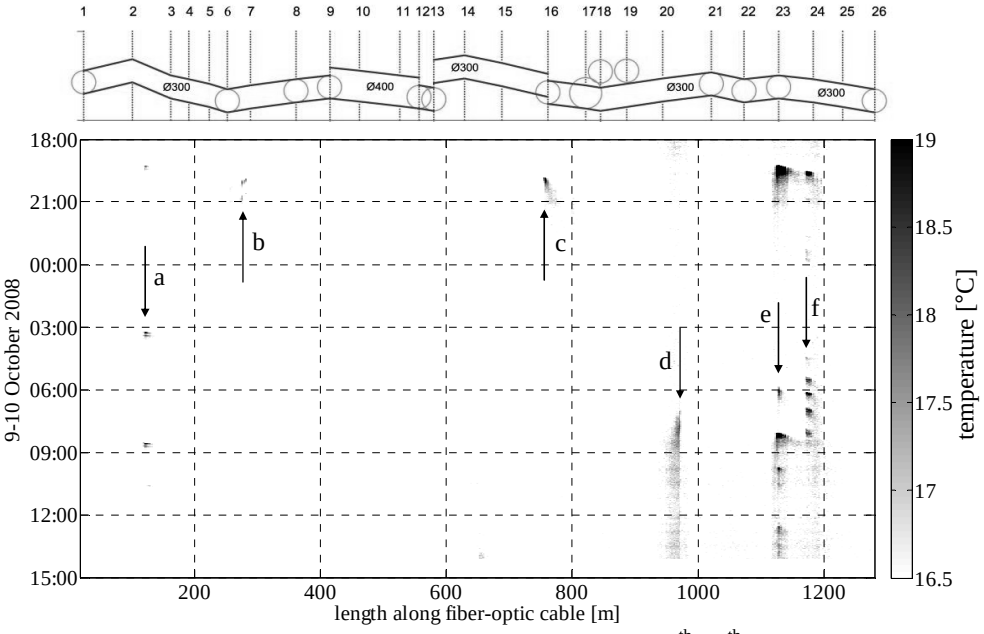

Figure 7-7: DTS monitoring results for Korendijk, October 9th-10th, 2008. In appendix L (Figure L-1) the original full-color graph is presented.

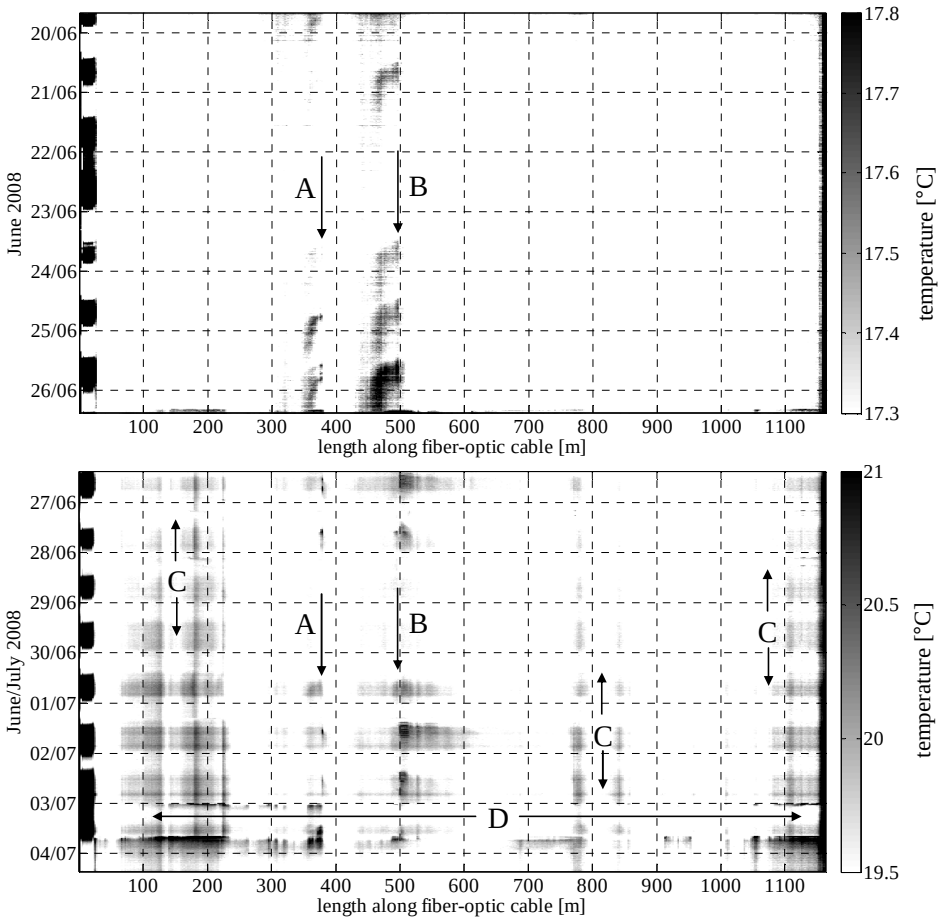

Figure 7-8: DTS monitoring results for Groningen, June 19th - July 4th, 2008. The first monitoring campaign (upper graph) took place in a partially submerged stormwater system; the second campaign (lower graph) took place in an emptied system. The original full-color graph can be found in appendix L (Figure L-2).

Groningen

In the Groningen catchment area normal receiving water levels exceed storm drain invert levels. As a result, a layer of water (~30 cm) is present in the stormwater sewers also under dry weather conditions. In this partially filled system, a first monitoring campaign was set-up (June 19th-26th, 2008) during which the fiber-optic cable was submerged in the water layer. A second campaign was held from June 26th until July 4th, 2008 after separating the storm drains from the receiving waters and emptying the drains for the duration of the campaign. During the latter campaign monitoring result represent 'empty' in-sewer conditions. Results are presented in Figure 7-8 and in appendix L (Figure L-2). The first 27m section of

the fiber-optic cable was not in the sewer system and hence recorded outside air temperatures. Predominant in-sewer temperatures differ for both graphs. In-sewer water temperatures in the partially submerged system range between 15°C and 17°C whereas air/water temperatures in the emptied storm drains vary between 17°C and 19°C. In both graphs at locations 'A' (x=378 m) and 'B' (x=500 m) high-temperature plumes are visible for working days, but not during weekends (21-22 and 28-29 June). The plumes have distinct characteristics: in partially filled situations temperature differences with the predominant values are small (0.5°C) and plumes are spread out in time and space whereas temperature differences in empty systems are larger (1.5°C) and more concentrated in time and space.

7.3.6 Discussion

Predominant in-sewer temperatures and temperature variations

For both the Korendijk and the Groningen cases, predominant in-sewer temperatures are presented in Figure 7-9. The data constitute in-sewer temperatures for three consecutive dry-weather days at locations along the studied sewer sections for which no anomalies in temperature readings have been recorded (Korendijk x=500 m; Groningen x=880 m). Korendijk in-sewer air/water temperatures in an 'empty' sewer system show a diurnal variation with values ranging between approximately 9°C and 10°C. This diurnal cycle can be attributed to variations in outside air temperatures in combination with heat exchange via storm drain inlets, manhole covers and outfalls. Superimposed on this diurnal variation is a high-frequent variation (~1 cycle per hour) with an amplitude around 0.4°C. The origin of the latter has not been found, but may be associated with instrument noise.

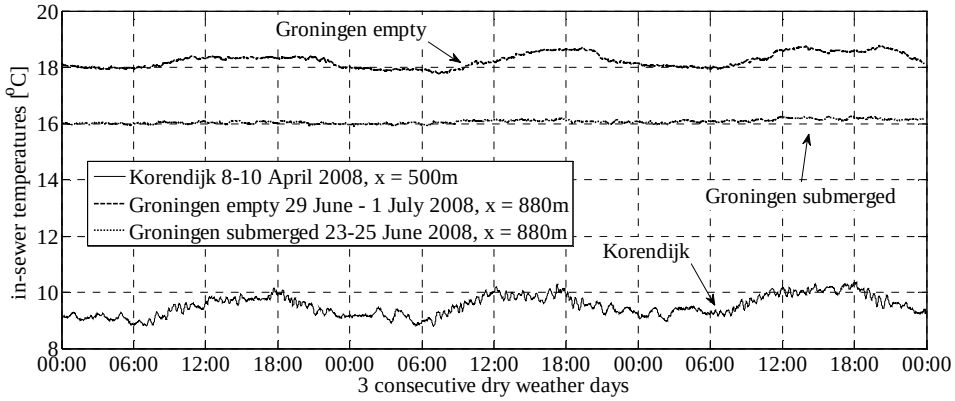

Figure 7-9: In-sewer temperature variations for three consecutive dry weather days in Korendijk and Groningen for locations without observed temperature anomalies.

In Groningen, in-sewer water/air temperatures in an empty storm sewer also show a diurnal variation with values varying between 18°C and 19°C. Compared to the Korendijk data, in-sewer temperatures in Groningen are higher due to a change in season: Groningen data were recorded in summer while Korendijk data were collected in early spring. When partially submerged, the same Groningen stormwater system shows in-sewer water temperatures around 16°C without a clearly distinguishable diurnal variation. Apparently, the large water mass in a water-filled storm drain prevents relatively quick diurnal temperature variations whereas the limited air/water mass in empty sewers is more easily influenced by outside temperature variations. For the same reason areas 'C' in Figure 7-8 are distinguishable for the emptied sewer system but not for the submerged system. The results in Figure 7-9 confirm the notion presented in section 7.3.3 that in-sewer temperatures for a stormwater system (section) without illicit connections are in the same range as soil, air and receiving water temperatures with (large) variations only on daily and seasonal basis.

Anomalous in-sewer temperatures and temperature variations

The Korendijk and Groningen results in Figure 7-7 and Figure 7-8 include multiple locations for which temperatures and temperature variations have been recorded that deviate from predominant in-sewer temperature behavior. As an example, in Korendijk at x=1124m (location 'e' in Figure 7-7) temperatures well above normal values are intermittently recorded, see Figure 7-10. During the night in-sewer temperatures are relatively stable at a value of approximately 12°C, but during day and evening hours temperatures can rise up to 27°C. It can be argued that these temperature increases are due to domestic wastewater discharges spilled into the stormwater system. First of all, water is the likely bearer of the energy that causes the temperature rise since peaks always move downstream along the considered sewer section (see Figure 7-7 for an overview and Figure 7-11 for the presentation of a warm water plume in detail). Secondly, the hours of the day (and for the industrial/commercial Groningen area also the days of the week) for which temperature peaks occur, coincide with peaks in human activities. Human involvement in the spills is further confirmed by the absolute temperature values of the spills, for in the Netherlands no natural sources are known that produce water over ~20°C. Raw domestic wastewater, however, can be (much) warmer. Over 60% of all consumed domestic water is heated in showers, baths and household appliances (Achttienribbe, 1993; Butler et al., 1995). Water temperatures can rise to ~40°C for baths and showers or to 30°C - 90°C for household appliances. Before water is discharged into the sewer system, temperatures drop as energy is lost during transport through house drains. Nevertheless, a house connection intermittently discharges wastewater that is likely warmer than ~20°C. Finally, the intermittent character as well as the duration of the peaks corresponds well with the characteristics of normal use of household appliances such as showers, laundry machines, etc.

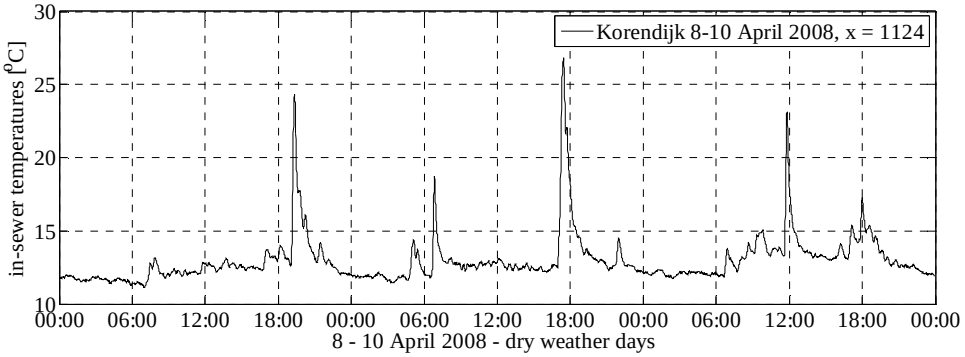

Figure 7-10: DTS monitoring results for Korendijk, April 8th-10th, 2008 at x=1124m (location 'e' in Figure 7-7)

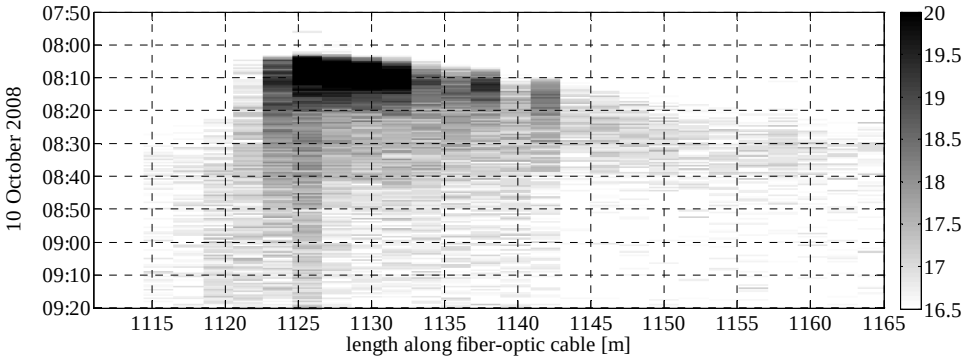

Figure 7-11: DTS monitoring results for Korendijk, zoom on warm water plume discharged at x=1124m for October 10th, 2008 around 08h00. Warm water moves downstream the sewer pipe (which is from left to right in this figure).

Although these four arguments make domestic wastewater discharges the *probable* source for the observed anomalous in-sewer temperatures, they do not prove *causality*. Conclusive evidence linking observed temperature peaks to domestic wastewater discharges was found during on-site verification of results by excavation and testing. For the Korendijk area a verification of results was performed opening warm water taps at suspected premises resulting in either visual or auditive confirmation of water entering the storm drains. Also, monitoring results showed increasing temperature values. In Groningen excavation work at the location of observed high-temperature plumes confirmed the existence of illicit connections.

Empty versus submerged stormwater systems
In many areas in the Netherlands stormwater sewers are submerged due to high water levels in receiving waters. A (partially) submerged sewer pipe contains an amount of water which means that a fiber-optic cable installed at the invert of that pipe is completely covered by a water layer and measures water temperatures. The water layer acts as a 'buffer' diluting discharges of warm wastewater. As a result, the fiber-optic cable will not measure the temperature of the discharge itself, but a 'mean value' of the mixture of the discharge and the water layer in the sewer pipe. For this mixture the temperature increase after a warm water discharge will be (much) lower than for the original discharge, approaching the detection limit of the DTS system. The question arises which discharge can still be detected by a fiber-optic cable at the invert of a submerged stormwater sewer. This can be roughly estimated using a simple theoretical approach presented in Figure 7-12.

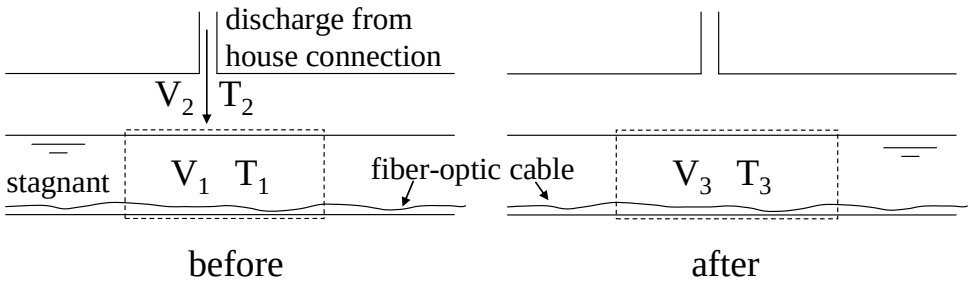

Figure 7-12: A discharge of volume V_2 and temperature T_2 into a partially submerged stormwater sewer with volume V_1 and temperature T_1. The mixture has volume V_3 and temperature T_3.

Assuming that a discharge with volume V_2 and temperature T_2 mixes fully and instantaneously with water volume V_1 of temperature T_1 in the sewer system, the mixture has a volume of V_3 and temperature T_3. Combining conservation of mass ($V_1 + V_2 = V_3$), conservation of energy ($V_1T_1 + V_2T_2 = V_3T_3$) and the in-sewer wastewater temperature change $\Delta T = T_3 - T_1$ it can be derived that:

$$\frac{V_2}{V_1} = \frac{\Delta T}{(T_2 - T_1) - \Delta T} \qquad (7.1)$$

As (nearly) the same cable section is monitoring T_1 and T_3 the temporal precision of the DTS system determines which observed in-sewer temperature change (ΔT) is significant and not due to random variation. As earlier presented in section 7.2.4 this depends on the type of DTS system, the programmed resolutions and the

distance to the instrument. Given a certain precision, the ability to detect a discharge is determined by the ratio of volumes V_1 and V_2 and the temperature difference. For instance, with a 0.1°C precision a discharge that is 5°C warmer than the in-sewer wastewater can only be discerned if the volume of the discharge (V_2) is larger than $1/49^{th}$ of the in-sewer volume that is influenced by the discharge (V_1). In practice, the ability to detect a warm water discharge will depend on many more factors such as the exact location of the discharge, pipe geometry, the temporal resolution of the measurement, the mixing process, possible flow in the sewer pipe, etc. Currently (2011), tests are carried out in an experimental set-up to study the detection limit of the DTS system under normal in-sewer conditions.

In the Groningen case study the same sewer section has been tested for empty as well as for submerged conditions. Results reveal warm water plumes for both conditions for the same two locations (Figure 7-8, at x=378m and x=500 m). The plumes however have different characters. For the submerged system, temperature variations are slower and spread out in time and space whereas temperature variations for the empty system are faster with discharged water remaining closer to its origin and cooling down more quickly. This is illustrated in Figure 7-13.

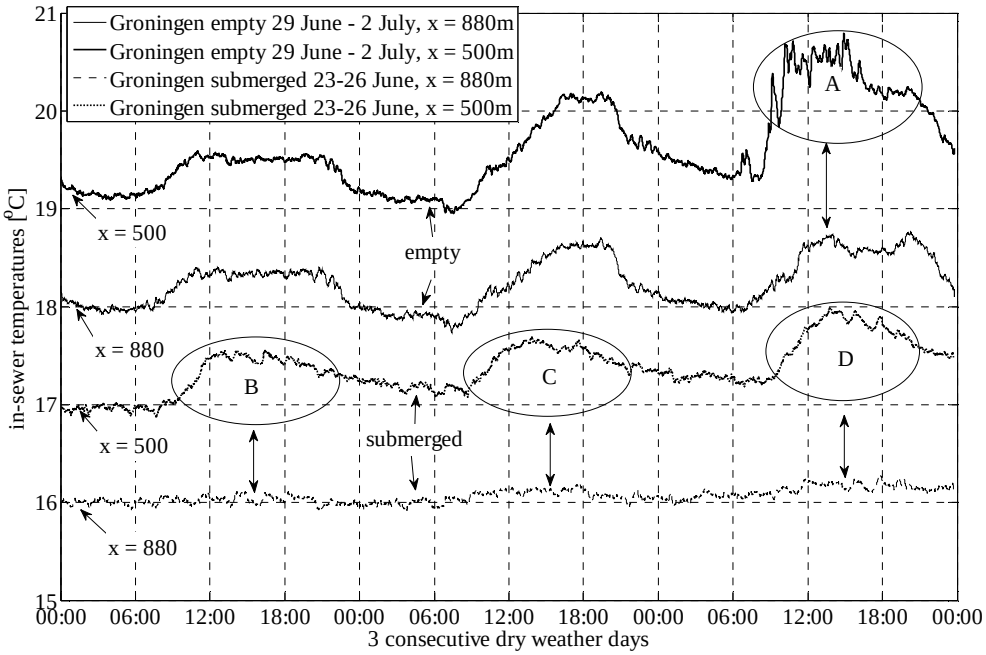

Figure 7-13: DTS monitoring results for Groningen. Results for three consecutive dry weather days at x=500m (illicit connection) and x=880m (normal conditions, no illicit connection) for both an emptied and a partially submerged stormwater system.

The graph presents temperature variations for both the empty and submerged systems during a three-day dry weather period at two distinct locations. Measurements at x=880m represent normal in-sewer temperature variations, namely a diurnal pattern for the empty system and a nearly constant temperature value for the submerged system (compare with the value presented in Figure 7-9). Measurements at x=500 m, however, show deviations from these standard patterns. In the emptied system, anomalies (area 'A') take the shape of relatively quick variations that cause slightly higher temperatures (~0.5°C) than expected considering the data for x=880 m. Areas 'B', 'C' and 'D' show that anomalies in a submerged system take a different form with gradual variations over the day that cannot be observed for locations without illicit connections. Despite their different appearances, anomalies in temperatures and temperature variations are detectable for both types of systems. In this case study illicit discharges can be detected using the DTS-monitoring system in both empty and submerged stormwater systems. Hence, in this case emptying the partially filled stormwater system is not required for DTS-monitoring to be successful.

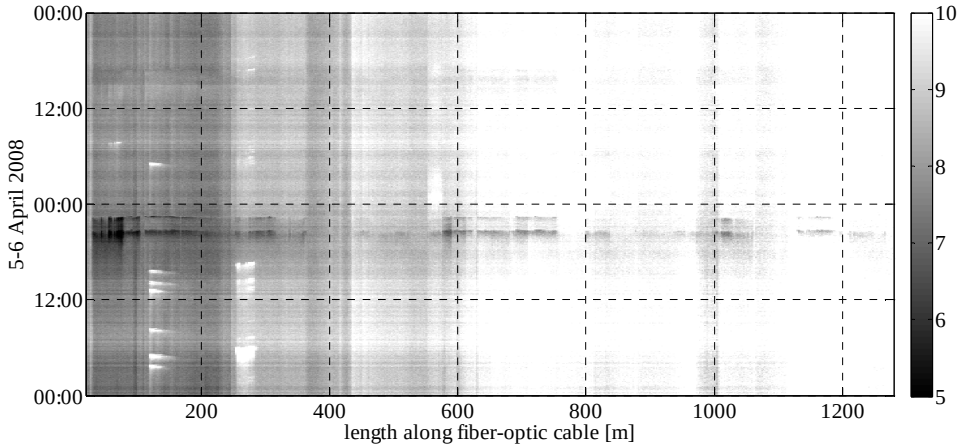

Figure 7-14: DTS data results for Korendijk, April 5th and 6th, 2008. The temperature range of the color bar next to the graph has been adjusted to accentuate values associated with precipitation in the early hours of April 6th. As a result, not all locations with illicit discharges are visible.

Influence of precipitation

During the monitoring campaigns in both Korendijk and Groningen precipitation influenced some of the results. For Korendijk, storm events have been recorded for April 6th 01h00 (≈ 5 mm) and 03h00 (≈ 3 mm). Relatively cold stormwater run-off entering the storm drains causes a temperature reduction over parts of the cable, see Figure 7-14. Temperature reductions are inhomogeneously distributed over the

cable possibly due to differences in run-off surfaces and an unbalanced run-off of stormwater to available storm drain inlets. Figure 7-15 demonstrates that temperature variations due to precipitation (areas 'A', 'B' and 'C') can have the same characteristics as temperature variations due to illicit discharges (e.g. areas 'D' and 'E'): a sudden temperature change within minutes with a recovery to normal temperatures within hours. For the Korendijk results, temperature changes due to precipitation (area 'C') can be identified as such since precipitation causes temperature reductions whereas illicit discharges cause temperature increases (areas 'D' and 'E').

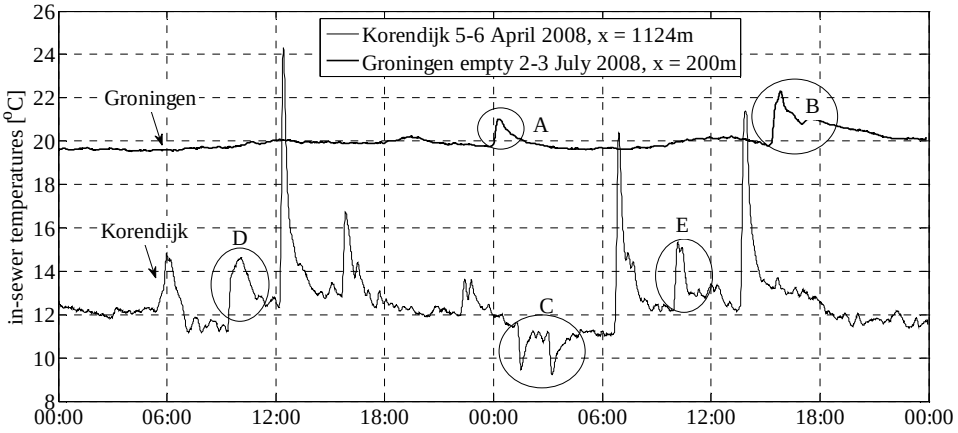

Figure 7-15: DTS monitoring results for Groningen (x=200m, July 2nd and 3rd, 2008) and Korendijk (x=1124m, April 5th and 6th, 2008). The influence of precipitation on monitoring results can be observed in areas 'A', 'B' and 'C'. Peaks 'D' and 'E' are due to discharges from illicit connections.

The Groningen results, however, show that precipitation can also cause a temperature *increase* in a stormwater sewer. A small storm event has been recorded for July 3rd 00h15 (≈ 2 mm), followed later that day by a larger storm event (≈ 14 mm) between 16h00 and 23h00 (areas 'A' and 'B' in Figure 7-15 and area 'D' in Figure 7-8) During run-off, stormwater is warmed up over heated asphalt surfaces after relatively warm days with maximum temperatures around 34°C. Again, only parts of the cable see this effect. Other parts of the storm drain may have received no stormwater or stormwater from different surfaces. Since the characteristics of in-sewer temperature variations are the same, the effects of illicit discharges on in-sewer temperatures can no longer be distinguished from the effects of precipitation. Hence, when searching for illicit connections, a correct interpretation of DTS-monitoring results requires using dry weather data only.

7.3.7 Conclusions

Fiber-optic distributed temperature sensing is a powerful tool to search for illicit connections in stormwater systems. Its near-continuous temperature monitoring in both time and space allows recording discharges of water with temperatures or temperature variations that differ from 'normal' stormwater system temperature characteristics. Normal characteristics for the case-studies presented in this paragraph constitute temperature values between approximately 5°C and 20°C and temperature variations only on a daily and seasonal basis. Domestic wastewater flows often show much higher temperatures with distinct variation patterns ('warm water plumes') and can hence be distinguished from normal situations. Excavation work and other verification efforts have confirmed the presence of illicit connections at the locations where warm water plumes have been observed with the DTS system.

In practice, precipitation can largely influence monitoring results. The case studies have shown both temperature rises as well as temperature reductions as a result of inflowing stormwater run-off. Hence, only dry-weather results should be used for illicit connection detection. Warm water discharges can more easily be detected in near-empty stormwater sewers, but monitoring data collected in a partially submerged system have demonstrated that illicit discharges can still be observed when the fiber-optic cable is situated in a stagnant layer of water. For this, the volume and/or temperature of the discharge need to be sufficiently large to cause a temperature increase that is beyond the detection limit of the DTS system. Other factors (such as the exact location of the cable, possible pollution around the cable, the mixing process of both flows etc.) will also play a role, the details of which are as yet not sufficiently studied. To maximize chances of observing an illicit discharge it is recommended to empty the stormwater system before performing DTS measurements.

In all, the use of a single instrument that performs the measurements and logs the data in an easy accessible and safe location and that can monitor up to several hundreds of monitoring locations at the same time and at a high frequency makes the DTS set-up very user-friendly and effective compared to other in-sewer monitoring devices.

7.4 Distributed temperature sensing in combined sewers

7.4.1 Introduction

Wastewater in combined sewer systems contains a considerable amount of thermal energy. This energy can be recovered from the sewer system by means of a heat exchanger and can subsequently be used to produce e.g. electricity or warm water. With increasing prices for energy from 'traditional' sources, an increasing number of such sewer energy recovery projects can be observed. Installation of heat recovery devices in a combined sewer system requires careful consideration of a suitable location. An important limitation is that the anticipated energy consumers should be located close to the heat recovery installation. Also, to optimize the amount of recoverable energy two conflicting mechanisms are to be considered: it increases with larger flows (i.e. further downstream in the sewer system), but also with higher wastewater temperatures that are expected in more upstream sections of a combined sewer system, as results in this chapter demonstrate. A concern for wastewater treatment plant operators is that heat recovery from in-sewer wastewater could result in lower influent temperatures. This could lead to a reduction in the efficiency of a nitrifying treatment plant (Wanner *et al.*, 2005). In response to this concern models have been developed to be able to study the dynamic behavior of in-sewer wastewater temperatures and to quantify the effect of the installation of heat recovery facilities on for instance wwtp influent temperatures (Dürrenmatt and Wanner, 2008). A difficulty with these models is a lack of data that can be used for calibration and validation. Data sets that describe wastewater temperatures in combined sewer systems in sufficient detail in both time and space are rare. Distributed temperature sensing with fiber-optic cables seems the appropriate tool to generate exactly such data sets. Application of DTS monitoring in combined sewer systems could therefore be of added value in the development of wastewater temperature models.

The objective of this paragraph is to study the feasibility of DTS application in combined sewer systems and to present and discuss data results collected with this monitoring system. For this, section 7.4.2 introduces the catchment area in which the application has been tested. Section 7.4.3 presents and discusses DTS monitoring results. Finally, section 7.4.4 considers a possible other use of DTS data collected in combined sewer systems: the calculation of flow ratios at confluences.

7.4.2 Test area: Ede

Distributed temperature sensing has been set up in the Rietkampen area in the municipality of Ede, the Netherlands. A fiber-optic cable was introduced in a

combined sewer system over a length of approximately 1850 meters. The studied sewer section drains an area of about 2 km^2 with predominantly a residential function (~15,000 inhabitants), some commercial functions (shops, cinema) and a hospital, see Figure 7-16. The Halo DTS instrument was connected to the downstream end of the cable and stored outside the sewer system in a small container. Approximately 200 m downstream from the Halo instrument a pumping station pumps all wastewater from the area to a nearby wastewater treatment plant. The lower graph of Figure 7-16 shows a longitudinal profile of the considered sewer section. Over the first 850 meters the sewer is a collector sewer without any individual house-connections. Along this section, nine side-connections contribute wastewater to the collector sewer, in the graph indicated by circles.

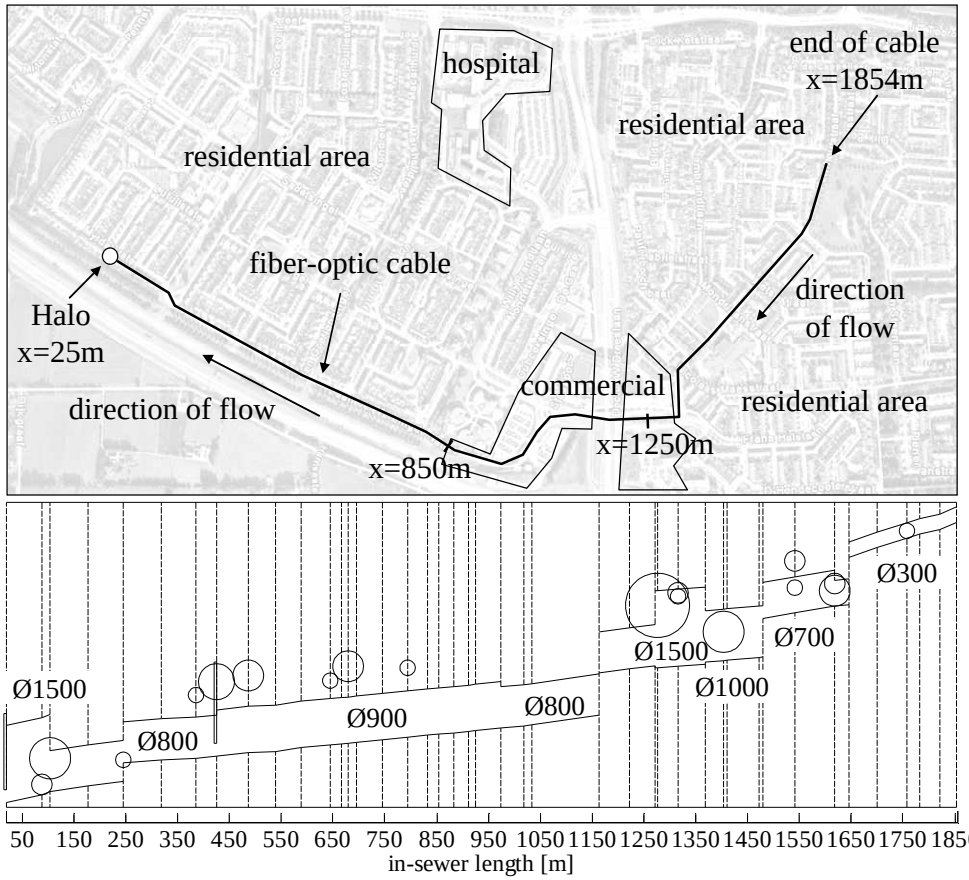

Figure 7-16: (upper graph) Rietkampen area in the municipality of Ede with location of Halo instrument and fiber-optic cable. Residential, commercial and hospital areas are indicated; (lower graph) Longitudinal profile of combined sewer section in which the fiber-optic cable is installed. Vertical dashed lines represent the locations of manholes; any side-connections are indicated by circles.

Between x=850 m and x=1250 m the sewer is a transport line that carries the wastewater underneath a main road without any house- or side-connections. A combined sewer overflow can be found at x=1280 m. Further upstream, the cable is situated in a 'normal' sewer system with many individual house-connections and contributary connections. Normal dry weather flows from the studied catchment area are on the order of 200 m^3/h. Flow decreases in the upstream direction; the most upstream sections can be without flow at moments without any domestic discharges.

A monitoring campaign was conducted December 15th-23rd, 2008. Programmed temporal and spatial resolutions were 30 seconds and 2 meters, respectively. Data collected at the most upstream section of the cable have a precision of approximately 0.15°C. For measurements closer to the Halo instrument this value further improves. To enhance the absolute accuracy of the temperature values a calibration procedure was performed prior to the monitoring campaign. At 5 locations along the cable the temperature of an ice-bath was measured with approximately 8m of fiber-optic cable as well as with 0.1°C accurate thermometers. Figure 7-17 presents per location the observed difference between thermometer value and DTS value, i.e. the offset. A linear fit with the y-intersect at an offset of 0°C at x=0 m (which is an internal measurement within the Halo instrument) yields a model for the offset of all locations along the cable. Using the model, data results have been corrected for the offset. Observed differences between model and observations (up to 0.6°C) could be due to the relatively short lengths of the tested cables or due to imperfections in the cable causing a step-wise temperature change. Also, errors with reference measurements in the ice-baths are possible.

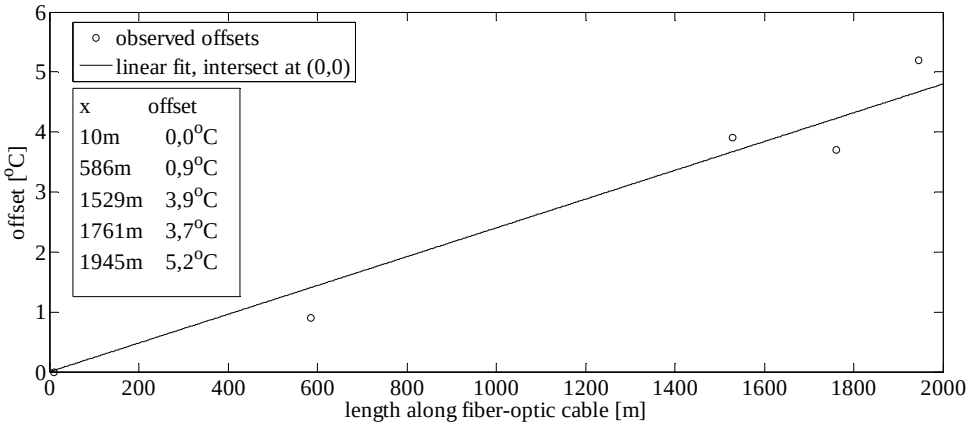

Figure 7-17: Calibration of DTS monitoring set-up in Ede, Rietkampen. At 5 locations along the fiber-optic cable reference temperature measurements give an offset for the DTS system.

7.4.3 Presentation and discussion of monitoring results

An overview of all results collected during the 8-days monitoring campaign (in full-color) can be found in appendix M (Figure M-1). Figure 7-18 presents the results for a typical dry weather day. The horizontal axis represents the length along the cable from x=20 m where the cable enters the sewer system to x=1854m at the end of the cable; the vertical axis represents a time-span of a day (December 18th, 2008). In total, the figure presents about 2.5 million individual temperature measurements by means of 917 x 2880 pixels (respectively 1834m divided by the 2m spatial resolution and one day divided by the 30s temporal resolution), which are colored according to the color map on the right hand side of the graph: values of 12°C and lower are colored white, values of 20°C and higher are colored black and any intermediate values are a shade of gray. The longitudinal profile of the sewer section (as earlier presented in Figure 7-16) is given directly above the temperature graph. Figure 7-19 presents the temperature variation along the fiber-optic cable for a single moment in time (December 18th, 09h15).

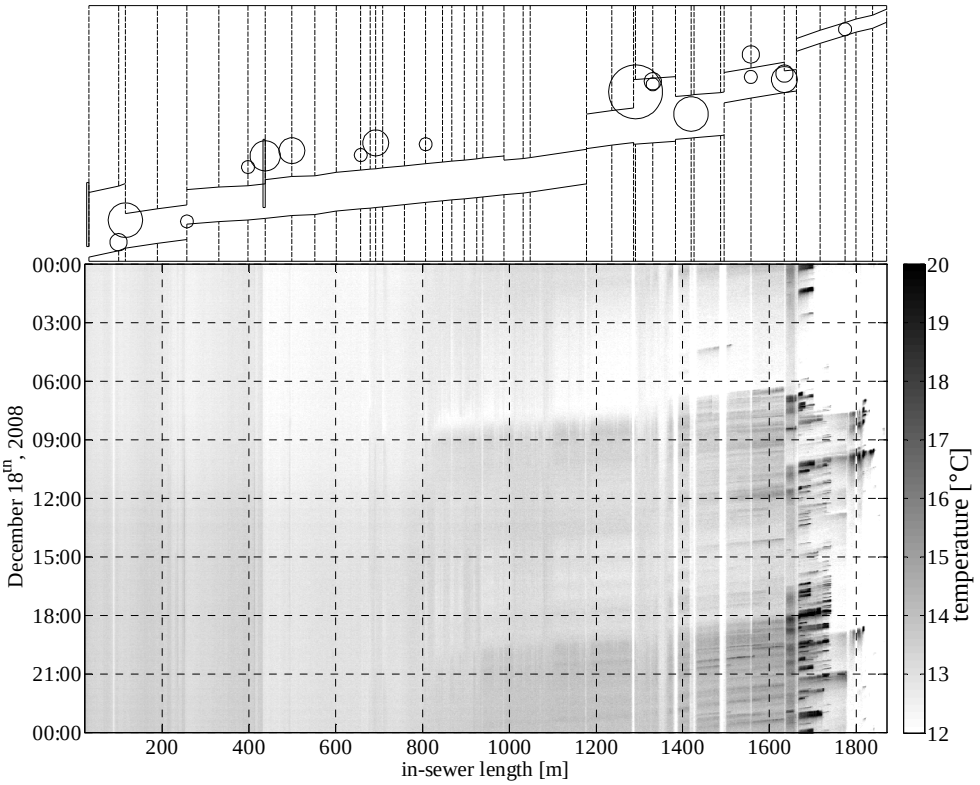

Figure 7-18: Results of DTS monitoring on a typical dry weather day in the combined sewer system of the Ede Rietkampen area, December 18th, 2008

The results show a distinction between on one hand the downstream two thirds of the cable (between x=0 m and x≈1200 m) and on the other hand the upstream one third (between x≈1200 m and x=1854 m). For the former in-sewer temperatures are fairly constant in time and space and range roughly between 12°C and 14°C; for the latter (and especially in the upper 300m) temperatures show a much larger temporal and spatial variation and values can be well outside the temperature range observed in the lower two thirds of the cable. Hereafter, a number of characteristics in the data results are discussed.

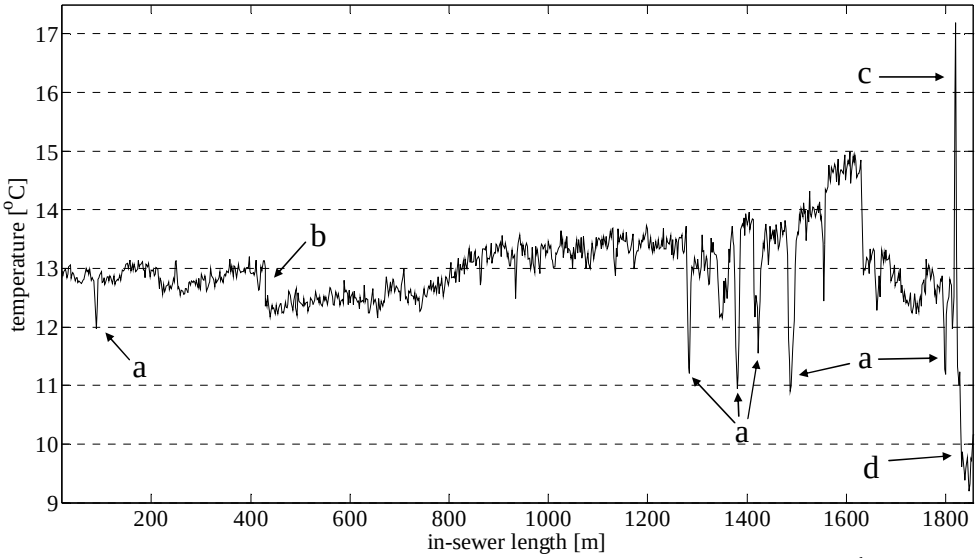

Figure 7-19: DTS monitoring results in the Ede Rietkampen area, December 18th, 09h15

Cable lifted from wastewater

Relatively low and constant temperature values around 11°C to 12°C (the 'vertical white lines' in Figure 7-18 and the sharp temperature drops indicated with 'a' in Figure 7-19) are often associated with locations where the cable is being lifted (just) above wastewater level, see Figure 7-20. This can be caused by an invert level difference in two pipes connected to the same manhole where the cable 'travels' from one level to the other via the shortest route hovering over the wastewater instead of following the z-shaped course of the wastewater. Also, at a number of sharp bends in the sewer line the cable was pulled too taut during installation, causing the cable to move up the circular concrete pipes to the widest part of the pipe and hence being lifted from the wastewater. At these locations relatively low in-sewer *air* temperatures instead of *wastewater* temperatures are recorded.

Figure 7-20: Locations where the fiber-optic cable is just above wastewater level due to an invert level difference (left picture) and due to the cable being pulled too taut around a sharp bend (right picture).

House connection discharges

Sharp and sudden temperature increases such as peak 'c' in Figure 7-19 are associated with individual discharges from house connections. Figure 7-21 presents the temperature data for a location (x=1818 m) that is suspected to be near a house connection. In the figure, temperatures intermittently increase up to 26°C. At other locations temperatures up to 35°C have been recorded. Logically corresponding to domestic use, temperatures rises occur mainly during morning and evening hours whereas hardly any warm water discharges are observed during the night. The low temperatures in the early hours of December 19th and 20th (areas 'a' in Figure 7-21) are due to the same phenomenon that causes the low temperatures over the last 30 meters of cable in Figure 7-19 (indicated with 'd'): no wastewater present in the sewer. Again, at these moments and locations in-sewer *air* temperatures rather than wastewater temperatures are recorded.

Discharges from individual house connections can be distinguished using DTS monitoring results, but only for the upstream 200 m of the cable, see Figure 7-22. Over this sewer section in-sewer flow is limited or not present, allowing the cable to register individual discharges. Peak temperature values are observed over short distances only. As the wastewater moves downstream along the (nearly empty) sewer pipe it cools down quickly: most discharges can no longer be recognized as such within 50 meters after the discharge location. Between x=1250 m and x≈1600 m household connections are also present, but the amount of energy in individual discharges proves to be too limited compared to the energy content of the main flow to be noticed by the DTS system. Further downstream the discharge of relatively warm wastewater from a side-connection at x=430m can be noticed: it causes a step-wise temperature increase in the main flow (in Figure 7-19 indicated by 'b'). The apparently large amounts of warm water are suspected to originate from the nearby hospital.

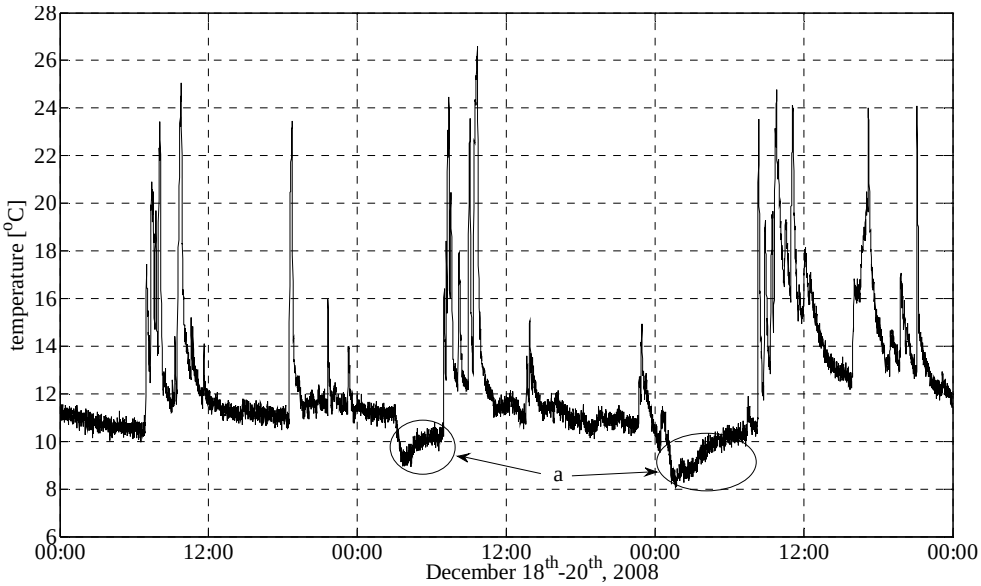

Figure 7-21: DTS monitoring results at x=1818 m for December 18th-20th, 2008

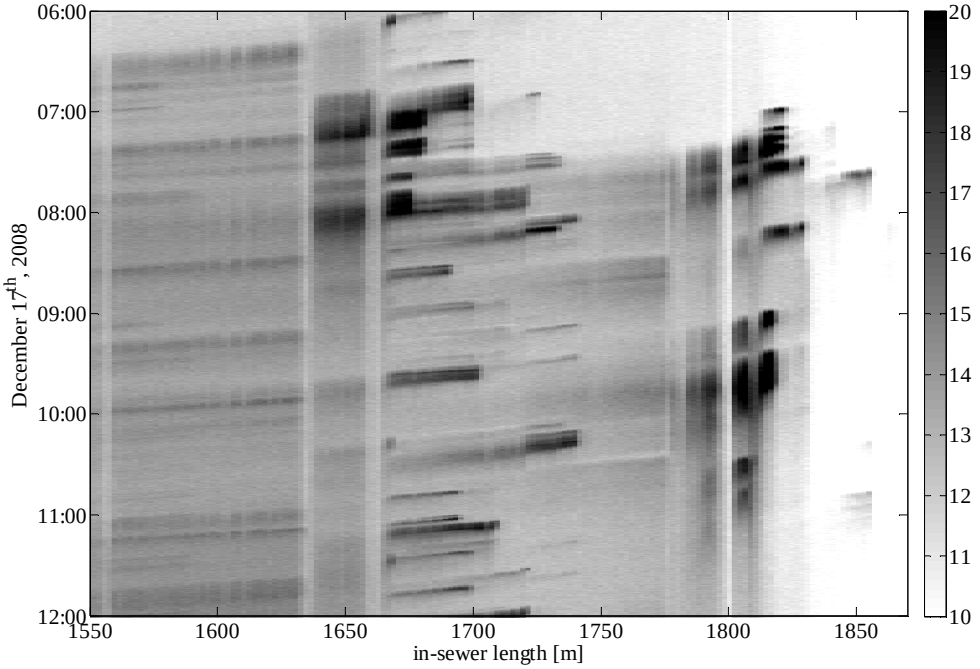

Figure 7-22: DTS monitoring results for December 17th, 2008 between 06h00 and 12h00, zoom on sewer section between x=1550 m and x=1850 m. The original full-color graph can be found in appendix M (Figure M-2).

Similar to the observation for stormwater sewers in section 7.3.6 results for combined sewer systems also show that discharges of warm water from individual house connections can be detected without difficulty in (nearly) empty sewer pipes. For (partially) submerged pipes, however, detection becomes less straightforward. Again, the question arises as to under which conditions the DTS system is still able to detect discharges from house or side-connections. The same approach as in section 7.3.6 is used but there are a number of differences, see Figure 7-23.

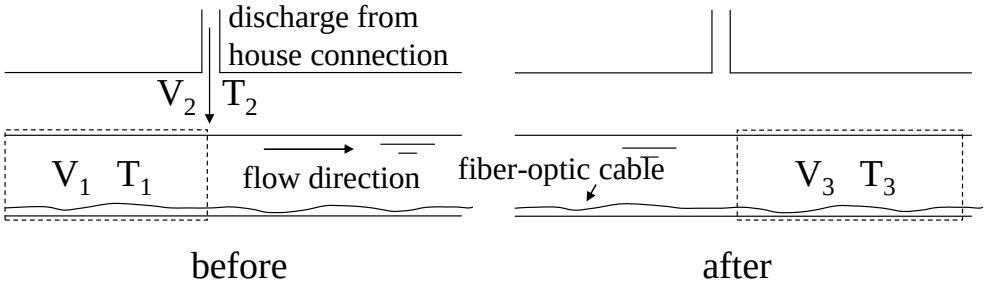

Figure 7-23: Discharge from a house or side-connection (volume V_2 with temperature T_2) into an upstream in-sewer volume V_1 with temperature T_1. The combined flows have volume V_3 and temperature T_3.

The water layer in a partially submerged *stormwater* sewer is often stagnant under dry weather conditions; water in a partially submerged combined sewer, however, is flowing. As a result, discharge volume V_2 will mix with an upstream volume V_1 and combine into downstream volume V_3. Again assuming full and instantaneous mixing and combining conservation of mass ($V_1 + V_2 = V_3$), conservation of energy ($V_1T_1 + V_2T_2 = V_3T_3$) and the in-sewer wastewater temperature change $\Delta T = T_3 - T_1$ it can be derived that (see equation 7.1):

$$\frac{V_2}{V_1} = \frac{\Delta T}{(T_2 - T_1) - \Delta T} \tag{7.2}$$

In-sewer temperatures T_1 and T_3 are now observed by different sections of the fiber-optic cable. Hence, it is the *spatial* precision of the DTS system that in this case determines the minimum in-sewer temperature change (ΔT) that is significant and not due to random variation. For example, assuming a 0.1°C precision and estimating ($T_2 - T_1$) ≈ 10°C from Figure 7-21 yields a volume ratio $V_1/V_2 \approx 100$. For equal flow rates this ratio suggests that - theoretically - after the collection of wastewater from approximately 100 households the next house connection can no longer be distinguished by the DTS system.

Inflow of stormwater run-off

The effect on in-sewer temperatures of stormwater run-off entering the combined sewer system can be observed in Figure 7-24. During the early hours of December 19th (02h40 - 03h40) and December 20th (23h30 - 02h00) respectively 1.3 mm and 1.8 mm of rain is observed at a nearby precipitation monitoring station. Prior to the events predominant in-sewer temperatures are on the order of 14°C. Then, upon inflow of relatively cold stormwater run-off, lower in-sewer temperatures of around 11°C are recorded, but primarily over the upper 1000 m of the cable. Over this cable section, the temperature decline is not simultaneous: the more upstream, the earlier the temperature reduction is observed. This is likely associated with the same mixing phenomenon as earlier described: less in-sewer wastewater in upstream sewer sections allows quicker in-sewer temperature variations. Downstream of x=850m almost no reaction to the storm event can be observed apart from lower temperatures at a few isolated locations that correspond to large side-connections. This non-reaction is likely due to the presence of flow-reduction weirs in the manholes at x=20m and x=430m (see Figure 7-16). During the storm event, total flow is probably larger than the maximum flow through the weirs, causing a backwater effect in the sections directly upstream from the weirs. Unfortunately, no water level measurements are available to confirm this assumption. The amount of wastewater in these sections largely increases, creating pools of nearly stagnant wastewater inhibiting (for the observed storm events) temperature changes due to the inflow of stormwater. The inflow of stormwater from large side-connections remains visible, but due to the stagnant character of the wastewater, the temperature variation remains a local phenomenon.

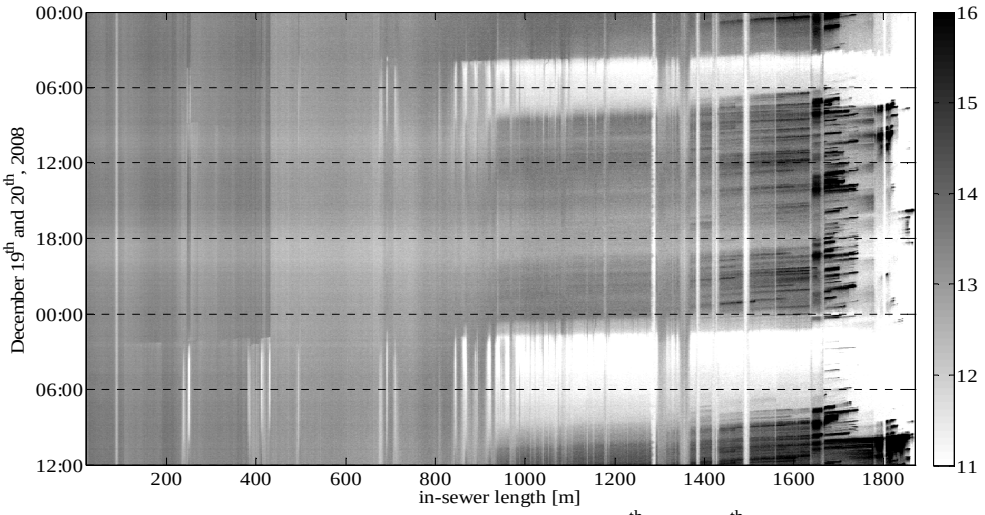

Figure 7-24: DTS monitoring results for December 19th and 20th, 2008 including two precipitation events. The original full-color graph can be found in appendix M (Figure M-3).

7.4.4 Flow measurements in part-full pipes based on DTS data

In-sewer flow monitoring in part-full pipes is a challenging task. As earlier described in section 1.3.2 common monitoring equipment (e.g. ultrasonic and electromagnetic sensors) suffers from uncertainty bands that are an order of magnitude larger than for full pipe measurements with reported errors up to 50% (Watt and Jefferies, 1996; Smits *et al*., 2007). As an alternative approach, this section considers the use of DTS data to determine flows in part-full pipes. More specifically, flow monitoring is considered in a free flow sewer section as presented in Figure 7-25: a confluence of flows 'A' and 'B' into a flow 'C'. For flow 'C' an existing (full pipe) flow monitoring device is present at location *p*, a distance *x* from the confluence manhole. The presented lay-out is a common situation in a branched sewer network in which, for instance, the existing flow monitoring at location *p* is situated in a pumping station and flow 'A' is a contributary flow into the main flow 'B'-'C'. The objective of this section is to present an idea on the possible use of DTS data to determine flow values in free flow pipes A and B using the data from the existing flow monitoring at location *p*. In other words, it considers the possibility of using the 'high quality' full-pipe flow monitoring at location *p* to derive good quality flow values further upstream by means of continuous in-sewer temperature data. The idea is presented, but cannot be verified due to lack of measurement data. For a proof-of-principle additional testing will be required.

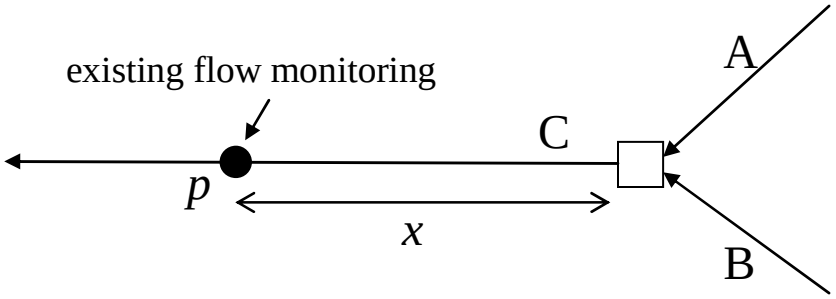

Figure 7-25: Confluence of flows A and B into flow C. For the latter flow monitoring is present at a distance *x* from the confluence manhole.

In the Ede Rietkampen area a sewer configuration as presented in Figure 7-25 can be found at a manhole near x=430m. At this manhole a temperature increase in the main sewer line ('B'-'C') can be observed in Figure 7-19 (indicated with 'b'). This is due to the inflow of relatively warm wastewater from a large side-connection (ø700 mm diameter, see Figure 7-16). Apart from temperatures in the main sewer, temperatures of wastewater in the side-connection have also been monitored by the DTS system by means of a loop in the cable. At the manhole, instead of continuing directly into the next part of the main sewer, the cable has been inserted into the

contributary sewer pipe in a loop of approximately 10 meters, see Figure 7-26 and Figure 7-27. The cable has been attached to a ø32 mm sand-filled PVC pipe that holds the cable in place at the invert of the contributary sewer pipe. This cable configuration allows simultaneous monitoring of wastewater temperatures in the main sewer (locations 'B' and 'C') as well as in the contributary sewer pipe ('A').

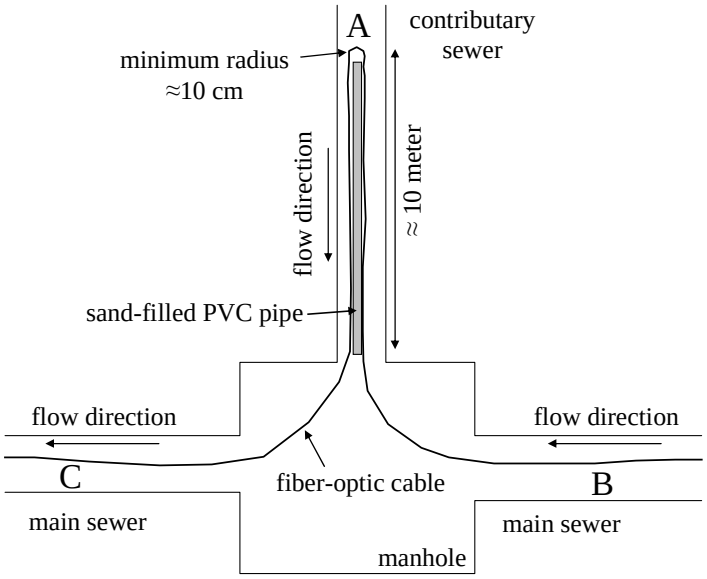

Figure 7-26: Lay out of the fiber-optic cable configuration at manhole x=430m.

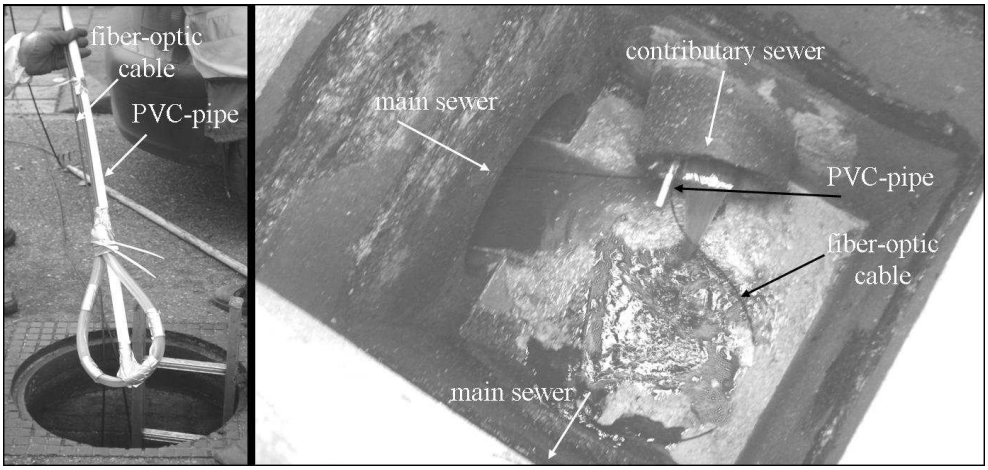

Figure 7-27: (left picture) Sand-filled PVC-pipe with fiber-optic cable attached; (right picture) cable loop inserted in a contributary sewer (different manhole than in Figure 7-26).

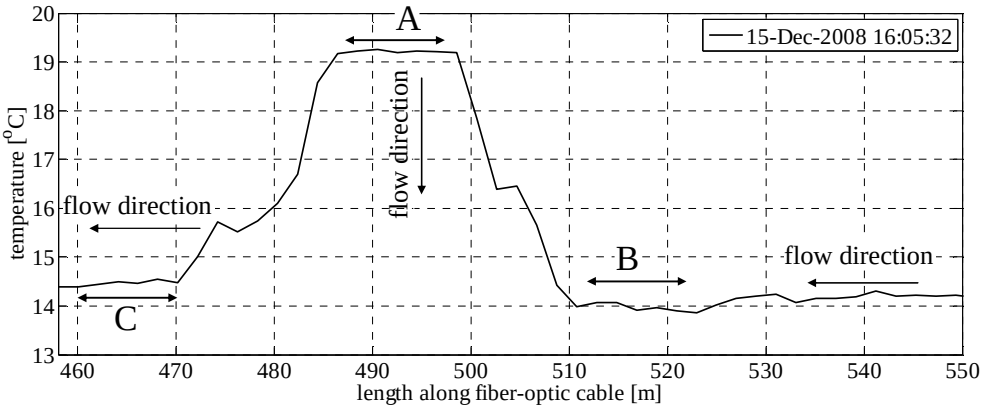

Figure 7-28: DTS data for the cable loop at x=430m: section 'B' represents wastewater temperatures upstream the confluence in the main sewer, section 'A' wastewater temperatures in the contributary sewer and section 'C' wastewater temperatures downstream the confluence.

Figure 7-28 presents DTS data for the cable loop at the x=430m manhole (notice that due to the presence of loops in the cable the length along the fiber-optic cable is unequal to in-sewer length presented in earlier figures). Section 'B' represents wastewater temperatures upstream the confluence (pipe B in Figure 7-26), section 'A' represents wastewater temperatures in the contributary sewer (pipe A) and section 'C' wastewater temperatures downstream the confluence (pipe C). In between sections the fiber-optic cable travels from pipe to pipe through air and hence measures in-sewer air temperatures (possibly influenced by wastewater that might be flowing along the cable). The data in Figure 7-28 confirm that wastewater in the side-connection is warmer than wastewater in the main sewer line: wastewater temperatures upstream the confluence are roughly 14.0°C, downstream the confluence around 14.5°C and in the contributary sewer about 19.2°C.

Figure 7-29 shows the same data as in Figure 7-28, but for two consecutive dry weather days. Each presented temperature value in Figure 7-29 is the mean value over a 10 meter cable section: for section 'B' between x=512m and x=522m, for section 'A' between x=487m and x=497m and for section 'C' between x=460m and x=470m (see Figure 7-28). In Figure 7-29 it can be noted that wastewater temperatures directly downstream the manhole are about 0.5-1.0°C higher than temperatures directly upstream the manhole. Wastewater temperatures from the contributary sewer are on average several degrees higher than in the main collector. All three temperature graphs show a diurnal variation with relatively high temperatures during the day and relatively low temperatures during the night.

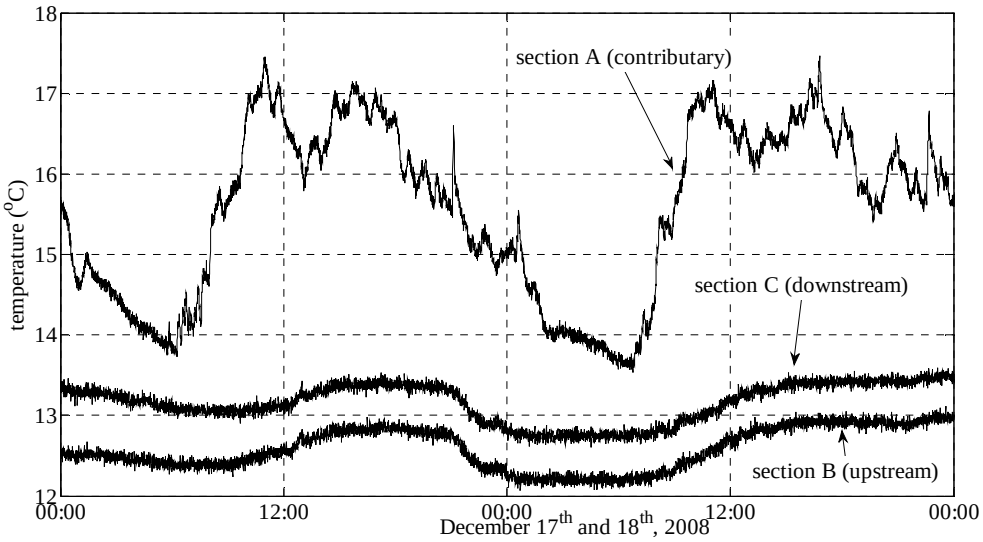

Figure 7-29: DTS monitoring results for December 17th and 18, 2008 in the direct vicinity of the manhole at x=430m: upstream the confluence ('B'), downstream the confluence ('C') and in the contributary sewer pipe ('A').

Wanner *et al.* (2004) show that - in undisturbed flow of about 100 L/s - wastewater temperature variations due to energy exchange with its surroundings over lengths of 1 km are on the order of 0.1°C. Hence, over short distances (10m in each direction in this case) wastewater energy loss to its surroundings is considered negligible. Therefore, for normal dry weather flow conditions and for a small time-span (<1 minute), the energy contained by the wastewater directly downstream the confluence of flows should be the sum of energy contained by wastewater directly upstream the manhole plus any energy in the contributary flow. In other words, wastewater temperatures in pipe C should be the flow-proportional average of wastewater temperatures at A and B. Using conservation of flow and energy the upstream flows (Q_A and Q_B) can be expressed as a percentage of the downstream flow (Q_C) using the measured temperature values:

$$Q_A = \frac{(T_C - T_B)}{(T_A - T_B)} Q_C \quad \text{and} \quad Q_B = \frac{(T_A - T_C)}{(T_A - T_B)} Q_C \tag{7.3}$$

It should be noted that these equations only apply when all flow directions are as indicated in Figure 7-26. In situations that annul the conservation of flow and energy over the three locations (such as backwater effects after a storm event) the

equations cannot be used. Applying equation (7.3) on the data of December 17th and 18th, 2008 (Figure 7-29) yields the relative flow contribution for Q_A (10-50%) and Q_B (50-90%) to Q_C, see Figure 7-30. With measured values for Q_C relative contributions can be transferred to absolute flow values for Q_A and Q_B.

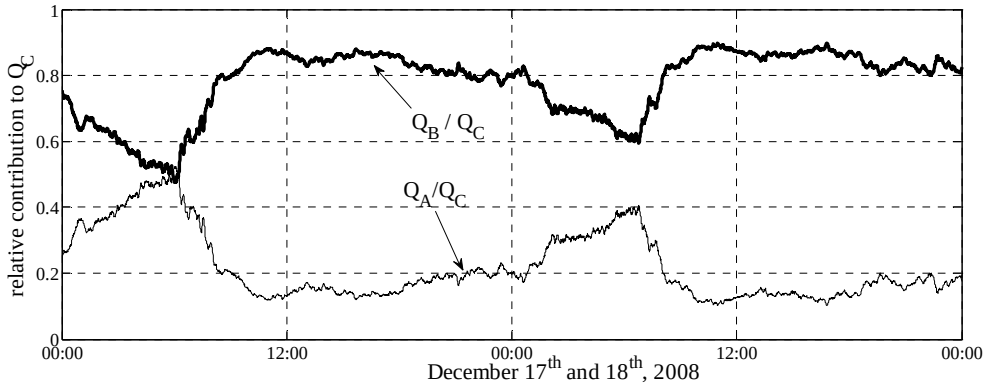

Figure 7-30: The relative contribution of Q_A and Q_B to Q_C for December 17th - 18th, 2008.

The derived relative contributions for the Ede Rietkampen case seem to be plausible considering the catchment areas of Q_A and Q_B (see Figure 7-16). However, no reference data sets on Q_A and Q_B are available that can be used to validate the results presented in Figure 7-30. As a result, no quality assessment of calculated values can be made and no proof-of-principle of the suggested flow monitoring method using DTS data can be given in this section. Testing in (for instance) a laboratory set-up with known flow values is required to verify whether the method can work in practice. Additional tests should also verify whether:

- the temperature as measured by the fiber-optic cable on the bottom of the sewer pipe correctly represents the mean temperature of the wastewater column above it;
- the cable lengths of 10 meter directly upstream and downstream the manhole are appropriate lengths that yield representative values for local wastewater temperatures;
- only negligible energy loss occurs in the direct vicinity of the manhole and
- (large-scale) pollution around the fiber-optic cable has an effect on the measurements.

Finally, for the method to be applicable a temperature difference must be present between the two upstream flows. For the Ede Rietkampen case study this has proven to be the case, but the consistency of this observation for other in-sewer confluences needs to be investigated.

7.4.5 Discussion and conclusions

Distributed temperature sensing in a combined sewer system provides a means to study a number of in-sewer processes with a level of detail that has hitherto been impossible with conventional sensors. A data set from a one-week monitoring campaign in an 1850m sewer section shows this level of detail with which in-sewer processes that affect in-sewer (wastewater) temperatures can be studied.

Discharges from individual house connections can be distinguished using DTS data, but only for (nearly) empty sewer pipes that are generally found upstream in a sewer network. For winter conditions (December 2008) observed peak temperature values from house-connections are within a range of 20°C to 35°C. These values are observed over short distances only. As the wastewater moves downstream along the sewer line it cools down quickly: most discharges can no longer be recognized as such within 50 meters after the discharge location. For (partially) submerged sewer pipes individual discharges can no longer be distinguished; in-sewer temperatures in such pipes are fairly constant in time and space and range roughly between 12°C and 14°C. The ability of the DTS system to detect individual discharges depends on its precision and the volume and temperature of the discharged wastewater in relation to the volume and temperature of the receiving water. In practice, other factors (such as the exact location of the cable, possible pollution around the cable, the mixing process of both flows etc.) will also play a role.

Using DTS results the process of stormwater run-off entering a combined sewer system can be observed in detail. For two (small) storm events a strong temperature reduction is observed over specific sections of the cable. After the storm events, temperatures gradually restore back to normal values. The question arises as to which extent the temperature variation during (parts of) the storm event is related to the dilution of wastewater. If during (a part of) the event wastewater temperature and pollutant concentrations prove to be well-correlated, the DTS measurements could provide insight into the in-sewer dilution process of pollutant parameters during the event.

The collected data set may be used as a data source for the calibration and validation of wastewater temperature models (see section 7.4.1). Also, with a dedicated cable configuration the confluence of wastewater flows can be observed with a potential to derive the relative contributions of contributary flows to a total flow. This application has been considered in theory only; no reference data sets are (as yet) available to provide a proof-of-principle. For the method to work a temperature difference is required between both contributary flows as well as free flow conditions around the confluence manhole.

In all, fiber-optic distributed temperature sensing is a powerful tool to study the water quality parameter ‘temperature’ in combined sewer systems The use of a single instrument that performs the measurements and logs the data in an easy accessible and safe location and that can monitor up to several hundreds of monitoring locations simultaneously makes the DTS set-up very user-friendly compared to other in-sewer monitoring devices.

Chapter 8. Concluding considerations

8.1 Introduction

Restating, the objective of this thesis has been twofold. The first objective has been the further development of in-sewer wastewater metrology. Specific discussions and conclusions on all applied monitoring techniques (precipitation, flow, UV/VIS and distributed temperature sensing) can be found in the respective chapters. In paragraph 8.2 a more general discussion is presented on the development of in-sewer wastewater metrology. A large part of the discussion is on data loss. The monitoring techniques addressed in this thesis are nearly all associated with data loss or with a significant effort to arrive at useful data sets. The reasons behind the data loss, however, are different but rather exemplary for the challenges faced in collecting proper data sets from wastewater systems in the Netherlands. The second objective has been the assessment of in-sewer wastewater quality dynamics. Paragraph 8.3 summarizes in-sewer processes that have been found to have an effect on the observed dynamics of wwtp Eindhoven influent. It also considers whether the observed phenomena have been reported by others in distinct catchment areas, in which case a degree of general validity can be assigned to the observation. Then, the paragraph briefly considers potential improvements in wastewater system operation using the acquired knowledge on wastewater quality dynamics of wwtp Eindhoven influent. Finally, the extreme loading event of May 7th, 2007 is once more discussed regarding the occurrence of such events in relation to a foreseen change in climatic conditions. The chapter concludes with a paragraph on privacy considerations when generating highly-detailed in-sewer measurements. The newly applied DTS technique offers the possibility to study in-sewer processes to a level of individual house connections. With such detailed data sets, certain aspects of residents' behavior can be studied with a potential of unintended use of the data.

8.2 Advancements and obstacles for in-sewer wastewater metrology

For the UV/VIS as well as the DTS monitoring technique it can be concluded that the application in sewer systems is feasible. For both sensor types installation set-ups have been conceived of which descriptions can be found in this thesis. Associated research question on sensor calibration, data uncertainty and data quality have been reflected on in chapters 5 and 7, respectively. Making these sensors available for in-sewer applications constitutes an important development in the collection of data on in-sewer wastewater quality parameters. The temporal (UV/VIS) and spatial (DTS) resolutions with which quality parameters can be

observed, improve significantly compared to conventional monitoring approaches. The availability of high-resolution data sets allows the study of wastewater system *dynamics*: the assessment of in-sewer processes with (much) smaller characteristic time and space scales than has hitherto been possible using data sets collected with conventional methods. Also, the repetitive observation of phenomena (e.g. the multitude of observed dry weather days and storm events in chapter 6, observation of an illicit connection over a number of days or weeks in chapter 7) allows the evaluation of (variations around) typical observed behavior. Hence, the use of UV/VIS and DTS data opens up new possibilities for the analysis of system behavior and performance.

It should be noted that the application of both techniques in the Netherlands is still in its infancy. As yet, the wwtp Eindhoven is one of few wastewater treatment plants where UV/VIS sensing is applied for detailed observation of influent quality. A wider application is expected with the increasing availability of off-the-shelf knowledge on installation requirements (see appendix G) and data validation (see paragraph 5.4) as well as with proven added value of detailed influent monitoring. A true *in-sewer* application of a UV/VIS sensor in the Netherlands does presently not exist. The DTS technique gradually gains acceptance among Dutch practitioners as a 'standard' method for the location of illicit connections in stormwater sewers. The number of municipalities in which the method has been applied is, however, still limited. Also, in some projects the DTS technique has been tested for other applications such as extraneous flow detection in combined sewer systems and the verification of the functionality of a stormwater separating manifold (Langeveld *et al.*, submitted).

It is stated with emphasis that any sensor applied in and around wastewater systems is generally not of the plug-and-play type as is frequently encountered in daily practice. Sensors as well as resulting data sets require constant and proper attention to guarantee an adequate description of the targeted process. This is illustrated in the current study by the large effort required to collect the precipitation, flow and wastewater quality data sets as well as by the data loss in the subsequent data quality assessments. The effort and data loss were expected for the application of a relatively new sensor type such as the UV/VIS sensors. For the precipitation and flow data sets, however, effort and data loss were larger than expected and - to a certain extent - avoidable. For the DTS monitoring technique data loss is not an issue. Hereafter, for each of the considered sensor/data types this is further considered.

For a correct installation, operation and maintenance of raingauges 'off-the-shelf' knowledge is widely available as is shown by the ample references provided in chapter 3. Also, the design and implementation of a properly and reliably functioning data communication system have been successful in many comparable

monitoring programs. Unfortunately, this knowledge has insufficiently been searched for and applied during the installation and use of the new monitoring network in the Eindhoven area. As a result, errors have been introduced in the network such as improper sensor installations, lacking calibrations, decreasingly stringent cleaning strategies over time and a frequently hampering data communication system. This has led to a relatively large data loss (46%, see paragraph 3.7) as well as to biased data sets. It can be concluded that this type of data loss is not due to lack of (technical) knowledge, but due to the non-application of existing knowledge as a result of *organizational* shortcomings. Measures to prevent the considered data loss include the set-up of a proper organizational structure around the monitoring project that ensures the search for and inclusion of existing knowledge as early as the preparatory phase of the project considering at an early stage all requirements for installation, calibration, operation, maintenance, logistics and data handling.

For the wastewater quantity data sets considered in chapter 4 the quality of raw data is good. Strictly speaking, data loss for these data sets is negligible. Nevertheless, a challenge for this data type has proven to be the transition from raw data to useful time-series (i.e. the flow time-series from the three catchment areas). Elaborate study within the context of this thesis has shown that a number of data operations are required to arrive at accurate and correct time-series that can be used for the data analyses presented in chapter 6. Areal inflow time-series are also available from a WDD database that contains many long-term data sets collected at the wwtp Eindhoven. Comparison of data from this database and the time-series generated in chapter 4 shows a number of discrepancies. Assessment of the differences reveals that corrections for the non-zero baseline and for Q_{OPEN} (see sections 4.3.4 and 4.4.2, respectively) are currently not included in the data handling in the WDD database. It can be concluded that the existing data source (i.e. the WDD database) has some flaws and should only be used with care. Consultation with experts in this field (e.g. Korving, 2010) confirms that the above observation is not uncommon when using monitoring data from existing databases or from sensors that are part of previously installed wastewater monitoring programs. Whenever assessing the potential to use existing data sources (instead of installing a new sensor or using raw data sets) it should be appreciated that those sources have often been compiled to meet different objectives and data needs than those of the newly started program. Therefore, a thorough examination of the origin of data as well as any data modifications prior to presentation of the data is deemed necessary when using existing sources in wastewater monitoring programs.

Data loss associated with the UV/VIS data sets adds to between 25% and 50% of the studied 19-months data sets. This is on the same order as for the precipitation data sets, but is not comparable: the installation and application of UV/VIS sensors is no ‘off-the-shelf’ knowledge (yet). An amount of data loss was therefore

anticipated during the development of a proper monitoring installation (as described in appendix G) and maintenance strategy. Upon closer consideration, the observed data loss in UV/VIS data sets is primarily associated with data gaps and with auto-cleaning system failure, see Table 5-8. The former are mainly due to absent sensors that were removed for repairs and the latter are primarily associated with a malfunctioning compressor. Retrospectively, a part of the data loss could have been prevented if a back-up would have been available for one or both of these systems. With a spare UV/VIS sensor and/or an additional compressor at the wwtp Eindhoven that could replace the original directly upon detection of system failure, data loss could have been limited. Costs for such back-ups are non-negligible (roughly €25,000 for a UV/VIS sensor and €2,000 for a compressor), but should be considered in relation to total costs for the monitoring program. These add for the UV/VIS monitoring installation that has been used to collect the data as presented in this thesis to roughly €200,000 (Verschoor, 2010). Costs include investment costs for the sensors and (multiple versions of) the by-pass installations as well as personnel costs for installation and maintenance. With a mean data yield of about 63% (see Table 5-8) it can be derived that every percent of useful data represents an investment of €200,000 / 63 = €3,200. Subsequently, it could be argued that any improvement to the monitoring set up that increases data yield by 1% and costs €3,200 or less is a good investment. In other words, if the availability of an additional compressor would have resulted in an improvement in data yield of at least (€2,000/€3,200) = 0.6%, the investment would have reduced the investment-to-data-yield ratio. For an additional UV/VIS sensor this percentage is 7.8%. Considering the data loss associated with each of these failure mechanisms, it can be concluded, retrospectively, that it would have been advantageous to have both back-up systems available.

It should be stressed in this context that the mere *availability* of back-up systems will not improve data yield; such can only be achieved in combination with a proper organizational structure. Essentially, before monitoring commences, an organization needs to be ready to receive and view the data, to diagnose data anomalies and to resolve any detected problems. Proper visualization tools as well as *a priori* knowledge on studied parameters are required as soon as monitoring commences to be able to directly detect anomalous data. Having detected incorrect data, the organization needs to be able to resolve the problem. In this context, resolving problems consists of (1) providing a platform to discuss and decide on a solution to the problem, (2) solution implementation by communicating the conceived solution to a responsible field unit, (3) central registration of metadata on the findings in, changes to or work carried out on the actual monitoring network and (4) verification whether the problem has actually been solved after solution implementation. As a monitoring program progresses, typical failure mechanisms and their associated solutions will be progressively known, reducing the need for extensive discussions.

8.3 Dynamics in wwtp influent flows and pollutant loads

An understanding of the variability of treatment plant influent flows and pollutant loads has been created studying the characteristics of the observed dry and wet weather hydrographs and pollutographs of the wwtp Eindhoven. Moreover, processes have been distinguished that influence the shape of both types of graphs.

For dry weather *flows* typical diurnal, weekday and long-term variations have been observed that are in line with the 'supply' of domestic and industrial wastewater and possible contributions from extraneous sources. Patterns are comparable to observations in many other areas. For dry weather pollutographs a distinction is made between suspended (TSS) and dissolved (CODf) compounds. The former show a pollutograph that is rather similar in shape compared to its associated hydrograph; the latter show much less variation in concentration values over a day. The *similarity* in shape for parameter TSS is not due to a diurnal change in 'supply', but is attributed to sedimentation and resuspension processes of in-sewer sediments upon variations of flow. This similarity has been observed by a number of other authors as well, but examples of catchment areas without well established correlations between flow and TSS values can also be found in literature. The latter can be caused by a site-specific factor: for area Riool-Zuid the discharge of highly polluted reject water from a sludge processing installation largely influences the shape of the observed pollutograph. A varying relative contribution of infiltration and inflow to total flow over the day attributes to the diurnal variation of both suspended and dissolved pollutants. Apart from shape similarity a *time-shift* between hydrograph and pollutographs has been observed. The variation in quality parameters lags behind flow variations by a number of hours. For dissolved compounds this has been attributed in literature to a wave celerity that is larger than the associated flow velocity. The same phenomenon for suspended solids has not often been noticed or described for other areas; possibly, an adaptation effect in the dynamics of suspended solids transport plays a role. Finally, for dry weather flows as well as for dry weather pollutant loads a catchment size effect has been observed: the smallest catchment area is associated with the largest deviations from mean values and vice versa. This is in line with a number of observations from other areas.

The foremost processes during wet weather are the additional supply of (storm)water and associated pollutants to the sewer system and the following increase in the release of pollutants from sediment layers and biofilms. As a result of both processes, at the wwtp Eindhoven for every storm event influent pollutant loads have been observed that are larger than their dry weather equivalents. Wet weather loads for parameter TSS are larger than for parameter CODf. Again, this expresses the relation between suspended solids concentrations and the variation of flow values. The smallest catchment area (Nuenen/Son) shows the relatively

largest wet weather peak loads whereas values are smaller for Riool-Zuid and Eindhoven, the largest catchment areas. This contradicts research from other areas where relative peak load magnitudes could not be related to catchment size. Calculated shares of the source of additional loads during wet weather flow (i.e. from run-off or from in-sewer stocks) are comparable to literature sources. Run-off generally contributes roughly 5-20%, in-sewer stocks approximately 50-80%. The repetitive character of load peaks for successive storm events suggests that contributing sewer systems are not flushed 'clean' during a storm event, but that the 'pollutant reservoir' is only partially depleted. Similar (literature) observations on the repeatability of peak loads during wet weather have not been found.

Flow and pollutant loadings into the wwtp Eindhoven show a more dynamic behavior than currently taken into account in the operation of the plant and contributing sewer system. The observed dynamics in influent loading can be employed to conceive improvements to system operation. For instance, the operation of the stormwater storage tank at the treatment plant can be optimized with information on fluctuations in pollutant parameters during large storm events. Also, short-term peaks in influent pollutant loads under dry weather conditions are detected, as is shown for e.g. suspended solids concentrations in Riool-Zuid influent in Figure 6-12 and for nitrate concentrations in Nuenen/Son influent in Figure 1-2. Some of these peaks can be associated with point discharges (such as the Mierlo sludge processing installation) and counteracted. A search for relatively 'clean' wastewater (i.e. wastewater diluted with stormwater arriving at the wwtp or CSO with pollutant concentrations lower than wwtp *effluent* standards that might be discharged directly onto receiving waters without treatment) shows that no such wastewater is found for 'normal' large storm events. As an illustration, the event presented in Figure 6-28 shows a minimum concentration level COD_{eq} of around 250 mg/L whereas the wwtp effluent standard is 125 mg/L (see Table 2-1). For the studied series of storm events, however, concentration levels decrease to a level nearing wwtp effluent standards for parameter COD_{eq} (presented in Figure 6-32) and TSS_{eq} (not presented). Much lower concentration levels are not to be expected: the maximum dilution of wastewater is determined by the (continuing) dry weather pollutant load arriving at the maximum wet weather flow rate. Other improvements to plant (and wastewater system) operation are currently being studied within the context of the Kallisto-project (see section 1.3.5) using a wwtp model that can handle short-term fluctuations of influent parameters.

The extreme wet weather loading event of May 7th, 2007 (that was discussed in chapter 6, see Figures 6-37, 6-38 and Table 6-13) with its clear adverse effects on wwtp operation has been presented in this thesis as an *exceptional* example of the dynamics in wet weather loadings to the wwtp Eindhoven. However, current developments in climatic conditions might result in a more frequent occurrence of similar influent loadings. The problems at the wwtp Eindhoven were attributed to

the arrival of an extreme pollutant loading which in turn was attributed to the combined occurrence of a long dry period (causing a prolonged accumulation of pollutants on street surfaces, in gully pots and in sewer pipes) and a subsequent storm event that was sufficiently large and intense for remobilization of the build-up pollutant layers and subsequent transport to the wwtp. Considering the KNMI climate change scenarios (Hurk *et al.*, 2006), it is expected that the combined occurrence of exactly these conditions will increase over the next decades in the Netherlands. As a result, extreme wwtp loadings with their adverse effects are also expected to occur more often. Considering climate change and its effect on an urban wastewater system should therefore include consideration of the effect of extreme pollutant loadings on wastewater system performance. Both the effects on the treatment plant operation as well as on CSO spills are to be taken into account. A study should investigate possibilities to prevent extreme loadings (e.g. remove in-sewer stocks prior to the event), to equip the wwtp with a form of advanced dynamic process control (e.g. temporarily reduce pollutant *load* influx into the biological treatment by by-passing a part of the wwtp influent), and/or to mitigate the effects (e.g. have a readily available calamity plan).

8.4 Highly detailed in-sewer measurements: privacy considerations

The objective of data collection and analysis - whether in wastewater systems or in other fields - is often to improve understanding of system behavior and to facilitate the search for possible improvements to the system. Data can also be misused when deployed for purposes other than the monitoring network was intended for. In this paragraph possible abuse of the DTS data as presented in chapter 7 is considered. Subsequently, as DTS data sets might prove to be the precursor of highly detailed in-sewer data sets on other quality parameters, the collection of such data sets is further elaborated on.

The results of in-sewer distributed temperature sensing show the level of detail with which in-sewer processes that affect (wastewater) temperatures can be monitored. With possible temporal and spatial resolutions on the order of, respectively, 30 seconds and 1 meter individual discharges of wastewater can be detected originating from single house connections. This detailed observation allows the owner of the data set to derive a “typical discharge pattern” for each observed house connection. Having established such a pattern, any deviation from the pattern can be simply detected. Also, the prolonged absence of spills can be noticed, which is likely associated with the absence of residents during e.g. a holiday period. Especially the latter information can be of interest to people intending to use it primarily to their own advantage. Careful consideration is therefore required before allowing (online) public availability of such data sets. It should be noted that the detection of individual discharges from house connections

is only possible under specific conditions that relate to the minimum detection limit of DTS monitoring systems. Considerations on minimum detection limits are presented in chapter 7.

A data set of the quality parameter 'temperature' of wastewater originating from a house connection basically holds information on the *occurrence* of discharges from that house connection. Other water quality parameters can provide additional information on the *contents* of the discharge. For instance, measurements of parameters COD and Kjeldahl nitrogen can be related to the number of people equivalents discharging to the location of measurement (see equation 6.1). Measurements of prescription drugs, pharmaceuticals and personal care products (PPCPs) and illicit drugs (of all of which remnants are present in wastewater, see Ternes, 1998; Daughton and Ternes, 1999) can provide information on the use of such substances in the observed household. Essentially, any substance that is found in either urine or faeces and that can be detected in wastewater can be related to residents' behavior and being. Monitoring of these wastewater quality parameters at the same temporal and spatial scale as with the DTS technique is not (yet) feasible. Some parameters can be observed online by means of rather substantial probes (e.g. COD with UV/VIS sensing as presented in chapter 5) whereas others still require sampling and subsequent laboratory analysis (e.g. PPCPs and illicit drugs, see for instance Zuccato *et al.*, 2008; Ort *et al.*, 2010). Efforts are ongoing, however, to develop measurement techniques that combine the easy data transmission and collection associated with fiber-optics and miniature sensors along or at the tip of fiber-optics. For instance, using this approach, measurements of dissolved oxygen along fiber-optic cables in water has been proven feasible (Wang *et al.*, 1999). Also, fiber-optic sensors for pH monitoring are already available on the market.

With these developments it is conceivable that within a time-span of one or more decades it will become possible to generate data sets comparable to the temperature DTS data sets presented in this thesis for many other quality parameters and constituents in wastewater. Such highly detailed in-sewer data sets will assist in further development of knowledge on a variety of processes in and outside the sewer system. Misuse of the data, however, might also be possible. Careful consideration will be required before allowing (public) availability of such data sets as questions about privacy may be raised. As an example, testing wastewater for illicit drugs has hitherto only been allowed at community-scale (Zuccato *et al.*, 2008). This way, findings cannot be tracked to any individual or specific location.

References

Achttienribbe G.E. (1993). De Nederlander en zijn watergebruik (in Dutch: Water usage in the Netherlands). *H_2O*, **26**(13), 349-350.

Almeida M.C., Butler D. and Friedler E. (1999). At-source domestic wastewater quality. *Urban Water*, **1**(1), 49-55.

Ankum P. (2003). Reader for CT4460: Polders, Drainage and Flood Control, edition September 2003. Delft University of Technology, the Netherlands.

Arcadis (2007). Sedimenttransport Dommel door Boxtel (in Dutch: Sediment transport in the river Dommel near Boxtel), Report 110502/OF7/200378/019/MR, Arcadis, Den Bosch, the Netherlands.

Ashley R.M. and Verbanck M.A. (1996). Mechanics of sewer sediment erosion and transport. *J. Hydraul. Res.*, **34**(6), 753-769.

Ashley R.M., Bertrand-Krajewski J.-L., Hvitved-Jacobsen T. and Verbanck M.A. (2004). Solids in sewers. Scientific and Technical Report No. 14. IWA Publishing, London, UK.

Bertrand-Krajewski J.-L., Briat P. and Scrivener O. (1993). Sewer sediment production and transport modeling: a literature review. *J. Hydraul. Res.*, **31**(4), 435-460.

Bertrand-Krajewski J.-L. and Bardin J.-P. (2002). Evaluation of uncertainties in urban hydrology: application to volumes and pollutant loads in a storage and settling tank. *Water Sci. Technol.*, **45**(4-5), 437-444.

Bertrand-Krajewski J.-L., Barraud S., Gibert J., Malard F., Winiarski T. and Delolme C. (2007). The OTHU case study: integrated monitoring of stormwater (Lyon, France). In: T.D. Fletcher and A. Deletic (eds.), Data requirements for Integrated Urban Water management. Taylor & Francis Urban Water series - UNESCO IHP, London, UK, Chapter 23, pp. 305-315.

Besluit Kwaliteitsdoelstellingen en Metingen Oppervlaktewater (BKMO) (1994). (in Dutch: Governmental Order for Quality Standards and Monitoring of Surface Waters). Staatsblad 1983, modified 1994.

Bos R. and Kruger - van der Griendt M. (2007). Overstortkalibratie in Petten (in Dutch: Calibration of overflow weirs at a test rig in Petten). *Rioleringswetenschap*, **7**(26), 22-43.

Boyd G.R., Palmer J.M., Zhang S., Grimm D.A. (2004). Pharmaceuticals and personal care product (PPCPs) and endocrine disrupting chemicals (EDCs) in storm water canals and Bayou St. John in New Orleans, Louisiana, USA. *Sci. Total Environ.*, **333**(1-3), 137-148.

Broeke J. van den (2009). Personal communication (representative of s::can, Vienna, Austria).

Brombach H. and Fuchs S. (2003). Datenpool gemessener Verschmutzungs-konzentrationen in Misch- und Trennkanalisationen (in German: Database of measured pollutant concentration levels in combined and separate sewer systems), *KA - Abwasser Abfall*, **50**(4), 441-450.

Brouwer R. (2000). Reader for CT4410: Irrigation and Drainage, edition March 2000. Delft University of Technology, the Netherlands.

Bourgeois W., Burgess J.E. and Stuetz R.M. (2001). On-line monitoring of wastewater quality: a review. *J. Chem. Technol. Biotechnol.*, **76**(4), 337-348.

Butler D. (1993). The influence of dwelling occupancy and day of the week on domestic appliance wastewater discharges. *Build. Environ.*, **28**(1), 73-79

Butler D., Friedler E. and Gatt K. (1995). Characterizing the quantity and quality of domestic wastewater inflow. *Water Sci. Technol.*, **31**(7), 13-24.

Butler D. and Davies J.W. (2004). Urban Drainage, 2nd Edition. E&FN Spon, London, UK.

Centraal Bureau voor de Statistiek (CBS) (2007). Provincie op Maat 2007 Noord-Brabant (in Dutch: Government Statistics for the province of Noord-Brabant in 2007), website http://www.cbs.nl, visited January 2009.

CIRIA (1998). Dry weather flows in sewers, Report 177, CIRIA, London, UK.

Clemens F.H.L.R. (1988). Transport of suspended solids in sewers. In: J.C. Hooghart (ed.), Urban Water ’88: Hydrological Processes and Water Management in Urban Areas. Unesco IHP National Committee, Zoetermeer, the Netherlands, pp. 213-221.

Clemens F.H.L.R. (2001). Hydrodynamic models in urban drainage: application and calibration. Ph.D. thesis, Delft University of Technology, the Netherlands.

Clemens F.H.L.R., Ashley R., Bouteligier R. and Berlamont J. (in preparation). Improving the modeling of quality of flow in combined sewers.

Dakin J.P., Pratt D.J., Bibby G.B. and Ross J.N. (1985). Distributed optical fibre Raman temperature sensor using a semiconductor light source and detector. *Electron. Lett.*, **21**(13), 569-570.

Daughton C.G. and Ternes T.A. (1999). Pharmaceuticals and personal care products in the environment: agents of subtle change? *Environ. Health Perspect*., **107**(suppl 6), 907-938.

Dickerson J.W., Hagedorn C. and Hassal A. (2007). Detection and remediation of human-origin pollution at two public beaches in Virginia using multiple source tracking methods. *Water Res.*, **41**(16), 3758-3770.

Dirksen J., Clemens F.H.L.R., Korving H., Cherqui F., Le Gauffre P., Ertl T., Plihal H., Müller K. and Snaterse C.T.M. (2011). The consistency of visual sewer inspection data. *Struct. Infrastruct. E.*, doi: 10.1080/15732479.2010.541265.

Dürrenmatt D.J. and Wanner O. (2008). Simulation of the wastewater temperature in sewers with TEMPEST. *Water Sci. Technol.*, **57**(11), 1809-1815.

EN-IEC (2003). Standard 60794:2003. Optical fiber cables.

Fankhauser R. (1998). Influence of systematic errors from tipping bucket raingauges on recorded rainfall data. *Water Sci. Technol.*, **37**(11), 121-129.

Glombitza U. and Hoff H. (2004). Fiber optic radar system for fire detection in cable trays. In: H. Luck, P. Laws and I. Willms (eds.), Proc. 13th Int. Conf. on Automatic Fire Detection "AUBE '04", Duisburg, Germany, September 14-16, 2004, pp. 1-23.

Graaf J. van der (1995). Reader for CT4481: Wastewater treatment I, edition January 1995. Delft University of Technology, the Netherlands.

Gromaire M.C., Garnaud S., Saad M. and Chebbo G. (2001). Contribution of different sources to the pollution of wet weather flows in combined sewers. *Water Res.*, **35**(2), 521-533.

Gruber G., Winkler S. and Pressl A. (2005). Continuous monitoring in sewer networks an approach for quantifications of pollution loads from CSOs into surface water bodies. *Water Sci. Technol.*, **52**(12), 215-223.

Gruber G., Bertrand-Krajewski J.-L., De Bénédittis J., Hochedlinger M. and Lettl W. (2006). Practical aspects, experiences and strategies by using UV/VIS sensors for long-term sewer monitoring. *Water Pract. Technol.*, **1**(1).

Grüning H. and Orth H. (2002). Investigations of the dynamic behavior of the composition of combined sewage using on-line analyzers. *Water Sci. Technol.*, **45**(4-5), 77-83.

Guo W., Soibelman L. and Garrett Jr. J.H. (2009). Automated defect detection for sewer pipeline inspection and condition assessment. *Autom. Constr.*, **18**(5), 587-596.

Hanna E. (1995). How effective are tipping-bucket raingauges? A review. *Weather*, **50**(10), 336-342.

Harremoës P. (2002). Integrated urban drainage, status and perspectives. *Water Sci. Technol.*, **45**(3), 1-10.

Henckens G.J.R. and Schuit A.D. (2002). Het monitoren van troebelheid in een rioolstelsel (in Dutch: Monitoring of turbidity in a sewer system). *Rioleringswetenschap*, **2**(5), 83-89.

Hochedlinger M. (2005). Assessment of combined sewer overflow emissions. Ph.D. thesis, Technische Universität Graz, Austria.

Hochedlinger M., Kainz H. and Rauch W. (2005). Assessment of CSO loads - based on UV/VIS spectroscopy of different regression methods. In: E. Eriksson, H. Genc-Fuhrman, J. Vollertsen, A. Ledin, T. Hvitved-Jacobsen and P.S. Mikkelsen (eds.), Proc. 10th Int. Conf. on Urban Drainage, Copenhagen, Denmark, 21-26 August 2005, CD-ROM.

Hoes O.A.C., Schilperoort R.P.S., Luxemburg W.M.J., Clemens F.H.L.R. and Giesen N.C. van de (2009). Locating illicit connections in storm water sewers using fiber-optic distributed temperature sensing. *Water Res.*, **43**(20), 5187-5197.

Huber E. and Frost M. (1998). Light scattering by small particles. *J. Water Supply Res. Technol. AQUA*, **47**(2), 87-94.

Huijsing J.H. (2009). Smart Sensor Systems. Why? Where? How? In: G.M.C. Meijer (ed.), Smart Sensor Systems. John Wiley & Sons, Ltd, West Sussex, UK, Chapter 1, pp. 1-19.

Huisman J.L., Burckhardt S., Larsen T.A., Krebs P. and Gujer W. (2000). Propagation of waves and dissolved compounds in sewers. *J. Environ. Eng.*, **126**(1), 12-20.

Hurk B.J.J.M. van den, Klein Tank A.M.G., Lenderink G., Ulden A.P. van, Oldenborgh G.J. van, Katsman C.A., Brink H.W. van den, Keller F., Bessembinder J.J.F., Burgers G., Komen G.J., Hazeleger W. and Drijfhout S.S. (2006). KNMI climate change scenarios 2006 for the Netherlands. Report WR-2006-01, KNMI, de Bilt, the Netherlands.

ISO (1975). Standard 2548:1975. Centrifugal, mixed flow and axial pumps - Code for acceptance tests - Class C.

ISO (1980). Standard 4185: 1980. Measurement of liquid flow in closed conduits - Weighing method.

ISO (1991). Standard 9104:1991. Measurement of fluid flow in closed conduits - Methods of evaluating the performance of electromagnetic flow-meters for liquids.

ISO (1992a). Standard 5667-10:1992. Water quality - Sampling - Part 10: Guidance on sampling of waste waters.

ISO (1992b). Standard 6817:1992. Measurement of conductive liquid flow in closed conduits - Method using electromagnetic flowmeters.

ISO (2002). Standard 15705:2002. Water quality - Determination of the chemical oxygen demand index (ST-COD) - Small-scale sealed-tube method.

Jewell C. (2001). A systematic methodology for the identification and remediation of illegal connections. In: s.n. (ed.), 2001 A collections systems odyssey: integrating O&M and wet weather solutions, Proc. of the Water Environment Federation, 2001**(**2), 669-683.

Jeanbourquin D., Sage D., Nguyen L., Schaeli B., Kayal S., Barry D.A. and Rossi L. (2010). Flow measurements in sewer systems based on image analysis: automatic flow velocity algorithm. In: s.n. (ed.), Proc. 7th Int. Conf. NOVATECH, Lyon, France, 28-30 June 2010, CD-ROM.

Johansson S., 1997. Seepage monitoring in embankment dams. Ph.D. thesis, Royal Institute of Technology, Sweden.

Jonge J. de (2009). Personal communication (representative of Waterschap De Dommel, Boxtel, the Netherlands).

Jørgensen H.K., Rosenørn S., Madsen H. and Mikkelsen P.S. (1998). Quality control of rain data used for urban runoff systems. *Water Sci. Technol.*, **37**(11), 113-120.

Kafi M., Gasperi J., Moilleron R., Gromaire M.C. and Chebbo G. (2008). Spatial variability of the characteristics of combined wet weather pollutant loads in Paris. *Water Res.* **42**(3), 539-549.

Koninklijk Nederlands Meteorologisch Instituut (KNMI) (2008, 2009). Data available via http://www.knmi.nl, visited October 2008; December 2009.

Korving H. (2010). Personal communication (representative of Witteveen+Bos consulting and engineering, Deventer, the Netherlands).

Krebs P., Merkel K. and Kühn V. (1999a). Dynamic changes in wastewater composition during rain runoff. In: I.B. Joliffe and J.E. Ball (eds.), Proc. 8th Int. Conf. on Urban Storm Drainage, 30 August - 3 September 1999, Sydney, Australia, pp. 920-927.

Krebs P., Holzer P., Huisman J.L. and Rauch W. (1999b). First flush of dissolved compounds. *Water Sci. Technol.*, **39**(9), 55-62.

Krejci V., Dauber L., Novak B. and Gujer W. (1987). Contribution of different sources to pollutant loads in combined sewers. In: W. Gujer and V. Krejci (eds.), Proc. 4th Int. Conf. on Urban Storm Drainage, 31 August - 4 September 1987, Lausanne, Switzerland, pp. 34-39.

Langergraber G., Fleischmann N. and Hofstädter F. (2003). A multivariate calibration procedure for UV/VIS spectrometric quantification of organic matter and nitrate in wastewater. *Water Sci. Technol.*, **47**(2), 63-71.

Langergraber G., Fleischmann N., Hofstädter F. and Weingartner A. (2004). Monitoring of a paper mill wastewater treatment plant using UV/VIS spectrometry. *Water Sci. Technol.*, **49**(1), 9-14.

Langeveld J.G. (2004). Interactions within wastewater systems. Ph.D. thesis, Delft University of Technology, the Netherlands.

Langeveld J.G., Haan C. de, Schilperoort R.P.S. and Klootwijk M. (submitted). Monitoring the performance of a storm water separating manifold with DTS. Submitted to the 12th Int. Conf. on Urban Drainage, Porto Alegre, Brazil, 11-16 September, 2011.

Larrarte F. (2008). Suspended solids within sewers: an experimental study. *Environ. Fluid Mech.*, **8**(3), 249-261.

Lijklema L., Tyson J.M. and Lesouef A.S. (1993). Interactions between sewer treatment plants and receiving waters in urban areas: a summary of the Interurba '92 workshop conclusions. *Water Sci. Technol.*, **27**(12), 1-29.

López-Higuera, J.M. (2002). Handbook of optical fiber sensing technology. John Wiley & Sons Ltd, West Sussex, UK.

Luxemburg W.M.J. and Savenije H.H.G. (2007). Reader for CT4440: Hydrological Measurements, edition May 2007. Delft University of Technology, the Netherlands.

Luyckx G. and Berlamont J. (2001). Simplified method to correct rainfall measurements from tipping bucket raingauges. In: R.W. Brashear and C. Maksimovic (eds.), Proc. Urban Drainage Modeling, Orlando, Florida, 20-24 May 2001, pp. 767-776.

Maksimović Č, Bužek L. and Petrović J. (1991). Corrections of rainfall data obtained by tipping bucket raingauge. *Atmos. Res.*, **27**(1-3), 45-53.

Man H. de (2008). On the applicability of discharge measuring techniques in partially filled conduits. M.Sc. thesis, Delft University of Technology, the Netherlands.

Man H. de, Clemens F.H.L.R., Veldhuis J.A.E. ten, Moens M.R. and Klootwijk M. (2008). Onderzoek naar de nauwkeurigheid van debietmetingen in deel gevulde leidingen (in Dutch: Assessment of the accuracy of flow measurements in part-full pipes). *Rioleringswetenschap*, **8**(31), 33-46.

Maribas A., do Carmo Lourenço da Silva M., Laurent N., Loison B., Battaglia P. and Pons M.-N. (2008). Monitoring of rain events with a submersible UV/VIS spectrophotometer. *Water Sci. Technol.*, **57**(10), 1587-1593.

Marsalek J. (1981). Calibration of the tipping-bucket raingage. *J. Hydrol.*, **53**(3-4), 343-354.

Métadier M. and Bertrand-Krajewski J.-L. (2009). From mess to mass: a methodology for calculating storm event pollution loads with their uncertainties, from continuous raw data. In: s.n. (ed.), Proc. 8th Int. Conf. on Urban Drainage Modelling & 2nd Int. Conf. on Rainwater Harvesting and Management, Tokyo, Japan, 7-12 September, 2009, CD-ROM.

Metcalf and Eddy (2003). Wastewater Engineering Treatment and Reuse, 4th edition. McGraw-Hill, New York, USA.

Ministerie van Verkeer en Waterstaat (Min.V&W) (2010). Water in Beeld 2010 (in Dutch: National water assessment 2010). The Hague, the Netherlands.

Moel P.J. de, Verberk J.Q.J.C and Dijk J.C. van (2004). Drinkwater - principes en praktijk (in Dutch: Drinking water - principles and practice). Sdu Uitgevers, The Hague, the Netherlands.

Mourad M. and Bertrand-Krajewski J.-L. (2002). A method for automatic validation of long time series of data in urban hydrology. *Water Sci. Technol.*, **45**(4-5), 263-270.

NEN (2009). Standard 6600-1. Water - Sampling - Part 1: Wastewater.

Niemczynowicz J. (1986). The dynamic calibration of tipping-bucket raingauges. *Nord. Hydrol.*, **17**(3), 203-214.

Nikolov N.A., Minkov I.N., Dimitrov D.K., Mincheva S.K. and Mirchev M.A. (1978). Hydraulic calculation of a submerged broad-crested weir. *Hydrotechnical Construction* , **12**(6), 631-634.

Olsson G. (2002). Lessons learnt at ICA2001. *Water Sci. Technol.*, **45**(4-5), 1-8.

Ort C., Lawrence M.G., Rieckermann J. and Joss A. (2010). Sampling for pharmaceuticals and personal care products (PPCPs) and illicit drugs in wastewater systems: are your conclusions valid? A critical review. *Environ. Sci. Technol.*, **44**(16), 6024-6035.

Otto M. (1999). Chemometrics: statistics and computer application in analytical chemistry, 2nd edition. Wiley-VCH Verlag GmbH & Co, Weinheim, Germany.

Overgaard S., El-Shaarawi A.H. and Arnbjerg-Nielsen K. (1998). Calibration of tipping bucket raingauges. *Water Sci. Technol.*, **37**(11), 139-145.

Perkampus H.-H. (1995). Encyclopedia of spectroscopy. Wiley-VCH Verlag GmbH & Co, Weinheim, Germany.

Pons M.-N., Le Bonté S. and Potier O. (2004). Spectral analysis and fingerprinting for biomedia characterisation. *J. Biotechnol.*, **113**(1-3), 211-230.

Pothof I. (2010). Personal communication (representative of Deltares Institute, Delft, the Netherlands).

Rauch W., Thurner N. and Harremoës P. (1998). Required accuracy of rainfall data for integrated urban drainage modeling. *Water Sci. Technol.*, **37**(11), 81-89.

Rieger L., Langergraber G., Thomann M., Fleischmann N. and Siegrist H. (2004). Spectral *in-situ* analysis of NO_2, NO_3, COD, DOC and TSS in the effluent of a WWTP. *Water Sci. Technol*., **50**(11), 143-152.

RIONED (2004). Leidraad Riolering, module C2100 rioleringsberekeningen en hydraulisch functioneren (in Dutch: Sewer Guidelines, module C2100 sewer calculations and hydraulic functioning). Stichting RIONED, Ede, the Netherlands

RIONED (2009a). Oppervlaktewaterkwaliteit: wat zijn relevante emissies? (in Dutch: Surface water quality: which emissions are relevant?). Stichting RIONED, Ede, the Netherlands.

RIONED (2009b). Riool in cijfers 2009/2010 (in Dutch: Sewer statistics in the Netherlands 2009-2010). Stichting RIONED, Ede, the Netherlands.

Scheer and Schilling (2003). Einsatz von Online-Messgeräten zur Beurteilung der Mischwasserqualität im Kanal (in German: application of online sensors for the assessment of in-sewer wastewater quality). *KA - Abwasser Abfall*, **50**(5), 585-595.

Schilling W. (1991). Rainfall data for urban hydrology: what do we need? *Atmos. Res.*, **27**(1-3), 5-21.

Schilperoort R.P.S., Dirksen J., Langeveld J.G. and Clemens F.H.L.R. (2008). Assessing characteristic time and space scales of in-sewer processes by analysis of one year of continuous in-sewer monitoring data. In: s.n. (ed.), Proc. 8th Int. Conf. on Urban Drainage Modelling & 2nd Int. Conf. on Rainwater Harvesting and Management, Tokyo, Japan, 7-12 September, 2009, CD-ROM.

Schilperoort R.P.S. and Clemens F.H.L.R. (2009). Fibre-optic distributed temperature sensing in combined sewer systems. *Water Sci. Technol.* **60**(5), 1127-1134.

Schmidt S.D. and Spencer D.R. (1986). The magnitude of improper waste discharges in an urban storm water system. *J. Water Pollut. Control Fed.*, **58**(7), 744-748.

Schütze M., Campisano A., Colas, H., Schilling W. and Vanrolleghem P.A. (2004). Real time control of urban wastewater systems - where do we stand today? *J. Hydrol.*, **299**(3-4), 335-348.

Selker J.S., Giesen N. van de, Westhoff M., Luxemburg W. and Parlange M.B. (2006a). Fiber optics opens window on stream dynamics. *Geophys. Res. Lett.*, **33**(24), art. no. L24401.

Selker J.S., Thévenaz L., Huwald H., Mallet A., Luxemburg W., Giesen N. van de, Stejskal M., Zeman J., Westhoff M. and Parlange M.B. (2006b). Distributed fiber-optic temperature sensing for hydrologic systems. *Water Resour. Res.*, **42**(12), art. no. W12202.

Sensornet (2009). Personal communication.

Sevruk B. (1996). Adjustment of tipping-bucket precipitation gauge measurements. *Atmos. Res.*, **42**(1-4), 237-246.

Sluis J.W. van, Hove M.D. ten and Boer B. de (1991). Final report of the 1982-1989 NWRW research program: conclusions and recommendations. Ministry of Housing, Urban Planning, and Environment, The Hague, the Netherlands.

Smith S.W. (1997). The scientist and engineers guide to digital signal processing. California Technical Publishing, San Diego CA, USA.

Smits J., Klootwijk M. and Moens M. (2007). Praktijktest debietmeters proefopstelling Breda (in Dutch: Flow sensors tested in a laboratory set-up in Breda). *Rioleringswetenschap*, **7**(28), 46-66.

Standard Methods for the Examination of Water and Wastewater (1998). 20th edition, American Public Health Association (APHA) / American Water Works Association (AWWA) / Water Environment Federation (WEF), Washington, USA.

Steiner M., Smith J.A., Burges S.J., Alonso C.V. and Darden R.W. (1999). Effect of bias adjustment and raingauge data quality control on radar rainfall estimation. *Water Resour. Res.*, **35**(8), 2487-2503.

STOWA (1996). Metingen aan rioolstelsels en oppervlaktewater. Leidraad voor metingen en meetprogramma's (in Dutch: Monitoring sewer systems and receiving

waters. Guidelines for monitoring programs). Report 1996-09, STOWA, Utrecht, the Netherlands.

STOWA (2001). Leidraad voor de bepaling van de ontwerpcapaciteit van rwzi's (in Dutch: Guidelines for the determination of the design capacity of wwtps). Report 2001-34, STOWA, Utrecht, the Netherlands.

STOWA (2007a). Regenwaterdatabase. De feiten over de kwaliteit van afstromend regenwater (in Dutch: Stormwater database. The facts on the quality of stormwater run-off). Report 2007-21, STOWA, Utrecht, the Netherlands.

STOWA (2007b). Gevolgen klimaatveranderingen onderzoeksvragen water-beheerders (in Dutch: Impact of climate changes. Research questions for Dutch waterboards). Report 2007-W08, STOWA, Utrecht, the Netherlands.

Stumwöhrer K., Matsché N. and Winkler S. (2003). Influence of changes of the wastewater composition on the applicability of UV-absorption measurements at combined sewer overflows. *Water Sci. Technol.*, **47**(2), 73-78.

Tauw (2002). Definitief ontwerp rwzi Eindhoven (in Dutch: Final design wwtp Eindhoven). Report R010-4222180TDG, Tauw bv, Deventer, the Netherlands.

Tauw (2007). Calamiteit rwzi Eindhoven, acute drijflaagvorming op de nabezinktanks (in Dutch: Calamity wwtp Eindhoven, acute formation of floating sludge layers on secondary clarifiers.) Report R001-4527996BAR, Tauw bv, Deventer, the Netherlands.

Taylor A.C. and Wong T.H.F. (2002). Non-structural storm water quality best management practices – A literature review of their value and life-cycle costs. Technical Report 02/13, Cooperative research center for catchment hydrology, Melbourne, Australia.

Teichgräber B., Stemplewski J., Althoff H. and Elkmann N. (2006). Remote controlled inspection device for large sewers. *Water Pract. Technol.*, **1**(4).

Ternes T.A. (1998). Occurrence of drugs in German sewage treatment plants and rivers. *Water Res.*, **32**(11), 3245-3260.

Torres A. and Bertrand-Krajewski J.-L. (2008). Partial Least Squares local calibration of a UV-visible spectrometer used for *in situ* measurements of COD and TSS concentrations in urban drainage systems. *Water Sci. Technol.*, **57**(4), 581-588.

Tuomari D. and Thompson S. (2003). “Sherlocks of storm water” effective investigation techniques for illicit connection and discharge detection. In: s.n. (ed.), Proc. Nat. Conf. on Urban Storm Water: enhancing programs at the local level, Chicago IL, USA, February 17-20, 2003, pp. 489-496.

Tyler S.W., Selker J.S., Hausner M.B., Hatch C.E., Torgersen T., Thodal C.E. and Schladow S.G. (2009). Environmental temperature sensing using Raman spectra DTS fiber-optic methods. *Water Resour. Res.*, **45**, art. no. W00D23.

Upton G.J.G. and Rahimi A.R. (2003). On-line detection of errors in tipping-bucket raingauges. *J. Hydrol.*, **278** (1-4), 197-212.

United States Environmental Protection Agency (US EPA) (1978). Management of small wasteflows. Report 600/2-78-173 (NTIS PB-286-560), Natl. Tech. Inf. Service, Springfield VA, USA.

United States Environmental Protection Agency (US EPA) (2004). Illicit discharge detection and elimination: a guidance manual for program development and technical assessments. Report X-82907801-0, US EPA Office of Research and Development, Cincinnati OH, USA.

Vanrolleghem P.A., Schilling W., Rauch W., Krebs P. and Aalderink H. (1999). Setting up measuring campaigns for integrated wastewater management. *Water Sci. Technol.*, **39**(4), 257-268.

Veldkamp R.G., Henckens G., Langeveld J.G. and Clemens F.H.L.R. (2003). Veldmetingen van troebelheid in relatie tot transportmechanismen in rioolstelsel (in Dutch: Turbidity measurements in relation to transport mechanisms in sewer systems). *Rioleringswetenschap*, **3**(9), 23-32.

Verschoor A. (2010). Personal communication (representative of Waterschap de Dommel, Boxtel, the Netherlands).

Wang W., Reimers C.E., Wainright S.C., Shahriari M.R. and Morris M.J. (1999). Applying fiber-optic sensors for monitoring dissolved oxygen. *Sea Technology*, **40(**3), 69-74.

Wanner O., Panagiotidis V. and Siegrist H. (2004). Wärmeenthahme aus der Kanalisation - Einfluss auf die Abwassertemperatur (in German: Heat recovery from the sewer system - influence on the wastewater temperature). *KA-Abwasser Abfall*, **51**(5), 489-495.

Wanner O., Panagiotidis V., Clavadetscher P. and Siegrist H. (2005). Effect of heat recovery from raw wastewater on nitrification and nitrogen removal in activated sludge plants. *Water Res.* **39**(19), 4725-4734.

Waterschap De Dommel (WDD) (2004). Beschikking WVO vergunning voor rwzi Eindhoven (Permit relating to the Pollution of Surface Waters Act for wwtp Eindhoven).

Waterschap De Dommel (WDD) (2005). Sewer system information files.

Waterschap De Dommel (WDD) (2007). Personal communication.

Watt I.A. and Jefferies C. (1996). Portable sewage flow sensors - their calibration and accuracy. *Water Sci. Technol.*, **33**(1), 127-137.

Weijers S. (2009). Personal communication (representative of Waterschap De Dommel, Boxtel, the Netherlands).

Weijers S., Jonge J. de, Zanten O. van, Benedetti L., Langeveld J., Menkveld H.W. and Nieuwenhuijzen A.F. van (accepted). KALLISTO: Cost effective and integrated optimization of the urban wastewater system Eindhoven. Accepted for presentation at 11th Spec. Conf. Design, Operation and Economics of Large Waste Water Treatment Plants, 4-8 September 2011, Budapest, Hungary.

Weiß G., Brombach H. and Haller B. (2002). Infiltration and inflow in combined sewer systems: long-term analysis. *Water Sci. Technol.*, **45**(7), 11-19.

Weyand M. (2002). Real-time control in combined sewer systems in Germany - some case studies. *Urban Water*, **4**(4), 347-354.

Willems P. (2006). Random number generator or sewer water quality model? *Water Sci. Technol.*, **54**(6-7), 387-394.

Willems P. (2008). Quantification and relative comparison of different types of uncertainties in sewer water quality modeling. *Water Res.*, **42**(13), 3539-3551.

Wirahadikusumah R., Abraham D.M., Iseley T. and Prasath R.K. (1998). Assessment technologies for sewer system rehabilitation. *Autom. Constr.*, **7**(4), 259-270.

Zuccato E., Chiabrando C., Castiglioni S., Bagnati R. and Fanelli R. (2008). Estimating community drug abuse by wastewater analysis. *Environ. Health Perspect.*, **116**(8), 1027-1032.

Appendix A. Monitoring network in wastewater system of wwtp Eindhoven

location	sensor	parameter(s)	in thesis?
wwtp influent pumping station inflow Riool-Zuid	s::can UV/VIS spectro::lyzer	-TSS, COD, CODf, NO3	√
wwtp influent pumping station inflow Riool-Zuid	pt100/preas 411	-temperature	-
wwtp influent pumping station inflow Eindhoven Stad	s::can UV/VIS spectro::lyzer	-TSS, COD, CODf, NO3	√
wwtp influent pumping station inflow Eindhoven Stad	pt100/preas 411	-temperature	-
wwtp influent pumping station inflow Eindhoven Stad	Evita Insitu 4100	-NH4	-
wwtp influent pumping station inflow Nuenen/Son	s::can UV/VIS spectro::lyzer	-TSS, COD, CODf, NO3	√
wwtp influent pumping station inflow Nuenen/Son	pt100/preas 411	-temperature	-
wwtp influent pumping station influent pumps 1 - 9	Danfoss MAG3100	-flow in full pipes	√
wwtp intermediary pumping station	s::can UV/VIS spectro::lyzer	-TSS, COD, CODf, NO3	-
wwtp intermediary pumping station	Evita Insitu 4100	-NH4 / PO4	-
22 locations (see also figure 3-1)	Rain-Ger tipping-bucket gauges	-precipitation	√
7 locations: Aalst, Bergeijk, Geldrop, Son Luijksgestel, Valkenswaard, Veldhoven	Flo-Tote 3 electromagnetic pt100	-flow in part-full pipes (velocity + level) -temperature	-
12 locations: Aalst, Duizel, Eersel, Heeze-Leende, Knegsel, Nuenen L., Son, Steensel, Sterksel, Weebosch, Westerh., Wintelre	various types	-flow in full pipes	-
3 locations: cs Valkenswaard, cs rwzi, cs de Meeren	bubblers	- water levels	-

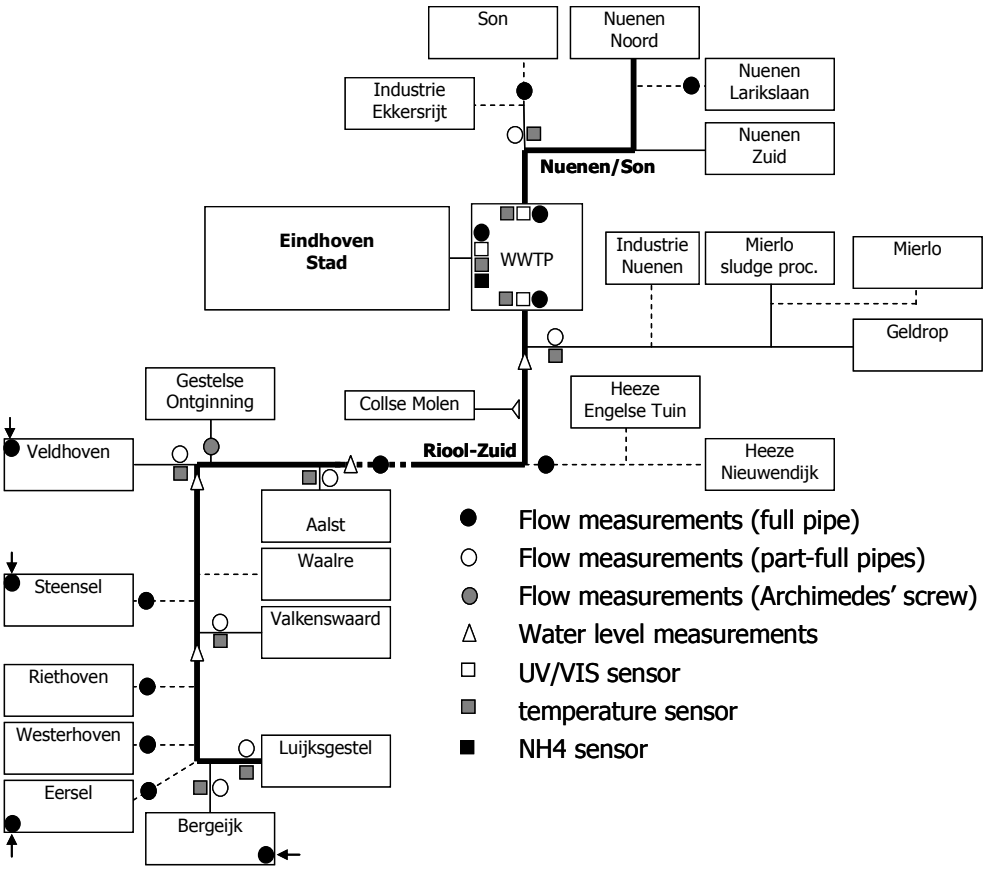

Figure A-1: The WDD monitoring network in the wastewater system of wwtp Eindhoven. Locations of raingauges can be found in Figure 3-1 in chapter 3.

Appendix B. Characteristics of municipal sewer systems discharging wastewater to the wwtp Eindhoven

Municipality	**Inhabitants**[1]	**Industry**[2]	**Total area**[1]	**Receiving waters**[1]	**Impermeable area**[2]
	[#]	[p.e.]	[km^2]	[km^2]	[km^2]
Bergeijk	18,094	7,721	101.79	0.74	2.16
Eersel	18,041	9,010	83.28	0.87	1.45
Eindhoven	209,699	68,800	88.84	1.14	20.82
Geldrop-Mierlo	37,823	30,250	31.39	0.36	2.69
Heeze-Leende	15,153	4,490	105.12	1.14	1.18
Nuenen	22,692	600	34.11	0.23	2.46
Son en Breugel	15,306	13,260	26.49	0.56	2.19
Valkenswaard	30,908	7,230	56.44	1.47	2.96
Veldhoven	43,284	6,330	31.92	0.19	3.60
Waalre	16,521	2,000	22.71	0.28	1.42
Total	**427,521**	**149,691**	**582.09**	**6.98**	**40.93**

Municipality	**Total length sewer system**[3]	**Combined**[3]	**Separate**[3]	**CSOs**[3]
	[km]	[%]	[%]	[#]
Bergeijk	133	97	3	17
Eersel	153	95	5	6
Eindhoven	1143	71	29	30
Geldrop-Mierlo	190	84	16	16
Heeze-Leende	81	96	4	22
Nuenen	122	79	21	26
Son en Breugel	120	79	21	13
Valkenswaard	144	83	17	15
Veldhoven	250	71	29	33
Waalre	91	98	2	4
Total	**2,427**	**78**	**22**	**182**

[1] source: CBS, 2007 (reference date January 1st, 2007)
[2] source: WDD, 2005
[3] source: WDD, 2011

Appendix C. Characteristics of connections to Riool-Zuid, Eindhoven Stad and Nuenen/Son

Connection		**Number of inhabitants**[1]	**Industry**[2]	**Impermeable area**[2]	**Capacity**[2,4]	**In-sewer storage**[2]		**Additional storage**[2,5]	
	Type[3]	[#]	[p.e.]	[km^2]	[m^3/h]	[m^3]	[mm]	[m^3]	[mm]
Bergeijk	ff	10,743	1,400	1.35	982	4,898	3.6	12,116	9.0
Luijksgestel	vv	2,943	811	0.29	273	1,910	6.6	3,700	12.8
Riethoven	ps	2,403	5,030	0.19	226	980	5.2	46	0.2
Westerhoven	ps	2,005	480	0.33	219	1,123	3.4	2,050	6.2
Eersel	ps	15,115	7,570	1.30	1,100	8,024	6.2	11,210	8.6
Steensel	ps	2,926	1,440	0.15	125	1,272	8.5	-	-
G.Ontginning	as	8,697	1,500	1.34	1,660	8,777	6.6	-	-
Geldrop	ff	34,787	5,090	1.89	1,930	15,948	8.4	12,700	6.7
Mierlo	ps	3,036	-	0.41	972	2,017	4.9	380	0.9
Industrie Nuenen	ps	-	4,160	0.39	125	449	1.2	-	-
Mierlo sludge processing	ff	-	21,000	-	325[6]	-	-	-	-
Heeze Nieuwendijk	ps	13,385	4,490	1.05	952	8,674	8.3	3,567	3.4
Heeze Engelse Tuin	ps	1,768	-	0.13	110	106	0.8	2,360	18.2
Valkenswaard	ff	30,908	7,230	2.96	2,679	24,439	8.3	2,592	0.9
Veldhoven	ff	43,284	6,330	3.60	4,145	21,555	6.0	5,447	1.5
Aalst	vv	10,736	2,000	0.97	804	8,892	9.2	12,660	13.1
Waalre	ps	5,785	-	0.45	250	3,087	6.9	780	1.7
Total RZ		**188,521**	**68,531**	**16.80**	**16,772**	**112,151**	**6.7**	**69,608**	**4.1**

[1] source: CBS, 2007 (reference date January 1st, 2007)
[2] source: WDD, 2007 (reference date January 1st, 2007)
[3] ff = free-flow; vv = vortex valve; ps = pumping station; as = Archimedean screw
[4] in case of free-flow connection: agreed guaranteed flow (agreement between municipality and WDD); in case of pumping station and Archimedean screw: installed capacity; in case of vortex valve: capacity to which flow is limited by the valve
[5] in settling tanks, retention ponds, helophyte filters, etc.
[6] only on weekdays during operating hours (08h00 - 16h00)

Characteristics of municipal sewer systems that discharge to other sewer systems are included in the characteristics of the receiving sewer system.

Connection		Number of inhabitants[1]	Industry[2]	Impermeable area[2]	Capacity[2,4]	In-sewer storage[2]		Additional storage[2,5]	
	Type[3]	[#]	[p.e.]	[km^2]	[m^3/h]	[m^3]	[mm]	[m^3]	[mm]
Nuenen/Son									
Nuenen Noord	ff	2,425	-	0.32	600	2,552	8.0	-	-
Nuenen Zuid	ff	16,614	600	1.78	964	6,945	3.9	4,931	2.8
Nuenen Lariksl.	ps	3,653	-	0.36	300	2,148	6.0	-	-
Son	ps	15,306	750	1.07	815	7,457	7.0	1,748	1.6
Industrie Ekkersrijt	ps	-	12,510	1.12	175	4,277	3.8	-	-
Total NS		**37,998**	**13,860**	**4.65**	**2,854**	**23,379**	**5.0**	**6,679**	**1.4**
Eindhoven Stad									
Eindh. Stad	ff	201,002	67,300	19.48	15,819	124,046	6.4	-	-
Total of 3 catchment areas (RZ, ES and NS)		**427,521**	**149,691**	**40.93**	**35,445**	**259,576**	**6.3**	**76,287**	**1.9**

[1] source: CBS, 2007 (reference date January 1st, 2007)
[2] source: WDD, 2007 (reference date January 1st, 2007)
[3] ff = free-flow; vv = vortex valve; ps = pumping station; as = Archimedean screw
[4] in case of free-flow connection: agreed guaranteed flow (agreement between municipality and WDD); in case of pumping station and Archimedean screw: installed capacity; in case of vortex valve: capacity to which flow is limited by the valve
[5] in settling tanks, retention ponds, helophyte filters, etc.

Characteristics of municipal sewer systems that discharge to other sewer systems are included in the characteristics of the receiving sewer system.

Appendix D. Automatic cross-check of WDD tipping bucket raingauge results

Upton and Rahimi (2003) developed an automated data quality assessment for a TBRG network in the United Kingdom. The UK raingauge network largely resembles that in the Eindhoven area: respectively 23 and 25 TBRGs in an area of 25x30 km and 23x28 km. In both areas sensors are inhomogeneously distributed over both rural and urban areas. It is therefore considered appropriate to apply their procedure - in somewhat adapted form - on the Eindhoven data. The total procedure comprises three single-gauge tests and four tests that can be applied to compare TBRGs in a network. In this study only the three most useful network tests are used. The three tests compare precipitation depth per event (test statistic z_n) and time between tips during an event (z_m and z_s). The objective of the statistics is to indicate that a specific sequence of tips or event *may* not be representing the precipitation process correctly; a subsequent manual interpretation remains necessary. Initially, boundary values as used for the UK network are used; later a sensitivity analysis demonstrates the effect of changing boundary values on the results for the Eindhoven data.

In Upton and Rahimi (2003) an event is defined as a rainy period between two dry periods that are each at least 2 hours long. A dry period is a period in which none of the gauges in the entire network tipped. The rainy period may contain any number of short dry periods, providing that each lasts less than 2 hours. Using this definition on the Eindhoven data a total of 901 events have been identified over the period July 1st, 2007 - November 1st, 2008. Of these, 377 events have a length of 1 minute during which a single gauge tipped only once or twice. For another 283 events the maximum of all sensor depths during the event does not exceed 0.5 mm. These pseudo-events are not further evaluated, reducing the number of 'real' events to 241. Fifty percent of these have a length up to 2.5 hours; another forty percent has a length between 2.5 and 24 hours; the two longest events lasted 5.5 and 9.5 days. This definition of an event is only used for the data quality assessment in this appendix; it differs from the definition of a storm event used in chapter 6.

To allow for possible spatial variability over the 600 km^2 area, a single WDD TBRG data set is not compared to all other WDD TBRG data sets; instead, each sensor is only compared to the seven nearest gauges. To guarantee comparison with at least three nearly always properly functioning raingauges, the results of the three NM gauges (>99% data yield, see Table 3-1) are always included for the z_n-statistic. Additionally, for this test statistic, the four closest neighboring sensors are added to make a total of seven. For the z_m and z_s-statistics the use of NM results is

not possible due to the 0.2 mm resolution of NM gauges; for these statistics the seven nearest neighboring WDD sensors have been used.

Test statistic z_n

For comparison of precipitation depths, the number of tips (n_g) at the considered WDD gauge during the considered event is used. This number is compared to $n_1,n_2,\ldots,n_7$, the number of tips recorded during the same event by four neighboring WDD gauges and the three NM gauges, sorted in ascending order. The statistic z_n is given by:

$$z_n = \begin{cases} 0 & \text{for } n_1 - 4 \le n_g \le n_7 + 4 \\ \left(n_g - m_n\right) / M_n & \text{otherwise} \end{cases} \qquad \text{(D.1)}$$

with m_n = n_4 or median of neighboring values;
M_n = median absolute deviation (MAD) from the median m_n .

In case the number of tips at the considered gauge lies within the extended range (by 4 on either side) of neighboring values, z_n equals zero; if not, the statistic is a measure for the deviation of n_g with respect to n_1 through n_7. For the method to be less sensitive to outliers caused by malfunctioning neighboring sensors, the median and MAD values are used as robust alternatives to respectively the mean value and standard deviation of neighboring values. Gauge data should be carefully inspected if boundary values for z_n are either

i. $z_n > 10$ or
ii. $z_n < -5$.

Hence, an event is considered suspicious if the total number of tips exceeds the range of neighboring sensors by 4 and if the resulting deviate becomes too large or too small. The upper and lower boundaries are asymmetrical since the distribution is skewed: tips have a finite lower bound of zero but no upper bound. The boundary values as presented here are developed by Upton and Rahimi (2003) for their UK data set. Hereafter, a sensitivity analysis for boundary values of test statistics is performed for the Eindhoven data.

Test statistics z_m *and* z_s

A comparison based on inter-tip times searches for unusual long inter-tip times that might point to a partially blocked sensor. For this, two parameters are used: $\tau_{g,m}$, the median inter-tip time and $\tau_{g,s}$, the shortest inter-tip time of the considered gauge during the considered event. These are compared to $\tau_{1,m}$, $\tau_{2,m},\ldots$, $\tau_{7,m}$ and $\tau_{1,s}$, $\tau_{2,s},\ldots$, $\tau_{7,s}$, the corresponding values for seven neighboring WDD sensors. The statistics are given by:

$$z_m = \begin{cases} 0 & \text{for} \quad \tau_{1,m} \le \tau_{g,m} \le \tau_{7,m} \\ \left(\tau_{g,m} - m_m\right) / M_m & \text{otherwise} \end{cases} \qquad \text{(D.2)}$$

with m_m = $\tau_{4,m}$ or median of neighboring values;
M_m = median absolute deviation (MAD) from the median m_m;
and

$$z_s = \begin{cases} 0 & \text{for} \quad \tau_{1,s} \le \tau_{g,s} \le \tau_{7,s} \\ \left(\tau_{g,s} - m_s\right) / M_s & \text{otherwise} \end{cases} \qquad \text{(D.3)}$$

with m_s = $\tau_{4,s}$ or median of neighboring values;
M_s = median absolute deviation (MAD) from the median m_s.

Gauge data should be carefully inspected if

$z_m > 10$ or $z_s > 10$.

Hence, an event is considered suspicious if the median or shortest inter-tip time exceeds the range of neighboring sensors and if the resulting deviate becomes too large. Large negative values of the deviate are often found to coincide with localized heavy rain.

Automated test results
The results of application of the three test statistics to the 20 WDD data sets are presented in Figure D-1. For comparison, the manually rejected data are included in the figure (i.e. grey areas in Figure 3-10 are the same as grey areas in Figure D-1). In total, 325 tip sequences have been identified that may not be representing the precipitation process correctly, see Table D-1. Of these, approximately 50% lie within a manually rejected sequence, the other half has not been identified in the manual assessment (i.e. false positive results of the automated procedure). Of the 137 manually rejected sequences, 81 (or 59%) contain at least one automatically detected doubtful tip sequence. The other 56 manually rejected sequences are not detected by the automated procedure and hence constitute false negative results. The results of the sensitivity analysis in Table D-1 show that results of the automated detection are only little sensitive to variation in critical values of test statistics.

Finding 59% of the manually rejected sequences, the performance of the automatic tests on the Eindhoven data is poor compared to the 90% obtained by Upton and Rahimi (2003). Also, the number of false positives is significant for the Eindhoven

data. Upon closer consideration of false positives and false negatives it is found that the general poor performance of the Eindhoven raingauge network stands at the basis of many false identifications. A frequently hampering data communication, an incomplete or incorrect metadata file and prolonged (partial) blockages of multiple gauges makes the application of an automated data quality assessment less straightforward. Closer consideration also revealed that some false positives are actually true positives: some incorrect sequences were overlooked during the manual assessment. Hereafter, some phenomena causing false positives and false negatives are considered in more detail.

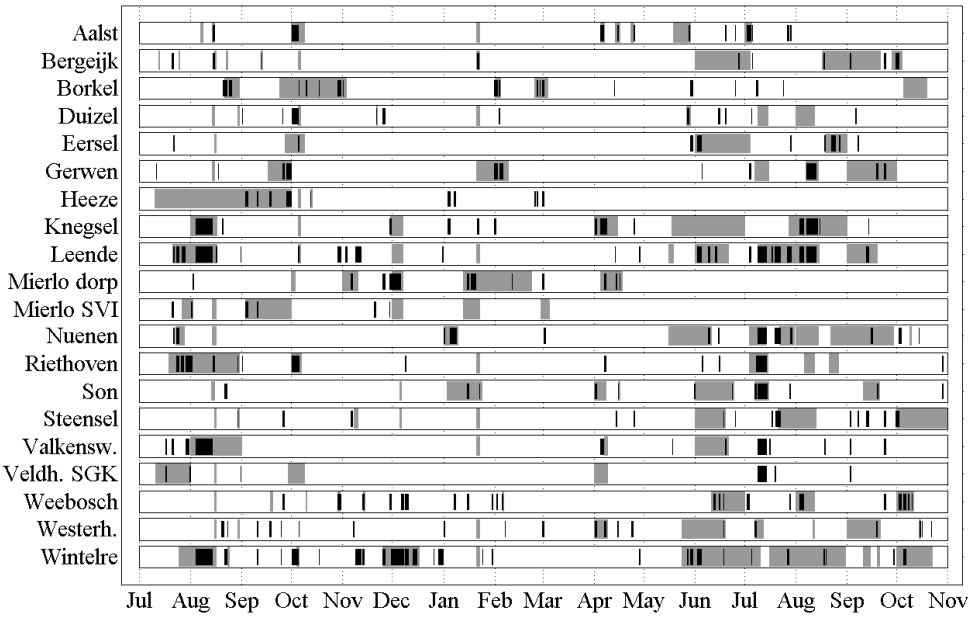

Figure D-1: Manually rejected data (in grey) and automatically detected doubtful tip sequences (in black) of 20 WDD TBRG data sets for the time-span July 1st, 2007 - November 1st, 2008.

False negatives

A false negative result of the automatic procedure constitutes a non-response to a sequence that has been rejected during the manual assessment. Examples are:

(1) All data during sensor cleaning (as reported by the metadata file) have been manually rejected since cleaning often results in a large number of tips not associated with precipitation. However, some reported cleaning

activities do not show in the data sets (which in itself suggests an incorrect metadata file), and are hence not detected by the automated procedure.

(2) A partially blocked sensor can continuously 'leak' stormwater to the tipping bucket. As a result, in some cases, no dry spells over 2 hours can be found and individual storm events are lumped into one prolonged event. Lumping events, the characteristics and anomalies of individual storm events are largely lost inhibiting the automated procedure to detect anomalous behavior.

(3) In case one or more of the neighboring sensors is malfunctioning, the z_n-statistic (precipitation depth) can yield false negatives. A malfunctioning neighboring sensor introduces a relatively large or small value in the range of $n_1,n_2,\ldots,n_7$. As a result, considering the equation, a suspiciously large or small precipitation depth of the considered gauge passes the automatic detection because the considered depth lies within the expanded range of neighboring values.

Table D-1: Automatically detected versus manually rejected sequences with false positives and false negatives; sensitivity analysis for critical values of test statistics.

	automatically detected sequences			manually rejected sequences		
	total	within manually rejected sequence	outside manually rejected sequence (false positive)	total	noticed by automatic detection	unnoticed by automatic detection (false negative)
U&R values	**325**	**169 (52%)**	**156 (48%)**	**137**	**81 (59%)**	**56 (41%)**
$z_n > 0$	390	179 (46%)	211 (54%)	137	83 (61%)	54 (39%)
$z_n > 5$	351	173 (49%)	178 (51%)	137	81 (59%)	56 (41%)
$z_n > 10$	**325**	**169 (52%)**	**156 (48%)**	**137**	**81 (59%)**	**56 (41%)**
$z_n > 15$	316	167 (53%)	149 (47%)	137	80 (58%)	57 (42%)
$z_n > 20$	313	165 (53%)	148 (47%)	137	78 (57%)	59 (43%)
$z_n < 0$	399	184 (46%)	215 (54%)	137	87 (64%)	50 (36%)
$z_n < -5$	**325**	**169 (52%)**	**156 (48%)**	**137**	**81 (59%)**	**56 (41%)**
$z_n < -10$	292	158 (54%)	134 (46%)	137	76 (55%)	61 (45%)
$z_m > 0$	402	180 (45%)	222 (55%)	137	83 (61%)	54 (39%)
$z_m > 5$	357	172 (48%)	185 (52%)	137	81 (59%)	56 (41%)
$z_m > 10$	**325**	**169 (52%)**	**156 (48%)**	**137**	**81 (59%)**	**56 (41%)**
$z_m > 15$	311	164 (53%)	147 (47%)	137	77 (56%)	60 (44%)
$z_m > 20$	304	162 (53%)	142 (47%)	137	75 (55%)	62 (45%)
$z_s > 0$	396	185 (47%)	211 (53%)	137	84 (61%)	53 (39%)
$z_s > 5$	363	179 (49%)	184 (51%)	137	82 (60%)	55 (40%)
$z_s > 10$	**325**	**169 (52%)**	**156 (48%)**	**137**	**81 (59%)**	**56 (41%)**
$z_s > 15$	330	170 (52%)	160 (48%)	137	81 (59%)	56 (41%)
$z_s > 20$	325	169 (52%)	156 (48%)	137	81 (59%)	56 (41%)

False positives

The automatic procedure yields a false positive result if it considers a tip sequence suspicious whereas the manual assessment has not rejected the event. Examples are:

(1) A malfunctioning data communication during a storm event causes a data gap and hence a zero precipitation depth for that sensor. The z_n-statistic detects the anomalous zero depth if values of surrounding gauges are significant. Since data gaps are not included in the 'manually rejected sequences' (only the grey areas from Figure 3-10 are grey areas in Figure D-1), the test result is strictly considered a false positive. However, the test results can be interpreted as a detection of a data gap. Inclusion of data gaps in the manually rejected sequences would reduce the number of false positives, but would at the same time increase the number of false negatives (e.g. data gaps without any precipitation).
(2) In case at least 4 out of 7 of the neighboring sensors malfunction, the median and MAD values in all three equations are determined by a misreporting sensor. As a result, an adequately operating sensor could be falsely regarded suspicious compared to the misreporting sensors.
(3) Several false positives are actually true positives: some incorrect sequences were overlooked during the manual assessment. Especially manual detection of erroneous data during small events (<3 mm) at the beginning of a clogging process, proofs to be difficult. Test statistics z_m and z_s, however, react to the increasing inter-tip times during such events. These incorrect sequences were removed from the data sets.

Conclusions

An automated data quality assessment of TBRG data sets becomes more successful as the quality of the data increases. Using the Upton and Rahimi (2003) procedure, it is relatively easy to detect an anomaly amidst good data. However, confronted with a hampering data communication, incomplete metadata files and blockages of multiple gauges in the Eindhoven data the success rate falls, introducing many false negatives. Only applying this automated procedure would leave approximately 40% of all erroneous data unnoticed. On the other hand, studying false positives reported by the automated procedure leads to the identification of doubtful sequences that were overlooked during the manual assessment. Therefore, the application of an automated procedure is useful to complement the results of a manual data assessment.

Appendix E. Comparison of WDD and NM data to KNMI gauge results

After the cross-check of TBRG results presented in paragraph 3.4 the second step in the data quality assessment of WDD gauges is the comparison of WDD TBRG results with KNMI Hellmann gauge results. The objective of this assessment is to search for and explain the sources of any structural differences between both data sources. Also, where possible, WDD data sets are corrected for biases. Preferably, precipitation sums are compared over a long time-period (e.g. a year) to reduce as much as possible the influence of temporal and spatial variation of rainfall. However, the longer the time-span considered, the larger the chance that data gaps and/or malfunctioning sensors influence the total sum over the considered time-span. In this appendix, sensor results are compared over a year (using equivalent sums) and over time-spans of a month (using actual observed sums). Section E.1 first describes the calculation (and conditions for calculation) of hourly precipitation depths from the 1-minute interval TBRG data sets. The hourly depths are used as the basis for further lumping precipitation into annual and monthly values. Also, the hourly values are used in paragraph 3.6 as the basis for areal precipitation calculations. In section E.2, annual equivalent sums are derived and compared to KNMI Hellmann data. In section E.3 the same is done for monthly observed precipitation. The origin of differences between WDD data and KNMI data is the focus of section E.4. Finally, in section E.5 the correction of WDD data sets based on calculated biases is explained.

E.1 Calculation of hourly precipitation depths

A comparison of precipitation depths is only sensible if these are based on complete and correct data sets. WDD data sets, however, contain many data gaps, the number of which has increased after removal of erroneous data in paragraph 3.4. For such data sets summation over a time-span can lead to underestimation of precipitation in case of rainfall during the data gaps. Considering this issue, this section describes the calculation of hourly precipitation sums and the conditions under which these values may be calculated to obtain (nearly) correct values. The hourly depths are used as the basis for further lumping precipitation into annual and monthly values. The (conditions for) calculations of annual and monthly values are discussed in the next sections.

A correct calculation of precipitation depths per hour is defined here as the summing of 60 values (1-minute interval data for 1 hour) for which a maximum of 5% (or 3 values) may be missing. Naturally, however strict this condition, it leaves

a chance that during those missing 3 minutes an amount of precipitation is not added to the sum. The mean recorded rainfall intensity over all WDD gauges is 0.14 mm/min. Hence, the expected missing depth in case of 3 minutes data loss in an hourly summation (during rainfall) would be on the order of 0.5 mm.

E.2 Calculation of annual equivalent sums and comparison to KNMI data

Annual equivalent sums of precipitation are calculated using the total precipitation sum of the 1-hour interval data sets and interpolating (or extrapolating) to a 365-day equivalent:

$$D_{365} = \frac{365}{L_{days}} D_{total} \qquad \text{(E.1)}$$

with D_{total} = total precipitation sum in data set [mm];
D_{365} = 365-day equivalent sum [mm];
L_{days} = length of data set [days].

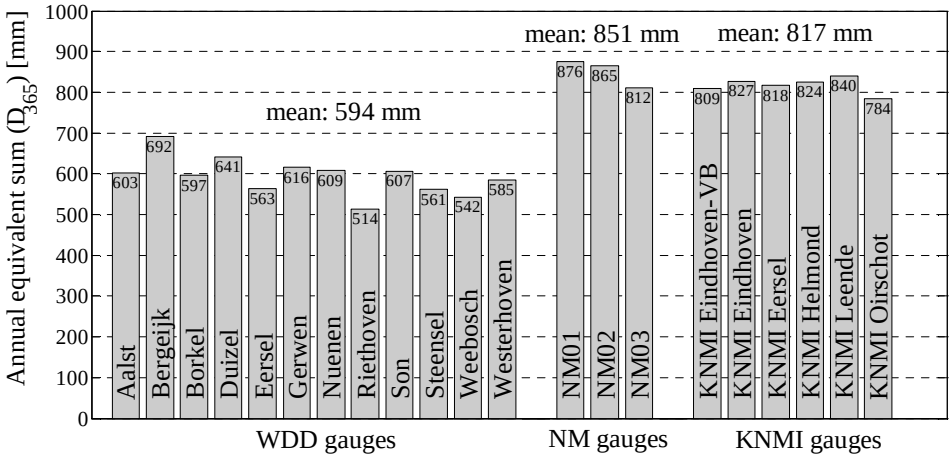

Figure E-1: Annual equivalent sums of precipitation (D_{365}) of 12 WDD, 3 NM and 6 KNMI raingauges.

Figure E-1 presents the calculated annual equivalent sums. It can be observed that WDD gauges systematically underestimate precipitation sums compared to NM and KNMI gauges by, on average, approximately 30%. The 6 KNMI Hellmann gauges show annual equivalent sums between 784 mm and 840 mm with a mean

value of 817 mm. NM gauges show a slightly higher mean sum of 851 mm. WDD gauges report an average sum of 594 mm, which is nearly 30% below the KNMI mean value. WDD equivalent sums range between 514 mm (Riethoven) and 692 mm (Bergeijk), which means that the largest sum for a WDD raingauge is more than 10% smaller than the smallest precipitation depth for any NM or KNMI gauge (784 mm, KNMI Oirschot).

Interpolation of incomplete precipitation data sets as presented in this section can only yield reliable estimates of annual precipitation sums if the fraction of missing or discarded data in the total data set is equal to the fraction of the total precipitation sum that was excluded from the calculation of D_{total}. In other words, for a correct interpolation, if for instance 20% of the data is rejected (i.e. 20% of the *time stamps* is rejected) also 20% of the recorded *precipitation* should be missing from the data set. If the missing and discarded data cover a relatively large fraction of wet-weather data (e.g. if storm events somehow cause the sensor malfunctioning), the interpolated value underestimates the total precipitation depth; if discarded and missing data have been mostly collected during dry weather, the interpolated value overestimates precipitation depth. For the WDD TBRG data sets this relation is considered in Table E-1.

Table E-1: Discarded and missing data at WDD gauges and, for the same time-spans, the corresponding rainfall at NM gauges.

	discarded and missing data in WDD data sets as percentage of 489-day total data set	during same time-spans, at NM gauges	
		observed precipitation sum	precipitation sum as percentage of total observed sum (over 489-day time-span)
WDD gauges	[%]	[mm]	[%]
Aalst	19	235	21
Bergeijk	40	430	39
Borkel	38	408	36
Duizel	18	246	22
Eersel	26	288	26
Gerwen	29	347	31
Nuenen	36	409	37
Riethoven	28	393	35
Son	29	338	30
Steensel	29	363	32
Weebosch	33	449	40
Westerhoven	27	301	27

Missing data in WDD data sets naturally cannot provide information on the amount of precipitation that was not measured; instead, the NM data sets are used as

reference 'true' values. For all time-spans for which WDD data is missing or discarded, the corresponding precipitation sum recorded at NM gauges is expressed as a percentage of the total sum recorded at NM gauges. As an example, 19% of the 489-day Aalst data set is missing. During the exact same time-spans for which Aalst data is missing, NM gauges have recorded 21% of their total sum recorded during the same 489-day time-span as the Aalst gauge. For most gauges near identical percentages indicate that interpolation of the incomplete data sets can be done without resulting in large over- or underestimations. For the Riethoven and Weebosch gauges differences are largest (7%) with a relatively large fraction of discarded wet weather data; interpolated values for these gauges are likely to underestimate the total precipitation sum recorded at these gauges. In line with this conclusion it can be noted that the Riethoven and Weebosch gauges report the smallest equivalent annual sums (D_{365}) of all WDD gauges in Figure E-1.

Based on equivalent annual sums it can be concluded that, as a group, WDD TBRGs systematically underestimate precipitation sums compared to KNMI gauges by approximately 30%. Exclusion of the interpolated values of the Riethoven and Weebosch gauges results in a mean underestimation of roughly 25%.

E.3 Calculation of observed monthly sums and comparison to KNMI data

For comparison of actual recorded values (instead of equivalent sums) over a relatively long time interval, precipitation sums per month have been calculated. To assess the performance of WDD gauges, results of 6 KNMI Hellmann type gauges are used as reference values. Figure E-2 presents for the considered 19-months time-span the monthly precipitation depths for KNMI gauges. April 2007 was an extremely dry month: recorded precipitation equals (almost) zero for all gauges. As expected, differences among KNMI gauges are generally smaller for winter months and larger for summer months due to differences in storm types. Also, generally speaking, summer sees more precipitation than winter.

Analogous to the calculation of hourly sums, monthly sums have only been calculated if a minimum amount of data is available. A correct summation for precipitation depths per month is defined here as the summing of 720 hourly precipitation values (for 30 day months) for which a maximum of 4 values (≈ 0.5%) may be lacking. This maximum number has been selected pragmatically: it is the smallest possible number for which for all 12 WDD gauges at least 2 monthly values could be calculated. However small the number, it leaves a chance that during these missing hours an amount of precipitation is not added to the sum. The mean recorded precipitation depth per hour (if larger than zero) over all WDD gauges is 0.68 mm/hour. Hence, the expected missing depth in case of 4 hours of lacking data in a monthly summation would be of the order of 2.5 mm. To make

sure no hourly values with high-intensity precipitation were excluded from monthly sums, all missing values have been verified using NM results as reference values. Most have been recorded during dry weather spells and only few during wet weather situations; a maximum depth of 1.7 mm has not been included in the monthly precipitation sum.

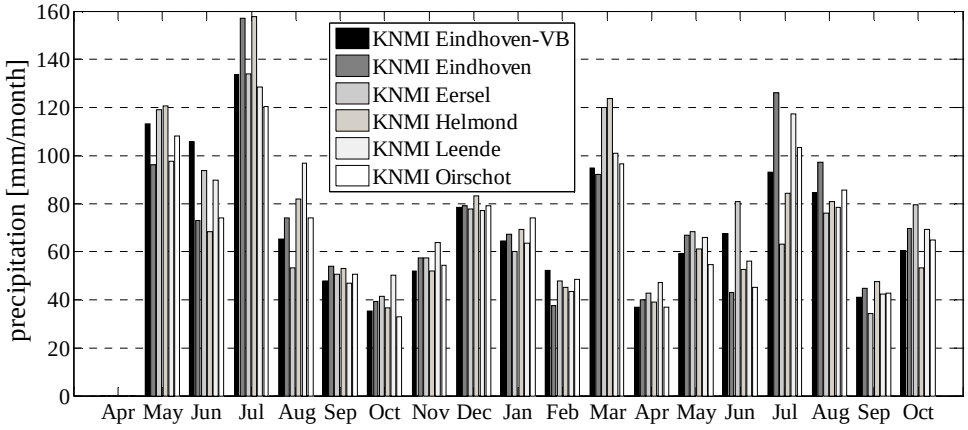

Figure E-2: Monthly precipitation depths for 6 KNMI Hellmann gauges in the Eindhoven area for the time-span April 2007 - November 2008 (source: KNMI, 2009)

Using the aforementioned criterion, for the majority of months no monthly precipitation sum could be calculated. For only 34 out of 192 months a total rainfall sum has been derived. For the other 158 months at least 5 hours of data were missing from the data sets. The 34 monthly sums have been recorded during 5 specific months: October, November and December 2007 and February and September 2008. Especially the absence of large data communication problems during these months yields near-complete data sets. Figure E-3 presents the relative deviation of calculated WDD monthly sums from the mean KNMI value. Mean KNMI values are plotted in gray squares; whiskers stretch to the minimum and maximum KNMI value per month (see Figure E-2). Table E-2 summarizes the position of the plotted WDD values with respect to KNMI mean and range. Only 2 sums are larger than KNMI mean values, the other 32 sums are below mean KNMI values. Two thirds of sums are outside (i.e. below) the range of observed values of KNMI gauges; one third is inside the range, but mostly in the lower whisker.

Results are inconsistent. For instance the Bergeijk gauge shows for November 2007 and February 2008 only minor deviations from the KNMI mean of respectively +5% and -3%. For December 2007, on the other hand, the difference is -23%. For this same month all 8 WDD sums are lumped together between -15%

and -40%, well outside the relatively small range of KNMI values. The next month, however, 6 out of 9 sums are within the KNMI range and 3 are well outside. Hence, since only 34 monthly sums are available and results are too inconsistent, no conclusions can be drawn about operation of a specific sensor or about operating conditions during a specific month. Nevertheless, the results in Figure E-3 and Table E-2 seem to confirm the conclusion from section E.2 that, on average, WDD gauges underestimate precipitation compared to KNMI gauges. Based on annual equivalent sums the underestimation yielded 25% to 30%; the 34 WDD monthly sums are on average approximately 20% smaller than KNMI mean values.

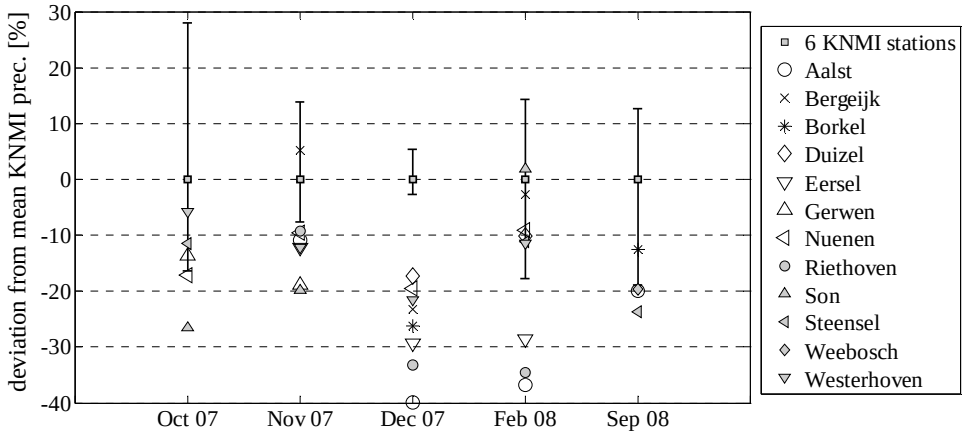

Figure E-3: Comparison of monthly precipitation depths between 12 WDD gauges and mean results of 6 KNMI gauges. For KNMI data the grey squares represent the mean value of the 6 gauges; the whiskers indicate the associated minimum and maximum values. For WDD gauges only months with less than 5 hours of missing data have been plotted.

Table E-2: Number and orientation with respect to KNMI mean and range of calculated monthly precipitation sums of WDD gauges

	Oct 07	Nov 07	Dec 07	Feb 08	Sep 08	**total**
number of calc. monthly sums	5	8	8	9	4	**34**
of which > KNMI mean	0	1	0	1	0	**2**
< KNMI mean	5	7	8	8	4	**32**
of which within KNMI range	3	1	0	6	1	**11**
outside KNMI range	2	7	8	3	3	**23**

E.4 Underestimation by WDD gauges assessed

In the previous two sections it was concluded that the WDD tipping-bucket raingauges systematically underestimate precipitation sums when compared to the

Hellmann type KNMI raingauges. Based on equivalent annual sums the underestimation was determined at 25%; using monthly precipitation sums the average underestimation was set at approximately 20%. The objective of this section is to search for (partial) explanations of the observed underestimation. The first factor considered is an initial lack of calibration of WDD gauges. Second, the contributions of random errors and systematic instrumentation and observation errors are studied.

Important in this context is to note that the aforementioned percentages are underestimations of WDD tipping-bucket raingauge results *compared to Hellmann gauge results*, and not compared to 'true' precipitation. When assessing these differences and their possible explanations, it is essential to keep in mind this 'triangle' of data: tipping-bucket results versus Hellmann gauge results and their respective relation with 'true' precipitation, as earlier described in paragraph 3.3. Generally, differences between Hellmann gauge results and 'true' precipitation are smaller than differences between TBRG results and 'true' precipitation.

Calibration of WDD gauges

Calibration of raingauges is comparing sensor performance with 'true' precipitation by subjecting the sensor to a known quantity of imitated rainfall. After installation in July 2007 the WDD tipping-bucket raingauges were *not* calibrated. After it became apparent that WDD TBRG results differed significantly from Hellmann gauge results (as presented in previous sections) a calibration was performed in September 2009. The sensor calibration comprised pouring a volume of water into the sensor at a constant rate of 30 mm/h and recording the number of tips, see Table E-3. For most sensors 50 ml was poured, which, with a bucket resolution of 0.1 mm and a funnel area of 200 cm^2, should equal 25 tips. The actual number of tips is smaller than 25 for all sensors, indicating that all 12 WDD gauges underestimate precipitation depths. The correction factor expresses the fraction of the actual number of tips over the expected number of tips. For 9 out of 11 sensors the correction factor ranges between 0.88 and 0.92 indicating roughly 10% underestimation of WDD gauge results versus 'true' precipitation. For the Son and Steensel gauges this percentage increases to around 15% and 25%, respectively.

This type of static calibration (subjecting the sensor to one specific rainfall intensity) basically describes the deviation between the nominal bucket volume (as stated by the manufacturer) and the true bucket volume. This can be a true volumetric difference, but the true bucket volume can also change due to e.g. the growth of biofilms on bucket walls. Also, the true bucket volume can 'include' any rainwater that is lost (i.e. spilled) during the movement of the bucket. This amount increases non-linearly with rainfall intensity. To be able to quantify this 'non-linearity'-effect, however, a dynamic calibration is required: subjecting the sensor to multiple rainfall intensities.

Table E-3: Static calibration of WDD tipping-bucket raingauges

WDD gauges	volume of water poured [ml]	actual number of tips [#]	correction factor [-]
Aalst	50	22	0,88
Bergeijk	50	23	0,92
Borkel*	-	-	-
Duizel	50	22	0,88
Eersel	50	22	0,88
Gerwen	50	22	0,88
Nuenen	50	23	0,92
Riethoven	50	22	0,88
Son	50	21	0,84
Steensel	100	37	0,74
Weebosch	50	22	0,88
Westerhoven	50	22	0,88
mean			**0,87**

* the Borkel raingauge was removed for renovation works prior to calibration

The calibration of WDD gauges shows that approximately half of the observed underestimation by WDD gauges can be attributed to a lacking initial calibration of sensors. The other half of the underestimation, however, is not explained. Additional sources of uncertainty that may lead to differences in data results between Hellmann gauges and TBRGs are studied in the next section.

Random and systematic errors in TBRG data results

Sources of uncertainty in raingauge data results have been described and quantified extensively in literature. Data errors are often divided into random and systematic errors. Random errors can be observed if two identical gauges (same instrumentation errors) at the same location (same observation conditions) give different results. Often mentioned examples of random errors in TBRG measurements are: mechanical and electrical disturbances of the gauge, data transmitting errors and clogging of the tipping bucket. In terms of *effects* on data results, clogging is not a true random error: a mechanical disturbance such as random variations in the force required to set the tipping bucket in motion (Marsalek, 1981) gives a random error (i.e. both higher and lower values about an unchanged mean value) whereas partial clogging of a TBRG results in predominantly *lower* precipitation depths, hence biasing results. Irrespective of definition, for WDD TBRG data sets erroneous results due to clogging have already been removed in previous sections; any further random errors do - by definition - not influence mean values of WDD TBRG data sets. Hence, random errors do not contribute to the observed systematic differences between KNMI Hellmann gauges and WDD tipping-bucket raingauges.

Systematic errors of tipping-bucket raingauges generally lead to underestimation of precipitation volumes. The origin of systematic errors can generally be traced to instrumentation errors or to observation conditions. *Observation conditions* can be influenced by a local wind effect: due to the presence of the elevated raingauge the wind field above the gauge is distorted and especially lighter precipitation particles are lost for the measurement. Also, sensors near a building or tree might suffer from wind shade: objects intercepting precipitation during specific wind conditions. Examples of *instrumentation errors* are:

(1) initial wetting of sensor walls after a dry period;
(2) initial inertia of the tipping mechanism;
(3) evaporation of accumulated water in the sensor;
(4) splashing (i.e. water reflected from the gauge due to impact with the funnel wall);
(5) sensor calibration errors (deviation of bucket volume, non-linearity not considered, wrong static calibration);
(6) improper leveling of a sensor and
(7) sensor ageing (e.g. changing bucket volume due to surface oxidation and contamination of bucket walls).

WDD TBRGs have not been fitted with siphons; hence, uncertainties typically associated with siphons (Maksimović *et al.*, 1991; Overgaard *et al.*, 1998) do not need consideration. Table E-4 presents measured and estimated losses due to both instrumentation errors and observation conditions.

Searching for errors that may explain underestimation of precipitation by WDD gauges non-linearity is considered first. Fankhauser (1998) states that non-linearity has only little influence on the long-term total recorded rainfall depth since high-intensity precipitation is relatively rare. Luyckx and Berlamont (2001) show that for intensities up to 30 mm/h (or 0.5 mm/min) non-linearity is not an issue. For intensities up to 180 mm/h (or 3 mm/min, the highest intensity in the WDD TBRG data sets) the error due to non-linearity gradually increases to around 20%. In the Eindhoven area data, approximately 99% of wet weather data remains below the 0.5 mm/min threshold. The remaining 1% of high-intensity data corresponds to approximately 7% of total recorded precipitation, which needs an estimated correction of around 5%. Hence, the influence of non-linearity on total recorded rainfall in the WDD data sets can be estimated at around 0,35% and is therefore indeed negligible.

The second considered error is the local wind effect. Sevruk (1996) concludes that the local wind effect does play an important role in explaining differences between Hellmann gauge results and TBRG results. Due to differences in sensor design (mainly the shape of the gauge body and thickness of the orifice rim) the wind-

fields directly above the gauges are affected in distinct ways, but predominantly so that TBRGs systematically yield lower precipitation depths than Hellmann gauges. In the study, for two gauges at the same location, the mean annual difference amounts to 14%. Differences are attributed to this local wind effect as well as to random errors. In the Eindhoven area no tipping-bucket gauge has been placed in the direct vicinity of a Hellmann gauge; therefore, no assessment of long-term differences in data results between the two sensor types can be made.

Table E-4: Main causes of systematic errors in TBRG precipitation measurements and their reported losses (after Rauch *et al.*, 1998).

Error caused by	Range of reported losses	Source
Instrumentation errors		
Wetting of funnel and/or bucket walls	[2 - 10] %	Marsalek, 1981; Sevruk, 1982, cited in Rauch *et al.*, 1998
	[0.02 - 0.09] mm	Niemczynowicz, 1986; Fankhauser, 1998
Inertia of tipping mechanism after dry period	"unexpectedly high"	Jørgensen *et al.*, 1998
Evaporation	[0 - 4] %	Sevruk, 1982, cited in Rauch *et al.*, 1998
	[0.001-0.004] mm/h	Fankhauser, 1998
Splashing	[1 - 2] %	Sevruk, 1982, cited in Rauch *et al.*, 1998
Sensor calibration errors, tipping bucket movement (non-linearity)	[-10 - 20] %	Marsalek, 1981; Niemczynowicz, 1986; Maksimovic *et al.*, 1991; Fankhauser, 1998; Luyckx and Berlamont, 2001
Leveling	"several percent"	Marsalek, 1981
Ageing	-4 %	Marsalek, 1981
Observation conditions		
Local wind effect	[2 - 15] %	Neff, 1977, cited in Upton and Rahimi, 2003; Hanna, 1995; Sevruk, 1996
Wind shade	"disastrous effect"	Upton and Rahimi, 2003
Overall systematic error	[5 - 10] %	Schilling, 1991

A third considered error source is wind shade. WDD TBRGs have been installed at or nearby WDD property (pumping stations, control stations) throughout the Eindhoven area. At many locations gauges have been installed in the lee of trees, buildings or other obstacles. Obstructions in the direct vicinity of raingauges can

cause wind shade and can consequently have an important effect on precipitation measurements. Upton and Rahimi (2003) report that during their experiments "one gauge was fixed for a time on the wall of a building with disastrous effects on its accuracy". A widely quoted rule (for instance in Hanna, 1995) is that any surrounding objects of height *h* should be situated at a distance *d* of at least 2*h* from the gauge (i.e. the *h*/*d*-ratio should be smaller than 0.5). At shorter distances the rainfall in the gauge is influenced by air flow deflections around the obstacles. In Table E-5 the *h*/*d*-ratios for all obstructions found near WDD and NM gauges are presented. For all WDD but the Bergeijk raingauge obstructions are reported with a ratio larger than 0.5. Also, many obstructions are found in the south-western wind direction, which is predominant in the Netherlands (KNMI, 2009). It is interesting to notice that the gauge with the lowest *h*/*d*-ratio (Bergeijk) records the largest annual equivalent sum, see Figure E-1. Considering the large number and orientation of obstructions close to WDD gauges it seems justified to conclude that wind shade has seriously affected the results of WDD TBRGs. Quantification of the effect is however not possible since no comparative tests have been performed.

Table E-5: For 12 WDD and 3 NM gauges the *h*/*d*-ratios for multiple obstructions around the sensors

gauge	***h*/*d*-ratios**	**gauge**	***h*/*d*-ratios**
Aalst	1.3	Son	1.0 ; 1.2
Bergeijk	0.5	Steensel	1.0 ; 1.1
Borkel	0.7	Weebosch	0.6 ; 8.0
Duizel	0.8 ; 1.7	Westerhoven	1.3 ; 3.8
Eersel	1.3 ; 6.0		
Gerwen	0.4 ; 0.8 ; 1.0	NM01	no obstructions
Nuenen	0.8 ; 1.0 ; 1.3	NM02	no obstructions
Riethoven	1.0 ; 4.0 ; 25	NM03	0.4

Conclusions

WDD tipping-bucket raingauges systematically underestimate precipitation sums when compared to the Hellmann type KNMI raingauges by 20% to 25%. A calibration performed on WDD gauges (two years after installation) has shown that approximately half of the underestimation could have been prevented by calibrating the sensors directly after installation. The other half may be explained mainly by observation conditions. Intrinsic differences in wind-induced errors exist between Hellmann gauges and TBRGs and a poor installation of WDD gauges has caused large-scale wind shading.

E.5 Correcting WDD data sets for quantified systematic errors

Correction of data sets for systematic errors can be implemented if systematic errors have been accurately quantified. Of the systematic errors described in the

previous section, only the error due to a missing calibration has been quantified per gauge. For the other errors only *qualitative* assessments are available that are of no use for data correction. Hence, WDD TBRG data sets have only been corrected for calibration errors using the correction factors presented in Table E-3. Figure E-4 presents the results. Application of the correction factors increases total recorded precipitation depths for all WDD sensors. As a result, the mean annual equivalent sum increases from 594 mm before to 683 mm after calibration. The difference with the same value for KNMI gauges (817 mm) reduces from 30% to 15%.

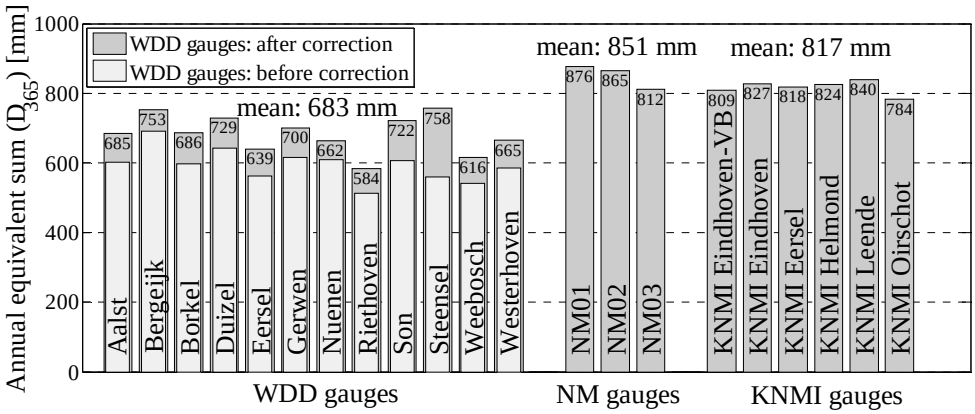

Figure E-4: Annual equivalent sums of NM and KNMI gauges and - before and after correction - of WDD gauges. For the applied correction factors, see Table E-3. For the Borkel gauge a mean correction factor of 0.87 is assumed.

Appendix F. Calculation of Q_{OPEN}

At the influent pumping station of wwtp Eindhoven a concrete wall divides the Eindhoven Stad and Riool-Zuid influent chambers. An opening in that wall allows wastewater to flow from one chamber into the other. The opening is rectangular with width w_o = 1.50 m and height h_o = 0.70 m. The thickness of the wall or crest length is l_c = 0.45 m with a crest level at +13.30 mNAP, see Figure F-1.

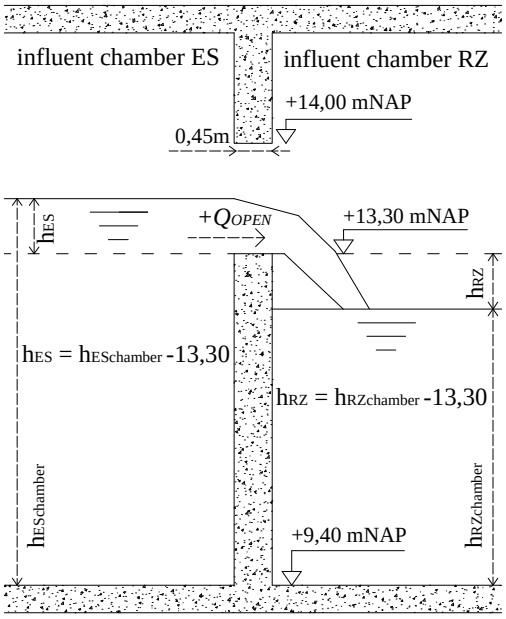

Figure F-1: Cross-section of the wall that divides the Eindhoven Stad (ES) and Riool-Zuid (RZ) influent chambers at the influent pumping station of the wwtp Eindhoven

If the water level in one or both influent chambers exceeds +13.30 mNAP wastewater flows from one chamber to the other. This flow is referred to as Q_{OPEN}. The flow is defined positive from the influent chamber of Eindhoven Stad to that of Riool-Zuid. The parameters h_{RZ} and h_{ES} are defined as the differences between the crest level of the opening and the water levels in the influent chambers of Riool-Zuid and Eindhoven Stad, respectively. Per combination of water levels different flow conditions occur. All described situations assume that h_{ES} exceeds h_{RZ}. If h_{RZ} exceeds h_{ES} all values for Q_{OPEN} should be multiplied by -1. The following five situations can be distinguished (Brouwer, 2000; Ankum, 2003).

1. Water levels in both influent chambers are below crest level or equal to each other:

$$\left(h_{ES} \le 0 \;\; \& \;\; h_{RZ} \le 0\right) \;\; \text{or} \;\; \left(h_{ES} = h_{RZ}\right) \tag{F.1}$$

Then:

$$Q_{OPEN} = 0 \tag{F.2}$$

2. Free-flow (non-submerged) conditions over a weir occur if (i) h_{ES} rises above crest level but remains below one and a half times the height of the opening and (ii) h_{RZ} remains below critical depth:

$$0 < h_{ES} \le \frac{3}{2} h_o \;\; \& \;\; h_{RZ} \le \frac{2}{3} h_{ES} \tag{F.3}$$

Then:

$$Q_{OPEN} = C_{w,f}\, w_o h_{ES}^{(3/2)} \tag{F.4}$$

with:

$C_{w,f}$ = weir coefficient for free flow conditions

The value of $C_{w,f}$ depends on the type of weir. If $h_{ES} < ½l_c$ the weir can be characterized as a broad-crested weir with a coefficient $C_{w,f,b}$ = 1.7 $m^{1/2}/s$. If $h_{ES} > ½l_c$ the opening is a sharp-crested weir with coefficient $C_{w,f,s}$ = 1.9 $m^{1/2}/s$.

3. Submerged conditions over a weir occur if (i) h_{ES} rises above crest level but remains below one and a half times the height of the opening and (ii) h_{RZ} rises above critical depth, but remains below the height of the opening:

$$0 < h_{ES} \le \frac{3}{2} h_o \;\; \& \;\; \frac{2}{3} h_{ES} < h_{RZ} < h_o \tag{F.5}$$

Then:

$$Q_{OPEN} = C_{w,s} w_o h_{ES} \sqrt{2g\left(h_{ES} - h_{RZ}\right)} \tag{F.6}$$

with:

$C_{w,s}$ = weir coefficient for submerged conditions

RIONED (2004) advises a weir coefficient of $C_{w,s}$ = 0.8 for submerged conditions. Nikolov *et al*. (1978) present a different approach to calculate a submerged broad-crested weir, but with similar results.

4. Free orifice flow occurs if (i) h_{ES} rises above one and a half times the height of the opening and (ii) h_{RZ} remains below the height of the opening:

$$h_{ES} > \frac{3}{2} h_o \quad \& \quad h_{RZ} \leq h_o \tag{F.7}$$

Then:

$$Q_{OPEN} = \mu h_o w_o \sqrt{2g\left(h_{ES} - \mu h_o\right)} \tag{F.8}$$

with:

μ = contraction coefficient

The value for μ depends on the ratio of h_o/h_{ES}, see Table F-1.

Table F-1: Contraction coefficients for various h_o/h_{ES} ratios (Brouwer, 2000)

h_o/h_{ES}	0,1	0,2	0,3	0,4	0,5	0,6
μ	0,61	0,62	0,63	0,65	0,68	0,72

5. Submerged orifice flow occurs if both h_{ES} and h_{RZ} rise above the height of the opening:

$$h_{ES} > h_o \quad \& \quad h_{RZ} > h_o \tag{F.9}$$

Then:

$$Q_{OPEN} = C_d h_o w_o \sqrt{2gh_{ES}} \tag{F.10}$$

with:

C_d = discharge coefficient for submerged orifice flow

Ankum (2003) gives an estimate for C_d for realistic ratios of $h_{ES}/h_o < 2$ and $h_{RZ}/h_o < 2$ in the influent chambers: $C_d \approx 0.15$.

Appendix G. Designing monitoring stations for UV/VIS sensors

The design of monitoring stations for the UV/VIS sensors at the influent pumping station of the wwtp Eindhoven has been a step-wise process. The monitoring set-up that has been used to generate the data sets presented in chapter 5 is the third version of the design. Two earlier designs have been rejected for a variety of reasons. This appendix presents the design process, the rejected designs and the reasons for rejection.

At the onset of the design process, the possibilities for sensor installation were restricted by a number of considerations. First of all, it was decided to monitor flows at the wwtp influent pumping station and not at the downstream end of the contributing sewer systems. Catchment area Eindhoven Stad transports its wastewater to the wwtp in two separate pipes, increasing the number of required UV/VIS sensors from three to four. Also, at the treatment plant, requirements for monitoring stations such as electricity and maintenance personnel could more easily be met. Within the influent pumping station, monitoring should take place before the three influent flows are mixed in the mixing flume to be able to monitor each inflow to the wwtp separately.

A second consideration was the choice between an *inline* installation (i.e. installing the sensor directly in the process) and a *by-pass* installation (i.e. diverting a small fraction of the targeted wastewater to a dedicated measurement environment in which the sensor is installed). Both installation types have been previously used in monitoring stations for UV/VIS sensors. Each solution has its distinct advantages and disadvantages (see Gruber *et al.*, 2006). For the influent pumping station at the wwtp Eindhoven it was decided that an inline sensor installation was not feasible for three reasons:

- any support structures for an inline installation (e.g. cables suspended from a floating pontoon or supports of a fixed structure) could not be attached to the walls of the influent chambers since these are lined with a coating to protect the concrete against corrosive gases;
- support structures that are (1) only suspended from the ceiling of the influent chambers, (2) moveable for easy maintenance access to the sensor and (3) able to withstand the large drag forces exerted on the sensor by the wastewater especially during wet weather flow, were rejected for reasons of costs;

- a sensor installed 7 m below ground level does not allow close observation during measurements which reduces the possibilities of diagnosis for a malfunctioning sensor.

Consequently, it was decided to use by-pass installations for the UV/VIS monitoring stations.

The first design of the UV/VIS monitoring station is presented in Figure G-1. A non-shredding pump (6 L/s for a normal dry weather head difference of 8m) suspended from a vertical truss construction pumps wastewater from the pumping station influent chambers into a hollow pipe in the truss and subsequently into the by-pass installation. The by-pass consists of two parallel ø10cm pipes: one containing the UV/VIS sensor and one serving as backup in case the first pipe needs to be removed for sensor maintenance and cleaning.

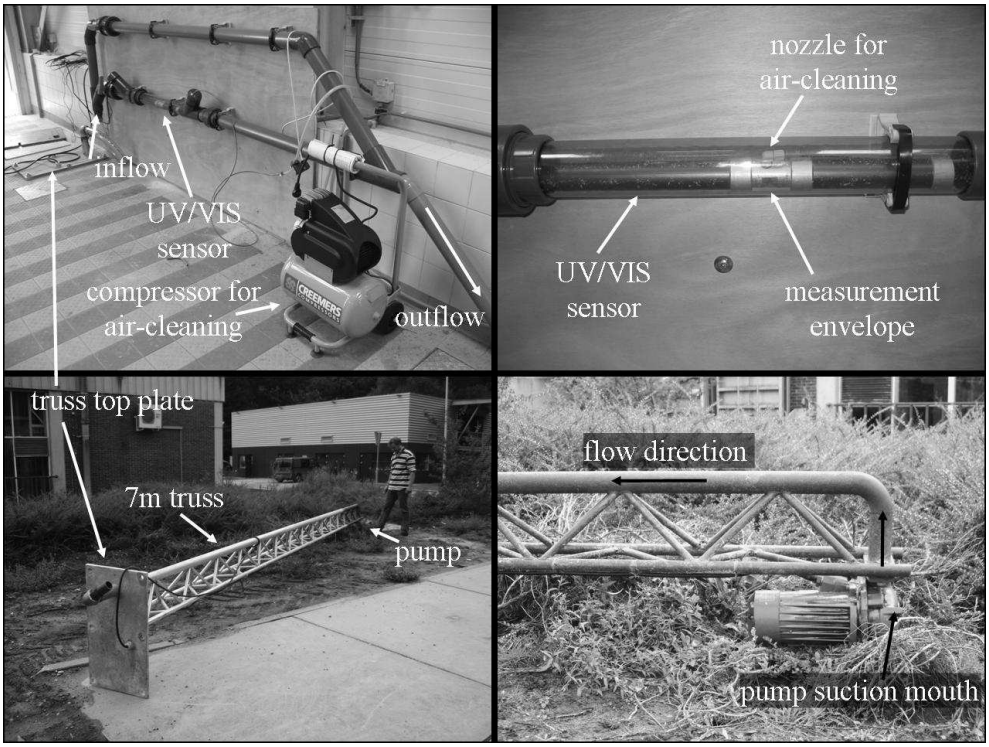

Figure G-1: (top left) first design of the monitoring set-up with two parallel pipes; (top right) one pipe contains the UV/VIS sensor; (bottom left) the 7m truss feeding the by-pass installation; (bottom right) the pump at the bottom of the truss feeding wastewater into a hollow section of the truss construction

Problems encountered with this first design concentrated on clogging of the pipe containing the UV/VIS sensor. After only a few hours of operation the pipe would be clogged mainly with tissues, sanitary products and other coarse materials from the wastewater that would get stuck behind the sensor. As a result, wastewater would be transported through the parallel pipe and would not be observed by the UV/VIS sensor.

In a second design, the pipe containing the sensor was replaced by two measurement vessels in series, see Figure G-2. Each vessel is fed with wastewater near the bottom of the vessel and the outflows are designed as overflow constructions near the top of the vessel. This way, short-circuit flows that would leave the sensor in stagnant water are prevented. The vessels have a diameter of 0.75 m with a water column of ~0.50 m between inflow and outflow level. Holding a total of approximately 350 L the wastewater in each vessel is fully renewed within one minute. In the first vessel the UV/VIS sensor is installed half way between the inflow and outflow levels. The second vessel allows for additional sensors.

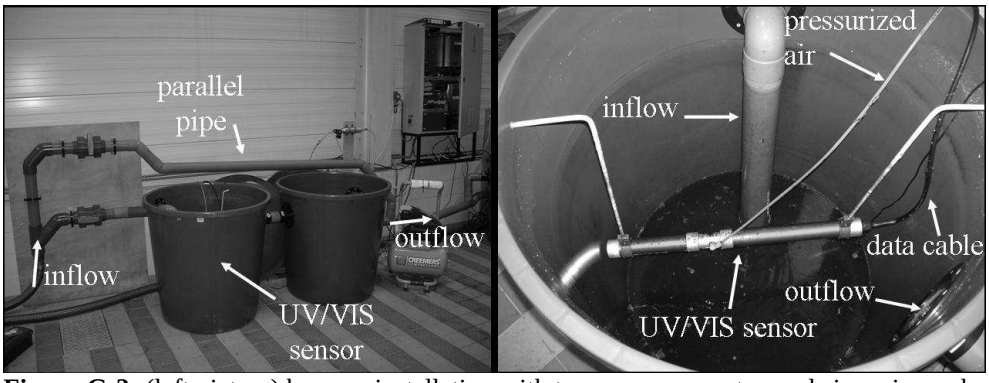

Figure G-2: (left picture) by-pass installation with two measurement vessels in series and a parallel pipe; (right picture) inside the first vessel the UV/VIS sensor is installed

Problems encountered with the second design concentrated on clogging of the (non-shredding) pumps that feed the by-pass installations. After a few days of operation, the pump suction mouths would get clogged, again mainly with tissues, sanitary products and other coarse materials, see Figure G-3. The sensitivity for clogging varied largely between the influent flows: the pump in influent chamber Riool-Zuid could clog after a few hours of operation already whereas the pump in influent chamber Nuenen/Son would last one to three weeks before clogging would occur. The gradual obstruction of the suction mouths led to a gradual decrease of

flow through the by-pass installations, ultimately resulting in a zero flow and stagnant water in the vessels.
Replacement of the non-shredding pumps with shredding pumps (of the same capacity) did not yield better results. Also, the construction of protective devices around the suctions mouths (such as large cages that prevent coarse materials to reach the suction mouths) did not improve the uptime of the pumps.

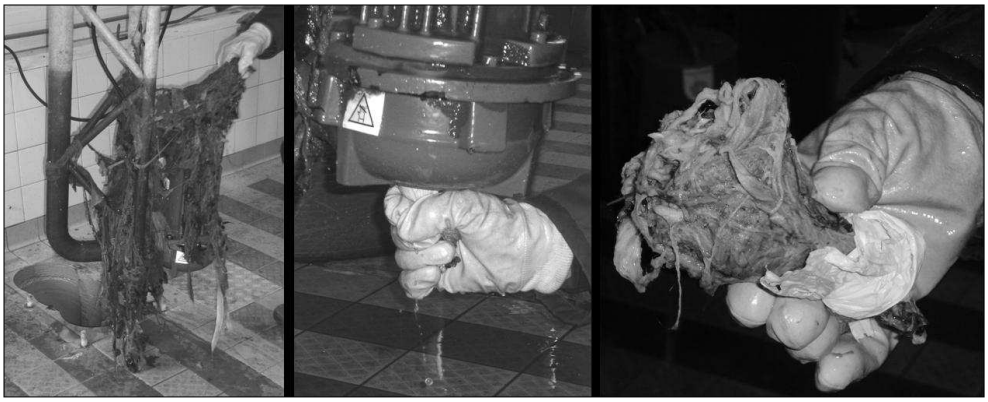

Figure G-3: (left picture) pollution around a by-pass pump as observed directly after the truss construction has been lifted from the wastewater; (middle picture) the suction mouth of the pump obstructed by a ball of tissue material and other coarse materials; (right picture) the obstruction after removal from the suction mouth

The main improvement introduced in the third design is the relocation of the by-pass pumps from the influent chambers to the pump suction chambers. The latter chambers are located behind the 25mm bar screens, see Figure G-4. The bar screens remove the majority of materials that cause the pumps to clog, hence largely reducing the frequency of this phenomenon. Since no lift installation is available near the pump suction chambers, the trusses have not been used; instead, simple chains are used to suspend the pumps from the chamber ceiling. Also in the third design, the parallel pipes have been removed as they no longer served a purpose.

The UV/VIS data considered in chapter 5 has been generated using this third monitoring station design. The presented set-up has, however, an important drawback: sediment gathers on the bottom of the vessels, see Figure G-5. The flow velocity in the vessels is too low to transport all coarse particles in the wastewater to the outflow level, resulting in the gradual build-up of a sediment layer on the bottom of the vessel. In case of resuspension of the sediment, measurements in the vessel can be influenced, resulting in erroneous data. To annul this error source

from the measurements, a fourth monitoring set-up has been implemented in 2009 (hence, *after* the collection of data sets presented in this chapter).

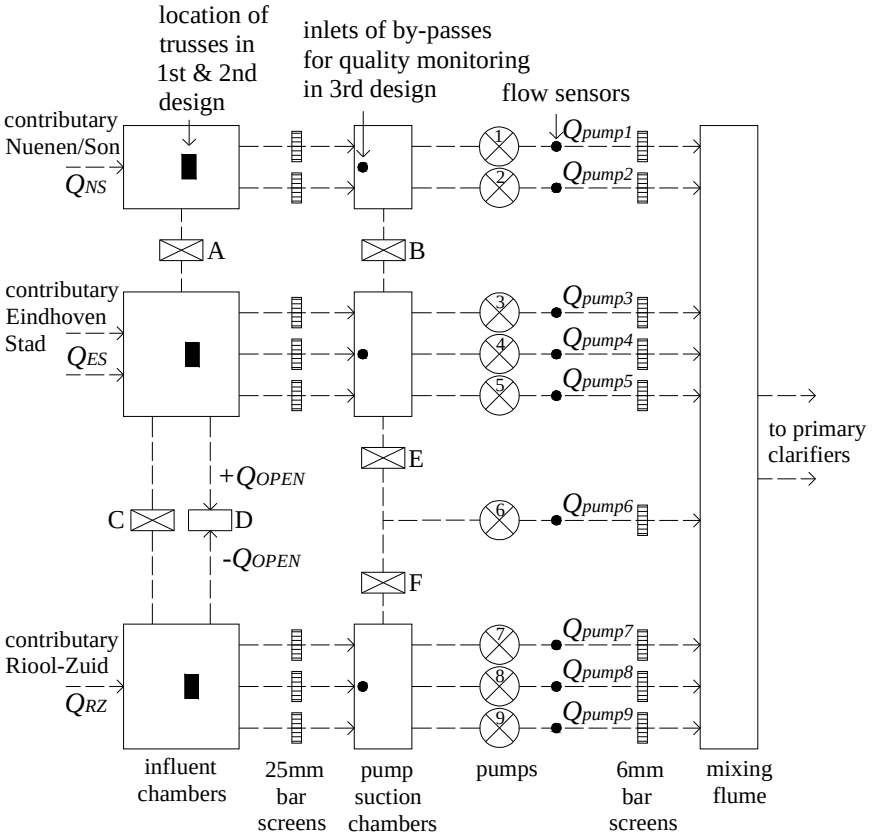

Figure G-4: Schematic lay-out of the influent pumping station at wwtp Eindhoven. Wastewater flows from left to right. In the first and second designs of the UV/VIS monitoring set-up pumps were suspended from truss constructions attached to the ceiling of the influent chambers; in the third design pumps were relocated to the pump suction chambers behind the 25 mm bar screens and suspended from the ceiling by simple chains.

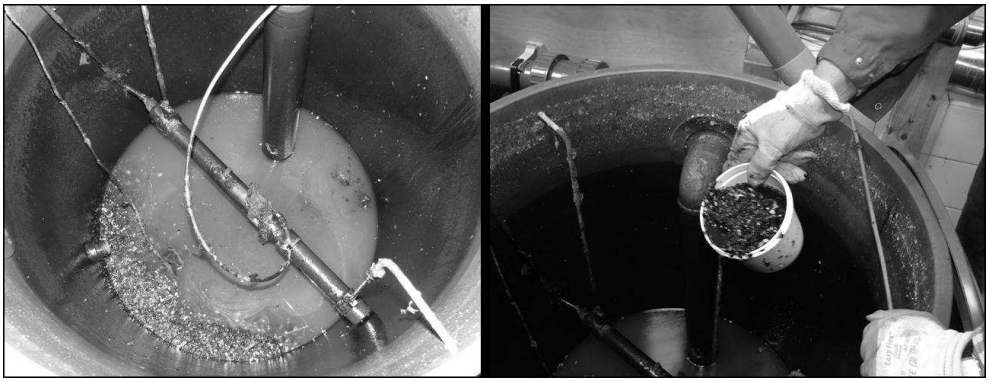

Figure G-5: Formation of sediment layers on the bottom of the measurement vessel

In the fourth design the plastic vessels have been replaced by non-corrosive steal flumes with a flat, ~15 cm wide invert and near-vertical side walls, see Figure G-6. The UV/VIS sensors are installed parallel to the flow direction, at approximately 3 cm from the invert. With this set-up it was expected to create an improved through-flow of wastewater and better entrainment of solids. This was *not* the case. As can be seen in Figure G-6 sediment layers were still observed, sometimes already after just a few hours of operation. Occasionally, the layers would grow to a depth that nearly the complete sensor would be buried.

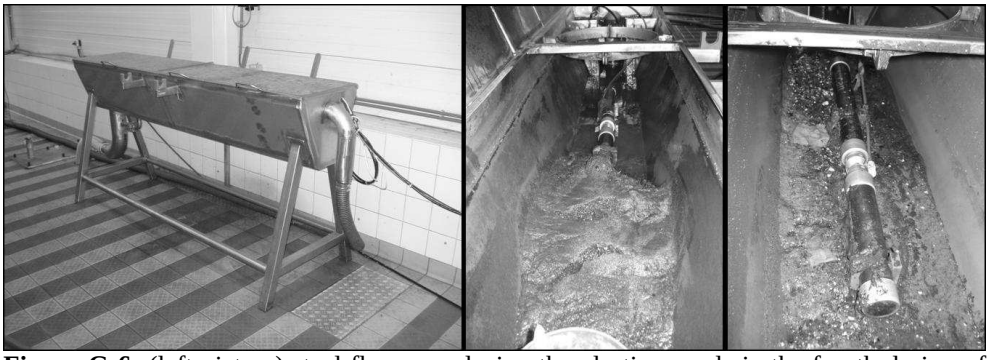

Figure G-6: (left picture) steal flumes replacing the plastic vessels in the fourth design of the set-up; (middle and right picture) sediment layers in the steal flumes

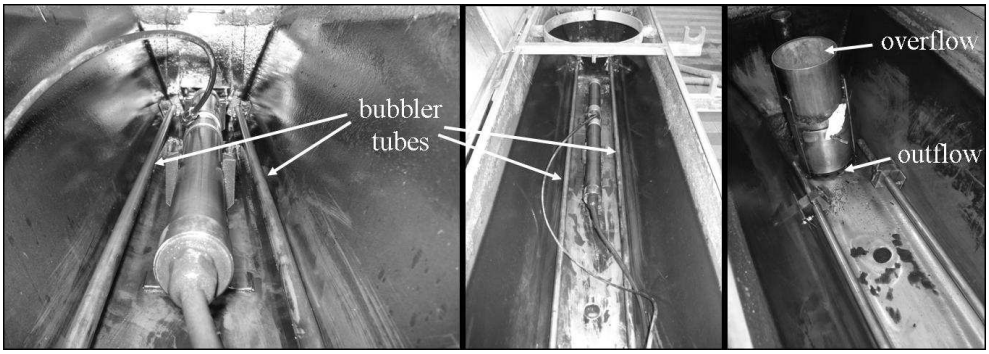

Figure G-7: (left and middle picture) the installation of bubbler tubes at the invert of the flume; (right picture) the outflow/overflow construction at the downstream end of the flume

To prevent the formation of sediment layers bubbler tubes were installed in the flumes, see Figure G-7. These consist of Ø1cm steal pipes positioned along the length of the flume at invert level. Small openings in the pipe are directed towards the bottom of the flume. The pipes are connected to the same compressed air installation as used for the regular cleaning of the UV/VIS sensor. This way, with each sensor cleaning a volume of air is blown into the flume and (assumedly) resuspends any sediments in the flume. After installation of the tubes the formation of sediment layers in the by-pass installation has largely ceased. With this set-up it has proven necessary to increase the compressed air volume that is available per cleaning cycle. As a part of the air volume is now used in the flume, a smaller volume is available for sensor cleaning. It has been observed that the remaining volume proved too small resulting in a gradual contamination of the measurement envelop.

In the first months of 2011 again a new design of the monitoring set-up will be implemented. The main improvement introduced in this fifth design is the relocation of the by-pass installations to a dedicated cabin *outside* the influent pumping station. The conditions in the pumping stations have proved to be too hostile for successful long-term monitoring. Despite elaborate protective devices corrosive gases have damaged electronics (e.g. for the data communication system) and compressors on numerous occasions. Also, on a number of occasions entry into the pumping station has not been possible due to the presence of hazardous gases rendering maintenance on the sensors impossible (sometimes for weeks on end). A final argument for relocation of the flumes is that a cabin provides improved hygienic working conditions compared to the influent pumping station.

Appendix H. Results of dry weather sampling campaign

This appendix presents per inflow and per parameter the results of the dry weather sampling campaign in two graphs. In the upper graph hourly laboratory results are set out against 2-minute interval results of the (still globally calibrated) UV/VIS sensors. In the lower graph the absolute (sensor value minus lab value), and relative (idem, with respect to lab value) differences between the laboratory and sensor values are presented.

The order of presentation is:

- DWF campaign, inflow Riool-Zuid, parameter TSS
- DWF campaign, inflow Riool-Zuid, parameter COD
- DWF campaign, inflow Riool-Zuid, parameter CODf

- DWF campaign, inflow Eindhoven Stad, parameter TSS
- DWF campaign, inflow Eindhoven Stad, parameter COD
- DWF campaign, inflow Eindhoven Stad, parameter CODf

- DWF campaign, inflow Nuenen/Son, parameter TSS
- DWF campaign, inflow Nuenen/Son, parameter COD
- DWF campaign, inflow Nuenen/Son, parameter CODf

DWF campaign, inflow **Riool-Zuid**, parameter **TSS**

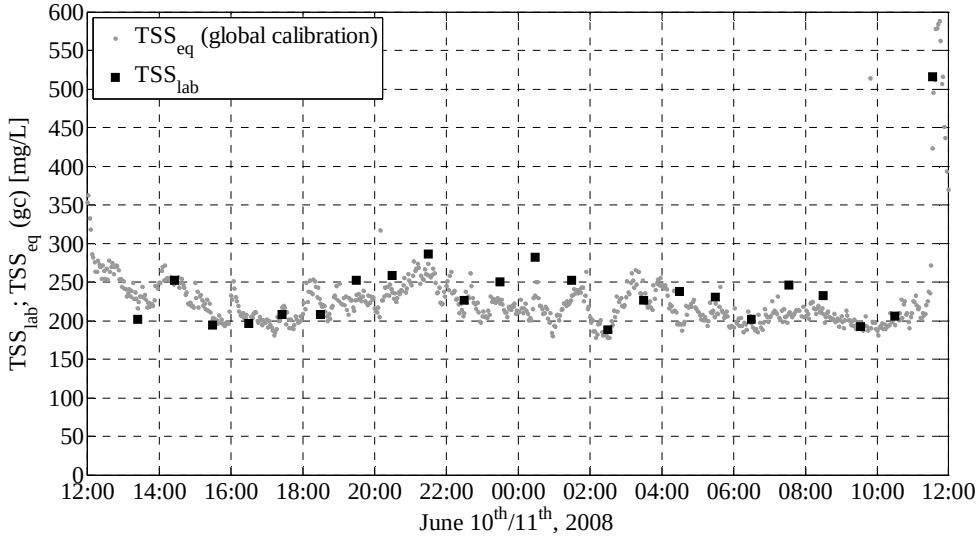

Figure H-1: Results of DWF sampling campaign: TSS_{eq} (as measured by the UV/VIS sensor at a 2-minutes interval, global calibration) versus TSS_{lab} (1 grab sample per hour) for wastewater from catchment area Riool-Zuid. The peak in both laboratory and sensor values around noon is a daily phenomenon for this catchment area (see chapter 6 for details). Despite a possible matrix change, the sample collected at 11h32 has *not* been excluded from the calibration data set. The laboratory analysis for the 12h28 sample failed.

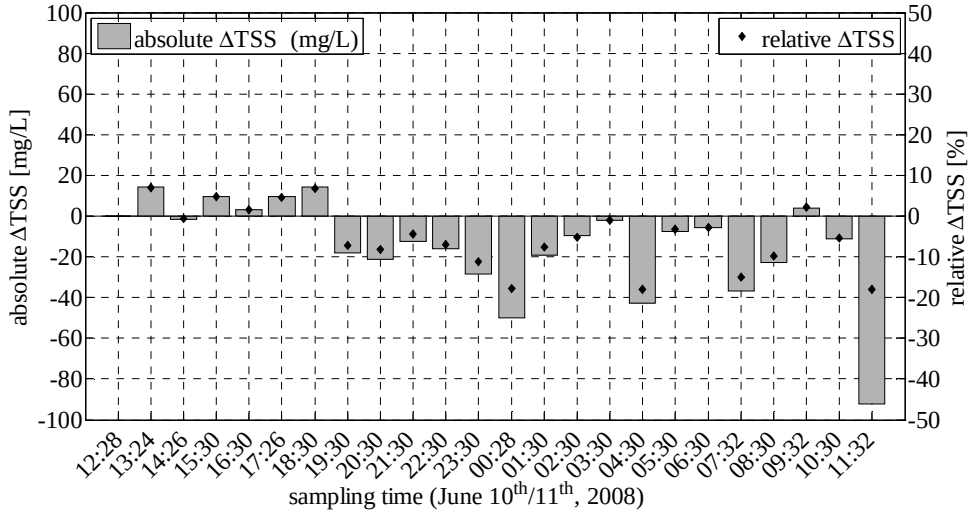

Figure H-2: Absolute (TSS_{eq} - TSS_{lab}, left axis) and relative (with respect to TSS_{lab}, right axis) differences between TSS results as presented in Figure H-1.

DWF campaign, inflow **Riool-Zuid**, parameter **COD**

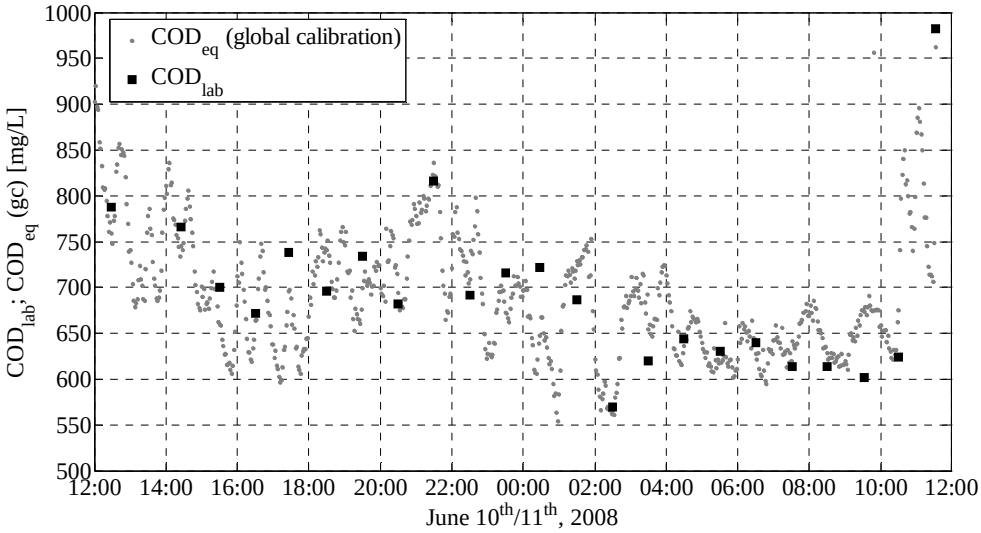

Figure H-3: Results of DWF sampling campaign: COD_{eq} (as measured by the UV/VIS sensor at a 2-minutes interval, global calibration) versus COD_{lab} (1 grab sample per hour) for wastewater from catchment area Riool-Zuid. The peak in both laboratory and sensor values around noon is a daily phenomenon for this catchment area (see chapter 6 for details). Despite a possible matrix change, the sample collected at 11h32 has *not* been excluded from the calibration data set. The laboratory analysis for the grab sample taken at 13h24 failed, hence no result is available.

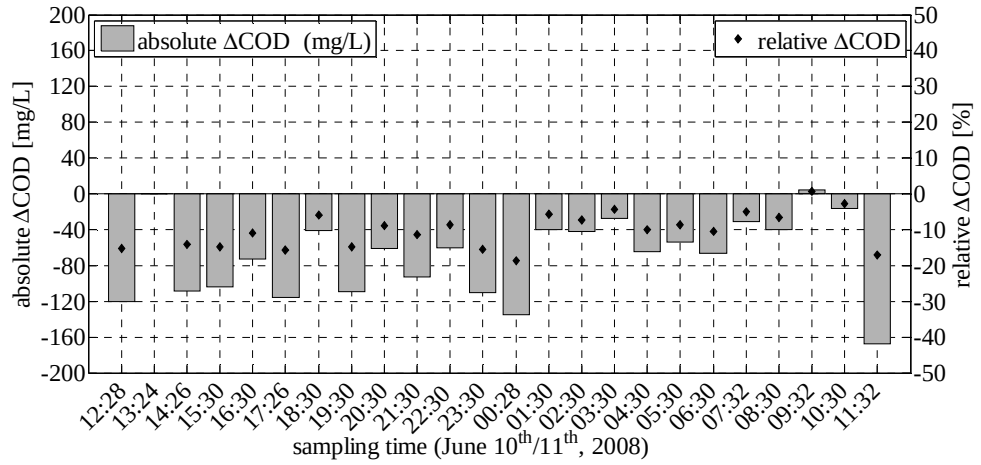

Figure H-4: Absolute (COD_{eq} - COD_{lab}, left axis) and relative (with respect to COD_{lab}, right axis) differences between COD results as presented in Figure H-3.

DWF campaign, inflow **Riool-Zuid**, parameter **CODf**

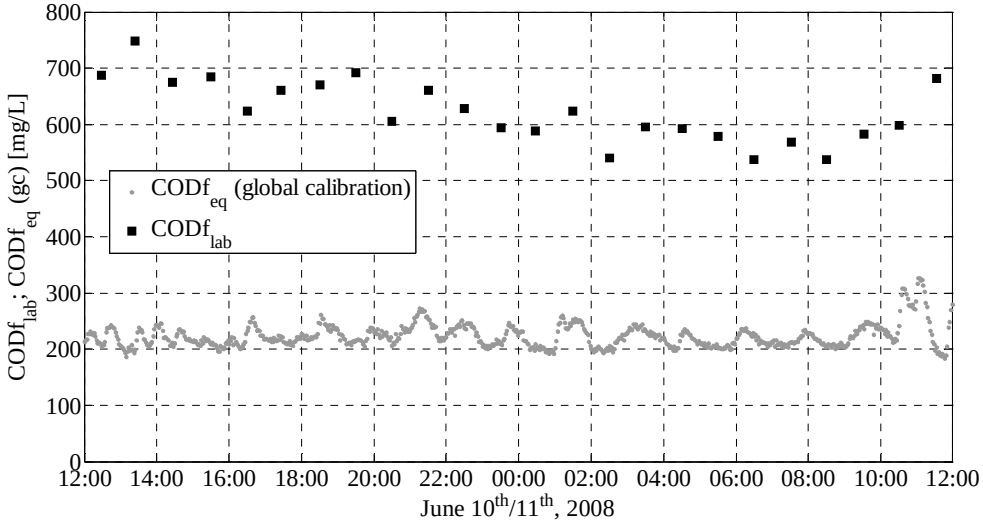

Figure H-5: Results of DWF sampling campaign: $CODf_{eq}$ (as measured by the UV/VIS sensor at a 2-minutes interval, global calibration) versus $CODf_{lab}$ (1 grab sample per hour) for wastewater from catchment area Riool-Zuid. The large differences are due to the use of a wrong filter for the laboratory analysis (see text in chapter 5 for details).

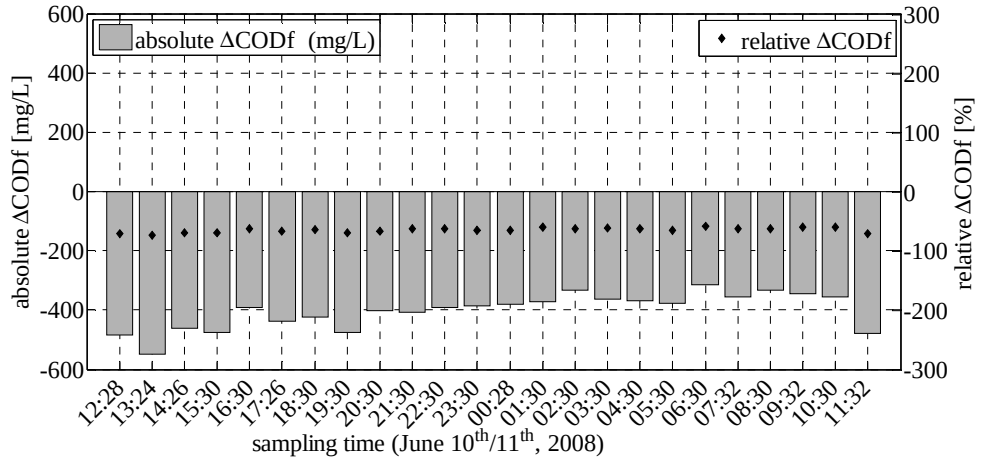

Figure H-6: Absolute ($CODf_{eq}$ - $CODf_{lab}$, left axis) and relative (with respect to $CODf_{lab}$, right axis) differences between CODf results as presented in Figure H-5.

DWF campaign, inflow **Eindhoven Stad**, parameter **TSS**

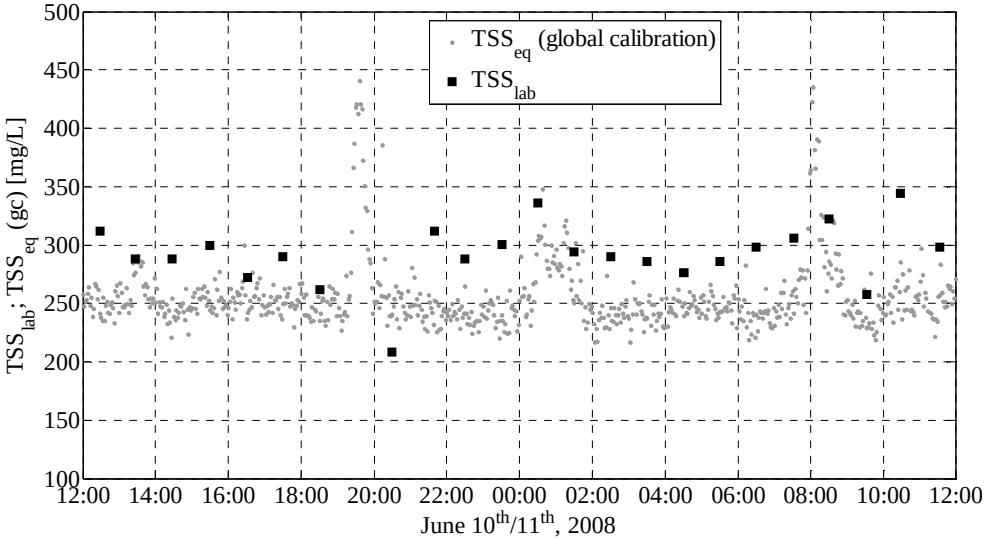

Figure H-7: Results of DWF sampling campaign: TSS_{eq} (as measured by the UV/VIS sensor at a 2-minutes interval, global calibration) versus TSS_{lab} (1 grab sample per hour) for wastewater from catchment area Eindhoven Stad. At 19h30 no grab sample was taken. The result of the 20h30 sample has not been used for the local calibration for suspicion of erroneous sampling (compare with COD_{lab} result in Figure H-9).

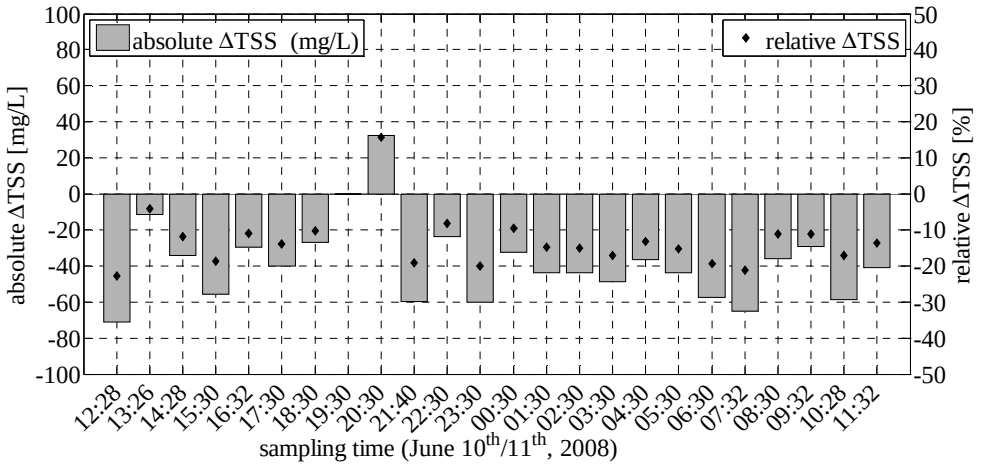

Figure H-8: Absolute (TSS_{eq} - TSS_{lab}, left axis) and relative (with respect to TSS_{lab}, right axis) differences between TSS results as presented in Figure H-7.

DWF campaign, inflow **Eindhoven Stad**, parameter **COD**

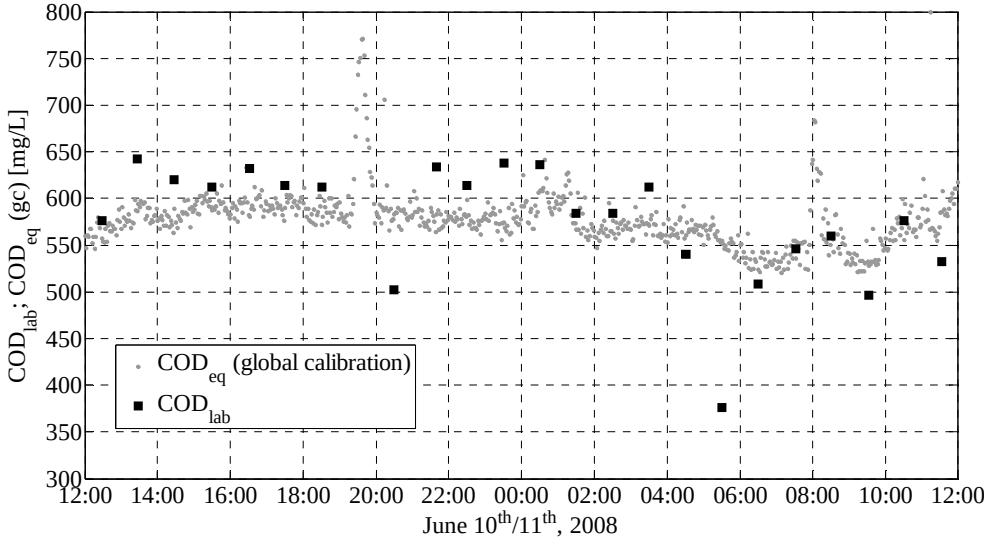

Figure H-9: Results of DWF sampling campaign: COD_{eq} (as measured by the UV/VIS sensor at a 2-minutes interval, global calibration) versus COD_{lab} (1 grab sample per hour) for wastewater from catchment area Eindhoven Stad. At 19h30 no grab sample was taken. The results of the 20h30 and 05h30 samples have been excluded from the local calibration due to suspected erroneous sampling and erroneous laboratory analysis, respectively.

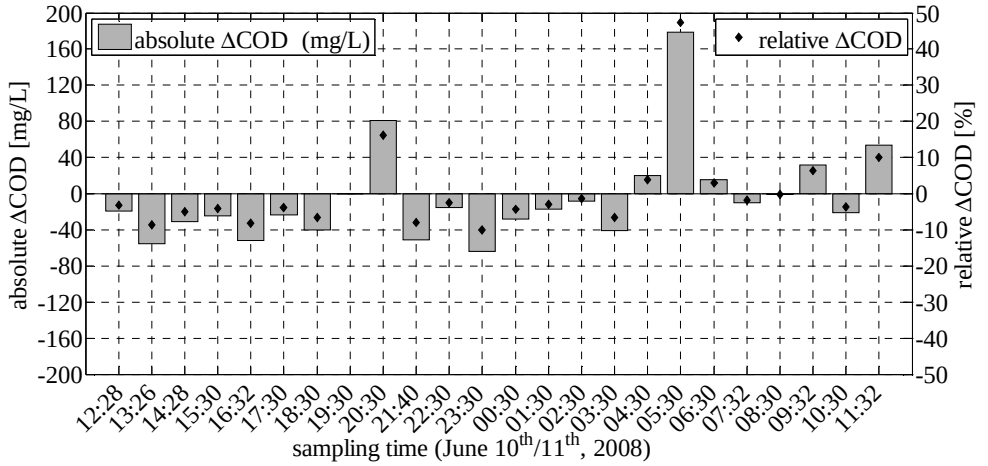

Figure H-10: Absolute (COD_{eq} - COD_{lab}, left axis) and relative (with respect to COD_{lab}, right axis) differences between COD results as presented in Figure H-9.

DWF campaign, inflow **Eindhoven Stad**, parameter **CODf**

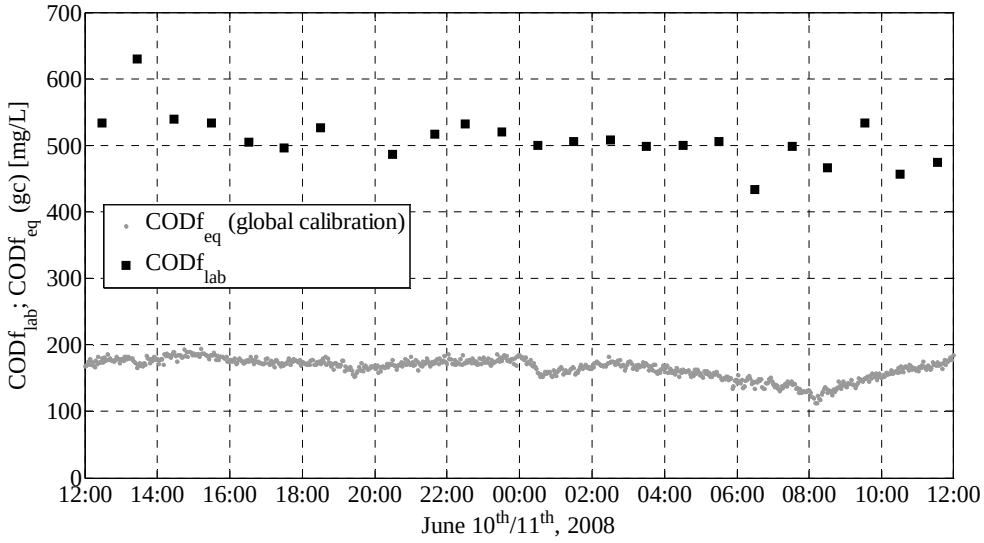

Figure H-11: Results of DWF sampling campaign: $CODf_{eq}$ (as measured by the UV/VIS sensor at a 2-minutes interval, global calibration) versus $CODf_{lab}$ (1 grab sample per hour) for wastewater from catchment area Eindhoven Stad. At 19h30 no grab sample was taken. The large differences are due to the use of a wrong filter for the laboratory analysis (see text in chapter 5 for details).

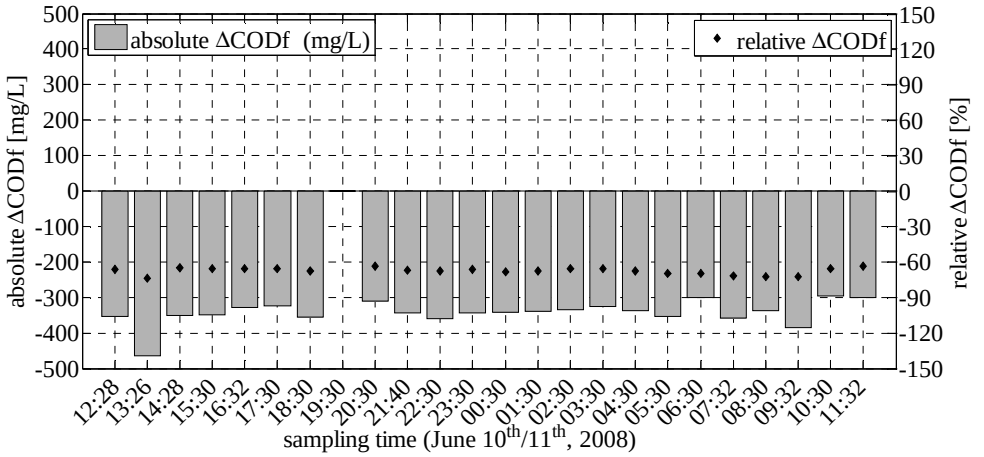

Figure H-12: Absolute ($CODf_{eq}$ - $CODf_{lab}$, left axis) and relative (with respect to $CODf_{lab}$, right axis) differences between CODf results as presented in Figure H-11.

DWF campaign, inflow **Nuenen/Son**, parameter **TSS**

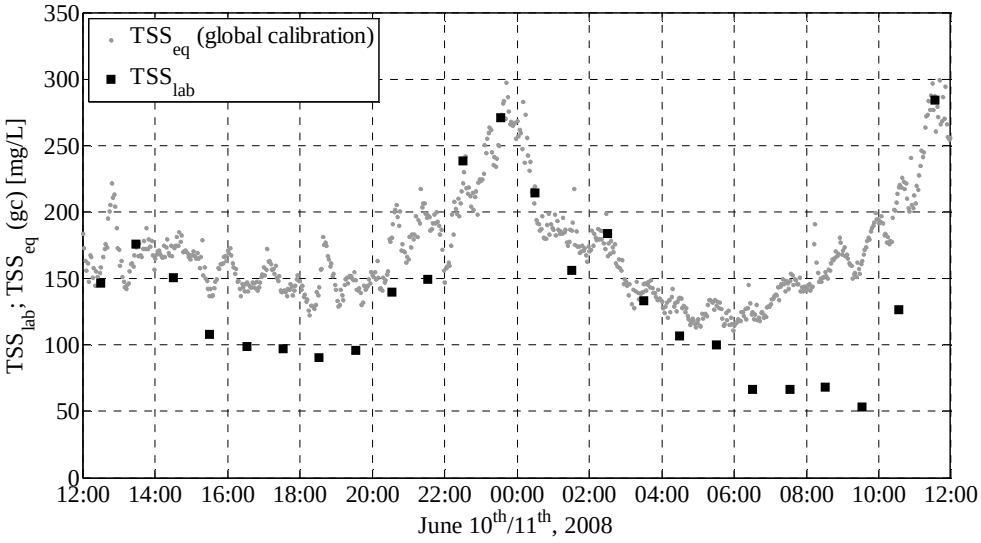

Figure H-13: Results of DWF sampling campaign: TSS_{eq} (as measured by the UV/VIS sensor at a 2-minutes interval, global calibration) versus TSS_{lab} (1 grab sample per hour) for wastewater from catchment area Nuenen/Son.

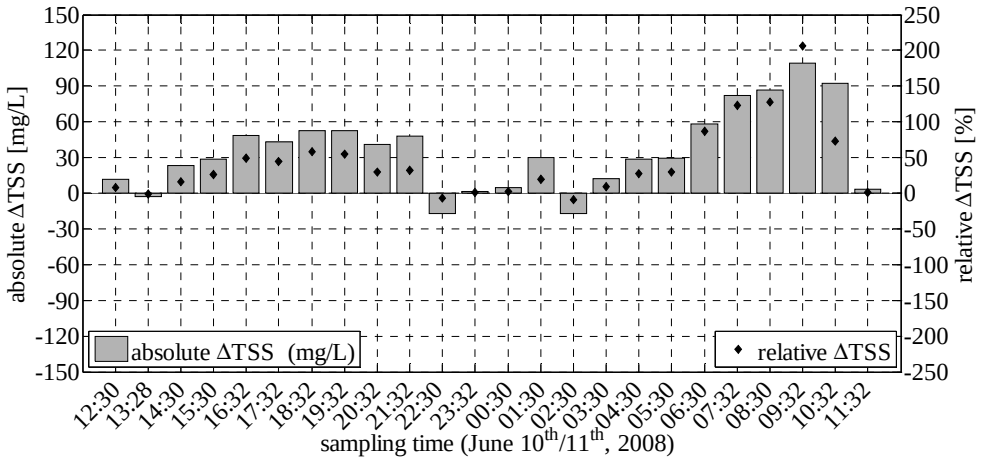

Figure H-14: Absolute (TSS_{eq} - TSS_{lab}, left axis) and relative (with respect to TSS_{lab}, right axis) differences between TSS results as presented in Figure H-13.

DWF campaign, inflow **Nuenen/Son**, parameter **COD**

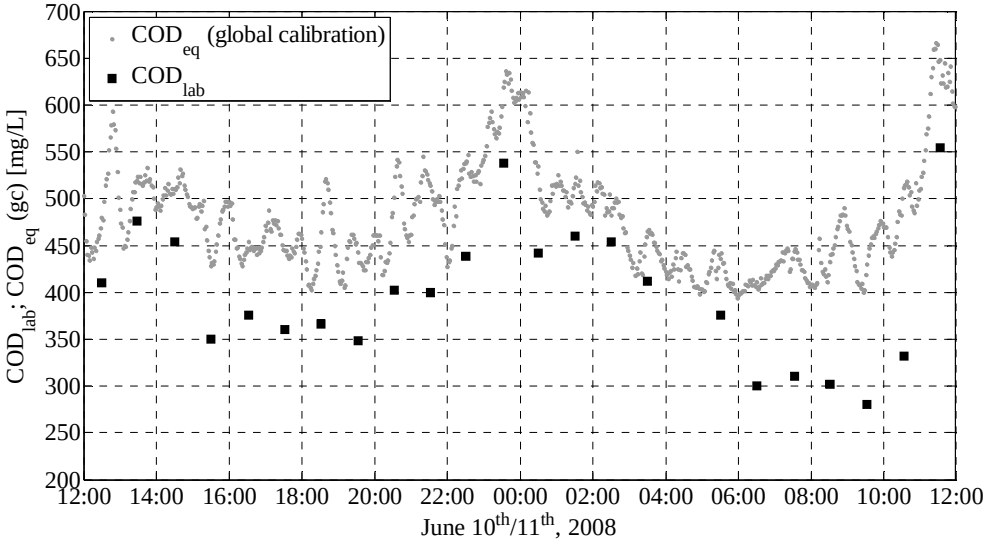

Figure H-15: Results of DWF sampling campaign: COD_{eq} (as measured by the UV/VIS sensor at a 2-minutes interval, global calibration) versus COD_{lab} (1 grab sample per hour) for wastewater from catchment area Nuenen/Son. The laboratory analysis for the grab sample taken at 04h30 failed, hence no result is available.

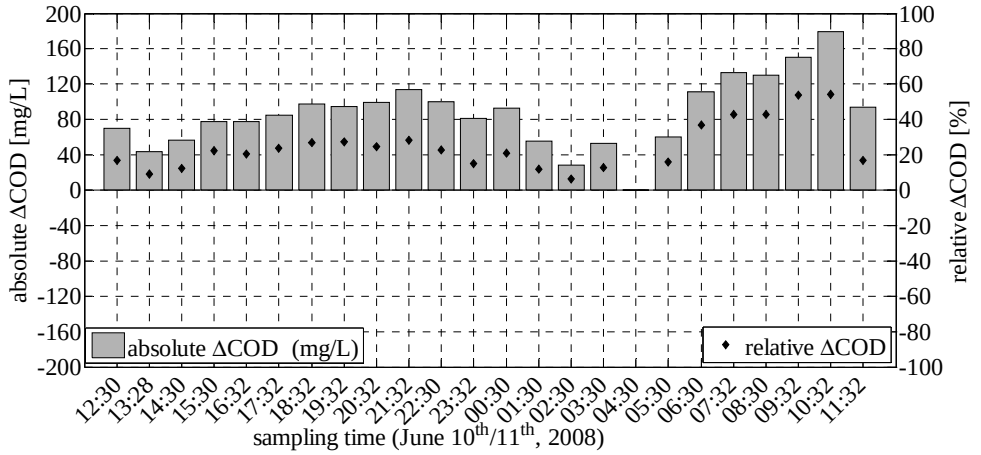

Figure H-16: Absolute (COD_{eq} - COD_{lab}, left axis) and relative (with respect to COD_{lab}, right axis) differences between COD results as presented in Figure H-15.

DWF campaign, inflow **Nuenen/Son**, parameter **CODf**

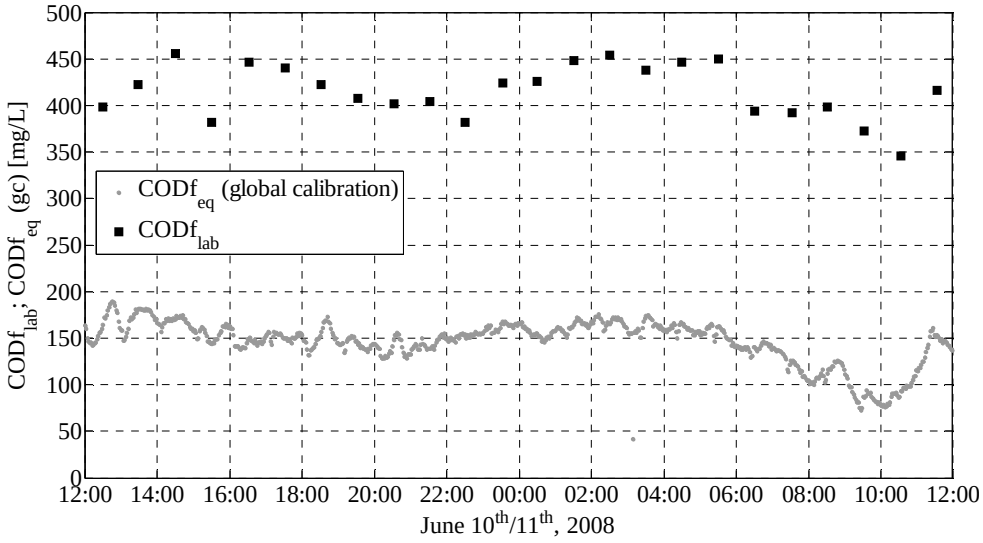

Figure H-17: Results of DWF sampling campaign: $CODf_{eq}$ (as measured by the UV/VIS sensor at a 2-minutes interval, global calibration) versus $CODf_{lab}$ (1 grab sample per hour) for wastewater from catchment area Nuenen/Son. The large differences are due to the use of a wrong filter for the laboratory analysis (see text in chapter 5 for details).

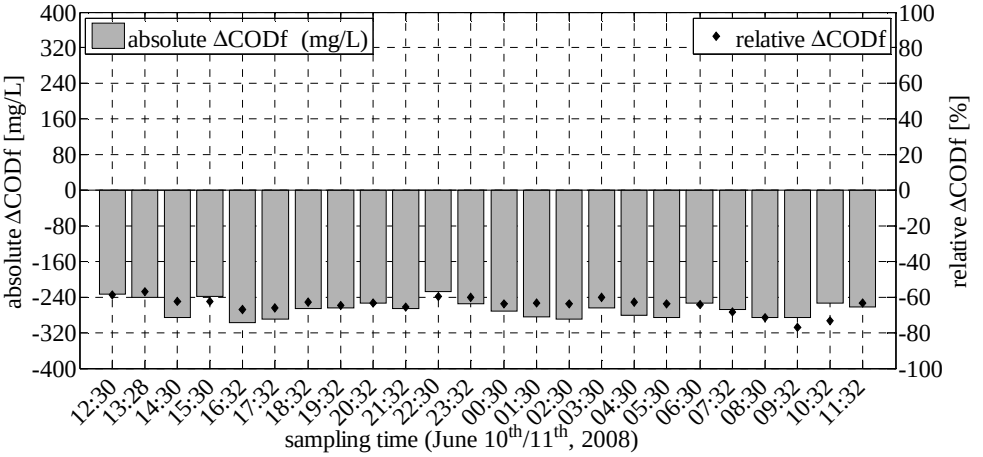

Figure H-18: Absolute ($CODf_{eq}$ - $CODf_{lab}$, left axis) and relative (with respect to $CODf_{lab}$, right axis) differences between CODf results as presented in Figure H-17.

Appendix J. Results of wet weather sampling campaign

This appendix presents per inflow an overview of the storm events showing the behavior of inflow to the wwtp, precipitation and the pollutant parameters TSS_{eq}, COD_{eq} and $CODf_{eq}$ throughout the complete storm events. Then, per pollutant parameter (in order TSS, COD, CODf) the results of the sampling campaign are presented in two graphs. In the upper graphs hourly laboratory results are set out against 2-minute interval results of the (still globally calibrated) UV/VIS sensors. In the lower graphs the absolute (sensor value minus lab value), and relative (idem, with respect to lab value) differences between the laboratory and sensor values are presented.

The order of presentation is:

- WWF campaign, inflow Riool-Zuid, overview storm event
- WWF campaign, inflow Riool-Zuid, parameter TSS
- WWF campaign, inflow Riool-Zuid, parameter COD
- WWF campaign, inflow Riool-Zuid, parameter CODf

- WWF campaign, inflow Eindhoven Stad, overview storm event
- WWF campaign, inflow Eindhoven Stad, parameter TSS
- WWF campaign, inflow Eindhoven Stad, parameter COD
- WWF campaign, inflow Eindhoven Stad, parameter CODf

- WWF campaign, inflow Nuenen/Son, overview storm event
- WWF campaign, inflow Nuenen/Son, parameter TSS
- WWF campaign, inflow Nuenen/Son, parameter COD
- WWF campaign, inflow Nuenen/Son, parameter CODf

WWF campaign, inflow **Riool-Zuid**, overview **storm event**

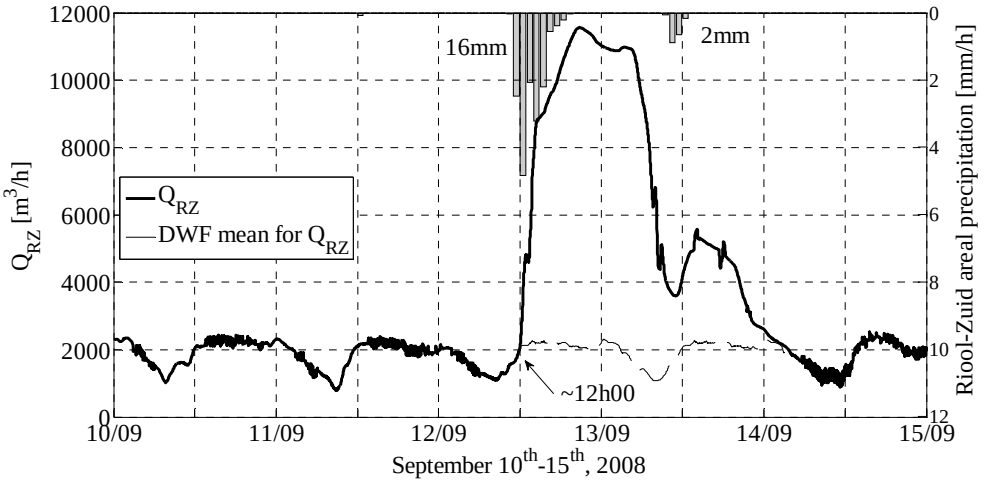

Figure J-1: Overview of inflow during the 16 + 2 mm storm events on September 12th and 13th, 2008. On September 12th after ~12h00 Q_{RZ} starts deviating from mean DWF flow.

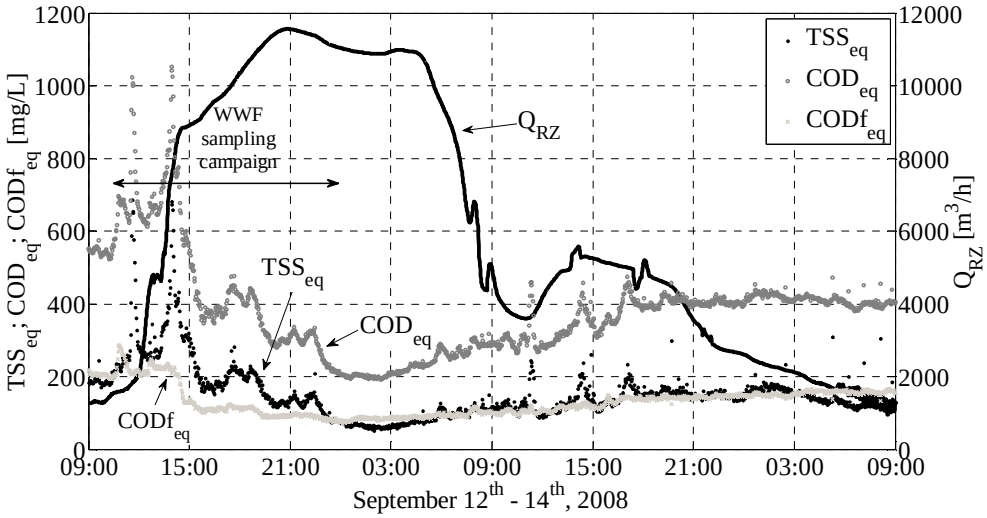

Figure J-2: Overview of behavior of Q_{RZ} and UV/VIS parameters during the complete storm events on September 12th and 13th, 2008. Samples for the WWF campaign have been taken during the first 12 hours of the storm event.

WWF campaign, inflow **Riool-Zuid**, parameter **TSS**

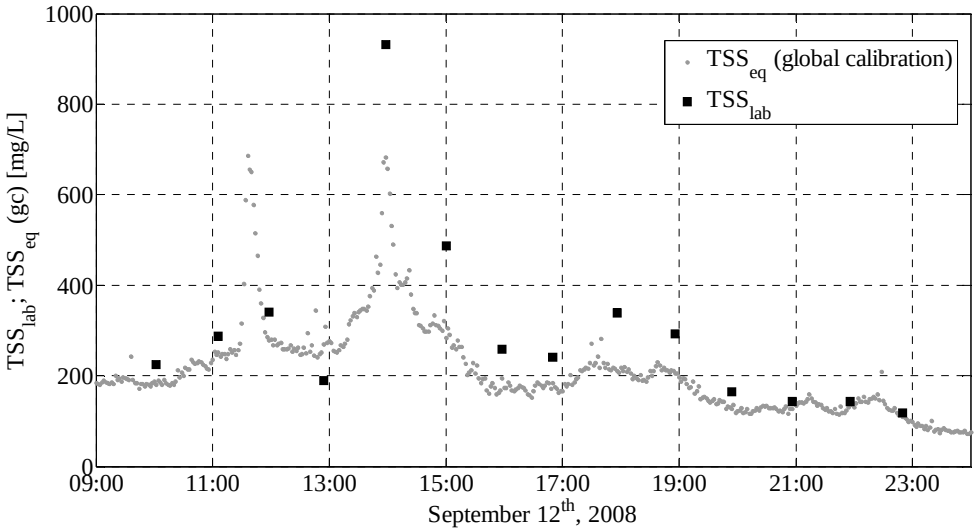

Figure J-3: Results of WWF sampling campaign: TSS_{eq} (as measured by the UV/VIS sensor at a 2-minutes interval, global calibration) versus TSS_{lab} (1 grab sample per hour) for wastewater from catchment area Riool-Zuid. All samples taken from 13h00 onwards are considered to be associated with wet weather flow conditions.

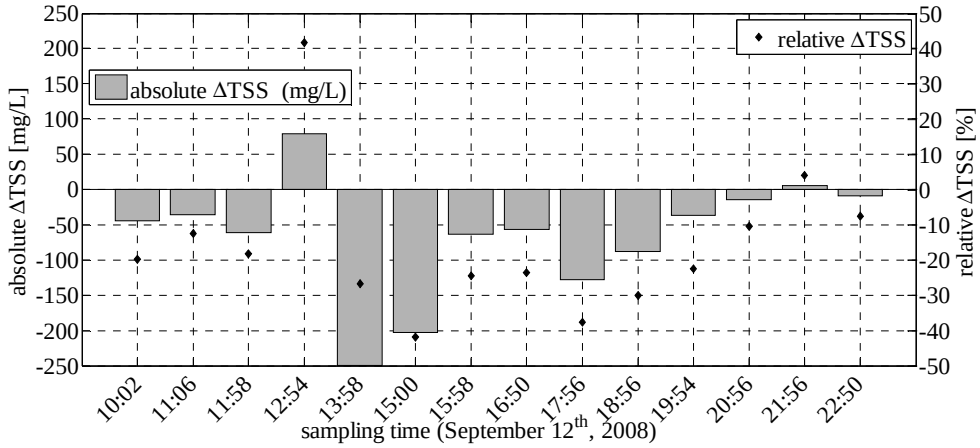

Figure J-4: Absolute (TSS_{eq} - TSS_{lab}, left axis) and relative (with respect to TSS_{lab}, right axis) differences between TSS results as presented in Figure J-3.

WWF campaign, inflow **Riool-Zuid**, parameter **COD**

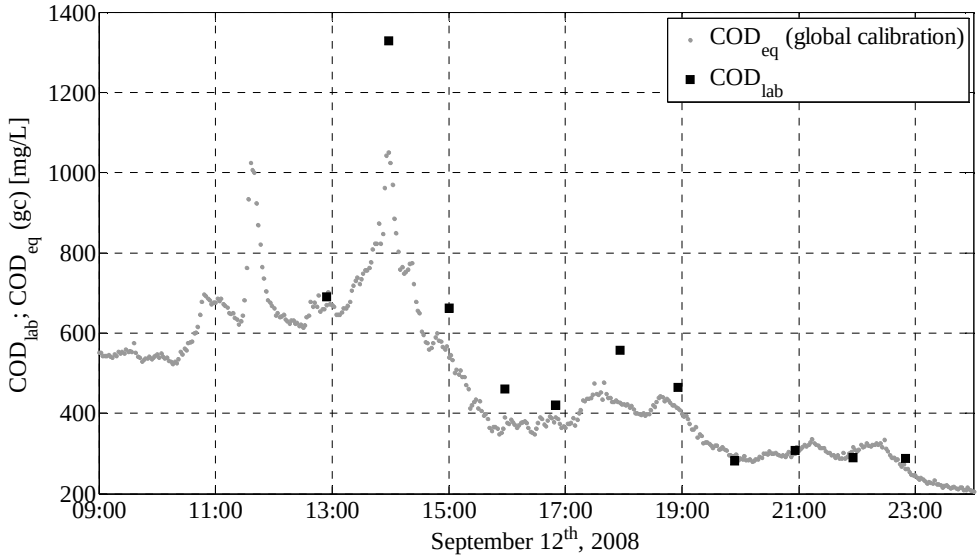

Figure J-5: Results of WWF sampling campaign: COD_{eq} (as measured by the UV/VIS sensor at a 2-minutes interval, global calibration) versus COD_{lab} (1 grab sample per hour) for wastewater from catchment area Riool-Zuid. The COD laboratory analyses of the first three samples (10h02, 11h06 and 11h58) failed. All samples taken from 13h00 onwards are considered to be associated with wet weather flow conditions.

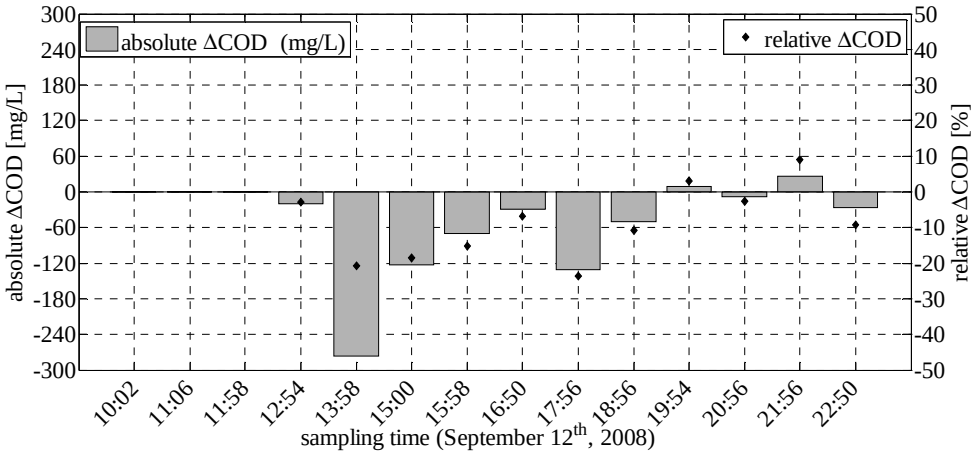

Figure J-6: Absolute (COD_{eq} - COD_{lab}, left axis) and relative (with respect to COD_{lab}, right axis) differences between COD results as presented in Figure J-5.

WWF campaign, inflow **Riool-Zuid**, parameter **CODf**

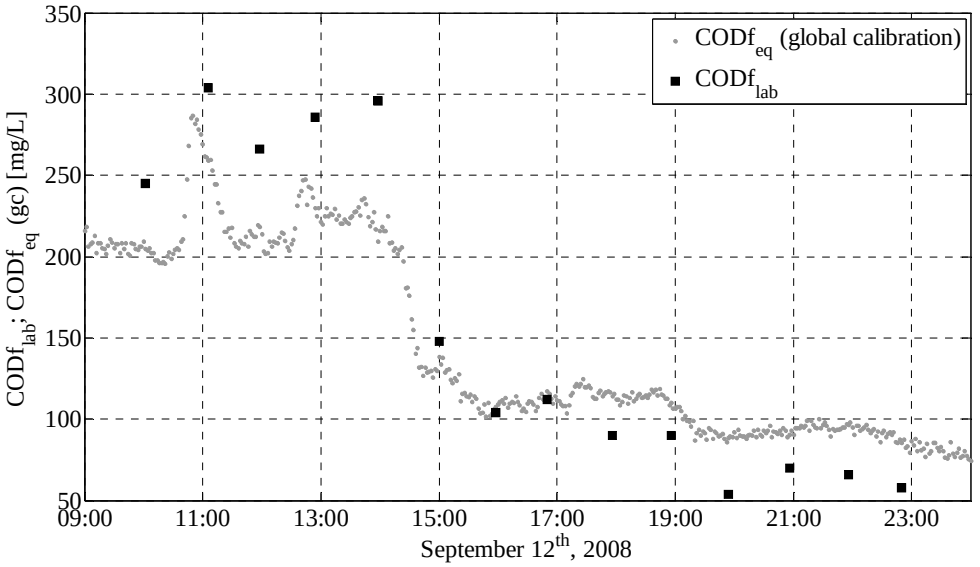

Figure J-7: Results of WWF sampling campaign: $CODf_{eq}$ (as measured by the UV/VIS sensor at a 2-minutes interval, global calibration) versus $CODf_{lab}$ (1 grab sample per hour) for wastewater from catchment area Riool-Zuid. Samples collected from 15h00 onwards have been used in the WWF calibration. The first four samples have been used in the DWF calibration for lack of results during the DWF sampling campaign; the 13h58 sample is considered to be associated with the transition between the two flow conditions.

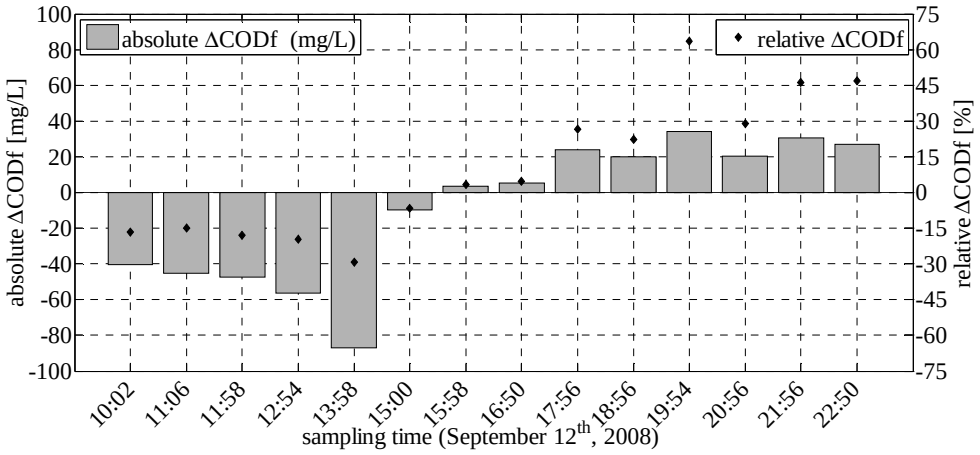

Figure J-8: Absolute ($CODf_{eq}$ - $CODf_{lab}$, left axis) and relative (with respect to $CODf_{lab}$, right axis) differences between CODf results as presented in Figure J-7.

WWF campaign, inflow **Eindhoven Stad**, overview **storm event**

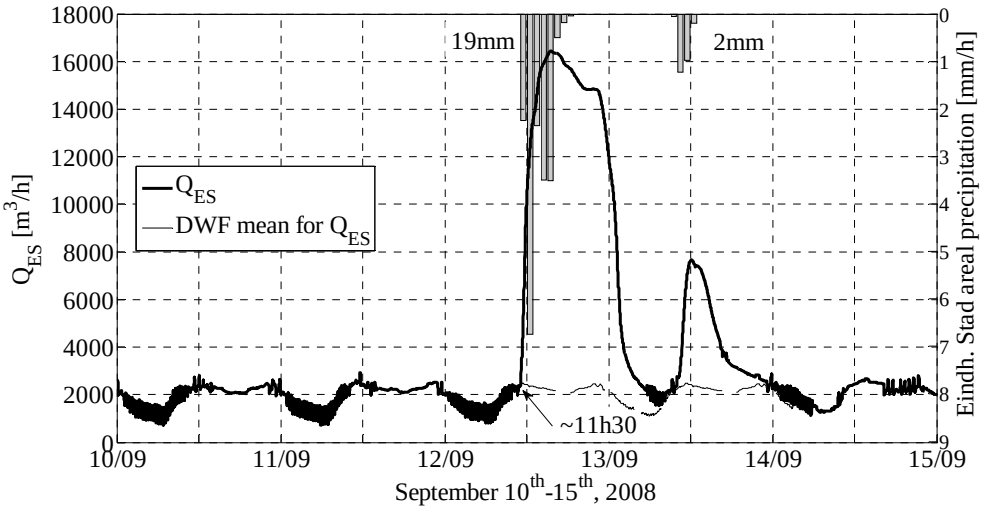

Figure J-9: Overview of inflow during the 19 + 2 mm storm events on September 12th and 13th, 2008. On September 12th after ~11h30 Q_{ES} starts deviating from mean DWF flow.

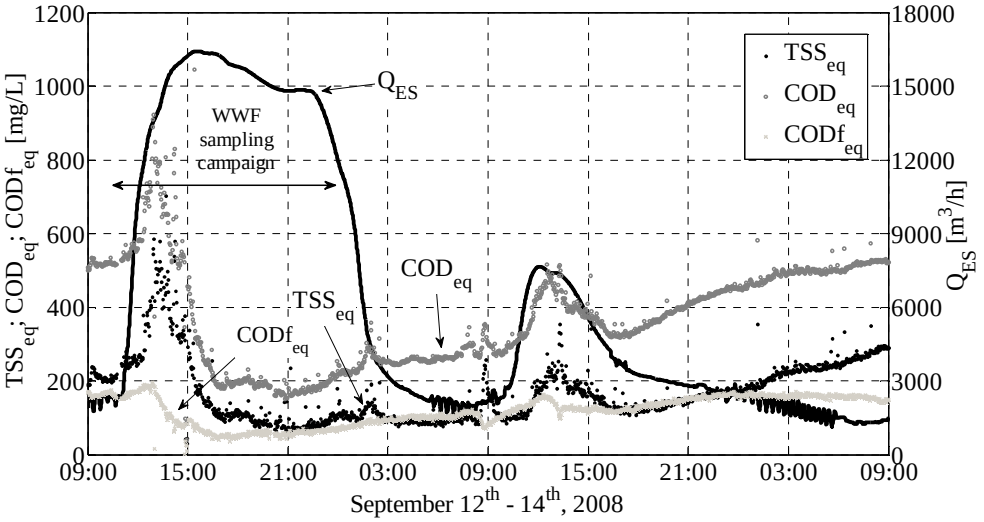

Figure J-10: Overview of behavior of Q_{ES} and UV/VIS parameters during the complete storm events on September 12th and 13th, 2008. Samples for the WWF campaign have been taken during the first 12 hours of the storm event.

WWF campaign, inflow **Eindhoven Stad**, parameter **TSS**

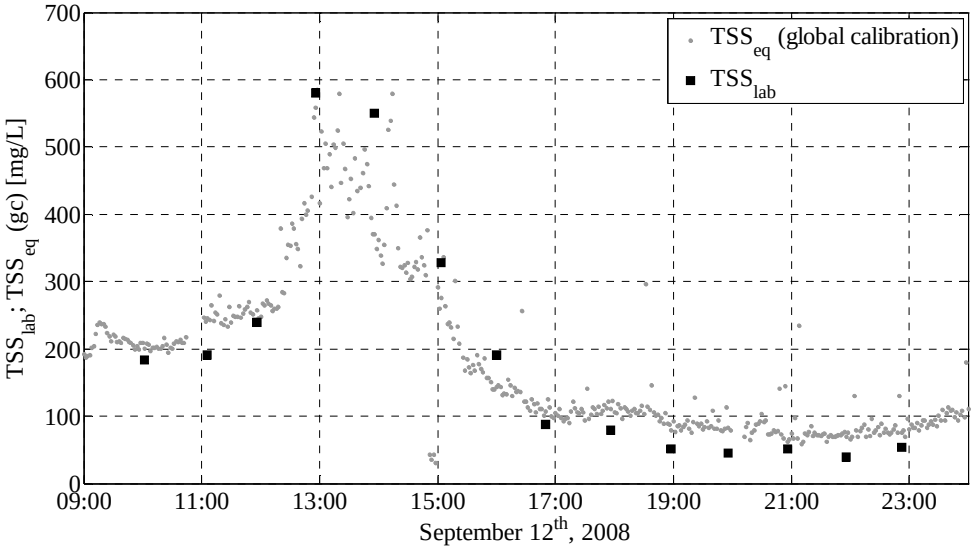

Figure J-11: Results of WWF sampling campaign: TSS_{eq} (as measured by the UV/VIS sensor at a 2-minutes interval, global calibration) versus TSS_{lab} (1 grab sample per hour) for wastewater from catchment area Eindhoven Stad. All samples taken from 13h00 onwards are considered to be associated with wet weather flow conditions.

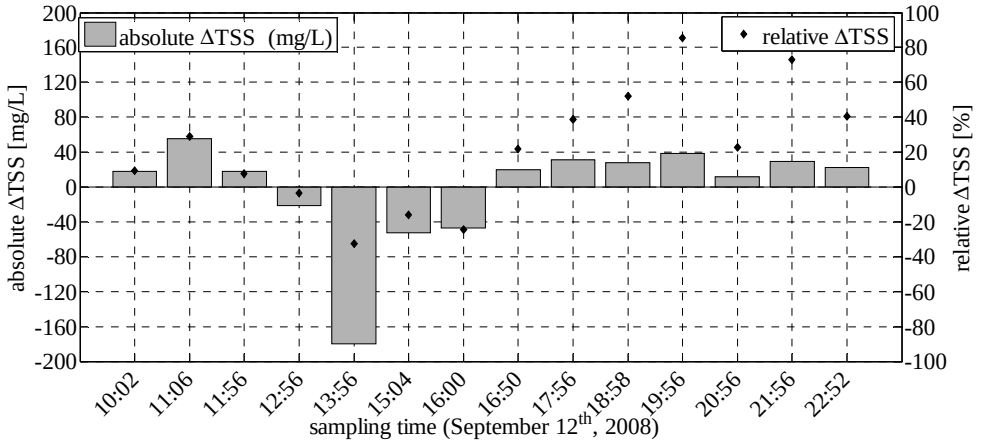

Figure J-12: Absolute (TSS_{eq} - TSS_{lab}, left axis) and relative (with respect to TSS_{lab}, right axis) differences between TSS results as presented in Figure J-11.

WWF campaign, inflow **Eindhoven Stad**, parameter **COD**

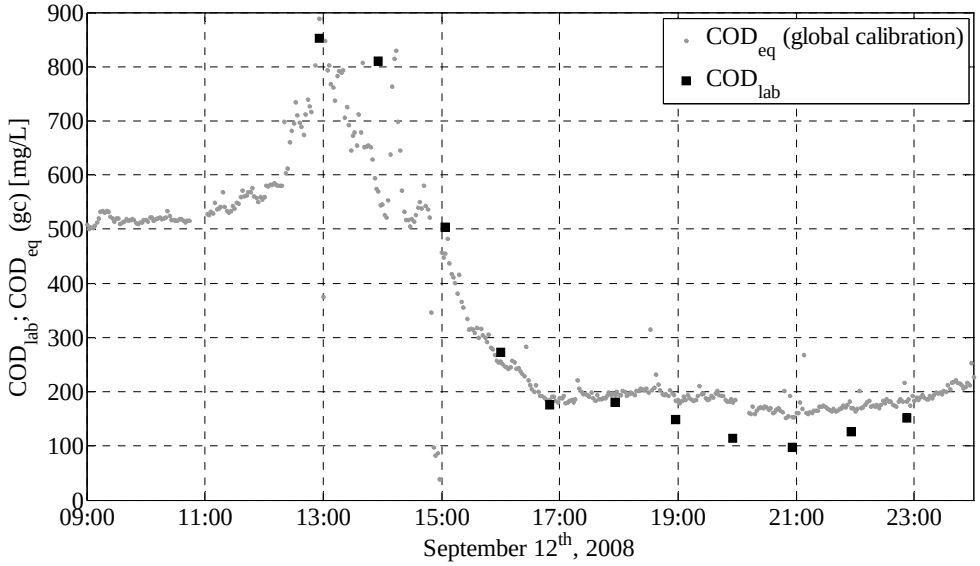

Figure J-13: Results of WWF sampling campaign: COD_{eq} (as measured by the UV/VIS sensor at a 2-minutes interval, global calibration) versus COD_{lab} (1 grab sample per hour) for wastewater from catchment area Eindhoven Stad. The COD laboratory analyses of the first three samples (10h02, 11h06 and 11h56) failed. All samples taken from 13h00 onwards are considered to be associated with wet weather flow conditions.

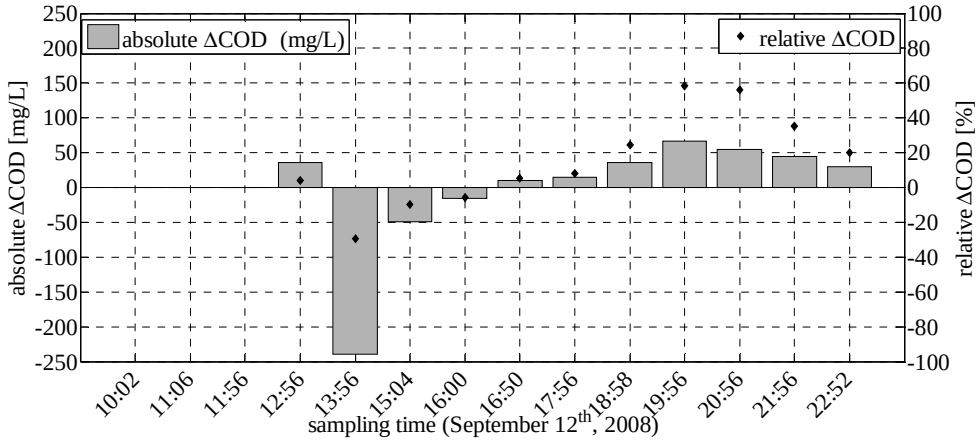

Figure J-14: Absolute (COD_{eq} - COD_{lab}, left axis) and relative (with respect to COD_{lab}, right axis) differences between COD results as presented in Figure J-13.

WWF campaign, inflow **Eindhoven Stad**, parameter **CODf**

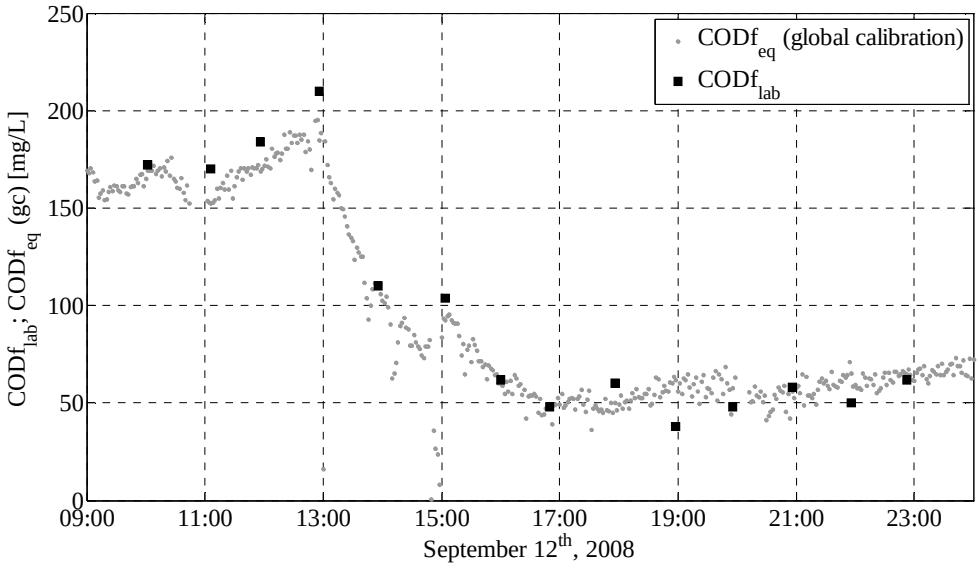

Figure J-15: Results of WWF sampling campaign: $CODf_{eq}$ (as measured by the UV/VIS sensor at a 2-minutes interval, global calibration) versus $CODf_{lab}$ (1 grab sample per hour) for wastewater from catchment area Eindhoven Stad. Samples collected from 14h00 onwards have been used in the WWF calibration. The first three samples have been used in the DWF calibration for lack of results during the DWF sampling campaign; the 12h56 sample is considered to be associated with the transition between the two flow conditions.

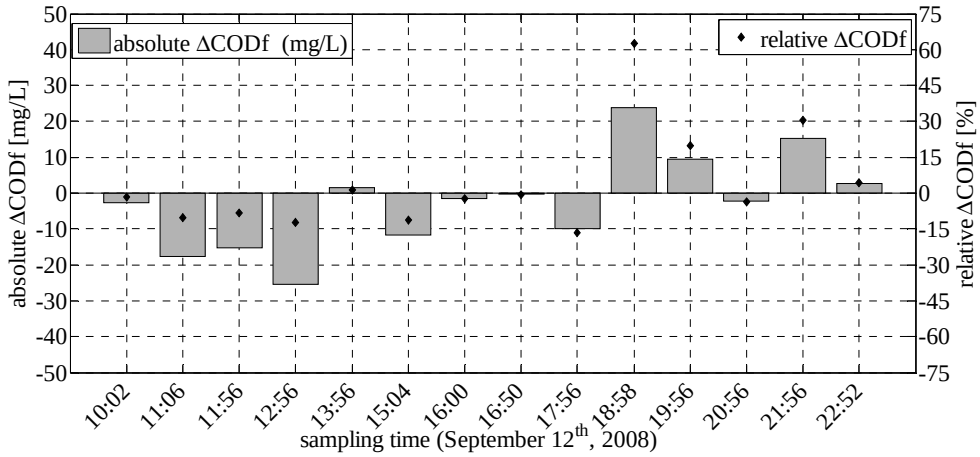

Figure J-16: Absolute ($CODf_{eq}$ - $CODf_{lab}$, left axis) and relative (with respect to $CODf_{lab}$, right axis) differences between CODf results as presented in Figure J-15.

WWF campaign, inflow **Nuenen/Son**, overview **storm event**

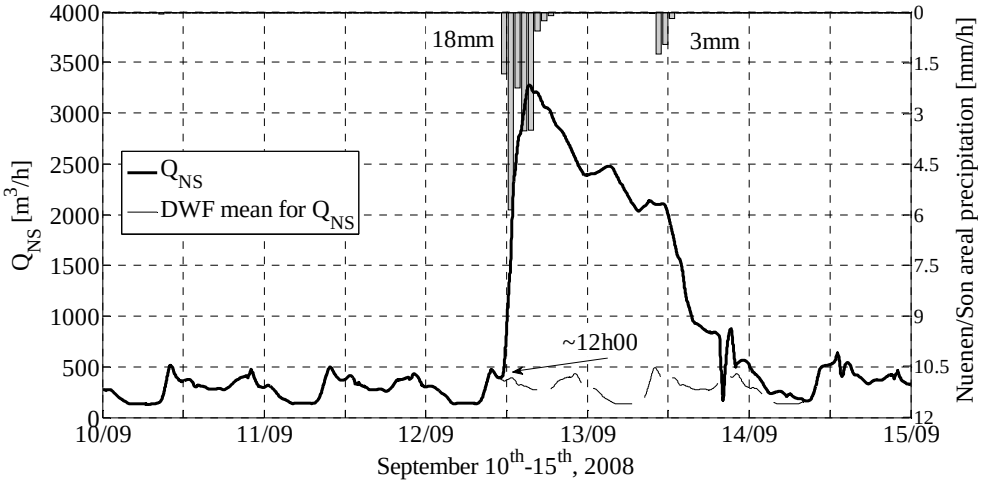

Figure J-17: Overview of inflow during the 18 + 3 mm storm events on September 12th and 13th, 2008. On September 12th after ~12h00 Q_{NS} starts deviating from mean DWF flow.

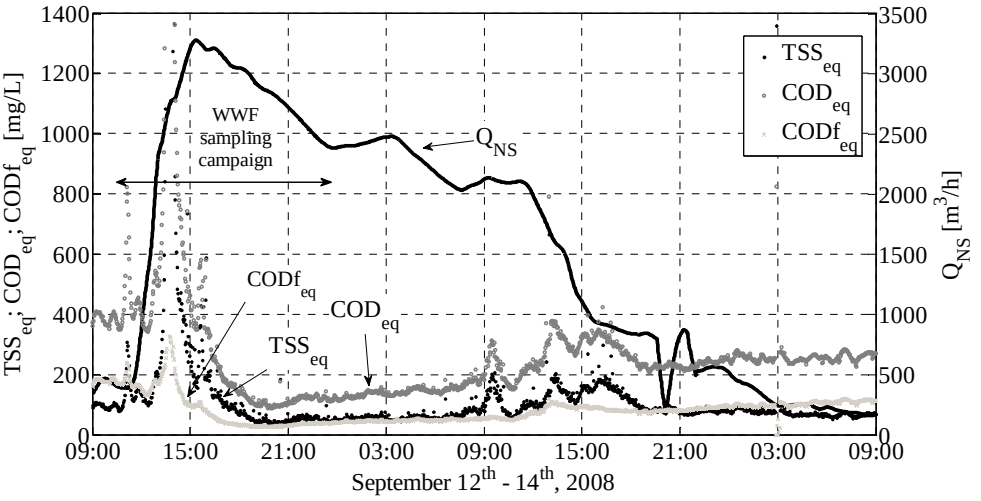

Figure J-18: Overview of behavior of Q_{NS} and UV/VIS parameters during the complete storm event on September 12th/13th, 2008. Samples for the WWF campaign have been taken during the first 12 hours of the storm event.

WWF campaign, inflow **Nuenen/Son**, parameter **TSS**

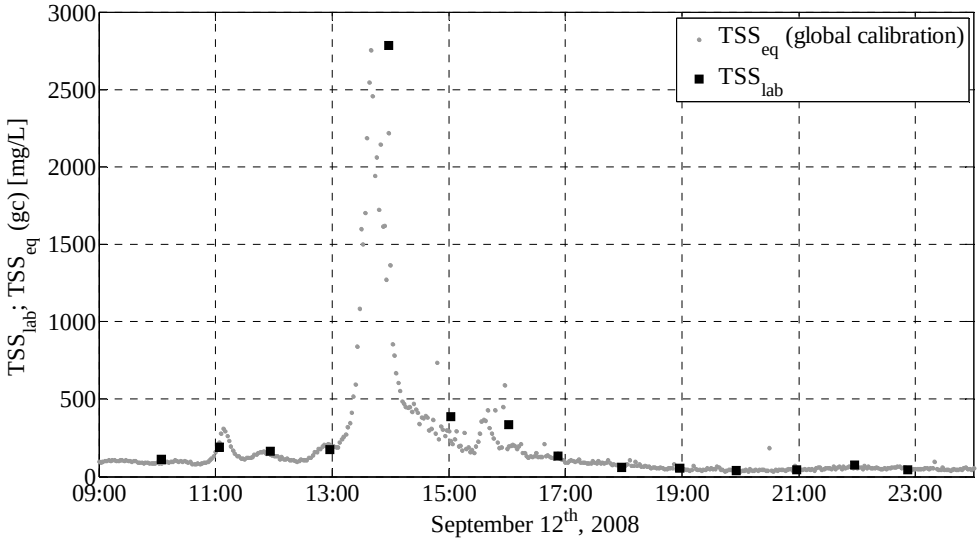

Figure J-19: Results of WWF sampling campaign: TSS_{eq} (as measured by the UV/VIS sensor at a 2-minutes interval, global calibration) versus TSS_{lab} (1 grab sample per hour) for wastewater from catchment area Nuenen/Son. All samples taken from 13h00 onwards are considered to be associated with wet weather flow conditions.

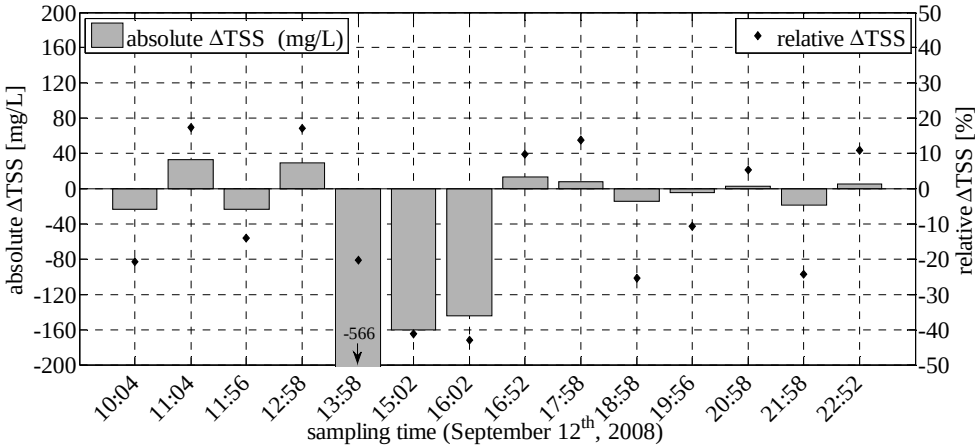

Figure J-20: Absolute (TSS_{eq} - TSS_{lab}, left axis) and relative (with respect to TSS_{lab}, right axis) differences between TSS results as presented in Figure J-19.

WWF campaign, inflow **Nuenen/Son**, parameter **COD**

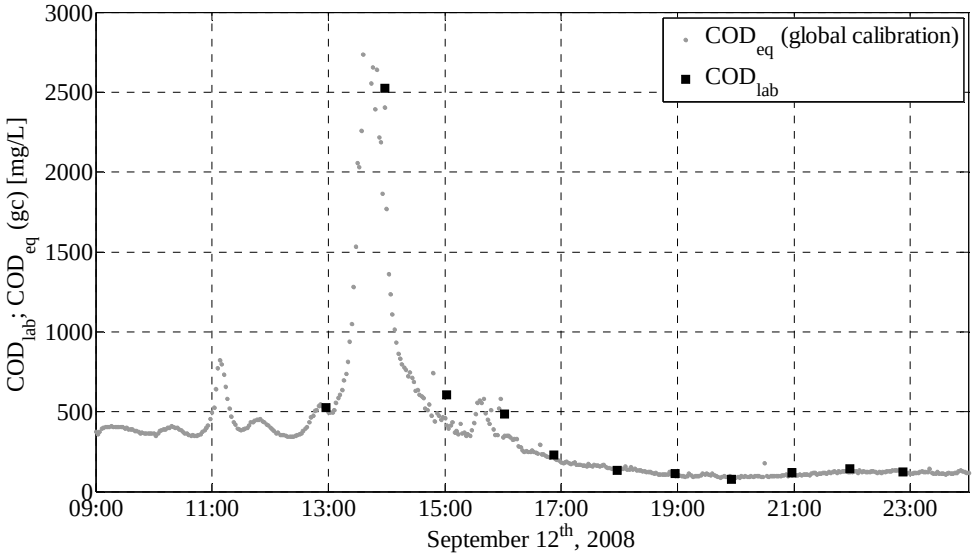

Figure J-21: Results of WWF sampling campaign: COD_{eq} (as measured by the UV/VIS sensor at a 2-minutes interval, global calibration) versus COD_{lab} (1 grab sample per hour) for wastewater from catchment area Nuenen/Son. The COD laboratory analyses of the first three samples (10h04, 11h04 and 11h56) failed. All samples taken from 13h00 onwards are considered to be associated with wet weather flow conditions.

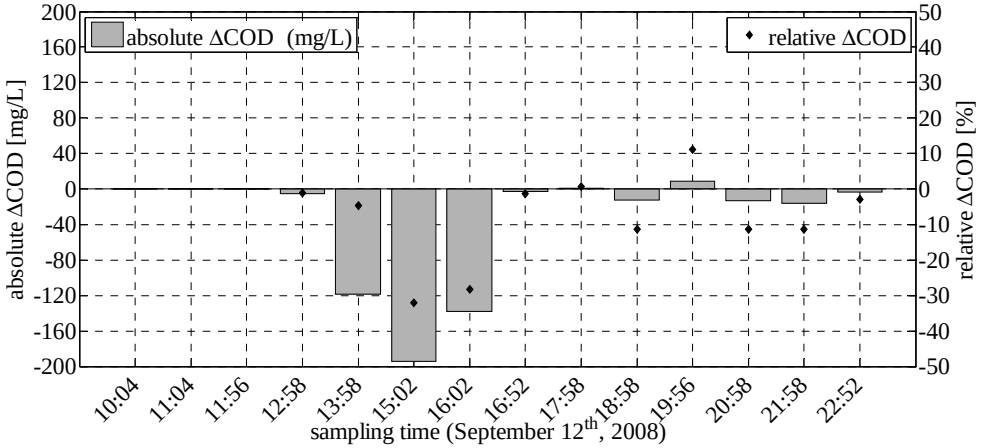

Figure J-22: Absolute (COD_{eq} - COD_{lab}, left axis) and relative (with respect to COD_{lab}, right axis) differences between COD results as presented in Figure J-21.

WWF campaign, inflow **Nuenen/Son**, parameter **CODf**

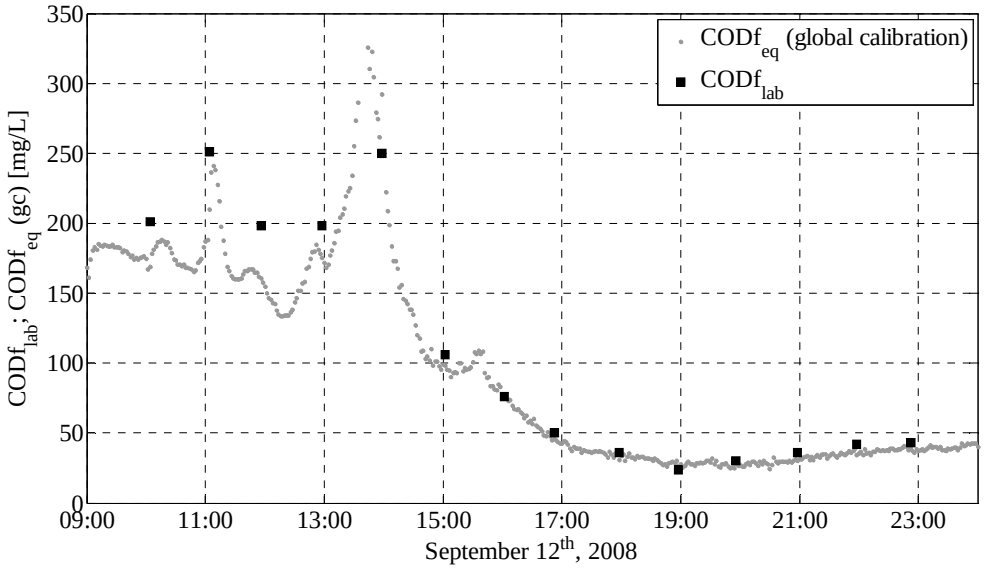

Figure J-23: Results of WWF sampling campaign: $CODf_{eq}$ (as measured by the UV/VIS sensor at a 2-minutes interval, global calibration) versus $CODf_{lab}$ (1 grab sample per hour) for wastewater from catchment area Nuenen/Son. Samples collected from 15h00 onwards have been used in the WWF calibration. The first four samples have been used in the DWF calibration for lack of results during the DWF sampling campaign; the 13h58 sample is considered to be associated with the transition between the two flow conditions.

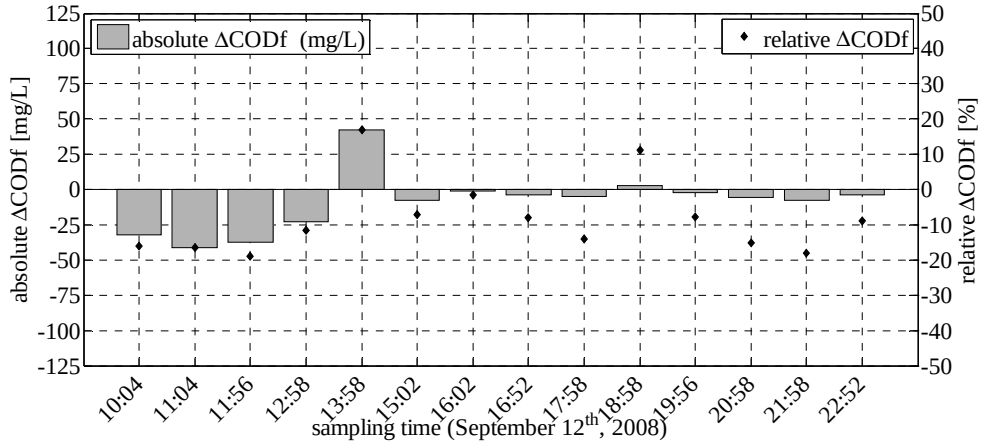

Figure J-24: Absolute ($CODf_{eq}$ - $CODf_{lab}$, left axis) and relative (with respect to $CODf_{lab}$, right axis) differences between CODf results as presented in Figure J-23.

Appendix K. Results of UV/VIS local calibration

This appendix presents per inflow, per pollutant parameter and per wastewater matrix the results of the local calibration process in two graphs. In the upper graphs the fit between UV/VIS sensor results (global calibration) and laboratory results is presented. Applying the fit on the sensor values, in the lower graphs the hourly laboratory results obtained during the DWF and WWF sampling campaigns are set out against both the globally as well as the locally calibrated results of the UV/VIS sensors. For all inflow/parameter combinations local calibration sets have been derived for two distinct wastewater matrices: DWF matrix and WWF matrix.

The order of presentation is:

- inflow Riool-Zuid, parameter TSS, DWF matrix
- inflow Riool-Zuid, parameter TSS, WWF matrix
- inflow Riool-Zuid, parameter COD, DWF matrix
- inflow Riool-Zuid, parameter COD, WWF matrix
- inflow Riool-Zuid, parameter CODf, DWF and WWF matrices

- inflow Eindhoven Stad, parameter TSS, DWF matrix
- inflow Eindhoven Stad, parameter TSS, WWF matrix
- inflow Eindhoven Stad, parameter COD, DWF matrix
- inflow Eindhoven Stad, parameter COD, WWF matrix
- inflow Eindhoven Stad, parameter CODf, DWF and WWF matrices

- inflow Nuenen/Son, parameter TSS, DWF matrix
- inflow Nuenen/Son, parameter TSS, WWF matrix
- inflow Nuenen/Son, parameter COD, DWF matrix
- inflow Nuenen/Son, parameter COD, WWF matrix
- inflow Nuenen/Son, parameter CODf, DWF and WWF matrices

inflow **Riool-Zuid**, parameter **TSS**, **DWF** matrix

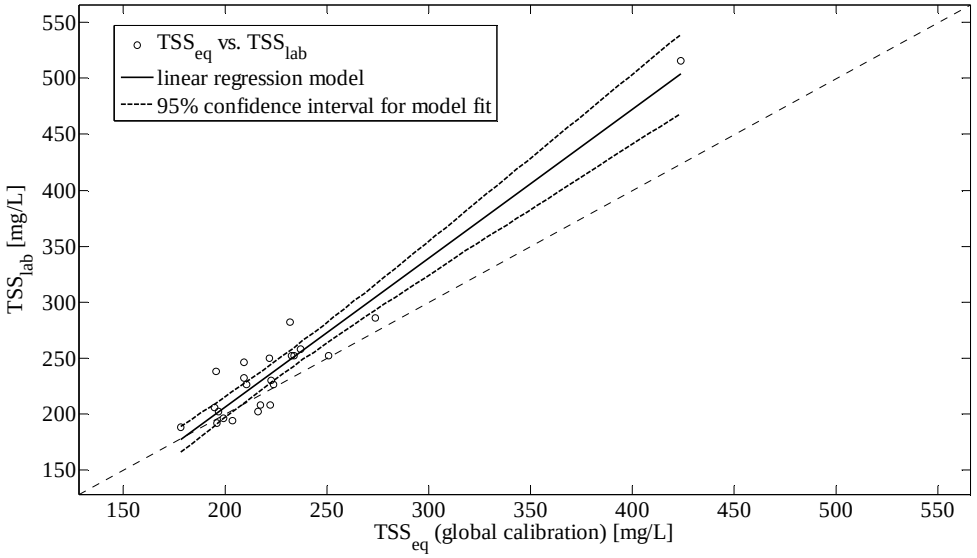

Figure K-1: TSS_{eq} (global calibration) vs. TSS_{lab} with linear regression model and confidence bounds.

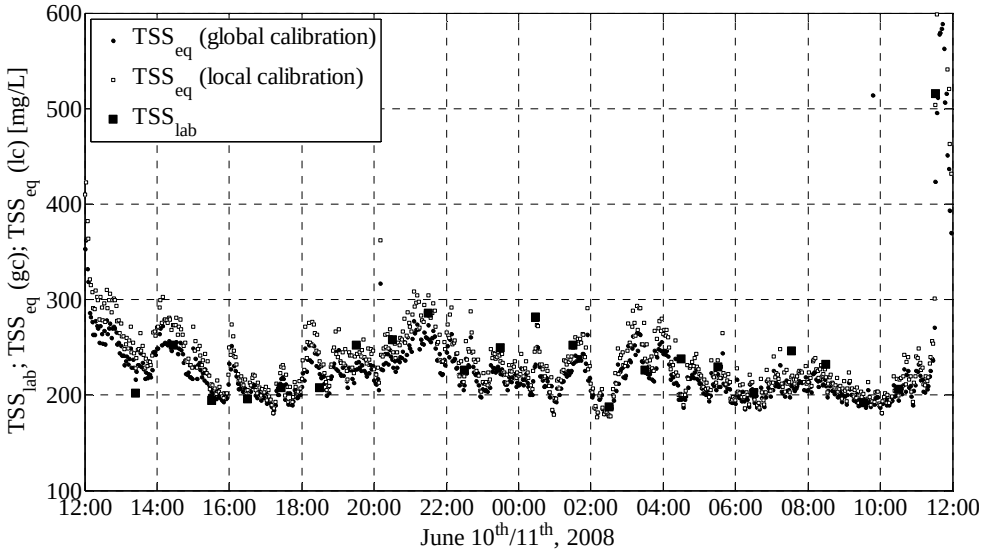

Figure K-2: Results of calibration for DWF matrix of inflow Riool-Zuid: TSS_{eq} (global calibration, 2-minute interval) converted into TSS_{eq} (local calibration, 2-minute interval) and compared to TSS_{lab} (1 sample per hour).

inflow **Riool-Zuid**, parameter **TSS**, **WWF** matrix

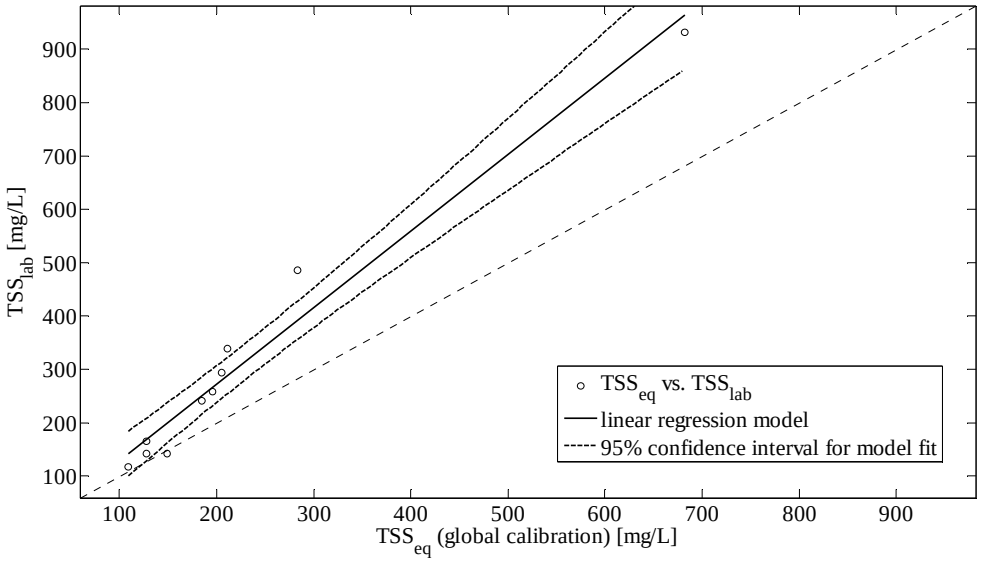

Figure K-3: TSS_{eq} (global calibration) vs. TSS_{lab} with linear regression model and confidence bounds.

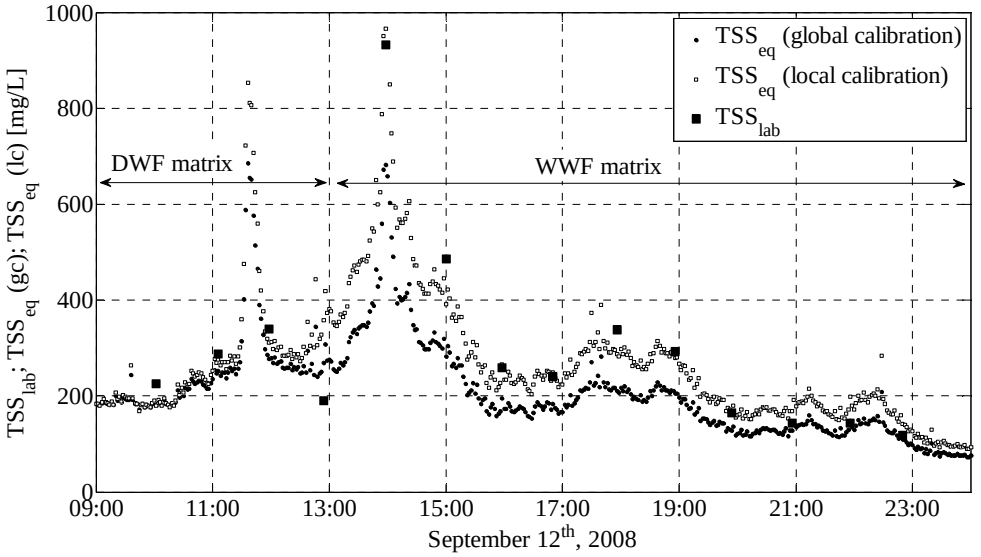

Figure K-4: Results of calibration for WWF matrix of inflow Riool-Zuid: TSS_{eq} (global calibration, 2-minute interval) converted into TSS_{eq} (local calibration, 2-minute interval) and compared to TSS_{lab} (1 sample per hour). Before 13h00, the DWF local calibration set is used based on the results presented in Figure K-2.

inflow **Riool-Zuid**, parameter **COD**, **DWF** matrix

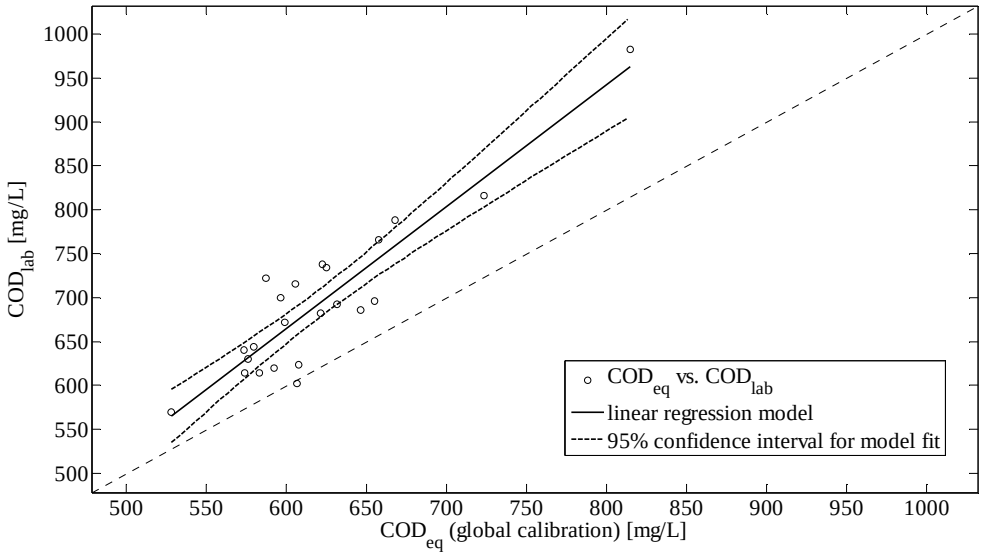

Figure K-5: COD_{eq} (global calibration) vs. COD_{lab} with linear regression model and confidence bounds.

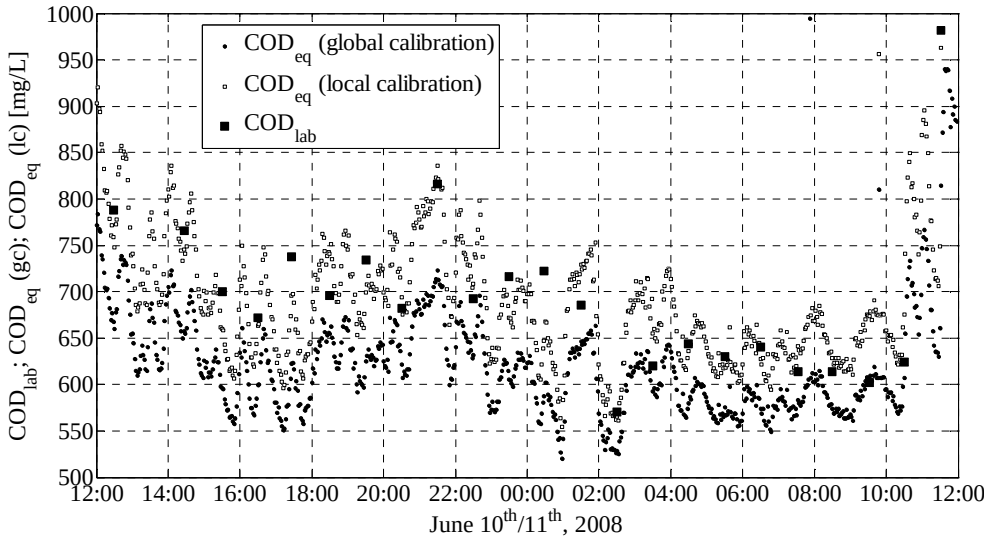

Figure K-6: Results of local calibration for DWF matrix of inflow Riool-Zuid: COD_{eq} (global calibration, 2-minute interval) transposed to COD_{eq} (local calibration, 2-minute interval) and compared to COD_{lab} (1 sample per hour).

inflow **Riool-Zuid**, parameter **COD**, **WWF** matrix

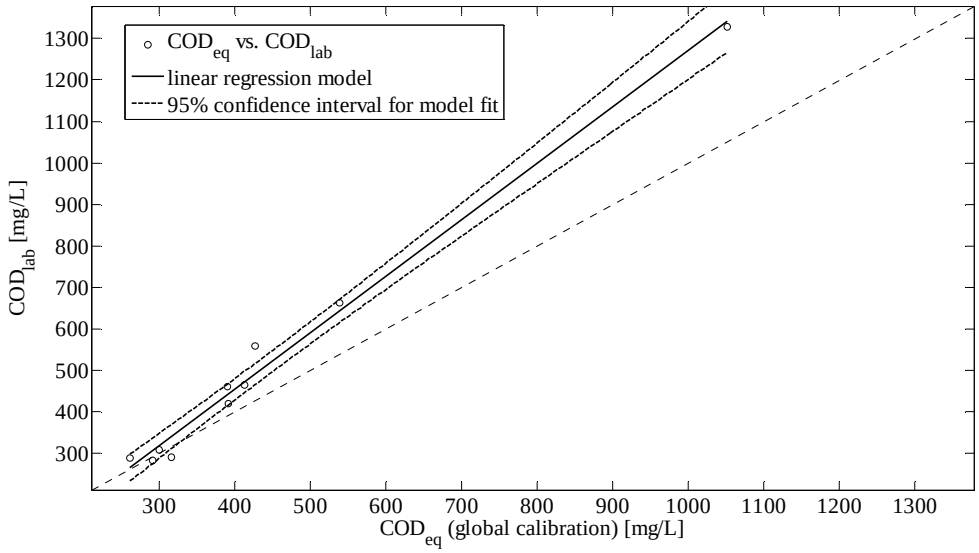

Figure K-7: COD_{eq} (global calibration) vs. COD_{lab} with linear regression model and confidence bounds.

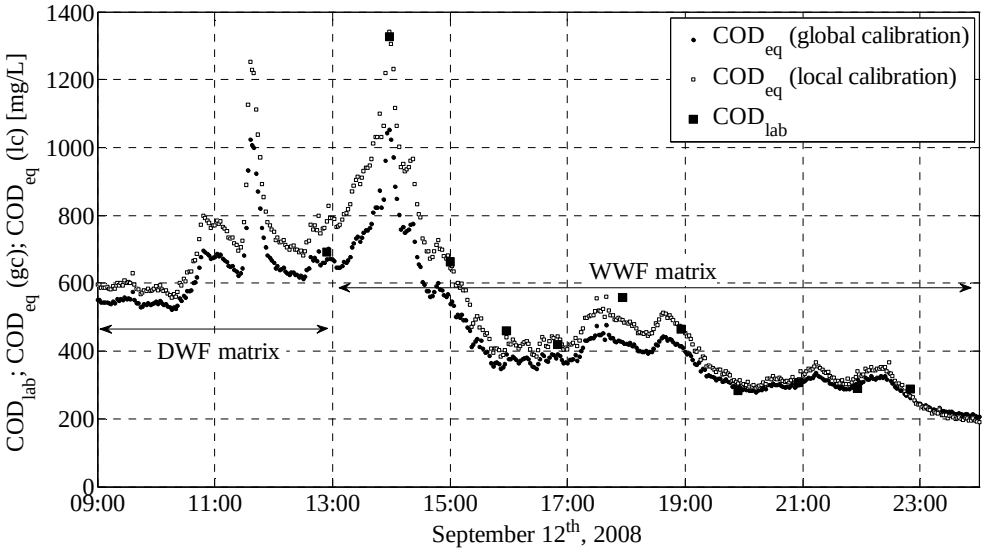

Figure K-8: Results of local calibration for WWF matrix of inflow Riool-Zuid: COD_{eq} (global calibration, 2-minute interval) transposed to COD_{eq} (local calibration, 2-minute interval) and compared to COD_{lab} (1 sample per hour). Before 13h00, the DWF local calibration set is used based on the results presented in Figure K-6.

inflow **Riool-Zuid**, parameter **CODf**, **DWF** and **WWF** matrices

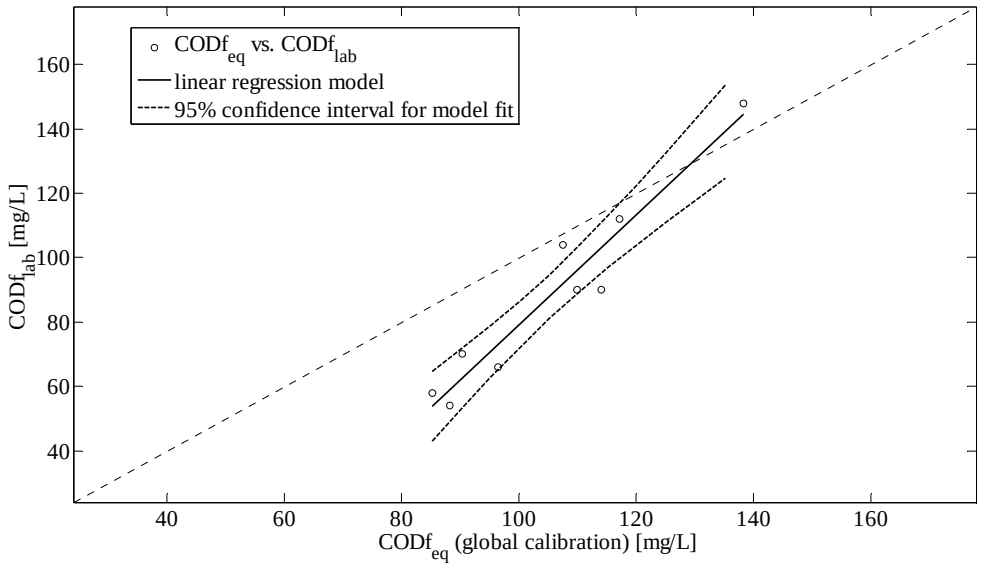

Figure K-9: For **WWF** matrix: $CODf_{eq}$ (global calibration) vs. $CODf_{lab}$ with linear regression model and confidence bounds.

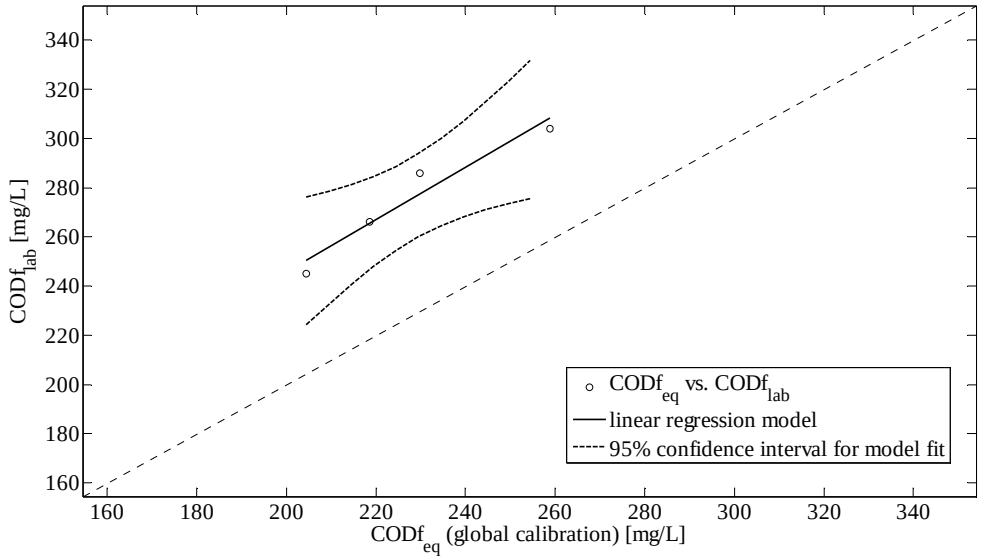

Figure K-10: For **DWF** matrix: $CODf_{eq}$ (global calibration) vs. $CODf_{lab}$ with linear regression model and confidence bounds. The number of samples for this matrix is limited and values are restricted to a small range. As a result, the regression model is founded on a small basis, which should be taken into account when considering locally calibrated values.

inflow **Riool-Zuid**, parameter **CODf**, **DWF** and **WWF** matrices (continued)

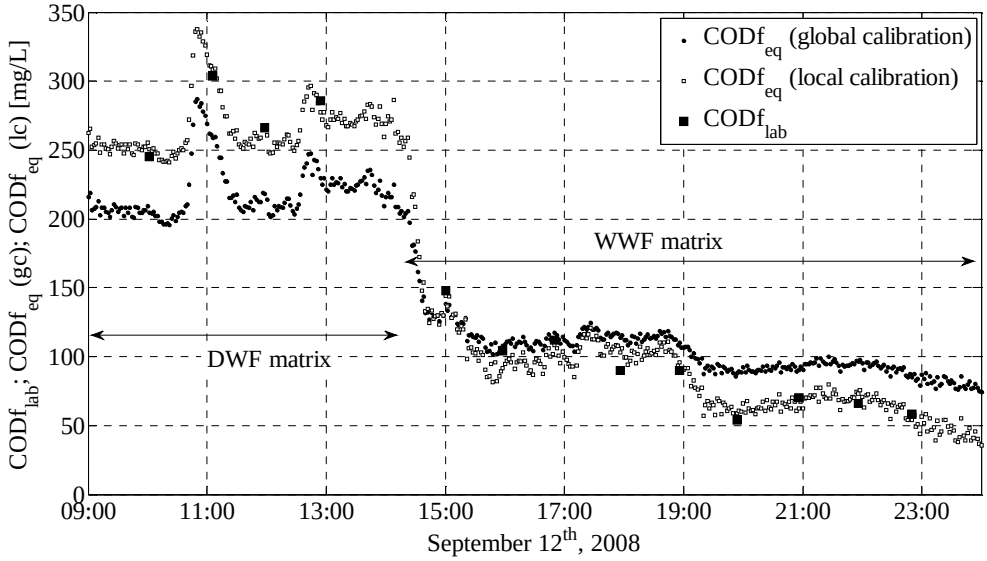

Figure K-11: Results of calibration for DWF and WWF matrices of inflow Riool-Zuid: $CODf_{eq}$ (global calibration, 2-minute interval) converted into $CODf_{eq}$ (local calibration, 2-minute interval) and compared to $CODf_{lab}$ (1 sample per hour). The calibration set as presented here is a linear combination of a DWF set (valid 09h00 - 14h00) and a WWF set (valid 14h00 - 24h00).

Please note that the results of the four grab samples collected during the *WWF* campaign prior to dilution have been used to derive a *DWF* local calibration set for lack of results (for CODf) during the DWF campaign.

inflow **Eindhoven Stad**, parameter **TSS**, **DWF** matrix

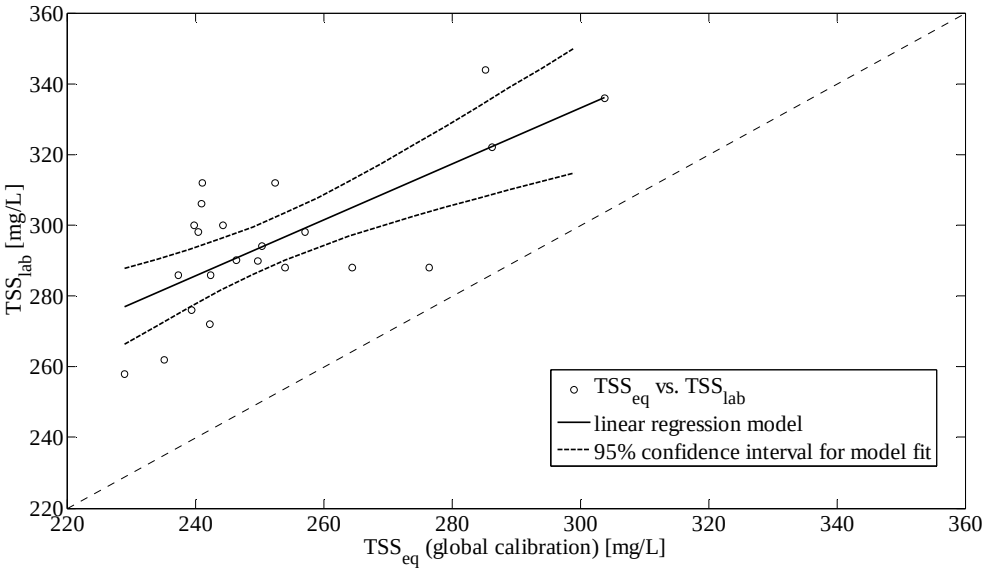

Figure K-12: TSS_{eq} (global calibration) vs. TSS_{lab} with linear regression model and confidence bounds.

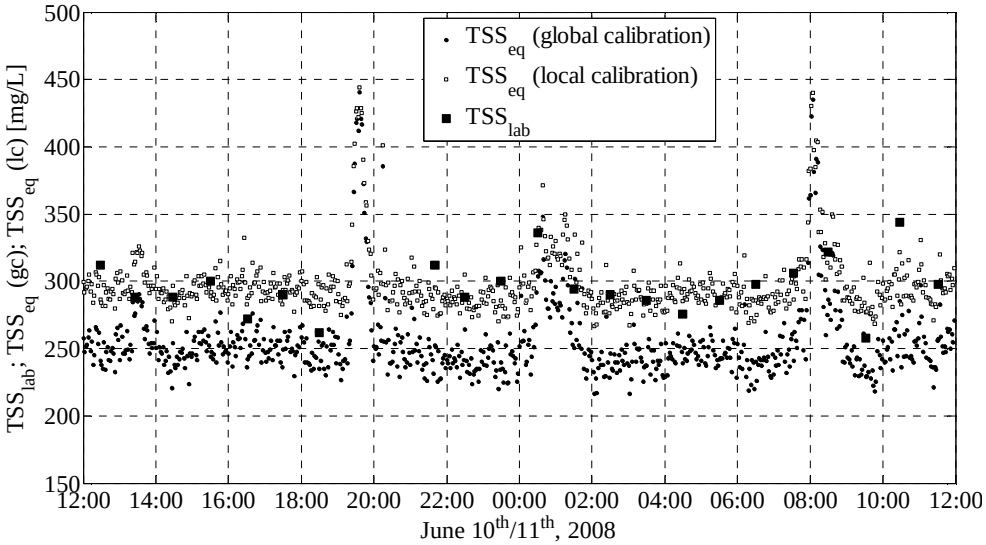

Figure K-13: Results of calibration for DWF matrix of inflow Eindhoven Stad: TSS_{eq} (global calibration, 2-minute interval) converted into TSS_{eq} (local calibration, 2-minute interval) and compared to TSS_{lab} (1 sample per hour).

inflow **Eindhoven Stad**, parameter **TSS**, **WWF** matrix

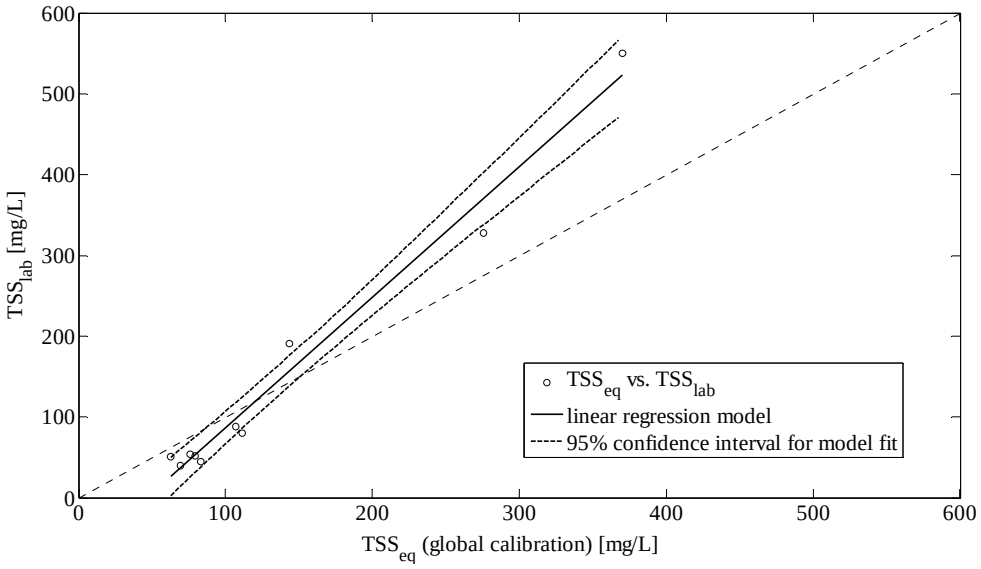

Figure K-14: TSS_{eq} (global calibration) vs. TSS_{lab} with linear regression model and confidence bounds.

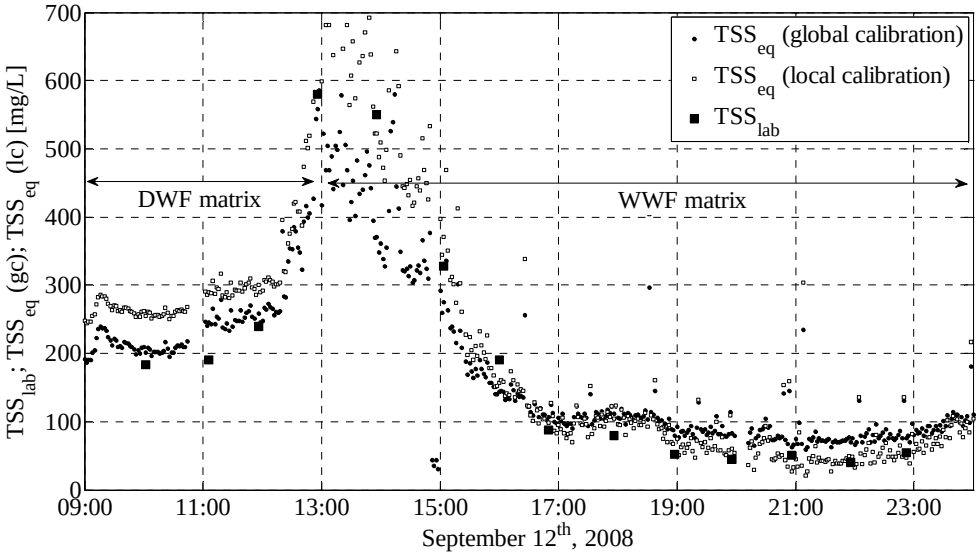

Figure K-15: Results of calibration for WWF matrix of inflow Eindhoven Stad: TSS_{eq} (global calibration, 2-minute interval) converted into TSS_{eq} (local calibration, 2-minute interval) and compared to TSS_{lab} (1 sample per hour). Before 13h00, the DWF local calibration set is used based on the results presented in Figure K-13.

inflow **Eindhoven Stad**, parameter **COD**, **DWF** matrix

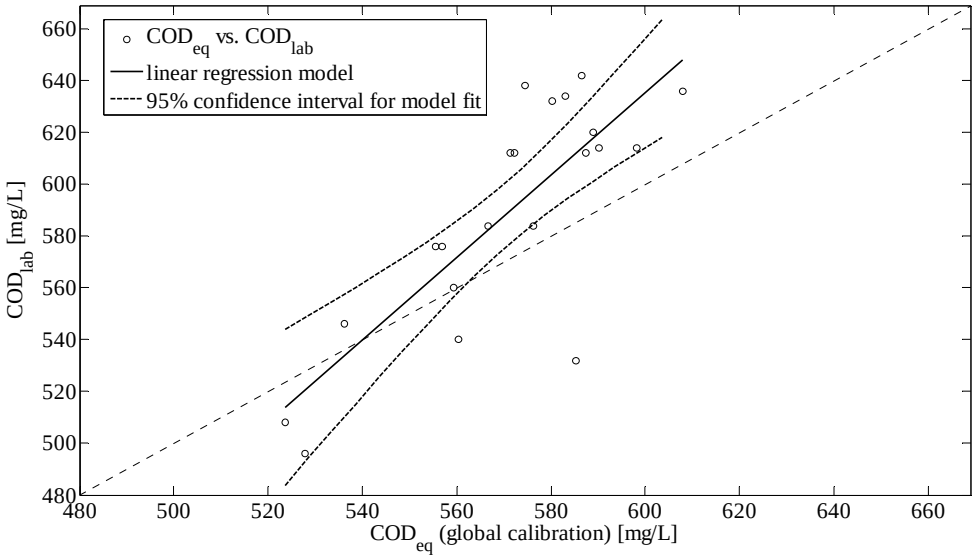

Figure K-16: COD_{eq} (global calibration) vs. COD_{lab} with linear regression model and confidence bounds.

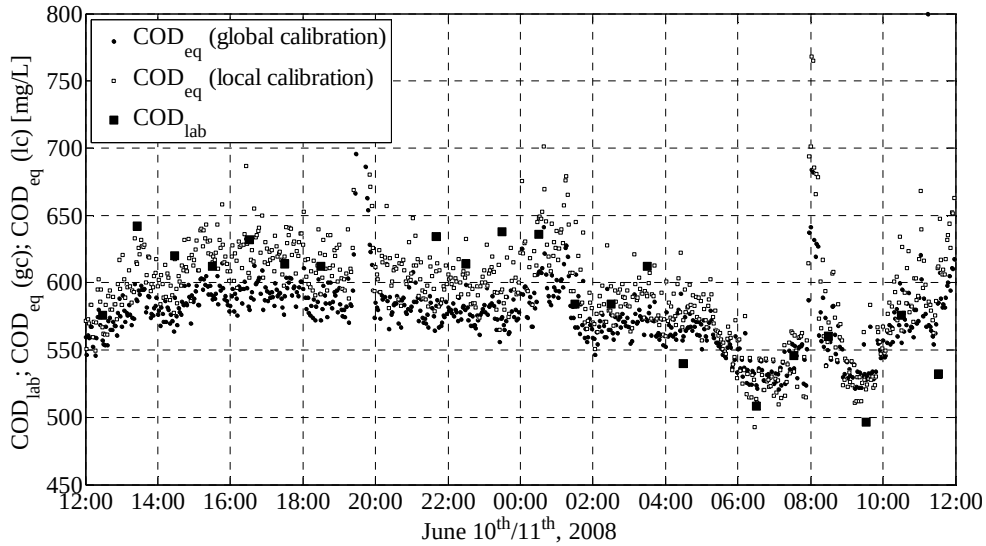

Figure K-17: Results of calibration for DWF matrix of inflow Eindhoven Stad: COD_{eq} (global calibration, 2-minute interval) converted into COD_{eq} (local calibration, 2-minute interval) and compared to COD_{lab} (1 sample per hour).

inflow **Eindhoven Stad**, parameter **COD**, **WWF** matrix

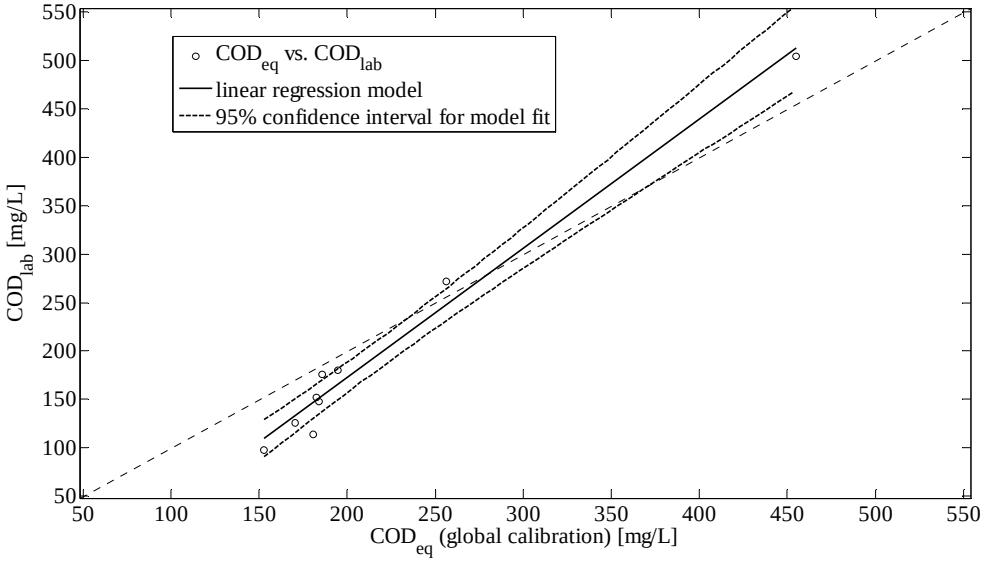

Figure K-18: COD_{eq} (global calibration) vs. COD_{lab} with linear regression model and confidence bounds.

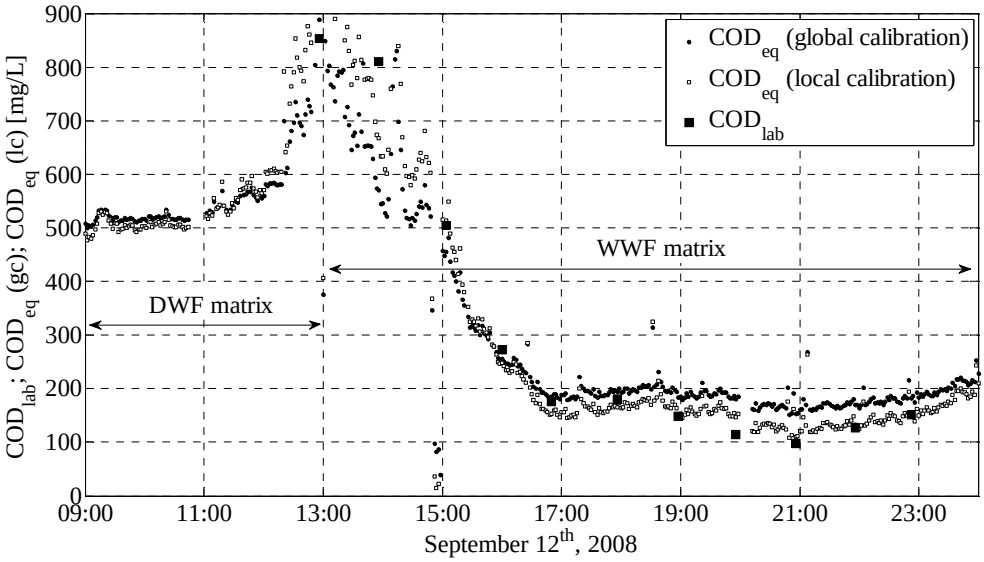

Figure K-19: Results of calibration for WWF matrix of inflow Eindhoven Stad: COD_{eq} (global calibration, 2-minute interval) converted into COD_{eq} (local calibration, 2-minute interval) and compared to COD_{lab} (1 sample per hour). Before 13h00, the DWF local calibration set is used based on the results presented in Figure K-17.

inflow **Eindhoven Stad**, parameter **CODf**, **DWF** and **WWF** matrices

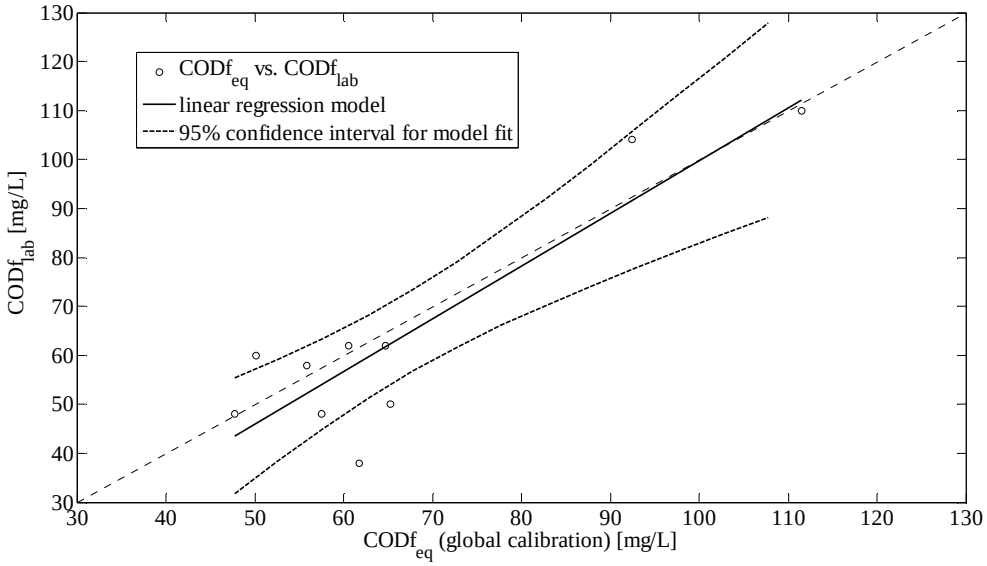

Figure K-20: For **WWF** matrix: $CODf_{eq}$ (global calibration) vs. $CODf_{lab}$ with linear regression model and confidence bounds.

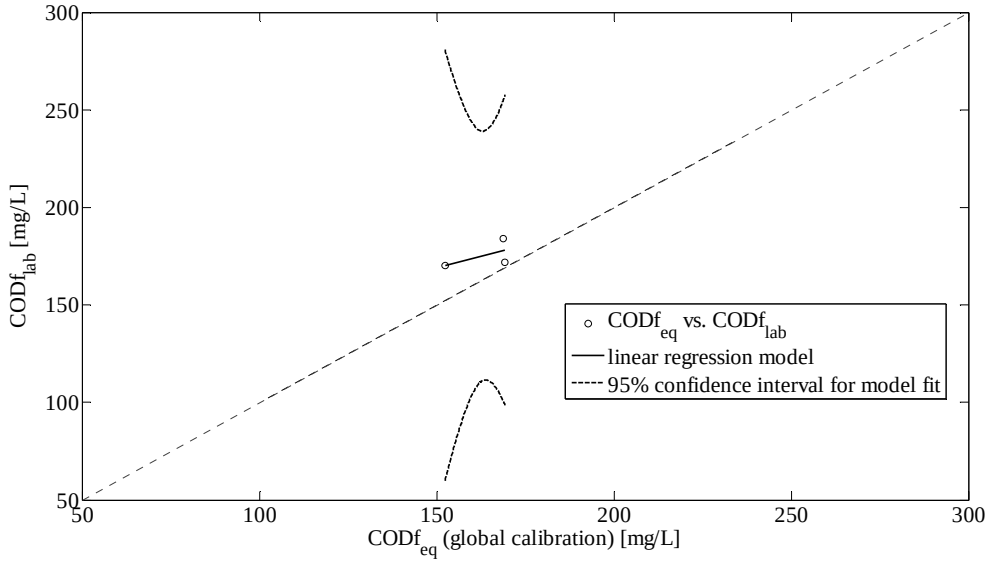

Figure K-21: For **DWF** matrix: $CODf_{eq}$ (global calibration) vs. $CODf_{lab}$ with linear regression model and confidence bounds. The samples collected for this matrix only cover a small bandwidth, hampering the calibration of values outside the bandwidth. Also, the number of samples is limited which hampers the detection of outliers. As a result, locally calibrated values for this parameter should be considered with care.

inflow **Eindhoven Stad**, parameter **CODf**, **DWF** and **WWF** matrices (continued)

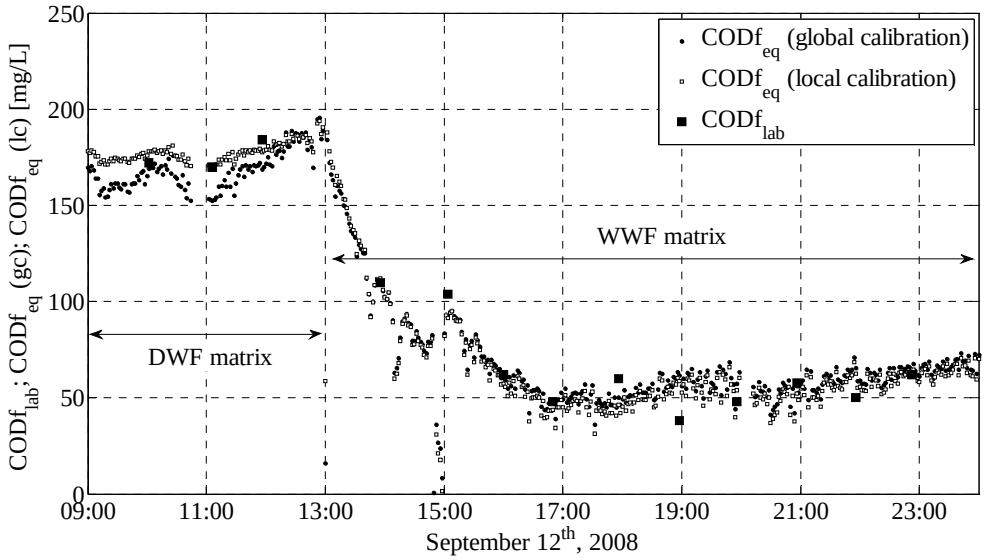

Figure K-22: Results of calibration for DWF and WWF matrices of inflow Eindhoven Stad: $CODf_{eq}$ (global calibration, 2-minute interval) converted into $CODf_{eq}$ (local calibration, 2-minute interval) and compared to $CODf_{lab}$ (1 sample per hour). The calibration set is a linear combination of a DWF set (09h00 - 13h00) and a WWF set (13h00 - 24h00).

Please note that the results of the three grab samples collected during the *WWF* campaign prior to dilution have been used to derive a *DWF* local calibration set for lack of results (for CODf) during the DWF campaign.

inflow **Nuenen/Son**, parameter **TSS**, **DWF** matrix

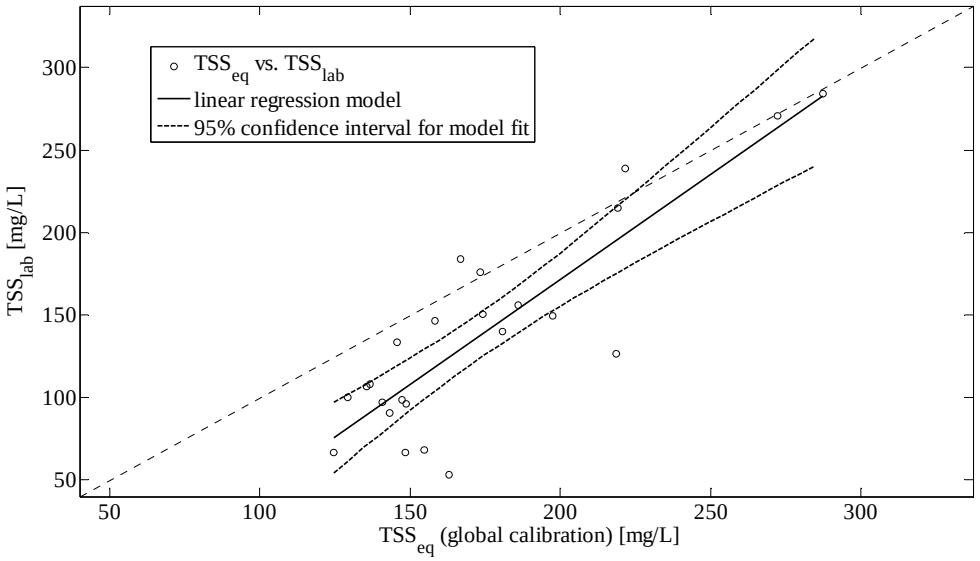

Figure K-23: TSS_{eq} (global calibration) vs. TSS_{lab} with linear regression model and confidence bounds.

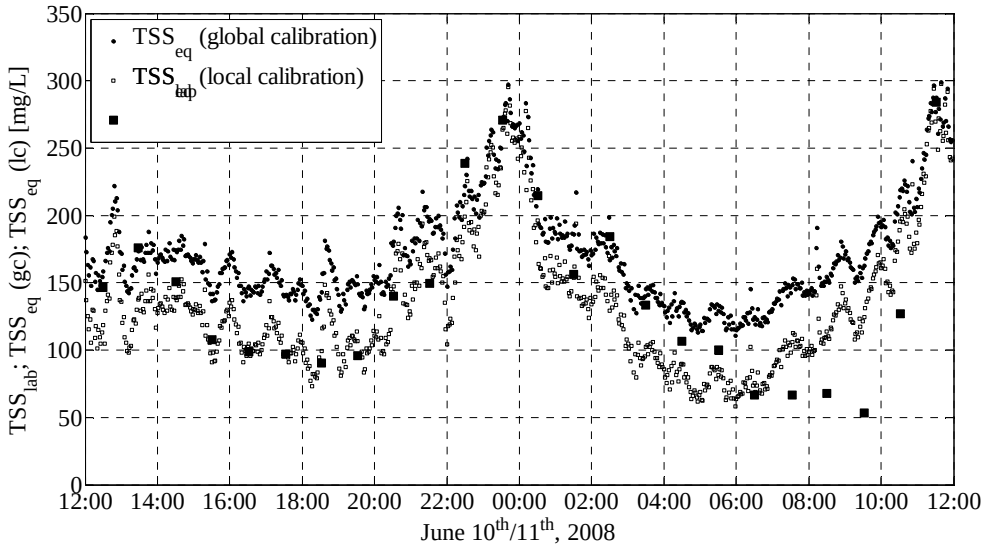

Figure K-24: Results of calibration for DWF matrix of inflow Nuenen/Son: TSS_{eq} (global calibration, 2-minute interval) converted into TSS_{eq} (local calibration, 2-minute interval) and compared to TSS_{lab} (1 sample per hour).

inflow **Nuenen/Son**, parameter **TSS**, **WWF** matrix

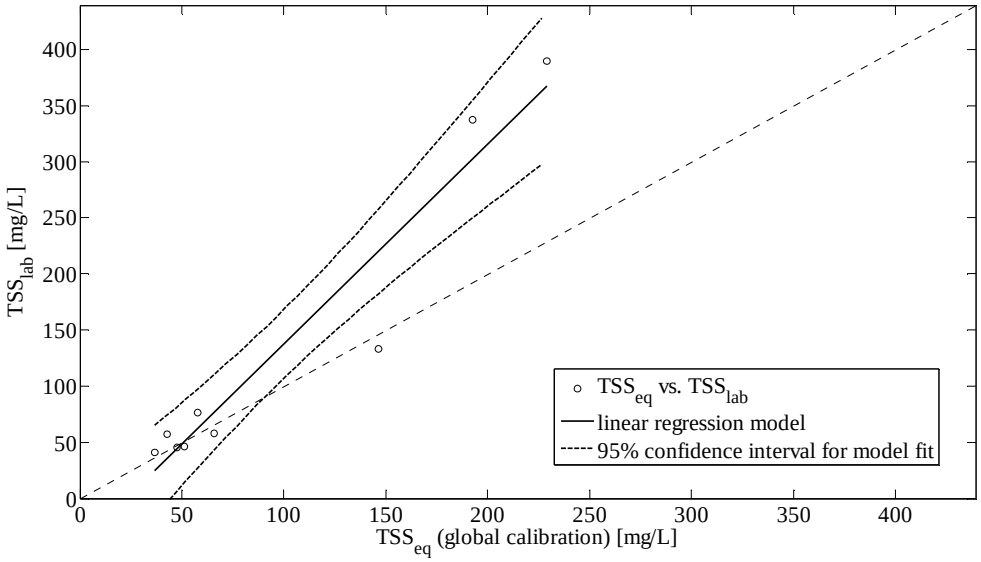

Figure K-25: TSS_{eq} (global calibration) vs. TSS_{lab} with linear regression model and confidence bounds.

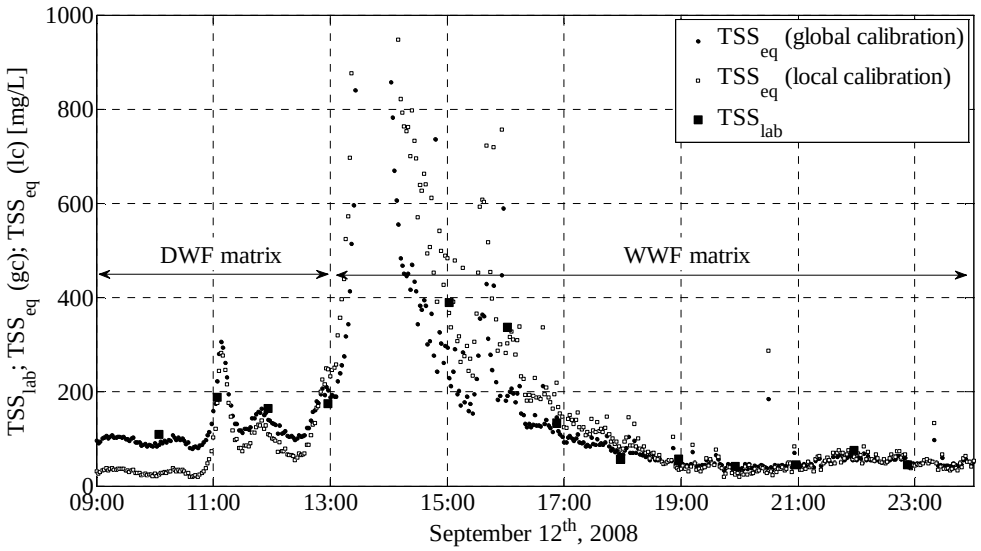

Figure K-26: Results of calibration for WWF matrix of inflow Nuenen/Son: TSS_{eq} (global calibration, 2-minute interval) converted into TSS_{eq} (local calibration, 2-minute interval) and compared to TSS_{lab} (1 sample per hour). Before 13h00, the DWF local calibration set is used based on the results presented in Figure K-24. The sample collected at 13h58 has been removed from the WWF laboratory data set prior to calibration.

inflow **Nuenen/Son**, parameter **COD, DWF** matrix

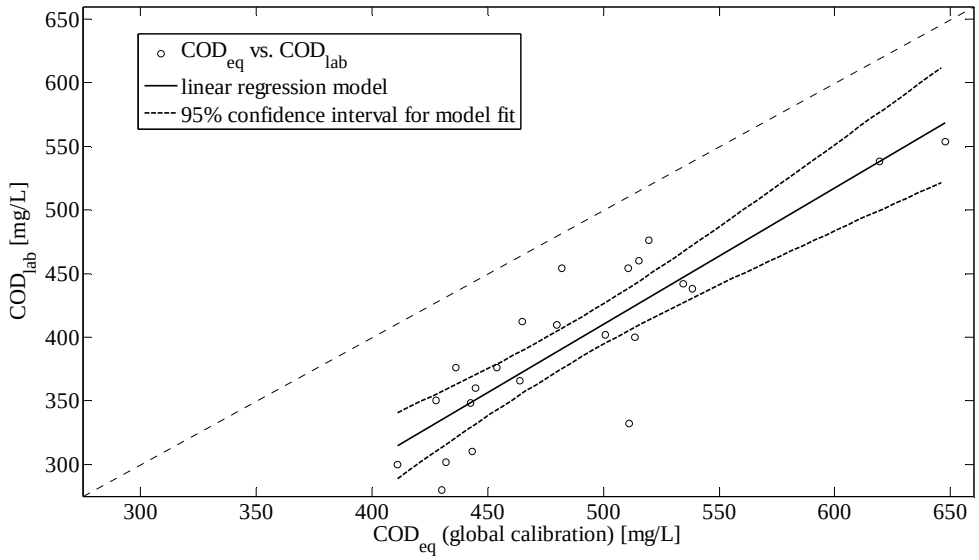

Figure K-27: COD_{eq} (global calibration) vs. COD_{lab} with linear regression model and confidence bounds.

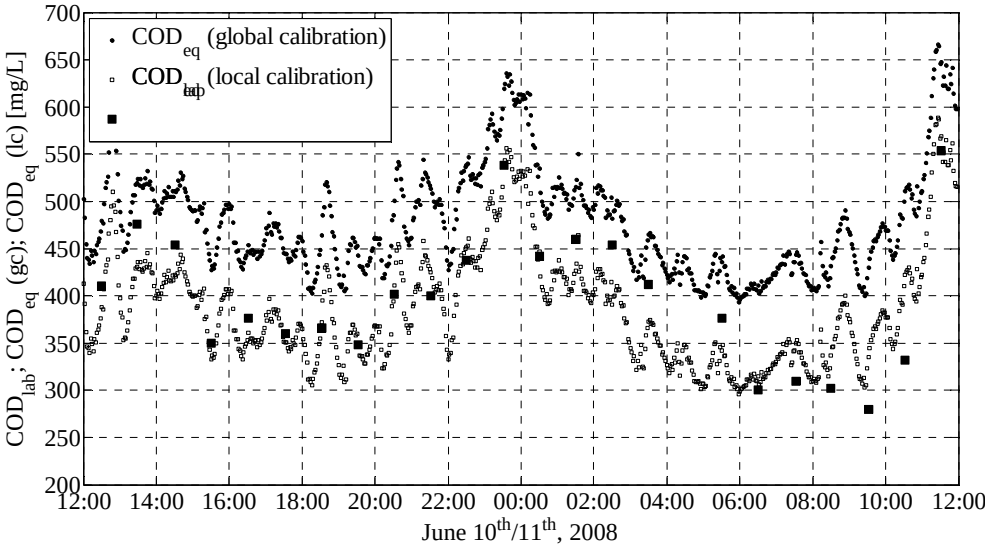

Figure K-28: Results of calibration for DWF matrix of inflow Nuenen/Son: COD_{eq} (global calibration, 2-minute interval) converted into COD_{eq} (local calibration, 2-minute interval) and compared to COD_{lab} (1 sample per hour).

inflow **Nuenen/Son**, parameter **COD, WWF** matrix

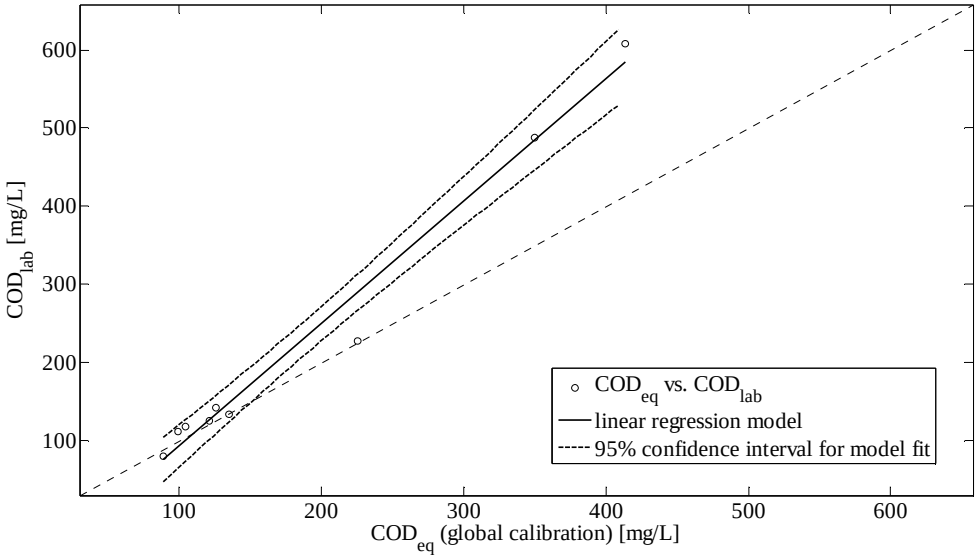

Figure K-29: COD_{eq} (global calibration) vs. COD_{lab} with linear regression model and confidence bounds.

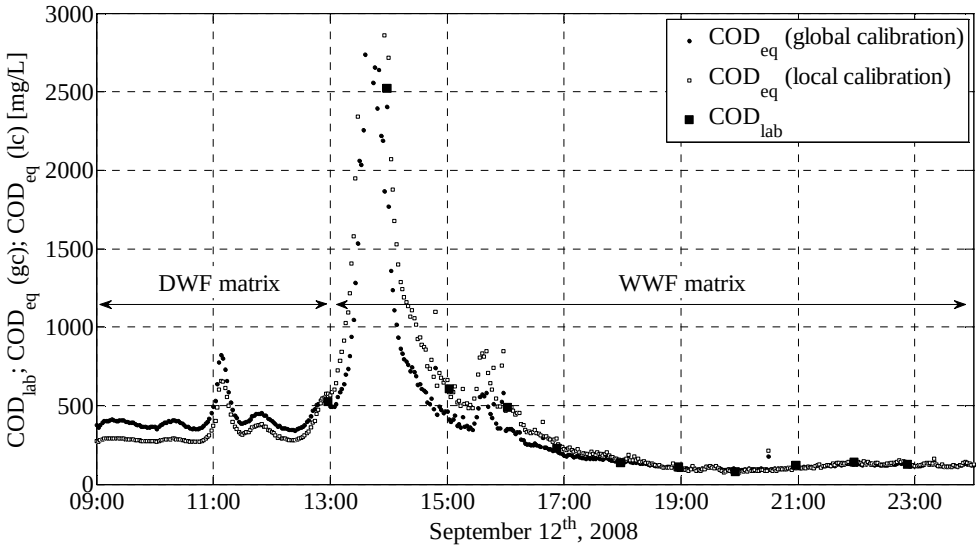

Figure K-30: Results of calibration for WWF matrix of inflow Nuenen/Son: COD_{eq} (global calibration, 2-minute interval) converted into COD_{eq} (local calibration, 2-minute interval) and compared to COD_{lab} (1 sample per hour). Before 13h00, the DWF local calibration set is used based on the results presented in Figure K-28. The sample collected at 13h58 has been removed from the WWF laboratory data set prior to calibration.

inflow **Nuenen/Son**, parameter **CODf**, **DWF** and **WWF** matrices

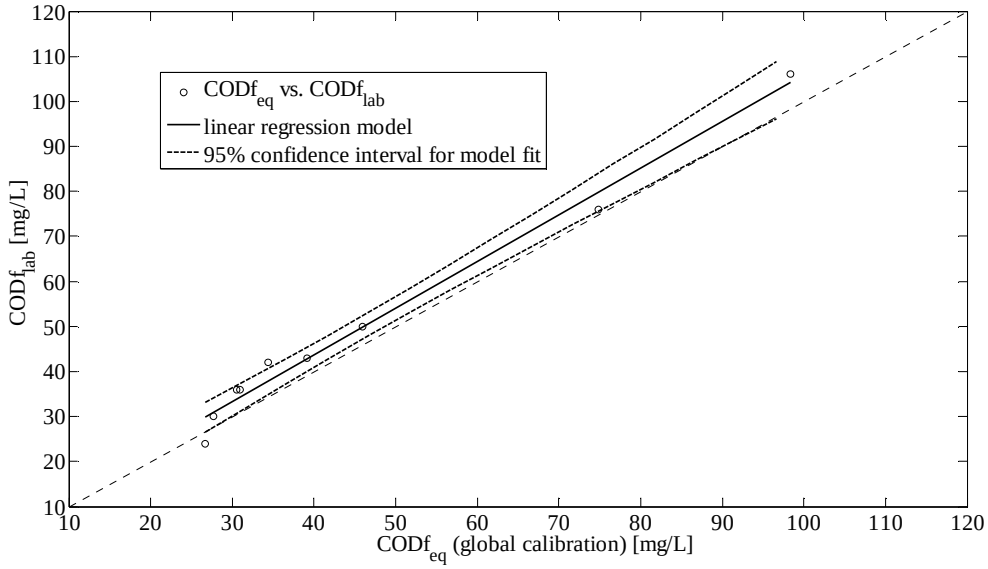

Figure K-31: For **WWF** matrix: $CODf_{eq}$ (global calibration) vs. $CODf_{lab}$ with linear regression model and confidence bounds.

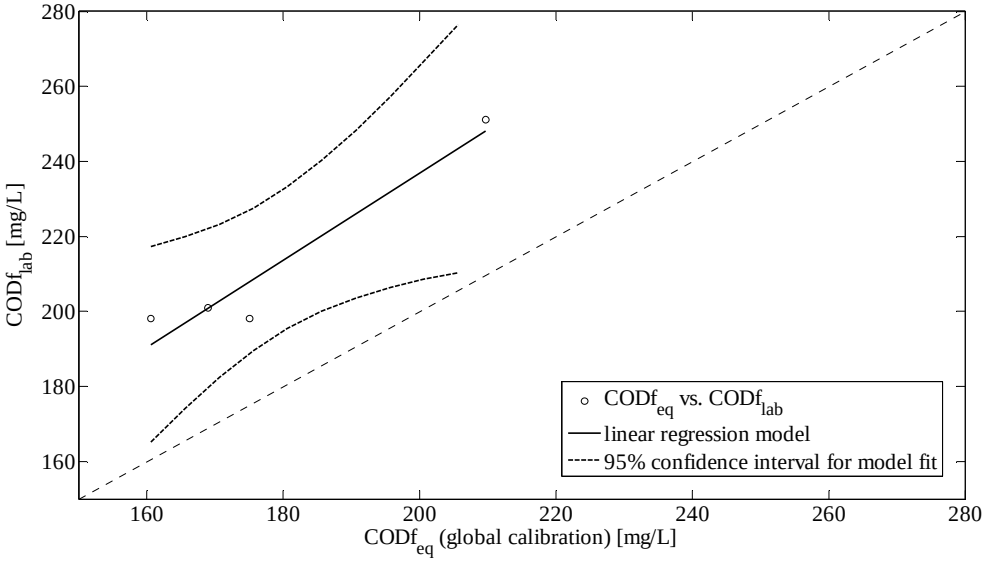

Figure K-32: For **DWF** matrix: $CODf_{eq}$ (global calibration) vs. $CODf_{lab}$ with linear regression model and confidence bounds. The samples collected for this matrix only cover a small bandwidth, hampering the calibration of values outside the bandwidth. Also, the number of samples is limited which hampers the detection of outliers. As a result, locally calibrated values for this parameter should be considered with care.

inflow **Nuenen/Son**, parameter **CODf**, **DWF** and **WWF** matrices (continued)

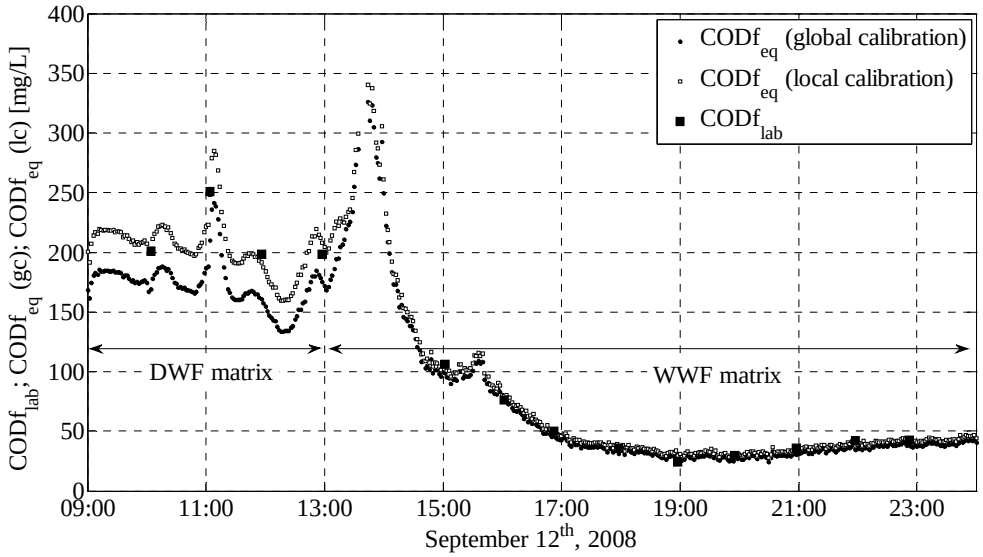

Figure K-33: Results of calibration for DWF+WWF matrices of inflow Nuenen/Son: $CODf_{eq}$ (global calibration, 2-minute interval) converted into $CODf_{eq}$ (local calibration, 2-minute interval) and compared to $CODf_{lab}$ (1 sample per hour). The calibration set is a linear combination of a DWF set (09h00 - 13h00) and a WWF set (13h00 - 24h00).

Please note that the results of the four grab samples collected during the *WWF* campaign prior to dilution have been used to derive a *DWF* local calibration set for lack of results (for CODf) during the DWF campaign.

Appendix L. DTS monitoring results in storm water sewers

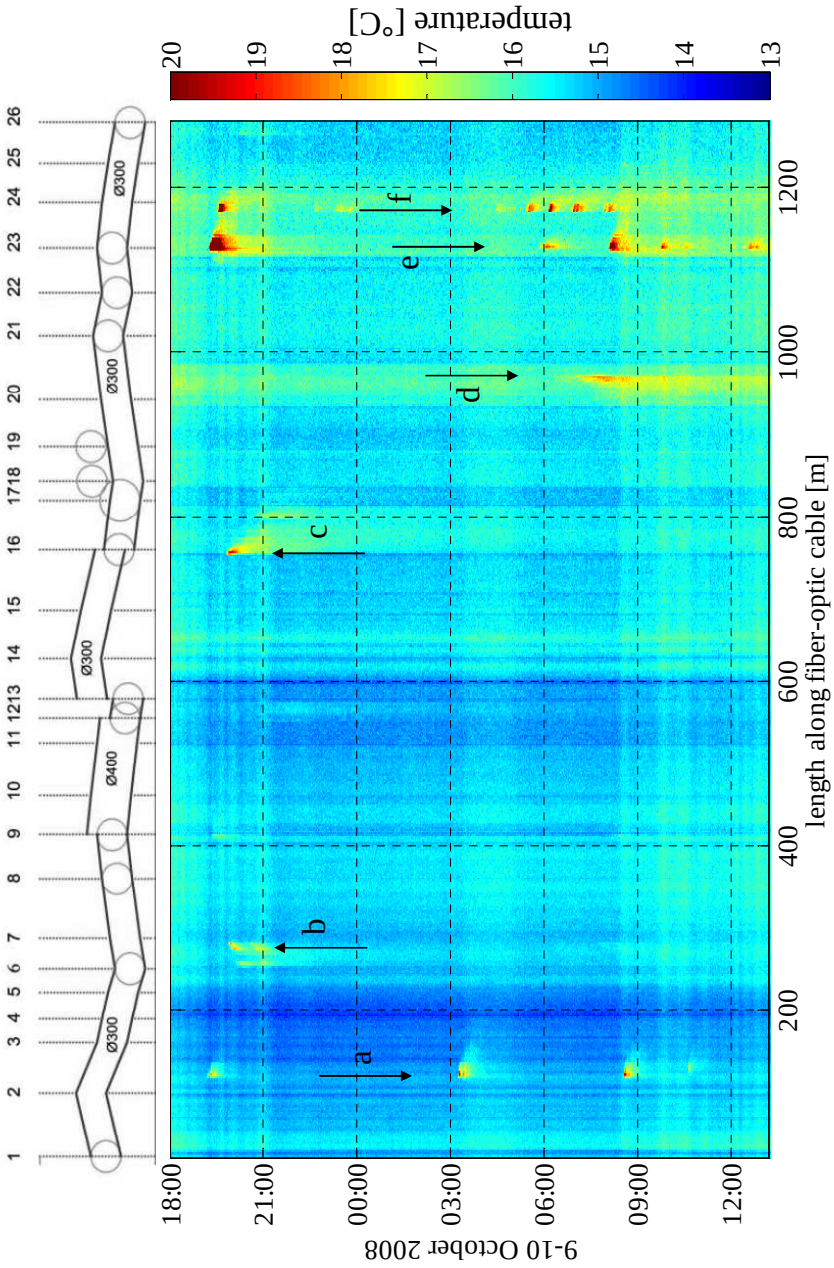

Figure L-1: DTS monitoring results for Korendijk, October 9th and 10th, 2008. Details of the graph are explained in section 7.3.5.

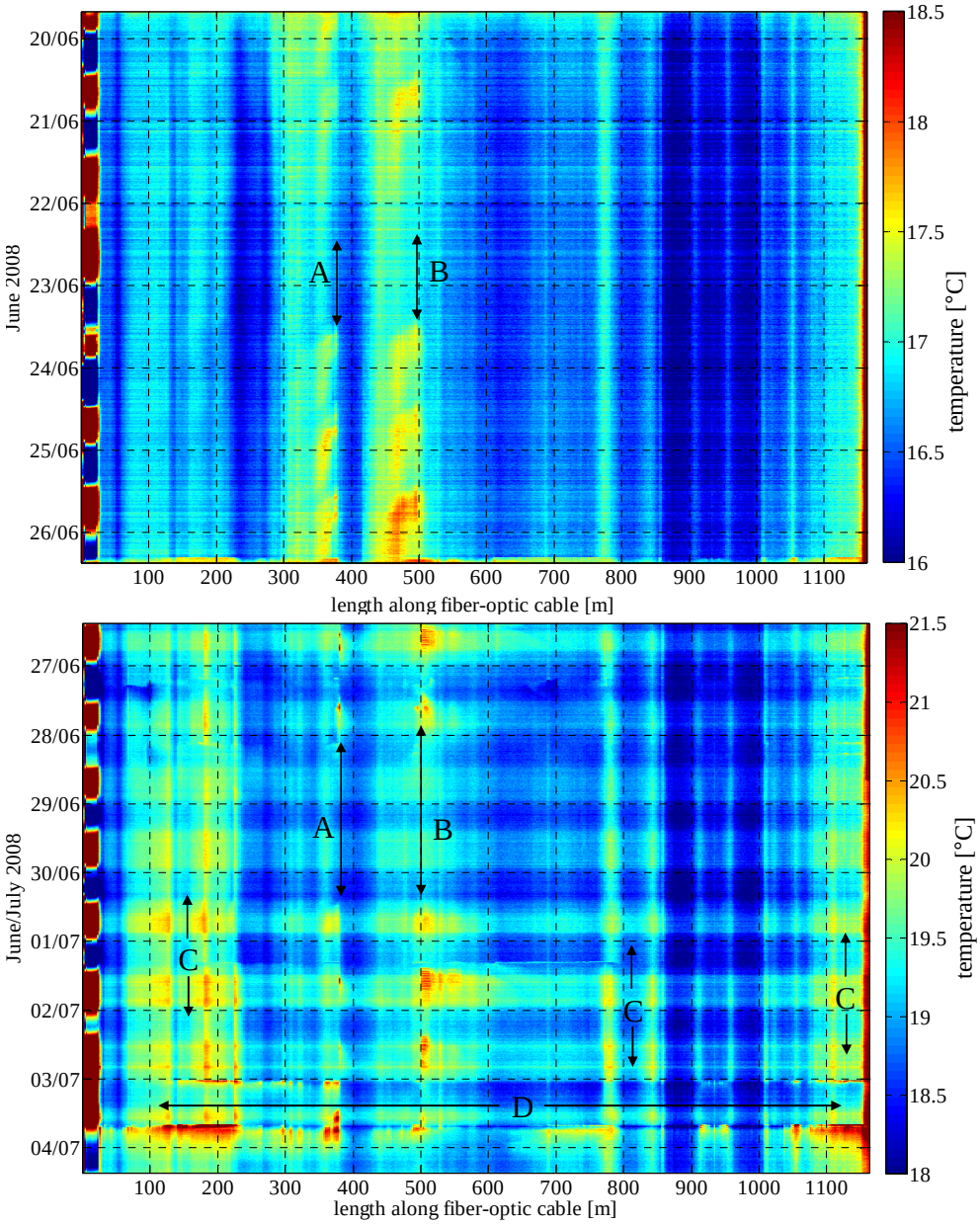

Figure L-2: DTS monitoring results for Groningen, June 19th - July 4th, 2008. Details of the graphs are explained in sections 7.3.5 and 7.3.6.

Appendix M. DTS monitoring results in combined sewer systems

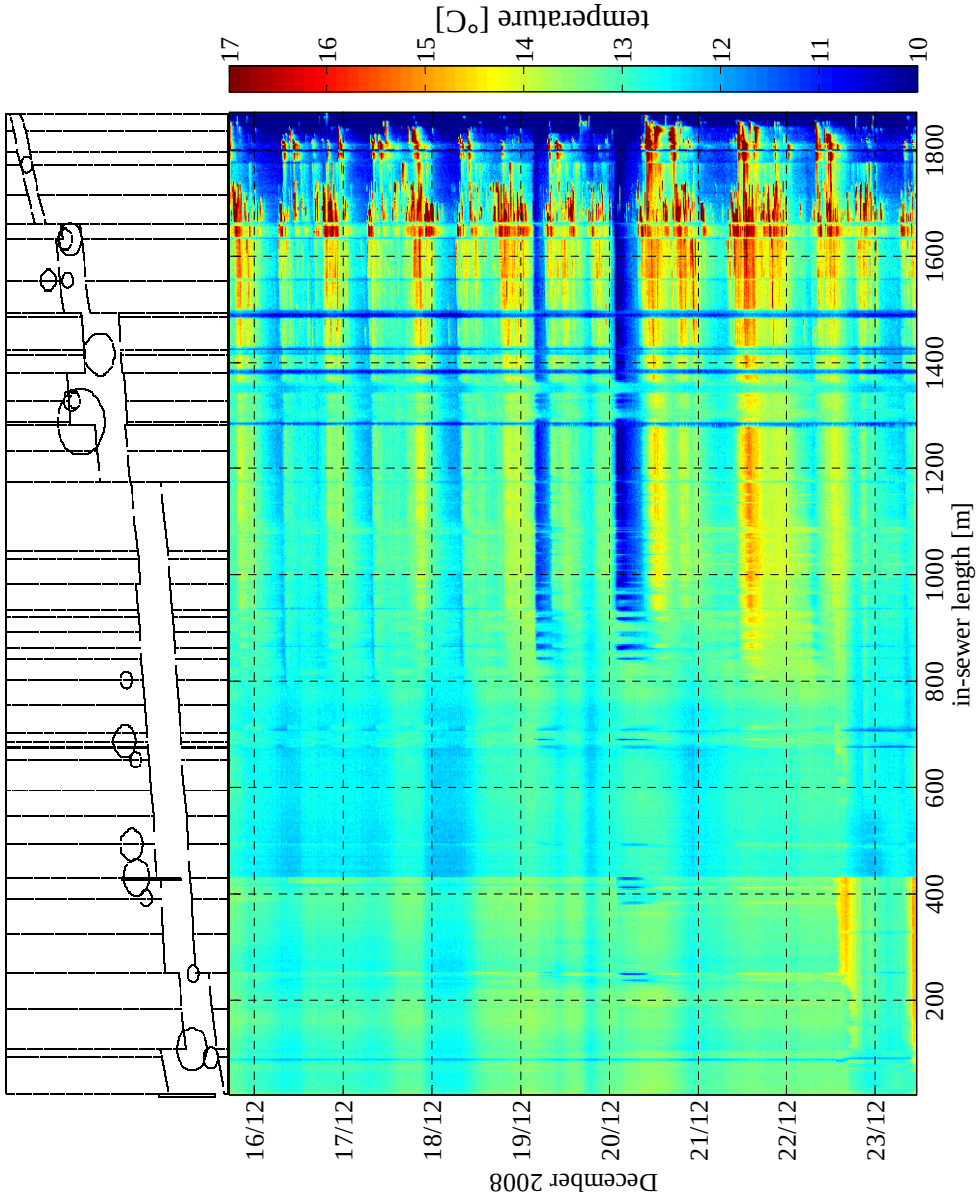

Figure M-1: DTS monitoring results in the combined sewer system of the Ede Rietkampen area, December 15th-23rd, 2008.

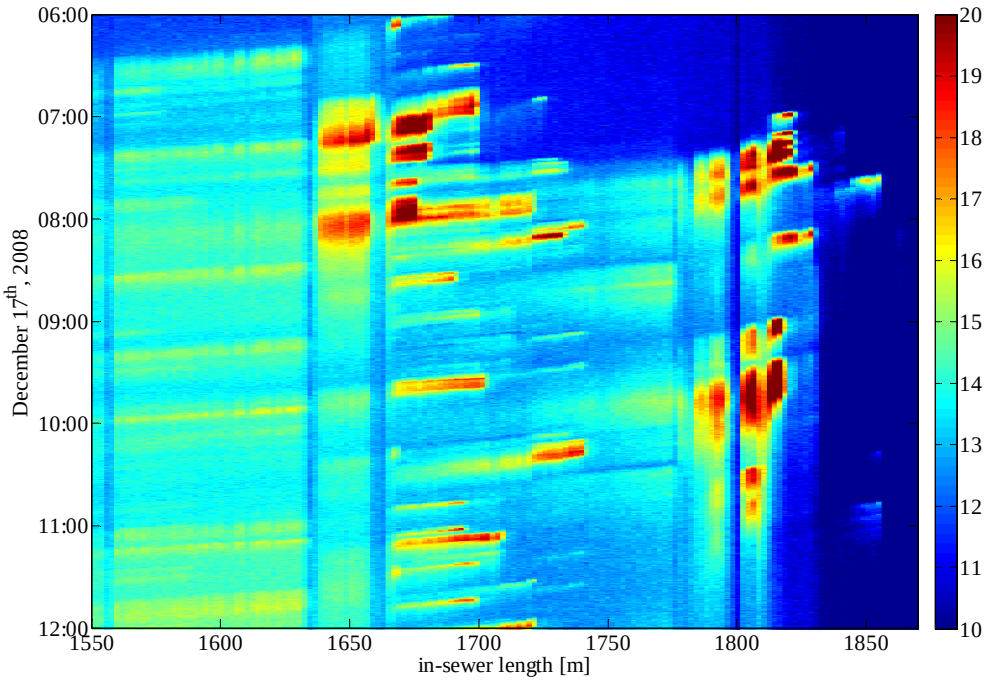

Figure M-2: DTS monitoring results for December 17th, 2008 between 06h00 and 12h00, zoom on data between x=1550 m and x=1850 m.

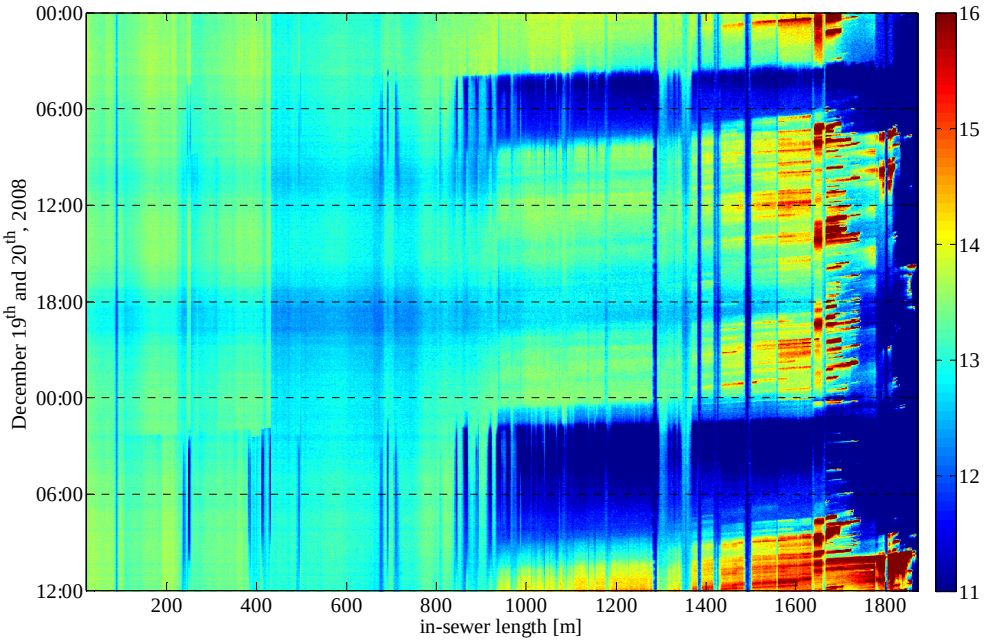

Figure M-3: DTS monitoring results for December 19th and 20th, 2008.

Summary

Monitoring as a tool for the assessment of wastewater quality dynamics

Chapter 1. Introduction

Discharges of (untreated) wastewater are still a major contributor to the total emission of pollutions to surface waters in the Netherlands. Over the last decades large efforts have been made in both practice and science to find ways to improve wastewater system performance and to hence reduce the impact system have on their environment. Optimization programs play an important role in these trials. Research shows that optimization strategies improve when aiming at *integrated* system optimization taking into account for *dynamics* in both water quantity and water *quality* parameters. Acquiring detailed and accurate descriptions of (the dynamics of) in-sewer wastewater quality parameters cannot be achieved using a modeling approach only. Partly because these models need data for calibration and validation purposes and partly because some processes appear to be too complicated to be correctly modeled, a tendency towards *monitoring* of wastewater processes can be observed. Monitoring of flow rates in sewer systems has a long tradition; large-scale trials of in-sewer wastewater quality monitoring, however, is of more recent date. The first objective of this thesis is the further development of in-sewer wastewater metrology. More specifically, it studies the in-sewer application of two novel sensor types: UV/VIS spectroscopy and DTS with fiber optics. The second thesis objective is the assessment of in-sewer wastewater quality dynamics using the UV/VIS and DTS data. The former sensor type has been applied in the influent pumping station of the wwtp Eindhoven; the latter has been tested in combined and separate sewer systems in the municipalities of Ede, Groningen and Korendijk.

Chapter 2. Eindhoven area wastewater system

The 750,000 p.e. wastewater treatment plant in Eindhoven receives wastewater from ten municipalities divided over three distinct catchment areas that differ in size and character. The sewer system of the city of Eindhoven (Eindhoven Stad, approximately 265,000 p.e.) is directly connected to the wwtp whereas wastewater from seven municipalities south of Eindhoven (260,000 p.e.) is collected in a 32 km long transport sewer (Riool-Zuid). Two municipalities north of Eindhoven (52,000 p.e.) discharge via a 5 km transport sewer (Nuenen/Son). Wwtp effluent is discharged to the river Dommel. Especially in dry summer months wwtp effluent can make up a large fraction of total flow in the river: up to 50% for dry weather, and even up to 90% for wet weather. As a result, (emergency) discharges of effluent can easily cause exceeding of surface water quality standards as well as severe damage to the ecology in the river. Hence, the operator of the wwtp (water

board De Dommel) has expressed the ambition to optimize the wastewater system in the Eindhoven area and investigates - among other options - the possibilities to apply a form of real-time control. For this, it has conceived and installed a monitoring network comprising precipitation, water quantity and water quality sensors.

Chapter 3. Precipitation monitoring

Precipitation is an important driving force behind in-sewer wastewater quantity and quality variations. Hence, 22 tipping-bucket raingauges have been installed in the Eindhoven area to collect high-frequent rain data. A thorough data quality assessment has been applied on the data sets. Manual and automatic checks for data gaps and anomalous data have resulted in rejection of approximately 50% of data. For comparison of long-term performance (in terms of recorded precipitation depths) data have been used from six other raingauges in the area operated by the Royal Netherlands Meteorological Institute. Results show that the tipping-bucket raingauges underestimate precipitation depths by around 20% to 25%. Half of this bias is explained by a lacking sensor calibration; data have been corrected for this error after an *a posteriori* calibration effort. The other half of the systematic error is likely due to unfavorable observation conditions: many tipping-buckets have suffered from wind shading due to nearby objects. For this error correction has not been possible. In conclusion, the overall monitoring performance of the tipping-buckets has been poor, but the (validated and corrected) data sets have nevertheless been used to derive precipitation time-series for the three studied catchment area using an inverse distance weighting method. As they have been used qualitatively rather than quantitatively, the poor quality of the precipitation times-series has had a limited influence on the outcome of data analyses in chapter 6.

Chapter 4. Flow monitoring

For calculation of pollutant *loads* arriving at the wwtp Eindhoven, data sets on both water quantity (chapter 4) as well as water quality (chapter 5) are required. To derive three time-series that represent the inflow of wastewater from catchment areas Riool-Zuid, Eindhoven Stad and Nuenen/Son into the wwtp Eindhoven, the data sets of nine flow sensors have been used. Each flow sensor monitors a wwtp influent pump; each catchment area is serviced by two, three or four influent pumps. Flow sensor data sets have first been assessed for quality, revealing almost no anomalous data but a systematic error due to non-zero baselines for non-operational pumps. Subsequently, the nine flow sensor data sets have been combined to obtain three time-series with flows from the considered catchment areas. In this process, a frequently changing allocation of one specific pump as well as flow over an internal weir at the influent pumping station have been taken into account. Data uncertainty assessment shows that around 99% of data has an associated uncertainty of less than 1%; during large storm events the uncertainty

can increase to around 10% due to a relatively large uncertainty associated with flow over the internal weir.

Chapter 5. Water quality monitoring

Wastewater quality data sets have been generated by means of three UV/VIS spectrometers (one per catchment area inflow) that provide high-frequent optical measurements of the wastewater in a dedicated by-pass installation. The long-term operation of a by-pass installation can be demanding. Targeted pollutant parameters are total suspended solids (TSS) and total and soluble chemical oxygen demand (COD and CODf). Dry weather and wet weather reference sampling campaigns have demonstrated that the sensors are capable of reproducing trends in the variation of pollutant concentration values. Using the manufacturer's calibration set (global calibration), relative errors between sensor and laboratory values for dry weather flow conditions are roughly within a range of ±25% (Riool-Zuid, Eindhoven Stad) or ±50% (Nuenen/Son). For wet weather flow conditions relatively large absolute errors have been observed during initial peak moments as well as relatively large relative errors during the dilution phase of the storm event. Using the reference samples, local calibration sets have been derived constructing a linear regression model between raw sensor values and laboratory reference values. All local calibration sets yield an improved fit between sensor and laboratory values. Some calibration sets can be disputed since they are based on too few reference samples; additional sampling is required for these calibration sets. An error estimate of locally calibrated sensor values is obtained accounting for sensor uncertainty and uncertainty in the calibration regression function. Concerns are the limited number and possible ill-representativeness of collected samples for a number of wastewater matrices. A quality assessment of the data sets has shown that 25 to 50% of the data is rejected. The majority of data loss is associated with (avoidable) errors that are non-intrinsic to the sensor. Hence, it is concluded that - with proper sensor and by-pass operation and maintenance - a data yield of more than 90% is achievable for wastewater quality monitoring with this type of sensor.

Chapter 6. Wwtp Eindhoven influent analysis

The dynamics of wastewater arriving at the wwtp Eindhoven from catchment areas Riool-Zuid, Eindhoven Stad and Nuenen/Son are studied in this chapter. *Dry weather* flows show, based on data of approximately 200 dry weather days, typical diurnal, weekday and long-term variations. Based on 100 to 150 dry weather days, diurnal and weekday variations can also be observed for water quality parameters. Suspended solids concentrations in wastewater are partly governed by flow variations. Hence, the shape of dry weather pollutographs for TSS and COD are largely similar to their equivalent for flow, leading to even larger pollutant *load* variations. Dissolved COD is less influenced by this phenomenon and shows a more constant dry weather pollutograph. For dry weather flows and pollutant loads

a catchment size effect has been observed: the smallest catchment area is associated with the largest deviations from mean values and vice versa.
Under *wet weather* conditions arriving pollutant loads at the wwtp Eindhoven are (much) larger than under dry weather conditions. Using data of approximately 65 storm events the arriving pollutant loads (averaged over 24 hours) have been calculated and compared to their dry weather equivalent. Results show that 'mean storm events' lead to the arrival of 2 to 3 times the suspended solids load for areas Riool-Zuid and Eindhoven Stad and 5.5 times the load for area Nuenen/Son. For dissolved COD these values are 1.6 to 1.7 and 2.0, respectively. As for dry weather conditions, a catchment size effect is observed for the magnitude of peak loads. Also, the larger peak factors for pollutant parameters associated with suspended solids again express the strong relation between these parameters and flow: large flows during wet weather conditions cause a much larger increase in TSS loads than in CODf loads. The largest observed 24-hour peak load into the wwtp Eindhoven (TSS: 6.8 and CODf: 4.3) occurred for a fairly large storm event in May 2007 after a long dry period. The extreme loading of the plant has had a large negative impact on plant operation for weeks on end. The origin of additional wet weather pollutant loads are predominantly in-sewer stocks. With an increase of flows, pollutants in in-sewer sediments and biofilms are released and transported towards the wwtp. For a series of successive storm event it has been observed that each event is again associated with pollutant loads larger than during dry weather. This shows that - even for a series of large storms - in-sewer stocks are in fact 'inexhaustible' and not depleted after the first storm.

Chapter 7. In-sewer temperature monitoring
Distributed Temperature Sensing (DTS) with fiber-optic cables is a monitoring technique that yields high-resolution data sets in both time and space of the wastewater quality parameter 'temperature'. A fiber-optic cable is installed at the invert of a sewer pipe and on one side connected to a dedicated measurement instrument. Such a monitoring set-up typically yields temperature values at an interval of 30-60 seconds for each 2m section along the cable. Absolute accuracies of ±0.1°C are feasible after field calibration. Temporal and spatial precisions depend on the details of the monitoring configuration. The application of DTS in stormwater sewers aims at locating illicit connections: unintentional inflows of (untreated) wastewater to a stormwater system. Spills of wastewater can be detected by their anomalous temperature characteristics when compared to normal values for stormwater systems. More specifically, higher temperatures and quick temperature variations suggest an illicit connection. As precipitation influences monitoring results, only dry weather data should be used for this application. Detection of spills is rather straightforward in near-empty sewers, but sufficiently large or warm spills can also be detected in (partially) submerged systems. On-site verification efforts have confirmed the presence of illicit connections at locations suggested by DTS monitoring results.

Distributed temperature sensing in *combined* sewer systems has been tested in a 2 km sewer section. Results show that DTS can be used to study a number of processes that affect in-sewer temperatures with a high level of detail. More specifically, discharges from individual house-connections can be studied, but only for sewer sections that contain a limited amount of (waste)water. Also, the process of stormwater entering a sewer system can be observed in detail. Temperature data sets from combined sewer systems may be used in the development, calibration and validation of in-sewer wastewater temperature models. Moreover, with a dedicated cable configuration the confluence of wastewater in free flow pipes can be observed with a potential to derive contributions of contributary flows to a total flow.

Chapter 8. Concluding considerations

Regarding the first objective of the thesis it can be concluded that the application of UV/VIS and DTS monitoring techniques in sewer systems has proven feasible and largely advances in-sewer wastewater metrology. Installation set-up, sensor calibration, data uncertainty and data quality have been presented in this thesis. A final consideration is on data loss. Precipitation monitoring has experienced an unexpectedly large loss of data which can be largely ascribed to not using readily available knowledge on e.g. installation and calibration. For the flow data sets the transition from raw data to useful time-series has been a bottleneck. Data loss for the UV/VIS data sets was anticipated as it is a novel technique. However, retrospectively, a large part of the loss could have been prevented with back-up systems and an improved organizational structure. These examples are exemplary for the challenges faced in collecting good data sets from wastewater systems in the Netherlands.

For the second objective of the thesis an understanding of the variability of treatment plant influent flows and pollutant loads has been generated studying the characteristics of the observed dry and wet weather hydrographs and pollutographs of the wwtp Eindhoven. Moreover, processes have been distinguished that influence the shape of both types of graphs. Site-specific processes have been observed as well as processes that have also been noticed for other catchment areas. The acquired knowledge of wwtp influent dynamics can be used to develop potential improvements to wastewater system operation. Examples are an improved operation of the wwtp stormwater storage and settling tank and the prevention of peak loads upon the arrival of reject water from the Mierlo sludge installation. The extreme loading event of May 7th, 2007 may prove to be exemplary for events that will occur more often as a result of foreseen changes in climatic conditions.

A final consideration is on privacy issues when generating highly-detailed in-sewer measurements. The newly applied DTS technique offers the possibility to study in-sewer processes to a level of individual house connections. With such detailed data sets certain aspects of residents' behavior can be observed which might lead to misuse of the data.

Nederlandse samenvatting

De dynamica van afvalwaterkwaliteit: een studie gebaseerd op metingen

Hoofdstuk 1. Introductie

Lozingen van (onbehandeld) afvalwater dragen nog steeds in belangrijke mate bij aan de emissie van verontreinigingen naar het Nederlandse oppervlaktewater. De afgelopen decennia zijn door wetenschap en praktijk grote inspanningen verricht om de prestaties van afvalwatersystemen te verbeteren en daarmee een vermindering te bewerkstelligen van de impact van afvalwatersystemen op hun omgeving. Optimalisatiestudies spelen hierin een grote rol. Onderzoek toont aan dat plannen voor optimalisatie effectiever worden naarmate deze meer gericht zijn op *geïntegreerde* systeemoptimalisatie en rekening houden met de *dynamiek* in waterkwantiteit- en *kwaliteit*sparameters. Voor het verkrijgen van een gedetailleerde en nauwkeurige beschrijving van de dynamiek van waterkwaliteitsparameters in rioolsystemen is het gebruik van alleen modellen niet toereikend. Deels voor het kalibreren en valideren van modellen en deels omdat sommige processen vooralsnog te gecompliceerd zijn om te kunnen modelleren, wordt steeds vaker *gemeten* aan afvalwaterkarakteristieken. Het meten van debieten in rioolstelsels wordt al veelvuldig toegepast; het meten van afvalwaterkwaliteit in riolering is een meer recente ontwikkeling. Het eerste doel van dit proefschrift is een bijdrage te leveren aan de ontwikkeling van metrologie in rioolstelsels. Meer in het bijzonder wordt de toepassing behandeld van twee relatief nieuwe typen sensoren: UV/VIS spectroscopie en DTS met glasvezelkabels. De tweede doelstelling van dit proefschrift is de studie naar dynamiek van afvalwaterkwaliteit in rioolstelsels. Voor deze tweede doelstelling wordt gebruik gemaakt van de UV/VIS en DTS data zoals deze gegenereerd is in meetopstellingen in respectievelijk de rwzi Eindhoven en de gemeenten Ede, Groningen en Korendijk.

Hoofdstuk 2. Het afvalwatersysteem in de regio Eindhoven

De rioolwaterzuivering Eindhoven (750,000 i.e.) behandelt het afvalwater van tien gemeenten verdeeld over drie stroomgebieden die verschillen in grootte en karakter. Het rioolstelsel van de stad Eindhoven (ongeveer 265,000 i.e.) is direct op de rwzi aangesloten terwijl het afvalwater van zeven gemeenten ten zuiden van Eindhoven (260,000 i.e.) verzameld wordt in een transportriool van 32 km lengte (Riool-Zuid). Twee gemeenten ten noorden van Eindhoven (52,000 i.e.) voeren afvalwater af naar de zuivering via een 5 km lang transportriool. Het effluent van de rwzi wordt geloosd op de rivier de Dommel. Vooral in de zomer kan dit effluent een aanzienlijk deel uitmaken van het totale debiet in de rivier: tot 50% tijdens droogweer en zelfs tot 90% tijdens regenweer. Verslechtering van de effluentkwaliteit resulteert dientengevolge snel in overschrijding van oppervlaktewater-

normen en brengt ernstige schade toe aan de ecologie in de rivier. De beheerder van de zuivering (Waterschap de Dommel) heeft de ambitie om het afvalwatersysteem in de regio Eindhoven verder te optimaliseren en onderzoekt, naast andere opties, de mogelijkheden om actieve sturing in het systeem toe te passen. Hiertoe is een meetnet geïnstalleerd voor neerslag-, waterkwantiteit- en waterkwaliteitsmetingen.

Hoofdstuk 3. Neerslagmetingen

Neerslag is een belangrijke drijvende kracht achter variaties van afvalwater-kwantiteit en -kwaliteit in rioolstelsels. In de regio Eindhoven is een meetnet bestaande uit 22 kantelbakregenmeters geïnstalleerd om hoogfrequente regendata te kunnen verzamelen. De datasets zijn uitgebreid gecontroleerd op kwaliteit van de data, zowel met de hand als met geautomatiseerde methodes. Ongeveer 50% van de beoogde data ontbrak of is afgekeurd. Neerslagdieptes over de lange termijn (jaar, maand) zijn vergeleken met gegevens van zes neerslagmeters van het KNMI. Deze vergelijking laat zien dat de geïnstalleerde kantelbakken de neerslagdiepte ongeveer 20% tot 25% systematisch onderschatten. Ongeveer de helft van de *bias* kan verklaard worden door een ontbrekende kalibratie; na afloop van de meetperiode zijn de sensoren alsnog gekalibreerd en is de dataset hiervoor gecorrigeerd. De andere helft van de systematische afwijking is waarschijnlijk te wijten aan ongunstige meetomstandigheden: veel kantelbakken hebben last gehad van windschaduw ten gevolge van te nabijgelegen objecten. Correctie voor deze fout is niet mogelijk. Concluderend kan gesteld worden dat het meetnet van neerslagsensoren matig gepresteerd heeft. Desalniettemin is de (gevalideerde en gecorrigeerde) data gebruikt om neerslag per stroomgebied af te leiden middels een ‘inverse distance weighting’ methode. Aangezien de neerslaggegevens vooral in kwalitatieve en minder in kwantitatieve zin zijn gebruikt, hebben voornoemde gebreken in de neerslaggegevens weinig invloed gehad op uiteindelijke analyse-resultaten in hoofdstuk 6.

Hoofdstuk 4. Debietmetingen

Voor de bepaling van vuil*vrachten* in het afvalwater dat de rwzi Eindhoven binnenstroomt, zijn debietmetingen (hoofdstuk 4) alsook waterkwaliteitsmetingen (hoofdstuk 5) noodzakelijk. Om het debiet uit de drie stoomgebieden Riool-Zuid, Eindhoven Stad en Nuenen/Son te kunnen bepalen, is gebruik gemaakt van de data van negen debietsensoren in het influentgemaal van de rwzi. Elke sensor meet het debiet dat verpompt wordt door één influentpomp; elk stroomgebied wordt bediend door twee, drie of vier influentpompen. De data van de debietsensoren zijn als eerste gecontroleerd op kwaliteit. Er is nauwelijks foutieve data geconstateerd, maar wel een systematische fout bij niet-werkende pompen. De data van de negen debietsensoren is vervolgens gecombineerd tot drie tijdreeksen met stroomgebied-debieten. Hierbij is rekening gehouden met een wisselende toewijzing van één bepaalde pomp en het debiet over een interne overstort in het influentgemaal. Meer

dan 99% van de debietgegevens heeft een onzekerheid van minder dan 1%. Alleen tijdens perioden van grote neerslag kan de totale meetonzekerheid oplopen tot rond de 10% ten gevolge een relatief grote onzekerheid in stroming over de interne overstort.

Hoofdstuk 5. Waterkwaliteitmetingen

Waterkwaliteitsmetingen in het influentgemaal van de rwzi Eindhoven zijn uitgevoerd met drie UV/VIS spectrometers (één per influentkelder) die in staat zijn middels een optisch meetprincipe hoogfrequente datasets te creëren. De sensoren zijn geïnstalleerd in speciaal ontwikkelde by-pass installaties die intensief onderhoud vergen. Beschouwde waterkwaliteitsparameters zijn zwevende stof (ZS) en totaal en opgelost chemisch zuurstof verbruik (CZV en CZVf). Monstername-campagnes tijdens droogweer en regenweer hebben aangetoond dat de sensoren goed in staat zijn om trends in parametervariaties te reproduceren. Voor droog-weersituaties liggen verschillen tussen sensorwaarden (fabrieksinstellingen of 'global calibration') en referentiewaarden (afgeleid in het laboratorium uit steek-monsters) binnen een marge van ruwweg ±25% (Riool-Zuid, Eindhoven Stad) en ±50% (Nuenen/Son). Tijdens regenweer zijn grote (absolute) verschillen geconstateerd in concentratiepieken aan het begin van een bui, maar ook grote (relatieve) verschillen in de daaropvolgende verdunningsfase. Door middel van regressieanalyse zijn nieuwe kalibratiesets ontwikkeld ('local calibration') die een betere fit laten zien tussen sensorwaarden en referentiewaarden. Enkele sets zijn (te) mager onderbouwd daar deze gebaseerd zijn op te weinig referentiewaarden. Een foutinschatting van meetwaarden van lokaal gekalibreerde sensoren combineert de onzekerheid in de regressielijn met de intrinsieke sensoronzekerheid. In de inschatting is uitdrukkelijk niet meegenomen de onzekerheid ten gevolge van een slecht onderbouwde regressielijn door bijvoorbeeld een te beperkt aantal referentiemonsters of niet-representativiteit van monsters. Een kwaliteitscontrole van de UV/VIS datasets laat zien dat 25% tot 50% van de data moet worden afgekeurd. Het grootste deel van het dataverlies is te wijten aan vermijdbare fouten in de meetopstelling. Er wordt geconcludeerd dat, met juiste uitgevoerde installatie en onderhoud van sensor en meetopstelling, een dataopbrengst van meer dan 90% mogelijk moet zijn met dit type sensor.

Hoofdstuk 6. Analyse van het influent van de rwzi Eindhoven

In dit hoofdstuk wordt de dynamiek bestudeerd van het afvalwater dat arriveert op de rwzi Eindhoven vanuit de stroomgebieden Riool-Zuid, Eindhoven Stad en Nuenen/Son. Uit de data van circa 200 *droogweerdagen* kunnen kenmerkende dag-, week- en jaarvariaties worden herleid. Standaard dag- en weekvariaties kunnen ook worden waargenomen voor waterkwaliteitsparameters. De concentratie zwevende stof in het afvalwater wordt mede bepaald door debietvariaties in het stelsel waardoor variaties in beide parameters veelal synchroon verlopen. De combinatie van beide parameters (i.e. *vrachten* zwevende stof) vertoont dientengevolge grotere

variaties dan de gemeten concentraties. Opgelost CZV wordt minder beïnvloed door dit fenomeen en vertoont weinig variaties gedurende droogweer. Zowel voor debiet als voor vuilvrachten kan een gebiedsgrootte-effect worden waargenomen: het kleinste stroomgebied vertoont de grootste parametervariaties en vice versa.
Tijdens *regenweer* zijn de aangevoerde vuilvrachten op de zuivering Eindhoven (veel) groter dan tijdens droogweer. Aangevoerde vuilvrachten tijdens circa 65 regenbuien zijn bepaald, gemiddeld over 24 uur en vergeleken met daggemiddelde vrachten tijdens droogweer. Resultaten tonen dat voor een 'gemiddelde regenbui' ongeveer 2 tot 3 maal zoveel zwevende stof vanuit Riool-Zuid en Eindhoven Stad komt en ongeveer 5.5 maal zoveel uit Nuenen/Son. Voor opgelost CZV zijn deze waarden respectievelijk 1.6 tot 1.7 en 2. Uit deze getallen blijkt dat voor de grootte van piekvrachten ook een gebiedsgrootte-effect optreedt. Tevens blijkt wederom de relatie tussen debiet en zwevende stof: toegenomen debieten tijdens regenweer-afvoer veroorzaken een grotere toename van vrachten zwevende stof dan van vrachten opgelost CZV. De grootst gemeten piekvracht naar de rwzi Eindhoven (ZS: 6.8 en opgelost CZV: 4.3) deed zich voor tijdens een relatief grote bui in mei 2007 na een lange periode zonder neerslag. Deze extreem grote hoeveelheid vuilvracht heeft het functioneren van de zuivering een tijdlang ontregeld. De extra vuilvrachten die tijdens regenweer op de rwzi arriveren, komen uit 'vuilvoorraden' in het riool. Door een toename van het debiet komt materiaal vrij uit sediment- en slijmlagen die zich in het riool bevinden. Metingen tonen aan dat bij een reeks opeenvolgende regenbuien elke bui wederom een toename in vuilvrachten op de zuivering laat zien. Daaruit kan worden geconcludeerd dat de vuilvoorraad in riolering in feite 'onuitputtelijk' is in de zin dat een rioolstelsel niet 'schoongespoeld' is na een eerste bui, maar voor elke nieuwe bui een wederom voorraad vuilvracht beschikbaar is.

Hoofdstuk 7. Temperatuurmetingen in het riool
Distributed Temperature Sensing (DTS) met glasvezelkabels genereert datasets met een hoge resolutie in tijd én ruimte van de temperatuur van afvalwater. Een glasvezelkabel wordt op de bodem van een rioolbuis gepositioneerd en aan één zijde verbonden met een meetinstrument. Veelal wordt elke 30 tot 60 seconden een temperatuurmeting verricht per sectie van 2m lengte van de kabel. Een absolute meetbetrouwbaarheid van ±0.1°C is haalbaar middels kalibratie. Meetnauwkeurigheden hangen af van de gekozen resoluties en meetopstelling. De toepassing van DTS in hemelwaterriolen richt zich op het lokaliseren van foutaansluitingen: onbedoelde lozingen van (onbehandeld) afvalwater op een regenwaterriool. Dergelijke lozingen kunnen worden gedetecteerd aan de hand van hun afwijkende temperatuurkarakteristieken: hoge temperaturen alsook snelle veranderingen in de temperatuur wijzen veelal op het binnenstromen van ruw afvalwater. Neerslag heeft ook een duidelijk effect op de temperatuur in het hemelwaterstelsel; voor deze toepassingen moet daarom alleen gebruik worden gemaakt van data verzameld tijdens droogweer. Foutaansluitingen kunnen vrij eenvoudig worden

gevonden in vrijwel lege rioolbuizen. In (gedeeltelijk) verdronken stelsels is het ook mogelijk, maar alleen als de lozing voldoende groot of warm is. Verificatie ter plaatse heeft aangetoond dat zich inderdaad foutaansluitingen bevinden op de locaties zoals aangeduid door de DTS meetgegevens.
DTS is ook toegepast in een gemengd rioolstelsel van circa 2 km lengte. De resultaten tonen aan dat de meetmethode goed gebruikt kan worden om een aantal processen in detail te kunnen bestuderen die de (afvalwater)temperatuur in het riool beïnvloeden. Zo kunnen lozingen vanuit huisaansluitingen in beeld gebracht worden, maar alleen voor strengen die weinig afvalwater bevatten. Ook de inloop van regenwater in het gemengde stelsel kan tot in detail worden bekeken. Temperatuurdata uit gemende rioolstelsels kan van toegevoegde waarde zijn in de ontwikkeling, de kalibratie en validatie van modellen die de afvalwatertemperatuur beschrijven. Ook lijkt het mogelijk om met een speciale kabelconfiguratie bij de samenkomst van twee afvalwaterstromen in vrijvervalleidingen de relatieve bijdrage van beide stromen te bepalen.

Hoofdstuk 8. Afrondende beschouwingen
The toepassen van UV/VIS en DTS meetsystemen in riolering is haalbaar gebleken en levert een belangrijke bijdrage aan de ontwikkeling van metrologie in rioolstelsels. In dit proefschrift zijn installatie, sensorkalibratie, dataonzekerheid en datakwaliteit aan bod gekomen. Een laatste beschouwing aangaande metrologie in rioolsystemen betreft het relatief grote verlies aan data dat opgetreden is bij verschillende meetcampagnes in dit proefschrift. Voor de neerslagmetingen is dit in essentie te wijten geweest aan het niet toepassen van bestaande kennis over installatie, kalibratie, etc. Voor de debietmetingen is niet zozeer veel data verloren gegaan als wel is de transitie van ruwe data naar nuttige tijdsreeksen een bottleneck gebleken. Voor de UV/VIS sensoren was geanticipeerd op dataverlies daar het een nieuwe meetmethode betreft. Achteraf beschouwd had een groot deel van het verlies voorkomen kunnen worden middels een aantal reservesystemen en een verbeterde opzet van de personele organisatie rondom de meetopstelling. De voornoemde voorbeelden zijn exemplarisch voor de uitdagingen waarvoor afvalwatersysteembeheerders in Nederland zichzelf gesteld zien bij het verzamelen van goede meetdata uit afvalwatersystemen.
Het bestuderen van de verzamelde data van het influent van de rwzi Eindhoven heeft geleid tot een beter begrip van de dynamica die daarin een rol speelt. Hiertoe zijn voor droogweer en voor regenweer karakteristieke curves afgeleid voor afvalwaterkwantiteit en - kwaliteit. Bovendien zijn processen beschouwd die een invloed hebben gehad op de kenmerken van deze curves. Sommige van deze processen zijn specifiek voor de regio Eindhoven, andere hebben ook toepassing in andere afvalwatersystemen. De verkregen kennis over de influentdynamiek kan worden toegepast in de optimalisatie van het beschouwde systeem. Voorbeelden hiervan zijn een betere inzet van de regenwaterbezinktank op de rwzi en het voorkómen van piekvrachten ten gevolge van lozingen uit de slibverwerking in

Mierlo. De eerder beschreven extreme piekvrachten tijdens een bui in mei 2007 zouden, gezien hun oorzaak, vaker kunnen gaan voorkomen als de voorziene veranderingen in het Nederlandse klimaat doorgang zullen vinden.
Een laatste beschouwing betreft de vergaring van privacy-gevoelige informatie met behulp van metingen in rioolstelsels. Met de DTS meettechniek is het mogelijk om tot op het ruimtelijk niveau van huisaansluitingen processen te bestuderen die zich in het rioolstelsel afspelen. Dergelijke gedetailleerde datasets lenen zich ook andere doeleinden dan waardoor de data verzameld is.

Abbreviations

-eq	equivalent
CCTV	closed-circuit television
COD	chemical oxygen demand
CODf	chemical oxygen demand filtered
CSO	combined sewer overflow
DTS	distributed temperature sensing
DWF	dry weather flow
ES	Eindhoven Stad (catchment area discharging to wwtp Eindhoven)
GPRS	general packet radio service
ICA	instrumentation, control and automation
KNMI	Koninklijk Nederlands Meteorologisch Instituut (Royal Dutch Meteorological Institute)
mNAP	meter above Normaal Amsterdams Peil (Amsterdam Ordnance Datum, used as vertical datum in level measurements)
NM	neerslagmeter (raingauges operated by the municipality of Eindhoven)
NS	Nuenen/Son (catchment area discharging to wwtp Eindhoven)
p.e.	population equivalent
PLF	peak load factor
RMSE	root mean squared error
RTC	real-time control
RZ	Riool-Zuid (catchment area discharging to wwtp Eindhoven)
SST	stormwater storage tank
TBRG	tipping bucket rain gauge
TSS	total suspended solids
TU Delft	Delft University of Technology
UTC	coordinated universal time
UV/VIS	ultraviolet / visible
WDD	Waterschap De Dommel (waterboard De Dommel)
WWF	wet weather flow
wwtp	wastewater treatment plant

List of publications

Peer reviewed journals

Schilperoort R.P.S., Gruber G., Flamink C.M.L., Clemens F.H.L.R. and Graaf J.H.J.M. van der (2006). Temperature and conductivity as control parameters for pollution-based real-time control. *Water Sci. Technol.*, **54**(11-12), 257-263.

Schilperoort R.P.S., Meijer H.A.J., Flamink C.M.L. and Clemens F.H.L.R. (2007). Changes in isotope ratios during domestic wastewater production. *Water Sci. Technol.*, **55**(4), 93-101.

Hoes O.A.C., Schilperoort R.P.S., Luxemburg W.M.J., Clemens F.H.L.R. and Giesen N.C. van de (2009). Locating illicit connections in storm water sewers using fiber-optic distributed temperature sensing. *Water Res.*, **43**(20), 5187-5197.

Dirksen J., ten Veldhuis J.A.E. and Schilperoort R.P.S. (2009). Fault tree analysis for data-loss in long-term monitoring networks. *Water Sci. Technol.*, **60**(4), 909-915.

Schilperoort R.P.S. and Clemens F.H.L.R. (2009). Fibre-optic distributed temperature sensing in combined sewer systems. *Water Sci. Technol.*, **60**(5), 1127-1134.

Schilperoort R.P.S., Dirksen J., Langeveld J.G. and Clemens F.H.L.R. (subm.). Assessing characteristic time and space scales of in-sewer processes by analysis of one year of continuous in-sewer monitoring data. Submitted to *Water Sci. Technol.*

Conferences and proceedings

Henckens G.J.R., Schilperoort R.P.S. and Clemens F.H.L.R. (2005). Monitoring network design using multiple storm events. In: Proc. 10th Int. Conf. on Urban Drainage, Copenhagen, Denmark, 21-26 August 2005, CD-ROM edition.

Schilperoort R.P.S., Meijer H.A.J., Flamink C.M.L. and Clemens F.H.L.R. (2006). Changes in isotope ratios during domestic wastewater production. In: Proc. 7th Int. Conf. on Urban Drainage Modeling, Melbourne, Australia, 2-7 April 2006, V2-23-30.

Schilperoort R.P.S., Gruber G., Flamink C.M.L., Clemens F.H.L.R. and Graaf J.H.J.M. van der (2006). Temperature and conductivity as control parameters for

pollution-based real-time control. In: Proc. 5th IWA World Water Congress, Beijing, China, 10-14 September 2006, CD-ROM edition.

Flamink C.M.L., Langeveld J.G., Schilperoort R.P.S., Clemens F.H.L.R. and Graaf J.H.J.M. van der (2006). Real time control of the integrated wastewater system: control potential for different loading conditions. In: Proc. 5th IWA World Water Congress, Beijing, China, 10-14 September 2006, CD-ROM edition.

Schilperoort R.P.S., Flamink C.M.L., Clemens F.H.L.R. and Graaf J.H.J.M. van der (2006). Long-term monitoring campaign in the wastewater transport system of WWTP Eindhoven, the Netherlands: the set-up. In: Proc. 2nd Conf. on Sewer Operation and Maintenance, Vienna, Austria, 26-28 October 2006, 361-367.

Schilperoort R.P.S. and Clemens F.H.L.R. (2007). Relations between wastewater temperature and wastewater quality during DWF and WWF. In: Proc. 5th Conf. on Sewer Processes and Networks, Delft, the Netherlands, 29-31 August 2007, 23-29.

Schilperoort R.P.S., Dirksen J., Clemens F.H.L.R. (2008). Practical aspects for long-term monitoring campaigns: pitfalls to avoid to maximize data yield. In: Proc. 11th Int. Conf. on Urban Drainage, Edinburgh, UK, 1-5 September 2008, CD ROM.

Schilperoort R.P.S. and Clemens F.H.L.R. (2009). Fiber-optic distributed temperature sensing in combined sewer systems. In: Proc. 10th IWA Conf. on Instrumentation Control & Automation, Cairns, Australia, 14-17 June 2009, CD ROM.

Dirksen J., Veldhuis J.A.E ten and Schilperoort R.P.S. (2009). Fault tree analysis for data-loss in long-term monitoring networks. In: Proc. 10th IWA Conf. on Instrumentation Control & Automation, Cairns, Australia, 14-17 June 2009, CD ROM.

Schilperoort R.P.S., Dirksen J., Langeveld J.G. and Clemens F.H.L.R. (2009). Assessing characteristic time and space scales of in-sewer processes by analysis of one year of continuous in-sewer monitoring data. In: Proc. 8th Int. Conf. on Urban Drainage Modeling, Tokyo, Japan, 7-12 September 2009, CD ROM.

Schilperoort R.P.S., Hoes A.O.C., Luxemburg W.M.J., Clemens F.H.L.R. and Giesen N.C. van de (2009). In-sewer temperature monitoring for the detection of illicit connections in stormwater sewers. In: Proc. 8th Int. Conf. on Urban Drainage Modeling, Tokyo, Japan, 7-12 September 2009, CD ROM.

Haan C. de, Langeveld. J.G., Schilperoort R.P.S. and Klootwijk M. (subm.). Locating and classifying illicit connections with Distributed Temperature Sensing.

Submitted to 12th Int. Conf. on Urban Drainage, Porto Alegre, Brazil, 11-16 September 2011.

Langeveld. J.G., Haan C. de, Klootwijk M. and Schilperoort R.P.S. (subm.). Monitoring the performance of a storm water separating manifold with DTS. Submitted to 12th Int. Conf. on Urban Drainage, Porto Alegre, Brazil, 11-16 September 2011.

Langeveld J.G., Schilperoort R.P.S., Weijers S.R., Jonge J. de and Flameling T. (subm.). Climate change and urban wastewater infrastructure: there is more to explore. Submitted to 8th Leading-Edge Conf. on Water and Wastewater Technologies, Amsterdam, the Netherlands, 6-10 June 2011.

National publications (in Dutch)

Schilperoort R.P.S. (2004). Natuurlijke waterisotopen voor de kwantificering van rioolvreemd water (in Dutch: Natural water isotopes for the quantification of extraneous flows). In: Proc. PAO course 'Interactions within the wastewater system', Rotterdam, the Netherlands, 15/29 October, 2004.

Schilperoort R.P.S. (2004). Natuurlijke waterisotopen voor de kwantificering van rioolvreemd water (in Dutch: Natural water isotopes for the quantification of extraneous flows). *Rioleringswetenschap*, **4**(16), 45-57.

Schilperoort R.P.S. (2005). Natuurlijke waterisotopen voor de kwantificering van rioolvreemd water (in Dutch: Natural water isotopes for the quantification of extraneous flows). In: Proc. 57th Vakantiecursus Drinkwatervoorziening en Riolering en Afvalwaterbehandeling, Delft, the Netherlands, 14 January, 2005, 75-86.

Helm A.W.C. van der and Schilperoort R.P.S. (2005). Verslag 57e Vakantiecursus Drinkwatervoorziening en Riolering en Afvalwaterbehandeling: van medicijnen wordt het water niet beter (in Dutch: Report of 57th TU Delft Sanitary Engineering Conference). *H_2O*, **38**(2), 4-6.

Schilperoort R.P.S. and Flamink C.M.L. (2005). Verslag 4e Internationale Conferentie over rioolprocessen en -netwerken (in Dutch: Report on 4th SPN conference). *Rioleringswetenschap*, **5**(17), 46-52.

Flamink C.M.L. and Schilperoort R.P.S. (2005). Interacties binnen het afvalwatersysteem (in Dutch: interaction within wastewater systems). *Afvalwaterwetenschap*, **5**(20), 100-105.

Smits J., Schilperoort R.P.S. and Flamink C.M.L. (2006). Vliegende putdeksels (in Dutch: Flying manhole covers). *Rioleringswetenschap*, **6**(21), 34-39.

Schilperoort R.P.S., Clemens F.H.L.R., Weijers S., Sikkes M. (2007). Meetcampagne in het afvalwatertransportsysteem naar de rwzi Eindhoven: keuzes tijdens de ontwerpfase (in Dutch). Rioleringswetenschap, 6(24), 49-57.

Schilperoort R.P.S. (2007). Temperatuur en geleidbaarheid als indicator parameters voor verdunning in een rioolsysteem (in Dutch: temperature and conductivity as indicator parameters for dilution in a sewer system). *Afvalwaterwetenschap*, **6**(2), 66-73.

Schilperoort R.P.S. (2007). Temperatuur en geleidbaarheid als indicator parameters voor verdunning in een rioolsysteem (in Dutch: temperature and conductivity as indicator parameters for dilution in a sewer system). In: Proc. 59th Vakantiecursus Drinkwatervoorziening en Riolering en Afvalwaterbehandeling, Delft, the Netherlands, 12 January 2007, 111-118.

Schilperoort R.P.S., Weijers S. and Sikkes M. (2007). Waterschap zet meetnet op voor afvalwater Eindhoven (in Dutch: Water board initiates monitoring for the Eindhoven area). *Land+Water*, **47**(1/2), 26-27.

Schilperoort R.P.S., Dirksen J., Langeveld J.G., Clemens F.H.L.R. (2009). De dynamiek in het aanvoerpatroon van de rwzi Eindhoven in beeld: een studie naar karakteristieke tijd- en ruimteschalen van RWZI influent op basis van 1,5 jaar hoogfrequente kwantiteits- en kwaliteitsgegevens (in Dutch). *Rioleringswetenschap*, **9**(34), 58-66.

Schilperoort R.P.S., Dirksen J., Langeveld J.G. and Clemens F.H.L.R. (2009). Piekvrachten naar rioolwaterzuivering Eindhoven in beeld (in Dutch: Assessment of peak loads to wwtp Eindhoven). *Land+Water*, **49**(12), 26-27.

Curriculum vitae

Rémy Peter Sander Schilperoort was born on August 7th, 1977 in Delft, the Netherlands. He attended high school (VWO, Oranje Nassau College) in Zoetermeer, the Netherlands from 1989 until graduation in 1995. Subsequently, he studied at Tulane University in New Orleans, Louisiana (USA) for two semesters in 1995/1996 with a focus on foreign languages and computer science. He continued studying at Delft University of Technology, faculty of Civil Engineering and Geosciences, majoring in Sanitary Engineering. In 1998/1999 Rémy interrupted his study for one year to become full-time board member of the faculty's student organization. In 2002 he spent 5 months at the Universidad de San Agustin in Arequipa (Peru) for an internship. In May 2004 he graduated with honors writing an MSc thesis on a novel isotope method to quantify extraneous flows in wastewaters in collaboration with INSA de Lyon (France).

Between 2004 and 2009 Rémy has held a PhD position at Delft University of Technology, faculty of Civil Engineering and Geosciences. The research project - funded by a consortium of water authorities and consulting firms - has primarily focused on wastewater system monitoring. In 2006 and 2007 he has co-organized the 5th International Conference on Sewer Processes and Networks (SPN 5) in cooperation with UNESCO/IHE.

Since August 2009 Rémy has been an independent consultant at Argus Analyse in Amsterdam, the Netherlands. He has worked for a number of clients advising on the application of wastewater monitoring systems. Starting July 2011 he will be employed by Royal Haskoning in Amsterdam and Nijmegen as a consultant in wastewater systems.

Acknowledgements

In conclusion a few words of appreciation. Many have helped me over the course of the last years and for this I would like to express my sincere gratitude.

First of all I would like to thank my supervisors François Clemens and Jaap van der Graaf. François, you've taught me a lot of good things, and not just about sewer systems. Jaap, your quick and sharp analyses surprise me every time. It has been a pleasure working with both of you.

My position at university leading up to this thesis would not have been possible without the financial support of Arcadis, Grontmij, Hoogheemraadschap Hollands Noorderkwartier, Royal Haskoning, Tauw, Waternet, Waterschap de Dommel, Waterschap Groot Salland and Witteveen+Bos. Moreover, representatives of these organizations have supported me with their valuable ideas and feed-back attending regular discussions on the research and its results. Thank you Egbert Baars, Henk Drost, Herman Evenblij, Simon Gaastra, Saskia Holthuijsen, Erwin Koetse, Jeroen Kluck, Jeroen Langeveld, Gert Lemmen, Michel Moens, Arjen van Nieuwenhuijzen, Jelle Roorda, Niels Schaart, Hielke van der Spoel, Henry van Veldhuizen, Stefan Weijers, Leo Wensveen and Jan Zuidervliet. I appreciate the faith you have put in me over these years.

A large part of the work for this thesis has been done in cooperation with as well as with support of Waterschap de Dommel. I am much indebted to the many 'Dommelaars' who have helped me out on many occasions. I want to specifically name Stefan Weijers, Jarno de Jonge, Robin Metz, Iwona Grabowska, Bianca Blom, Jesse Flohr, Aart Verschoor, Krista Noppen and Jurgen Nous. Michel Sikkes, without you I'd probably still be lost somewhere in the woods between Valkenswaard and Bergeijk. Thanks for all your effort to show me around.

The work on DTS has been partly done in cooperation with colleagues of the Water Resources Management section. Olivier Hoes and Wim Luxemburg, thanks for your help and for sharing some of your data. Also, Laura Tanis of the municipality of Ede is acknowledged for allowing us to test DTS monitoring in the Ede sewer systems.

Everyday working life in Delft has been made enjoyable by pleasant colleagues: Adrien, Aldo, Anke, Annelies, Arie, Diana, Jaap, Maria, Mieke, Petra, Sigrid, Stephan and Vivian. Tonny, your assistance in lab-related issues has been very valuable. To my current and former 'sewer-colleagues' Cathelijne, Christof, Ivo, Marco, Marie-Claire, Matthieu and Vincent: thanks for all the fun we shared going

to conferences and field trips, enjoying many dinners and even more beers. Marie-Claire, we kicked buttocks organizing SPN!

A special word for two colleagues who have become more than just that: Jojanneke Dirksen and Jeroen Langeveld. Jojanneke, your contribution to this thesis has been significant for which I am most grateful. Apart from the work, you're a fun person to spend time with. Jeroen, your contribution to my work cannot be overestimated, thanks. I've thoroughly enjoyed our discussions and hope they will continue as future colleagues at Royal Haskoning.

This thesis would not have been possible without all the coffees and lunches served by the employees of (in alphabetical order): hotel Américain, café Amsterdam, de Bakkerswinkel, de Blaffende Vis, Blond&Blont, Coffee Plaza, café Dantzig, café Entredok, café Finch, Harlem, café de Jaren, Katoen, café Kobalt, café Koosje dochter van Stevens, café Luxembourg, café Milo, NAP / het Badhuis, OBA (thanks Lotte for being a sister in arms!), Pacific, Pakhuis de Zwijger, café het Paleis, de Ponteneur, de II Prinsen, Razmataz, café Ruysch, café Schenkelhoek, café de Sluyswacht, 't Smalle, café Sowieso, café Stevens, Stout!, Tabak, café de Tijd, café Thijssen, café de Tuin, de Vergulde Gaper, Vertigo/Filmmuseum, Walem, 't Weeshuis, café Wester, and de Winkel van Sinkel. I much appreciate it.

Derk-Jan, Rik and Tonie, friends for nearly 15 years. I hope it's just the beginning.

Marieke, Elodie and Féline, I'm really finished now. I could not be happier and prouder than with my three women.

Rémy Schilperoort
Amsterdam, May 2011